Marvin Alfredo Anganoy Criollo

As relações filogenéticas de *Hyloxalus* Jiménez de la Espada 1870 (Anura: Dendrobatidae)

The phylogenetic relationships of *Hyloxalus* Jiménez de la Espada 1870 (Anura: Dendrobatidae)

São Paulo

2022

Marvin Alfredo Anganoy Criollo

As relações filogenéticas de *Hyloxalus* Jiménez de la Espada 1870 (Anura: Dendrobatidae)

The phylogenetic relationships of *Hyloxalus* Jiménez de la Espada 1870 (Anura: Dendrobatidae)

EXEMPLAR CORRIGIDO

Tese apresentada ao Instituto de Biociências da Universidade de São Paulo, para a obtenção de Título de Doutor em Ciências Biológicas, na Área de Zoologia.

Orientador(a): Prof. Dr. Taran Grant

São Paulo

2022

Anganoy-Criollo, Marvin
The phylogenetic relationships of Hyloxalus Jiménez de la Espada 1870 (Anura: Dendrobatidae) / Marvin Anganoy-Criollo ; orientador Taran Grant -- São Paulo, 2022.
378 p. + anexo

Tese (Doutorado) -- Instituto de Biociências da Universidade de São Paulo. Programa de Pós-Graduação em Zoologia.

1. Phenotypic characters. 2. Total evidence. 3. Successive outgroup expansion. 4. Dendrobatoidea. 5. Hyloxalinae. I. Grant, Taran, orient. II. Título.

Comissão Julgadora:

Prof(a). Dr(a).

Prof(a). Dr(a).

Prof(a). Dr(a).

Prof(a). Dr(a).

Prof. Dr. Taran Grant
Orientador

Nomenclatural Disclaimer

The taxonomic changes presented herein, including new taxa, combinations, and synonymy, are disclaimed as nomenclatural acts and are not available, in accordance with Article 8.3 of the International Code of Zoological Nomenclature.

A minha família, Paulo Nicolás Anganoy Lamadrid e
Faride Lamadrid, e meus pais, Luz Marina Criollo
e Alfredo Anganoy.

Agradecimentos

Muitas pessoas e instituições ajudaram nessa pesquisa, sem eles eu não tivera conseguido realizar a tese. Eu agradeço especialmente a:

Meu orientador, o Prof. Dr. Taran Grant pela ajuda constante, todos os ensinamentos, as discussões, e os conselhos.

Ao Prof. Dr. John D. Lynch pelos ensinamentos, discussões e conselhos durante longo dos anos como herpetólogo.

Ao Dr. Pedro Dias, pela imensa ajuda com girinos de anuros em geral.

Ao Dr. Boris Blotto, Dr. David Sánchez, Dr. Denis J. Machado, Dr. Jimmy Cabra, Dr. John D. Lynch, Dr. John Jairo Ospina, Dra. Mariane Targino, Dr. Martín Pereyra, Dr. Pedro Dias, e a Dra. Rachel Montesinos pelas discussões em taxonomia, desenvolvimento, sistemática, filogenia e evolução.

À Dra. Adriana Jeckel, M.Sc. Isabella Cavalcanti, Dr. Andrés Brunetti, e os técnicos Phillip Lenktaitis e Enio Mattos pela ajuda na histologia, e discussões em glândulas de rãs.

Ao Dr. Edgar Gamero, Dr. Jairo Moreno, a Dra. Julia Benetti e a Manuel Antunes pela discussões em biologia molecular, e procedimentos na obtenção de DNA. À M.Sc. Clarissa Garbi Molinari quem ajudou-me muito no laboratório de biologia molecular.

À meus colegas do Laboratório de Anfíbios, Adriana Jeckel, Rachel Montesino, Pedro Dias, Carola Yovanovich, Gabriel Cohen, Mariane Targino, Rafael dos Santos Henrique, Denis Machado, Isabela Cavalcanti, Jhon Jairo Ospina, David Andrés, Boris Blotto, Marco Rada, Julia Primon, Rafaela Perez, João Marcos Pereira, e Paulo Pinheiro, por todos os momentos longo desses anos.

À minha família, Paulo Nicolas Anganoy e Faride Lamadrid, pela companhia, amor, e todo o apoio incondicional neste processo. A meus pais e irmãos, Luz Marina Criollo, Alfredo Anganoy, Jhonatan Anganoy e Daisy Anganoy pela força constante e apoio.

À todas as pessoas que ajudaram com o trabalho de campo na Colombia e no Ecuador: Adolfo Ortega, Andrés Aponte, Andrés Viuche, Ariel Lozano, Brian Giraldo, Carolina Reyes Puig, V. Catalina Gutierrez, Cesar Mongui, Duvan Zambrano, Cristian Castro, Edwin Beltran, Esteban Betancourt, Fiorela Delgado, Fraibel Giraldo, Gustavo Gonzales, Gustavo Pisso, Ivan Mauricio Pareja, Jaime Ortega, José Guzman, Juan Sebastian Forero, Maria Paulo Enciso, Mario Castellanos, Merilyn Caballero, Pablo Portilla, Paola Triviño, Raiza Castañeda, e Sigifredo Clavijo. Também, eu agradeço à todas as famílias que nos acolheram no campo.

Aos professores e curadores que abriram as portas de seus laboratórios, facilitaram o acesso ao material, informação e fotos, e fizeram empréstimos: Darrel Frost, Frank T. Burbrink, David Kizirian, David Dickey, e Margaret G. Arnold (AMNH), Mark Wilkinson e Barry Clark (BMNH), Erika J. Ely (CAS-SUA), Manuel Bernal e Sigifredo Clavijo (CZUT-A), Pablo Venegas (CORBIDI), John D. Lynch (ICN), Rafe Brown, Richard Glor, e Melissa Mayhew (KU), Danny Urrego (ITM, before CJS-H), Andrew Crawford (ANDES-A), Aline Staskowian Benetti e Hussam Zaher (MZUSP), José P. Pombal Jr., e Manoela Woitovicz Cardoso (MNRJ), Belisario Cepeda e Fernando Santander (PSO-CZ), Addison Wynn, Steve Gotte e Esther Lagan (MCZ-A), Beatriz Alvarez Dorda (MNCN), Kevin de Queiroz e Addison Wynn (NMNH, ex-USNM), Cameron Siler e Jessa L. Watters (OMNH), Santiago Ron (QCAZ), Diego Cisneros e Carolina Reyes (USFQ) Claudia Koch,

Morris Flecks e Inna Rech (ZFMK), Michael Franzen (ZSM), e Mark-Oliver Rödel e Frank Tillack (ZMB).

Aos meus amigos de toda a vida. Eles me apoiaram emocionalmente desde meus primeiros dias como herpetólogo.

À Fundación Centro de Estudios Interdisciplinarios Básicos y Aplicados – CEIBA, Colombia, ano 2016, pela ajuda econômica no doutorado.

O presente trabalho foi realizado com apoio da Coordenação de Aperfeiçoamento de Pessoal de Nível Superior – Brasil (CAPES) – Código de Financiamento 001, e à Fundação de Amparo à Pesquisa do Estado de São Paulo (FAPESP Procs., 2012/10000-5, and 2018/15425-0), pelo apoio econômico parcial.

Índice

General Introduction

Hyloxalus Jiménez de la Espada, 1870 currently comprises 63 species (Frost 2021), making it the largest genus of the poison frogs, superfamily Dendrobatoidea. Most of the species of this genus exhibit a cryptic coloration (brown, black) with lateral stripes on their body; however, some species have bright coloration on the dorsal or ventral surface of the body. The species of this genus are distributed in northwestern South America, between Brazil, Colombia, Ecuador, and Peru countries. These occupy the Andes mountains and the adjacent Chocoan and Amazonian lowlands, occupying different habitats from the streams, ponds, grasslands, forest, and paramos, in almost sea level to above 4000 m. of elevation.

Hyloxalus is supported by abundant molecular synapomorphies, and their monophyly has been recovered recurrently since its resurrection (Grant et al. 2006, Santos et al. 2009, 2014, Pyron and Wiens 2011, Pyron 2014, Grant et al. 2017, Jetz and Pyron 2018, Guillory et al. 2019); however, internal relationships of the *Hyloxalus* have been reviewed partially (Páez-Vacas et al. 2010, Acosta-Galvis and Vargas-Ramírez 2018); moreover, there are inconsistencies in the topological position of some clades between previous studies. Thus for instance the topological placement of *H. nexipus, H. sylvaticus*, and *H. pulcherrimus* varies between phylogenies previously proposed (see Grant et al. 2006, 2017, Santos et al. 2009, 2014, Santos and Cannatella 2011, Pyron and Wiens 2011, Pyron 2014, Jetz and Pyron 2018, Guillory et al. 2019).

In this genus, some groups has been recognized by the shared presence of the morphological characters, but subsequent studies revealed that these are non-natural neither homologous. For example, the anal sheath in the *H. edwardsi* group (Lynch 1982), the black arm gland of the *H. ramosi* group (Grant and Castro 1998, Grant and

Ardila 2002, Grant et al. 2006, 2017), and the pale dorsolateral stripe of the *H. azureiventris* group (Grant et al. 2006). In other cases, some groups have been proposed on the basis of the genotype evidence; for example, the *H. bocagei* group (Páez-Vacas et al. 2010) and the *H. subpunctatus* group (Acosta-Galvis and Vargas-Ramírez 2018); nevertheless, the paraphyly was reported for the *H. bocagei* group (Grant et al. 2017).

Furthermore, in *Hyloxalus* some systematics problems are persistent. For example, more than one-third of the species (21 species of the genus) is known only from the original description and there are no additional data of these (e.g., *H. pinguis*, Rivero and Granados-Díaz 1990; see also Rivero 1991a, b; Rivero and Serna 1986, 2000 "1995" and Duellman 2004), complex species and species with a wide distribution has not been reviewed and their identity remains unclear (e.g., *Hyloxalus lehmanni, H. breviquartus, H. elachyhistus, H. littoralis, H. pulchellus*; Coloma 1995, Grant et al. 2006), and about of this genus are tentatively assigned to this based on phenotype resemblance only.

Added to this, unambiguously phenotypic synapomorphies are unknown for the genus, and various characters of adults of *Hyloxalus* (e.g., lateral stripes, extension of toe webbing, cryptic coloration, dorsal skin texture, swelling finger IV) are shared with species of the other genera, including of the family Aromobatidae. This difficult the assignation of the species to the genus without molecular data. However, the species of the *Hyloxalus* exhibit differences in external morphological (*e.g., H. chocoensis* have extensive toe webbing and lack of oblique, ventral, and dorsal lateral stripes, and *H. subpunctatus* with basal toe webbing and complete oblique lateral stripe), which can be used to test the *Hyloxalus* relationships.

Nevertheless, a few studies reported variation in the hyoid musculature, urogenital system, integument of the ventral skin, and also in behavior in *Hyloxalus* and other dendrobatoids (Trewavas 1933, Bhaduri 1953, Myers et al. 2012, Grant et al. 2017, Quiguango-Ubillús and Coloma 2008). Likewise, in tadpoles of this genus and also in superfamily there is variation in its morphology and anatomy, which has been proposed as characters (Myers 1987, Haas 1995, Grant et al. 2006, Sánchez 2013, Dias et al. 2021); however, the tadpoles of 33 species of *Hyloxalus* remain unknown, and larval morphology, both external and internal, of the genus is poorly understood (Haas 1995, Anganoy-Criollo 2013). In addition, the review of the homoplastic characters of the superfamily revealed new characters, resulting in new synapomorphies at distinct levels for this group (e.g., Cavalcanti et al. 2021). Therefore, the study of this variation could provide new characters useful to test the *Hyloxalus* relationships.

Despite this, the recent phylogenies in Dendrobatoidea used only genomic data (e.g., Guillory et al. 2019, 2020, Muell et al. 2022), and the phenotype characters are less used and studied. Therefore, based on the above mentioned, I review the phenotype of the adult and larvae of the *Hyloxalus* to define new characters and also I generate new genotype evidence to test the *Hyloxalus* relationships. Phylogenetic results are used to reevaluate the taxonomy of this genus and to understand the phenotype evolution in this anuran group. The main aim of this study is to test the phylogenetic relationships of *Hyloxalus* employing distinct sources of evidence by mean a parsimonious total evidence analysis.

In the first chapter, the homology of the cloacal sheath and the phylogenetic position of the *Hyloxalus edwardsi* group are evaluated. I examined the adult morphology and the anatomy associated with the cloacal sheath. The phylogenetic

position of this group is corroborated by means of the new genotype data of a new species of this group, which is also described. Topological position of this species was severely tested by the successive outgroup expansion method (Grant 2019).

In the second chapter, the *Hyloxalus* phylogeny is evaluated with the increase of terminals and characters, both phenotype and genotype. For this, I reviewed the morphology of adults and larvae from most species of this genus and also several species across Dendrobatoidea to test the characters previously proposed, identify new characters, and test phylogenetic relationships of *Hyloxalus*. Moreover, five mitochondrial and five nuclear molecular markers of the unsequenced species and the representatives of the other populations and species are amplified. All new evidence generated, together with the phenotype and genotype data available for this genus was analyzed in a total evidence analysis using parsimony as optimality criteria to infer the phylogenetic relationships. The homology and topology hypotheses of the ingroup (*Hyloxalus*) are severely tested as possible through the successive outgroup expansion to identify the outgroup with the greatest chances of refuting the hypothesis because is expected an impact on the phylogeny with the addition of the new evidence (i.e., terminals and characters). The phylogeny with the greatest explanatory power is used to infer the *Hyloxalus* relationship. New unambiguous phenotype synapomorphies are provided for different clades within *Hyloxalus,* and also for other Dendrobatoidea clades. Phylogeny is used to propose a monophyletic taxonomy in *Hyloxalus*, and to analyze the phenotype evolution.

In the third chapter, the homology of the black arm gland—a dark arm swelling of the adult males of nine species of *Hyloxalus*—is evaluated, given this character was found as homoplastic within *Hyloxalus* previously (see Grant et al. 2017). External morphology and histology are used to characterize the integumentary

structure. These data provide evidence to propose characters both external morphology and integument and also test the glandular nature of this arm swelling. The external morphology characters are optimized in the largest *Hyloxalus* phylogeny generate in the second chapter to study their evolution. The systematic and biological implications of the findings are analyzed.

Capítulo 1

Submetido à publicação: Herpetologica, maio de 2021.

The Enigmatic *Hyloxalus edwardsi* Species Group (Anura: Dendrobatidae): Phylogenetic Position and a New Species

MARVIN ANGANOY-CRIOLLO[1,3], ANDRES VIUCHE-LOZANO[2], MARIA PAULA ENCISO-CALLE[2], MANUEL HERNANDO BERNAL[2], AND TARAN GRANT[1]

[1] Department of Zoology, Institute of Biosciences, University of São Paulo, 05508-090, São Paulo, SP, Brazil.

[2] Grupo de Herpetología, Eco-Fisiología and Etología. Departamento de Biología. Universidad del Tolima. 730006299, Ibagué, Colombia.

[3] CORRESPONDENCE: e-mail, marvinanganoy@gmail.com

ABSTRACT: *Hyloxalus edwardsi* and *H. ruizi* are high Andean dendrobatid frogs that inhabit the Cordillera Oriental of Colombia. Both species were grouped in the monophyletic *H. edwardsi* group on the basis of the synapomorphic presence of an elongated cloacal sheath and absence of a tarsal keel and vocal slits. Until now, the generic allocation of this species group has been uncertain. The group was provisionally placed in *Colostethus* sensu lato and formerly in *Hyloxalus* due to the presence of diagnostic characters of this genus (e.g., finger IV not swollen, absence of dorsolateral and ventrolateral stripes, and extensive toe webbing); however, no species of the group were included in previous phylogenetic analyses. Moreover, both species are critically endangered and recent field trips to their type localities have yielded no additional specimens. Nevertheless, on the western flank of the Cordillera Oriental of Colombia, we discovered a population possessing the elongated cloacal sheath and a weak tarsal keel, but with other morphological traits differing from the two known species of the *H. edwardsi* species group. Based on this material and the revision of *H. edwardsi* species group, we herein describe this population as a new species, revise the elongated cloacal sheath and other two key morphological characters, and tested the phylogenetic position of this group with the addition of the new species. Our results corroborate the hypothesis that this group is part of *Hyloxalus* and that there is morphological variation in this genus, such as the modifications found in the *m. sphincter ani cloacalis* that is associated to the cloacal sheath, and in the distal subarticular tubercles of hand, which are relevant to the relationships of *Hyloxalus*.

Key words: Bosque de Galilea; Cloacal sheath; Dendrobatoidea; *M. sphincter ani cloacalis; M. rectus abdominis*; Successive outgroup expansion.

LYNCH (1982) described the Andean dendrobatid species *Colostethus edwardsi* Lynch 1982 and *C. ruizi* Lynch 1982, noting that they could be distinguished from all other species of *Colostethus* Cope 1866 by the synapomorphic presence of an elongate cloacal sheath and absence of tarsal keels and vocal slits. Later, Rivero (1990 "1988") referred to the clade as the *C. edwardsi* group. Grant et al. (2006) resurrected *Hyloxalus* Jiménez de la Espada 1870 for almost half of the species of the former *Colostethus*, and although neither *C. edwardsi* nor *C. ruizi* was included in their phylogenetic analysis, they were referred to *Hyloxalus* on the basis of the absence of a swollen finger IV and dorsolateral and ventrolateral stripes and presence of toe webbing, and indirectly, their Andean distribution. Therefore, although the monophyly of the *H. edwardsi* group has a strong evidential basis, clear affinities to other dendrobatoids are lacking, and resolving the group's phylogenetic placement is one of the top priorities for Dendrobatoidea (Grant et al. 2017).

Little is known about the biology of *Hyloxalus edwardsi* group. Both species inhabit the high Andean forests of Cordillera Oriental of Colombia above 2410 m elevation (Lynch 1982) and one, *H. edwardsi*, is cavernicolous (Cueva de las Moyas, type locality). Both species are classified as Critically Endangered (IUCN RedList 2020), with neither having been observed in more than 25 years (*H. edwardsi* was last collected in 1994 and *H. ruizi* in 1979). Expeditions to the type localities of both species by MAA in 2016–2017 failed to detect them, and no tissue samples, tadpoles, call recordings, or other information are available for these species.

During fieldwork in a remote Andean forest on the western flank of the Cordillera Oriental of Colombia in late 2016, MPE-C and AV-L collected a specimen of *Hyloxalus* apparently belonging to the *H. edwardsi* species group. Given the importance of the discovery, in early 2017 we returned to the locality, and collected

additional specimens, which enabled us to obtain enough evidence both to confirm its placement in the *H. edwardsi* group and determine that it is not conspecific with either of the nominal species of the group. The newly collected material also allowed us to test the *H. edwardsi* group's phylogenetic position using DNA sequences and morphology, and examine in detail the evidence for its monophyly and internal relationships.

MATERIAL AND METHODS

Field Work and Study Area

Fieldwork was conducted 25–31 August 2016 and 28 January–4 February 2017 at "Bosques de Galilea," Villarica municipality, Tolima department, at 1654–2217 m elevation on the western flank of the Cordillera Oriental of Colombia (ca. 3° 48' N, 74° 36' W). The Andean forest of the Bosques de Galilea covers an elevational gradient from 1300 to 3000 m and is a biological corridor connecting the Paramos of the Parque Natural Nacional Sumapaz and the forest of the Magdalena Valley (Alcaldia Municipal de Villarica 2003; Alcaldia Local de Sumapaz 2012; Parques Naturales Nacionales de Colombia 2018). Despite the great expanse of Bosques de Galilea (33000 ha), distributed among the municipalities of Icononzo, Villarrica, Dolores, Purificación, Prado, and Cunday in Tolima, this area is unprotected and is threatened by clearcutting to harvest timber, hunting, mining, illicit crops, and conversion of forest into grassland for livestock (Alcaldia Municipal de Villarica 2003; Corporación Autónoma Regional del Tolima 2019).

The specimens of the new species were found in the fast-flowing stream "La Quebrada Wolf," a tributary of the Magdalena River that flows into the Río Negro River and in the dam of the Prado River. The stream has reddish water (due to high

tannin concentration) and abundant moss-covered rocks, is 4–5 m wide, and is surrounded by low (5–15 m) montane wet forest.

Following capture and photography, specimens were euthanized and fixed following standard procedures (McDiarmid 1994) and deposited in the amphibian collection of the Instituto de Ciencias Naturales, Universidad Nacional de Colombia (ICN) where they were stored in 70% ethanol. Prior to fixation, tissue samples were collected from the thigh muscle of three specimens (MAA 1260, MAA 1266, MAA 1269) and preserved in 95% ethanol, and the skin was removed from MAA 1266 and preserved in methanol.

Laboratory Work and Data Collection

Measurements were taken with a dial caliper to the nearest 0.1 mm. Males with vocal slits on both sides of the mouth and/or enlarged testes were scored as adults, those with only one vocal slit and/or moderate sized as subadults, and those lacking slits on both sides and possessing small testes as juveniles. Females with expanded, convoluted oviducts and enlarged oocytes were considered to be adults, those with only weakly expanded, non- or weakly convoluted oviducts and poorly differentiated oocytes to be subadults, and those with small, undifferentiated oocytes and unexpanded, straight oviducts to be juveniles. Adults of the new species are unknown for both sexes, so all measurements should be interpreted as minimum values. The characters and character-states follow Grant et al. (2006, 2017). The method of Kaplan (1997) was used to evaluate the length of finger II and III. The toe webbing formula is that of Savage and Heyer (1967; see also Myers and Duellman 1982; Savage and Heyer 1997). Skeletal characters were scored from 3D reconstructions obtained by X-ray micro-computed tomography using a SkyScan 1176 scanner (Bruker, Kontich, Belgium, at 9 μm voxel resolution and 43 Kv) and

SkyScan NRecon (v.1.6.6.0, Bruker, Kontich, Belgium) and CTVox (v.2.3.0, Bruker, Kontich, Belgium) software.

To better distinguish the cloacal sheath from the condition found in other dendrobatoids, we dissected the extrinsic cloacal musculature of the new species, *H. edwardsi*, *H. ruizi*, and other dendrobatoids (Appendix I). Terminology for the extrinsic musculature of the cloaca follows van Dijk (1955, 1959), with modifications where required. Nomenclature for abdominal musculature follows Burton (1980). Abbreviation for herpetological collections are ICN (Instituto de Ciencias Naturales, Universidad Nacional, Bogotá, Colombia), KU (University of Kansas Natural History Museum, Lawrence, USA), PSO-CZ (Colección Zoológica, Universidad de Nariño, Pasto, Colombia), MZUSP (Museu de Zoologia da Universidade de São Paulo, São Paulo, Brasil), UTCZ (Colección Zoologica, Universidad del Tolima, Ibagué, Colombia), and UV-CD (Colección Vertebrados de Docencia, Universidad del Valle, Cali, Colombia). Field numbers TG (T. Grant) and MAA (M. A. Anganoy) are reported when specimens have not yet been deposited.

DNA was extracted from tissue samples using the Qiagen DNeasy kit. Five mitochondrial (12S, tRNAval, and 16S [comprising the H-strand transcription unit 1] and MT-CYB, MT-CO1) and five nuclear (H3F3C, RHO, RAG1, SIAH1 and RNA28S) loci, were amplified and sequenced using primers and protocols previously employed by Grant et al. (2006: 55, 2017: S4). PCR products were purified using the Agencourt AMPure XP DNA Purification and Cleanup kit (Beckman Coulter Genomics, USA) and sequenced in both directions by a commercial laboratory. Newly generated sequences were deposited on GenBank under accession numbers XXXX–XXXXX**.**

Phylogenetic Analysis

We merged our new data plus the available DNA sequences of *Hyloxalus felixcoperari* (GenBank accession numbers: MG637362, 637364–65), recently described by Acosta-Galvis and Vargas-Ramírez (2018), into the dataset of Grant et al. (2017: Appendix 4) to test the phylogenetic position of the new species (and, by proxy, the *H. edwardsi* group). The final dataset comprised 15 loci (see Grant et al. 2017: Table 1) and 189 phenotypic characters. Although we identified novel characters in the musculature of the elongate cloacal sheath and subarticular tubercles of the fingers, we did not include them in our phylogenetic analysis because a complete morphological revision to evaluate their variation in Dendrobatoidea was beyond the scope of this study, but we describe and discuss the observed variation below.

The complete dataset of Grant et al. (2017) comprises 564 terminals, including 495 dendrobatoid terminals treated as the ingroup in that study, and required approximately 150,000 CPU-hours for analysis. Given the less ambitious objective of the present study of discovering the phylogenetic placement of the new species, thorough analysis of such a large dataset would be both unnecessary and counter-productive, since most of the computational effort and time would be directed at parts of the tree that are so distant from the new species that they are irrelevant to the research question. As such, on the basis of preliminary analyses corroborating the placement of new species within *Hyloxalus,* we focused our analyses primarily on that clade by including all *Hyloxalus* terminals from Grant et al. (2017), plus the recently described *H. felixcoperari* (DNA sequences from Acosta-Galvis and Vargas-Ramírez 2018) in our analyses and using successive outgroup expansion (Grant 2019) to limit taxon sampling.

We conducted a total evidence analysis (Kluge 1989) of the genomic and phenomic data under the parsimony optimality criterion, applying equal weights to all classes of transformation events, following the justification of Kluge and Grant (2006). We conducted analyses in POY v.5.1.1 (Wheeler et al. 2015), which uses tree-alignment (e.g., Sankoff 1975; Sankoff and Cedergren 1983; Wheeler 1996; Varón and Wheeler 2012, 2013) to test hypotheses of nucleotide homology dynamically by optimizing unaligned DNA sequences directly onto alternative topologies (Kluge and Grant 2006; Wheeler et al. 2006; Grant and Kluge 2009) while simultaneously optimizing prealigned transformation series (e.g., morphology) as standard character matrices. Specifically, we used the command *search* to perform timed driven searches composed of random addition sequence Wagner builds, Subtree Pruning and Regrafting (SPR) and Tree Bisection and Reconnection (TBR) branch swapping (RAS + swapping; Goloboff 1996), Parsimony Ratcheting (Nixon 1999), and Tree Fusing (Goloboff 1999), alternating between standard direct optimization (Wheeler 1996) and static-approximation, which searches using the implied alignment (Wheeler 2003a) of the best tree in memory. For final refinement following successive outgroup expansion, we calculated the cost of the optimal tree using approximate iterative pass optimization (Wheeler 2003b) and submitted the implied alignment to additional searches in TNT v.1.5 (Goloboff et al. 2008; Goloboff and Catalano 2016; equal costs for all transformations, gaps treated as fifth state), stopping when a stable consensus was reached five times (TNT command: *xmult = level 10 chklevel 5 consense 5*). We estimated clade support (Grant and Kluge 2008a) by calculating Goodman-Bremer values (GB; Goodman et al. 1982; Bremer 1988; Grant and Kluge 2008b) in TNT v.1.5 (Goloboff et al. 2008; Goloboff and Catalano 2016) using the implied alignment and the parameters specified in the bremer.run

macro (for details see Goloboff et al. 2008; macro available at www.lillo.org.ar/phylogeny/tnt). All compute-intensive analyses were run on Ace, a high-performance computing cluster housed at the Museum of Zoology of the University of São Paulo composed of 12 quad-socket AMD Opteron 6376 16-core 2.3-GHz CPU, 16 MB cache, 6.4 GT/s compute nodes (= 768 cores total), 10 with 512 GB RAM DDR3 1600 MHz (32 × 16 GB) and two with 256 GB (16 × 16 GB), and QDR 4x InfiniBand (32 GB/s) networking.

RESULTS

Hyloxalus ***jhoncito*** sp. nov.

(Figs. 1A, 2A, 3A, 4A, 5)

Holotype.—ICN 0000 (Field number MAA 1260) a subadult female from La Quebrada Wolf, Bosques de Galilea, Villarica, Tolima, Colombia, 2142 m; GPS coordinates N 3° 48′ 13.4″, W 74° 36′ 32.3″, collected by Andrés Viuche, María P. Enciso, Raiza Castañeda, Ariel Lozano, Viviana Gutiérrez and Marvin Anganoy on 2 February 2017.

Paratypes.—ICN 0000 (MAA 1269, juvenile female), general locality and collector data same as the holotype, but 2172 m and N 3° 48′ 12.9″, W 74° 36′ 29.7″. **ICN 0000** (MAA 1266, juvenile male), locality and collector data same as the holotype, but 2217 m and N 3° 48’ 20″, W 74° 36′ 19.1″, on 3 February 2019. CZUT 2156 (juvenile male), data locality as the holotype; collected by Andrés Viuche, María P. Enciso, Ariel Lozano on 28 August 2016.

Diagnosis.—A species of *Hyloxalus* with an elongate cloacal sheath, distal subarticular tubercle on finger II–III (variable occurrence on finger II) and hyperdistal subarticular tubercle on fingers IV–V, a complete oblique lateral stripe (absent in juvenile male CZUT 2156), and extensive toe webbing (I 1 – 1^{+} II 1 – 2 III 2 – 3 IV 3

– (2^{-} – 2) V), and lacking dorsolateral and ventrolateral lateral stripes, no swollen finger IV, no black arm gland, and the median lingual process and cloacal tubercles are absent. Adult snout–vent length (SVL) unknown (maximum observed SVL = 25.2 mm; subadult female holotype MAA 1260).

Hyloxalus jhoncito differs from all other species of *Hyloxalus* (and all other dendrobatoids) except those of the *H. edwardsi* group in possessing an elongate cloacal sheath (Fig. 4A) and distal and hyperdistal subarticular tubercles on fingers II–V (Fig. 3A). Within the *H. edwardsi* group, *H. jhoncito* differs from both known species in possessing a weak tarsal keel extending from the inner metatarsal tubercle (tarsal keel comprising an inconspicuous dermal thickening not extending to the metatarsal tubercle in *H. ruizi*; tarsal keel entirely absent in *H. edwardsi*; Fig. 3A–C). It further differs from *H. ruizi* by having more extensive toe webbing (I 1.5–2 II 1.5–2.5 III 2–3 IV 3– 2 V in *H. ruizi*) and mottled ventral coloration (immaculate in *H. ruizi.* Fig. 1, 3). *H. jhoncito* most resembles *H. edwardsi* in sharing mottled or spotted ventral coloration and extensive toe webbing, but it differs in possessing fringes on the fingers (absent in *H. edwardsi*) and larger finger discs (1.2–1.3 times the adjacent phalanx of finger IV in *H. jhoncito*, and 1.0–1.1 times in *H. edwardsi.* Fig. 3A, 3B).

Measurements of holotype (mm).—The holotype MAA 1260 is a subadult female. SVL 25.2; forearm length from proximal edge of palmar tubercle to outer edge of flexed elbow 6.0; hand length from proximal edge of palmar tubercle to tip of finger IV 6.9; tibia length from outer edge of flexed knee to heel 11.4; foot length from proximal edge of outer metatarsal tubercle to tip of fourth toe 12.2; head width between angle of jaws 8.3; head length diagonally from corner of mouth to tip of snout 9.5; eye length from posterior to anterior corner 3.4; eye to naris distance from anterior corner of eye to center of naris 2.3; distance between centers of nares 3.5;

snout length from anterior corner of eye to tip of snout 3.9; interorbital distance 2.7; diameter of tympanum 1.2.

Morphology.—A composite description is presented to include the variation of the subadult female holotype, one juvenile female, and two juvenile males. Adults are unknown. Proportions are reported for three specimens, including the holotype (we did not include measurements of MAA 1266 because it was skinned prior to formalin fixation, but we did use it to score other characters).

Largest juvenile male (CZUT-A 2156) 21.6 mm SVL, testes white in both juvenile males. Vocal slits absent, unknown in adults. Juvenile and subadult females 21.1–25.2 SVL (n = 2). Body slender. Head slightly narrower than body (at level of scapula); head length 38–44% SVL and head width 32–38% SVL; head longer than wide, 1.1–1.2 times head width. Snout rounded or weakly rounded in dorsal perspective, rounded in profile; snout sloping, projecting beyond upper lip. *Canthus rostralis* straight, rounded. Loreal region flat, vertical, sloping outward to lip. Eye length 31–37 % of head length. Eye–naris distance 63–69 % of eye length, 87–88 % of snout length. Nares slightly projected, directed laterad, visible in anterior and dorsal views, not visible in ventral view, surrounded by low, fleshy rim. Tympanum well defined, posterodorsal third concealed by low supratympanic bulge, length of visible tympanum 33–38% of eye length. Teeth present on maxillary arch; vomerine odontophores absent. Tongue elliptical, anterior one-half attached, median lingual process absent.

Forearm 21–24% of SVL. Hand length 27–29% of SVL, 1.2–1.3 times forearm length. Finger discs expanded; discs of fingers II < III < IV = V (character 7: state 0 for finger disc II, character 8: 1 for finger disc III, and character 9: 2 for finger disc IV and V, Grant et al. 2006: 65), disc on finger IV 1.2–1.3 times wider that

adjacent phalanx. Fringes present on all fingers (stronger on preaxial side but still present on postaxial side). Finger II equal to finger III (when appressed or measured, finger II 4.0–5.1 mm, finger III is 4.1–5.2 mm; character 5: state 2 of Grant et al. 2006: 64). Finger III extending to level of distal subarticular tubercle of finger IV; finger V surpassing distal subarticular tubercle of finger IV, almost reaching finger disc. Relative length of appressed fingers IV > V > III > II. Finger IV not swollen, carpal pad and metacarpal ridge absent. Subarticular tubercle formula (1 or 2)-2-3-3. All subarticular tubercles protuberant, rounded; hyperdistal subarticular tubercles on finger III–V weak (see below); thenar tubercle elongate, palmar tubercle subtriangular; palmar tubercle 2–3 times larger than thenar tubercle (Fig. 3A).

Tibia 45–48% of SVL, foot 46–50% SVL. Toes disc unexpanded, equal to adjacent phalanges (state 0 of Grant et al. 2006: 72). Disc on Toe IV slightly narrower than disc on finger IV, 1.0–1.2 times width of adjacent phalanx. Relative length of appressed toes IV > V = III > II > I. Disc of Toes III and V reaching level of penultimate subarticular tubercle of Toe IV. Toe webbing formula I 1 – 1^{+} II 1 – 2 III 2 – 3 IV 3 – (2^{-} – 2) V. Fringes present on both sides of all toes, equal to one half of toe width. Outer metatarsal fold present, continuous with postaxial fringe of Toe V, almost reaching outer metatarsal tubercle. Tarsal keel weak, straight, extending proximolaterad from inner metatarsal tubercle, not elevated proximally. Subarticular tubercles 1-1-2-3-2. Subarticular tubercles rounded, protuberant except basal subarticular tubercle of the Toe IV, which is weak and either rounded or bifid. Inner metatarsal tubercle elongate. Outer metatarsal tubercle round, diameter one half that of inner metatarsal tubercle. Median metatarsal tubercle absent (Fig. 3A).

Dorsal surface smooth, with fine granules on posterior dorsum, sacrum and hindlimbs (thighs and shanks), and flanks of body; ventral surfaces smooth. One to

three postrictal tubercles present. Cloacal tubercles absent. Preaxillary area with postrictal bulge. Elongate cloacal sheath extending to midlevel of thighs (Fig. 4A). Tubercles on eyelid absent (but two low, flat tubercle-like protuberances present in life in MAA 1260, MAA 1269, and CZUT 2156).

Color in preservative (70% ethanol).—Dorsum brown with irregular dark brown spots or blotches; sometimes, these forming a band at interorbital region. Eyelid and snout with dark brown and dull white blotches. Flanks brown with dark brown spots; lateral head with black band extending from tip of snout to tympanum or above arm insertion; lower half of loreal region pale brown; tympanum brown with dark brown dots; postrictal tubercles with dark brown base and white tips; upper lip dull white with dark brown spots. Oblique lateral stripe absent in CZUT 2156, otherwise extending from groin to eyelid, pale cream, bordered dorsally and ventrally by dark brown blotches. Ventrolateral flanks dull white or light brown with dark brown spots. Ventral surfaces cream or dull white with dark brown blotches. Forelimbs dorsally brown with dark brown spots or bands on forearm, ventrally cream with dark brown spots or mottling. Hindlimbs dorsally yellowish brown or brown with dark brown spots or bands, ventrally cream with dark brown mottling on thighs; concealed surface of shank translucent white. Hand brown with dark brown blotches. Inner half of dorsal surface of the feet and the tarsus translucent white, while the outer half yellowish brown with dark brown spots; finger and toes with some white spots; palmar and plantar surfaces cream with dark brown stippling. Iris dull gray, pupil dull white.

Color in life.—Based on field notes and photos in life of MAA specimens (MAA1260, 1266, 1269. Fig. 5). Dorsum greenish yellow, greenish brown, or yellowish brown with copper dots and dark brown blotches along vertebral line and

interobital region. Dull white dots on sacral region. Lateral head with black band from tip of snout to tympanum or above arm insertion, area below of this band dull white to pale yellow with dark brown blotches. Postrictal tubercles white. Flanks pale yellow to yellowish brown with dark brown blotches. Oblique lateral stripe dull white, pale yellow, or orange copper. Venter and gular-chest region dark brown with white spots and mottling. Fore- and hindlimbs dorsally greenish yellow or yellowish brown with dark brown bands or blotches, ventrally reddish, inner half of the dorsal surface of the shank and feet dull pinkish white, upper arm and forearm with diffuse dark brown spots or bands. Toes and fingers pale yellow to dark brown with white spots or bands. Iris orange copper with fine black reticulation, and pupil ring gold.

Distribution and natural history.—*Hyloxalus jhoncito* is known only from the type locality (Fig. 6A–B). The frogs were found active on rocks, the stream bank, and along the edge of the stream between 18:00–24:00 (Fig. 6C). All specimens jumped quickly into the water and hid beneath rocks, even after only minor disturbances. Despite extensive searching along the same stream during the day, no frogs, tadpoles, or vocalizations were detected. *Hyloxalus jhoncito* occurs in sympatry with another apparently undescribed species of *Hyloxalus* (cf. *H. subpunctatus*), as well as the toad *Atelopus subornatus* (Bufonidae), the frogs *Hyloscirtus bogotensis* (Hylidae), *Centrolene notostictum* (Centrolenidae), and *Pristimantis* sp. (Craugastoridae) and the salamander *Bolitoglossa pandi* (Plethodontidae).

Etymology.—The specific epithet is a tribute to the preeminent herpetologist John D. Lynch, who described the first two species of this group and provided evidence for its monophyly. For more than half a century, John has dedicated his life to studying the seemingly never-ending yet rapidly disappearing amphibians and reptiles of the Neotropics, especially Colombia. And for decades, John's students

have referred to him as “Jhoncito,” which is the Spanish diminutive of the intentionally misspelled and quintessentially Colombian name, Jhon (sic), used here as a noun in apposition.

Remarks.—Adults of *Hyloxalus jhoncito* are unknown, so measurements and proportions should be interpreted with caution. Nevertheless, ontogenetic variation in the characters that differentiate *H. jhoncito* from the other species of the *H. edwardsi* group is either absent (e.g., tarsal keel, toe webbing) or inadequate to support a hypothesis of conspecificity (ventral coloration); moreover, the juveniles (e.g., ICN 6382, ICN 21944) of the *H. edwardsi* show no variation in diagnostic characters used here regards its adult. Juveniles of *H. ruizi* are scarce and unavailable to us. Given that the subadult female holotype (25.2 mm SVL) is smaller than the juvenile female *H. edwardsi* (27.5 mm SVL, ICN 6377) and *H. ruizi* (29.8 mm SVL, ICN 5418) reported by Lynch (1982), we predict that adult *H. jhoncito* will prove to be smaller than adults of the other two species of the *H. edwardsi* group (*H. edwardsi*: 27.5–37.3 mm SVL; *H. ruizi*: 32–38.5 mm SVL).

Given our limited field observations, few conclusions can be reached about the natural history of *Hyloxalus jhoncito.* All specimens were captured in close association with fast-flowing water. Myers et al. (1991) observed that the aquatic species *Aromobates nocturnus* spent more of its time in the water than adjacent to it, in contrast to the riparian dendrobatoids that occupy the rocks, banks, or fallen vegetation at the edge of streams and only dive into water when disturbed (Grant et al. 2016). Our observations are inadequate to determine if *H. jhoncito* is aquatic or riparian. Similarly, although all specimens were found during crepuscular or nocturnal periods (1800–2400 h) and none of our diurnal searches succeeded in detecting specimens or vocalizations, it is not uncommon to observe and disturb

sleeping individuals of diurnally active species of dendrobatoids and other anurans (e.g., *Atelopus* spp., *Amazophrynella* spp.), and, although two of the three specimens observed by MAA were clearly alert and in an active position (i.e., head and chest elevated, in contrast to sleeping individuals, in which the head and entire body are flattened against the substrate), we cannot dismiss the possibility that we disturbed them or sleeping prior to being disturbed before observing them. Finally, given the lack of adult male specimens, the occurrence of vocal slits (consequently vocal sac) in *H. jhoncito* is unknown. Given that all other adult male *Hyloxalus* species we have examined possess vocal slits, their confirmed absence in all three species would be another unambiguous synapomorphy of the clade. Regardless, species that lack vocal slits can still emit advertisement calls (e.g., *Pristimantis erythropleura*; Lynch 1996), so it is unknown if any of the species of the *H. edwardsi* group employ acoustic communication.

Although no species of *Hyloxalus* is known to sequester lipophilic alkaloids (Grant et al. 2017), the hyloxaline *Paruwrobates erythromos* possesses several classes of alkaloids (Daly et al. 1987), and the ventral coloration (red or orange tinge and contrasting black and white marbling) of *H. jhoncito* is suggestive of aposematism. Nevertheless, gas-chromatography/mass spectrometry of the methanol extract of the skin of *H. jhoncito* (sample MAA 1266) failed to detect any alkaloids (A. M. Jeckel and R. Saporito, personal communication; for methods see Saporito et al. 2006; Jeckel et al. 2015).

In *Hyloxalus jhoncito* the oblique lateral stripe (OLS) is either complete or absent (for definition and variation, see Grant et al. 2006. Fig. 2A). Lynch (1982: 367) reported that the OLS (and dorsolateral and ventrolateral stripes) is absent in the *Hyloxalus edwardsi* group, but he also stated that the largest individuals of *H.*

edwardsi had “hints of yellowish dorsolateral stripe from eye to above arm” (p. 370) in life and described the holotype of *H. ruizi* as having a “slightly paler stripe from eye to above insertion of upper arm (remnant of dorsolateral stripe?)” (p. 372). We did not observe a dorsolateral stripe in any specimens, but we observed both the presence and absence of the OLS in both adults and juveniles of both *H. edwardsi* and *H. ruizi*. When present, the OLS is either complete (i.e., it extends from the groin to the eye) or partial, extending from the eye to above the arm (Fig. 2B–C). Although a posterior partial OLS extending from the groin toward the arm has been reported for numerous species (Grant et al. 2006), this is the first report of an anterior partial OLS.

Phylogenetic Placement of the *Hyloxalus edwardsi* Group

In all analyses, *Hyloxalus jhoncito* was monophyletic and nested within a clade composed of *H. cepedai*, *H. felixcoperari*, *H. picachos*, *H. subpunctatus*, and *H.* sp. AguaAzul (i.e., the *H. subpunctatus* clade of Acosta-Galvis and Vargas-Ramírez 2018). However, its sister-species relationships varied in the first rounds of successive outgroup expansion (Table 1; supplementary figures). In analysis 1 (7 outgroup terminals), the sister species of *H. jhoncito* was *H. picachos* (Table 1; supplementary figure 1), whereas in analysis 2 (with 21 outgroup terminals) it was *H. cepedai* + *H.* sp. AguaAzul (supplementary figure 2). In analysis 3 (28 outgroup terminals), the sister species relationship between *H. jhoncito* and *H. picachos* was again supported (supplementary figure 3), and both that relationship and the other relationships of the *H. subpunctatus* clade remained constant in all subsequent rounds of successive outgroup expansion (Fig. 7; supplementary figure 4–6).

In contrast, subsequent rounds of outgroup expansion continued to have a major effect on hyloxaline relationships more generally (see supplementary figures). With the inclusion of a few colostethines and rooting on the aromobatid *Rheobates*

palmatus in analysis 3, the monophyly of both Hyloxalinae and *Hyloxalus* was rejected. *Paruwrobates* moved from being sister to *Ectopoglossus* to a deeply nested position, and the *Hyloxalus bocagei* group was optimally placed as sister to a large clade composed of the *H. subpunctatus* clade, *Paruwrobates,* Colostethinae, Dendrobatinae, and all remaining *Hyloxalus*. Those relationships persisted with the inclusion of additional colostethines and dendrobatines in analyses 4 (36 outgroup terminals) and 5 (62 outgroup terminals) but were overturned in analysis 6, which included additional aromobatids and four non-dendrobatoid lineages (68 outgroup terminals; rooted on the hylid *Boana boans*; Fig. 7; supplementary figures).

Morphological Evidence for the Monophyly and Internal Relationships of the *Hyloxalus edwardsi* Group

Although our phylogenetic analysis included only one species of the *Hyloxalus edwardsi* group, we identified morphological evidence in support of both the monophyly of the three known species and a sister-group relationship between *H. edwardsi* and *H. ruizi*.

Cloacal sheath.—The elongate cloacal sheath of *Hyloxalus edwardsi* and *H. ruizi* was described as comprising an "…anal opening extended to midlevel of lower level of thighs by an anal [cloacal] sheath" (Lynch 1982: 367), and we observed the same condition in *H. jhoncito* (Fig. 4A–C). Other species have been described as possessing this character-state (e.g., *Nephelobates* of La Marca 1994); however, Grant et al. (2006) restricted its presence to the two species of the *H. edwardsi* group and noted the difficulty in distinguishing it due to preservation artifacts, which we corroborated in our survey of taxa for the present study. Nevertheless, our dissections of the extrinsic cloacal musculature revealed modifications of the *m. sphincter ani cloacalis* (SAC) and *m. rectus abdominis* (RA) of *H. edwardsi*, *H. jhoncito*, and *H.*

ruizi that are absent in all other examined dendrobatids and, therefore, support the monophyly of the group.

The SAC encircles the distal portion of the cloaca, originating from the mid-ventral cloaca and ascending dorsad on both sides to meets in a symphysis on the mid-dorsal cloaca. Distally, the SAC inserts on the dermis (Ecker and Haslam 1889; Gaupp 1904; van Dijk 1955, 1959), with the distal-most portion of the SAC forming a distinct slip (Fig. 8A**)**. In most dendrobatoids (Appendix I), a few fibers of this slip insert on the dermis dorsal to the cloaca, while most fibers insert on the dermis ventral to the cloaca immediately adjacent to the cloacal aperture (Fig. 8B). In the three species of the *Hyloxalus edwardsi* group, the distal slip extends distad to the level of the pubic symphysis, inserting along the dermis and on the posterior branch of the RA tendon of origin (see below; Fig. 8C–E).

The RA comprises a pair of laminar muscles that originate from the ventral pubis and quickly fuse and extend anteriad to cover the abdominal surface (Burton 1980; Duellman and Trueb 1994). In most dendrobatoids, each half of the RA originates via a short, unbranched tendon attached to the ventral pubis, but in the three species of the *Hyloxalus edwardsi* group this tendon is divided into two branches, an anterior branch attached to the ventral pubis, and a posterior branch projected distad to attach to the ventral fibers of the distal slip of the SAC (Fig. 8D–E).

Hyperdistal subarticular tubercles.—The subarticular tubercles are integumentary enlargements of variable shape and protrusiveness situated ventral to the digital articulations. Like the pads of digital discs, the epithelium of subarticular tubercles is composed of polygonal (in surface view), flat-topped epithelial cells covered by a dense array of columnar nanopillars, providing enhanced adhesion to

both terrestrial and aquatic substrates (Noble and Jaeckle 1928; Federle et al. 2006; Barnes et al. 2013; Drotlef et al. 2014). Most dendrobatoids possess 1–1–2–2 subarticular tubercles on fingers II–V, respectively, with a proximal subarticular tubercle ventral to the articulation of the metacarpal + proximal phalanx on all fingers, a distal subarticular tubercle beneath the articulation of the proximal + penultimate phalanges on fingers IV–V, and no subarticular tubercle beneath the distal-most articulation between the distal and adjacent (proximal or penultimate) phalanges. However, all three species of the *Hyloxalus edwardsi* group possess a small but well-defined subarticular tubercle beneath the articulation between the distal and adjacent phalanges of all fingers (i.e., 2–2–3–3 subarticular tubercles on fingers II–V, respectively; Fig. 3). Insofar as this tubercle is distal to the "distal" subarticular tubercles of fingers IV and V, we refer to it as "hyperdistal" (see also Ospina-Sarria and Duellman 2019). Inasmuch as these hyperdistal tubercles are unknown in other dendrobatoids, their presence is a putative synapomorphy that supports the monophyly of the *H. edwardsi* group.

Tarsal keel.—Interspecific variation in the tarsal keel was summarized by Grant et al. (2006). Among the closest relatives of the *Hyloxalus edwardsi* group (see above), the tarsal keel is short, tubercle-like in *H. cepedai* (holotype, USNM 146926), *H. picachos* (paratypes ICN 42620, 42632, sister species of the *H. edwardsi* group) and *H. subpunctatus* (Grant et al. 2017). Lynch (1982) characterized the *H. edwardsi* group as lacking the tarsal keel (as the inner tarsal fold), explicitly describing it as absent in *H. edwardsi* but clarifying that in *H. ruizi* it is "evident only as slightly thickened area (no fold is present, at least not the sort of fold ending in a sickle-shaped tubercle typical of *Colostethus*)" (p. 372). Our observations corroborate Lynch's account. Specifically, *H. edwardsi* lacks any external trace of the tarsal keel,

while in *H. ruizi* the tarsal keel is an approximately straight line of slightly elevated integument that does not reach the inner metatarsal tubercle. In *H. jhoncito*, the tarsal keel is also straight or slightly curved, but it is more elevated than in *H. ruizi* and extends from the metatarsal tubercle. Although additional evidence is required to root the *H. edwardsi* group and determine character polarity, the observed variation is suggestive of character additivity and either the progressive loss or gain of a straight tarsal keel.

DISCUSSION

Relationships

The placement of the *H. edwardsi* species group among other dendrobatoids remained unknown until now due to a lack of evidence. The evidence used by Lynch (1982) allowed him to establish the monophyly of the group, but he was unable to identify synapomorphies shared with any other group of dendrobatoids. Our morphological analyses corroborate both the monophyly of the group, including three new discrete putative synapomorphies (viz., presence of a posterior branch of the *m. rectus abdominis* tendon of origin, insertion of the ventral fibers of the elongated distal slip of the *m. sphincter ani cloacalis* on the posterior branch of the *m. rectus abdominis* tendon of origin, presence of hyperdistal subarticular tubercles on fingers), and the lack of phenotypic synapomorphies relating the *H. edwardsi* group to any specific clade of dendrobatoid.

Grant et al. (2006) hypothesized that this group is part of *Hyloxalus*, partially on the basis of the absence of swelling on finger IV, but the distribution of that character has proven to be more complex than previously believed, with several species of *Hyloxalus* exhibiting a clearly swollen finger IV (including *H. cepedai* and *H. picachos*, now known to be close relatives of the *H. edwardsi* group; Grant et al.

2017). Nevertheless, the results of our phylogenetic analysis including DNA sequences of *H. jhoncito* corroborate Grant et al.'s (2006) hypothesis, with *H. jhoncito* nested deep within *Hyloxalus.*

Specifically, we found that *Hyloxalus jhoncito* is part of a group of Andean *Hyloxalus* from the Cordillera Oriental of Colombia formed by *H. cepedai*, *H. picachos*, *H. subpunctatus*, and *Hyloxalus* sp. AguaAzul, rendering the *H. subpunctatus* clade of Acosta-Galvis and Vargas-Ramírez (2018) paraphyletic. This relationship was unexpected, not only due to the lack of discrete phenotypic synapomorphies but also the lack of resemblance in external morphology. For example, the closest relatives of the *H. edwardsi* group are *H. cepedai* and *H. picachos*, which are diminutive species (maximum adult size about 19.5 mm in *H. cepedai* and 18.8 mm in *H. picachos*; Morales 2002 "2000"; Ardila-Robayo et al. 2000 "1999") with finger IV swelling and basal toe webbing between toes II–IV, whereas *H. edwardsi* species are larger, lack external evidence of finger IV swelling (known in *H. edwardsi* and *H. ruizi*), and have more extensive webbing between all toes.

Taxon Sampling

We defined the taxon sampling of this study to test the relationships of the *Hyloxalus edwardsi* group, represented by *H. jhoncito,* as severely as possible. For decades, it has been well understood and widely recognized that (1) taxon sampling can have a major impact on results and (2) all else being equal, taxon sampling should be as dense as possible (e.g., Hillis 1998; Zwickl and Hillis 2002; Heath et al. 2008). As such, given that our preliminary tests corroborated Grant et al.'s (2006) placement of the group in *Hyloxalus,* we included all the species of *Hyloxalus* analyzed by Grant et al. (2017) and the recently discovered *H. felixcoperari.* Further, given that even

distantly related outgroup taxa can affect ingroup relationships, we employed successive outgroup expansion (Grant 2019) as both a scientifically defensible basis to select outgroup taxa and limit outgroup sampling and a means of examining the empirical effects of outgroup sampling on relationships.

Our results showed that, although increased taxon sampling affected the relationships of *H. jhoncito*, its sister-group relationship to *H. picachos* stabilized quickly in the early rounds of outgroup expansion. In contrast, the broader relationships among hyloxalines more generally continued to be highly variable during successive outgroup expansions, affecting the monophyly of Hyloxalinae and *Hyloxalus* and the placement of species and clades within *Hyloxalus*. These results mirror those of Grant (2019), who also found that ingroup relationships were affected by successive outgroup expansion.

Despite the well-known relevance of taxon sampling, several recent studies have claimed decisively to have resolved the relationships of a variety of taxa on the basis of large amounts of data per terminal but only a fraction of the taxa used in other studies without even considering the possible taxon sampling effects. Among dendrobatoids, Guillory et al. (2019) analyzed data from up to 1719 ultraconserved element loci—a truly impressive amount of character data— sequenced for only 57 terminals (Table S1, Fig. S1) representing 34 species of 13 dendrobatid genera and an outgroup sample of 2 species of aromobatids (3 terminals of *Allobates femoralis*, 1 terminal of *Allobates* sp.). Many of the relationships they recovered corroborated previous findings based on much less data per terminal but many more taxa. However, they also recovered relationships that are refuted by more character-sparse but taxon-dense studies. For example, in their results Hyloxalinae was recovered as sister to Colostethinae instead of Dendrobatinae a relationship that has consistently

been recovered in studies using comparatively small taxon samples (28 dendrobatoid terminals in Clough and Summer 2000; 20 in Vences et al. 2000; 54 in Santos and Cannatella 2011) and refuted in studies based on larger taxon (Santos et al. 2003, 2009, 2014; Vences et al. 2003a; Grant et al. 2006, 2017; Pyron and Wiens 2011; Pyron 2014), a fact that should have at least given the authors pause when interpreting their results. However, the only concern raised about taxon sampling refers to their inability to place unsampled genera (p. 9).

This is not to say that Guillory et al. (2019) were unconcerned with phylogenetic methods. For example, they clarified that concern about the statistical consistency of parsimony had compelled them to conduct their study and emphasized that their placement of *Minyobates* as sister to *Adelphobates* agreed with "recent studies" (viz., Twomey and Brown 2008; Santos et al. 2009; Pyron and Wiens 2011) that, like their own, used a parametric method (maximum likelihood or Bayesian inference) instead of the nonparametric parsimony method. Of course, other equally recent studies using parametric methods also refuted the *Minyobates* + *Adelphobates* relationship (Pérez-Peña et al. 2010; Brown et al. 2011), but more importantly, Guillory et al. (2019) neglected to cite any of the counter-arguments against parametric methods and in favor of parsimony (e.g., Farris 1999; Goloboff 2003; Grant and Kluge 2003; Padial et al. 2014) or observe that the parsimony-based studies they cited (viz., Grant et al. 2006, 2017) also included phenomic characters and inferred nucleotide homology on the basis of tree-alignment instead of similarity-based alignments, thereby presenting a theoretically and empirically complex problem in the most simplistic terms while failing to critically examine their own results. Indeed, given the disproportionate impact that phenomic evidence has been shown to have on total evidence phylogenetic analyses of predominantly molecular

datasets (e.g., de Sá et al. 2014; Sánchez-Pacheco et al. 2014), we suggest that its inclusion is of paramount importance in elucidating the evolutionary history of this clade.

Morphological Characters

Our results suggest that the presence of hyperdistal subarticular tubercles on fingers, the insertion of the ventral fibers of the elongated distal slip of the *m. sphincter ani cloacalis* (SAC) on the posterior branch of the *m. rectus abdominis* (RA) tendon of origin, and the presence of a posterior branch of the RA tendon of origin are unambiguous putative synapomorphies of the *Hyloxalus edwardsi* species group, given that no other dendrobatoids appear to possess these character-states. However, more extensive revision of these characters is necessary to corroborate these hypotheses and determine if additional states exist, with the subsequent inclusion of these characters in a phylogenetic analysis to rigorously test their homology and evolutionary transformations.

The most comprehensive revision of the extrinsic cloacal musculature is that of van Dijk (1959, also see 1955), and the evolution of the SAC was examined by Drewes et al. (2013). Although revision of the extrinsic cloaca musculature across Anura was beyond the scope of the present study, we agree that such a revision is required, both to document and explain the variation not considered in previous studies (e.g., Noble 1922, Burton 1983) and clarify the homology of the muscles described with different nomenclatures (e.g., compared Van Dijk 1959 versus Dunlap 1966; see Burton 1983). Nevertheless, there is agreement that the SAC is the posterior-most muscle that encircles the cloaca, with fibers originating mid-ventrally on the cloaca and ascending dorsad around both sides of the cloaca to meet mid-dorsally, and the distal-most portion of the muscle forming a slip of fibers that insert

on the dermis ventral to the cloaca (Gaupp 1904; Van Dijk 1959; Drewes et al. 2007, 2013).

The SAC of dendrobatoids conforms to previous descriptions; however, the distal slip is uniquely modified in the *Hyloxalus edwardsi* species group, extending distad to the level of the pubic symphysis and inserting on the dermis and the posterior branch of the RA tendon of origin. Among non-dendrobatoids, elongation of the distal slip of the SAC to the level of the pubic symphysis was also reported in the bufonids *Vandijkophrynus angusticeps* and *Rhinella marina* by van Dijk (1959) and Drewes et al. (2007, 2013), respectively, and we also observed this elongation in *R. ornata* (uncatalogued specimen, MZUSP), *R. paraguas* (UV-CD 1503), and *Osornophryne bufoniformis* (PSO-CZ 2496). Nevertheless, in these species the distal slip inserts on the pubis, not the dermis and the RA, thereby refuting the primary homology of the elongation of the distal slip in these two groups.

The functional significance of the SAC has not been fully clarified. Although the designation of the SAC as a "sphincter" implies that it constricts the distal portion of the cloacal tube, evidence for that hypothesis is lacking. Alternatively, Drewes et al. (2007, 2013) proposed that SAC contraction helps depress the urostyle, thereby influencing the volume and pressure of the pubic lymphatic sac and the return of lymph from the hind limbs to the cardiovascular system. The consequences of ventral insertion of the fibers of the distal slip of the SAC on the dermis and posterior branch of the RA tendon of origin at the level of the pubic symphysis in the *Hyloxalus edwardsi* group is unknown. Similarly, the occurrence of the derived state in juveniles and adults of both sexes suggests that the function is unrelated to reproduction.

Variation in the occurrence of tubercles on the hands of dendrobatoids has been reported previously. Silverstone (1976) and Caldwell and Myers (1990)

documented the absence of the thenar tubercle in some dendrobatines, and Grant and Rodríguez (2001) described variation in the subarticular tubercles of finger V among some species of *Allobates*, both of which were subsequently coded as transformation series for phylogenetic analysis (Grant et al. 2006: characters 26 and 3, respectively). Our observations of distal (fingers II and III) and hyperdistal (fingers IV and V) subarticular tubercles indicate that this character system is more diverse and complex than has been appreciated. A thorough inspection is necessary to determine additional variation and transformations in the subarticular tubercles. Based on current knowledge, hyperdistal tubercles evolved at least three times in Dendrobatoidea: once in Aromobatidae (*Aromobates nocturnus*) and twice in Dendrobatidae (*Ectopoglossus isthminus* and the *H. edwardsi* species group).

We identified new morphological characters that provide evidence for the monophyly of the *Hyloxalus edwardsi* species group. Nevertheless, recognition of the *H. edwardsi* group as a separate genus would either render *Hyloxalus* paraphyletic (just as it would have *Colostethus* when the first species were discovered; Lynch, 1982) or require many more genera to be recognized than current evidence warrants. However, we agree with Grant et al. (2017) that increased taxon and character sampling will enable recognition of multiple genera within this clade.

Acknowledgments.—We are grateful to J. D. Lynch, J. Ospina-Sarria, B. Blotto, M. Rada, M. Targino, P. Pinheiro, P. H. S. Dias, D. J. Machado, and R. Montesinos for discussion, the curators of the amphibians collection of the Instituto de Ciencias Naturales of Universidad Nacional de Colombia (J. D. Lynch), the Colección Zoológica de la Universidad del Tolima (M. H. Bernal), the Natural History Museum of the University of Kansas (R. Brown and R. Glor), the Museu de Zoologia da Universidade de São Paulo (H. E. D. Zaher), and A. M. Jeckel and R. A.

Saporito for testing the skin of *Hyloxalus jhoncito* for alkaloids. Fieldwork was assisted by V.C Gutierrez, R. Castañeda and A. Lozano. The MicroCT reconstruction was performed by P. Lenktaitis. The *Hyloxalus picachos* photo was provided by G. Medina. MAA is grateful to F. Lamadrid Feris for the discussions and the unconditional support during the doctoral studies and Paulo Anganoy Lamadrid for daily motivation. Specimen collection was authorized by the Ministerio de Ambiente y Desarrollo Sostenible of Colombia (ANLA, resolutions 255 of 2014 and 701 of 2016). This research was supported by the São Paulo Research Foundation (FAPESP Procs., 2012/10000-5, and 2018/15425-0), and the Coordenação de Aperfeiçoamento de Pessoal de Nível Superior (CAPES Finance Code 001). MAA was supported by a doctoral scholarship from the Fundación Centro de Estudios Interdiciplinarios Básicos y Aplicados (CEIBA 2016) and a The Kurt Milton Pickett Intercontinental Student Travel Award award given to MAA provided support to present this research at the 2017 meeting of the Willi Hennig Society. MPE-C, AV-L, and MHB scholarship grant support were provided by Fondo de Investigaciones, Universidad del Tolima, Project Number 270220516, and TG was supported by a research fellowship from the Brazilian National Council for Scientific and Technological Development (CNPq Proc. 306823/2017-9).

LITERATURE CITED

Acosta-Galvis, A.R., and M. Vargas-Ramírez. 2018. A new species of *Hyloxalus* Jiménez De La Espada, 1871 ‘‘1870’’ (Anura: Dendrobatidae: Hyloxalinae) from a cloud forest near Bogotá, Colombia, with comments on the *subpunctatus* clade. Vertebrate Zoology 68:123–141.

Alcaldía Local de Sumapaz. 2012. Plan ambiental local de Sumapaz, 2013–2016. Secretaria Distrital de Ambiente, Bogotá, Colombia. Retrieved from

http://www.ambientebogota.gov.co/documents/10157/2883180/PAL+Sumap%C3%A1z+2013-2016.pdf. Accessed on 28 February 2020.

Alcaldía Municipal de Villarrica. 2003. Esquema de ordenamiento territorial municipio de Villarrica, Tolima, Proyecto de acuerdo, 2003. Alcaldia de Villarrica, Tolima, Colombia. Retrieved from https://repositoriocdim.esap.edu.co/handle/123456789/10502. Accessed on 29 February 2020.

Ardila-Robayo, M.C., A.R. Acosta-Galvis, L.A. Coloma. 2000 "1999". Una nueva especie de *Colostethus* Cope 1867 (Amphibia: Anura: Dendrobatidae) de la Cordillera Oriental de Colombia. Revista de la Academia Colombiana de Ciencias Exactas, Físicas y Naturales 23:239–244.

Barnes, W.J.P., M. Baum, H. Peisker, and S.N. Gorb. 2013. Comparative Cryo-SEM and AFM studies of hylid and rhacophorid tree frog toe pads. Journal of Morphology 274:1384–1396.

Bremer, K. 1988. The limits of aminoacid sequence data in angiosperm phylogenetic reconstruction. Evolution 42:795–803.

Brown, J.L., E. Twomey, A. Amézquita, M.B. Souza, J.P. Caldwell, S. Lötters, R. von May, P.R. Melo-Sampaio, D. Mejía-Vargas, P. Perez-Peña, M. Pepper, E.H. Poelman, M. Sanchez-Rodriguez, and K. Summers. 2011. A taxonomic revision of the neotropical poison frog genus *Ranitomeya* (Amphibia: Dendrobatidae). Zootaxa 3083:1–120.

Burton, T.C. 1980. Phylogenetic and functional significance of cutaneous muscles in Microhylid frogs. Herpetologica 36:256–264.

Burton, T.C. 1983. The musculature of the papuan frog *Phrynomantis stictogaster* (Anura, Microhylidae). Journal of Morphology 175:307–324.

Caldwell, J.P., and C.W. Myers. 1990. A new poison frog from Amazonian Brazil, with further revision of the *quinquevittatus* group of *Dendrobates.* American Museum Novitates 2988:1–21.

Clough, M., and K. Summers. 2000. Phylogenetic systematics and biogeography of the poison frogs: Evidence from mitochondrial DNA sequences. Biological Journal of the Linnean Society 70:515–540.

Corporación Autónoma Regional del Tolima. 2019. Plan de gestión ambiental regional del Tolima 2013–2023. 01–201. Available at https://www.cortolima.gov.co/sites/default/files/images/stories/boletines/marzo2013/PGAR_2013_2023_TOLIMA_DIC_2012.pdf. Accessed on 30 October 2019. Corporación Autónoma Regional del Tolima, CORTOLIMA, Ibagué, Tolima, Colombia.

Daly, J.W., C.W. Myers, and N. Whittaker. 1987. Further classification of skin alkaloids from neotropical poison frogs (Dendrobatidae), with a general survey of toxic/noxious substances in the Amphibia. Toxicon 25:1023–1095.

de Sá, R.O., T. Grant, A. Camargo, W.R. Heyer, M.L. Ponssa, and E. Stanley. 2014. Systematics of the neotropical genus *Leptodactylus* Fitzinger, 1826 (Anura: Leptodactylidae): Phylogeny, the relevance of non-molecular evidence, and species accounts. South American Journal of Herpetology 9:S1–S128.

Drewes, R.C., M.S. Hedrick, S.S. Hillman, and P.C. Witthers. 2007. Unique role of skeletal muscle contraction in vertical lymph movement in anurans. Journal of Experimental Biology 210:3931–3939. https://doi:10.1242/jeb.009548

Drewes, R.C., S.S. Hillman, M.S. Hedrick, and P.C. Withers. 2013. Evolutionary implications of the distribution and variation of the skeletal muscles of the anuran

lymphatic system. Zoomorphology 132:339–349. https://doi:10.1007/s00435-013-0190-7

Drotlef, D.M., E. Appel, H. Peisker, K. Dening, A. del Campo, S.N. Gorb, and W.J.P. Barnes. 2014. Morphological studies of the toe pads of the rock frog, *Staurois parvus* (family: Ranidae) and their relevance to the development of new biomimetically inspired reversible adhesives. Interface Focus 5: 20140036. http://dx.doi.org/10.1098/rsfs.2014.0036

Duellman, W.E., and L. Trueb. 1994. Biology of Amphibians. McGraw Hill. Inc. New York, USA.

Dunlap, D.G. 1966. The development of the musculature of the hindlimb in the frog, *Rana pipiens*. Journal of Morphology 119:241–258.

Ecker, A., and G. Haslam. 1889. The Anatomy of the Frog. Oxford, Clarendon Press, USA.

Farris, J.S. 1999. Likehood and inconsistency. Cladistics 15:199–204.

Federle, W., W.J.P. Barnes, W. Baumgartner, P. Drechsler, and J.M. Smith. 2006. Wet but not slippery: Boundary friction in tree frog adhesive toe pads. Journal of the Royal Society Interface 3:689–697.

Gaupp, E. 1904. Lehre von integument und von den sinnesorganen. Pp.3–439 in Anatomie des Frosches (A. Ecker's and R. Wiederseim's, eds.). Friedrich Vieweg und Sohn, Braunschweig, Germany.

Goloboff, P.A. 1996. Methods for faster parsimony analysis. Cladistics 12:199–220.

Goloboff, P.A. 1999. Analyzing large data sets in reasonable times, solutions for composite optima. Cladistics 24:774–786.

Goloboff, P.A. 2003. Parsimony, likelihood, and simplicity. Cladistics 19:91–103.

Goloboff, P.A., and S.A. Catalano. 2016. TNT version 1.5, including a full implementation of phylogenetic morphometrics. Cladistics 32:221–238.

Goloboff, P.A., J.S. Farris, and K.C. Nixon. 2008. TNT, a free program for phylogenetic analysis. Cladistics 24:774–786.

Goodman, M., C.B. Olson, J.E. Beeber, J. Czelusniak. 1982. New perspectives in the molecular biological analysis of mammalian phylogeny. Acta Zoologica Fennica 169:19–35.

Grant, T. 2019. Outgroup sampling in phylogenetics: Severity of the test and successive outgroup expansion. Journal of Zoological Systematics and Evolutionary Research 2019:1–16. https://doi.org/10.1111/jzs.12317

Grant, T., and A.G. Kluge. 2003. Data exploration in phylogenetic inference: Scientific, heuristic, or neither. Cladistics 19:379–418.

Grant, T., and A.G. Kluge. 2008a. Clade support measures and their adequacy. Cladistics 24:1051–1064.

Grant, T., and A.G. Kluge. 2008b. Credit where credit is due: The Goodman-Bremer support metric. Molecular Phylogenetics and Evolution 49:405–406.

Grant, T., and A.G. Kluge. 2009. Parsimony, explanatory power, and dynamic homology testing. Systematics and biodiversity 7:357–363. https://doi.org/10.1017/S147720000999017X

Grant, T., and L.O. Rodríguez. 2001. Two new species of frogs of the genus *Colostethus* (Dendrobatidae) from Peru and a redescription of *C. trilineatus* (Boulenger, 1883). American Museum Novitates 3355:1–24.

Grant, T., D.R. Frost, J.P. Caldwell, R. Gagliardo, C.F.B. Haddad, P.J.R. Kok, and W.C. Wheeler. 2006. Phylogenetic systematics of dart-poison frogs and their

relatives (Anura: Athesphatanura: Dendrobatidae). Bulletin of the American Museum of Natural History 299:1–262.

Grant, T., M. Rada, M. Anganoy-Criollo, A. Batista, P.H. Dias, A.M. Jeckel, D.J. Machado, and J.V. Rueda-Almonacid. 2017. Phylogenetic systematics of dart-poison frogs and their relatives revisited (Anura: Dendrobatoidea). South American Journal of Herpetology 12:1–90.

Guillory, W.X., M.R. Muell, K. Summers, and J.L. Brown. 2019. Phylogenomic reconstruction of the neotropical poison frogs (Dendrobatidae) and their conservation. Diversity 2019:1–14.

Heath, T.A., S.M. Hedtke, and D.M. Hillis. 2008. Taxon sampling and the accuracy of phylogenetic analyses. Journal of Systematics and Evolution 46:239–257. https://doi.org/10.3724/SP.J.1002.2008.08016

Hillis, D.M. 1998. Taxonomic sampling, phylogenetic accuracy, and investigator bias. Systematic Biology 47:3–8. https://doi. org/10.1080/106351598260987

IUCN. 2020. The IUCN Red List of Threatened Species. Version 2020-2. Available at https://www.iucnredlist.org. Accessed on 04 November 2020. International Union for Conservation of Nature and Natural Resources, Switzerland.

Jeckel, A.M., T. Grant, and R.A. Saporito. 2015. Sequestered and synthesized chemical defenses in the poison frog *Melanophryniscus moreirae*. Journal of Chemical Ecology 41:505–512. DOI: 10.1007/s10886-015-0578-6

Jiménez de la Espada, M. 1870. Fauna neotropicalis species quaedam nondum cognitae. Jornal se Sciencias, Mathematicas, Physicas e Naturaes 3:57–65.

Kaplan, M. 1997. A new species of *Colostethus* from the Sierra Nevada de Santa Marta (Colombia) with comments on inter-generic relationships within the Dendrobatidae. Journal of Herpetology 31:369–375.

Kluge, A.G. 1989. A concern for evidence and a phylogenetic hypothesis of relationships among *Epicrates* (Boidae, Serpentes). Systematic Biology 38:7–25.

Kluge, A.G., and T. Grant. 2006. From conviction to anti-superfluity: Old and new justifications for parsimony in phylogenetic inference. Cladistics 22:276–288.

La Marca, E. 1994. Descripción de un nuevo género de ranas (Amphibia: Dendrobatidae) de la Cordillera de Mérida, Venezuela. Anuario de Investigación 1991:39–41.

Lynch, J.D. 1982. Two new species of poison-dart frogs (*Colostethus*) from Colombia. Herpetologica 38:366–374.

Lynch, J.D. 1996. *Eleutherodactylus erythropleura*. Catalogue of American Amphibians and Reptiles 623:1–3.

McDiarmid, R.W. 1994. Preparing amphibians as scientific specimens. Pp. 289–296. In Measuring and Monitoring Biological Diversity. Standard Methods for Amphibians (Heyer W.R., M.A. Donnelly, R.W. McDiarmid, L.C. Hayek and M.S. Foster, eds.). Smithsonian Institution Press, USA.

Morales, V. 2002 “2000”. Sistemática y biogeografía del grupo *trilineatus* (Amphibia, Anura, Dendrobatidae, *Colostethus*) con descripción de once nuevas especies. Publicaciones de la Asociación de Amigos de Doñana 13:1–59.

Myers, C.W., and W.E. Duellman. 1982. A new species of *Hyla* from Cerro Colorado, and the other tree frog records and geographical notes from western Panama. American Museum Novitates 2752:1–32.

Myers C.W., O.A. Paolillo, and J.W. Daly. 1991. Discovery of malodorous and nocturnal frog in the family Dendrobatidae: Phylogenetic significance of a new genus and species from the Venezuela Andes. American Museum Novitates 3002:1–33.

Nixon, K.C. 1999. The parsimony ratchet, a new method for rapid parsimony analysis. Cladistics 15, 407–414.

Noble, G.K. 1922. The phylogeny of the Salientia I. The osteology and the thing musculature; their bearing on classification and phylogeny. Bulletin of the American Museum of Natural History 46:1–87.

Noble, G.K., and M.E. Jaeckle. 1928. The digital pads of the tree frogs. A study of the phylogenesis of an adaptation structure. Journal of Morphology and Physiology 45:259–292.

Ospina-Sarria, J.J., and W.E. Duellman. 2019. Two new species of *Pristimantis* (Amphibia: Anura: Strabomantidae) from southwestern Colombia. Herpetologica 75:85–95.

Padial, J.M., T. Grant, and D.R. Frost. 2014. Molecular systematics of terraranas (Anura: Brachycephaloidea) with an assessment of the effects of alignment and optimality criteria. Zootaxa 3825:1–132.

Parques Naturales Nacionales de Colombia. 2018. Parque Natural Nacional Sumapaz. Available at http://www.parquesnacionales.gov.co/portal/es/parques-nacionales/parque-nacional-natural-sumapaz/ Accessed on 29 October 2018. Parques Naturales Nacionales de Colombia y El Ministerio de Ambiente, Colombia.

Perez-Peña, P.E., G. Chávez, E. Twomey, and J.L. Brown. 2010. Two new species of *Ranitomeya* (Anura: Dendrobatidae) from eastern Amazonian Peru. Zootaxa 2439:1–23.

Pyron, R.A. 2014. Biogeographic analysis reveals ancient continental vicariance and recent oceanic dispersal in amphibians. Systematic Biology 63:779–797.

Pyron, R.A., and J.J. Wiens. 2011. A large-scale phylogeny of Amphibia including over 2800 species, and a revised classification of extant frogs, salamanders, and caecilians. Molecular Phylogenetics and Evolution 61:543–583. https://doi: 10.1016/j.ympev.2011.06.012.

Rivero, J.A. 1990 "1988". Sobre las relaciones de las especies del género *Colostethus* (Amphibia, Dendrobatidae). Memoria de la Sociedad de Ciencias Naturales La Salle 42:3–32.

Sánchez-Pacheco, S.J., O. Torres-Carvajal, V. Aguirre-Peñafiel, P.M. Nunes, L. Verrastro, G.A. Rivas, M.T. Rodrigues, T. Grant, and R.W. Murphy. 2018. Phylogeny of *Riama* (Squamata: Gymnophthalmidae), impact of phenotypic evidence on molecular datasets, and the origin of the Sierra Nevada de Santa Marta endemic fauna. Cladistics 34:260–291.

Sankoff, D. 1975. Minimal mutation trees of sequences. SIAM Journal on Applied Mathematics 28:35–42.

Sankoff, D., and R.J. Cedergren.1983. Simultaneous comparison of three or more sequences related by a tree. Pp. 253–263 in Time Warps, String Edits, and Macromolecules: The Theory and Practice of Sequence Comparison (Sankoff, D., and J. B. Kruskal, eds.). Addison-Wesley Pub, USA.

Santos, J.C., and D.C. Cannatella. 2011. Phenotypic integration emerges from aposematism and scale in poison frogs. Proceeding of the National Academy of Sciences United States of America 108:6175–6180. https://doi. org/10.1073/pnas.1010952108

Santos, J.C., L.A. Coloma, and D.C. Cannatella. 2003. Multiple, recurring origins of aposematism and diet specialization in poison frogs. Proceedings of the National

Academy of Sciences of the United States of America 100:12792–12797. https://doi.org/10.1073/pnas.2133521100

Santos, J.C., L.A. Coloma, K. Summers, J.P. Caldwell, R. Ree, and D.C. Cannatella. 2009. Amazonian amphibian diversity is primarily derived from late Miocene andean lineages. PLOS Biology 7:1–14. https://doi.org/10.1371/journal.pbio.1000056

Santos, J.C., M. Baquero, C. Barrio-Amoros, L.A. Coloma, L.K. Erdtmann, A.P. Lima, and D.C. Cannatella. 2014. Aposematism increases acoustic diversification and speciation in poison frogs. Proceedings of the Royal Society B: Biological Sciences 281:20141761–2014176. https://doi.org/10.1098/rspb.2014.1761

Saporito, R.A., M.A. Donnelly, H.M. Garraffo, T.F. Spande, and J.W. Daly. 2006. Geographic and seasonal variation in alkaloid-based chemical defenses of *Dendrobates pumilio* from Bocas del Toro, Panama. Journal of Chemical Ecology 32:795–814. DOI: 10.1007/s10886-006-9034-y

Savage, J.M., and R. Heyer. 1967. Variation and distribution in the tree-frog genus *Phyllomedusa* in Costa Rica, Central America. Beiträge zur Neotropischen Fauna 5:111–131.

Savage, J.M., and R. Heyer, R. 1997. Digital webbing formulae for anurans: A refinement. Herpetological review 28:131.

Silverstone, P.A. 1976. A revision of the poison-arrow frogs of the genus *Phyllobates* Bibron *in* Sagra (family Dendrobatidae). Natural History Museum of Los Angeles County 27:1–53.

Twomey, E. and J.L. Brown. 2008. Spotted poison frogs: Rediscovery of a lost species and a new genus (Anura: Dendrobatidae) from northwestern Peru. Herpetologica 64:121–137.

Van Dijk, D.E. 1955. The ‘tail’ of *Ascaphus*: A historical résumé and new histological-anatomical details. Annals of the University of Stellenbosch 31:1–71.

Van Dijk, D.E. 1959. On the cloacal region of Anura in particular of larval *Ascaphus*. Annals of the University of Stellenbosch 35:169–249.

Varón, A., and W.C. Wheeler. 2012. The tree alignment problem. BMC Bioinformatics 13:1–14. https://doi:10.1186/1471-2105-13-293

Varón, A., and W.C. Wheeler. 2013. Local search for the tree alignment problem. BMC Bioinformatics 14:1–12. https://doi:10.1186/1471-2105-14-66

Vences, M., J. Kosuch, S. Lotters, A. Widmer, K.H. Jungfer, J. Kohler, and M. Veith. 2000. Phylogeny and classification of poison frogs (Amphibia: Dendrobatidae), based on mitochondrial 16S and 12S ribosomal RNA gene sequences. Molecular Phylogenetics and Evolution 15:34–40. https://doi:10.1006/mpev.1999.0738

Vences, M., J. Kosuch, R. Boistel, C.FB. Haddad, E. La Marca, S. Lotters, and M. Veith. 2003. Convergent evolution of aposematic coloration in Neotropical poison frogs: A molecular phylogenetic perspective. Organisms, Diversity and Evolution 3:215–226. https://doi: 10.1078/1439-6092-00076

Wheeler, W.C. 1996. Optimization alignment: The end of multiple sequence alignment in phylogenetics? Cladistics 12:1–9.

Wheeler, W.C. 2003a. Implied alignment: A synapomorphy-based multiple sequence alignment method. Cladistics 19:261–268.

Wheeler, W.C. 2003b. Iterative pass optimization of sequence data. Cladistics 19:254–260.

Wheeler, W.C., N. Lucaroni, L. Hong, L.M. Crowley, and A. Varón. 2015. POY version 5: Phylogenetic analysis using dynamic homologies under multiple optimality criteria. Cladistics 31:189–196.

Wheeler, W.C., L. Aagesen, C.P. Arango, J. Faivovich, T. Grant, C. D'Haese, D. Janies, W.L. Smith, A. Varon, and G. Giribet. 2006. Dynamic homology and phylogenetic systematics: A unified approach using POY. American Museum Novitates, American Museum of Natural History, USA.

Zwickl, D.J., and D.M. Hillis. 2002. Increased taxon sampling greatly reduces the phylogenetic error. Systematic Biology 51:588–598.

APPENDIX I

Specimens Dissected to Examine the Extrinsic Cloacal Musculature

Aromobatidae: *Allobates femoralis* (KU 205289), *A. juanii* (KU 189425), *A. talamancae* (PD 49), *A. olfersioides* (KU 93159), *Aromobates haydeeae* (KU 181033, KU 181040), *A. mayorgai* (KU 133213), *A. nocturnus* (KU 220986), *A. orostoma* (KU 106702), *Mannophryne collaris* (ICN 3241), *M. cordillerana* (MZUSP 94591), *M. herminae* (MZUSP 8094), *Rheobates palmatus* (ICN 1454, 8535, 8689, 35479).

Bufonidae: *Rhinella ornata* (uncataloged specimen at MZUSP), *Rhinella paraguas* (CD 1503), *Osornophryne bufoniformis* (PSO-CZ 2496).

Dendrobatidae: *Adelphobates galactonotus* (TG3683), *Ameerega braccata* (MZUSP100230)*, A. flavopicta* (MZUSP100112, TG3191), *A. hahneli* (MZUSP55668), *Colostethus agilis* (ICN 6412), *C. inguinalis* (ICN47962), *C. mertensi* (ICN 8212, 8220, KU 139596), *"C". ruthveni* (ICN 35712), *Dendrobates auratus* (MZUSP 100174), *Ectopoglossus atopoglossus* (KU289251), *E. confusus* (KU 166157, MZUSP 101190), *E. lacrimosus* (KU170244, ICN 13425), *E.saxatilis* (IaVH 14615), *Epipedobates darwinwallacei* (MZUSP15605), *E. machalilla* (KU142485), *Hyloxalus abditaurantius* (ICN9843, 9848, 9856), *H. cepedai* (USNM 146926, ICN 44491), *H. edwardsi* (ICN 2770, 6384, 6389, 21914, 21936, 21944), *H. excisus* (ICN-CMV 332), *H. jhoncito* (MAA 1266), *H. lehmanni* (ICN16281), *H. maculosus* (ICN23609, 24253), *H. picachos* (ICN 42620, 42632), *H. ruizi* (ICN 5416), *H. sanctamariensis* (MAA 1402), *H. subpunctatus* (ICN 1721, 5733, 35350, 12729, 12733), *H. vergeli* (ICN 35431), *H.* sp. Supatá (ICN55869), *H.* sp. Inzá (LVP 398), *H.* sp. Tambito (ICN 35526), *Leucostethus brachistriatus* (ICN 9814, 9815), *Oophaga pumilio* (PD 50), *Paruwrobates andinus* (PSO-CZ 626), *P. whymperi* (KU 221620).

Hylodidae: *Hylodes phyllodes* (uncataloged specimen at MZUSP).

Ranidae: *Lithobates catesbeianus* (uncataloged specimen at LabAnfibios IBUSP)

TABLE 1.—Summary of the successive outgroup expansion analysis to test the phylogenetic position of the new species in poison frogs, Dendrobatoidea. Analysis included 100 *Hyloxalus* terminals and a variable number of the outgroup terminals (number in parenthesis). "*n*" is the total number of terminals in each analysis. In Outgroup, "+", indicate the additional terminals added to the previous analysis.

Analysis	*n*	Outgroup	Root	Sister species	Relationships of the sp. nov.
1	106 (6)	*Ectopoglossus, Paruwrobates, Phyllobates*	*Phyllobates lugubris*	*Hyloxalus picachos*	(((*H. jhoncito*+*H. picachos*) (*H. cepedai*+*H.* sp_AguaAzul)) (*H. felixcoperari*+*H. subpunctatus*))
2	120 (20)	1+ *Phyllobates* spp., *Minyobates, Oophaga,"Colostethus"*	*Silverstoneia flotator*	*Hyloxalus cepedai* + *Hyloxalus* sp_AguaAzul	((((*H. cepedai*+*H.* sp_AguaAzul) *H. jhoncito*) *H. picachos*) (*H. felixcoperari*+*H. subpunctatus*))
3	127 (27)	2 + *Adelphobates, Ameerega, Colostethus, Dendrobates, Epipedobates, Excidobates, Silvertoneia*	*Rheobates palmatus*	*Hyloxalus picachos*	(((*H. jhoncito*+*H. picachos*) (*H. cepedai*+*H.* sp_AguaAzul)) (*H. felixcoperari*+*H. subpunctatus*))
4	136 (35)	3 + *Andinobates, Leucostethus, Ranitomeya*	*Rheobates palmatus*	*Hyloxalus picachos*	(((*H. jhoncito*+*H. picachos*) (*H. cepedai*+*H.* sp_AguaAzul)) (*H. felixcoperari*+*H. subpunctatus*))

5	162 (61)	4 + 4–5 spp. per genus.	*Rheobates palmatus*	*Hyloxalus picachos*	(((*H. jhoncito*+*H. picachos*) (*H. cepedai*+*H.* sp_AguaAzul)) (*H. felixcoperari*+*H. subpunctatus*))
6	168 (67)	5 + *Allobates, Rheobates, Anomaloglossus* (Aromobatidae), and *Crossodactylus* (Hylodidae), *Thoropa* (Cycloramphidae), *Melanophryniscus* (Bufonidae)	*Boana boans*	*Hyloxalus picachos*	(((*H. jhoncito*+*H. picachos*) (*H. cepedai*+*H.* sp_AguaAzul)) (*H. felixcoperari*+*H. subpunctatus*))

FIGURES CAPTIONS

FIG. 1.—Body of *Hyloxalus edwardsi* group species in dorsal and ventral views. The holotype of *H. jhoncito*, a subadult female, MAA 1260 (A), *H. edwardsi,* an adult male, ICN 8560 (B), *H. ruizi*, an adult female, ICN 5417, paratype (C).

FIG. 2.—Body of *Hyloxalus edwardsi* group species in lateral view. *H. jhoncito*, a subadult female, MAA 1260 (A), *H. edwardsi,* an adult female, ICN 21936 (B), *H. ruizi*, an adult female, ICN 5416 (C).

FIG. 3.—Hand and foot of *Hyloxalus edwardsi* group species in ventral view. *H. jhoncito*, a subadult female, MAA 1260 (A), *H. edwardsi*, hand of adult male, ICN 21937; foot of a subadult male, ICN 6382 (B), *H. ruizi*, an adult female, ICN 5416 (C).

FIG. 4.—Cloacal sheath of *Hyloxalus edwardsi* group species. *H. jhoncito*, a subadult female, MAA 1260 (A), *H. edwardsi*, a juvenile female, ICN 21944 (B), *H. ruizi*, an adult female, ICN 5416 (C).

FIG. 5.—*Hyloxalus jhoncito*, subadult female in life, in lateral (A) and ventral (B) views (MAA 1260).

FIG. 6.—Distribution of the *Hyloxalus edwardsi* group and type locality of the new species with a red star (A), Los Bosques de Galilea (B), and La Quebrada Wolf (C).

FIG. 7.—The phylogenetic position and the relationships of the *Hyloxalus edwardsi* group, represented by *H. jhoncito*. Summary of the strict consensus of 52 most parsimonious trees (29746 steps) from analysis 6. Branch value are Goodman-Bremer support values.

FIG. 8.—Variation of the *m. sphincter ani cloacalis* (SAC) in dendrobatids. Lateral (A) and ventral (B) view of the SAC in *Hyloxalus maculosus* (adult male, ICN 23609). Ventral (C and D) and ventro-lateral (E) view of slip of the SAC of *H. edwardsi* (D and E, a juvenile female ICN 21944; C, an adult female ICN 21936). See in A the presence of the slip of the SAC (sSAC), and in B the insertion of the sSAC in the dermis, below of the cloacal aperture. In C the sSAC extends distad, attaching to the dermis, here the skin cut is at the posteroventral pubic level. In D and E the insertion of the sSAC to posterior branch of the *m. rectus abdominis* (RA) tendon of origin. Other abbreviations: P. *m. piriformis*, U. Urostyle tip.

FIGURES CHAPTER 1

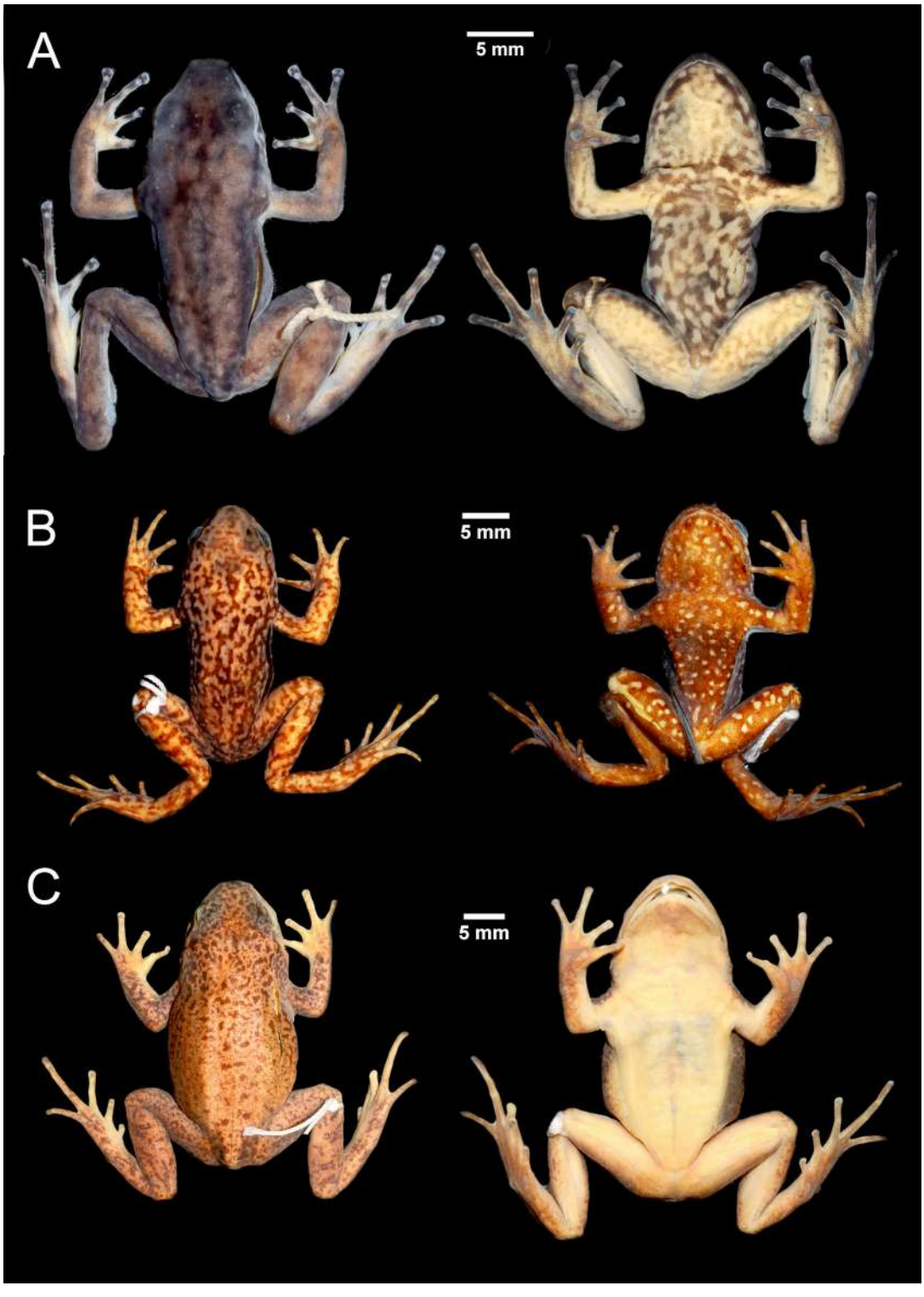

FIGURE. 1.—Body of *Hyloxalus edwardsi* group species in dorsal and ventral views. The holotype of *H. jhoncito*, a subadult female, MAA 1260 (A), *H. edwardsi,* an adult male, ICN 8560 (B), *H. ruizi*, an adult female, ICN 5417, paratype (C).

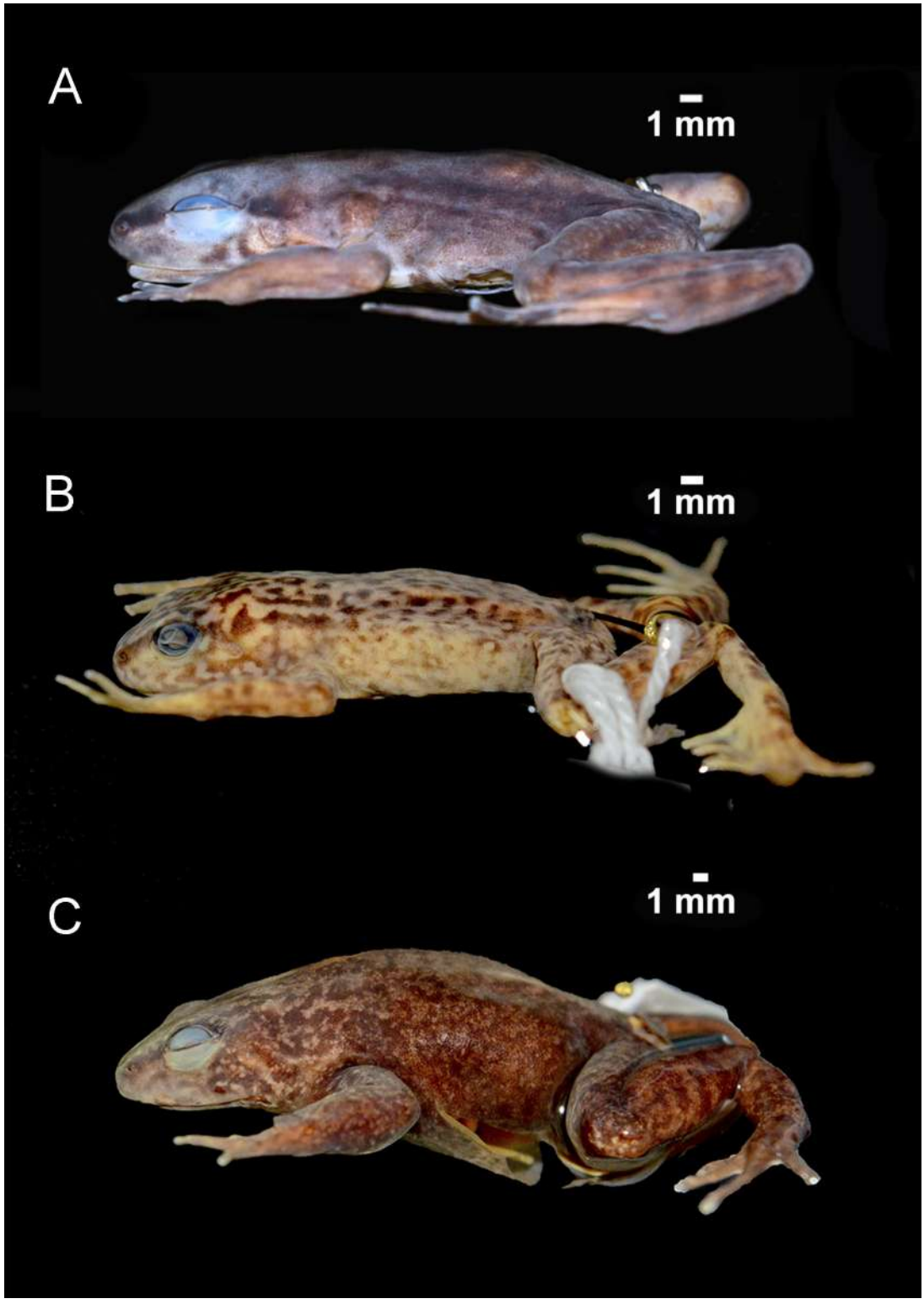

FIGURE 2.—Body of *Hyloxalus edwardsi* group species in lateral view. *H. jhoncito*, a subadult female, MAA 1260 (A), *H. edwardsi,* an adult female, ICN 21936 (B), *H. ruizi*, an adult female, ICN 5416 (C).

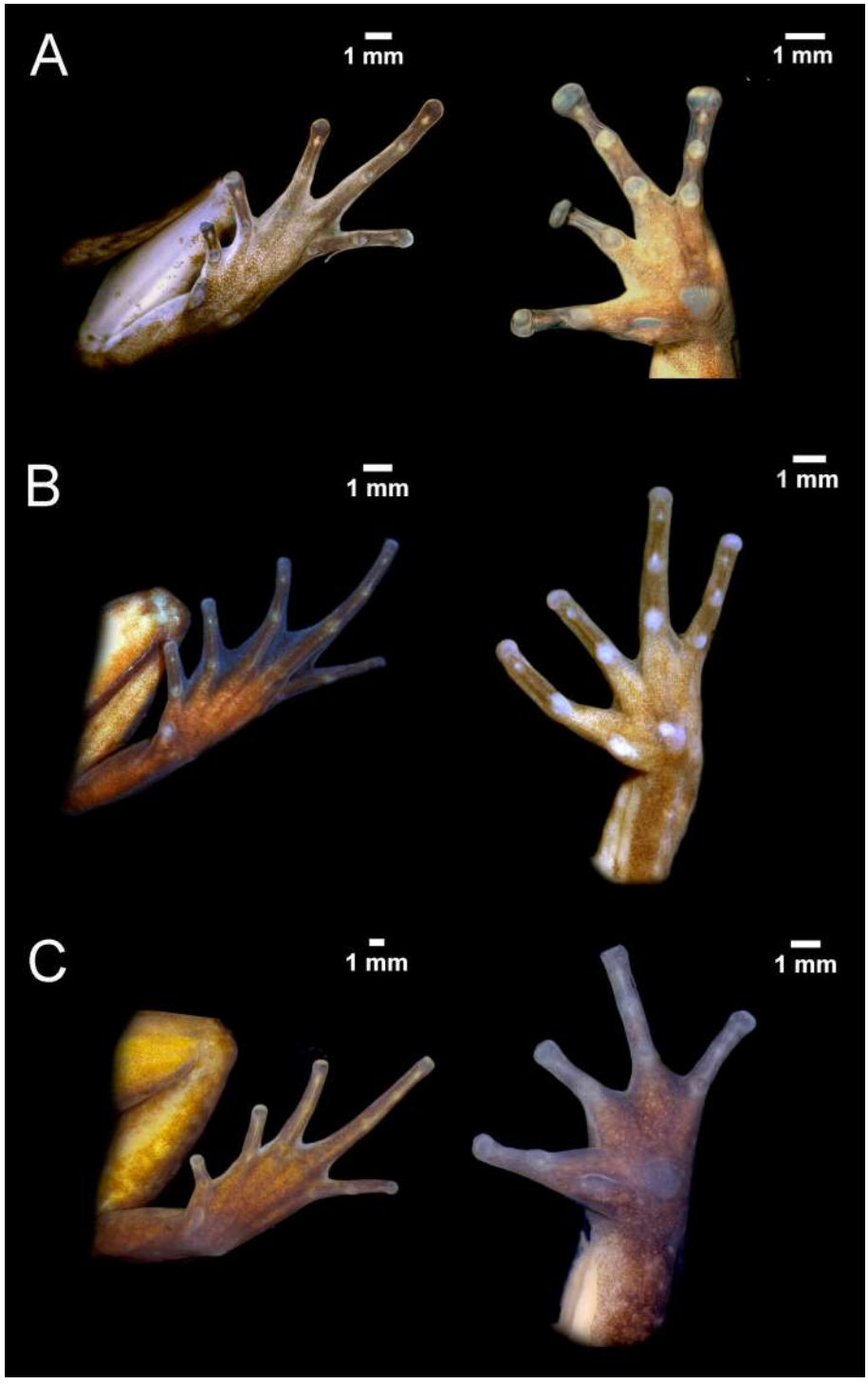

FIGURE. 3.—Hand and foot of *Hyloxalus edwardsi* group species in ventral view. *H. jhoncito*, a subadult female, MAA 1260 (A), *H. edwardsi*, hand of adult male, ICN 21937; foot of a subadult male, ICN 6382 (B), *H. ruizi*, an adult female, ICN 5416 (C).

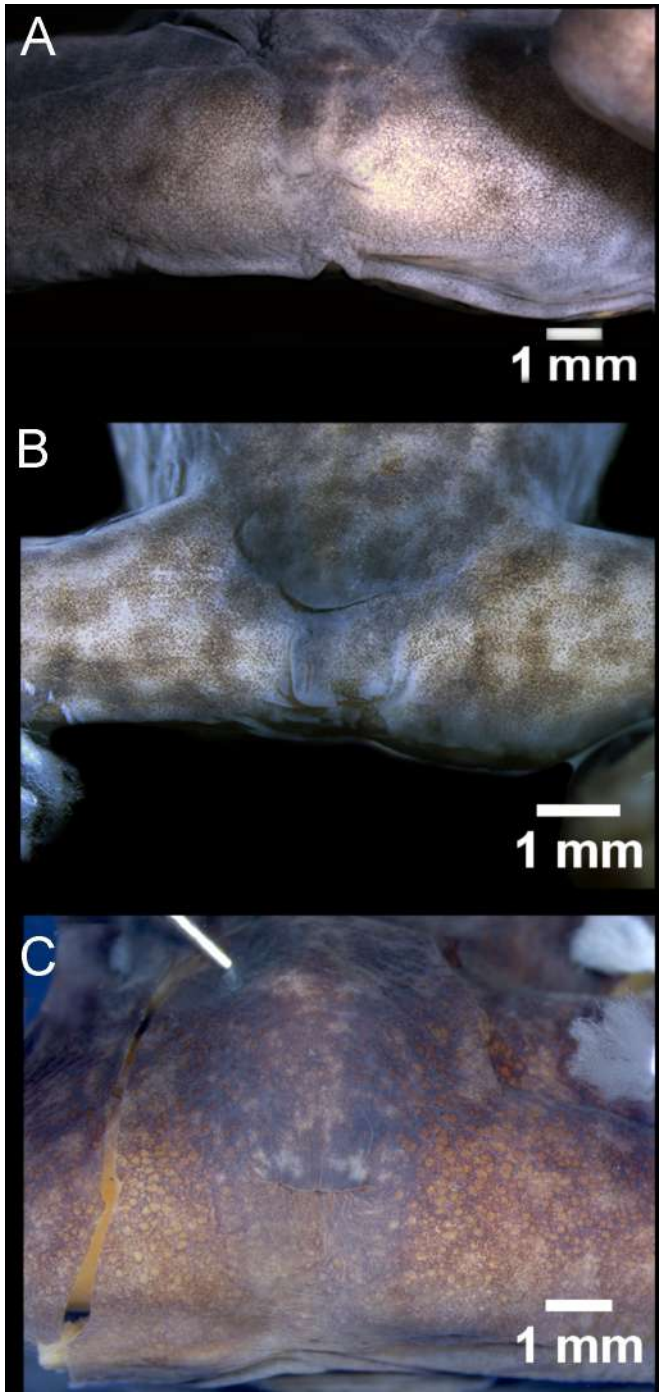

FIGURE 4.—Cloacal sheath of *Hyloxalus edwardsi* group species. *H. jhoncito*, a subadult female, MAA 1260 (A), *H. edwardsi*, a juvenile female, ICN 21944 (B), *H. ruizi*, an adult female, ICN 5416 (C).

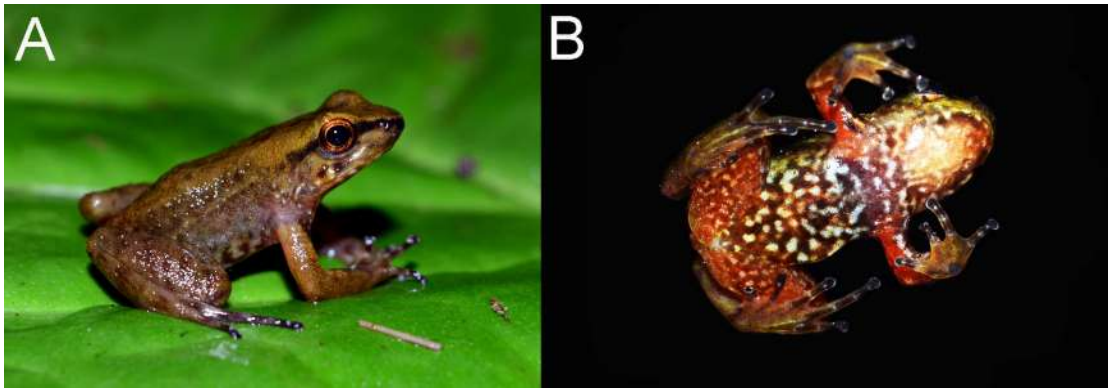

FIGURE 5.—*Hyloxalus jhoncito*, subadult female in life, in lateral (A) and ventral (B) views (MAA 1260).

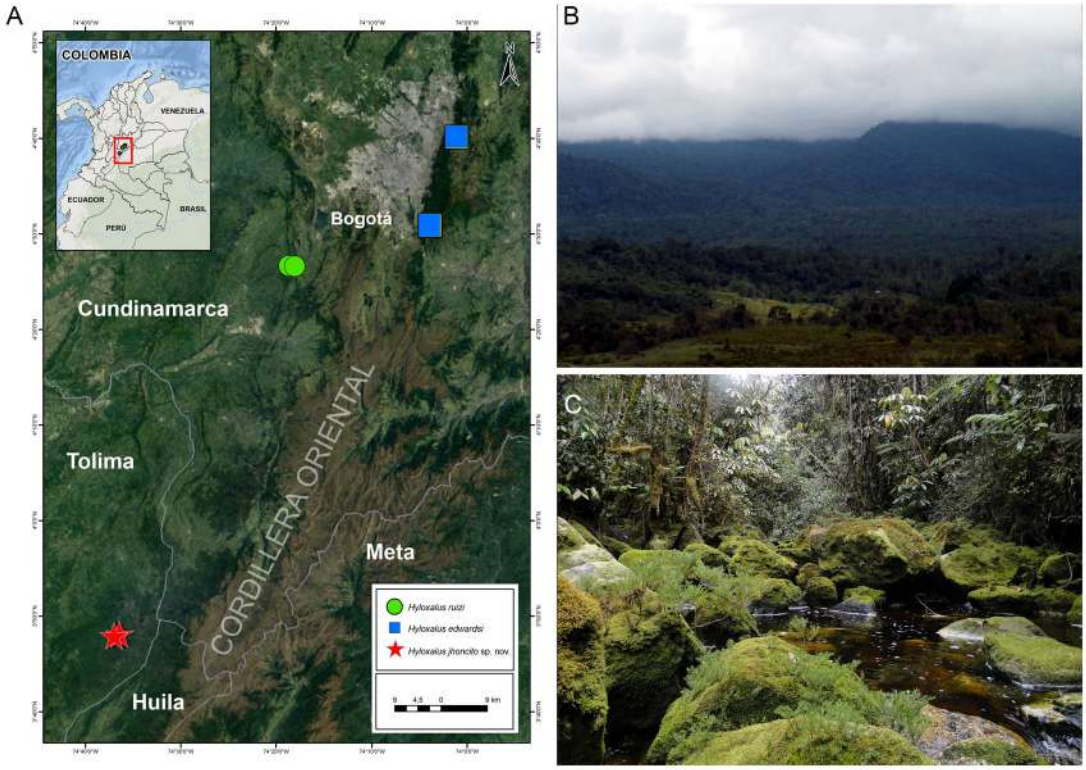

FIGURE 6.—Distribution of the *Hyloxalus edwardsi* group and type locality of the new species with a red star (A), Los Bosques de Galilea (B), and La Quebrada Wolf (C).

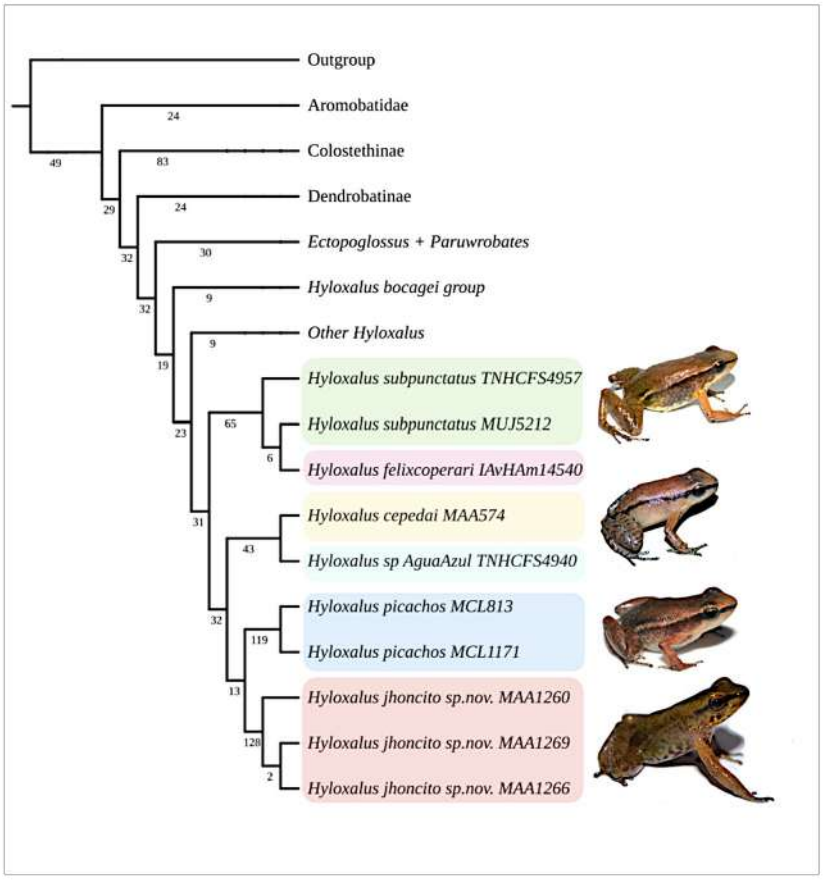

FIGURE 7.—The phylogenetic position and the relationships of the *Hyloxalus edwardsi* group, represented by *H. jhoncito*. Summary of the strict consensus of 52 most parsimonious trees (29746 steps) from analysis 6. Branch value are Goodman-Bremer support values.

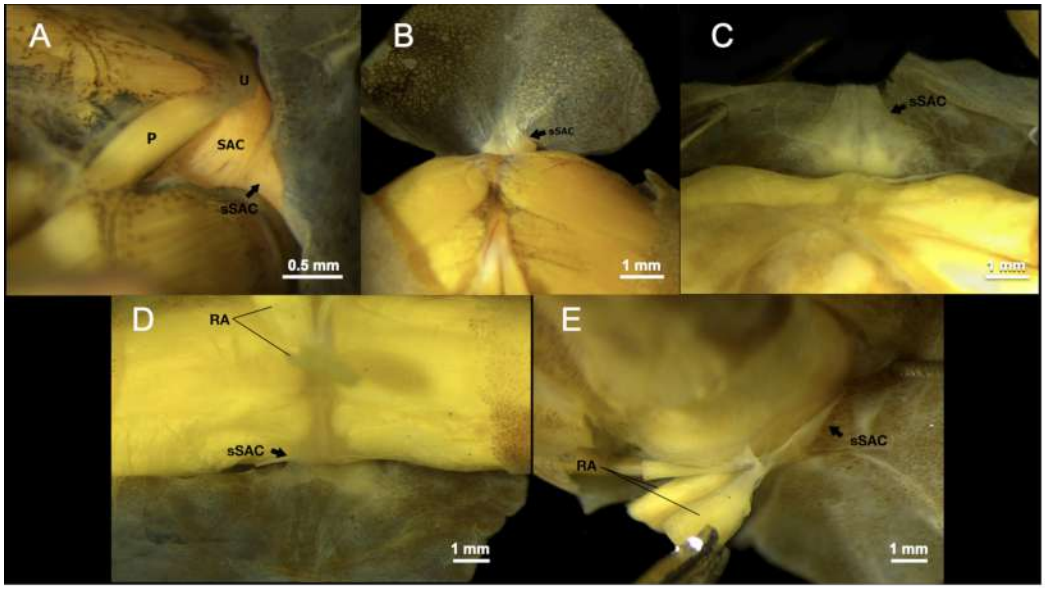

FIGURE. 8.—Variation of the *m. sphincter ani cloacalis* (SAC) in dendrobatids. Lateral (A) and ventral (B) view of the SAC in *Hyloxalus maculosus* (adult male, ICN 23609). Ventral (C and D) and ventro-lateral (E) view of slip of the SAC of *H. edwardsi* (D and E, a juvenile female ICN 21944; C, an adult female ICN 21936). See in A the presence of the slip of the SAC (sSAC), and in B the insertion of the sSAC in the dermis, below of the cloacal aperture. In C the sSAC extends distad, attaching to the dermis, here the skin cut is at the posteroventral pubic level. In D and E the insertion of the sSAC to posterior branch of the *m. rectus abdominis* (RA) tendon of origin. Other abbreviations: P. *m. piriformis*, U. Urostyle tip.

1. Most parsimonious tree of the first successive outgroup expansion analysis in the genus *Hyloxalus* (Dendrobatidae)

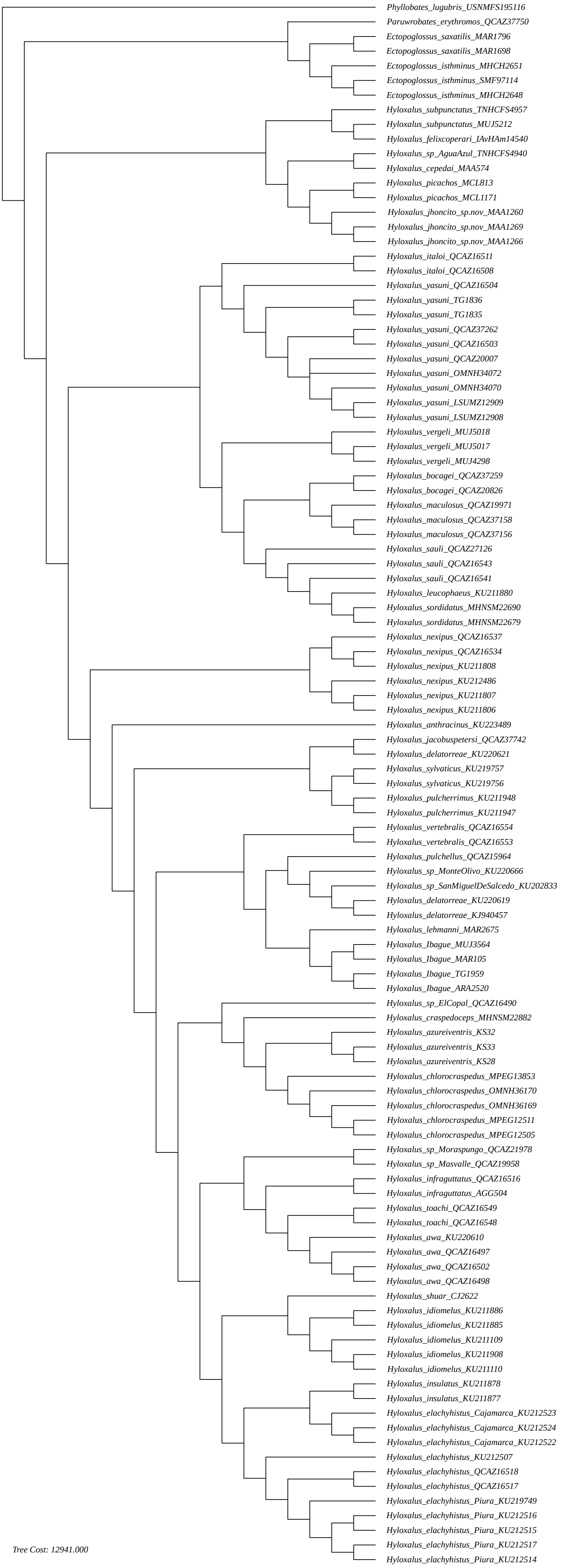

Tree Cost: 12941.000

2. Most parsimonious tree of the second successive outgroup expansion analysis in the genus *Hyloxalus* (Dendrobatidae)

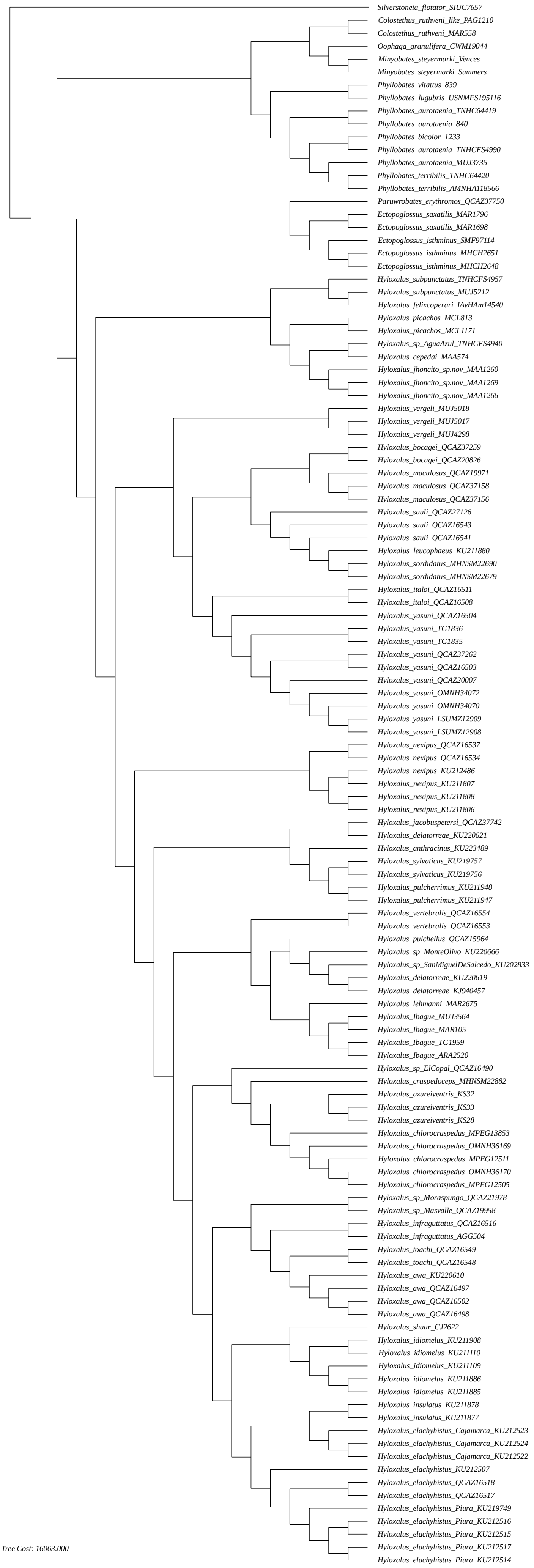

Tree Cost: 16063.000

3. Most parsimonious tree of the third successive outgroup expansion analysis in the genus *Hyloxalus* (Dendrobatidae)

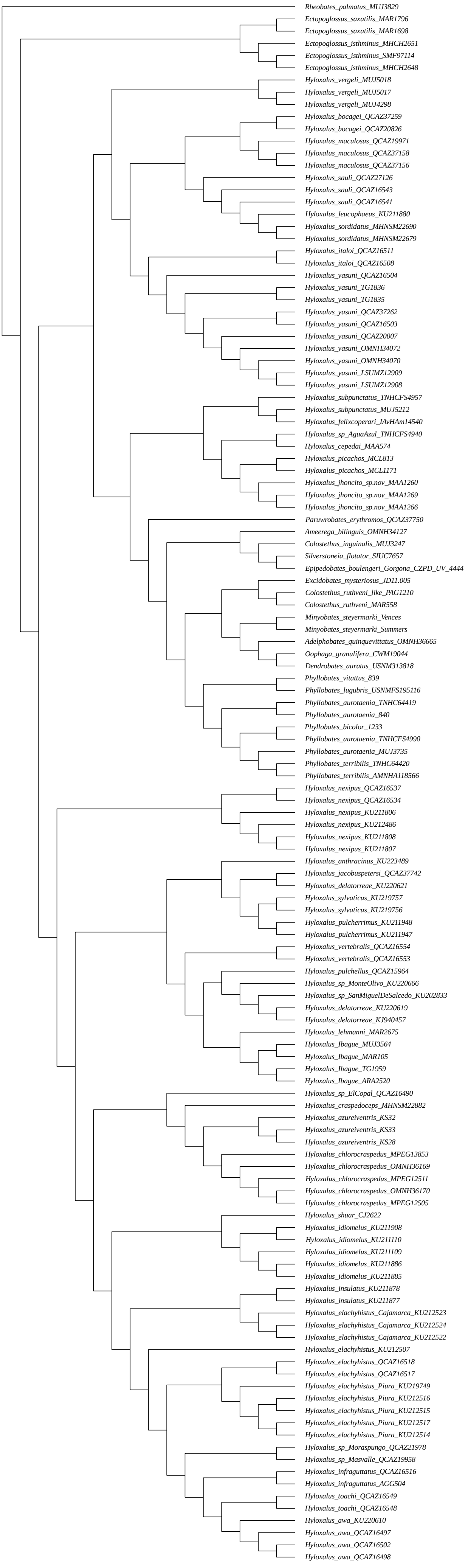

Tree Cost: 18682.000

4. Most parsimonious trees of the fourth successive outgroup expansion analysis in the genus *Hyloxalus* (Dendrobatidae)

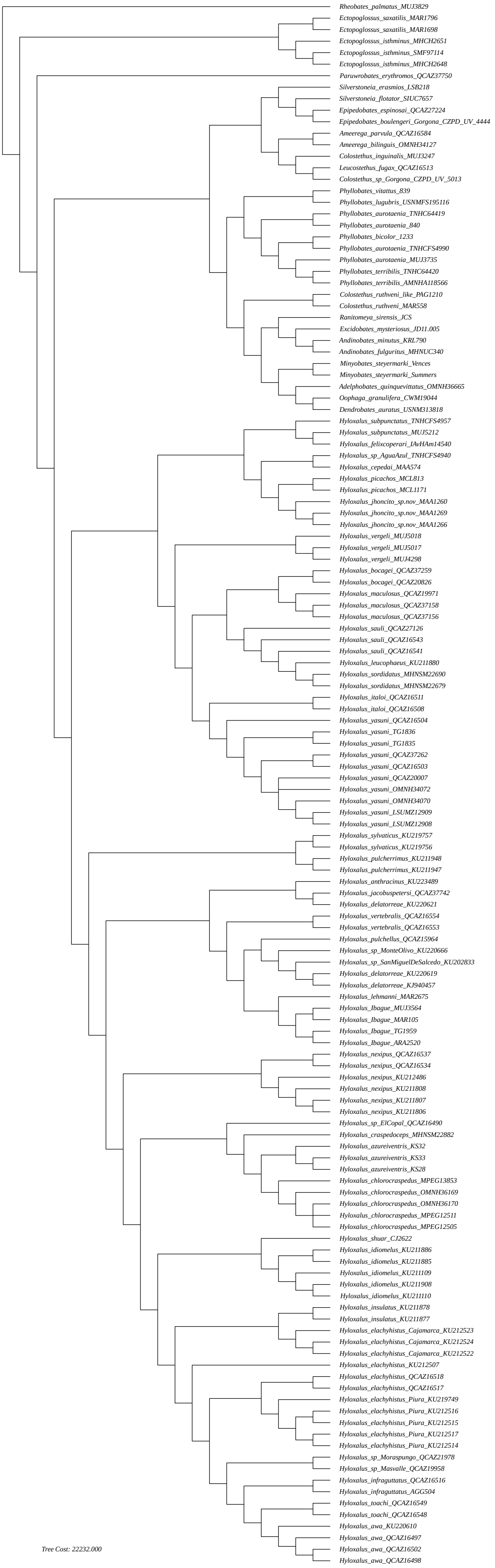

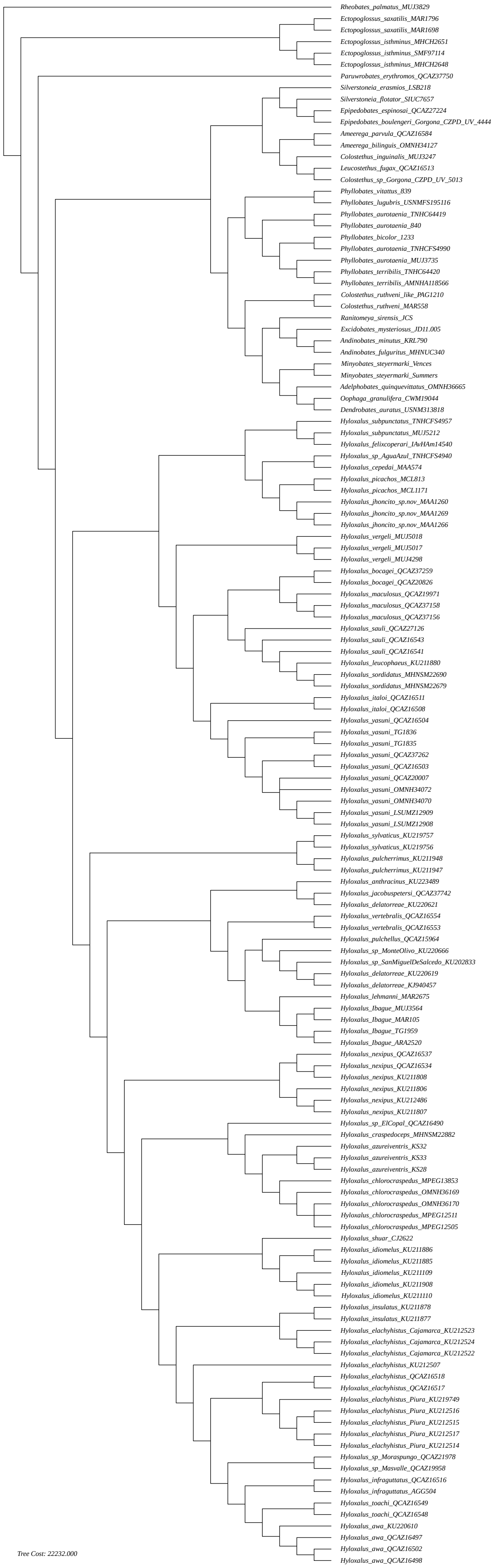

Tree Cost: 22232.000

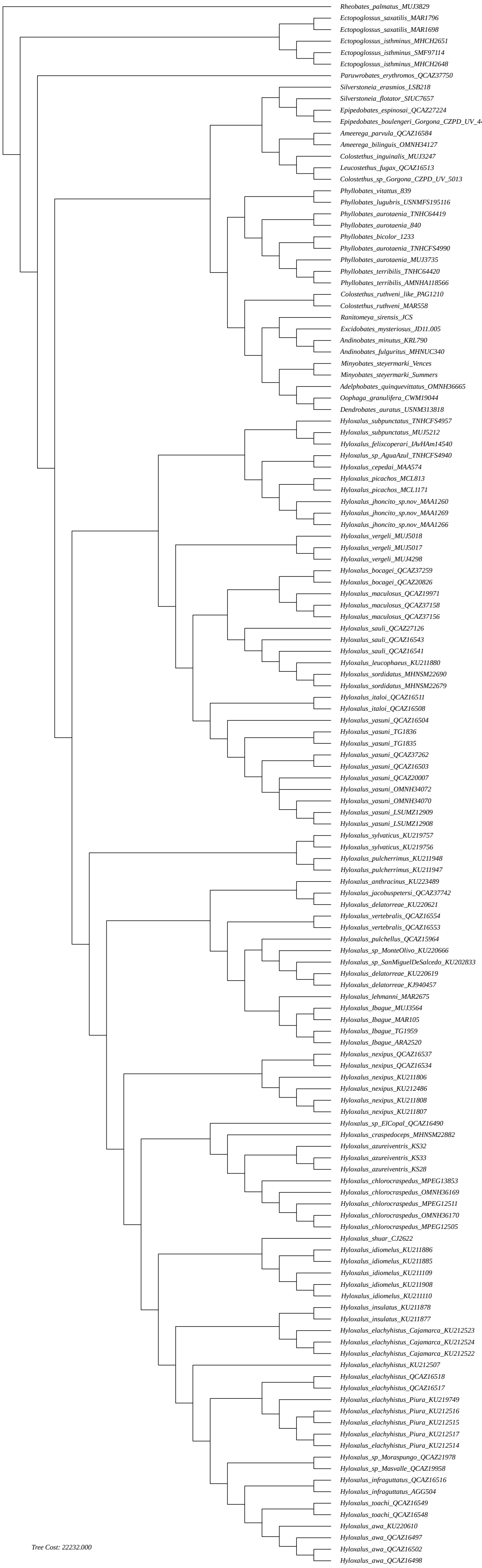

Tree Cost: 22232.000

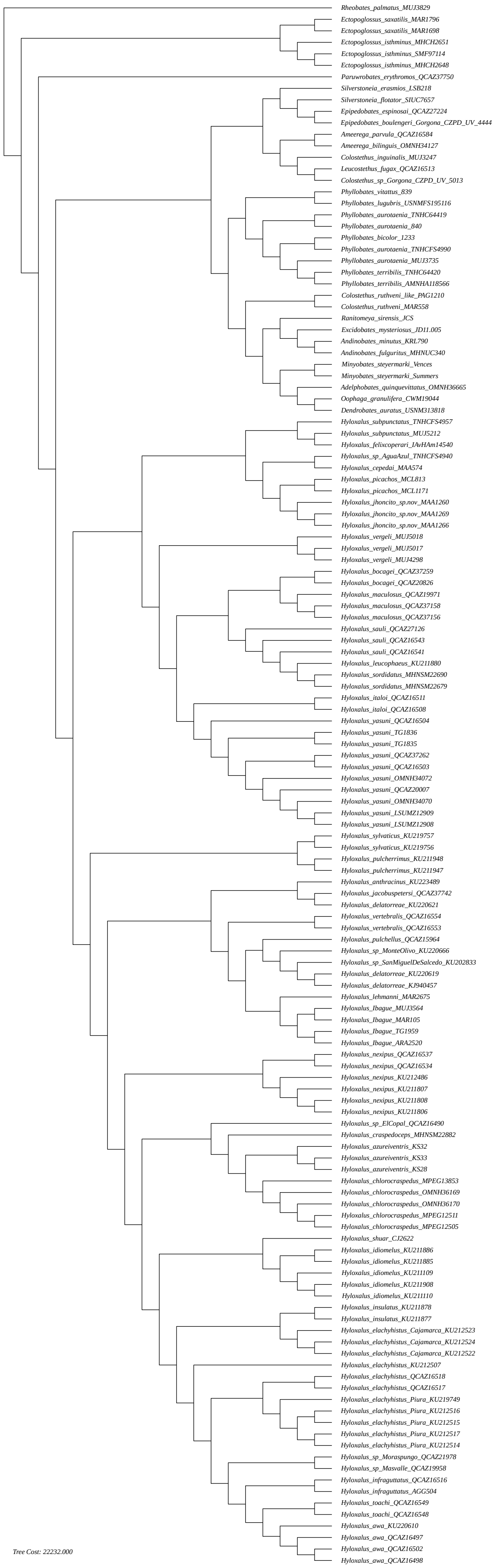

Tree Cost: 22232.000

5. Most parsimonious trees of the fifth successive outgroup expansion analysis in the genus *Hyloxalus* (Dendrobatidae)

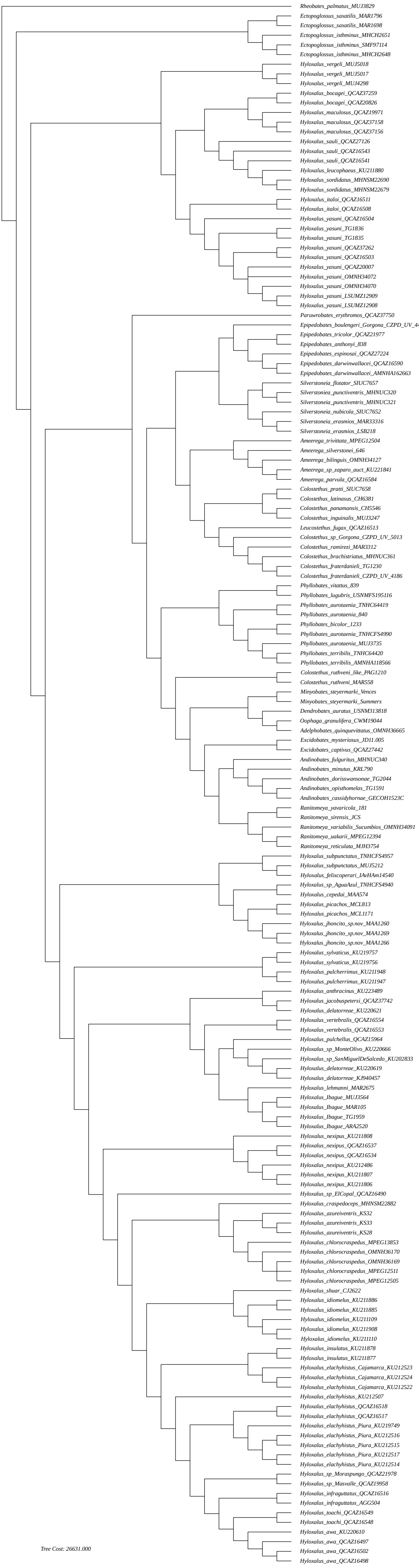

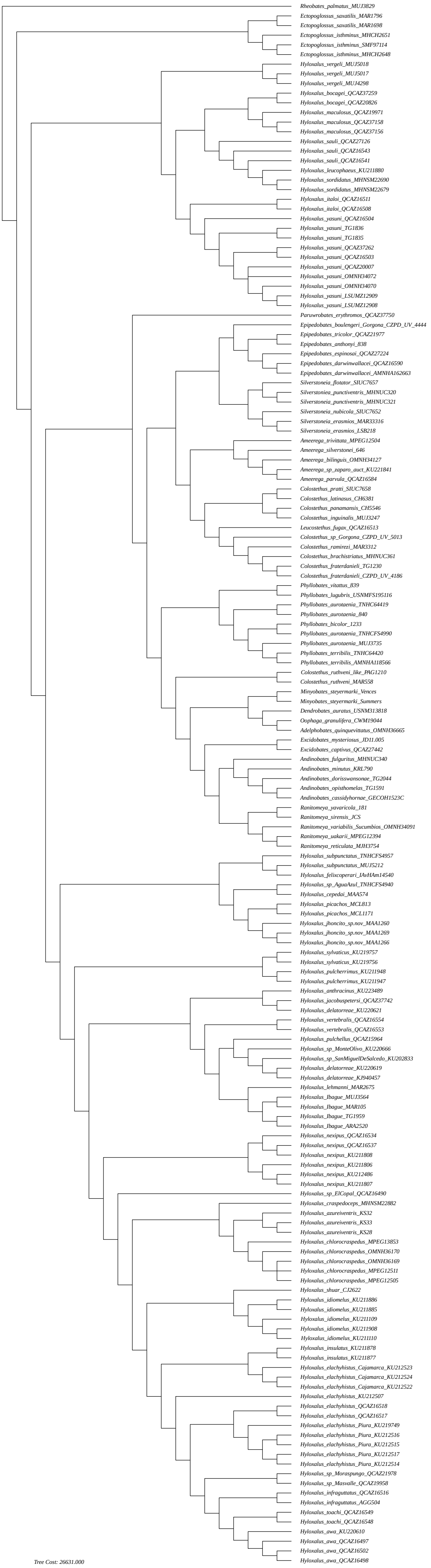

Tree Cost: 26631.000

Tree Cost: 26631.000

6. Most parsimonious trees of the sixth successive outgroup expansion analysis in the genus *Hyloxalus* (Dendrobatidae)

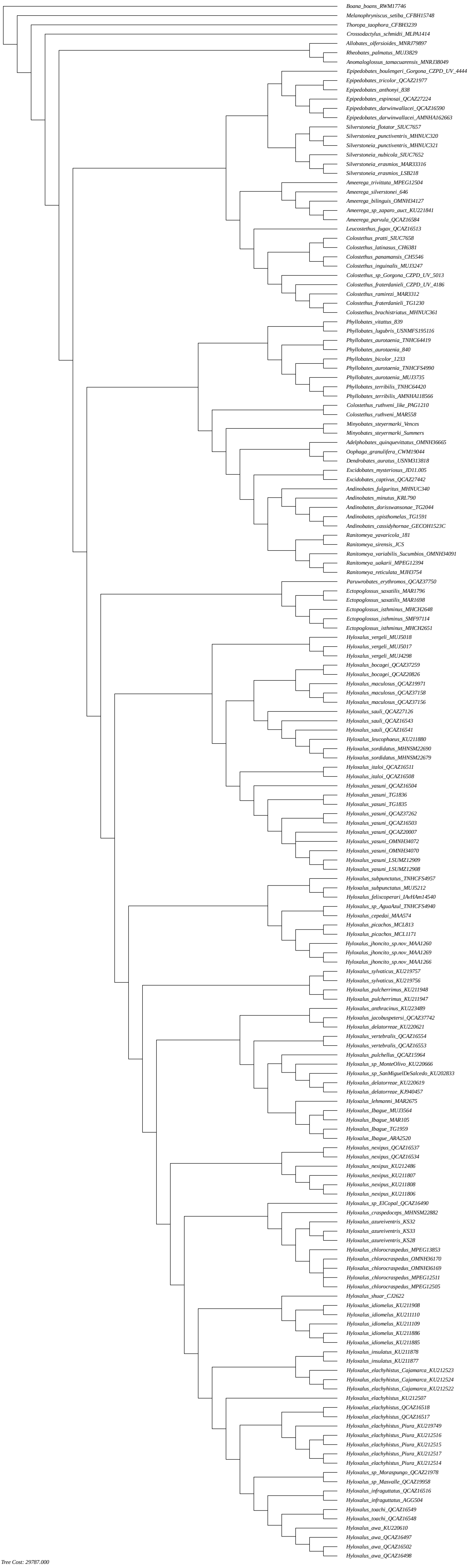

Tree Cost: 29787.000

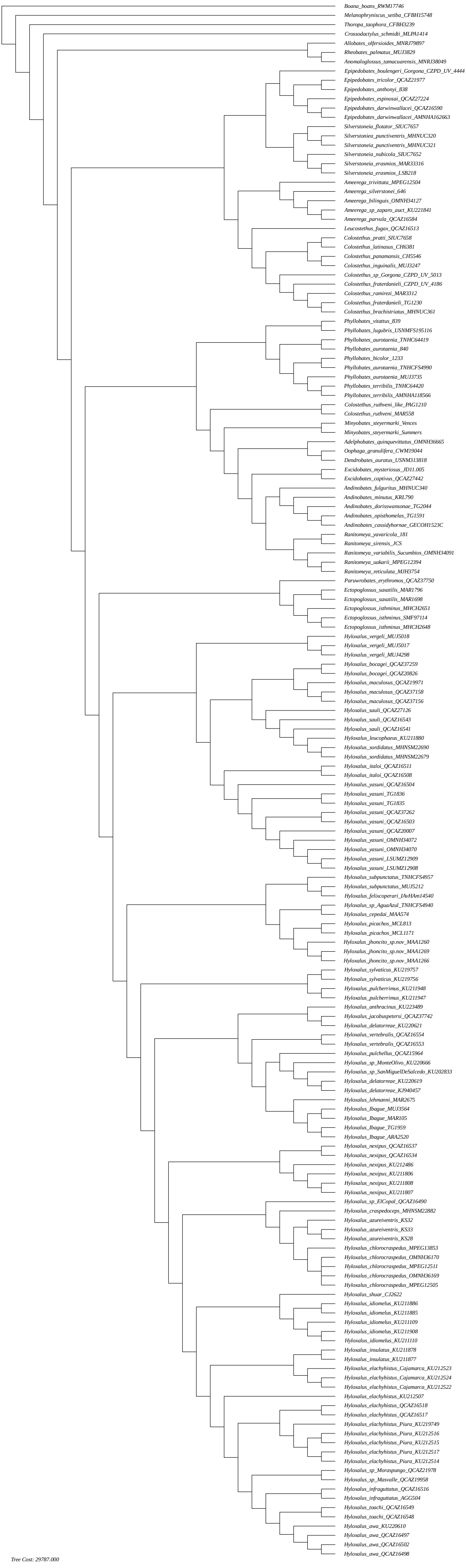

Tree Cost: 29787.000

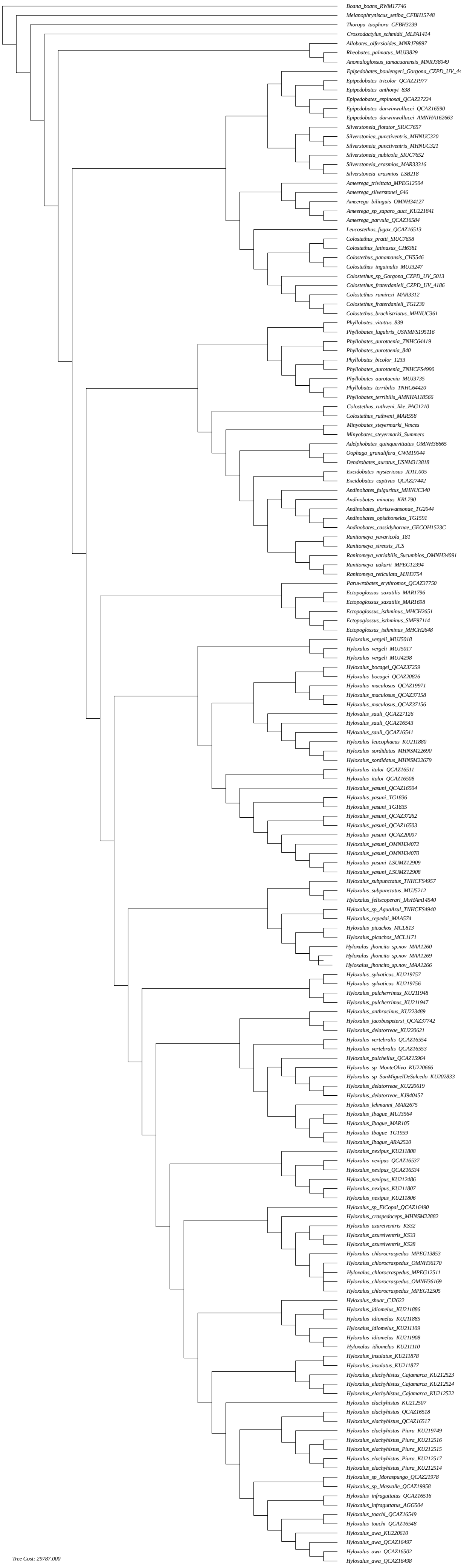

Tree Cost: 29787.000

Capítulo 2

The Phylogenetic Relationships of *Hyloxalus* Jiménez de la Espada 1870 (Anura: Dendrobatoidea: Dendrobatidae)

MARVIN ANGANOY-CRIOLLO

Department of Zoology, Institute of Biosciences, University of São Paulo, 05508-090, São Paulo, SP, Brazil.

ABSTRACT: *Hyloxalus* contains 63 nominal species, being the largest genus of the neotropical poison-dart frogs, Dendrobatoidea (Aromobatidae and Dendrobatidae). Nevertheless, despite some progress on the phylogeny of this genus in recent years, there are inconsistence between studies in the monophyly of some internal groups (e.g., the *H. bocagei* group), and in the placement of some species (e.g., *H. nexipus*, *H. sylvaticus*, and *H. pullcherrimus*). Moreover, the previously proposed groups in this genus have not been monophyletic, making of its phenotypic synapomorphies homoplasies (e.g, *H. ramosi* group and the black arm gland, and *H. azureiventris* group and the dorsolateral stripes); phenotypic synapomorphies are unknown for the genus; and a half of species (31 species) are assignment to *Hyloxalus* tentatively. In this study, I tested the phylogenetic relationship of *Hyloxalus* with additional species and populations. For this, I examined the adult and larval morphology of the 84% (53 species) of the nominal species and eleven unnamed species of *Hyloxalus,* evaluating the previously proposed phenotype characters and proposing 206 new characters (70 characters from adult, and 136 from tadpoles). In addition, I generate new molecular DNA sequences of the five species never been

sequenced before, and also of the known and undescribed species. Dataset for the phylogenetic analysis includes these new evidence together the available phenotype and molecular DNA data of this genus and their relatives. Due to the large increased in the taxon and character samples, the *Hyloxalus* (i.e., ingroup) monophyly and its internal relationships were tested as severely as possible through the successive outgroup expansion, performing nine total evidence analysis with parsimony as optimality criterion. The phylogenetic relationships of this genus was inferred when the topological relationships were relatively insensitive to the outgroup taxa addition. Successive outgroup expansion revealed that the ingroup topological relationships are affected at difference levels of inclusiveness, impacting drastically the monophyly of the genus and subfamily; and although, the ingroup topology tends to be stable in the last rounds, the topological position of the some clades, such as the clade *H. nexipus*, the clade *H. sylvaticus* and *H. pulcherrimus*, and the clade *Hyloxalus* sp. Bongara and *Hyloxalus* sp. PAV, recurrently vary. I recognize three large clades into this genus, the *H. bocagei, H. subpunctatus*, and *H. pulchellus* clades. The last clade being sister to the closely related *H. bocagei* and *H. subpunctatus* clades. This relationship is congruent with previous studies, although the current analysis contains more taxa. Unambiguous phenotypic synapomorphies optimize for each one of these three clades, and also for other minors clades within *Hyloxalus*. Based on this phenotypic evidence, I assigned to one of these three clades a few species of this genus and other dendrobatoids for which genotypical data are unavailable, but possess these synapomorphies. Additionally, *H. faciopunctulatus, H. pinguis*, and *H. sanctamariensis* are phylogenetic positioned for first time, and relevantly, the incertae sedis "*Colostethus*" *poecilonotus* was found as a member of *Hyloxalus*, closely related to *H. azureiventris* and *H. chlorocraspedus.* A complex species is recognized

in the populations assigned to *H. subpunctatus*, and based on the phenotypic and genotypic evidence, the subspecies *Prostherapis subpunctatus walesi* Cochran and Goin (1970) is elevate at species level. There are other undescribed species related to *H. arliensis, H. craspedoceps, H. elachyhistus, H. insulatus, H. lehmanni,* and in *H. nexipus*, which revealing the underestimated *Hyloxalus* diversity. Others finding including: phylogeny recovers the monophyly and relationships of Dendrobatoidea superfamily, except for subfamily Anomaloglossinae; and new unambiguous phenotypic synapomorphies optimize at distinct level of inclusiveness. Based on the current phylogeny, I analyzed the evolution of the key phenotypic characters for *Hyloxalus*.

Key words: Phylogenetic Systematic; Successive Outgroup Expansion; Hyloxalinae; phenotypic Synapomorphies; Evolution.

INTRODUCTION

With 63 formally recognized species (Frost 2021), *Hyloxalus* Jiménez de la Espada (1870) is the most diverse genus of the neotropical superfamily Dendrobatoidea. Species of this group inhabit the northwestern South America, in Brazil, Colombia, Ecuador, and Peru. The genus is centered on the Andean mountain range but also extends into the adjacent lowland forest of the Chocó and Amazon. Species are found in diverse habits, such as open grasslands, vegetation and rocks along stream, leaf litter of montane, tropical and subxerophytic forests, in caves, and paramos, from almost the sea level to high Andean ecosystems (roughly 4000 m. of elevation). Species are riparians, developing most biological activities beside to the water, in change other species, although part of the reproductive cycle is water dependent (e.g., deposit and development of the tadpoles), are terrestrial, because territory and social interactions occur away the streams. Most *Hyloxalus* have cryptic,

brown coloration, often with bright spots or blotches on the groin, axilla, and shank. A few species possess bright coloration suggestive of aposematism, as in the true dendrobatid poison frogs (*Ameerega*, *Epipedobates*, *Paruwrobates*, and Dendrobatini), but to date none has not been found to possess lipophilic alkaloids (Grant et al. 2006, 2017: S57). Tadpoles of this genus develop in pools, streams, and pools formed in the trunk of the fallen tree above 1 m of the ground and, as in most other poison frogs, after hatching, tadpoles are transported on the dorsum of adults to a water body where they complete their development. Natural history for this genus is known for few species (*H. awa*, *H. azureiventris*, *H. felixcoperari*, *H. subpunctatus*, *H. toachi*; Mudrack 1959, Stebbins and Hendrickson 1959, Fandiño et al. 1997, Lötters et al. 2000, Quiguango-Ubillús and Coloma 2008, Acosta-Galvis and Vargas-Ramírez 2018). The male carry the tadpoles, although in *H. awa* and in *H. felixcoperari* is the female. These has cephalic amplexus as most other dendrobatoids, but this is absent in *H. azureiventris*; and the male exclusively or both sexes (in *H. awa*) care the clutch.

Prior to Grant et al. (2006), most of the cryptic colored species were allocated in the then-*Colostethus sensu lato*; however, their phylogenetic total evidence analysis of the poison frogs showed that about a half species of this genus, inhabiting the Andean chain and the adjacent lowland regions, are more closely related to the aposematic clades (e.g., *Dendrobates, Oophaga, Ameerega, Epipedobates*) of the Dendrobatidae family, while the other half of the cis-Andean species remained distantly related in the Aromobatidae family, included in the genus *Allobates*. Thus, Grant et al. (2006) resurrected *Hyloxalus* from the synonymy with *Colostethus* Cope (1866) for this large clade of the Dendrobatidae. This genus is more closely related to Dendrobatinae rather than Colostethinae. With the addition of further taxa and

characters (molecular data mainly), subsequent studies supported the monophyly of the genus, but there are differences in the relationships among its parts (Santos et al. 2009, 2014, Santos and Cannatella 2011, Grant et al. 2017, Pyron and Wiens 2011, Pyron 2014, Jetz and Pyron 2018). Exemplified in the ambiguous position of *H. nexipus.* This species is sister to the clade conform by *H. azureiventris, H. chlorocraspedus,* and *Hyloxalus* sp. ElCopal in Grant et al. (2006); however subsequently, this was found sister to *H. anthracinus* (Santos et al. 2009), or sister to the clade comprise from *H. azureiventris* to *H. awa* (Pyron and Wiens 2011, Jetz and Pyron 2018) or from *Hyloxalus* sp. ElCopal to *H. awa* (Grant et al. 2017). Santos et al. (2014) found that two previously unanalized species, *Ameerega erythromos* and *Colostethus jacobuspetersi*, are the sister of *Hyloxalus* and part of *Hyloxalus*, respectively. Grant et al. (2017) revisited the poison frog phylogeny and corroborated Santos et al.'s (2014) findings, with their expanded taxon sample resulting in the trans-Andean median lingual process-possessing species (*Ectopoglossus*) and the revalidated *Paruwrobates* being placed in Hyloxalinae as the sister clade of *Hyloxalus*.

Despite the extensive phenotypic evidence that has accumulated (Grant et al. 2006, 2017), phenotype synapomorphies are unknown for *Hyloxalus*; nevertheless, five species groups have been proposed on the basis of morphological characters, as follow. (1) Lynch (1982) proposed the *H. edwardsi* group (as *Colostethus*) to include *H. edwardsi* and *H. ruizi* on the basis of their synapomorphic elongated cloacal sheath. La Marca (1994) reported this character in the *Nephelobates alboguttatus* group (now in *Aromobates*), and Grant (1998) reported it in *Colostethus lynchi*, but Grant et al. (2006) concluded that it is confined to the *H. edwardsi* group. (2) In the later 1990s and early 2000s, Grant and co-workers used the black arm gland, a dark

cutaneous swelling found on the internal surface of the distal upper arm and the proximal lower arm of adult males, to delimit the *H. ramosi* group (Grant and Castro 1998, Grant and Ardila-Robayo 2002, Grant et al. 2006). However, the monophyly of this group was rejected by Grant et al. (2017), because four members of this group (*H. anthracinus, H. arliensis, H. lehmanni*, and *H. nexipus*) are not closely related, refuting the homology of this character. (3) The brightly colored species of *Hyloxalus* (*H. azureiventris*, *H. chlorocraspedus,* and *H. nexipus*) were nested in a clade in Grant et al. (2006), and the presence of dorsolateral stripes was postulated as an unambiguous synapomorphy for these species, and *H. patitae* and *H. eleutherodactylus*; however, that group was not recovered in later analyses (e.g., Santos et al. 2009, Grant et al. 2017). On the basis of molecular data, Páez-Vacas et al. (2010) proposed the *Hyloxalus bocagei* group for species with extensive toe webbing, formerly confused with *H. bocagei*, *H. fuliginosus*, or *H. maculosus*, but the group do not included *H. leucophaeus, H. sordidatus*, and *H. vergeli* (see Grant et al. 2017). (5) Finally, although without phenotype synapomorphies, one more group has been recognized in the *Hyloxalus* literature, the *H. subpunctatus* group, which includes the *H. cepedai*, *H. felixcoperari*, *H. picachos*, *H. subpunctatus*, and *Hyloxalus* sp. Aguazul (Santos et al. 2009, Páez-Vacas et al. 2010, Acosta-Galvis and Vargas-Ramírez 2018). Again, the group is paraphyletic with respect to the *H. edwardsi* group (see Chapter 1). All these changes show that relationships of *Hyloxalus* are still cause of confusion in the phylogeny of poison frogs.

Although *Hyloxalus* is the largest genus of the dendrobatid frogs, only about half of the nominal species (49% of the 63 formally recognized species) have been included in previous phylogenetic analyses, and the remaining species are tentatively assigned to this genus based on their morphological resemblance to analyzed species.

However, generic assignation is somewhat difficult because, in addition to the lack of phenotypic synapomorphy for *Hyloxalus*, the characters present in *Hyloxalus* are shared with other aromobatid (e.g., *Allobates*, *Aromobates*) and dendrobatid (e.g., *Colostethus*) genera. This is exemplified by the taxonomic history of *H. cepedai* (Morales 2002) and *H. picachos* (Ardila-Robayo et al. 2000), both of which were described as *Colostethus* and later transferred to *Allobates* due to their resemblance to species of this genus (Grant et al. 2006). However, once genomic and phenotype data were analyzed, Grant et al. (2017) found them to be nested within *Hyloxalus*. Another example related to aposematic genera is the taxonomic history of *H. azureiventris*, described as *Phyllobates* (Kneller and Henle 1985), and transferred sequentially to *Dendrobates* (Myers and Burrowes 1987)*, Epipedobates* (Myers 1987)*, Cryptophyllobates* (Lötters et al. 2000)*, Ameerega* (Frost et al. 2006)*,* and *Hyloxalus* (Grant et al. 2006). Adding to this, several species tentatively allocated to *Allobates* and *Colostethus* (e.g., *A. ranoides*, *C. agilis, C. mertensi, C. thorntoni*, and *C. ucumari*) closely resemble species of *Hyloxalus* or *Paruwrobates* (see Grant et al. 2017). Further, some *Hyloxalus* are morphologically similar to the Colostethinae (e.g., *H. maquipucuna*, Vigle et al. 2020).

Other systematic problems of no-lesser importance persist in *Hyloxalus*; for instance, half of the species of the genus (46% species) are known from the type series or type locality (e.g., *H. aeruginosus*, *H. excisus*, *H. pinguis*, *H. utcubambensis*; Duellman 2004, Rivero and Serna 2000 “1995”, Rivero and Granados-Díaz 1990, Morales 1994). Moreover, several crucial species are in need of taxonomic revision (e.g., *H. delatorreae*, *H. elachyhistus*, *H. lehmanni*, *H. subpunctatus*; Coloma 1995, Grant and Ardila-Robayo. 2002, my data), and doubts about the assignment of populations to nominal species are common (e.g., *H. breviquartus*, *H. littoralis*;

Coloma 1995, Morales 1998), exacerbating the problem and hindering progress in the knowledge about the relationships within *Hyloxalus*.

Nevertheless, the extensive morphological variation in *Hyloxalus* could potentially provide new phenotype evidence to test phylogenetic hypothesis. For example, the species vary in size (e.g., maximum SVL 19.5 mm in *H. cepedai*, Morales 2002 "2000"; 31.5 mm in *H. shuar*, Coloma 1995), toe webbing (e.g., absent in *H. delatorreae* Coloma 1995; extensive in *H. faciopunctulatus,* Rivero 1991), coloration (e.g., cryptic in *H. bocagei,* Páez-Vacas et al. 2010; bright in *H. azureiventris*, Lötters et al. 2000, 2007), and lateral stripes (present in *H. subpunctatus*, Stebbins and Hendrickson 1959, Grant et al. 2006; absent in *H. chocoensis,* Myers 1991, Myers and Grant 2009), among others. Moreover, other studies have reported variation in musculature of the dendrobatoids (Dunlap 1960), or also these suggested to review other character systems, such as phalanges of the fingers and the integument of the venter or the black arm gland (Myers et al. 2012, Grant et al. 2017).

Therefore, all aforementioned makes it clear that the phylogenetic relationships of *Hyloxalus* need revision. Thus, given the extensive morphological variation in the genus, I examined this variation to test the phenomic characters proposed previously, and thanks to the new tissue samples get of the several nominal and undescribed species, I provide new genomic data for the genus. Altogether all of this evidence were used to test the phylogenetic relationships within *Hyloxalus*, by means a total evidence analysis with direct optimization.

MATERIALS AND METHODS

Taxon Sampling

Taxon sampling expanded on the datasets of Grant et al. (2017) and Anganoy-Criollo et al. (in prep; or Chapter 1). Given the many persistent problems in the species taxonomy of *Hyloxalus*, samples from all available populations were included to assess their taxonomic status. In addition to the *Hyloxalus* terminals included in those studies, I obtained tissue samples of other populations and species of *Hyloxalus* from Colombian and Peruvian amphibian collections, including *H. faciopunctulatus*, *H. littoralis*, *H. pinguis*, *H. sanctamariensis*, and "*Colostethus*" *poecilonotus,* analyzed here for the first time. I also carried out fieldwork to obtain new samples of key, previously unanalyzed species for which molecular data or tissues were not available, possess relevant character proposed in the literature, and could potentially be part of this genus or subfamily. Fieldwork was limited by access to collecting permits, sociopolitical problems (especially in Colombia), funding, and time. In total, I conducted fieldwork to search for 11 key species in historical and potential localities in Colombia and Ecuador (see **Table 1**). Unfortunately, I was only able to collect two of the key species (*H. cepedai* and *H. pinguis*; but see also new terminals included in Chapter 1). Nevertheless, additional populations of *H. arliensis*, *H. awa*, *H. bocagei*, and *H. subpunctatus* were discovered, as well as populations of six unnamed *Hyloxalus* species (*Hyloxalus* sp. AguaBonita, *Hyloxalus* sp. Alban, *Hyloxalus* sp. MesasGalilea, *Hyloxalus* sp. Junin, *Hyloxalus vergeli* Ibagué, *Hyloxalus* sp. QuebradaWolf). Specimens were euthanized, fixed, and preserved in 70 % ethanol (post-metamorphs) or 10% formaldehyde (larvae) following standard protocols (McDiarmid, 1994**)** and deposited in the Laboratorio de Anfibios, Instituto de Ciencias Naturales, Universidad Nacional de Colombia (ICN) and Laboratorio de Zoología Terrestre, Colegio de Ciencias Biológicas y Ambientales, Universidad San

Francisco de Quito (USFQ). Tissue samples were fixed in 95% ethanol and stored in the Laboratorio de Anfibios, Instituto de Biociencias, Universidade de São Paulo, São Paulo.

Given the aim of this study to test the topological relationships of *Hyloxalus* and the underlying character-state homology as severely as possible, successive outgroup expansion was employed to define the final outgroup sample (Grant 2019). In this approach, the ingroup is determined a priori and outgroup representatives are incrementally added on the basis of their expected ability to refute hypotheses of ingroup topology and homology hypotheses until the ingroup (i.e., *Hyloxalus*) hypotheses are stable (insensitive to outgroup expansion) in at least three continuous successive rounds

Adult phenotypic data were obtained from specimens of 53 species of *Hyloxalus* (i.e., 85% of total), but to test homology and characters, I also included 9 species (i.e., 90% of total) of the remain Hyloxalinae subfamily, 41 species (61%) of the Colosthethinae subfamily, and 23 (37%) of Dendrobatinae subfamily in the Dendrobatidae family. Furthermore, 14 species of Allobatinae (25%), 6 species of Anomaloglossinae (18%) and 7 species of Aromobatinae (18%) in the Aromobatidae family were reviewed (see **Table 2** for details). I examined type specimens and other reference material from *Hyloxalus* and other dendrobatoids and also studied photographs of the type specimens of the aromobatids *Allobates ranoides* and *Rheobates palmatus* and the dendrobatids *Ameerega bilinguis*, *A. boehmei*, *A. rubiventris*, *A. berohoka*, *Dendrobates claudiae*, *Epipedobates narinensis*, *Hyloxalus bentancuri*, *H. borjai*, *H. breviquartus*, *H. cevallosi*, *H. marmoreoventris*, *H. vergeli,* and also one of the junior synonyms of *H. subpunctatus, Phyllobates subpunctatus walesi*. In scored larval characters for 30 species (48%) of *Hyloxalus* and 1

Paruwrobates (*Ectopoglossus* larvae are unknown), as well as tadpoles of other dendrobatoids, covering most of the diversity of the superfamily (**Table 2**). The final matrix contains 326 terminals, with 189 belonging to the ingroup (*Hyloxalus*) and 137 to the outgroup.

Character Sampling

The final phenotypic matrix comprise 376 characters (characters are listed in the **Appendix 1**; matrix in Hennig format is provided in **Appendix 2**). The 189 external morphological, musculoskeletal, and behavioral characters of Grant et al. (2006, 2017) were analyzed and reformulated when necessary to improve the homology hypothesis based on the current phenotypic variation. Modifications were made to characters 4 (distal tubercle on finger IV), 5 (finger V length), 6 (relative lengths of Fingers II and III), 20 (metacarpal ridge/fold), 21 (finger IV swelling in adult males), 22 (morphology of Finger IV swelling in adult males), 27 (thenar tubercle), 28 (black arm gland in adult males), 46 (metatarsal fold), 58 (ventrolateral stripe occurrence), 59 (ventrolateral stripe structure), and 81 (vocal sac occurrence) of Grant et al. (2017: Appendix 1). Characters 21 and 22, related to the swelling of finger IV were divided into eight characters following Cavalcanti et al. (2021). Additionally, on the basis of my revision of the adult morphology of *Hyloxalus* and their relatives, I identified 70 new characters (sensu Grant and Kluge 2004), of which 62 pertain to external morphology and 8 from musculature. Reformulation and new characters are found in the Phenotypic Characters section of the Results. Larval characters from external morphology and the chondrocranium were taken from the unpublished doctoral thesis of P. H. Dias (2018b); however, for the final larval characters used in this study, I considered the tadpole variation and characters found in Anganoy-Criollo (2013), Anganoy-Criollo and Cepeda-Quilindo (2017), Dias et al.

(2018a, c, 2021), and also the unpublished master thesis of Anganoy-Criollo (2014) related with the dendrobatoid chondrocranium. On the basis of this information, the larval characters of Grant et al. (2006, 2017) were reformulated, except the character 93 (caudal coloration), 94 (oral disc occurrence), 95 (oral disc morphology), 96 (lateral indentation of oral disc), 97 (marginal labial papillae size), and 102 (larval jaw sheath). In total, 135 larval characters are used in this study.

When the direct examination of characters was not possible, data were obtained from the following publications: Myers and Daly (1980), Aichinger (1991), Myers (1991), Morales (1992), Rodriguez and Myers (1993), Haddad and Martins (1994), Myers and Donelly (1997), Myers et al. (1998, 2012), Lötters et al. (2005, 2007, 2009), Kok et al. (2006a, b, 2010), Rueda et al. (2006), Mueses-Cisneros et al. (2008), Quiguango-Ubillús and Coloma (2008), von May et al. (2008), Brown and Twomey (2009), Myers & Grant (2009), Barrio-Amorós et al. (2010, 2011), Fouquet et al. (2015, 2018), Kok (2010), Páez-Vacas et al. (2010), Brown et al. (2011), Vaz-Silva and Maciel (2011), Amézquita et al. (2013), Batista et al. (2014), Schulze et al. (2015), Neves et al. (2017), Serrano-Rojas et al. (2017), Acosta-Galvis and Pinzón (2018), Brown et al. (2019), French et al. (2019), and Klein et al. (2020).

My examination of phenotypic characters systems was far from exhaustive. For example, it is likely that additional characters could be found in the hand and foot muscles (Blotto et al. 2020, B. Blotto in litt. 02/12/2020), structural composition of the ventral skin (Myers et al. 2012, Grant et al. 2017: S22), and behavior (e.g., Quiguango-Ubillús and Coloma 2008). Time constraints prevented me from scoring additional characters from these systems, but these and other character systems merit study to further test the relationships of *Hyloxalus*

In addition to phenotype evidence, I included the 15 genes used by Grant et al. (2017: S7). Besides to the data obtained from GenBank (**Table 3**), I generated molecular sequences of five mitochondrial (12S, tRNAval, and 16S [comprising the H-strand transcription unit 1] and MT-CYB, MT-CO1) and five nuclear (H3F3C, RHO, RAG1, SIAH1, and RNA28S) genes for 92 terminals.

Laboratory and Molecular Methods

External morphology and muscles of the adults and tadpoles (stages 26–41; Gosner 1960) were observed with a stereoscopic microscope Zeiss Stereo Discovery V8. To confirm dermal modifications (e.g., folds, granules, tubercles, fringes etc.), I made gross dissection and sometimes apply lugol and alcian blue solutions, following the recommendation of Grant et al. (2006: 62). When possible, conditions were confirm by direct inspection of live specimens in the field or from photos (Lynch and Duellman 1997, Cisneros and McDiarmid 2007, Duellman and Lehr 2009). Finger length was measured with a dial caliper to the nearest 0.1 mm, from palmar tubercle base to the finger disc tip (Kaplan 1997). Osteological characters were coded from 3D reconstructions obtained by X-ray micro-computed tomography using SkyScan 1176 scanner (Bruker, Kontich, Belgium, at 9 μm voxel resolution and 43 Kv) with the CTVox v.2.3.0 (Bruker, Kontich, Belgium) and SlicerMorph 1–4 (Fedorov et al. 2012) softwares. To obtain the chondrocranial character, tadpoles between stages 26–41 were cleared and double-stained with the Dingerkus and Uhler (1977) procedure. Histological preparations were done from the skin of the upper and lower arm of specimens stored in 70% ethanol. Skin sections were embedded in historesin (glycol methacrylate; Leica Microsystems Nussloch GmbH, Nussloch/Heidelberg, Germany), sectioned at 5 μm, and stained with toluidine blue and basic and basic fuchsin. Cuts

were studied and photographed using a Leica DM750 M microscope equipped with a Leica ICC50 W digital camera.

Whole cellular DNA was extracted from hindlimb muscle or liver tissue stored in 95–100% ethanol with the Qiagen DNeasy (Qiagen, Valencia, CA, USA) extraction kit. The mitochondrial and nuclear genes were amplified following the procedures described in Grant et al. (2006: 55). Amplification was done with standard PCR. An initial denaturing step of 3 min at 94 °C, 35–40 cycles of 1 min at 94 °C, 1 min at 45–62 °C, and 1–1.25 min at 72 °C, and the final extension step of 6 min at 72 °C. PCR products were purified with the Agencourt AMPure XP DNA Purification and Cleanup kit118 (Beckman Coulter Genomics, USA), and after sequencing in both directions (3’ → 5’ and 5’ → 3’) in Macrogen Inc. (South Korean) to double-check for sequencing and edition errors. Chromatograms, contigs, and consensus were read and generated in Sequencher 5.2.3 (Gene Codes Corporation, USA). Primers used for PCR amplification are listed in **Table 4**.

Phylogenetic Analysis

Phenotypic transformation series were compiled in Mesquite v. 3.4 (Maddison and Maddison 2016). When there were multiple terminals for one species, phenotypic characters were duplicated based on the arguments of Grant et al. (2006: 56–57). Loci that failed to amplify for some terminals or were not available in Genbank were treated as missing. Polymorphism as ambiguity were coded when two or more character-states occurs in the semaphoront (see Grant and Kluge 2003: 402–403, 2004: 25).

Nucleotide homology.—Due to nucleotides lacking the structural and developmental complexity like other character types, as morphology or behavior, it is cannot test homology independently. Moreover, DNA sequences vary in length,

which entails additional problem to establish homology between sequences. The multiple sequences alignment resolve this problem by mean of the correspondence between pair of sequences, inserting gaps to compensate the differences. So, each position is inferred as putative homology (static homology) (Wheeler 1996). Nevertheless, the resultant alignment is product of the different parameters or indels (insertions, deletions) cost, generating distinct solutions for a same DNA dataset, that support contradictory trees hypothesis (Grant et al. 2006). Moreover, in this case homology is treat as similarity, rather than nucleotide historical identity (i.e., evolutionary transformations; Grant and Kluge 2004, Kluge and Grant 2006; Grant and Kluge 2009). Alternatively, the direct optimization method optimize simultaneously sequences directly onto tree reconstructions (dynamic homology), avoiding the parameters or indels cost previous to the alignment, and competitive alignment hypotheses are test heuristically in the search of the most optimal tree (Wheeler 1996). In this method, indels are considered equivalent to the other transformations events (Wheeler 1996; Wheeler et al. 2006). Thus in this study, nucleotide homology is test by direct optimization on the tree, implemented in POY software (Wheeler et al. 2006, 2014). Previously to the dynamic homology procedure, each gene was prealigned in MAFFT v. 7.490 with default parameters to identify the conserved nucleotide regions and so delimit the homologous blocks to accelerate the tree search and avoid the errors by the different fragment lengths (Wheeler et al. 2006).

Choice optimality criteria.—My interest is obtain an optimal tree hypothesis that minimized the number of the transformation events to explain the characters-states variation in the terminals studied (Kluge and Grant 2006). Thus, I select unweighting parsimony as optimal criteria follows the reasons exposed in Padial et al.

(2014) and Kluge and Grant (2006). This is non-statistical, non-parametric and conservative method, because this do not impose probability or frequencies to infer character transformations, this reduce the assumptions necessaries to explain the evidence and the transformation events to the only evolutionary assumption, that is, descent with modification, and this treats faithful the ambiguous data (e.g., missing data) as such (Padial et al. 2014). Moreover, in this approach with the minimization of the transformation events is maximizing the explanatory power of the hypothesis (Kluge and Grant 2006, Grant and Kluge 2009, Kluge 2009).

Conversely, other methods to infer phylogenetic relationships, such as maximum likelihood, bayesian inference and weighting parsimony, impose additional assumptions to the evidence (e.g., evolutionary models), the transformation event are deduce by mean the use of probabilities, and the ambiguities are treat as evidence when there is none (Padial et al. 2014). Thus the evolution of the life history is considered by mean of the universal probabilistic laws (in contra of phylogenetic systematic as ideographic science; see Grant and Kluge 2004) and therefore the evidence is treat as classes (not as a historical individual; see Grant and Kluge 2004). For this reasons, I do not use the statistical, parametric, and evidentially ambivalent approaches.

Total evidence analysis.—All phenotypic and genotypical evidence was analyzed simultaneously in a total evidence analysis (Kluge 1989), applying equal weights to all classes of transformation events, following the justification of Kluge and Grant (2006). The theoretical and empirical advantages of the total evidence approach has been demonstrated previously (Grant and Kluge 2003, Rokas et al. 2003, Grant et al. 2006, Cabra-García and Hormiga 2019). Total evidence evaluates all available evidence both in terms of taxa and characters to test independently and

simultaneously each character hypothesis by mean the character congruence to identify the phylogenetic hypothesis with greatest explanatory power (Popper 1963, Kluge 1989, Grant and Kluge 2003, Kluge 2004, Grant et al. 2006).

I conducted analysis in POY v.5.1.1 (Wheeler et al. 2015), which uses tree-alignment (e.g., Sankoff 1975; Sankoff and Cedergren 1983; Wheeler 1996; Varón and Wheeler 2012, 2013) to test hypothesis of nucleotide homology dynamically by optimizing unaligned DNA sequences directly on alternative topologies (Kluge and Grant 2006; Wheeler et al. 2006; Grant and Kluge 2009), while simultaneously optimizing prealigned transformation series (e.g., morphology) as standard character matrices. Specifically, I used the command *search* to perform timed driven searches composed of random addition sequence Wagner builds, Subtree Pruning and Regrafting (SPR) and Tree Bisection and Reconnection (TBR) branch swapping (RAS + swapping; Goloboff 1996), Parsimony Ratcheting (Nixon 1999), and Tree Fusing (Goloboff 1999), alternating between standard direct optimization (Wheeler 1996) and static-approximation, which searches using the implied alignment (Wheeler 2003a) of the best tree in memory. I used the same search strategy for each successive outgroup expansion but increased search duration to account for the greater computational complexity of more terminal-rich analyses (**Table 5**).

For final refinement, I calculated the cost of the optimal tree(s) of each analysis using approximate iterative pass optimization (Wheeler 2003b) and submitted the implied alignment to additional searches in TNT v.1.5 (Goloboff et al. 2008; Goloboff and Catalano 2016; equal costs for all transformations, gaps treated as fifth state), stopping when a stable consensus was reached five times (TNT command: *xmult = level 10 chklevel 5 consense 5*).

I estimated clade support (Grant and Kluge 2008a) by calculating Goodman-Bremer values (GB; Goodman et al. 1982; Bremer 1988; Grant and Kluge 2008b) in TNT v.1.5 (Goloboff et al. 2008; Goloboff and Catalano 2016) using the implied alignment and the parameters specified in the bremer.run macro (for details see Goloboff et al. 2008; macro available at www.lillo.org.ar/phylogeny/tnt). To enable comparison of support values across analyses, I also calculated the ratio of explanatory power (REP), defined as $(S'–S)/(G–S)$, where S is the cost of the most parsimonious tree(s), S' is the cost of the most parsimonious tree lacking the clade in question, and G denotes the length of the least parsimonious tree, which is equal to the ratio of the observed GB to the maximum possible GB, or GB/GB_{max} (Grant and Kluge, 2007, 2010). To estimate G, in POY I set the cost of all transformations to -1 and performed timed driven search of each implied alignment.

All compute-intensive analyses were run on Ace, a high-performance computing cluster housed at the Museum of Zoology of the University of São Paulo composed of 12 quad-socket AMD Opteron 6376 16-core 2.3-GHz CPU, 16 MB cache, 6.4 GT/s compute nodes (= 768 cores total), 10 with 512 GB RAM DDR3 1600 MHz (32 × 16 GB) and two with 256 GB (16 × 16 GB), and QDR 4x InfiniBand (32 GB/s) networking.

Unambiguous synapomorphies common to all the most parsimonious trees were identified, plotted, and visualized using Mesquite v. 3.40 (Maddison and Maddison, 2016), YBYRÁ (Machado 2015), and TNT v.1.5 (Goloboff et al., 2008; Goloboff and Catalano, 2016). YBYRÁ generates color codes boxes categorizing the unambiguous synapomorphies as (1) unambiguously optimized, private (i.e., exclusive to the clade in question), and homoplastic, blue; (2) unambiguously optimized, non-private, and homoplastic, red; and (3) unambiguously optimized,

private, and present in all descendants, black (Machado 2015). I plotted key unambiguous synapomorphies only for selected clades of *Hyloxalus* and dendrobatoids. In the Results, the GB value reported in the analysis of the topological changes in the successive outgroup expansion correspond to the less value of the two adjacent nodes (up or down) to the interest node.

Terminology and Abbreviations

The taxonomy of Dendrobatoidea superfamily follows Grant et al. (2017), with the *Leucostethus* of Marin et al. (2018). Outside of Dendrobatoidea, I follows Frost (2021). In general, muscle terminology follows Ecker and Haslam (1889), Gaupp (1904), Noble (1922) and Duellman and Trueb (1994). Specifically, Dunlap (1960) for pelvic and hindlimb musculature, Burton (1980) for abdominal musculature, van Dijk (1959, also see 1955) and Anganoy-Criollo et al. (in press, Chapter 1) for extrinsic cloacal musculature, and Duellman and Trueb (1994) for arm musculature. A muscular slip is considered if a distinctive bundle fasciculus is separated from adjacent fasciculus of the same muscle by epimysium (Grant et al. 2006: 50). Terminology of the adult osteology follows Trueb (1993), and Duellman and Trueb (1994), and for sesamoids to Ponssa et al. (2010), and Abdala et al. (2019). For larvae, McDiarmid and Altig (1999) were used for external morphology, and Haas (1995, 1997) for chondrocranium and hyobranchial apparatus.

I examined material from the following collections: British Natural History Museum (BMNH), Colección Zoológica, Universidad de Nariño (PSO-CZ), Colección Zoológica, Universidad de Tolima (CZUT-A), Herpetology Division of the American Museum of Natural History (AMNH), Instituto de Ciencias Naturales, Universidad Nacional de Colombia (ICN), Instituto de Investigaciones de Recursos Biológicos Alexander von Humboldt (IAvH), Kansas University Natural History

Museum (KU), Museo de Ciencias Naturales de La Salle, Instituto Tecnológico Metropolitano (ITM, before Colegio San Jose de La Salle, CJS-H), Museo de Historia Natural, Universidad de los Andes (ANDES-A), Museu de Zoologia, Universidade de Sao Paulo (MZUSP), Museu Nacional de Rio de Janeiro (MNRJ), Museum für Naturkunde (ZMB), Museum of Comparative Zoology, Harvard University (MCZ-A), National Museum of Natural History, Smithsonian Institution (NMNH, ex-USNM), Sam Noble Oklahoma Museum of Natural History (OMNH), Zoological Research Museum Alexander Koenig (ZFMK), and Zoologische Staatssammlung München (ZSM). Uncatalogued specimens are identified with field series of Marvin Anganoy (MAA), Duvan Zambrano (DFZ), Pedro Henrique Dias (PD), and Taran Grant (TG).

RESULTS

Phenotypic Characters

First, the character of Grant et al. (2006, 2017) are commented, and second the characters proposed herein are enlisted and discussed. In the former case, when I found discrepancies in a particular character, these are annotated, re-formulated and/or discussed, otherwise those are enlisted only in Appendix 1.

The Characters of Grant et al. (2006, 2017)

Characters enumeration follows the numbering of Grant et al. (2017):

Character 1. Palmar skin: (0) taut; (1) loose.

Grant et al. (2017) defined this character and reported the derived state in *Ectopoglossus*, while the remaining dendrobatoids has the primitive condition. However, I also observed loose palmar skin in *Anomaloglosssus surinamensis* (KU220993, KU 220996. **Figure 1**) and the species of the *A. degranvillei* group (*A. blanci, A. degranvillei, A. dewynteri*; see Fouquet et al. 2018: Figure 2, 5, 7).

Character 3. Supernumerary tubercles on hand: (0) absent; (1) present.

Poison frogs lack supernumerary tubercles on the palm (see Grant et al. 2006, 2017; and data here). However, five species of the *Ameerega braccata* group (sensu Guillory et al. 2019; *A. flavopicta,* MZUSP 100112–16; *A. braccata,* MZUSP 100230–32; *A. berohoka,* MNRJ67262–63; *A. boehmei,* ZFMK 77442, 77444; and *A. munduruku,* see Neves et al. 2017: Fig. 2C) has these tubercles at the base of each finger (**Figure 2**). These are unconfirmed in two species of this group (*A. boliviana* and *Ameerega* sp. MatoGrosso1). Despite the little intraspecific variation observed in occurrence of this tubercles, the presence of supernumerary tubercles was overlooked by decades in poison frogs (e.g., see Savage 1968, Silverstone 1975, 1976, Haddad and Martins 1994: Fig., 1, 4). In change, others authors describes these, but they are unnoticed the finding. For example; Rodrigues and Myers (1993: 6, Fig. 4) stated there are "small tubercles discernible on hands of some specimens [of *A. macero*], as on proximal part of first finger between subarticular tubercle and inner metacarpal tubercle"; and Neves et al. (2007) refer it as "one intercalar tubercle on finger I (or II in my terminology) [in *A. munduruku*]". Conversely, Coloma (1995: 32) described these tubercles in *H. fuliginosus,* but the specimens reported by him lack of these. Moreover, Dubois et al. (2021: 138) reported as a diagnosis feature of the superfamily, but without offers data neither evidence to support this statement.

Character 6. Relative lengths of fingers II and III: (0) II << III (1.2 or more times longer); (1) II < III; (2) II = III; (3) II > III.

The length of the finger II is a historically very useful character in poison frog systematic (Silverstone 1975**,** Kaplan 1997, Grant et al. 2006). To detect differences, finger II is compared to the finger III either by pressing them against each other (i.e., appressing them), or by measuring the distance from the base of the palmar tubercle

to the tip of each finger (Grant et al. 2006: character 5, Grant et al. 2017: character 6). Grant et al. (2006) reported that the length of finger III is invariable, reaching the midlevel of the subarticular tubercle of finger IV, and consequently, they used it to delimit the variation in the finger II; however, I detected variation in finger III length (see below **character 190**), making it impossible to determine if variation in the relative length of finger II is due to variation in the length of finger II or finger III.

As such, instead of scoring variation in the length of finger II by comparing it to finger III, I compared it to finger IV (specifically, the distance from the base of the palmar tubercle to the tip of the finger), which appears to be constant. The comparison between fingers II and IV from 139 species of poison frogs, including 10 species used to evaluate intraspecific variation (see **Appendix 3**), show that the variation in a single species is large, and that the interspecific variation is continuous, where the finger II represents 57–86% of finger IV. Thus at moment, the available methods are not allow to delimit the character-states in the length of the finger II. Despite this, although the character 5 of Grant et al. (2006) is not tenable, variation in this finger in poison frogs is undeniable (e.g., the long finger II of *Ameerega trivittata* compared to the much shorter finger II of *Adelphobates quinquevittatus* or *Oophaga pumilio*). Alternative methods or tools that allow to evaluate directly the variation in the phalangeal and metacarpal bones could be helps to defined the multiple characters and character-states involved in each finger (Grant et al. 2006).

Character 81. Vocal sac occurrence: (0) absent; (1) present.

The vocal sac is a composite structure of the three anatomical distinct components, the internal lining or mucosa, the superficial submandibular musculature, and the gular skin. The air passage to the vocal sac is by mean the vocal slits, that are small, elongated apertures, situated on either side of the tongue, that

communicate the vocal sac with the buccal cavity (Noble 1931, Tyler 1971, Elias-Costa et al. 2017, and Targino et al. 2019). Grant et al. (2017) coded the occurrence of the vocal sac in adult males following Liu (1935). In dendrobatoids the occurrence of the vocal sac is linked with the gular skin modification which is often detectable externally, and more precisely by the presence of vocal slits in adult males.

Most adult males of the Dendrobatoidea have open vocal slits; however, Lynch (1982) reported the absence of the vocal slits in *Hyloxalus edwardsi* and *H ruizi*, which he used as evidence to group them as sister species; moreover, gular skin in the adult males of both species is unmodified. Myers (1982: 5) reported polymorphism in a species of the *Ranitomeya* (as *Dendrobates quinquevittatus*, but see Caldwell and Myer 1990) from Mishana, Río Nanay, Perú. Myers (1982) also reported the absence of vocal slits in adult males of *R. reticulata*, although Grant et al. (2006: 246, appendix 7) employing the same specimens of *R. reticulata* (AMNH 103619–30, 103638–73) coded them as present. Grant and Castro (1998) also reported intraspecific variation among adult males of the *Colostethus fraterdanieli* complex, whereby some adult males lack open vocal slits. Another particular case is *Ameerega berohoka*, for which Vaz-Silva and Maciel (2011) stated that the vocal slits are absent in the adult male holotype but did not clarify the condition of other males; however, the presence of gular skin modification is evident in the photos of the holotype (MNRJ 67263) in my possession, suggesting that the vocal sac (and vocal slits) are present.

Character 85. Median lingual process (MLP): (0) absent; (1) present.

Among dendrobatoids, the genera *Anomaloglossus* (Aromobatidae) and *Ectopoglossus* (Dendrobatidae) are the only ones to possess the MLP. Nonetheless, revision of five paratopotypes of the *Paruwrobates andinus*, deposited at the

Colección Zoologica, Universidad de Nariño, Colombia (PSO-CZ), revealed the presence of a short MLP in three specimens (PSO-CZ 623, 625, 627), although this is retracted in other three specimens, including one paratype (PSO-CZ 624, 626, KU 212533), and only the PSO-CZ 624 has an evident pit (**Figure 3**). Previous studies with this species, do not reported the MLP presence in this species (see Myers and Burrowes 1987, Grant et al. 2017).

New Characters.

Character enumeration is the proposed in this study (see Appendix 1)

A) Adult external morphology.

Ventral body skin.—The ventral and anteroventral skin is smooth in most poison frog, although some shagreen or faintly granulated texture is observed at high magnification (Grant et al. 2006). Moreover, it is undeniable that preservation affects ventral skin structure so that inadequately preserved individuals can exhibit slight granulation when the species has smooth ventral skin, or in the opposite case, the granules or warts are lost. Nevertheless, well-preserved specimens of some *Hyloxalus* has rounded flat granules, close to each other (granular skin) or separate, low tubercles (warty skin) in this region. When present, granules or warts cover the ventral skin from the chin or chest to the posterior abdomen (**Figure 4A, 4B**), and extends to the ventrolateral flank of the body from the arm insertion to the groin. However, in some species these are restricted to the ventrolateral flanks of the body, while the ventral abdominal region is smooth (**Figure 4C**). This provide support to the independence of these regions and characters.

Early in the last century, Boulenger (1919) described the ventral skin of *Hylixalus granuliventris* (now under the synonymy of *Rheobates palmatus*) as “throat and belly strongly granulate”. In *Hyloxalus*, Rivero (2000 “1995”) described a

granular ventrolateral flank in *H. excisus*, and I confirmed this condition. Moreover, *Andinobates bombetes* (Myers and Daly 1980), *A. tolimensis* (Bernal et al. 2007), *Oophaga granulifera* (Silverstone 1975), and *Ranitomeya sirensis* (Aichinger 1991) also possess a granular ventral skin.

Character 170 (**Figure 4**): Ventral body skin, structure: (0) smooth, (1) granular, (2) warty.

Character 171 (**Figure 4**): Ventrolateral body skin, structure: (0) smooth, (1) granular, (2) warty.

Sexual dimorphism was observed in *Hyloxalus craspedoceps*, so the ventrolateral flanks are granular in adult males and smooth in adult females.

Middle ear.—The anuran tympanic middle ear is composed of a tympanic membrane (TM), tympanic annulus (TA), middle ear cavity (*cavum tympanicum*), and middle ear bone (columella, stapes, plectrum; Wever 1985, Pereyra et al. 2016). The tympanic membrane is a disc of modified thin, often translucent, non-glandular skin that is tightly bound to the outer edge of the TA, a cartilaginous funnel that forms the middle ear cavity (Wever 1985: 43, Pereyra et al., 2016:2). In Dendrobatoidea, only the anteroventral portion of the middle ear is visible externally, because the *m. depressor mandibulae* covers its posterodorsal portion (Myers and Daly 1979: 8, Myers and Ford 1986, Myers et al. 1991, Grant et al. 2006).

In the taxonomy of poison frogs, the term “tympanum” has been used to refer to either the external visibility of the tympanic membrane, the tympanic annulus, or both of them. Moreover, in some species, the term “indistinct or inconspicuous tympanum” is used to describe the absence of the TM and/or TA ambiguously (e.g., Martins 1989, Fouquet et al. 2018); nevertheless, in a few descriptions, the presence of TM or TA is specified (e.g., Lima et al. 2009). In systematic studies, these terms

produce confusion more than a precise description of the occurrence of the tympanic middle ear structures. Therefore, the use of these terms is not recommended (Lynch and Duellman 1997: 28).

In the literature of this anuran group, the skin that covers the middle ear structures is called the TM, while the raised ring of skin around the edge of the tympanum is used as evidence of the occurrence of a TA (**Figure 5A, 5C**). Gross dissections of the dendrobatoid tympanic middle ear reveal that the skin is commonly adhered to a translucent or semi-translucent connective tissue disc bound to the TA covering the auditory cavity; skin is also bound to the TA. However, in a few species the skin is free, loose of the connective tissue disc and TA (e.g., *Anomaloglossus surinamensis, Allobates wayuu*), or sometimes this is tightly adhered to both structures (e.g., *Dendrobates leucomelas* and *D. tinctorius*). In addition, the thickness of the skin on the tympanic middle ear varies, being somewhat thin but not translucent, or in the extreme case it is thin when skin is tightly adhered. In both case, the TA is visible externally. Contrarily, when the skin in loose, this is thick (i.e., thickness as same as surrounding skin areas), and the TA is not detectable externally. The connective tissue disc, like the TA, is present in all examined dendrobatoids. In consequence, the middle ear cavity of poison frogs is covered by both structures, the skin—by definition considered as TM, and by the connective tissue disc, of unknown origin (homology), that directly covers the *cavum tympanicum* (**Figure 5E**), here considered as an internal TM.

Comparisons of the tympanic middle ear between dendrobatoids with bufonids (*Rhinella ornata* uncatalogued specimen; *Osornophryne bufoniformis* PSO-CZ 2496, *Rhinella paraguas* UV-CD 1503), and hyloids (*Hylodes phyllodes*, uncatalogued specimen) reveal clear differences. First, the TM and TA in the

examined bufonids and hylodids matching the standard definition, i.e., TM is very thin, translucent, apparently non-glandular skin, continuous with the adjacent skin, tightly bound to the TA. Second, there is no indication of an internal TM (disc of connective tissue) underlying the TM in bufonids and hylodids (**Figure 5D, 5F**). And third, in Dendrobatoidea the contact between the skin with the TA and the internal TM is intruded by the *m. depressor mandibulae* on the posterodorsal portion, separating in different grades these structures. Moreover, skin of poison frogs no reaching the fineness of the TM of bufonids and hylodids, and in some cases, this appear be glandular (e.g., *Allobates talamancae*; **Figure 5A**). These differences entail question about correspondence of the dendrobatoid internal and external TM regards the TM of other frogs. Traditionally, the TM have been considered as very modified skin (Wever 1985, Pereyra et al. 2016), and it is not the case in poison frogs, and on the other hand, the internal TM of the dendrobatoids appear be similar to the TM, but I have not evidence to confirm this similarity. Given this ambiguities, with the evidence at hand, it difficult to determine with certainty the transformation series involves in the tympanic middle ear structures; although, undeniable the internal TM of poison frogs is absent in other frogs examined here.

Functionally, the TM transmit the sound to the middle ear cavity (Mason 2007). However, in poison frogs there are two structures, the internal and external TM, involved in the transmission of the acoustic signal; nevertheless, the external TM is separate posterodorsally from the tympanic middle ear by the *m. depressor mandibulae* without entire adhesion to the TA, and without properly seal of the all cavity, which would impede in some degree the sound transmission; in change, the internal TM cover and seal entirely the middle ear cavity, acting as a membrane

fulfilling the role of the TM. Additional experiments are required to confirm the role the dendrobatoid internal and external TM.

Given the ambiguities exposed above, here I propose a transformation series for the occurrence of the internal TM, although it is possible propound other characters, such as the presence of the TM, the available evidence is not sufficient to distinguish between alternative hypothesis homology. Additionally, I propose a character for the variation of the skin adhesion to the tympanic middle ear.

Character 172 (**Figure 5**): Internal tympanic membrane, occurrence: (0) present, (1) absent.

A internal tympanic membrane is found in poison frogs. Hylodids and bufonids examined here, lack of this.

Character 173 (**Figure 5**): Skin on the tympanic middle ear: (0) adhered, (1) loose.

In poison frogs, the skin that covers the tympanic middle ear is adhered or tightly adhered to connective tissue disc and to the TA (state 0); however, in few species (e.g., *Anomaloglossus stepheni, A. surinamensis*, and *Allobates wayuu.* **Figure 5B**) this skin is loose, free of the internal structures (1).

In the literature of this superfamily, *Anomaloglossus beebei, A. stepheni*, and the species of the *A. degranvillei* group were reported with an indistinct or inconspicuous tympanum (Martins 1989, Kok and Kalamandeen 2008, Fouquet et al. 2018). Likewise, on the basis of the study of Savage (2002) and Kok and Kalamandeen (2008), Pereyra et al. (2016: supplementary information) scored the absence of the TM in *Allobates talamancae*, *Anomaloglossus kaiei*, *Oophaga pumilio*, respectively. However, I examined specimens of the *A. talamancae* (PD 49) and *O. pumilio* (PD 50), and the skin is attached to the connective tissue disc and to the TA,

which are detectable externally (contra Pereyra et al. 2016). Available figures of *A. kaiei* in Kok et al. (2006a: Figure 4, 5), *A. beebei* in Kok and Kalamandeen (2008: 72, Figures 43, 83a) and *A. stepheni* in Fouquet et al. (2019: Figure 2) show the TA, for which here is inferred as state 0; nevertheless, the well-preserved specimens of *A. stepheni* (MZUSP 69178, 70477), examined in this study, has a loose skin. Variation found in this species could be explained by the complex species under this name (Vacher et al., 2017). Specimens of Fouquet et al. (2018) are from eastern end of the distribution of the species (Voltzberg, Suriname), while the MZUSP are from southwestern distribution (Amazonas and Pará, Brazil). Specimens of the *A. degranvillei* group were not available to corroborate the occurrences of these structures, therefore I report the condition follows Fouquet et al. (2018).

Subarticular tubercles of the fingers.—Subarticular tubercles are specialized adhesive epithelial structures, located beneath each digital articulation, with variable shape and protuberance degree (Noble and Jaeckle 1928, Barnes et al. 2013, Anganoy-Criollo et al. in prep). In Dendrobatoidea, the subarticular tubercles formulae of the fingers is commonly 1-1-2-2. However, Grant and Rodriguez (2001) reported variation in the presence of the distal subarticular tubercle of finger V, and consequently, this was formulated as a character in Grant et al. (2006: character 3, 2017: character 4). Recently, Anganoy-Criollo et al. (in press. Figure 3) documented an additional distal subarticular tubercle on each finger of the species of *Hyloxalus edwardsi* group, the presence of the distal subarticular tubercle in finger II and III, and the hyperdistal subarticular tubercle in finger IV and V (formulae: 2-2-3-3). These authors also noted the existence of hyperdistal subarticular tubercle in *Ectopoglossus ithsminus* and *Aromobates nocturnus*. Furthermore, the distal subarticular tubercle of finger IV is absent in *E. absconditus* and *E. saxatilis* (see

Grant et al. 2017: S16, S20, Figure 13A), which shows that there are losses in other fingers in addition to the finger V.

Character 4 of Grant et al. (2017) was reformulated and additional transformational series were added to reflect observed variation in each finger. There is a proximal–distal dependence in the occurrence of the subarticular tubercles, whereby the proximal subarticular tubercle always is present when there is a distal subarticular tubercle, leading me to treat the characters for fingers IV and V as additive (see also Fabrezi and Alberch 1996).

I scored the occurrence of the distal subarticular tubercle of finger V in *Andinobates bombetes* and *Ranitomeya sirensis* as polymorphic because Myers and Daly (1980:5) and Aichinger (1991: 2) mentioned the absence of this tubercle, while this character was coded as present in Grant et al. (2006). This tubercle also is absent in *Andinobates abditus* (Myers and Daly 1976: 4).

Character 174: Distal subarticular tubercle on finger II, occurrence: (0) absent, (1) present.

Character 175: Distal subarticular tubercle on finger III, occurrence: (0) absent, (1) present.

Character 176: Subarticular tubercles on finger IV: (0) basal, (1) basal+distal, (2) basal+distal+hyperdistal. Additive.

Character 177: Subarticular tubercles on finger V: basal (0); basal+distal (1); basal+distal+hyperdistal (2). Additive.

Shape of the subarticular tubercles of the finger.—In poison frogs, there are some studies about the variation of the subarticular tubercles (Myers and Daly 1979, Caldwell and Myers 1990, Grant and Rodrigues 1998, Duellman 2004). Variation in occurrence was proposed as characters by Grant et al. (2006: character 3

and 26), while the other features of the subarticular tubercles have not been evaluated. Like other dermal structures, preservation affects subarticular tubercles, making the character coding somewhat difficult. But a revision of hand tubercles in well-preserved specimens shows significant variation in shape at its base (in palmar view) and in the degree of protrusion (in profile) that are not discussed in the literature of this group.

In profile, subarticular tubercles are low, flat, or slightly rounded (flattened tubercle. **Figure 6A**), or these are enlarged, conical, rounded tubercles that protrude distally (projected tubercle. **Figure 2**); notwithstanding, the protrusiveness is not uniform in all tubercles of the digit. Thus, in the finger IV and V, the proximal subarticular tubercle is projected, while the distal subarticular tubercle is flat and low, although this does not occur in the opposite way. And rarely, the proximal subarticular tubercle is projected on finger II–III and flattened on the finger IV–V. This variation support to code each tubercle as independent character: moreover, character state distribution does not reveal otherwise.

Initial inspection in alizarin red-stained *manus* bones in *Hyloxalus arliensis* and *A. flavopicta*, which have projected subarticular tubercles, revealed the presence of a sesamoid between the metacarpal and proximal phalanx of fingers II–IV (in *H. arliensis*) or fingers II–V (in *A. flavopicta*), and between the medial phalangeal articulations of finger IV in *H. arliensis* and fingers IV and V in *A. flavopincta*, just below of the basal and proximal subarticular tubercles, respectively. Furthermore, in *H. arliensis* there is a ventral bone projection arise from ventrodistal end of the metacarpals and from ventrodistal end of the medial phalanges of finger IV and V. One or both of these bone structures are observable in micro-CT reconstructions in species with projected subarticular tubercle of the aromobatids genus *Allobates* and

Anomaloglossus, and dendrobatids genus *Ameerega*, *Epipedobates*, and *Hyloxalus*; however, sometimes is difficult elucidated between sesamoid or bone projection in micro-CT reconstructions, due it is necessary to increase the density in the software to detect these bones, which generating an apparent single a continuous structure. Contrastingly, there are no indication of any of these bone structures in micro-CT reconstruction in the species with flattened subarticular tubercles (**Figure 7**, **Table 6**). Despite of the apparent correlation between projected subarticular tubercles and presence of the sesamoid or the bone projection or vice versa, some species with flattened tubercles has bone projection (e.g., *H. nexipus, H. vergeli*), which indicate these bones are not always the cause of the tubercle projection (**Table 6).** I am aware that there is more than one independent character here, but at this time, I do not have sufficient data of these bone structures to elucidate their homology, character and distribution, and advocate to used tubercle protrusiveness as character, and as a way to hypothesized the occurrence sesamoids or projections, with pendent corroboration.

Previously, Myers and Daly (1979: 4, Figure 4) used the protrusiveness of subarticular tubercles of the foot to diagnosis *Ameerega silverstonei* from *Phyllobates bicolor* (see below). And Duellman (2004: 10–11) described variation in the shape and protuberance of the subarticular tubercles of the fingers in Peruvian *Hyloxalus.* I examined most of the species reported by him and noted some disparities. For example, I coded flattened tubercles on the hand of *H. mittermeieri*, while it was stated as distinctive and subconical tubercles by Duellman.

In general, in palmar (ventral) view, all tubercles appear to be circular or rounded at the base, with some variation to the point of having ovoid tubercles. However, the basal subarticular tubercle of finger II and III can have a notably

elongated shape at the base (length > 1.5 times width. **Figure 6B, 6C**). As such, I propose the following characters:

Character 178: Basal subarticular tubercle of finger II, protrusiveness: (0) flattened, (1) projected. Compare **Figure 6A** and **Figure 2**.

Character 179: Basal subarticular tubercle of finger III, protrusiveness: (0) flattened, (1) projected.

Character 180: Basal subarticular tubercle of finger IV, protrusiveness: (0) flattened, (1) projected.

Character 181: Basal subarticular tubercle of finger V, protrusiveness: (0) flattened, (1) projected.

Character 182: Distal subarticular tubercle of finger IV, protrusiveness: (0) flattened, (1) projected.

Character 183: Distal subarticular tubercle of finger V, protrusiveness: (0) flattened, (1) projected.

Character 185 (**Figure 6 B, 6C**): Basal subarticular tubercle of finger II, shape: (0) rounded, (1) elongated.

Character 186 (**Figure 6 B, 6C**): Basal subarticular tubercle of finger III, shape: (0) rounded, (1) elongated

State 0 includes the rounded to slightly ovoid tubercles and only is considered an elongated tubercle when its length is 1.5 times larger than its width (state 1).

Relative width of basal subarticular tubercle of fingers II and III.—In ventral view, the basal subarticular tubercle width varies in poison frogs. In most species, the basal subarticular tuberclea are narrow than the corresponding fingers (i.e., their width does not reach or surpass the width of the finger; state 0, **Figure 8A, 8D**). In others, the width of the basal subarticular tubercle of finger II and/or III

surpasses that of finger, and the lateral margins of the fingers are interrupted by the tubercle circumference (state 1, **Figure 8B**). Independence in the basal subarticular tubercle of finger II from III is based on the character distribution and variation between fingers.

Character 186 (**Figure 8A, 8B**): Relative width of the basal subarticular tubercle of finger II: (0) lesser or equal than its finger, (1) wider than its finger.

Character 187 (**Figure 8A, 8B**): Relative width of the basal subarticular tubercle of finger III: (0) lesser or equal than its finger, (1) wider than its finger.

Thenar tubercle size.—The systematic value of the thenar tubercle has been previously discussed in dendrobatoids (see Silverstone 1975, Caldwell and Myers 1996, Grant et al. 2006). Grant et al. (2006) proposed character 26 (or character 27 in Grant et al. 2017) for the occurrence and the degree of variation of the thenar tubercle protuberance. I agree with Grant et al. (2006: 69), and likewise, the preservation artifacts (as was mentioned above), difficult the distinction between the absence and a conspicuous thenar tubercle. In addition, I detected variation in the size of the thenar tubercle in palmar view, and as a way to reflect this variation, the thenar tubercle size was compared to the basal subarticular tubercle of finger II (the times that this tubercle fills in the basal subarticular tubercle), because the size variation in this last tubercle is negligible.

It is important to note that the size in the character of Grant et al. (2006) refer to the thenar tubercle size in profile, unlike the size in ventral view. Also, the distribution in the variation of the size shows independence between profile and palmar view. For example, the large conspicuous and well-defined thenar tubercle of *Mannophryne cordillerana, Hyloxalus delatorreae*, and *H. vergeli* is small in ventral

view (it is half than basal subarticular tubercle), justifying the independence between Grant et al's (2006) character and the variation observed here.

Character 188 (**Figure 8A, 8C, 8D**): Relation between thenar tubercle and the basal subarticular tubercle of finger II: smaller (0), equal (1), or larger (2) than the basal subarticular tubercle.

To avoid ambiguities, a small thenar tubercle (state 0) is considered when it is a lesser or equal than half basal subarticular tubercle. A large tubercle (state 2) is equal or larger than 1.5 times the basal subarticular tubercle. When this is larger than half to lesser than 1.5 times the basal subarticular tubercle, thenar is considered as equal (state 1).

Thenar tubercle shape.—At the base, the thenar tubercle is ovoid in most poison frogs, though an elongated tubercle also is observed in this anuran group. Character distribution in poison frogs shows independence between the size and shape of the thenar tubercle. The elongated tubercle condition is defined as in character 186 (see above).

Character 189 (**Figure 8A, 8D**): Thenar tubercle, shape: (0) rounded, (1) elongated.

Finger III and V length.—The finger III length varies and does not always reaches the distal half of the distal subarticular tubercle of the finger IV (in contra of Grant et al. 2006: 64), and this variation implies effects in codification and homology of the finger II length, for this reason the character 6 of Grant et al. (2017) was rejected. In case of the finger V, length variation was evaluated regard to the distal subarticular tubercle of the finger IV by Grant et al. (2006: character 4); nevertheless, in *Hyloxalus* there are additional variation within the state 0 and 2 of this character, no reported previously (see below, Character 210).

The differences in both finger length is delimited when these are comparing with finger IV and its subarticular tubercles. Variation in the finger IV is so minimal and apparently constant in poison frog superfamily; moreover, finger III and IV variation is not product of the finger IV changes, because in this case would be expected a covariation in the finger III and IV length, but this does not occur, and variation in each finger is independent. For example, in *Hyloxalus anthracinus* and *H. craspedoceps*, the finger III no reaching the distal subarticular tubercle of finger IV, whilst its finger V surpassing or reaching the distal subarticular tubercle, respectively. Then, to delimited and qualify the relative length variation in finger III and V, this is coded in the same way as Grant et al. (2006), that is, the finger III and V length are pressed against the finger IV and compared to its subarticular tubercles.

Character 190 (**Figure 9A, 9B**): Finger III length: (0) not reaching the distal subarticular tubercle of finger IV, (1) reaching the distal subarticular tubercle of finger IV.

In the state 0, the disc of finger III does not reaches the distal subarticular tubercle of the finger IV. In state 1, the disc of the finger III reaches the half or is at the level of the distal subarticular tubercle of finger IV.

Character 191 (**Figure 9B–9F**): Finger V length: (0) barely surpassing the basal subarticular tubercle of finger IV, (1) extending to just before of the distal subarticular tubercle of finger IV, (2) reaching or at same level than distal subarticular tubercle of finger IV, (3) surpassing the distal subarticular tubercle of finger IV, (4) reaching the hyperdistal subarticular tubercle or the disc of finger IV.

The character 4 of Grant et al. (2006) is redefined to include the variation found in *H. breviquartus* and the species of the *H. edwardsi* group. *H. breviquartus* was described by Rivero and Serna (1986) from Urrao, Antioquia, Colombia and its

specific epithet is due to the shorter finger V. A specimen in the ICN amphibian collection matches with this species, and its finger V does not reach the distal subarticular tubercle (state 2 of Grant et al. 2006). However, when this is compared to other species with this "same" condition (e.g., *A. olfersoides*, *A. insperatus*), finger V barely surpasses the basal subarticular tubercle and does not extend further (state 0, here). In contrast, in *H. breviquartus*, finger V surpasses the basal subarticular tubercle and extends to just before the distal subarticular tubercle (state 1). State 2 is equivalent to state 1 of Grant et al. (2006: character 4). In the species with finger V surpassing the distal subarticular tubercle of finger IV, it barely surpasses the basal subarticular tubercle without extending beyond (state 3), but in the species of *Hyloxalus edwardsi* group (*H. edwardsi*, *H. jhoncito*, *H. ruizi*), the finger V extends well beyond, to reaches the hyperdistal subarticular tubercle or the disc base of finger IV (state 4).

Metacarpal ridge/fold.—Grant et al. (2006, character 19) defined and discussed the metacarpal ridge/fold in dendrobatoids and mixed occurrence and morphology in their transformational series. This was redefined by Grant et al. (2017, character 20) to evaluate the occurrence only. Considerations of Grant et al. (2006) to coding this character are pertinent and are followed here (e.g., gross inspection in various individuals, several transversal incisions). Reevaluation of this character in *Hyloxalus* and other dendrobatoids show the difficulty to distinguish between fold and ridge and allows to confirm the presence of metacarpal ridge/fold in species that it was coded as absent (e.g., *Hyloxalus bocagei*, *H. pulchellus*, *H. sauli*, *H. subpunctatus* and *H. toachi*). Moreover, unexpected differences in the metacarpal ridge/fold in *Hyloxalus* and relatives were found.

In most species, the metacarpal ridge/fold is continuous with the postaxial fringe of the finger V, and extends proximad by the outer edge of the palm towards the palmar tubercle, ending at proximal two-third of the palm without contact with palmar tubercle; however, in a few species this ending at one-half of the palm. Conversely in other species, this is in contact with the palmar tubercle. Distally also there is variation, so this ridge/fold is not continuum with the postaxial fringe of the finger V, forming a separated, elongated ridge/fold. In addition, in *Hyloxalus toachi* and some *Ameerega*, this is reduced to a tubercle-like, near to the palmar tubercle, without ridge/fold. As part of this variation, sometimes the ridge/fold ending proximally as a slight and low protuberance, and when there is a tubercle-like, ridge traces extending to the basal subarticular tubercle are discernible. Beside of the occurrence character of Grant et al. (2017, character 20), morphology, and distal/proximal extension variation is proposed as character.

Character 192 (**Figure 10A, 10E–F)**: Metacarpal ridge/fold, morphology: (0) ridge/fold, (1) tubercle-like.

Character 193 (**Figure 10A, 10D**): Metacarpal ridge/fold, distal extension: (0) continuous with postaxial fringe of finger V, (1) non-continuous with postaxial fringe of finger V.

Character 194 (**Figure 10A–10D**): Metacarpal ridge/fold, proximal extension: (0) reaching one-half of palm, (1) reaching two-third of palm, (2) in contact with the palmar tubercle.

Swelling on the fingers.—Grant et al. (2006) highlighted the relevance and evolution of the swelling on the finger IV in the dendrobatoids systematics; moreover, they characterized the different swelling types in this anuran group, and proposed two characters, the occurrence and the morphology of the swelling finger IV. Also, they

claim that in most cases, the swelling is weak and can be undetectable (p. 67–68). For this reason, it is necessary to compare fingers of both sexes, as done Myers et al. (1998: Figure 4; **Figure 11D**). For a detailed revision of the systematic history, evolution, and relevant aspects of swelling finger IV see Grant et al. (2006: 67–68; 2017: S66; and Cavalcanti et al. 2021).

While in Dendrobatoidea, the finger IV swelling is widespread (see Grant et al. 2017), in *Hyloxalus* (and also in Hyloxalinae), the occurrence have been reported for three species only, *H. cepedai* (Morales 2002 "2000"), *H. jacobuspetersi* (Grant et al. 2017), and *H. picachos* (Ardila-Robayo et al. 2000); however, Cavalcanti et al. (2021) also reported metacarpal swelling of finger IV in *H. anthracinus* and *H. nexipus*. Recently, Cavalcanti et al. (2021) reviewed the swelling at the hand, and they found glandular integument, with specialized mucous, dimorphic sexually, distributed on the phalanges and the metacarpal of each finger in poison frogs; moreover, they redefined the characters of the external morphology. Thus in this study, I follows the characters of the external morphology of Cavalcanti et al. (2021).

Character 195: Phalangeal swelling on finger II of adult males, occurrence: (0) absent, (1) present.

I observed phalangeal swelling of finger II exclusively in *Hyloxalus jacobuspetersi*. In addition, Cavalcanti et al. (2021) reported the presence of the specialized mucous gland on finger II for this species. Character 6 of Cavalcanti et al. (2021).

Character 196 (**Figure 11A**): Phalangeal swelling on finger III in adult males, occurrence: (0) absent, (1) present.

Adult males of the *Hyloxalus walesi* (see below for justification of specific status), and *H. jacobuspetersi* have phalangeal swelling on finger III. Character 7 in Cavalcanti et al. (2021).

Character 197 (**Figure 11A, 11F**): Phalangeal swelling on finger IV in adult males, occurrence: (0) absent, (1) present.

Character 20 and 21 of Grant et al. (2006, 2017), respectively. Character 1 of Cavalcanti et al. (2021).

Character 198: Phalangeal swelling on finger IV of adult males, expansion: (0) dorsal and preaxial, (1) dorsal, preaxial, and postaxial.

Definition is found in Cavalcanti et al. (2021: character 2. See Grant et al. 2006: Figure 28).

Character 199: Preaxial phalangeal swelling on finger IV of adult males, degree: (0) weak, (1) strong.

Character 21 and 22 of Grant et al. (2006, 2017). Character 3 of Cavalcanti et al. (2021).

Character 200 (**Figure 11B, 11C, 11E**): Basal swelling on finger IV of adult males, occurrence: (0) absent, (1) present.

Basal swelling is a glandular dilatation on both sides of the finger IV base, extending from the proximal end of the basal subarticular tubercle to the proximal terminus of finger IV (or the metacarpal portion of the finger, visible externally). Comparison between adult males and females or histological evidence is necessary to detect it. Character 4 of Cavalcanti et al. (2021).

Character 201 (**Figure 11E**): Metacarpal swelling in adult males, occurrence: (0) absent, (1) present.

The metacarpal swelling is onto wrist skin between the metacarpal bones of the finger II–IV (e.g., *H. anthracinus*). Character 5 of Cavalcanti et al. (2021).

Character 202: Phalangeal swelling on finger V of adult males, occurrence: (0) absent, (1) present.

Present in adult males of *H. walesi* and in *H. jacobuspetersi*. Character 8 of Cavalcanti et al. (2021).

Ulnar tubercles.—Ulnar tubercles are dermal elevations, occurring as a row along the outer ventrolateral edge of the ulna (Duellman and Lerh 2009). These are common in other neotropical frogs (e.g., *Pristimantis*, Lynch and Duellman 1997), and vary from low to enlarged with rounded to acuminated tip. The most proximal tubercle to the wrist is known as the antebrachial tubercle.

Ulnar tubercles have not been reported previously in dendrobatoids. However, a revision of the forearm of the dendrobatoids shows the presence of the ulnar tubercles. When ulnar tubercles occur, there is a row of three to four low, rounded tubercles (e.g., *H. aeruginosus*); nevertheless, most species only exhibit the antebrachial tubercle, and there are not other proximal tubercles (**Figure 12**). In many cases, on the outer edge of the ulna, there is a row of two or three pale spots (e.g., *H. elachyhistus*), but gross dissection of these structures shows no dermal modification. In concordance with variation recorded, an occurrence and structure characters are proposed.

Character 203 (**Figure 12**): Ulnar tubercles, occurrence: (0) absent, (1) present.

Character 204 (**Figure 12**): Ulnar tubercles, structure: one tubercle, antebrachial, (1) row of tubercles.

Swelling on the distal end of the upper arm and lower arm.—Grant and Castro (1998; and also see Grant and Ardila 2002, Grant et al. 2006, 2017) described the "black arm gland" (as black arm band) as a black swelling of the skin, apparently glandular tissue, on the ventral surface at the distal end of the upper arm, sometimes extends distally to the inner surfaces of the lower arm in the adult males. Despite intra-population variation in protrusiveness and coloration was well-known; recently, Acosta-Galvis et al. (2020) restricted the name to "arm gland" to include species with pale (in references to the dull white color in *Hyloxalus arliensis*) and dark/black arm gland; however, examination of the extensive material of the species with pale condition show a dark gray or black swelling also. The character was proposed as synapomorphy for the *H. ramosi* group, that included nine species of *Hyloxalus* (Grant and Castro 1998, Grant et al. 2006, 2017); however, the homology of the black arm gland was rejected by Grant et al. (2017) because four species of this group, used in this study (*H. anthracinus*, *H. arliensis*, *H. lehmanni*, and *H. nexipus*), were not closely related.

I evaluated histologically the distal end of the upper arm and the proximal end of the lower arm in order to explore the glandular nature of this structure (see Chapter 3). Main results in the integument of the adult males with swelling of some species of the non-natural *H. ramosi* group show clusters of largest, mucous and serous glands, in comparison with adult females of the same species, who have scattered ordinary mucous and serous glands. These cluster of largest glands, sexually dimorphic, also are present in one species with not evident external swelling; contrary, other species with external swelling lack these glands, and in this case, these are ordinary glands, like adult females. Moreover, species with external swelling has accumulation of melanophores in the dermis, which covers all large glands, except one species who

have large glands almost free or with scarce melanophores quantity. The *tela subcutanea* also is modified in adult males with external swelling, with an enlarged space, where there are melanophores deposits, but this enlarged space is absence even in species with or without external swelling. On the basis of the histological complexity of the "black arm gland", I opt to call it as *swelling of the distal upper arm and proximal lower arm,* because the external swelling always is not glandular and there is white skin due to the scarce melanophores quantity (not in the same way of Acosta-Galvis et al. 2020). I propose the following characters to encompass the external variation of this structure. The histological results and the integumentary characters are formulated and discussed in the Chapter 3.

Character 205 (**Figure 13**): External swelling at the distal upper arm and the proximal lower arm of the adult males, occurrence: (0) absent, (1) present.

In addition to the species reported with swelling previously, I report the presence in *Hyloxalus craspedoceps* and *H. pinguis*.

Character 206 (**Figure 13**): Distal swelling of the upper arm and the proximal lower arm of the adult males, extension: (0) restricted to the distal end of the upper arm, (1) also extending to the proximal lower arm.

To code this character it is necessary to observe several adult males per species. My data come from multiple adult males of *H. anthracinus, H. arliensis, H. lehmanni, H. nexipus, H. pinguis*, and one undescribed species *Hyloxalus* sp. *fascianigrus*-like; moreover, also histological confirmation. In state 0, the swelling is restricted to the distal end of the upper arm without extension to the lower arm; while in state 1, the swelling is either on the upper arm, and extends to the proximal lower arm.

Basal subarticular tubercle on toe IV.—Poison frogs have one tubercle on toes I and II, two on toes III and V, and three on toe IV, but two species of the *Hyloxalus edwardsi* group (*H. edwardsi* and *H. ruizi*) lack the basal subarticular tubercle in toe IV (see Anganoy-Criollo et al. in press). As far as I know, no previous report was done about the absence of this tubercle in poison frogs, except for *Allobates caeruleodactylus* (Lima and Caldwell 2001: 185) and *Ectopoglossus saxatilis* (see Grant et al. 2017: S21, Figure B).

Character 207 (Figure 14A–B. 226): Basal subarticular tubercle of toe IV, occurrence: (0) absent, (1) present.

Character 208 (**Figure 14A, 14C. 227**): Relation between basal and proximal subarticular tubercle of toe IV, size: (0) small (≤1/2), (1) slightly lesser or equal (>3/4).

There are species with a small basal subarticular tubercle on the toe IV (in plantar view), this is lesser than or equal to the half of the proximal subarticular tubercle (state 0); otherwise, this tubercle is slightly lesser or about equal than proximal subarticular tubercle (state 1).

Protrusiveness of the subarticular tubercles of the toes.—Myers and Daly (1979: Fig. 4) noted that *Ameerega silverstonei* has prominent subarticular tubercles, and they used it to distinguish from the low, non-protuberant subarticular tubercles of the *Phyllobates bicolor*. Despite of this, variation in protrusiveness has been overlooked in poison frogs. In other neotropical anurans groups, such as *Pristimantis*, the protuberance degree in the subarticular tubercles of the hand and foot were considering as systematic character (Ospina-Sarria and Angarita-Sierra 2020, also see Lynch 1998, Ospina-Sarria and Duellman 2019).

In profile, the subarticular tubercles on toes of the poison frogs are flattened or projected (**Figure 15**), and commonly, there is not variation in protrusiveness between tubercles of each toe (although see preservation artifacts above); in change, in a few dendrobatoids genera, the tubercle protuberance varies between subarticular tubercles and between the toes, being the basal subarticular tubercles projected and the proximal and/or distal tubercles flattened, or projected on the first to third toe, and flattened on the fourth and fifth toe. This provide evidence to the independence of each tubercle, which is supported also by the character state distribution. On the other hand, the subarticular tubercles base shape is rounded or ovoid from plantar view, and only the basal subarticular tubercle of the toe II–IV show an elongated shape (i.e., its length is 1.5 times larger than its width). Like the subarticular tubercles of hand (see above), I coded separately the protuberance degree of each subarticular tubercle of toe and the shape of the basal subarticular tubercle at the base.

Character 209: Basal subarticular tubercle of toe I, protrusiveness: (0) flattened, (1) projected.

Character 210: Basal subarticular tubercle of toe II, protrusiveness: (0) flattened, (1) projected.

Character 211: Basal subarticular tubercle of toe III, protrusiveness: (0) flattened, (1) projected.

Character 212: Basal subarticular tubercle of toe IV, protrusiveness: (0) flattened, (1) projected.

Character 213: Basal subarticular tubercle of toe V, protrusiveness: (0) flattened, (1) projected.

Character 214: Proximal subarticular tubercle of toe III, protrusiveness: (0) flattened, (1) projected.

Character 215: Proximal subarticular tubercle of toe IV, protrusiveness: (0) flattened, (1) projected.

Character 216: Proximal subarticular tubercle of toe V, protrusiveness: (0) flattened, (1) projected.

Character 217: Distal subarticular tubercle of toe IV, protrusiveness: (0) flattened, (1) projected.

Character 218 (**Figure 14A, 14C–D**): Basal subarticular tubercle of toe II, shape: (0) rounded or ovoid, (1) elongated.

Character 219 (**Figure 14A, 14C–D**): Basal subarticular tubercle of toe III, shape: (0) rounded or ovoid, (1) elongated.

Character 220 (**Figure 14A, 14C–D. 239**): Basal subarticular tubercle of toe IV, shape: (0) rounded or ovoid, (1) elongated.

Shape of the inner metatarsal tubercle.—There is an inner metatarsal tubercle at the toe I base in poison frogs. Previous studies reported an elongated or elliptical, or rarely an oval or ovoid inner metatarsal tubercle (e.g., Coloma 1995, Duellman 2004, Myer and Grant 2009). My revision of this tubercle in poison frogs agree with previously reported, because the inner metatarsal tubercle varies in shape (from a plantar view), with two defined shapes. A rounded to ovoid tubercle, and in other cases, an elongated tubercle. Moreover, there is little intra-specified variation (except the variation induced by the preservation artifact).

Character 221 (**Figure 14A, 14E**): Inner metatarsal tubercle, shape: (0) rounded or ovoid, (1) elongated.

Species with rounded or ovoid tubercle are those with a tubercle as long as width or when the tubercle length is lesser to 1.5 times than its width (state 0) and

species with an elongated tubercle are those that tubercle length is twice larger than width (state 1).

Metatarsal fold.—Grant et al. (2006: 73, character 46) proposed one character to account for the presence of and variation in the metatarsal fold. The character was unmodified in Grant et al. (2017: character 47). I found variation in the metatarsal fold extension. To test the homology independently, first I divided the character of Grant et al. (2006) in occurrence and variation of its morphology, and second, a character about extension is proposed.

Character 222: Metatarsal fold, occurrence: (0) absent, (1) present.

Character 223: Metatarsal fold, degree: (0) weak, (1) strong.

Character-states definition like to Grant et al. (2006: character 46)

Character 224 (**Figure 16**): Metatarsal fold, extension: (0) reaching half of plantar surface, (1) reaching the proximal 2/3 of plantar surface, (2) reaching the outer metatarsal tubercle level.

The metatarsal fold extends proximad toward of the outer metatarsal tubercle, reaching this tubercle level, but without contact, because the proximal end of the fold is most post-axial than outer metatarsal tubercle (state 2). In other species (e.g., subfamily Hyloxalinae) the proximal end of the metatarsal fold only reaches or slightly surpass the two third of the basal subarticular tubercle–outer metatarsal tubercle distance and do not extend beyond proximally (state 1). And in a few species, the fold only reaches half of the basal subarticular tubercle–outer metatarsal tubercle distance (state 0).

Additional to known variation (see Grant et al. 2006), in some species of the *Hyloxalus bocagei* group (*H. excisus* assigned here, *H. maculosus*, *H. vergeli*, and

two undescribed species), the metatarsal fold is strong but the proximal end is weak, or it is strong near to the toe and weak in most of its extension (e.g., *H. vergeli*).

Length of toe III and V.—Toe length was not evaluated in previous systematic studies of the poison frogs (e.g., Myers et al. 1991, Grant et al. 2006, 2017); although sporadically, there a comparison between the length of toes in the species descriptions, without major comment about this variation. Nevertheless, considerable variation in toe length in other neotropical anurans group was recorded; for example, in terraranan frogs, the length variation was used to recognize groups within these frogs (Lynch and Duellman 1997). Thus, I evaluated the length of toes III and V regard the proximal subarticular tubercle of toe IV. Similar to finger length, variation in the length of toe IV is minimal, but additional tools could help to test the variation.

Character 225 (**Figure 17A–B**): Toe III length: (0) reaching antepenultimate subarticular tubercle of toe IV, (1) surpassing antepenultimate subarticular tubercle of toe IV. Additive.

When the toe III is pressing against the toe IV, the disc of toe III reaching the proximal subarticular tubercle of toe IV (state 0), or it surpass and extend beyond the proximal subarticular tubercle (state 1).

Character 226 (**Figure 17**): Toe V length: (0) not reaching proximal subarticular tubercle of toe IV; (1) reaching proximal subarticular tubercle of toe IV; (2) surpassing proximal subarticular tubercle of toe IV. Additive.

The state 0 is when the disc of the toe V not reaching the proximal edge of the proximal subarticular tubercle of toe IV. In state 1, the disc of toe V reaching the proximal subarticular tubercle, and both are about the same level. And in state 2, the disc of toe V surpass and extends beyond the proximal subarticular tubercle.

B) Adult coloration pattern.

Ventrolateral stripe.—Variation in the ventrolateral stripe (VLS) in Dendrobatoidea is most complex than described previously, as much as two types of the VLS occur in poison frogs. Silverstone (1976) described and recognized the two ventrolateral stripes in *Allobates femoralis*, as follow: *"*[v]entral to this [ventrolateral] stripe ran a second ventrolateral stripe... (p. 31)"; nevertheless, as far as I know, no other study mentioned both VLS. A revision of the ventrolateral stripe in Dendrobatoidea agree with the Silverstone's observation, and decisively these two types of the VLS can be distinguish depending where these are located on the ventrolateral flank. The first VLS runs at the upper end of the ventrolateral flank, and the second one runs lower at ventrolateral flank (**Figure 18**). Both stripes co-occur in individuals of *Allobates* (Aromobatidae)*,* in *Adelphobates,* and in *Ranitomeya* (Dendrobatidae), which denies the homology between both stripes; therefore, to improve the homology, I recognized two VLS types (see below). These characters were evaluated from preserved specimens and, when was possible, in alive specimens by photo or field notes (Grant et al. 2006: character 54).

Character 227 (Figure 18–19): Ventrolateral stripe A, occurrence: (0) absent, (1) present.

The ventrolateral stripe A runs by the upper end of the ventrolateral flank, extending from groin to arm insertion region, interconnecting with labial stripe (when it is present, see below). This pass above of the arm insertion, although sometimes, this stripe is in contact with dorsal arm insertion, without interruption in the continuity between both stripes. In other species, there are not contrasting pigmentation between ventrolateral stripe A and the abdomen, doing difficult the

codification of this line in preserved specimens; however, differences in light pigments help to detected the line (**See Figure 18, 19A**).

Character 228: Ventrolateral stripe A, structure: (0) wavy series of elongate spots, (1) straight.

Like as Grant et al. (2006: Figure 39, 2017: character 59). Most *Allobates* with A-type has a straight VLS, however exists exception. Moreover, in *Phyllobates vittatus* the elongated spots, that sometimes forming a wavy VLS are located on upper ventrolateral flanks.

Character 229 (**Figure 19**): Ventrolateral stripe B, occurrence: (0) absent, (1) present.

Ventrolateral stripe B runs on lower end of the ventrolateral flank, from groin to arm insertion region; however, unlike of VLS-A, this is interrupted by the arm insertion, and do not interconnected directly with labial stripe (when it is present). Sometimes, pale coloration of the arm insertion, gives the appearance of the continuity between stripes (e.g., the southern populations of *Hyloxalus lehmanni*); nevertheless, differences between those stripes from axilar ground coloration are easily discernible by detection of the iridophores and melanophores (see also Grant and Castro 1998: 379). In addition, due to the position, this line can be confused with the coloration of the ventral pale spots, but like to VLS type A, differences in pigments composition and also structure (straight line or elongated spots) are perceptible. *Hyloxalus* with VLS show this stripe type.

Grant et al. (2006: character 54, 2017: character 58) reported presence of VLS for *Hyloxalus azureiventris* and *H. chlorocraspedus*; nevertheless, although some rounded or elongated pale spots are present on the ventrolateral flank, revision of the type specimens and photos in life of both species (e.g., Lötters et al. 2007) show that

these are not trace of VLS. In change, the same authors (like as Coloma 1995) coded VLS absent for *H. sauli*; however, the type specimens revised by me show the presence of VLS B type (KU 109318, KU 122217-20, KU 149709; see also Edwards 1974: Fig. 2D, Coloma 1995: Plate 1A, Páez-Vacas et al. 2010: Fig. 4C).

Character 230 (**Figure 19B – C**)**:** Ventrolateral stripe B, structure: (0) wavy series of elongate spots; (1) straight.

Testis.—Testis size varies ontogenetically, being smaller in juveniles and reaching its maximum size in adults, and furthermore, it is presumed that testis size appears be a function of the sexual activity, with intraspecific variation in testis size (Grant et al. 1997). Nevertheless, Coloma (1995) reported notable interspecific variation in poison frogs, with a large testis in adult male *Ectopoglossus confusus* (as *Colostethus chocoensis*), contrasting with the small testes in adult males of the other studies Ecuadorian species. Large testes extend almost along the entire kidney length, while small testes cover approximately one third of kidney length (p. 12, Figure 5); nonetheless, very few studies specify the testis size (e.g., Grant et al. 1997, Grant and Ardila-Robayo 2002, Grant 2007a, b) and it is unknown the systematic and phylogenetic relevance of this character.

In order to discover the transformational series in testis size in dendrobatoids, I evaluated the relative testis size regard to the kidney and eye length, as a way to control variation introduce by each reference point and because these were previously used to testis size quantification. Data are from adult males of Hyloxalinae frogs mainly, available for this research. Large adult males with presence of the secondary sexual characters (e.g., both vocal slits open, swelling in the finger IV or on the distal end of the upper arm, or dark coloration on the throat) were included as much as possible, to recorded the maximum testis size.

I check and reviewed the testis size in species for which the size was reported. I confirmed that testis of *Ectopoglossus confusus* (KU 166158, adult male, paratype) is equal to kidney length and 1.1 times of eye length. For *E. atopoglossus* also was reported a large testis (Grant et al. 1997), and I found that testis is 1.5 times of eye length and it is equal to kidney length in the adult male (KU289252). Grant (2007) reported that testis is 0.3–0.5 of eye length in *Colostethus ucumari*. My measurement in three types (ICN 28556, ICN 38768–69) agree with him, and show that it is 0.3–0.5 of kidney length. Grant and Ardila-Robayo (2002) stated that one male of *Hyloxalus saltuarius* have the testis equal than eye, contrarily other two adult males have testis 0.6 of eye length. I checked one paratype adult male of *H. saltuarius* (ICN 43467), and its testis is 0.5 of eye length and 0.3 of kidney length. Finally, Grant et al. (2007) stated that testis is about 0.6 of eye length in *Allobates niputidea*, but specimens of this species were not available in this research.

Also, I found intra-specified variation in testis size; for example, testis size varies between 0.2–0.5 times kidney length in *Hyloxalus vergeli* (*n* = 19), *Hyloxalus* sp_R (*n* = 20), and *Rheobates palmatus* (*n* = 12), and 0.3–0.6 times of kidney length in *H. subpunctatus* (*n* = 10), while the testis is 0.2–0.4 times of eye length in *H. vergeli, Hyloxalus* sp_R and *R. palmatus* and from 0.5–0.8 of eye length in *H. subpunctatus*. These four species may be considered to have small testis (0.2–0.6 of kidney length, and 0.2–0.8 of eye length) in concordance with previously reported and regard to the species with large testis. The variation in the relative proportion between testis/kidney length in the other species included here falls within variation described; however, in a few species, such as *Allobates olfersioides* (specimens from Rio de Janeiro, Brazil), *Colostethus mertensi,* and *H. vertebralis*, although testes are small (0.3–0.6 of kidney length), they are 0.5–1 times of eye. In those species that

was diagnosis a large testis, and those found here, despite a few adult males by species were available (1–2 males, except *H. abditaurantius* with 4 adult males), testis reaching large proportion of the kidney and eye length, so testis is 0.9–1 times of kidney length and from 1.1–2 times of eye length. Variation recorded in testis/eye proportion show a continuous variable, which as well as the testis variation, related to eye size variation; unlike, the testis/kidney relation show a gap between small (0.2–0.6 of kidney length) or large (is 0.9–1 of kidney length) testis. In addition, the kidney size of most species show no obviously difference, being about 40% of snout-vent length.

Character 231 (**Figure 20**): Testis of the adult males, size: (0) small, 0.2–0.6 of kidney length, (1) large, 0.9–1 of kidney length.

C) Adult myology.

M. compressor cloacae.—The *m. compressor cloacae* surround the cloaca at distal urostyle level, originating from anterior to mid-dorsal iliac symphysis, ascending and inserting to each ventrolateral side of the urostyle, extending posteriod to urostyle tip (Ecker and Haslam 1889, Gaupp 1904, Van Dick 1955, 1959). In poison frogs, account of this muscle is almost absent as far I known, and only the *m. sphincter ani cloacali* was described and discussed in dendrobatoids (Anganoy-Criollo et al. in press). My revision of the *m. compressor cloacae* in these frogs agrees with the previously studies. It is noteworthy that anteriorly this muscle inserts ventral and is covered by the *m. pyriformis*, and extends posteriod to the urostyle tip, and sometimes a few fibers pass and meets in a short symphysis, just before of the *m. sphincter ani cloacalis*; nonetheless, in other dendrobatoids this muscle is divided medially at the *m. pyriformis* level and separates in two portions, one portion inserts anterior and is not covered by the *m. pyriformis*, and the posterior one that insert

ventral and barely posterior to *m. pyriformis*. Thus, the transformational series involves the anterior portion insertion of the *m. compressor cloacae* in relation to the *m. pyriformis*.

Character 232 (**Figure 21**): *M. compressor cloacae,* anterior portion insertion: (0) inserting ventrally, covered by the *m. pyriformis*, (1) inserting anteriorly, uncovered by the *m. pyriformis*.

Distal slip of the *m. sphincter ani cloacalis*.—Anganoy-Criollo et al. (in press) revised the *m. sphincter ani cloacalis* in various poison frogs, finding variation in the ventral insertion of its distal slip and in the *m. rectus abdominis* tendon origin. Ventrally, the distal slip inserts on the dermis, ventral to the cloaca, or extending distad to the level of the pubic symphysis, inserting on the dermis and merge with the posterior branch of the *m. rectus abdominis* tendon origin, given the RA tendon origin is divided in two branches, the anterior attached to the ventral pubis and the posterior branch projecting distad to attach with fibers of the distal slip of the *m. sphincter ani cloacalis*. Otherwise, in most cases, the *m. rectus abdominis* tendon origin is unbranched, inserts on ventral pubis only. Here, the sampling in Dendrobatoidea was expanded, corroborating these finding, and in addition, the distal slip occurrence variation was observed in poison frogs.

Character 233 (Figure 22): Distal slip of *m. sphincter ani cloacalis*, occurrence: (0) absent, (1) present.

Character 234: Distal slip of *m. sphincter ani cloacalis*, ventral insertion: (0) proximal, ventral to cloaca, on dermis, (1) distal, pubic symphysis level, on dermis and posterior branch of the *m. rectus abdominis* tendon origin. See figures in Chapter 1.

Character 235: Posterior branch of the *m. rectus abdominis* tendon origin, occurrence: (0) absent, (1) present.

M. tensor fascia latae.—The *m. tensor fascia latae* originates from the ventral iliac shaft and insert on the fascia of the *m. cruralis* at the first third to mid-level of the thigh, and its insertion tendon also covers the *m. glutaneus magnus* (Dunlap 1960, McDiarmid 1971, Prikryl 2009). This muscle has been subject of several studies in anurans, finding variation in thick, shape, size, and origin of this muscle (e.g., Limese 1964, Fabrezi et al. 2014), but the variation in the origin has played an important role in anuran systematic studies. Thus, previous researches proposed two (anterior and posterior) or three (anterior, middle, and posterior) origins of *m. tensor fascia latae*. The anterior origin originates near to the proximal tip or anterior iliac shaft, a medial origin arise from the ventral half of the iliac shaft, and the posterior origin arise from posterior third of iliac shaft (Dunlap 1960, McDiarmid 1971, Prikryl 2009). In addition, intraspecific variation in the *m. tensor fascia latae* origin was reported in one toad of genus *Mertensophryne* (Tihen 1960).

Noble (1922) evaluated the variation of this muscle in different poison frogs, including aromobatids *Aromobates alboguttatus* (as *Phyllobates alboguttatus*), *Mannophryne collaris* (*Hyloxalus collaris*), and *Rheobates palmatus* (as *H. granuliventris*), and dendrobatids *Ameerega braccata*, *A. parvula*, *A. trivittata* (as *Dendrobates*), *Colostethus inguinalis* (as *P. inguinalis*), *Dendrobates auratus,* and *D. tinctorius* (both as *D. tinctorius*), *H. fuliginosus*, *H. infraguttatus* (as *P. infraguttatus*), *H. subpunctatus* (as *P. subpunctatus*), and *Oophaga. histrionica, O. pumilio*, and *O. sylvatica* (all as *D. typographus*); however, he does not report condition or differences in the *m. tensor fascia latae* origin between them. After, Dunlap (1960) included two dendrobatoids in your study about hindlimbs musculature, *M. trinitatis* (as *P.*

trinitatis) and *D. tinctorius*, and both were considered to have a posterior origin (i.e., *m. tensor fascia latae* originate along of the posterior third of the iliac shaft). Additional studies no included other poison frogs.

I reviewed the *m. tensor fascia latae* origin in Hyloxalinae and other poison frogs. In general, my result agrees with previous studies, without intraspecifid variation, but with differences in the muscle origin. Usually, the fibers of the TFL arise from the posterior third of the ventral iliac shaft (posterior origin), projecting posteriod and quickly runs parallels to the *m. cruralis* to insert as a tendon on the fascia at the middle femur length; nevertheless, other species, including the *Rheobates palmatus* and *Colostethus inguinalis* that was revised by Noble (1922), show a medial origin, given that this muscle extends continuously to the middle iliac shaft. No anterior origin was recorded in dendrobatoids studied. These variations, together the previously recorded, allow to embrace the three-origin points proposal, with anterior, middle and posterior origin (as were defined above).

Character 236 (**Figure 23**): *M. tensor fascia latae*, origin: (0) anterior, (1) medial, (2) posterior.

M. gracilis minor.—In all dendrobatoids reviewed here, the *m. gracilis minor* originates by its own short tendon from pelvic rim and extends distad on the dorsal face of the *m. gracilis major* as a narrow, thin muscle, to unite just before to the insertion of the *m. gracilis major*, sharing a common tendinous insertion (Myers et al. 1991). This muscle, even if very thin in a few cases, is present in all poison frogs, including the species of *Mannophryne* examined here revised. Although, I could not study *M. trinitatis*, Myers et al. (1991) reported implicitly the occurrence of this muscle in this species (contra Dunlap 1960: 15). Sometimes, the muscular fibers are interrupted and replace by a short tendon interval at the proximal first third of *m.*

gracilis minor, attached to the dermis by means the tendinous or muscular fibers (Dunlap 1960, Myers et al. 1991)—the second origin of *m. gracilis minor*; but in other species contrary, there is no indication the attachment to the femur dermis. The muscles in *Dendrobates tinctorius* was said to insert independently of the *m. gracilis major* (Dunlap 1960: 16), but the specimen used here of this species (MZUSP 139803) have similar condition than other poison frogs. Grant et al. (1997) reported that this muscle is indistinguishable from *m. gracilis major* after one third of its distance in *Ectopoglossus atopoglossus*; however, my observation based in the adult male (KU 289252) and adult female (KU 289251) reveal otherwise, the muscle is very joined but well differentiable from the *m. gracilis major*. Other variation observed was associated with preservation or postmortem effects, because the muscle is adhered to the skin in well preserved specimens, and it is free in those specimens that skin suffered alteration by inadequate handling; for example, in a specimen of *Anomaloglossus stepheni* (MZUSP 70477), the muscle is attached to the skin in the left leg, while is free on the right leg.

Character 237 (**Figure 24**): Second origin of *m. gracilis minor*, from dermis: (0) absent, (1) present.

M. extensor carpi radialis.—In dendrobatoids, the *m. extensor carpi radialis* originates by mean of two slips (or heads in previous studies, e.g., Duellman and Trueb 1994), the internal slip arise from distal humerus, proximal to the *m. flexor antibranchi lateralis superficialis* (or *m. brachioradialis*), and the external slip arises from epicondylus of the humerus. The slips join distally and continues as a flat tendon, passing dorsolateral to the radiale, inserting between the carpal 5-4-3 and element Y (Ecker and Haslam 1889, Davis and Burton 1982: 511, Duellman and Trueb 1994, Diogo and Ziermann 2014. Carpal terminology of Fabrezi and Alberch

1996). Commonly, the internal slip is thin through of its extension, and represent about 1/4 of external slip width, and joined at about distal second-third on the ventral face of external slip (**Figure 25A**); nevertheless, in a few Hyloxalinae frogs, the internal slip is thick and robust proximally (being about equal than external slip width), the origin covering roughly half humerus, extends distad inserting at the second-third on the external slip, or inserting on the external slip distal tendon, at level the radiale (**Figure 25B– C**). Variation in the thickness and insertion of the internal slip are proposed as the following transformation series:

Character 238 (**Figure 25**): Internal slip of the *m. extensor carpi radialis*, width of the origin: (0) thin, (1) robust.

The width of the internal and external slips is evaluated at its proximal end, near to the humerus. A thin internal slip reaches about one quarter of the external slip width (state 0), while a robust internal slip is as width as external slip (state 1).

Character 239 (**Figure 25**): Internal slip of the *m. extensor carpi radialis*, insertion: (0) at about distal two-third of external slip, (1) at the external slip distal tendon, roughly at radiale level.

Other Potentially Informative Morphological Variation

Coloration on the supralabial region.—The supralabial region is comprised above of the upper lip and below of the tympanic middle ear (TME), eye and loreal region, and extends from anterior shoulder to snout tip. In preserved specimens of Hyloxalinae frogs, the coloration of this region varies from pale color entirely (e.g., *Hyloxalus shuar*) to almost dark entirely (e.g., *H. exasperates*, *Paruwrobates whymperi*), and between these extremes, many species have dark or white coloration in distinct quantities and structures (dots/spots/blotches). Moreover, in *H. azureiventris* and *H. chlorocraspedus* there is a pale line runs from arm insertion to

the eye, passing below of TME, and ventrally do not reaching the upper lip (**Figure 26**). This line was named as labial stripe, and was used in the diagnosis of poison frogs (e.g., Silverstone 1976, Rodriguez and Myers 1993).

Rodriguez and Myers (1993) defined this stripe as the "...labial stripe commences below the middle or anterior edge of eye...and extends posteriorly under eye and tympanum to the anteroproximal part of upper arm (p. 6)."; and recently, Brown et al. (2011) defined it as the "stripe that extends from shoulder around upper lip (p. 17)". Despite there being co-occurrence and continuity between labial stripe and ventrolateral stripe, the former differ from the ventrolateral stripe in occurrence, length, and structure; moreover, Silverstone (1976) already made distinction between labial stripe from ventrolateral stripe in the revision of the then-*Phyllobates*; for example, in description of *Allobates zaparo* (p. 34) and *Epipedobates anthonyi* (p. 27). This variation provide support by the independence between both stripes.

Nevertheless, the variation found in labial stripe in dendrobatoids complicate the definition and codification of the character(s). Thus in preserved specimens, the sharpness of the line varies, from well defined (e.g., *H. azureiventris* or *Ameerega* spp. **Figure 26**) to ill-defined (e.g., *Hyloxalus anthracinus*, *H. elachyhistus*). In the last case, this stripe is generating by lack of the melanophores, or there are not contrasting pigments between white labial stripe and white region. In other species, there are elongated white spots/blotches, sometimes forming a line. In addition, the pale upper lip may be confused with this line. Added to this complex variation, members of the Dendrobatinae subfamily (except most *Ranitomeya* and "*Colostethus*" *ruthveni* group) has uniform coloration on the supralabial region (dark in preservative) with the presence of the rounded pale spots (e.g., *Dendrobates tinctorius*, *Oophaga histrionica*, *O. pumilio*). A regionalization of the lateral head and

the evaluation of the coloration can provide clues about of the transformational series involved.

Skin structure on the oblique lateral stripe.—Commonly in poison frogs the skin on the oblique lateral stripe (OLS) is smooth as the lateral body skin; however, in some specimens the three *Hyloxalus* species (*H. anthracinus, H. sylvaticus* and *H. pulcherrimus*), the skin on this line show some degree of structure but intraspecific variation is extensive. In adult males with black coloration in most of its body and some adult females of *H. anthracinus,* or a few specimens of *H. sylvaticus* and *H. pulcherrimus*, the skin on OLS is raised along of its extension from groin to shoulder; nonetheless, other individuals in these species show a smooth skin. Transversal gross dissection in skin show a thickness integument on the OLS in these individuals. This raised OLS is also observed in frogs of the genus *Hylodes* (e.g., Haddad and Pombal 1995: Figure 1, Salles et al. 2009: Figure 11, Pirani et al. 2010, Malagoli et al. 2017: Figure 1). Preservation artifact and intraspecified variation do not allow me stablished a character, therefore I refrained to formulate this. I thinks that a histological evaluation could be give insight about of the integument differences observed in those species.

Phylogenetic Systematic of *Hyloxalus*

General Results

The total evidence analyses with dynamic homology in POY found one or two most parsimonious tree (MPT) in each analysis of the successive outgroup expansion. Analysis of the implied alignments in TNT found more MPTs of the same length as POY in all but the sixth and ninth analyses, in which the TNT trees are one step shorter than the POY tree (**Table 5**).

The final analysis (ninth round of the successive outgroup expansion), which will be used the discussion of phylogenetic relationships of *Hyloxalus* has 54672 steps in POY after iterative pass refinement; the TNT analysis of the implied alignment resulted in 345 trees of 54671 steps. Phylogenetic results are presented in successive outgroup expansion result and after, the ingroup relationships.

Successive Outgroup Expansion

The ingroup sample of *Hyloxalus* includes 188 terminals. The successive outgroup expansion affect in different degrees the internal relationship of *Hyloxalus*, including interspecific relationships and the topological position of the large clades, even compromising ingroup monophyly. The topological position of certain clades is variable throughout the analysis. Recovered trees are given in **Appendix 4** and relevant differences are specified in **Table 7**. To facilitate presentation of the result, below I use the following names:

1) *Hyloxalus subpunctatus* clade: *H. cepedai*, *H. felixcoperari* (included population of *Hyloxalus* sp. Supata and *Hyloxalus* sp. Tequendama), *H. picachos*, *H. sanctamariensis*, *H. subpunctatus*, *H. walesi* (re-validated at species level in this study, see below), and the unnamed *Hyloxalus* sp. Aguabonita, *Hyloxalus* sp. AguaAzul, *Hyloxalus* sp. Junin, *Hyloxalus* sp. QuebradaWolf, *Hyloxalus* sp. *edwardsi* group (representative of *H. edwardsi* group), and *Hyloxalus* sp. Sumapaz.

2) *Hyloxalus bocagei* clade: *H. bocagei*, *H. faciopunctulatus*, *H. italoi*, *H. leucophaeus*, *H. maculosus*, *H. sauli*, *H. sordidatus*, *H. vergeli*, and *H. yasuni*, and unnamed species *Hyloxalus* sp. Amazonas, *Hyloxalus vergeli*_Ibague, *Hyloxalus* sp. Inza.

3) *Hyloxalus nexipus* clade: Terminals named as *H. nexipus*.

4) *Hyloxalus sylvaticus* + *H. pulcherrimus* clade.

5) *Hyloxalus jacobuspetersi* + *H. delatorreae* (KU220621) clade.

6) *Hyloxalus pulchellus* clade: *H. arliensis*, *H. delatorreae* (KJ940457, KU220619–20), *H. lehmanni*, *H. pinguis*, *H. pulchellus*, *H. vertebralis*, the undetermined *Hyloxalus* sp. MonteOlivo and *Hyloxalus* sp. SanMiguelDeSalcedo, and unnamed *Hyloxalus* sp. Alban and *Hyloxalus* sp. MesasGalilea.

7) *Hyloxalus azureiventris* clade: *H. azureiventris*, *H. chlorocraspedus*, *H. craspedoceps*, and *Hyloxalus* sp. ElCopal.

8) *Hyloxalus* sp. Bongara + *Hyloxalus* sp. PAV clade.

9) *Hyloxalus infraguttatus* clade: *H. awa*, *H. infraguttatus*, *H. toachi*, *Hyloxalus* sp. Moraspungo, *Hyloxalus* sp_Masvalle.

10) *Hyloxalus shuar* + *H. idiomelus* clade.

11) *Hyloxalus elachyhistus* clade: *H. elachyhistus*, *H. insulatus*, *H. littoralis* and *H. elachyhistus* Cajamarca, *H. insulatus* Amazonas.

12) *Hyloxalus anthracinus:* It is not placed in any of the above groups because its placement varied.

The first analysis (**analysis 1**) included an outgroup sample of five *Ectoploglossus* and, one *Paruwrobates*, and *Phyllobates lugubri*s as the root. This analysis recovered Hyloxalinae, *Ectopoglossus* and *Hyloxalus* as monophyletic (*Paruwrobates* monophyly was not tested, because only a single terminal was analyzed). *Paruwrobates* is sister to *Ectopoglossus*, and both are sister to *Hyloxalus*. Within the ingroup, the *H. subpunctatus* clade (including the *H. edwardsi* group) is sister to all other *Hyloxalus*. Within this clade, the *H. edwardsi* group (as defined in Chapter 1) + *Hyloxalus* sp. Sumapaz is sister to a clade that contains *H. cepedai*, *H. picachos*, *H. sanctamariensis*, and *Hyloxalus* sp. AguaAzul. Next, the *H. bocagei* clade is sister of the remaining *Hyloxalus*. Among the remaining *Hyloxalus*, the *H.*

nexipus clade is sister to the other remainder of *Hyloxalus*; *H. sylvaticus* + *H. pulcherrimus* form a clade with *H. jacobuspetersi* + *H. delatorreae* (KU220621), and these, in turn, are nested with the *H. pulchellus* clade; the *H. azureiventris* clade is sister to the clade composed of *Hyloxalus* sp. Bongara + *Hyloxalus* sp. PAV, followed by the *H. infraguttatus* clade, *H. shuar* + *H. idiomelus,* and finally the *H. elachyhistus* clade (**Figure 27**). In this last clade, with the exception of *H. elachyhistus* from Cajamarca, the other terminals of this species form a clade, while the Cajamarca lineage is more closely related to *H. insulatus* and *H. littoralis* (**Figure 29**).

In the first expansion (**analysis 2**) with 18 outgroup terminals, including six terminals of the first analysis, plus 12 Dendrobatinae and the tree rooted in *Silverstoneia flotator,* Hyloxalinae monophyly and the intergeneric relationships of the first analysis remained unchanged; however, in this analysis the *Hyloxalus bocagei* clade is sister to the *H. subpunctatus* clade; *H. sylvaticus* + *H. pulcherrimus* are not nested with *H. delatorreae* (KU220621) + *H. jacobuspetersi* (which are part of the *H. pulchellus* clade) and are instead sister to a large clade bracketed by *H. nexipus* and *H. littoralis*; the *H. nexipus* clade is clustered with the *H. azureiventris* clade, but this clade is more basal than in the previous analysis, branching after *H. sylvaticus* + *H. pulcherrimus*. The relationships within the clade comprising *Hyloxalus* sp. PAV and *H. littoralis* are unchanged (**Figure 27**).

In the second expansion (**analysis 3**), the outgroup sample was expanded to 26 terminals in total, added three terminals of Dendrobatinae, four Colostethinae (including "*Colostethus*" *poecilonotus*), and the tree was rooted on the aromobatid *Rheobates palmatus*. Hyloxalinae and its genera are monophyletic, and the intergeneric relationships are unaffected by the outgroup expansion; however within

the *Hyloxalus*, the *H. subpunctatus* and *H. bocagei* clades are not sister, and both return to the placement of the analysis 1, as do the clades *H. nexipus* + *H. azureiventris* clades. Once again, *H. sylvaticus* + *H. pulcherrimus* and *H. jacobuspetersi* + *H. delatorreae* (KU220621) form a clade. *Hyloxalus anthracinus* is not related to the *H. pulchellus* clade, as in the first analysis, but is instead sister to the clade of *H. sylvaticus* + *H. pulcherrimus* and *H. jacobuspetersi* + *H. delatorreae* (KU220621). Finally, *Hyloxalus* sp. Bongara + *Hyloxalus* sp. PAV are placed more basal than the first analysis, branching between *H. pulchellus* and *H. azureiventris* clades. The unassigned "*Colostethus*" *poecilonotus* falls within the *H. azureiventris* clade as sister to *H. azureiventris* and *H. chlorocraspedus.* Other relationships encompassing *Hyloxalus* sp. Moraspungo and *H. littoralis* are the same as in previous analyses (**Figure 27**).

In the third expansion (**analysis 4**), with 36 outgroup terminals (including "*Colostethus*" *poecilonotus*) and the same root, the effect on the topology was much greater than in previous analyses. First, the monophyly of Hyloxalinae and the sister relationship between *Ectopoglossus* and *Paruwrobates* are rejected, with these genera shifting to basal positions adjacent to the root. Within *Hyloxalus*, the *H. bocagei* and *H. subpunctatus* clades are again sisters; the clade composed of *H. sylvaticus* + *H. pulcherrimus*, *H. jacobuspetersi* + *H. delatorreae* (KU220621) and *H. anthracinus* are nested within the *H. pulchellus* clade; the *Hyloxalus* sp. Bongara + *Hyloxalus* sp. PAV clade and the *H. shuar* + *H. idiomelus* clade are positioned between the *H. azureiventris* and *H. infraguttatus* clades (**Figure 27)**. The two terminals of *H. elachyhistus* (CORBIDI 4292 and KU212507) leave this clade, and, like the *H. elachyhistus* Cajamarca lineage, are closely related to *H. insulatus* and *H. littoralis* (**Figure 29**).

In the fourth expansion (**analysis 5**), with a considerable increase in the Colostethinae (23 additional terminals) sample and eight additional Dendrobatinae, the ingroup relationships also were severely affected. Hyloxalinae remains nonmonophyletic, but in this analysis the *H. bocagei* clade is sister to all terminals except *Rheobates palmatus* (the root) and *Ectopoglossus*, *Paruwrobates* is sister to Dendrobatinae + Colostethinae, which are collectively sister to the remaining *Hyloxalus*. The *H. nexipus* clade is sister to the *H. azureiventris* clade, as in the second analysis, but these are placement basal, sisters to the remaining *Hyloxalus* except *H. subpunctatus* clade. The *H. shuar* + *H. idiomelus* clade returns to the position found in the first to third analyses, that is, sister to the *H. elachyhistus* clade (**Figure 27**).

Further changes within the major clades also occurred. Within the *H. bocagei* clade, the clade bracketed by *H. bocagei* and *H. maculosus* is sister to *H. vergeli* from Ibagué and *Hyloxalus* sp. Inza instead of the clade bracketed by *H. faciopunctulatus* and *H. yasuni*. In the *H. subpunctatus* clade, *H. picachos* is sister to the *Hyloxalus edwardsi* group + *Hyloxalus* sp. Sumapaz clade. Finally, "*Colostethus*" *poecilonotus* is sister to *H. craspedoceps,* and the two terminals of *H. elachyhistus* (CORBIDI 4292 and KU212507) return to the position in analysis 3 (**Figure 29**).

With the inclusion of more aromobatids (4 additional terminals) and three non-dendrobatoids (rooting in the hylid *Boana boans*) in the fifth expansion (**analysis 6**), *Hyloxalus* is again monophyletic, although Hyloxalinae remains non-monophyletic because *Ectopoglossus* + *Paruwrobates* are sister to all other dendrobatids. Within *Hyloxalus*, *H. bocagei* group is sister to the all other *Hyloxalus*, a previously unrecovered position; *H. sylvaticus* + *H. pulcherrimus* are no longer related to the *H. pulchellus* clade, which is nested within a clade with *H. anthracinus*,

H. jacobuspetersi, and *H. delatorreae* (KU220621); *H. nexipus* clade is sister to the *H. azureiventris* clade like the analysis 5, but they are sisters to the clade bracketed by *Hyloxalus* sp. ElCopal and *H. littoralis*; *Hyloxalus* sp. ElCopal is not longer part of the *H. azureiventris* clade as in previous analyses, instead it is sister to the *H. shuar* + *H. idiomelus* clade, *H. infraguttatus* clade, and *H. elachyhistus* clade. Within *H. subpunctatus* clade, *H. picachos* is sister to *H. cepedai* instead the *H. edwardsi* group + *Hyloxalus* sp. Sumapaz. In the *H. elachyhistus* clade, the terminals CORBIDI 4292 and KU 212507 again leave this clade and are sisters to *H. elachyhistus* Cajamarca, *H. insulatus* and *H. littoralis*, as in analysis 4. Within *H. bocagei* clade, *H. bocagei* and its closely species change to a basal placement, sister to the all *H. bocagei* clade but *H. vergeli* Quinchas (**Figure 28–29**).

The sixth expansion (**analysis 7**) retained the same non-dendrobatoids but expanded the sample of Aromobatidae (10 terminals) and Colostethinae (7 additional terminals). In this analysis, Hyloxalinae and *Hyloxalus* are monophyletic, *Paruwrobates* and *Ectopoglossus* are sisters, and both are sister to *Hyloxalus* (cf. Grant et al. 2017). Within *Hyloxalus*, the *H. bocagei* and *H. subpunctatus* clades are sisters, as recovered in analysis 2 and 4; *H. nexipus* returns to its position as sister to the large clade that includes *H. anthracinus* and *H. littoralis*; *H. sylvaticus* + *H. pulcherrimus* are nested with *H. anthracinus*, *H. delatorreae* (KU220621), and *H. jacobuspetersi*, which comprise the sister clade to the *H. pulchellus* clade; *Hyloxalus* sp. ElCopal is again part of the *H. azureiventris* clade, and "*Colostethus*" *poecilonotus* is sister to *H. azureiventris* + *H. chlorocraspedus*; *Hyloxalus* sp. Bongara + *Hyloxalus* sp. PAV returns to the position of the analysis 4, sister to *H. shuar, H. idiomelus*, *H. infraguttatus* clade, and *H. elachyhistus* clade. Unexpectedly, *H. shuar* and *H. idiomelus* do not form a clade but instead are successive sister to the

large clade comprising *H. infraguttatus* and *H. littoralis*. The *H. elachyhistus* terminals again form a clade (except the Cajamarca lineage). Finally, in the *H. bocagei* clade, *H. bocagei* and its closely species are sisters to *H. faciopunctulatus* + *H. italoi* + *H. yasuni* as in analysis 4; and within the *H. subpunctatus* clade, *H. picachos* again is sister to the *Hyloxalus edwardsi* group + *Hyloxalus* sp. Sumapaz clade (**Figure 28–29**).

The seventh expansion (**analysis 8**) increased the sample of aromobatid genera (18 additional terminals). The *Hyloxalus* relationships are similar to those of analysis 7, except for the clades whose position changes frequently. Thus, *H. nexipus* is clustered with *Hyloxalus* sp. Bongara + *Hyloxalus* sp. PAV and returns to the position between the *H. pulchellus* and *H. azureiventris* clades; *H. sylvaticus* + *H. puchlerrimus*, *H. anthracinus*, and *H. jacobuspetersi* + *H. delatorreae* (KU220621) are not a clade, although they are closely related to the *H. pulchellus* clade; and *H. shuar* and *H. idiomelus* are sister species once more, again forming the sister clade of the *H. elachyhistus* clade, while *H. infraguttatus* is the sister of both these clades (**Figure 28**).

The outgroup sample for the eighth expansion (**analysis 9**) comprised 136 outgroup terminals, including 11 additional aromobatids and seven additional non-dendrobatoids. Most *Hyloxalus* relationships are the same in analysis 7 and 8, with the same, variably placed clades changing position. Specifically, *H. nexipus* is no longer related to *Hyloxalus* sp. Bongara + *Hyloxalus* sp. PAV, returning to a more basal placement as sister to the large clade that includes *H. sylvaticus* and *H. littoralis*; and *H. shuar* + *H. idiomelus* are again sister to *H. infraguttatus* and the *H. elachyhistus* clade (**Figure 28**), and within the *H. subpunctatus* clade, *H. picachos* is once more sister to *H. cepedai* (**Figure 29**).

The consistent ingroup monophyly (with the consistent placement of "*Colostethus*" *poecilonotus* within it since it was first included in analysis 3) since analysis 6 and lack of variation in the relationships of most ingroup terminals and clades in analyses 7, 8, and 9 suggests that their relationships are stable to outgroup sampling (Grant, 2019). Similarly, the persistent variation in the placement of the same, few clades and terminals across outgroup expansions suggests that their instability is not due to outgroup sampling (i.e., additional expansion outgroup sampling is unlikely to decisively refute or corroborate any of the alternative placements of these taxa) but rather to either ingroup sampling (i.e., missing taxa from the ingroup sample) or character sampling (i.e., lack of evidence, conflicting/ambiguous evidence).

The three species and three clades whose position remained unstable in analyses 7, 8, and 9 are *Hyloxalus anthracinus*, *H. nexipus*, and *H. picachos* and *H. sylvaticus* + *H. pulcherrimus*, *Hyloxalus* sp.Bongara + *Hyloxalus* sp. PAV, and *H. shuar* + *H.idiomelus*, respectively. Among all nine analyses, *H. anthracinus* occupied three different positions in the optimal topologies. Its position as sister to the *H. pulchellus* clade in analyses 8 (GB = 13) and 9 (GB = 1) was also optimal in analyses 1 (GB = 10) and 2 (GB = 12); however, in analyses 3 (GB = 4) and 4 (GB = 1) it was sister to a clade composed of *H. delatorreae* KU220621 + *H. jacobuspetersi* and *H. pucherrimus* and *H. sylvaticus*, and in analyses 5 (GB = 7), 6 (GB = 9), and 7 (GB = 6) it was sister to *H. delatorreae* KU220621 + *H. jacobuspetersi*. *Hyloxalus nexipus* also occupied three different positions, including the final position (analysis 9, GB = 1) as sister to a large clade bracketed by *H. pulcherrimus* and *H. littoralis*, also recovered in analyses 1 (GB = 22), 3 (GB = 32), 4 (GB = 1), and 7 (GB = 1), nested inside that clade as sister to *Hyloxalus* sp.Bongara + *Hyloxalus* sp. PAV and together

forming the sister to the clade bracketed by the *H. azureiventris* clade and *H. littoralis* in analysis 8 (GB=10), and as sister to the *H. azureiventris* clade in analyses 2 (GB = 19), 5 (GB = 21), and 6 (GB = 16). In the final analysis, *H. picachos* is sister to *H. cepedai* (analysis 9, GB = 24), where it was also placed in analyses 1 (GB = 18), 2 (GB = 23), 3 (GB = 19), 4 (GB = 23), and 6 (GB = 20), but in analyses 7 (GB = 1) and 8 (GB = 15) it was sister to the *Hyloxalus edwardsi* group + *Hyloxalus* sp. Sumapaz clade, where it was also placed in analysis 5 (GB = 13). Among the persistently unstable clades, the *H. sylvaticus* + *H. pulcherrimus* clade was most unstable, occupying six different positions in the nine analyses (**Figure 27**); its position in analysis 9 not optimal in any of the other analyses and has minimal support (GB = 1). In contrast, the *Hyloxalus* sp.Bongara + *Hyloxalus* sp. PAV clade was optimally placed in only two positions, as sister to the clade bracketed by *H. shuar* and *H. littoralis* in analyses 1 (GB = 20), 2 (GB = 1), 3 (GB = 13), 4 (GB = 15), 5 (GB = 16), 6 (GB = 10), and 7 (GB = 18), and in a more basal position adjacent to the clade bracketed by the *H. azureiventris* clade and *H. littoralis*, either as the sister of that clade (analysis 9, GB = 21) or as sister to *H. nexipus* (analysis 8, GB = 10). Similarly, *H. shuar* and *H.idiomelus*, which form a clade in all analyses except analysis 7, are optimally placed in only two alternative positions, as the sister of the clade bracketed by *H. infraguttatus* and *H. littoralis* in analyses 4 (GB = 11), 6 (GB = 8), and 9 (GB = 7), or slightly tipward as sister to the clade bracketed by *Hyloxalus elachyhistus* KU212507 and *H. littoralis* in analyses 1 (GB = 4), 2 (GB = 4), 3 (GB = 6), 5 (GB = 3), and 8 (GB = 7).

The iterative pass optimization of the ninth analysis produce a more parsimonious tree (54672 steps). To follow, *Hyloxalus* relationships are discuss and in the case of the position-changing clades, the alternative placement are commented.

The Phylogenetic Relationships

The relationships of the other Dendrobatoidea.—A detailed revision of the phylogeny of the poison frogs was not the aim of this study; however, I record some relevant results about the generic and suprageneric relationships of the Dendrobatoidea, and discuss some relevant characters. The taxon sample in Aromobatidae was not addressed to test their relationships, therefore these are prone to the change.

The higher relationships. The monophyly of superfamily, families, and subfamilies of Dendrobatidae was recovered as proposed by Grant et al. (2006, 2017; see also Santos et al. 2009, Jetz and Pyron 2014; **Figure 30**); nevertheless, Aromobatidae subfamilies differ from previous studies. The main contrariety is that *Anomaloglossus* are not sister to the *Rheobates*, as in Grant et al. (2006, 2017; see also Santos et al. 2009, Jetz and Pyron 2018), and therefore the Anomaloglossinae monophyly was not recuperated. Contrariwise, *Rheobates* is sister to the Aromobatinae (*Aromobates* and *Mannophryne*) as was found by Santos and Canatella (2011) and Pyron (2014). Pyron and Wiens (2011) proposed a different relationship, where *Rheobates* is sister to all other Aromobatidae (**Appendix 5**).

The presence of the internal tympanic membrane (character 172: 0) is a new derived shared character for Dendrobatoidea. This structure is absent in the other anurans examined herein (e.g., Bufonidae, Hylodidae, Leptodactylidae); however, this character does not optimize as unambiguously phenotypic transformation given the lack of data in the sampled outgroup. Outside of Dendrobatoidea, data were obtained from species not included in this phylogenetic analysis.

The generic relationships. The monophyly of all poison frogs genera study herein was corroborated, like Grant et al. (2006, 2017; see Myers et al. 1991,

Twomey and Brown 2008, and Brown et al. 2011, Marin et al. 2018). The exception is for *Adelphobates*, *Dendrobates,* and *Oophaga,* because one species was used by each genus (**Appendix 5**).

The *Allobates* relationships recovered are equal to Grant et al. (2017). For this genus, eight unambiguous phenotypic transformations optimize at the node (see **Figure 31**). Among these characters, noticeably the pale ventrolateral stripe (VLS) A-type (character 227: 1) is an unambiguous phenotypic synapomorphy for the genus. This type of the VLS is absent in other aromobatid and dendrobatids, because these have a B-type (including *Hyloxalus*). Furthermore, the VLS A and B-type coexist in *A. femoralis* group, making the B-type (230: 1) a synapomorphy for this group. Other unambiguous phenotypic synapomorphies for *Allobates* are the basal subarticular tubercle projected of the finger V (character 181: 1), and the small (smaller than half of the proximal) subarticular tubercle of the toe IV (character 208: 0).

Four phenotypic characters optimize to the *Anomaloglossus* (**Figure 31, Appendix 6**), from these, the metacarpal ridge proximally extends to the palmar tubercle (character 194: 2) is present in the examined species. This could be a synapomorphy for the genus if the occurrence will be corroborated in other *Anomaloglossus*. Three phenotypic synapomorphies are shared by two species of the *A. stepheni* group (*A. degranvillei* and *A. stepheni*) included in this study: the loose skin on the tympanic middle ear (173: 1), and the absence of the oral disc (85: 0) and the upper sheath (89: 0). These last two larval characters are also found in *A. baeobatrachus* (see Fouquet et al. 2019), that also part of the *A. stepheni* group.

A warty skin on the venter (character 170: 2) was scored for *Rheobates palmatus*; however, this does not optimize as the phenotypic synapomorphy for the genus *Rheobates*. Recently, I confirmed this condition in *R. pseudopalmatus*. Other

dendrobatoids with texture on the ventral skin, show granular skin. Three unambiguous phenotypic transformations define *Aromobates*, all of these related to the expansion of the finger discs (see **Figure 31**). In *Mannophryne*, two phenotypic characters are unambiguous transformations, including the presence of the dermal collar (character 55: 1; **Figure 31**. see also La Marca 1989, Grant et al. 2006).

In the Dendrobatidae family, all Colostethinae genera are supported by unambiguous phenotypic synapomorphies. *Silverstoneia* has 23 unambiguous phenotypic transformations between adult and larval characters; 22 for *Ameerega;* 12 for *Epipedobates;* six for *Colostethus;* and two for *Leucostethus* (**Figure 32, Appendix 6;** see also Grant et al. 2017, Dias et al. 2020). Among these, two putative larval synapomorphies (presence of shelf, character 265: 1; dark transverse band on the ventral body, 271:1) were proposed by Anganoy-Criollo and Cepeda-Quilindo (2017) and subsequently by Dias et al. (2018a) were corroborated as derived shared characters for *Epipedobates*. In *Ameerega*, the presence of supernumerary tubercle (character 3: 1) is a phenotypic synapomorphy for the clade composed by *A. berohoka*, *A. boehmei*, *A. braccata,* and *A. flavopicta*. These tubercles are also present in the non-analyzed *A. munduruku*. These five species plus *A. boliviana* and *Ameerega* sp. MatoGrosso1 compose the *A. braccata* group (of Guillory et al. 2019). The occurrence of the supernumerary tubercles is unconfirmed in *A. bolivianus* and *Ameerega* sp. MatoGrosso1. Nevertheless, these tubercles are homoplastic within the genus, because these also occurs in *A. macero* (follow Rodriguez and Myers 1993). There are no supernumerary tubercles in other poison frogs reviewed here (in contra of Dubois et al. 2021: 138). Intergeneric Colostethinae relationships differ from previous studies, given that the optimal tree recuperates *Leucostethus* sister to the

Colostethus instead than *Leucostethus* sister to the *Ameerega* as previously proposed (e.g., Grant et al. 2017, Jetz and Pyron 2018, Marin et al. 2018, Vigle et al. 2020).

The relationships between the Dendrobatinae genera are equal to Grant et al. (2017), except for the *Adelphobates*, *Oophaga,* and *Dendrobates* (ADO clade of Grant 2019) relationships, and the placement of the *Minyobates*. The relationships of these genera have been contradictory to the relationships of the poison frogs (see Grant 2019). For example, herein *Adelphobates* is sister to the *Oophaga* rather than *Dendrobates*, a hypothesis do not found in other large phylogenies. Other studies found *Oophaga* sister to the *Dendrobates* (Grant et al. 2006, Santos et al. 2009, Santos and Cannatella 2011, Santos et al. 2014, Pyron 2014 Jetz and Pyron 2018), or in another case, *Adelphobates* sister to the *Dendrobates* (Grant et al. 2017, Grant 2019). Second, in this study *Minyobates* is sister to the clade composed of *Andinobates*, *Excidobates*, and *Ranitomeya* (AER clade of Grant 2019), differing from other studies because *Minyobates* is sister to the AER and ADO clade (Grant et al. 2006, 2017), or only sister to *Adelphobates* (Santos et al. 2009, Pyron and Wiens 2011 Pyron 2014), or sister to the ADO clade (Jetz and Pyron 2018). Recently, the relationship of this genus as sister to the AER or ADO was found equally parsimoniously (Grant 2019). My optimal tree recovers unambiguous phenotypic transformations for the node of the Dendrobatini tribe, and for the genus *Andinobates*, *Phyllobates*, *Ranitomeya,* and the "*Colostethus*" *ruthveni* group (**Figure 32, Appendix 6**).

Hyloxalinae subfamily and their relationships.—The optimal tree recoveries a monophyletic Hyloxalinae with high support (GB = 54) and with one unambiguous phenotypic transformation (toe length reaches the proximal subarticular tubercle of the toe IV, character 226:1; **Appendix 1. Figure 30**). The subfamily is

composed by the sister genera *Ectopoglossus* and *Paruwrobates*, and *Hyloxalus* (see below) as its sister clade, like previous phylogenetic hypothesis (i.e., Grant et al. 2017, Santos et al. 2014). Among the Dendrobatidae, Hyloxalinae is sister Dendrobatinae rather than Colostethinae. The last is sister to both subfamilies (Santos et al. 2003, 2009, 2014, Pyron and Wiens 2011, Pyron 2014, Grant et al. 2006, 2017, Jetz and Pyron 2018); however, contrarily Guillory et al. (2019, see also Clough and Summer 2000, Vences et al. 2000, Santos and Cannatella 2011) found the Hyloxalinae sister to Colostethinae instead Dendrobatinae. This difference is related to the taxon sample density (for discussion see Chapter 1), because phylogenies with large taxon sample refute the Guillory et al. relationships, which employed a reduce taxon samples, despite the large molecular data amount used. The node of Dendrobatinae plus Hyloxalinae is well supported (GB = 33), and two unambiguous phenotypic transformations optimize at node, including the possession of the flattened basal subarticular tubercle on the toe I and II (character 209: 0, 210: 0, respectively. **Figure 30**).

The relationships between *Paruwrobates* and *Ectopoglossus* is supported by one unambiguous phenotypic synapomorphy. Unlike Grant et al. (2017) proposed two synapomorphies proposed. The pale abdomen with discrete dark spotting/reticulation/marbling in the adult females optimized at node of both genera herein (character 60: 1); while in Grant et al. (2017) in addition to this synapomorphy, the adult female with pale throat and with discrete dark spotting/reticulation/marbling also optimize as synapomorphy (Grant et al. 2017: character 69: 1, 67: 4). Moreover, the unambiguous phenotypic synapomorphies proposed by *Ectopoglossus* by Grant et al. (2017) also were recovered in this study, except the weakly expanded toe disc IV

(Grant et al. 2017: character 35: 1), instead of this, the weakly expanded toe disc II is added to this list (character 27: 1. **Figure 30**).

My examination of the most species of *Ectopoglossus* and all *Paruwrobates* allowed me to detect some highlighted findings. I found that there is loose palmar skin in the aromobatid *Anomaloglossus degranvillei*, which was exclusive and synapomorphy to *Ectopoglossus.* The adult males of *E. atopoglossus* (KU 289252) and *E. absconditus* (KU 189526) have dorsal and preaxial swelling along the finger IV, this character was scored as absent for the genus. The dots on the venter that are large serous glands (Myers et al. 2012, Grant et al. 2017: S22–S23) reported for *E. astralogaster* and *E. saxatilis* previously, also are present in *E. confusus* (KU 166157, 221616). Furthermore, like that *E. confusus,* the testis in the adult males of *E. atopoglossus* and *E. ithsminus* is large (0.9–1 of kidney length).

Grant et al. (2017) do not provide unambiguous synapomorphies for *Paruwrobates*; however, they diagnose this genus from its sister genus, *Ectopoglossus,* by lack of the median lingual process (MPL) and the toe webbing (present and extensive in *Ectopoglossus*), taut palmar skin (loose), finger II about equal to III (II<III), and the lipophilic alkaloids sequestration ability known only for *P. erythromos* (Grant et al. 2017). Nevertheless, the examination of the paratype and topoparatypes of the *P. andinus,* the type species of the genus*,* reveals a short bump-like MPL (PSO-CZ 623, 625, 627 or LP 432, 536, 820 in Myers and Burrowes 1987 respectively), a pit of the MPL in PSO-CZ 624, and MPL absent in three specimens (PSO-CZ 624, 626*,* including the paratype KU 212533. **Figure 3**) of this species. The MPL was not reported previously (see Myers and Burrowes 1987, Grant et al. 2006, 2017). Moreover, the adult male PSO-CZ 623 has a basal and phalangeal swelling on the preaxial and dorsal surface of the finger IV (character 197: 1, 198: 0), and the

venter of this specimen has white and yellowish dots, reminiscent of those of *Ectopoglossus*.

The MLP (or failing that, a pit), swelling on the fingers, and dots on the venter are absent in the other two *Paruwrobates* species (*P. erythromos*, and *P. whymperi* of San Francisco de las Pampas), but these are present and shared with *Ectopoglossus*. Moreover in *Ectopoglossus, E. absconditus* is a toe webless species, like *Paruworbates*. Unfortunately, species of *Paruwrobates* and *Ectopoglossus* appear to be locally extinct (De la Riva et al. 2020, Grant and Bolivar 2014; my data), and tissue samples of *P. andinus* and the other key species (e.g., *E. absconditus*) are unavailable to date, which prevents to test the relationships and monophyly of both genera.

Relationships of the *Hyloxalus*.—Complete ingroup relationships and synapomorphies are found in the Appendices 5 and 6. A condensed *Hyloxalus* phylogeny is in **Figure 33.** Three large clades comprise *Hyloxalus* Jiménez de la Espada 1870 as discussed in the successive outgroup section: the *H. bocagei*, *H. pulchellus*, and *H. subpunctatus* clades.

The *Hyloxalus bocagei* clade and *H. subpunctatus* clade (which includes the *H. edwardsi* group) are well-supported (Goodman-Bremer value, GB =35) sister taxa, delimited by three unambiguous phenotypic transformation from larvae: the vent tube ventrally directed in an angle of 30–45° (character 293: 1), presence of stitches on the anterior pit line (300: 1), and stitches on the middle pit line (302: 1. **Figure 34**).

The *Hyloxalus bocagei* clade was proposed by Páez-Vacas et al. (2010) for the species previously confused with *H. bocagei* and *H. fuliginosus* (see Coloma 1995, Santos et al. 2003). They included in this group *H. bocagei*, *H. maculosus,* and *H. sauli*, and also described two new species, *H. italio* and *H. yasuni.* Additionally,

although molecular evidence was lacking, they suspected that *H. faciopunctulatus,* and *H. fuliginosus* are part this group based on phenotypic similarity. The *H. bocagei* clade of Páez-Vacas et al. is paraphylectic, because *H. leucophaeus*, *H. sordidatus*, *H. vergeli* also are nested inside the *H. bocagei* group (Grant et al. 2017). The present phylogeny corroborate the paraphyly and the inclusion of *H. faciopunctulatus* and one undescribed species, *Hyloxalus vergeli* from Ibague, in the *H. bocagei* clade. Thus, this group is conform by twelve species: *H. bocagei*, *H. faciopunctulatus*, *H. italoi*, *H. leucophaeus*, *H. maculosus*, *H. sauli*, *H. sordidatus*, *H. vergeli*, *H. yasuni*, and undescribed species *Hyloxalus vergeli*_Ibague, *Hyloxalus* sp. Amazonas, *Hyloxalus* sp. Inza (**Figure 34**). The clade has low support (GB = 1), but 10 unambiguous phenotypic synapomorphies optimize at node, including the presence of fringe on the preaxial side of the finger III (character 11: 1), on the preaxial side of the finger IV (13: 1), and on the preaxial side of the toe I (31: 1), extensive toe webbing (32: 4, 33: 2, 38: 3 or 4; 39: 5), fringe on the posaxial side toe V (40: 1), presence of palatines (126: 1), and separation between the nasal and sphenethmoid bones (129: 0). *H. fuliginosus*—type species of *Hyloxalus* Jiménez de la Espada (1870)—is assigned to this group based on phenotypic similarity with *H. bocagei* (see Coloma 1995, Grant et al. 2006), moreover, this species possess all unambiguously synapomorphies of this clade.

The internal relationships in the *Hyloxalus bocagei* clade recovers in this study differ from previous phylogenies (Páez-Vacas et al. 2010, Santos et al. 2014, Grant et al. 2017), and in addition the successive outgroup expansion show alternative topological rearrange within this clade (see above). For example, *H. bocagei* and *H. maculosus* are sister species in Páez-Vacas et al. (2010), Santos et al. (2014) and Grant et al. (2017), instead in my analysis these are not closely related species,

because *H. bocagei* is sister to the clade of *Hyloxalus* sp. Amazonas + *H. leucophaeus* + *H. sordidatus* + *H. sauli* + *H. maculosus. H. sauli* is sister to *H. bocagei* and *H. maculosus* in Páez-Vacas et al. (2010) and Santos et al. (2014), but in this and other studies, *H. sauli* is sister closely related to *H. leucophaeus, H. sordidatus*, and *H. maculosus* (see, Grant et al. 2017. **Figure 34**).

Hyloxalus vergeli Hellmich (1940) inhabits the middle Magdalena valley on the western flank of the Cordillera Oriental and eastern flank of the Cordillera Central of Colombia (Cochran and Goin 1970, Ruiz-Carranza et al. 1996, Clavijo-Garzón et al. 2018, Ovalle et al. 2019), and as well the La Tatacoa desert, in the Huila department (Acosta-Galvis 2012). Distribution of this species is disjunct and separate by the dry forest of the Magdalena valley basis. Grant et al. (2017) employed the La Tatacoa terminals (Tamarindo, Neiva, Huila, Colombia) in their analysis. I increased the taxon sampling of this species with populations from Cordillera Oriental (Serrania de las Quinchas, Boyacá deparment; Gigante, Huila department) and Cordillera Central of Colombia (Ibagué and Chaparral, Tolima department; Inza, Cauca department; Neiva, Huila department). The optimal tree recovered a clade for these terminals, except for the Serrania de las Quinchas, which is sister to all *H. bocagei* clade (as defined here).

Uncorrected pairwise 16S distance between of these samples suggest three independent lineages (see **Table 8**), that are coincident with morphological differences found in adults and tadpoles between populations, as was predicted by Anganoy-Criollo (see Acosta 2012). Nevertheless, new material and genotypic data from the type locality of *Hyloxalus vergeli* (Fusagasuga municipality, Cundinamarca, 1800 m) are not available, because the natural ecosystem in this site has been devastated by the uncontrolled growth of Fusagasuga city. Nevertheless, on the basis

of morphological comparisons with type (ZSM 110/1937) and topotypic material, I conclude that the *H. vergeli* terminal from Serrania de las Quinchas (ALOP 191) represents *H. vergeli* sensu stricto. Consequently, *H. vergeli* sensu stricto is restricted to the western slope of Cordillera Oriental of Colombia in the middle Magdalena valley, and the populations referred to as *H. vergeli* Ibagué and *Hyloxalus* sp. Inza (including the La Tatacoa population of Grant et al. 2017) are undescribed species (**Figure 34**).

Uncorrected pairwise 16S genetic distance between of *H. faciopunctulatus* and the remaining species of the *H. bocagei* group range from 6.5–15.6%, with the lowest values corresponding to *H. yasuni* (6.5–7.0 %). Similarly, the uncorrected pairwise 16S genetic distance between of *Hyloxalus* sp. Amazonas (CORBIDI 9423) and other species of the *H. bocagei* clade range between 3.3–14.1%, being most similar to *H. sauli* (3.3–3.4%); nevertheless, the three terminals of *H. sauli* used here (QCAZ16541, QCAZ16543, QCAZ27126), none of which are from the type locality (Santa Cecilia, Napo, Ecuador, 340 m), do not compose a monophyletic clade. Samples are from Yasuni National Park, Francisco de Orellana (QCAZ16541 and QCAZ16543) and from Río Arajuno, Napo, in Ecuador (QCAZ27126:). Genetic distance in 16S between Yasuni National Park samples is 0.0%, while between these samples regards the Río Arajuno is 1.5%. Although genetic distance is low, the phylogenetic relationship suggests different species within *H. sauli* and *Hyloxalus* sp. Amazonas. The taxonomy of *H. sauli* merits attention. Additionally, I added two terminal from Pongo de Rentema, Amazonas, Peru, 664 (MNCN 47510 and 47511) to *H. italoi*.

The *Hyloxalus subpunctatus* clade comprise similar species with oblique lateral stripes and unexpanded finger discs—*H. cepedai*, *H. felixcoperari*, *H.*

picachos, *H. sanctamariensis*, *H. subpunctatus*, *H. walesi* (see below), and five undescribed species (*Hyloxalus* sp. Aguabonita, *Hyloxalus* sp. *edwardsi* group, *Hyloxalus* sp. Junín, *Hyloxalus* sp. QuebradaWolf, *Hyloxalus* sp. Sumapaz). These species inhabiting the Andean slopes and the highlands of the Cordillera Oriental of Colombia. The clade is well-supported (GB = 58), and 16 unambiguous phenotypic transformations occur at this node, including the unexpanded finger III disc (character 6: 1), complete oblique lateral stripe (52: 1), granular ventrolateral body flanks (171: 1), basal subarticular tubercles on the fingers projected (178–181: 1), phalangeal swelling on the finger IV (197: 1), anterior projection of the suprascapula heavily calcified (122: 1), a shorter, less robust and well defined zygomatic (124: 3), and the anterior portion of the *m. compressor cloacae* uncovered and inserting anteriorly to the *m. pyriformis* (232: 1). In the larvae optimize the lateral eyes orientation (282: 0), rounded narial opening (285: 1), a conical vent tube (290: 0), and the acuminate tip of the *processus anterior dorsalis* in the suprarostral cartilage (328: 1). The adults prefer habits independent of streams (up to ca. 30 m or more from water. Character 108: 2. **Figure 35**).

The *H. edwardsi* group (*H. edwardsi*, *H. ruizi*, and the undescribed *Hyloxalus*. sp. *edwardsi* group; see Chapter 1 of this thesis) is represented by the *Hyloxalus*. sp. *edwardsi* in the phylogeny of this study. For this species optimize the presence of distal (on finger II and III) and hyperdistal (on finger IV and V) subarticular tubercles, and the anatomical transformations of the *m. sphincter ani cloacali* slip and the *m. rectus abdominis* origin. These are synapomorphies of the *H. edwardsi* group (see Chapter 1). Additionally, a bulk of phenotypic transformations provide support, including the finger V reaching the hyperdistal subarticular tubercle (character 191: 4), a robust *m. extensor carpi radialis* origin (238: 1), and the internal slip of this

muscle inserting at the external slip tendon insertion (239: 1). Unexpectedly, the terminal from Páramo de Sumapaz, Cundinamarca, Colombia (MAA 1401) that closely resembles *H. subpunctatus* is sister to the *Hyloxalus edwardsi* group (**Figure 35**). This relationship is well-supported node (GB = 28) and was recovered in all successive outgroup expansion (see above); however, the *Hyloxalus* sp. Sumapaz lacks of the external morphological synapomorphies of the *H. edwardsi* group (character 191: 4, 238: 1), but this share the presence of tarsal keel, extending to the inner metatarsal tubercle, with *H. ruizi*, *Hyloxalus* sp. edwardsi group. The *H.* edwardsi group + *Hyloxalus* sp. Sumapaz clade is sister to the cis-Andean clade of *H. cepedai*, *H. picachos*, and *H. sanctamariensis* instead with *H. picachos,* as found in the Chapter 1. This relationships lack of the phenotypic transformations, but molecular evidence support the node with GB = 19.

The recently described *Hyloxalus sanctamariensis* is positioned phylogenetically for first time, being sister to the *H. picachos* and *H. cepedai*. These species inhabit the eastern slope of the Cordillera Oriental of Colombia, between Caqueta to Boyacá departments. These are small species (SVL = 15–20 mm; unknown data for *Hyloxalus* sp. AguaAzul; Ardila-Robayo et al. 2000 "1999", Acosta-Galvis and Pinzón 2018, this study) with phalangeal swelling on the finger IV in the adult male (in contra of Acosta-Galvis and Pinzón 2018) and complete solid oblique lateral stripe (except in *H. cepedai,* partial and diffuse). High GB value (GB = 25) and 21 unambiguous phenotypic transformations support the clade (**Figure 35**), including the absence of the basal subarticular tubercle on the toe IV (character 207: 0), tadpoles with massive upper jaw sheath (263: 1), and larvae without white spots on the antero- and posteroventral body surface (315: 0, 317: 0). Other synapomorphies are reported in **Appendix 6**. Uncorrected pairwise genetic distances

in 16S supports the recognition of the three species (*H. cepedai*, *H. picachos* and *H. sanctamariensis*); therefore, the *Hyloxalus* sp. AguaAzul, erroneously considered as *H. ranoides* by Santos et al. (2009), and the terminal MAA 528 from Casanare are *H. cepedai* (see **Table 9**).

Most terminals in the following clade are representatives of the populations which had been considered as *Hyloxalus subpunctatus*, including the terminals assigned to the synonym *Phyllobates subpunctatus walesi* (Cochran and Goin 1970). This clade is well-supported (GB = 41) and only the occurrence of the dark lower labial stripe (56: 1) optimize as unambiguously phenotypic synapomorphy. Cochran and Goin described the subspecies *P. s. walesi* from the Andean Páramos of Boyacá department, Colombia, and distinguished it from *H. subpunctatus* on the basis the tibia length differences; however, Edwards (1971) synonymized it under *H. subpunctatus.* Currently, all populations resembling *H. subpunctatus* from the slopes of Cordillera Oriental and from the Altiplano Cundiboyasence, between 1750–4020 m., are including in this species (Ruiz-Carranza et al. 1996, Bernal and Lynch 2008, Anganoy-Criollo 2013). Nevertheless, Acosta-Galvis and Vargas-Ramírez (2018) described a new species, similar to *H. subpunctatus,* from San Francisco, Cundinamarca (2500 – 2577 m) as *H. felixcoperari*, too nested in the *H. subpunctatus* clade. They also discussed the taxonomic status of the TNHCF 4957 from Chiquinquira, Boyacá, and concluded that there are more than one species in the terminals named as *H subpunctatus.*

I increased the samples in *Hyloxalus subpunctatus* and the result reveals a diverse, cryptic morphological clade. Initially, the terminals from Bogotá and from neighbor localities (MAA 167, MAA1054, MUJ5212) form a clade, closely related to the *Hyloxalus* from western slopes of the Cordillera Oriental of Colombia, between

2142–2483 m (*H. felixcoperari, Hyloxalus* sp. Aguabonita, *Hyloxalus* sp. QuebradaWolf), and the sample *H. subpunctatus* TNHCF4957 is sister to this clade. Second, the populations from the Páramos of Boyacá (as *H. walesi* in the three, see below) are not closely allied to *H. subpunctatus* sensu stricto; in change, this is sister to the undescribed *Hyloxalus* sp. Junin (Junín, Cundinamarca, 2058 m) which occurs at eastern slope of this Cordillera. Both species are sister to the bracketed clade between *H. subpunctatus* TNHCF4957 and *Hyloxalus* sp. AguaBonita (**Figure 35**). Uncorrected pairwise 16S genetic distances between these populations are low, even though there are not overlap in the intraspecific genetic variation (**Table 10**). Furthermore, revision of the adults and tadpoles of these samples show morphological differences between these lineages; for example, *H. subpunctatus* s.s. differ from *Hyloxalus*. sp. Aguabonita and *Hyloxalus*. sp. Junin in foot morphology; the larval upper jaw sheath distinguish the *H. subpunctatus* s.s. from *Hyloxalus* sp. QuebradaWolf (in contra Anganoy-Criollo 2013). Moreover, the phalangeal swelling on the fingers III–IV, and on fingers III–V in the adult males of both *H. subpunctatus* s.s. and population from high-Andean Boyacá (or *P.s. walesi*) respectively, allow differentiate these species from their closely relatives. All of this phylogenetic, genetic and morphological evidence point to the lineage diversification within this clade, that in addition of the nominal species (*H. subpunctatus* and *H. felixcoperari*), allow recognized as undescribed species to *Hyloxalus* sp. Aguabonita, *Hyloxalus* sp. Junin and *Hyloxalus* sp. QuebradaWolf, and justify raise up to species level *Phyllobates subpunctatus walesi* Cochran and Goin (1970. See below). It is to note that there are two additional junior synonymies under *H. subpunctatus*, *Prostherapis variabilis* Werner (1899) and *Prostherapis tarsalis* Werner (1916); however, a careful revision of the type specimens of these species is necessary.

The next large division within of the genus is composed by the remaining species of *Hyloxalus*, the clade comprising between the *H. nexipus* to *H. littoralis,* here named as the *Hyloxalus pulchellus* clade. Despite the frequent topological changes of the *H. anthracinus*, *H. nexipus*, *H. sylvaticus* + *H pulcherrimus*, *H. shuar* + *H. idiomelus*, and *Hyloxalus* sp. Bongara + *Hyloxalus* sp. PAV, the monophyly and most of the internal relationships of this clade are stable in last three SOE analyses. The clade also have been recovers in previous studies (e.g., Grant et al. 2017, Santos et al. 2009, 2014, Santos and Cannatella 2011, Pyron and Wiens 2011, Pyron 2014, Jetz and Pyron 2018). Samples of the 23 nominal species compose it, including *H. anthracinus*, *H. arliensis, H. awa*, *H. azureiventris*, *H. chlorocraspedus*, *H. craspedoceps*, *H. delatorreae*, *H. elachyhistus*, *H. idiomelus*, *H. infraguttatus*, *H. insulatus*, *H. jacobuspetersi*, *H. lehmanni*, *H. littoralis*, *H. nexipus*, *H. pinguis*, *H. pulchellus*, *H. pulcherrimus*, *H. shuar*, *H. sylvaticus*, *H. toachi*, *H. vertebralis,* and the *"Colostethus" poecilonotus* (see below), and various undetermined and undescribed species. Species in this group has not toe webbed or toe are webbed basally, with exception of *H. nexipus*, who has extensive toe webbing. The rounded or ovoid inner metatarsal tubercle (character 221: 0) optimize ambiguously as phenotypic synapomorphy for the clade and this is supported with a high GB value (GB = 49. **Figure 36**). The type species of the two generic junior synonyms of *Hyloxalus* are in this clade, *H. pulchellus* type species of the *Phyllodromus* Jiménez de la Espada (1875), and *H. azureiventris* type species of *Cryptophyllobates* Lötters et al. (2000).

Hyloxalus nexipus is sister to all other remaining species of the *H. pulchellus* clade (**Figure 36**). This topological position is supported by high GB value (= 49). This relationships was optimally recovered in the study of Santos and Cannatella

(2011) and Guillory et al. (2019). However, Grant et al. (2006) recovered *H. nexipus* as sister to the *H. azureiventris* and *H. chlorocraspedus*. This relationship was consistent with external features—bright colored *Hyloxalus* with dorsolateral stripe. After, Santos et al. (2009) recovered *H. nexipus* sister to *H. anthracinus*, and these are sister to the clade bracketed between *H. vertebralis* to *H. awa.* This relationship is similar to their later studies, except that *H. anthracinus* and *H. sylvaticus* were no included in Santos et al. (2014). Grant et al. (2017) found *H. nexipus* embedded within *H. pulchellus* clade*,* branching between the clade of *H. pulchellus* and all other remaining species of this clade. This position also was recovered in Pyron and Wiens (2011) and Pyron (2014).

The taxonomic status of *Hyloxalus nexipus* Frost (1986) was discussed most recently by Santos et al. (2014). This species is distributed on the eastern slopes and foothills of the Andes of southern Ecuador and northern Peru (Coloma 1995, Duellman 2004). Duellman (2004) noted that Peruvian specimens inhabit lower elevations than Ecuadorian specimens, but did not detect any diagnostic characters. Grant et al. (2006) noted that the terminal sequenced by Santos et al. (2003) from near to Mendez, Morona Santiago, Ecuador (QCAZ 16534) differs from the San Martín, Peru terminal (KU 211806–08, KU 212486) in at least 45 transformation and, therefore, might not be conspecific. Likewise, Santos et al. (2014) found that the two Peruvian terminals (KU 211808, 212486) they analyzed are sister to the Ecuadorian terminal (QCAZ16537). Nevertheless, Grant et al. (2017) found the six Ecuadorian and Peruvian terminals they analyzed to form a polytomy. Uncorrected pairwise genetic distances between 16S of those terminals are larger when these are compared between Morona Santiago and San Martin populations, likewise within of this last

populations (**Table 11, Figure 36**). Clearly, additional research is necessary to resolve the species identity of these populations.

As part of this problem *Colostethus citreicola* Rivero (1991) is junior synonym of *H. nexipus*. In my morphological revision of *Hyloxalus*, I found no differences between the type material of *H. nexipus* and *C. citreicola*. Nevertheless, within *H. nexipus* populations, some adult characters do not match at least between northern and southern populations of this species, because one paratype (KU194164) plus the Amazonas, Peru population differ from San Martin populations in the ventrolateral stripe occurrence.

The next clade is formed by a pair of species, *Hyloxalus sylvaticus* and *H. pulcherrimus* with a well-supported (GB = 76). This clade is sister to the all other species of the *H. pulchellus* clade, but with a low GB value (GB = 1), although sharing eight unambiguous phenotypic transformations (**Figure 36**). The relationship as sister species was recovered previously (Grant et al. 2006, 2017. Santos et al. 2009, Pyron and Wiens 2011, Jetz and Pyron 2018), unlike to their topological position within the *H. pulchellus* clade. The position here recovered also was found by Santos et al. (2009), but other studies found this pair of species closely related to *H. anthracinus*, *H. delatorreae*, and/or *H. jacobuspetersi* (e.g., Grant et al. 2006, Pyron and Wiens 2011, Pyron 2014) like to the SOE analyses 3–5 and 7. In turn, Pyron and Wiens (2011) and Grant et al. (2017) found to *H. sylvaticus* and *H. pulcherrimus* closely related to either the *H. azureiventris* group or to the *H. pulchellus* group, respectively.

On the other hand, morphological distinction between *H. pulcherrimus* and *H. sylvaticus* was not provided by Duellman (2004: 34); however, Grant et al. (2006) found mitochondrial cytochrome B differences between these species. My

examination of the type material of both species show differences in the metacarpal ridge occurrence, finger II length, and the projection of the basal subarticular tubercles of the toes.

In the *Hyloxalus pulchellus* clade, the next clade is composed of similar species with oblique lateral stripe with middle and small size, distributed in the Andes of Colombia and Ecuador, *viz*., *H. anthracinus*, *H. arliensis*, *H. delatorreae*, *H. jacobuspetersi*, *H. lehmanni*, *H. pinguis*, *H. pulchellus*, *H. vertebralis* and the undetermined *Hyloxalus* sp. SanMiguelDeSalcedo, *Hyloxalus* sp. MonteOlivo, and the undescribed *Hyloxalus* sp. MesasGalilea and *Hyloxalus* sp. Alban. Five unambiguous larval phenotypic transformations optimize to this node (**Figure 36**. **Appendix 6**), which has GB = 15. The internal relationships of this group previously proposed are quite contrasting between studies (Santos et al. 2009, Pyron and Wiens 2011, Grant et al. 2017, see **Figure 27–28**). This is due to the variable topological position of *H. anthracinus*, *H. sylvaticus* + *H. pulcherrimus*, and *H. jacobuspetersi* + *H. delatorreae* (KU220621); however, there are some consistent relationships between previous phylogenies. For example, *H. jacobuspetersi* is sister of *H. delatorreae* (KU220621), and they are sister to the clade comprise by *H. arliensis*, *H. delatorreae, H. pulchellus*, *H. vertebralis*, *Hyloxalus* sp. SanMiguelDeSalcedo and *Hyloxalus* sp. MonteOlivo (Grant et al. 2017, Acosta-Galvis et al. 2020). *H. vertebralis* is sister of that clade in Santos et al. (2009), Grant et al. (2017), and Jetz and Pyron (2018). *H. arliensis* and *H. lehmanni* are sister species (Grant et al. 2017, Acosta-Galvis et al. 2020). Given these consistences, the *Hyloxalus pulchellus* group is restricted to the clade bracketed by *H. vertebralis* to *H. arliensis* (**Figure 36**).

Within the *Hyloxalus pulchellus* group, the *H. delatorreae* terminals are not closed relatives, because the KU220621 (of Grant et al. 2006) is clustered with *H.*

jacobuspetersi, and the other two *H. delatorreae* terminals (KU 220619 of Santos et al. 2009, and KJ940457 of Santos et al. 2014) are nested with *H. pinguis, H. pulchellus*, *Hyloxalus* sp. MonteOlivo, and *Hyloxalus* sp. SanMiguelDeSalcedo. This polyphyly was also recovered and discussed by Grant et al. (2017: S57), who noted that three KU specimens are paratypes (KU200619–21). My examination of the *H. delatorreae* type series did not revealed morphological differences, and the possible explanations provided by Grant et al. are not discarded, that is, that two species are in *H. delatorreae* or one of the aliquoted are not of this species.

Hyloxalus H. arliensis and *H. lehmanni* were included in the polyphyletic *H. ramosi* group on the basis the shared presence of the black arm gland (swelling on the distal end of the upper arm and lower arm; character 205 herein; Grant and Castro1998, Grant et al. 2006, Grant et al. 2007). Now are nested within the *H. pulchellus* clade, and the black arm gland is homoplastic, because this occurs in other distantly related *Hyloxalus* to the *H. arliensis* and *H. lehmanni* (e.g., *H. anthracinus*, *H. nexipus*). However, this external swelling is also found in other two species of the *H. pulchellus* group, the undescribed *Hyloxalus* sp. Alban and *Hyloxalus* sp. MesasGalilea, closely related to *H. arliensis* and *H. lehmanni.* My histological studies indicate that adult male *H. pinguis,* which lack conspicuous swelling or dark skin, also possess glandular modifications in this region (e.g., glandular integument with cluster of hypertrophied mucous glands) also present in *H. lehmanni* (see Chapter 3). The other species related to *H. pinguis* (i.e., *H. delatorreae*, *H. pulchellus*, *Hyloxalus* sp. SanMiguelDeSalcedo, *Hyloxalus* sp. MonteOlivo) also lack arm swelling, but histological data are necessary to determine if the specialized mucous glands are also absent. *H. vertebralis* sister to this clade, also lack of the arm swelling.

Rivero and Granados-Diaz (1990) described *Colostethus pinguis* (now *Hyloxalus*, Grant et al. 2006) from high elevation of the Cordillera Central of Colombia in Cauca department (Malvasa, Valle de Paletará, Totoró, Cauca 2995 m). Additionally, populations from southwestern Colombian have also been referred to *H. pulchellus* (as *Colostethus taeniatus*, which is a junior synonym of *H. pulchellus*, Ruiz-Carranza et al. 1996: 378, Acosta-Galvis 2000: 297–298, Anganoy-Criollo 2013), generating uncertainty in the taxonomic status of the *H. pinguis*. Terminals identified as *H. pinguis* here (GAP 195, MAA 1248–1250) are sister to the *Hyloxalus* sp. MonteOlivo instead *H. pulchellus* (**Figure 36**). Moreover, uncorrected pairwise 16S genetic distance between of these three populations are consistent with the recognition of two species, *H. pinguis* and *H. pulchellus* (**Table 12**). In addition, Coloma (1995: 47) reported morphological differences between individuals of *Hyloxalus* sp. MonteOlivo and *H. pulchellus*.

I added phenotypic similar samples to the clade of *Hyloxalus lehmanni* (Silverstone 1971) and *H. arliensis* Acosta-Galvis et al. (2020). *H. lehmanni* is widely distributed in the Andean forest of the Cordillera Central and Occidental of Colombia, and the northwestern Andes of Ecuador. Coloma (1995) suspected that Ecuadorian populations are not con-specified with *H. lehmanni,* but until date diagnostic morphological characters are unknwon between these populations (Coloma 1995, Grant and Castro 1998, Grant and Ardila 2002). The type locality of *H. lehmanni* falls in northern extreme of the Cordillera Central Colombia (Santa Rita, Antioquia, Colombia), and the sample of *H. lehmanni* analyzed by Grant et al. (2017) is from eastern flank of the middle Cordillera Central, 2450 m (Herrera, Rio Blanco, Tolima). Conversely, the two terminals analyzed here are from Farallones de Cali on eastern Cordillera Occidental, 2430 m (FC 656–657). Both localities far from the type

locality. The three terminals are clustered in a clade (**Figure 36**); however, uncorrected pairwise genetic distances in 16S provide evidence of the two lineages in the samples considered as *H. lehmanni* (**Table 13**). Additional data from the type locality and throughout its distribution are necessary to resolve this problem.

Hyloxalus arliensis Acosta-Galvis et al. 2020 was included in previous analyses as *Hyloxalus* sp. Ibagué (Grant et al. 2006). Adults resemble *H. lehmanni*, and both species were found as sister taxa (Grant et al. 2017; this study), but the species differ in size and genetic distance in the 16S (Acosta-Galvis et al. 2020), and moreover in the extension of the arm swelling. *H. arliensis* inhabits the eastern slope of the Cordillera Central of Colombia at Tolima department and the western slope of Cordillera Oriental, at Boyacá, Cundinamarca and Santander departments, between 565–1300 m. of elevation (Grant et al. 2006, Acosta-Galvis et al. 2020). Here, I added 10 more terminals that resemble *H. arliensis* from Tolima (Ibagué, Libano, Villarica municipalities) and Cundinamarca (Albán and Caparrapí municipalities) departments. The optimal tree recovers the samples from Ibagué (DFZ411, 413), Libano (MAA 1381, 1400B), and Caparrapí (RC 1423, 1439) embedded among *H. arliensis* terminals, with low 16S genetic distances, corroborating their conspecificity. Nevertheless, terminals from Villarica (*Hyloxalus* sp. MesasGalilea, MAA 1272, 1281, 1283) and Albán (*Hyloxalus* sp. Alban ANDES-A 2923) form the sister clade of *H. arliensis,* and the 16S distances are high (**Table 13**). These findings corroborate Grant and Ardila-Robayo's (2002: 258) observation that the taxonomy these species is unresolved and there are still several apparently undescribed species.

Two undetermined species of northern Peru comprise the sister clade to remaining Ecuadorian and Peruvian *Hyloxalus* (**Figure 37**). The *Hyloxalus* sp. PAV (CORBIDI 11007) is from Laguna de los Condores, San Martín department, 2826 m,

while the *Hyloxalus* sp. Bongara (CORBIDI 12891) is from Catarata La Chinata, Amazonas department, 1984 m. The node have a GB = 32 and the relationship with other species of *H. pulchellus* clade is supported with a GB = 21. Uncorrected pairwise distance between 16S of these samples (7.2%) provide support to recognized two species. Individual of these species look like to *H. idiomelus*; however, the last is distantly related, and nested with *H. shuar*.

The *Hyloxalus azureiventris* clade is compose by *H. azureiventris* (Kneller and Henle 1985), *H. chlorocraspedus* (Caldwell 2005), *H. craspedoceps* (Duellman 2004), *Hyloxalus* sp. ElCopal, and by the first-time analyzed "*Colostethus" poecilonotus* Rivero (1991). This species will transfer to their respective genus below. "*C." poecilonotus* remained as *incertae sedis* in Dendrobatoidea from Grant et al. (2006) to nowadays, because they were unable to allocate this species in any of their genera due to the lack of evidence. Rivero (1991) described "*C." poecilonotus* from Utcubamba Valley, between Bagua Grande Alva to Chachapoyas, Amazonas, Peru, 500 m. The available sample come from a neighboring site, La Peca, Bagua, Amazonas department, Peru 1405 m. In spite the elevation difference, the adult morphology of this population agrees with paratypes MCZ89106–07, confirming its identity. Within *H. azureiventris* clade, three species of this group have a dorsolateral stripe (data unknown for *Hyloxalus* sp. ElCopal), and two of them (*H. azureiventris*, *H. chlorocraspedus*) are brightly colored. "*C." poecilonotus* is sister to the last two species; however in contrast with these, this species has complete oblique lateral stripe, lack dorsolateral and ventrolateral stripes, and the adults of this population has brown coloration, except that some individuals has yellow spots on the hidden body parts (axilla, groin, and tarsus) and blue blotches at the ventrolateral abdomen. The relationship between these three species is supported by GB value = 15, and five

unambiguous phenotypic transformations (**Figure 37**): a projected distal subarticular tubercle of finger IV (character 182: 1), projected basal subarticular tubercle of toe I–III (character 209 – 211: 1), and projected proximal subarticular tubercle of toe III (character 214: 1).

Previous studies recovered *Hyloxalus azureiventris* sister to the *H. chlorocraspedus*, but their close relatives varies between hypothesis; thus for example, *H. nexipus* was considered part of this group (Grant et al. 2006), *Hyloxalus* sp. ElCopal is or is not closely allied (Santos et al. 2009, Grant et al. 2017, respectively), and in other cases *H. craspedoceps* is member of this group (Grant et al. 2017, Jezt and Pyron 2018). Furthermore, based on phenotypic resemblance, Grant et al. (2006) suggested included in this group to *H. patitae* (Lötters et al. 2003a) and *H. eleutherodactylus* (Duellman 2004). Likewise, other species that can be part of this group is *H. exasperatus,* because morphologically is similar to the species of this group (e.g., dorsolateral stripe present). Moreover, the occurrence of the dark swelling on the distal upper arm (former black arm gland) in the adult males of *H. craspedoceps,* also is present in *H. exasperatus*.

Additionally, the analyzed samples of *H. craspedoceps* show differences in uncorrected pairwise genetic distance between 16S of the analyzed population, i.e., between terminal of Chazuta, Peru (MNCN 47538–39) and of Lamas–San Jose de Sisa, Peru (CORBIDI 6804, MHNSM 22882. **Table 14**). These values surpass the intra-population variation and suggesting more than one species are probably involved, despite the geographic nearness.

Two phenotypic transformations and GB = 6 optimize at the node of the clade of the Ecuadorian *Hyloxalus shuar* and the Peruvian *H. idiomelus.* Both species are sister to the *H. infragruttatus* and *H. elachyhistus* clades (**Figure 38**). This

relationship also was recovered by Grant et al. (2017). Although other studies found the same position, these used only *H. idiomelus* (Santos et al. 2009, Pyron and Wiens 2011, Jetz and Pyron 2018). Nonetheless, SOE analysis show one additional placement, as sister only to the *H. elachyhistus* clade, and the monophyly of this clade was not recovered in analysis 7. I corroborated the morphological differences reported in *H. shuar* populations by Coloma (1995: 51), that is, there are differences in hand, foot and ventral coloration differences between populations, which guarantee a further revision of this species.

The *Hyloxalus infraguttatus* clade is compose by three nominal species, *H. awa*, *H. infraguttatus*, *H. toachi,* and two undetermined terminals, *Hyloxalus* sp. Moraspungo, *Hyloxalus* sp. Masvalle, all from the Ecuadorian pacific slope. The clade is well-support (GB = 19); however, no unambiguously phenotypic synapomorphies optimize at node. The internal relationships of this group have been recovery previously (Santos et al. 2009, 2014, Pyron and Wiens 2011, Grant et al. 2017, Jetz and Pyron 2018). This clade is sister to the *H. elachyhistus* clade, supporting in a GB = 7 and three larval phenotypic unambiguous transformation (**Figure 38, Appendix 6**). This relationships was recovered in previous studies (Grant et al. 2006, 2017, see also Santos et al. 2009, 2014, Pyron and Wiens 2011, Pyron 2014, Jetz and Pyron 2018). The SOE analysis show other sister group relationship, because the *H. infraguttatus* clade also is sister to the *H. shuar* + *H. idiomelus* and *H. elachyhistus* clade (**Figure 27–28**).

The *Hyloxalus elachyhistus* clade is the last large clade in the *H. pulchellus* clade. This group contains the *H. elachyhistus*, *H. insulatus* and *H. littoralis*, and the undescribed species *H. elachyhistus*_Cajamarca, *H. elachyhitus*_Lambayaque, *H. insulatus*_Amazonas, all of these with two dark marks on gular-chest region of the

adults and oblique lateral stripe. This node is supported by a GB = 7, and 16 unambiguous phenotypic transformation (**Figure 39**). Within this clade, the terminals assigned to *H. elachyhistus* are monophyletic, except by the *H. elachyhistus* from Cajamarca, Perú which is sister to *H. insulatus* and *H. littoralis* (also see Grant et al. 2006). My study included samples named as *H. elachyhistus* representatives of the southern Ecuador and northern Peru populations; however, complex species and taxonomic difficulties had been recognized in *H. elachyhistus* (Coloma 1995, Grant et al. 2006). Grant et al. (2006: 139) concluded that the population of Piura, Perú is *H. elachyhistus*, while the Cajamarca population is a new species. The uncorrected pairwise distances of 16S analyzed herein reinforce the result of Grant et al., because there is 6.1–6.9 % of difference between Piura and Cajamarca populations (**Table 15**), which not overlap with intrapopulation genetic variation (0.0–2.4%). Piura is the nearest site to the type locality of this species (Loja, Loja, Ecuador, 2150 m; 52 km airline distance), then the Piura lineage (KU 212514–17) could be considered as *H. elachyhistus* (see also Duellman and Wild 1993, Grant et al. 2006). Furthermore, the three terminals from Torata–Balsas road, El Oro province (QCAZ16517–18, KU 212507) are not nested in a clade, because the KU 212507 terminal is sister to the terminal from Lambayaque, Perú (CORBIDI 4292). In change, the QCAZ16517–18 are closely related to the Piura lineage. Genetic distances of 16S between the KU 212507 + CORBIDI 4292 and others *H. elachyhistus* clades reveal values at interspecific level, justify the recognition of the other species within this species (**Table 15**). Difference in temporal variables in the advertisement call between the Lambayaque, Piura and Cotopaxi lineages provide support to the complex species within *H. elachyhistus* (Koch et al. 2011, Santos et al. 2014: supplementary material 2). Despite the progress made in *H. elachyhistus*, DNA data from type locality of this

species are not available yet; however, in the light of the current results, the molecular data from the type locality are necessary to resolve the taxonomic problem.

Duellman (2004) described *Colostethus insulatus* from middle elevation of the Marañon Valley, Perú (1260–2600 m). In this study, this species is part of the *H. elachyhistus* clade, sister to the Peruvian *H. littoralis*, unlike to Grant et al. (2006, 2017) who found the *H. insulatus* sister to the *H. elachyhistus* Cajamarca. Additionally, the terminals assigned to *H. insulatus* herein are non-monophyletic, because the specimens from Bolivar, La Libertad (2653 m, CORBIDI 5650) and Limón, Celedín, Cajamarca (2092 m, CORBIDI 5656) are closely related to *H. littoralis* instead of the remaining terminals of *H. insulatus,* which compose a clade. These remaining *H. insulatus* terminals are from the northern of the distribution of this species, between Pedro Ruiz Gallo, Bagua, and La Peca (Amazonas department), and from Jaen (Cajamarca department. **Figure 39**). The uncorrected pairwise distance between 16S of these groups (2.3–2.8%) are relatively low among *Hyloxalus* (see above), but these surpassing the intraspecific variation (0.0 % and 0.1 %), suggesting the existence of more than one species within *H. insulatus* (**Table 16**). Molecular data of the type locality of *H. insulatus* (17 ENE from Balsas, Chachapoyas, Amazonas) are not available; however, besides the geographic proximity to the type locality, the adult morphology of the individuals of Limón and Bolivar (CORBIDI 5650, 5656) agrees with type material and in consequence herein these are considered as *H. insulatus*. In change, the population from Amazonas and Cajamarca needs additional information to corroborate its specific status.

Finally, the last species of the *Hyloxalus elachyhistus* clade is the poorly known *H. littoralis* (Péfaur 1984). Records of this species show a disjunct distribution. This species was described from a pond in Chorrillos, on the coast of

Lima, about the sea level, 5 m (Péfaur 1984). Now, population of the type locality is loss, but the species also was recorded in the Pantanos de Villa, Chorrillos, Lima, and also in Huánuco (2100–2800 m) and Ancash (3100 m) departments (Morales 1998). Morales (1998) compared the Lima population regards Andean populations (Huánuco and Ancash), and on the basis the vocalization, morphology and coloration similarities, he concluded that all populations are *H. littoralis.* Moreover, on the basis of the distribution of the most *Hyloxalus* species of Peru (then-*Colostethus*), Morales though that the type locality population was introduced, while the Andean populations are naturals. The Andean localities are far away from type locality (roughly of 260 kms in northeastern direction and 375 kms in north direction of Lima in airline distance, respectively), these are at higher elevation and has Andean ecosystems. Additional records between the coast and the Andes have been provided (Aguilar et al. 1997, Lerh et al. 2002). Herein, I included terminals from Lima (Pantanos de Villa, 3 m. of elevation) and Huánuco (Chinchao and Pachitea, 970 – 2739 m), and these form a clade (GB = 13. **Figure 39**), and astonishingly, the uncorrected pairwise genetic distances between 16S of these samples are low and supports considered as one species (**Table 16**). On the other hand, although Duellman (2004) do not provided a diagnosis of *Hyloxalus insulatus* from *H. littoralis*, and the adults of both species are relatively similar, the genetic distances between species is 1.2–1.5 %, without overlapping with the intrapopulation variation (0.0–0.1%); furthermore, morphological differences in toe webbing justifying the recognition of these species as independent lineages.

Toward a Monophyletic *Hyloxalus* Taxonomy

Hyloxalus is a large, diverse, phenotypically heterogeneous genus in Dendrobatoidea. Grant et al. (2006) resurrected this generic name for the clade of

Dendrobatidae that contain roughly half species of the then-*Colostethus* sensu lato. Given the large species content and variability in *Hyloxalus*, they anticipated that "additional partitioning [of *Hyloxalus*] will be warranted as knowledge of the group increases (Grant et al. 2006: 169)". Ten years after, Grant et al. (2017) showed that other dendrobatoids species are part or closely related to the *Hyloxalus* rather Aromobatidae or Colostethinae. Thereby, Grant et al. (2017) redefined *Hyloxalus* with the inclusion of the species with phalangeal swelling on the finger IV (e.g., *H. cepeda*i, *H. picachos*), they proposed *Ectopoglossus* for the trans-Andean species with the median lingual process, and resurrected *Paruwrobates* Bauer (1994) to include two Andean species before located in *Ameerega*.

Grant et al. (2006) also noted that in *Hyloxalus* there are type species of the other available generic names synonymized with *Hyloxalus. H. pulchellus* the type species of *Phyllodromus* Jiménez de la Espada (1875), and *H. azureiventris* the type species of *Cryptophyllobates* Lötters, Jungfer, and Widmer (2000). *Hylixalus* Boulenger (1882b) is a junior objective synonym of *Hyloxalus* (Grant et al. 2006, Myers and Grant 2009). Both type species (*H. pulchellus* and *H. azureiventris*) were included in this study; however, the type species of *Hyloxalus* (*H. fuliginosus* Jiménez de la Espada 1871''1870'') was not analyzed, because genotype data are not available until now. Nevertheless, adult of the *H. fuliginosus* resembles to *H. bocagei* and their relatives (i.e., *H. bocagei* clade) with subtle differences between them, which suggests propinquity, as concluded previously Coloma (1995), Grant et al. (2006), and Páez-Vacas et al. (2010). Thus *H. bocagei*—the subsequent older name in the *H. bocagei* clade—can be treated as a proxy of *H. fuliginosus* (Grant et al. 2006) and therefore *Hyloxalus* Jiménez de la Espada can apply to the clade of *H. bocagei.*

Otherwise, whether this relationship will not be corroborated, taxonomic rearranged are necessary.

Moreover, the taxon and character sample was increased in *Hyloxalus* in this study, revealing the monophyly of *Hyloxalus*, and also recovering the monophyly of the three large clades—*Hyloxalus bocagei* clade, *H. subpunctatus* clade, *H. pulchellus* clade. These clades were insensitive to the successive outgroup expansion, maintaining consistently the specific content in each analysis. Most internal relationships in the *H. pulchellus* clade were stable, with exception of the frequent change position of *H. anthracinus*, *H. nexipus*, and the clade *H. sylvaticus* + *H. pulcherrimus*, *H. shuar* + *H. idiomelus*, and *Hyloxalus* sp. Bongara + *Hyloxalus* sp. PAV. Unambiguous phenotypic synapomorphies optimize in each large clade, which allows for a reliable diagnosis. Therefore, in the light of our finding, *Hyloxalus* is divided to recognize the three large clades as generic units. I give to each clade the oldest available generic name; nevertheless for the nonce, in one clade I maintained the unnamed group. Furthermore, the content of each genus/group is based on the species employed in this study. For a few species, I used phenotypic evidence as well as possible to allocate the species otherwise these are left as *incertae sedis* within Hyloxalinae.

SUBFAMILY: **Hyloxalinae** Grant et al. 2006: 5, 168.

Type genus.—*Hyloxalus* Jiménez de la Espada 1871 “1870”, by implicit etymological designation by Dubois (2017).

Immediately more inclusive taxon.—Dendrobatidae Cope, 1865

Sister group.—Dendrobatinae Cope (1865).

Content.—Four genus and a species group: *Ectopoglossus*, *Hyloxalus, Paruwrobates*, *Phyllodromus*, and the “*Hyloxalus*” *subpunctatus* group.

Diagnosis and support.—Goodman-Bremer value = 54. My analysis recovered one unambiguous phenotypic synapomorphies for the subfamily, toe V reaching the proximal subarticular tubercle of the toe IV (character 226: 1). Most of the evaluated hyloxalinaes have this condition; however, in a few species (in *H. azureiventris, H. leucophaeus, H. picachos, H. pulchellus* group (except, *H. pinguis*), *H. sanctamariensis, H. toachi,* and "*C." poecilonotus*) the toe V do not reach the proximal subarticular tubercle of the toe IV. Only in *Ectopoglosus ithsminus,* the toe V surpasses the proximal subarticular tubercle of the toe IV.

The characterization and diagnosis provided for *Hyloxalus* by Grant et al. (2006: 169), and consequently applied to their Hyloxalinae subfamily, is applicable in this case, except for the swelling on the finger IV in some species (see below).

Comments.—In the current proposal, Hyloxalinae encompasses four genera plus one clade without a generic name; however, various species of the subfamily remain without assignation to one of these clades. In another case, the species assignation is tentative.

GENUS: ***Ectopoglossus*** Grant et al. 2017: S11.

Type species.—*Ectopoglossus saxatilis* Grant et al. (2017: S18) by original designation.

Immediately more inclusive taxon.—Hyloxalinae Grant et al. (2006).

Sister group.—*Paruwrobates* Bauer (1994).

Content.—*Ectopoglossus absconditus* Grant et al. (2017), *E. astralogaster* (Myers et al. 2012), *E. atopoglossus* (Grant et al. 1997), *E. confusus* (Myers and Grant, 2009), *E. isthminus* (Myers et al. 2012), *E. lacrimosus* (Myers, 1991), and *E. saxatilis* Grant et al. (2017).

Diagnosis and support.—Goodman-Bremer value = 78. Unambiguous phenotypic synapomorphies optimizing for this genus are: (1) dorsal skin smooth posteriorly (character 0: 0), (2) palmar skin loose (1: 1), (3) toe disc II weakly expanded (27: 1), (4) fringe on preaxial toe I (31: 1), (5) one phalanx free of the webbing on the postaxial toe I (32: 4), (6) one phalanx free of the webbing on the postaxial toe III (36: 6), (7) two phalanges free of the webbing on the preaxial toe IV (37: 6), (8) two phalanges free of the webbing on the postaxial toe IV (38: 6), (9) one phalanx free of the webbing on the preaxial toe V (39: 5), (10) fringe on postaxial toe V (40: 1), and (11) median lingual process present (76: 1). In addition, there is a dorsal and preaxial swelling along phalanges of the finger IV in adult males of *Ectopoglossus atopoglossus* (KU 289252) and *E. absconditus* (KU 189526); testis is large (0.9–1 of kidney length) in adult males of *E. atopoglossus*, *E. confusus*, and *E. ithsminus*; and there is a large serous gland in the dots on the ventral skin of *E. astralogaster, E. confusus,* and *E. saxatilis*.

Comments.—Diagnosis from closely related genera of Grant et al. (2017: S12) is adequate (but see comment above). Genus composition is unmodified from Grant et al. (2017) given that additional new molecular data are unavailable, because the populations and species are threatened, and these suffer drastic local reduction (see Coloma 1995, Grant and Bolivar 2014), or the type localities of some species are in away areas or with socio-politicals problems (e.g., the Pacific slope of Colombia).

Relationships within *Ectopoglossus* are unknown, but a close relationship based on median lingual process morphology was proposed by Grant et al. (2017). *E. atopoglossus*, *E. confusus* and *E. lacrimosus* (or South American group) have elongated, tapered, bluntly pointed, posteriorly reclined, non-retractile MLP. In change *E. absconditus*, *E. astralogaster*, *E. ithsminus,* and *E. saxatilis* (Middle

American group) have a low, blunt, bump-like, retractile MLP. My revision show variation in the internal slip origin of the *m. extensor carpi radialis* in *Ectopoglossus*. The origin is robust in *E. atopoglossus* and *E. lacrimosus*, while it is thin in *E. confusus,* suggesting a sister species relationship in the south American clade. Additional evidence (e.g., molecular data) is necessary to test the internal relationships.

GENUS: ***Hyloxalus*** Jiménez de la Espada 1871 "1870".

Type species.—*Hyloxalus fuliginosus* Jiménez de la Espada 1871 "1870" by subsequent designation of Savage (1968).

Immediately more inclusive taxon.—Hyloxalinae Grant et al. (2006)

Sister group.—*Hyloxalus subpunctatus* group, as defined here.

Content.—*Hyloxalus bocagei* Jiménez de la Espada (1871 "1870"), *H. excisus* (Rivero and Serna 2000 "1995"), *H. faciopunctulatus* (Rivero 1991), *H. fuliginosus* Jiménez de la Espada (1871 "1870"), *H. italio* (Páez-Vacas et al. 2010), *H. leucophaeus* (Duellman 2004), *H. maculosus* (Rivero 1991), *H. sauli* (Edwards 1974), *H. sordidatus* (Duellman 2004), *H. vergeli* (Hellmich 1940), *H. yasuni* (Páez-Vacas et al. 2010).

Diagnosis and support.—Goodman-Bremer value = 1. Unambiguous phenotypic synapomorphies optimizing for this genus are: (1) fringe on the preaxial side of the finger III (character 11: 1), (2) fringe on the preaxial side of the finger IV (13: 1), (3) fringe on the preaxial side of the toe I (31: 1), (4) one phalanx free of the webbing on the postaxial of the toe I (32: 4), (5) two phalanges free of the webbing on the preaxial of the toe II (33: 2), (6) three or three and half phalanges free of the webbing on the postaxial of the toe IV (38: 3/4), (7) one phalanx free of the webbing on the preaxial of the toe V (39: 5), (8) fringe on the postaxial side of the toe V (40:

1), (9) presence of palatines (126: 1), and (10) nasal and sphenethmoid bones separated (129: 0).

Comments.—This clade was first recognized by Páez-Vacas et al. (2010) for cis-Andean webbed species related to the *H. bocagei, H. fuliginosus, H. maculosus*; moreover, they supposed that other unsequenced phenotypically similar species can be part of this group, such as *H. faciopuntulatus* and *H. vergeli*. Subsequent studies recovered the group, revealed that this was paraphyletic, and included the trans-Andean *H. vergeli* (Grant et al. 2017, Pyron 2014). Different relationships for the *H. leucophaeus* + *H. sordidatus* have been proposed, because sometimes these are closely related to *H. subpunctatus* clade (Pyron and Wiens 2011, Santos et al. 2014, Jetz and Pyron 2018) or these are closely related to the *H. bocagei.* The last relationship was corroborated in the current proposal, being either sister to *H. sauli* (Grant et al. 2017) or *H. maculosus* (this study).

Species in the current *Hyloxalus* have extensive toe webbing; nevertheless, there are additional species with this feature in Hyloxalinae, for example, "*H" nexipus* that is part of other genus recognized herein (see below) or also in most species of the genus *Ectopoglossus*. Moreover, other unsequenced species have toes extensively webbed, such as *H. abditaurantius*, *H. betancuri*, and *H. chocoensis*, which resemble species of the current *Hyloxalus*; however, these possess other character-states (e.g., throat coloration, dorsolateral stripe) absent or uncommon in this genus, which cause doubts of their close to *Hyloxalus*. Thus, I left these species as *incertae sedis.*

GENUS: ***Paruwrobates*** Bauer 1994.

Type species.—*Paruwrobates andinus* (Myers and Burrowes 1987) by original designation.

Immediately more inclusive taxon.—Hyloxalinae Grant et al. (2006).

Sister group.—*Ectopoglossus* Grant et al. (2017).

Content.—*Paruwrobates andinus* (Myers and Burrowes 1987), *P. erythromos* (Vigle and Miyata 1980), *P. whymperi* (Boulenger 1882a).

Diagnosis and support.—A single species, *Paruwrobates erythromos*, was included in present phylogenetic analysis. The diagnosis of Grant et al. (2017: S24) is adequate, except that *P. andinus* possess a short, bump-like, blunt retractile median lingual process.

Comments.—The characters and molecular data (taken from Vigle et al. 2020) were increased for *Paruwrobates erythromos*, without generating changes in the known phylogenetic placement. The detection of the MPL in *P. andinus* was unexpected because in the literature (i.e., Myers and Burrowes 1987, Grant et al. 2006) was reported as absent. They employed the type series specimens deposited at Instituto Alexander von Humboltd (IAvH) and the herpetology collection of the Kansas University (KU) available until now; nevertheless, five additional specimens were deposited in the private collection Reserva Natural La Planada (type locality; see Myers and Burrowes 1987: 2). In the year 2002, this collection was donate to the Colección Zoológica of the Universidad de Nariño, Pasto, Colombia (PSO-CZ). I revised this collection and found three *P. andinus* with MPL (PSO-CZ 623, 625, 627), another with a pit (PSO-CZ624) and others have not the process neither pit (PSO-CZ 626), likewise the paratype KU 212533. Additionally, the adult male of this species has a weak phalangeal swelling on the Finger IV and dots on the ventral skin. Nonetheless, the other two *Paruwrobates* lack these characters (see also Vigle and Miyata 1980, Myers and Burrowes 1987, Coloma 1995, Grant et al. 2006). I reviewed a few specimens of each species (four *P. erythromos*, one *P. whymperi*) which may

be insufficient material to detect the discussed character-states because in the dendrobatoids is well-known that detection of the swelling fingers and a retractile MPL depends of the examination of multiple adult males.

Myers and Burrowes (1987) get attention on the advertisement calls to test the sister species hypothesis between *Paruwrobates andinus* and *P. erythromos*. Due to the call of *P. andinus* was unavailable for this time, they only described call of *P. erythromos* and defined this as "a long train of harsh but not very loud chirps" or retarded chirp call, which is only display by this species (Grant et al. 2017: S25). Recently, De la Riva et al. (2020) provided call description of *P. andinus* and although they compared with *P. erythromos*, *Ectopoglossus*, and *Ameerega* species, they do not discuss whether calls support closely related species hypothesis neither stressed if it is a retarded chirp call; nevertheless, similarity was explicit (p. 184)". Despite of the noise in *P. andinus* call (see De la Riva et al. 2020: Figure 2), a re-examination of the calls of both *Paruwrobates* show that these are a series of repetitive short notes, notes are spectrally pulsed with frequency modulate, around of 4.1–4.7 Khz (see details in Myers and Burrowes 1987, De la Riva et al. 2020), which can be considered as support for a retarded chirp call in *P. andinus*. Whether sister relations between *P. andinus* and *P. erythromos* is corroborated, then the MPL, swelling on Finger IV and dots on ventral skin would be shared between *Ectopoglossus* + *Paruwrobates*; otherwise, the phylogenetic value of this call type is limited.

Larval morphology is another potential source of evidence to test relationships. The phylogenetic significance has been highlight in Dendrobatoidea (Silverstone 1976, Anganoy-Criollo and Cepeda Quilindo 2017, Dias et al. 2021). Wassensug and Heyer (1988) analyzed the internal oral morphology of the larvae of

P. whymperi (but species identity is doubtful, see Coloma 1995 and Grant et al. 2017); unfortunately, larvae of the other *Paruwrobates* are unknown to test its phylogenetic relevance.

The content of *Paruwrobates* with three species is maintained in this study, given the phenotypic resemblance between species (see Myers and Burrowes 1987: 16, Coloma 1995: 56, Grant et al. 2017: S24); although, the arguments above discuss warrant a genus revision,, including other types of evidence (e.g., genetic data). A potential species to be part of this genus is *Ectopoglossus absconditus.* This species is phenotypically similar to *Paruwrobates,* because in addition to the occurrence of the dorsolateral stripes, and absence of the toe webbing (see Grant et al. 2017: S15), this species has a short, blunt, bump-like retractile MPL, which are shared with *P. andinus*; nevertheless, the synapomorphic loose palmar skin of *Ectopoglossus* is against of this hypothesis. This is but proof of our limited knowledge about phylogenetic relationships in these genera.

GENUS: ***Phyllodromus*** Jiménez de la Espada (1875).

Cryptophyllobates Lötters, Jungfer, and Widmer (2000). Type species, *Phyllobates azureiventris* Kneller and Henle (1985), by original designation.

Type species.—*Phyllodromus pulchellum* Jiménez de la Espada (1875), by monotypy.

Immediately more inclusive taxon.—Hyloxalinae Grant et al. (2006)

Sister group.—Unnamed clade composed by *Hyloxalus* Jiménez de la Espada (1871 "1870") and "*Hyloxalus" subpunctatus* group.

Content.—*Phyllodromus anthracinus* (Edwards 1971) **new combination**, *P. arliensis* (Acosta-Galvis et al. 2020) **new combination***, P. awa* (Coloma 1995) **new combination**, *P. azureiventris* (Kneller and Henle 1985) **new combination**, *P.*

chlorocraspedus (Caldwell 2005) **new combination**, *P. craspedoceps* (Duellman 2004) **new combination**, *P. delatorreae* (Coloma 1995) **new combination**, *P. elachyhistus* (Edwards 1971) **new combination**, *P. idiomelus* (Rivero 1991) **new combination**, *P. infraguttatus* (Boulenger 1898) **new combination**, *P. insulatus* (Duellman 2004) **new combination**, *P. jacobuspetersi* (Rivero 1991) **new combination**, *P. lehmanni* (Silverstone 1971) **new combination**, *P. littoralis* (Péfaur 1984) **new combination**, *P. nexipus* (Frost 1986) **new combination**, *P. pinguis* (Rivero and Granados-Díaz 1990) **new combination**, *P. poecilonotus* (Rivero 1991) **new combination**, *P. pulchellus* (Jiménez de la Espada 1875), *P. pulcherrimus* (Duellman 2004) **new combination**, *P. shuar* (Duellman and Simmons 1988) **new combination**, *P. sylvaticus* (Barbour and Noble 1920) **new combination**, *P. toachi* (Coloma 1995) **new combination**, *P. vertebralis* (Boulenger 1899) **new combination**.

Diagnosis and support.—Goodman-Bremer value = 49. One phenotypic character-state optimize ambiguously as synapomorphy, (1) the rounded or ovoid inner metatarsal tubercle (character 221: 0). In addition, the species of this group are characterized by: (1) dorsal skin granular posteriorly, (2) ventrolateral body skin smooth, (3) antebrachial tubercle present commonly, (4) complete pale oblique lateral stripe (absent in *P. chlorocraspedus*, and partial in *P. azureiventris, P. craspedoceps, P. nexipus*), (5) dorsolateral stripe absent (except *P. azureiventris, P. chlorocraspedus, P. nexipus*), (6) ventrolateral stripe usually absent (except a B-type VLS present in *P. arliensis P. delatorreae, P. lehmanni, P. toachi*), (7) basal subarticular tubercles on fingers projected usually, (8) swelling along the phalanges of the finger IV absent (except *P. jacobuspetersi, P. shuar*), (9) toes are unwebbed or

basally webbed (with exception of *H. nexipus*), (10) median lingual process absent, and (11) dark throat collar absent.

Comments.—*Phyllodromus* contains a third of the species that were allocated in the former *Hyloxalus*. There are additional undescribed species belonging to this genus (see *Hyloxalus* relationship). Internal relationships changed in a few species in the successive outgroup expansion analysis (see above), which refrained me from the additional division in this genus until the increasing the knowledge of those clades. Conversely, some clades within this genus have character-states that could be synapomorphies for some clades, which would warrant further partitions. For example, the species in the *P. elachyhistus* and *P infraguttatus* clades (as defined above) has basal toe webbing, gular chest marks, and the metatarsal fold extending to the proximal 2/3 of plantar surface. In the case of the *H. nexipus* clade, the arm swelling is present in Ecuadorian and Peruvian populations, and in addition, whether the basal swelling on the finger IV in the adult males is corroborated for other populations/species, this will be a derived character-state for this clade.

The distal swelling on the upper arm and proximal lower arm is present in six closely related species within the *Phyllodromus pulchellus* group (as defined here), *P. arliensis*, *P. lehmanni, P. pinguis, Phyllodromus* sp. Albán, *P. lehmanni*-like, *Phyllodromus* sp. MesasGalilea), but this is absent (or undetected) in remain species of this clade. Whether the presence of the glandular integument will be confirme in these species, this swelling could be homologous at this taxonomic level. Anatomical integumentary similarities of the distal swelling are studied in the Chapter 3.

The types species of *Cryptophyllobates* (type species is *P. azureiventris*)—the only available generic name in synonym under *Phyllodromus.* This belongs to the *H. azureiventris* group, unfortunately, unambiguous phenotypic synapomorphies are

unknown. Species of this group have dorsolateral stripe and bright coloration, with exception of *H. poecilonotus*.

UNNAMED TAXON: "*Hyloxalus*" *subpunctatus* group.

Type species.—*Prostherapis subpunctatus* Cope (1899).

Immediately more inclusive taxon.—Hyloxalinae Grant et al. (2006).

Sister group.—*Hyloxalus* Jiménez de la Espada (1871 "1870").

Content.—"*Hyloxalus*" *cepedai* (Morales 2002 "2000"), "*H*". *edwardsi* (Lynch 1982), "*H*". *felixcoperari* (Acosta-Galvis and Vargas-Ramírez 2018), "*H*". *picachos* (Ardila-Robayo et al, 2000 "1999"), "*H*". *ranoides* (Boulenger 1918) **new combination**, "*H*". *ruizi* (Lynch 1982), "*H*". *sanctamariensis* (Acosta-Galvis and Pinzón 2018), "*H*". *subpunctatus* (Cope 1899), "*H*". *walesi* (Cochran and Goin 1970) **new combination**.

Diagnosis and support.—Goodman-Bremer value = 58. Unambiguous phenotypic synapomorphies that defined and diagnosis this group are: (1) unexpanded finger III disc (character 6: 1), (2) complete oblique lateral stripe (52: 1), (3) granular ventrolateral body flanks (171: 1), (4) basal subarticular tubercles on the fingers projected (178–181: 1), (5) phalangeal swelling on the finger IV (197: 1); (6) anterior projection of the suprascapula heavily calcified (122: 1), (7) a shorter, less robust and well defined zygomatic (124: 3), (8) the anterior portion of the *m. compressor cloacae* uncovered and inserting anteriorly to *m. pyriformis* (232: 1), (9) larval eyes oriented laterally (282: 0), (10) rounded larval narial opening (285: 1), (11) a conical larval vent tube (290: 0), (12) acuminate tip of the *processus anterior dorsalis* in the suprarostral cartilage (328: 1), and (13) adults are independent of streams (up to ca. 30 m or more from water. Character 108: 2).

Comments.—There is no generic available name for this group, and I left it as an unnamed group at moment. In addition to the nominal species included, there are various undescribed species cryptically masked under *H. subpunctatus* (see above). Most of these species inhabit the Andean ecosystems of the Cordillera Oriental de Colombia, but *H. picachos* extends to the lowland of the amazonian forest. Within this group is allocated the *H. edwardsi* group (see Chapter 1), a clade supported with multiple morphological and anatomical synapomorphies.

Comments of the Some Unsequenced and Key Species

I obtained morphological data of some unsequenced *Hyloxalus*; however, for those species, no molecular data were available due to scarce or inadequate material for DNA analysis. Based on this phenotypic evidence, I assign tentatively these species to one of the three clades: *Hyloxalus* (or *H. bocagei* clade), *Phyllodromus* (or *H. pulchellus* clade), or the *H. subpunctatus* clade. I am aware of the limitation of taking taxonomic conclusions based on morphology or phenotypic resemblance; exemplified in *Ectopoglossus*, because of their resemblance with distant related genus *Anomaloglossus* (see also the chapter 1). Nevertheless, in addition to the phenotypic resemblance, these species have unambiguous synapomorphies of some of these clades. Contrarily, to leave the species in the current proposal is to deny the present knowledge; in change, this provisional allocation is a more restrictive scientific hypothesis that will be refuted with future research. Moreover, my aim is to provide this additional evidence and recall attention to those species to motivate new studies.

***Colostethus borjai* Rivero and Serna 2000 "1995". —**Rivero and Serna (2000, "1995) described this species with three adult specimens from Amalfi, Antioquia, Colombia, northern Cordillera Central of Colombia, between 1000–1500 m. of elevation. They assigned it to the IX group (for a criticizing see Coloma 1995,

Grant et al. 2006), and subsequently, was placed tentatively on *Hyloxalus* based on phenotypic data (Grant et al. 2006). From its description, tissue and additional specimens have been unavailable to test its relationships. Nevertheless, two adult males (KU 189437, 189440) and two adult females (KU 189438–39) from San Pedro and Caldas, Antioquia department are indistinguishable from this species. The types and these specimens have a complete pale oblique lateral stripe, lack dorsolateral and ventrolateral stripe, finger II larger than III, finger and toe disc unexpanded, toes unwebbed, fingers without swelling, ventrolateral flank of body smooth, the metacarpal ridge as tubercle-like, and maximum SVL is 19.3 mm in adult males (adult male holotype being 20 mm, Rivero and Serna 2000 "1995") and 21.1 mm in adult females. The only difference between this new material and types is the throat color in adult males, because Rivero and Serna stated that holotype has "vientre ennegrecido en la garganta y las ¾ partes anteriores del abdomen (p. 58)", while the throat in the KU specimens is cream with dark brown spots. Although no variation in ventral coloration for males was discussed in the original description (one adult male was described), the other characters allow not denied that these are the same species.

Phenotypically, the resemblance of this species to the *Hyloxalus pinguis* or *H. pulchellus* is undeniable, but the tubercle-like metacarpal ridge/fold (character 192: 1) differs from both species (a ridge in *H. pinguis* and *H. pulchellus*). Other differences are found in the ventral coloration, and finger and toe disc width. To date, only *H. toachi* possesses tubercle-like metacarpal ridge/fold among the forme *Hyloxalus*. Moreover, unambiguously synapomorphies of the adults of the *H. subpunctatus* group (e.g., granular ventrolateral body skin) and *Hyloxalus* (e.g., extensive toe webbing) are absent *H. borjai*. Therefore, on the basis of the shared presence of metacarpal

ridge, and morphological resemblance, I placement provisionally this species in *Phyllodromus*, with pendent corroboration.

***Colostethus excisus* Rivero and Serna 2000 "1995".—**Rivero and Serna (2000 "1995") described *C. excisus* with a single adult male specimen (CSJ 0176) from Quebrada La Ayura, Envigado, Antioquia, Colombia, 2200 m. After, Grant et al. (2006) transferred this species to *Hyloxalus*. Based on the original description, this species has extensive toe webbing, with oblique lateral stripe, granular ventrolateral flanks of the body (free translation of "flancos finamente granulares"; Rivero and Serna 2000 "1995": 47), and SVL = 24.0 mm. Additional specimens are found in the ICN (15813**,** 18417, 18594) and KU (189424) amphibians collections from Cocorna, Medellin, between 950–1125 m. Despite the altitudinal differences, the morphology of these specimens matches with features of *C. excisus*. Moreover, this species has a complete pale oblique lateral stripe, straight ventrolateral stripe B-type, extensive toe webbing (I1–2II1–2III1.5–3IV3.5–2V), throat and abdomen stippled dark in adult males and pale with scarce dark dots in adult females, dorsum with dark brown irregular spots, forming an inverted V-shape at interorbital region. In addition to these features, this species possesses the unambiguous phenotypic transformation (except the palatines) of the *H. bocagei* group. On the basis of this phenotypic evidence, I included this species *Hyloxalus*.

***Colostethus marmoreoventris* Rivero 1991.—**Rivero (1991: 3–4) described *Colostethus marmoreoventris* with an adult male from Rio Negro, Tungurahuga, Ecuador (1125 m). Later, Coloma (1995: 43–44) provided an account and compared it with *Hyloxalus fallax* given that both species lack lateral stripes and webbing on toes. He diagnosis them through the ventral coloration differences. Moreover, he noted the resemblance with then-*Epipedobates* or *Dendrobates* species. After, the

species was transferred to *Hyloxalus* on the basis the morphological evidence only (Grant et al. 2006). I conducted a fast field trip to the type locality, and despite the forest matrices remaining near to Rio Negro town, the result was negative. There are no additional specimens of the species. The characters and the adult morphology of the holotype are commonly found in the aromobatids *Allobates femoralis* group (e.g., wider basal tubercle of the finger II, finger II larger than finger III, tarsal keel as tubercle-like; also see Grant et al. 2006: 161–162) instead *Hyloxalus, Phyllobates* or the *H. subpunctatus* group. The *A. femoralis* group has strong granular dorsal skin texture and basal toe webbing between toe II–IV, which are undetectable in *H. marmoreoventris*; however, skin on the dorsum of the holotype suffered abrasion. The resemblance between *H. marmoreoventris* and *A. femoralis* group makes me suspect that this is an *Allobates* rather than Hyloxalinae. Additional data are necessary to corroborate its phylogenetic placement.

***Colostethus peculiaris* Rivero 1991.—**This species was described by Rivero (1991: 13–14) from Pailas, 2195 m. This locality is between Sevilla de Oro and Méndez, Provincia Morona Santiago, on the eastern slope of the Ecuadorian Andes. The species was transferred to *Hyloxalus* based on phenotypic characters (Grant et al. 2006), but the phylogenetic position still remains unknown. The specified epithet is in allusion to the short webbing between fingers II and III; moreover, Rivero reported the presence of the two pectoral spots (p. 14) and placed it in their group I (i.e., species with pectoral spots, finger IV no swollen, and lack of the dorsolateral and lateral stripes). Likewise, Coloma (1995) characterizes the spots in the *H. peculiaris* account. I examined the holotype (USNM 282664, by photos) and paratype (USNM 282666), and the fingers webbed is by preservation artifact instead of the loose palmar skin like *Ectopoglossus*; moreover, the type specimens have no median

lingual process, which is a synapomorphy of this genus. Although the adult female USNM 282666 was stated to possess a large pectoral spot (Rivero 1991: 14), this specimen has melanophores stippling on the skin of the throat, darkening this region partially; additionally, there are dark pigments on the hyomandibular sinus located posterior to the interhyoideous muscle. The pigments on the skin and the sinus generate the apparent pectoral dark spot reported by Rivero, but these spots are absent. Grant et al. (2006: 79–80) discussed this phenomenon, that is, different types of pigmentation on the throat influence the pattern coloration and also the character coding. On the other hand, toes of the *H. peculiaris* are extensively webbed and fringed laterally, and this is phenotypic similar to the species of *Hyloxalus* (e.g., coloration pattern, toe webbing, size), and has the unambiguous synapomorphies of this genus thus I assigned to this genus provisionally.

***Dendrobates ranoides* Boulenger 1918.—**Taxonomic problems of this species remain unresolved. The species is known from the holotype only (Grant et al. 2017). A detailed account is provided by Grant et al. (2017: S59 – S60). Briefly, Boulenger (1918) described *Dendrobates ranoides* from Quatiquia [Guatiquia] river, Villavicencio, [Meta], Colombia, 400 feet. Silverstone (1971) removed from synonym with *Allobates brunneus*, where it was put by Dunn (1957) and allocated in *Colostethus*. Currently, this is in *Allobates*, due to the presumed relationship with *A. brunneus* (Grant et al. 2006). Recently, Grant et al. (2017: S31, S59) discussed the identity of the misidentified *A. ranoides* terminals of Santos et al. (2009) and Muñoz-Ortiz et al. (2015), concluding that these samples are not *A. ranoides*; moreover, they supplied photos in dorsal, ventral and lateral view of the holotype (Grant et al. 2017: Figure S1), and a key characters of the species (p. S60) to clarify the identity of *A. ranoides*. Despite this, Rejaud et al. (2020) again used the terminals and identification

(*A. ranoides*) of Muñoz-Ortiz et al., without considered that these was reidentified as *A. aff. juanii* by Grant et al. (2017: S31).

*Allobates ranoide*s is characterized by having a complete pale oblique lateral stripe; small, irregularly shaped spots on ventral surfaces of throat, belly, and limbs, and adult female with SVL = 22.4 mm (Grant et al. 2017). Furthermore, the skin is granular on the ventrolateral flanks of the holotype (see Grant et al. 2017: Figure S1, and Boulenger 1918: 428). These characters resemble with the adult morphology of the *Hyloxalus subpunctatus* group (e.g., complete pale oblique lateral stripe, basal toe webbing, irregular dark spots on most venter, and SVL between 20.1–24 mm), and the holotype has the unambiguously phenotypic synapomorphies of the *H. subpunctatus* group, as was defined here (e.g., ventrolateral body flanks granular, Character 171: 1). In addition, the type locality fall into the distribution of the *H. subpunctatus* group (easter slope of the Cordillera Oriental of Colombia). On the other hand, with the redescription of the *A. brunneus* by Lima et al. (2009), *A. ranoides* is easily distinguished from *A. brunneus* and from most *Allobates,* because this species has a complete oblique lateral stripe (diffuse in *A. brunneus*), dorsolateral and ventrolateral stripes absent (present in *A. brunneus*), paracloacal marks absent (present in *A. brunneus*), and dark spots on the ventral skin in females (free, pale in *A. brunneus*). Thus, on the basis of the phenotypic characters to maintain *A. ranoides* in *Allobates* is questionable, and otherwise, I recommend to transfer to the *H. subpunctatus* group. New specimens and evidence are necessary to test the current hypothesis.

DISCUSSION

The discussion is divide in three main part, the method to select the outgroup sample, the *Hyloxalus* relationships, and the evolution of the relevant characters proposed in this study.

Successive Outgroup Expansion

One of the aim of this research was to test the ingroup relationships as severe as possible; for this reason, question arose about how to choose the outgroup samples and how many terminals are necessary to provide a rigorous test of ingroup relationship. These questions recovers relevance because either the closely related taxa or also the distant related taxa have an effect in the ingroup relationships (Wheeler 1990, Holland et al. 2003, Grant 2019). Moreover, in poison frogs have been demonstrated that sometimes the addition of one species is sufficient to changes the known relationships. For example, the inclusion of one *Leucostethus* species showed the paraphyly of this genus (of Grant et al. 2017), and brought with it other species of the *L. fraterdanieli* group placed before in *Colostethus* (Marin et al. 2018); or the "*Hyloxalus"* sp. *edwardsi* group ("*Hyloxalus" jhoncito* sp. nov.) was merged in the dataset of Grant et al. (2017) and this species changed the relationship in the "*H". subpunctatus* group (**Chapter 1**). Likewise, the relevance of the character sampling in phylogenetic inference is well-known (Rokas et al. 2003, Hillis et al. 2003, Rokas and Carroll 2005, Heath et al. 2008), and the phenotypic characters has an impact in the topology and in the clade support in the total evidence phylogenies, in spite the disproportionate imbalance between phenotypic and genotypic characters (de Sá et al. 2014 or Sánchez-Pacheco et al. 2017, Cabra-García and Hormiga 2019).

In this study, the ingroup sample was increased considerably, passing from 96 former *Hyloxalus* terminals in Grant et al. (2017) to 189 terminals (i.e., 93 terminals added)—the largest *Hyloxalus* phylogeny until date. Furthermore, herein the

transformation series was increased substantially, given that characters proposed here represent 55 % of the final phenotypic matrix (i.e., 206 increased, a matrix with 376 characters in total). Therefore, an impact on the ingroup (i.e., the former *Hyloxalus*) relationships was expected, and the outgroup selected must have the capacity to supply a severe test of the ingroup topology and homology hypotheses. For this reason, I used the successive outgroup expansion (SOE) of Grant (2019) because this address the empirical identification of the outgroup by choosing the taxa that have higher probability to refute the hypotheses, increasing the outgroup sequentially until to topology will be insensitive.

The results of the successive outgroup expansion show that ingroup relationships are impacted at different levels throughout the analysis, changing the topological placement of the species, clades, until the ingroup monophyly. This agrees with the findings of Grant (2019) and Chapter 1 because the selected outgroup terminals added successively alters the ingroup relationships; however, most of the ingroup topology was stable in the final three rounds of the SOE.

In this study, the ingroup monophyly and the relationships of the large clades —*H. pulchellus* clade sister to the *H. subpunctatus* clade + *H. bocagei* clade was recovered and insensitive in the last three SOE analyses, which motivated to halt the successive outgroup expansion (Grant 2019); nevertheless, some species or clades vary persistently throughout the analysis. These are *Hyloxalus anthracinus, H. nexipus, H. picachos*, and the clades *H. sylvaticus* + *H. pulcherrimus*, *H. shuar* + *H. idiomelus, Hyloxalus* sp. Bongara + *Hyloxalus* sp. PAV clade (see **Table 7**). The ambiguity in the topological position of these unstable clade is not related to the SOE, because these clades change their position in the initial and in the final SOE rounds,

where the outgroup is almost as larger as the ingroup (outgroup with 118 and 136 terminals in the analysis 8 and 9, respectively).

Moreover, those unstable species or clades also have a different topological placement when previous studies are compared. For example, Santos et al. (2009) recovered the *H. sylvaticus* + *H. pulcherrimus* sister to the large clade bracketed by *H. anthracinus* and *H. awa* (equivalent to *H. nexipus* and *H. littoralis* herein). This position was recovered in analysis 2 of this study (see **Figure 27–28**). *H. nexipus* is sister to *H. azureiventris* clade in Santos et al. (2003) and Grant et al. (2006), and this relationship was found in the analyses 2, 5, and 6 of this study. Evidently, the available evidence of each unstable species or clade and their close relatives is not sufficient to resolve the relationships. Therefore, this variation in topological position is not a product of the SOE but rather of the ingroup evidence (e.g., terminals and characters). In addition, this reveals that the SOE allowed to identifing those ingroup topological regions where the relationships are weak, and where is necessary additional evidence to resolve the phylogenetic incongruences. I expect that with further evidence of those changing clades in *Hyloxalus,* their relationships will be discovered.

Thus, the outgroup selection is not a trivial practice, because the outgroup impacts direct on the ingroup relationship. As was discussed by Grant (2019), the selection of the outgroup terminals must be based on the prior knowledge (e.g., terminals resembling to the ingroup terminals, or terminals with characters also present in ingroup, homoplasic character) to choose those that has the greatest chance to test the hypothesis (i.e., topology and homology) as severely as possible, which increase the severity of test of the hypothesis, and non-limited to the closely related

species (e.g., or sister group), in unconstrained and simultaneously analyses with all ingroup samples until that its topology be insensitive to the outgroup increasing.

The Monophyly of *Hyloxalus*

The current total evidence analysis of the genotype and phenotype evidence corroborated that *Hyloxalus* is monophyletic, corroborating that previous unanalyzed species are part of this genus. Thus, the unsequenced *Hyloxalus faciopunctulatus*, *H. pinguis, H. littoralis, H. sanctamariensis* are part of this genus as were hypothesized (Grant et al. 2006, Acosta-Galvis and Pinzón 2018). In addition, *H. fasciopunctulatus* is nested within the *H. bocagei* clade as speculated by Páez-Vacas et al. (2010), and the incertae sedis "*Colostethus*" *poecilonotus* is nested in the *H. azureiventris* group.

Three large clades compose this genus, the *H. bocagei* clade, *H. subpunctatus* clade, and the *H. pulchellus* clade. Monophyly of these clades is consistently recovered in the SOE done herein, supported in unambiguously phenotypic synapomorphies, and on the GB clade support. This corroborates the statement of Grant et al. (2006) that with more evidence, the groups or clades can be identify in this genus. Therefore, on the basis of the analyzed evidence, each group is recognized as naturals genera in this study: *Hyloxalus* (*H. bocagei* clade), *Phyllodromus* (*H. pulchellus* clade), and the un-ranked "*H*." *subpunctatus* group, for which there is not an available generic name.

A comparison between the available poison frog phylogenies shows differences within the relationships of each of these genera. Within *Hyloxalus* is notorious the difference found in the relationship of the *H. maculosus*, because this is sister to *H. bocagei* in Santos et al. (2009), Páez-Vacas et al. (2010), Grant et al. (2017), and in Acosta-Galvis and Vargas-Ramírez (2018), or closely related to the *H. leucophaeus* + *H. sordidatus* instead *H. bocagei* in this study. Conversely, the internal

relationships of the *"H". subpunctatus* clade agree between studies (Grant et al. 2017, Acosta-Galvis and Vargas-Ramírez 2018, this study) with no major differences; although, the *"H". edwardsi* group (*"H". edwardsi, "H". jhoncito* sp. nov., *"H". ruizi*) relationships obtained in the Chapter 1 differ from this study in if *"H". picachos* is its sister group. Within *Phyllodromus*, my SOE analysis shows some unstable species and clades, which also have a distinct topological position between previous studies (see Santos et al. 2003, 2009, 2014, Santos and Cannatella 2011, Grant et al. 2006, 2017, Pyron and Wiens 2011, Pyron 2014, Jetz and Pyron 2018, Acosta-Galvis et al. 2020). Other relationships in this genus are consistent. Further researches are necessary to unravel the relationships of these unstable species.

In the genera recognized here, all species do not share some features. For instance, within the *"H". subpunctatus* group the dorsolateral stripes are present in *H. cepedai* but absent in the sister *H. picachos,* or in *Phyllodromus* these are present in *P. azureiventris* and absent in *P. poecilonotus*; the toe webbing is extensive in the "*H". edwardsi* group, while this is basal in their sister "*Hyloxalus"* sp. Sumapaz. Nonetheless, unambiguous phenotypic synapomorphies provide evidence to support the three genera, and to place some unsequenced species in one of these genera or doubt the phylogenetic closeness. In these cases, genotypic evidence is crucial to corroborate the hypothesis, reinforcing the necessity to incorporate new specimens and new genetic evidence to test the relationship of the unsequenced species, even further in the face of the reduction of the populations and local extinction in Hyloxalinae (Grant and Bolivar 2014; De la Riva et al. 2021).

An alternative to obtain the genotypic data when there are not fresh material is by mean of the historical DNA analysis. This is a powerful tool that allowed to obtain this data from museum specimens (Lyra et al. 2020, Rancilhac et al. 2020). With this,

the phylogenetic placement would be examined. There are various hyloxalines of interest that can be subjected to this procedure for which additional specimens are unavailable, so to mention some examples of the relevant species are found: *Ectopoglossus absconditus, "H". abditaurantius, "H". aeruginosus, "H". alessandroi, "H". edwardsi, "H". chocoensis, "H". exasperatus, "H". fuliginosus, "H". maquipucuna, and Paruwrobates andinus,* and also species assigned tentatively to other aromobatid (e.g., *Allobates ranoides, A. wayuu*) and dendrobatid genera (e.g., *Colostethus agilis, C. mertensi, C. ucumari*). These species could be refute the current hypothesis giving their phenotypic resemblance (see Grant et al. 2017: S24, S69, Melo-Sampaio 2020: 55–56, Vigle et al. 2020).

Grant et al. (2006, 2017) provided an extensive phenotypic characters revision from adults and larval morphology, behavior and from alkaloid profiles. Various of these characters were used in systematic of this superfamily previously (e.g., Noble 1923, Dunn 1924, Savage 1968, Silverstone 1975, 1976, Edwards 1971, 1974, Daly et al. 1978, Myers 1987, Myers and Burrowes 1987**,** Myers and Daly 1976a, b, Myers and Donnelly 2001, Myers et al. 1978, 1991, 2012, Lynch 1982, Duellman and Simmons 1988, Zimmermann and Zimmermann 1988, Caldwell and Myers 1990, Coloma 1995, La Marca 1995, Kaplan 1997, 2004, Morales 2002 "2000", Caldwell et al. 2002, Grant and Castro 1988, Grant and Rodriguez 2001, Grant and Ardila-Robayo 2002, Grant and Myers 2013, Grant et al. 1997, Poelman et al. 2010, Sánchez 2013. Details are in Grant et al. 2006: 9–37). After that, some additional phenotypic characters have been proposed (Anganoy-Criollo and Cepeda Quilindo 2017, Dias et al. 2018a, c, 2021, Grant and Bolivar 2021, Cavalcanti et al. 2021), and the genotypic data are more and more predominant in the systematic review of poison frogs in the

last decade (e.g., Marin et al. 2018, Brown et al. 2019, Fouquet et al. 2019, Guillory et al. 2019. 2020).

My revision of the adult and larval phenotype in the former *Hyloxalus* and other Dendrobatoidea show additional and new characters which can provide evidence to test the relationships. Some of these were redefined from already proposed character (e.g., fingers length, metacarpal fold/ridge, black arm gland, ventrolateral stripe, larval external morphology), others are new characters from external adult morphology (e.g., subarticular and supernumerary tubercles, ulnar tubercles, the texture of ventral skin), the musculature of the arm, hindlimb and the cloacal (e.g., *m. extensor carpi radialis*, *m. rectus abdominis*, *m. sphincter ani cloacali*, *m. compressor cloacae*, *m. tensor fascia latae*), and from larval chondrocranial anatomy (e.g., suprarostral and infrarostral cartilage, crista parotida). Some of these characters were proposed for other anuran groups (e.g., ulnar tubercle in Lynch and Duellman 1997, Duellman and Lerh 2009; *m. tensor fascia latae* Dunlap 1960, McDiarmid 1971, Prikryl 2009); however, their variation was unnoticed or unscored in poison frogs. See the Phenotypic Characters above or **Appendix 1** for a detailed lists. All of this phenotypic evidence highlight the role of the morphology in the present genomic era (Giribet 2015, Lee and Palci. 2015, Pyron 2015)

Recently, Cavalcanti et al. (2021) shows an impressive glandular variation in the skin of the fingers and hand related to the swollen fingers in adult males of poison frogs; moreover, they suggest promissory variation in the anatomy of the other secondary sexual characters of poison frogs, as the supracarpal pad (Myers and Donnelly, 2001; Grant et al, 2006) and in the black arm gland (or distal swelling of the arm, herein. Grant and Castro-Herrera 1998; Grant and Ardila-Robayo 2002). My

anatomical study of the distal swelling of the arm corroborates that this swelling is glandular, but also there are additional dermal and hypodermal variations (see Chapter 3).

Other characters analyzed in this study with potential phylogenetic value, but that need further examination, are the phalanges length of the fingers and toes, the occurrence of the sesamoids and ventro-distal projection on the finger phalanges, the middle ear tympanum, the skin structure of the oblique lateral line, and the adult head coloration in this genus. Besides these characters, other studies reported variation in hand and hyoid musculature (Burton 1998a, Blotto et al. 2020, Trewavas 1933), urogenital system (Bhaduri 1953), and glands on the ventral skin (Myers et al. 2012, Grant et al. 2017). Despite the scarce data for *Hyloxalus*, behavior also can provide characters (see Castillo-Trenn and Coloma 2008, Quiguango-Ubillús and Coloma 2008). Furthermore, the internal oral cavity (Wassersug and Heyer 1988; Dias et al. 2018c, 2021) and musculature of the tadpole (Haas 1995, Haas 2001, Dias et al. 2021) are rich character sources.

This variation, together with standard and new tools and methods (histology, SEM microscopy, micro-computed tomography, synchrotron X-ray microtomography, confocal microscopy; Arch et al. 2012, Haas et al. 2014, Pardo et al. 2017, Fidalgo et al. 2020) can provide new data to test and refined the homology hypotheses and supply new phenotypic characters for phylogenetic inferences and phenotype evolution.

Remarkably, this study reveals an unrecognized diversity within the former *Hyloxalus* with undescribed taxa hidden in widely distributed species (e.g., *Phyllodromus elachyhistus, P. lehmanni, P. nexipus,* and *"H". subpunctatus*), or new taxa in species without taxonomic problems (e.g., *P. insulatus, P. sauli* and *H.*

vergeli) or revalidation of the species in synonymy (e.g., "*H". walesi*). To date, this was the largest genus in all superfamily Dendrobatoidea (63 species; Frost 2021). Most species inhabit ecosystems of the tropical Andes chain, which is the most species-rich region and a biodiversity hotspot in the world (Myers et al. 2000). This region shows high speciation and diversification rates in amphibians (Hutter et al. 2017), such in poison frogs (Santos et al. 2009), centrolenids (Hutter et al. 2013), and *Pristimantis* (Lynch and Duellman 1997). Together with my data, this show that diversity in each recognized Hyloxalinae genera is large than known.

Despite this, the amazing growth in the poison frog diversity in the recent decades (see Grant et al. 2006), these genera are of the few that their diversity remains undescribed since the resurrection of the then-*Hyloxalus* by Grant et al. (2006). Thus, only five species have been described in the last fifteen years in the systematic contributions of this group (i.e, Páez-Vacas et al. 2010, Acosta-Galvis and Pinzón 2018, Acosta-Galvis and Vargas-Ramírez 2018, Acosta et al. 2020), which is a relatively low number in comparison with other poison frog groups with comparable diversity, as *Allobates* (22 species described since 2006, Frost 2021; see Jaramillo et al. 2021: Figure 1).

This low rate of diversity is related to the persistent taxonomic problems in this group (e.g., species known only from the original description, lack of the systematic studies of the complex species, doubts about the specific status of the nominal species or other populations), unsampled far away ecosystems to search the nominal species few-known, relatively low or overlapping morphological variation between populations, the lack of the additional evidence (e.g., DNA data, advertisement call) for key species; and the decline of some Hyloxalinae species

(Lynch and Grant 1998, Coloma 1995, Lips et al. 2005, Grant and Bolivar 2014). All of this masks and tangle the diversity in these three genera.

Comment on the Phenotypic Evolution

In this section, I discuss the phenotypic evolution in the former *Hyloxalus,* focusing on the key characters proposed here (e.g., supernumerary tubercles) that are relevant in the poison frogs evolution. For this, it is necessary the following considerations. Given character and taxon samples affect on the phylogenetic relationships, then the incorporation of new characters, character-states, and terminals could entail other evolutionary scenarios. Thus, the current inferences are prone to be questioned or reformulated, because these are a product of the available evidence, that is, the character samples are not complete for all data sets, and the taxon sample is unbalanced towards the Dendrobatidae family. Moreover, another consideration is concerning to the sister group, because this determines the character-states optimization, or the primitive–derive hypotheses. The sister group of the former *Hyloxalus* is *Ectopoglossus* + *Paruwrobates* which have been a relationship consistently recovered (Santos et al. 2014, Grant et al. 2017, herein); however, the sister group of the Dendrobatoidea is controversial (Frost et al., 2006; Grant et al., 2006, 2017; Pyron and Wiens, 2011; Pyron, 2014; Jetz and Pyron 2018). Therefore, to reduce the ambiguity, I used only the characters that optimize unambiguously. Also, the current section is motivated to generate additional discussion and studies on phenotype evolution in poison frogs.

Supernumerary tubercles.—Supernumerary tubercles are integumentary projected modifications situated on the palm or sole of the anurans, varying in size, projection, and in quantity. These are common structures in Bufonidae, Cycloramphidae, Hylodidae, Leptodactylidae, Strabomantidae (Lynch 1971,

McDiarmid 1971, Caramaschi and Sazima 1984, Lynch and Duellman 1997, Giaretta et al. 1993, Pombal et al. 2002, Nascimento et al, 2005). These tubercles resembles to the toe pad and subarticular tubercles which are epithelial modification with hexagonal or polygonal (in ventral view) cell with flat surface, that providing enhance adhesion to the substrate (Noble and Jaeckle 1928, Barnes et al. 2013, Drotlef et al. 2016). The adhesion to the surface increase with put in contact other body surface parts, as all ventral surface of the hand and toe (Endlein et al. 2017), including the supernumerary tubercles.

Supernumerary tubercles are lost in the common ancestor of dendrobatoids, and these are acquired twice independently within *Ameerega*, evolving at the node of the four analyzed members of the *A. braccata* group (sensu Guillory et al. 2019; *Ameerega berohoka, A. boehmei, A. braccata, A. flavopicta*), and these are polymorphic in *A. macero* (Rodriguez and Myers 1993). Moreover, one unanalyzed species of the *A. braccata* group was corroborated the presence of these tubercles (*A. munduruku*), but in the other two members, the *A. bolivianus* and *Ameerega* sp. MatoGrosso1, the occurrence was not confirmed. If the supernumerary tubercles will be confirmed in these species, this could be optimized as a synapomorphy for the *A. braccata* group. At nonce, these are shared derived character-state for four *A. braccata* species.

Most of the species *Ameerega braccata* group occupies the savannas and gallery forest of the Cerrado biome (Haadad and Martins 1994, Lötters et al. 2009, Forti et al. 2010, Vaz Silva and Maciel 2011, Andrade et al. 2013, French et al. 2019), except *A. bolivianus* (Yungas forest; Kohler et al. 2006) and *A. munduruku* (Amazonian forest; Neves et al. 2017), and these are found associated to the rocky or rupestrian habitats, using rocks crevices or surfaces of stone as shelter, for

reproduction, or as calling site (Haddad and Martins 1994, Costa et al. 2006, Lötters et al. 2009, Magrini et al. 2010, Neves et al. 2017, French et al. 2019, Eterovick et al. 2020). Additional tubercles on palm can improve adhesion to the substrate, and although is possible to speculate a correlation between habitat and supernumerary tubercles, there is no evidence for that, therefore studies are necessary to corroborate this supposition. Other dendrobatids that inhabited similar habitat (*H. edwardsi* and *Hyloxalus* sp. *edwardsi* group, cavernicolous and riparian species; Lynch 1982, and see Chapter 1) also has additional subarticular tubercle on the hand, insinuating morphological adaptation to the environment.

Protrusiveness of the subarticular tubercles on Fingers.—For definition and function of the subarticular tubercles see Chapter 1 and supernumerary tubercles above. Poison frogs have subarticular tubercles on the finger commonly, but the protrusiveness degree varies among Dendrobatoidea (see Character 178–183, **Appendix 1**), with relatively constant variation in some genera of poison frogs. For example, most Dendrobatinae—sister group of Hyloxalinae—reviewed here have flat subarticular tubercles in all fingers, but in "*Colostethus*" *ruthveni* group (sensu Grant et al. 2017) and *Adelphobates quinquevittatus* the basal subarticular tubercles on all fingers are projected, like as the distal on the finger IV (although with polymorphism in "*C*". *ruthveni*-like). In Hyloxalinae, protrusiveness variation is relatively conserved, varying among the *H. pulchellus* clade, and optimize as an unambiguous synapomorphy for *H. subpunctatus* clade.

The flattened basal subarticular tubercles on fingers are the ancestral state in *Hyloxalus* and Hyloxalinae. These derive as project basal subarticular tubercles on the fingers in the *H. subpunctatus* clade, retained the ancestral state for the distal subarticular tubercles (i.e., flat tubercles), with exception of the finger V in *H.*

sanctamariensis. Within this clade, the *H. edwardsi* group also retains the plesiomorphic condition in all tubercles. The basal subarticular tubercles on fingers of the *H. pulchellus* clade, minus *H. nexipus*, also evolved independently as projected tubercles; however, most species of this clade retained the simplesiomorphic flat distal subarticular tubercle, with the derived condition on the distal of finger IV and V in three species of the *H. pulchellus* group (*H. arliensis, H. pinguis, H.vertebralis*), two species of the *H. azureiventris* group (*H. chlorocraspedus, H. poecilonotus*), and in *H. shuar* and *H. toachi*, and only on the finger V in *H. infraguttatus*. Optimization of the distal subarticular tubercle of the finger IV is ambiguous to the *H. pulchellus* group due to polymorphism in *H. pulchellus*.

Hyloxalus with flattened subarticular tubercles occupy riparian habitats (character 109: 1; Coloma 1995, Páez-Vacas et al. 2010, Acosta 2012, and data herein), while the *Hyloxalus* with projected subarticular tubercles are terrestrial (independent of the water, individuals are found up to 30 m. from the stream. Character 109: 2; Stebbins and Hendrickson 1959, Acosta-Galvis and Vargas-Ramírez 2018, Acosta-Galvis and Pinzón 2018, my data), except *H. anthracinus, H. craspedoceps, H. pulcherrimus, H. sylvaticus*, and *H. elachyhistus* group). The ancestral reconstruction of the habitat shows that the ancestor of Hyloxalinae inhabited a riparian ecosystem, and evolved independently to a water-independent lifestyle in the ancestor of the *H. subpunctatus* clade, of the *H. pulchellus* group, and in the species *H. azureiventris, H. chlorocraspedus*, *H. shuar,* and *H. toachi*. Also, the terrestrial habitat optimizes as a synapomorphy for *H. subpunctatus* clade (character 108: 2). This relation confirms, in this case, that lifestyle transition was accompanied by the change in the phenotype (Grant et al. 2006: 176), acquiring the projected basal subarticular tubercles for a terrestrial habitat. Nevertheless, the clear deviation to this

pattern is the *H. elachyhistus* clade, because species are riparian with projected basal subarticular tubercles. Likewise, the Dendrobatinae are terrestrial with flattened subarticular tubercles in most of them. Additional research can be help to understand the convergent evolution of the subarticular tubercles and the habitat in poison frogs.

Finger lengths and the Finger V length.—Grant et al. (2017: S66) recognized the use of the relative length of the finger II and III as diagnosis character in poison frogs, and although for some clades of dendrobatoid optimize as a synapomorphy (e.g., II larger III in *Allobates*, and II lesser III in Hyloxalinae), they recognized the extensive variation among these clades. In order to evaluate the finger II variation, a finger III constant in length was assumed (Grant et al. 2006). A broader revision of the Hyloxalinae frogs and a standard quantitative analysis in fingers II and III reveals variation in the finger III, which denies the Grant et al.'s (2006) supposition, like the proposed finger II homology (Character 6 of Grant et al. 2017).

In the same way, the finger V length has a diagnosis value in poison frogs (Grant et al. 2017: S66), and the revision of the hyloxalines frogs shows additional character states in this finger (character 191). My results show a constant variation of the character states proposed here; for instance, the finger V of the most *Anomaloglossus* evaluated extends before the distal subarticular tubercle of the finger IV (state 1), or it reaches the hyperdistal subarticular tubercle of the finger IV in the *Hyloxalus edwardsi* group; however, in another case it is highly variable within a clade, such as in the *H. pulchelus* clade that there is almost proportionally species with the plesiomorphic condition of Hyloxalinae (i.e., state 3, finger V surpassing the distal subarticular tubercle of the finger IV), or with derived state 2 (finger V reaching the distal subarticular tubercle of the finger IV), and a few species with the

state 1. Moreover, the optimization is ambiguous at superfamily and families (Aromobatidae and Dendrobatidae) levels.

The extensive observed variation and the complex optimization scenario in fingers length show our scarce knowledge to decipher the involve homologies, but a skeletal evaluation can improve and refined the homologies proposed (Grant et al. 2017: S67); nevertheless, all phalanges of the fingers show some degree variation, and even though, the identified character-state can be defined ostensively, operationally the phalanx need to be compare with a reference point without or little variation to described the observed variation (Grant and Kluge 2004).

Swelling on the fingers.—Many adult males of the poison frogs possess the sexually dimorphic swelling on the fingers, that is associated with the clustered specialized mucous glands, hypothesized to secrete pheromones to stimulate the female in the cephalic amplexus, when the male puts the fingers below or in front of the female nares (Grant et al. 2017, Cavalcanti et al. 2021); nonetheless, despite the presence of one type of the specialized gland (type I, commonly), sometimes there is not an evident swollen on fingers (Cavalcanti et al. 2021). In addition to the histological characterization of the four specialized mucous glands, Cavalcanti et al. (2021) identify and defined three swelling types in the hands: the phalangeal swelling that occurs in all fingers, the basal and the metacarpal swelling restricted to the finger IV. This variation was conceptualized in eight transformation series, which were implemented herein (for details also see the Character 195–202, **Appendix 1**). They also reported swelling occurrence in species for which it was unknown and arguing that type I specialized mucous gland is a synapomorphy for Dendrobatoidea.

Regarding the external morphology, my results agree with Cavalcanti et al. (2021), but I found phalangeal swelling on finger IV in other *Hyloxalus* not analyzed

by them and for which was unknown until now, such as *H. subpunctatus*, *H. walesi*, *H. sanctamariensis*, and *H. shuar*, and also in *Paruwrobates andinus.* The first couple species also have phalangeal swelling on the fingers III and V; furthermore, I detected phalangeal swelling on the Finger III of the *A. stepheni* and in the "*Colostethus*" *ruthveni* group, unlike Cavalcanti et al. (2021), and basal and metacarpal swelling in *P. andinus*.

Phalangeal swelling on the finger IV (Character 197) evolved independently multiple times in poison frogs, and the absence optimizes in the most recent common ancestor (MRAC) of Dendrobatoidea. In Aromobatidae, the most recent ancestor of *Anomaloglossus* had swelling, optimizing as a synapomorphy for the genus. The swelling is found as well in some species of *Aromobates* and *Allobates,* but optimization is ambiguous. The ancestor of the Dendrobatidae lacked swelling, and three clades gained the derived condition: in Colostethinae as predicted by Cavalcanti et al. (2021), with reversions in a few *Ameerega*; in the "*Colostethus*" *ruthveni* group; and in the *Hyloxalus subpunctatus* clade, with secondary loss in *H. felixcoperari* and *Hyloxalus* sp. QuebradaWolf. The occurrence also evolved in *H. jacobuspetersi* and *H. shuar*. Like the superfamily, the MRAC of Hyloxalinae and *Hyloxalus* retained the plesiomorphic condition.

The absence of the phalangeal swelling on the fingers II, III, and V (Character 195, 196, 202, **Appendix 1**), and of the basal swelling in finger IV, and the metacarpal swelling is a plesiomorphy for Dendrobatoidea and Hyloxalinae, and only the phalangeal swelling on the finger III is a synapomorphy for "*Colostethus*" *ruthveni* group. The basal swelling is acquired independently in three *Anomaloglossus* (*A. baeobatrachus*, *A. stepheni*, and *A. tamacuarensis*), and two *Hyloxalus* (*H. nexipus* and *H. anthracinus*). *H. anthracinus* also has metacarpal

swelling. *Hyloxalus* was considered to lack finger swollen (see Grant et al. 2006); however, Santos et al. (2014) and Grant et al. (2017) found three dendrobatids (*H. jacobuspetersi*, *H. cepedai,* and *H. picachos*) with phalangeal swelling on the finger IV as part of *Hyloxalus.* The histology of the four *Hyloxalus* species from 63 nominal species was analyzed to date (Cavalcanti et al. 2021) and likewise lacks data on the amplexus of most *Hyloxalus* (see Mudrak 1969, Fandiño et al. 1997, Quiguango-Ubillús and Coloma 2008, Lötters et al. 2000). Given the result of Cavalcanti et al. (2021), I suspect that the phalangeal swelling in Hyloxalinae possesses specialized sexual dimorphic mucous glands, which will need corroborate with histological studies.

Toe V length.—The phylogenetic value of the toe V length have not been tested in poison frogs (Character 226). My results show a conserved variation with diagnosis utility in some clades. For example, it not reaching the proximal subarticular tubercle of the finger IV in *Epipedobates* and *Silverstoneia* (state 0) or it reaches the proximal subarticular tubercle of the finger IV in *Aromobates*, *Mannophryne* and *Rheobates* (state 1). This last condition as well as present in many Hyloxalinae frogs, changing for state 0 in a few *Hyloxalus* or to state 2 (it surpass the proximal subarticular tubercle of the finger IV) in *Ectopoglossus ithsminus*.

The state 0 optimize at Dendrobatoidea node, while the state 1 was gained multiple independent times in poison frogs. In Aromobatidea, the derived state 1 evolve at the node of the *Aromobates*, *Mannophryne* and *Rheobates*, in two *Anomaloglossus* (*A. baeobatrachus*, *A. stepheni*) although optimization is ambiguous in the node that is shared with *A. degranvillei*, because this has the plesiomorphic condition, and in *Allobates kingsburyi*. Most Colostethinae and Dendrobatinae retain the simplesiomorphous state 0, except the *Leucostethus fraterdanieli* group,

Ameerega braccata, *A. berohoka*, *A. flavopicta*, *A. parvula*, *Oophaga granulifera* and in *Ranitomeya sirensis* and *R. variabilis* who which evolve the derived state 1. Likewise, this state (finger V reaches the proximal subarticular tubercle of the finger IV) evolved in the MRAC of Hyloxalinae, with reversions to state 0 in *H. leucophaeus*, *H. sanctamariensis*, *H. picachos*, *H. delatorreae*, *H. poecilonotus*, *H. azureiventris*, and in *H. toachi*, and with polymorphism in *H. elachyhistus*. Most species of the *H. pulchellus* group, excluding *H. vertebralis* and *H. pinguis*, retain the simplesiomophy also (i.e., state 0). Alike the fingers, a comparative study of the phalanges in toes could be supply insight in homology and the masked characters in the toe length.

Ventrolateral skin of body texture.—Anuran integument is the large external organ, implicit in several functions, including physical protection, chemical defense, osmoregulation, respiration, immunity, sensorial perception, temperature regulation, and water balance (Duellman and Trueb 1994, Fox 1994). The skin of the ventral region and ventral surface of the hindlimbs of the frogs is specialized and most permeable to the water, ions, and air exchanges (Bentley and Main 1972, Ogushi et al. 2010). Integument has some degree of texture, that even the apparent smooth skin has an irregular surface. Most notable is the presence of warts, granules, or tubercles distributed in almost all body. These epidermal projections vary in size, shape, and tip shape (Duellman and Lehr 2009). These structures increment the skin surface in favor of the hydric balance, thus in a terrestrial habitat this favors water absorption, whereas in an aquatic habitat regulates the respiration (Duellman and Trueb 1994, Young et al. 2005, Ogushi et al. 2010)

The ventral body skin of the poison frogs is smooth generally, but some taxa have warts or granules on the ventrolateral body skin surface. The ancestral

reconstruction shows that ventrolateral texture was smooth in the MRAC of Dendrobatoidea, and texture was acquired in various clades of the superfamily. A warty skin evolved exclusively in *Rheobates palmatus* and *Mannophryne cordillerana*. The condition could be turned into synapomorphy for *Rheobates* because I confirmed the condition in *R. pseudopalmatus*, for which phenotypic data was not included. It is now, that the derived granular condition evolved multiple times in unrelated clades into Dendrobatidae, although the common ancestor of the family and subfamilies retain the simplesiomorphic smooth skin. In change, the granular flanks were gained independently in *Colostethus ruthveni* group, *Oophaga granulifera*, *Ranitomeya sirensis, H. anthracinus, H. sauli, H. vertebralis,* and *Hyloxalus* sp. Inza, as well as in the common ancestor of the *Hyloxalus subpunctatus* clade, with a single reversion in *Hyloxalus* sp. *edwardsi* group. The ancestral and derived character-state occurs in *H. bocagei* and *H. craspedoceps*. The results suggest that the transition to the terrestrial lifestyle was accompanied by modification in ventral body skin texture. Certainty, the granular ventrolateral flanks in *Hyloxalus* play a role in one or more biological functions, even more, when there are species with terrestrial and riparian lifestyle in this genus; for example, the *Hyloxalus subpunctatus* clade are terrestrial and has granular ventrolateral body flanks; however, although the anuran integument knowledge is broad, little is known regard that in poison frogs.

Anterior insertion portion of the *m. compressor cloacae* regard the *m. pyriformis*.—As the name indicates, the implicit function of the *m. compressor cloacae* is related to the sphincter control in anurans (Van Dijk 1959), because this, with other extrinsic cloacal muscles, depressed the urostyle, influencing the lymphatic fluid movement (Drewes et al. 2007, 2013). Nevertheless, as far as known direct

evidence of the functional role is unknown. Same as the *m. sphincter ani cloacali* (see Chapter 1), a revision of the *m. compressor cloacae* is needed, and also homology and characters are necessary. This muscle is broadly distributed in Anura (see Ecker and Haslam 1889, Van Dijk 1955, 1959, Drewes et al. 2013), and present in all Dendrobatoidea evaluated.

The accounted variation in *Hyloxalus* and poison frogs show that the anterior insertion portion of the *m. compressor cloacae* is uncovered or covered by the *m. pyriformis* in poison frogs and the phylogenetic analysis show that this variation is unambiguously optimized and diagnosed in some clades. Thus, the most recent ancestor of Dendrobatoidea retains the symplesiomorphic condition of the anterior insertion *m. compressor cloacae*, that is, covered by the *m. pyriformis*, whereas the derived condition—uncovered anterior insertion—is acquired independently multiple times in the superfamily. Thus out of the ingroup, it is uncovered in *Allobates magnussoni*, in three *Epipedobates* (*E. darwinwallacei, E. espinosai, E. machalilla*), and in various *Ameerega* (*A. braccata, A. flavopicta, A. parvula, A. petersi, A. picta*). This condition (uncovered anterior insertion) optimizes as unambiguous synapomorphy at the Dendrobatini tribe with reversion in *Adelphobates quinquevittatus*. The MRAC of *Hyloxalus* and its subfamily maintain the symplesiomorphy, and the derived shared condition optimize as unambiguous synapomorphy in the *H. subpunctatus* clade and in the *H. pulchellus* clade (minus *H. nexipus*), reversing in several species in each clade, even though the derived condition is lost and synapomorphy for the clade of *Hyloxalus shuar* and *Hyloxalus idiomelus*. Moreover, the derived condition only occurs in *H. leucophaeus* in the *H. bocagei* clade.

Occurrence of a second origin of *m. gracilis minor*.—The second origin of the *m. gracilis minor* occurrence is highly variable in poison frogs, but there is a tendency to the absence or presence in some clades. Most Aromobatidae lack a second origin (but *Aromobates nocturnus* and *Anomaloglossus baeobatrachus*), while in most *H. subpunctatus* clade is present (unverified in undescribed species); nonetheless, the absence was recovered as a derived shared character for the *H. bocagei* clade (excluding *H. vergeli* Quinchas), and the clade of *Andinobates*, *Excidobates,* and *Ranitomeya*. On the other hand, due that this muscle attaches to the dermis, it is suspected that any of its movements influence the volume and pressure of the interfemoral lymph sac (Drewes et al. 2007). Additional studies are needed to improve the phylogenetic and evolutionary value.

M. extensor carpi radialis.—There is sexual dimorphism in the forearm muscle in anurans (Ecker and Haslam 1889, Gaupp 1896, Duellman et al. 1997, Peters and Aulmer 2000, Clark and Peters 2006; Magalhães et al. 2018, Pinheiro et al. 2021), like as in the *m. extensor carpi radialis* (Navas and James 2007, Hoyos and Salgar 2016). Navas and James (2007) suggested that the sexual difference in the *m. extensor carpi radialis*, like other forearm muscles, enable the male to improve of the hold the female in the amplexus (Oka et al. 1984, Peters and Aulmer 2000, Lee 2001, Wells 2007: 392 – 396). Nevertheless, the forearm muscles in poison frogs received little attention, but my evaluation demonstrated variation in the *m. extensor carpi radialis*, mainly in robustness and insertion of its internal slip. The general pattern in Dendrobatoidea is a thinner internal slip (i.e, it is one quarter more than the external slip width), inserting on the external slip ventral surface about at distal two-third of its distance. In the *Hyloxalus edwardsi* species group (*H. edwardsi*, *H. ruizi*, *Hyloxalus* sp. *edwardsi* group) and *Ectopoglossus atopoglossus* has a deviated pattern, because

the internal slip is robust (as wide as external slip at their origin), and in the *H. edwardsi* group inserts on the external slip tendon insertion, roughly to the radiale level. This variation is not intersexual or related to maturity, so also adult males as adult females and juveniles show similar conditions.

The first chapter provided phenotypic evidence that support the monophyly of the *Hyloxalus edwardsi* group and the robust internal slip of the *m. extensor carpi radialis* is another synapomorphy for this clade, while it is an autapomorphy for *E. atopoglossus*. With this at hand, the derived robust internal slip of the *m. extensor carpi radialis* evolved twice independent times in Dendrobatidae, and the internal slip inserting on the external slip tendon insertion evolved uniquely in the *H. edwardsi* group.

The hand and forearm muscles convergences have been related to the lifestyle and habitat in other frogs (e.g., Burton 1998b, Manzano et al. 2008), possibly related to the lotic habitats (Pinheiro et al. 2021), as well as with the fighting behavior (Wells 2007, Magalhães et al. 2018); notwithstanding, in addition to the behavior data, the functional role of those evolutionary acquisitions in the riparian *H. edwardsi* group and *E. atopologlossus* are unknown.

Acknowledgments.—I very grateful with my advisor, Dr Taran Grant, for your teaching, patient, and support. I thankful to the curators and/or managers Darrel Frost, Frank T. Burbrink, David Kizirian, David Dickey, and Margaret G Arnold (AMNH), Mark Wilkinson and Barry Clark (BMNH), Erika J. Ely (CAS-SUA), Manuel Bernal and Sigifredo Clavijo (CZUT-A), Pablo Venegas (CORBIDI), John D. Lynch (ICN), Rafe Brown, Richard Glor, and Melissa Mayhew (KU), Danny Urrego (ITM, before CJS-H), Andrew Crawford (ANDES-A), Aline Staskowian Benetti and Hussam Zaher (MZUSP), José P. Pombal Jr., and Manoela Woitovicz

Cardoso (MNRJ), Belisario Cepeda and Fernando Santander (PSO-CZ), Addison Wynn, Steve Gotte and Esther Lagan (MCZ-A), Beatriz Alvarez Dorda (MNCN), Kevin de Queiroz and Addison Wynn (NMNH, ex-USNM), Cameron Siler and Jessa L. Watters (OMNH), Santiago Ron (QCAZ), Diego Cisneros and Carolina Reyes (USFQ) Claudia Koch, Morris Flecks and Inna Rech (ZFMK), Michael Franzen (ZSM), and Mark-Oliver Rödel and Frank Tillack (ZMB) for access, space, loans of the specimens. I specially grateful with Faride Lamadrid and Paulo Nicolas Anganoy, my family, for daily support and unconditional love. Specimen collection was authorized by the Ministerio de Ambiente y Desarrollo Sostenible of Colombia (ANLA, resolutions 255 of 2014 and 701 of 2016). Grant doctoral scholarship was provided by the Fundación Centro de Estudios Interdisciplinarios Básicos y Aplicados – CEIBA (2016), and partial economical support was provided by the Brazilian Coordenação de Aperfeiçoamento de Pessoal de Nível Superior (CAPES Finance Code 001) and São Paulo Research Foundation (FAPESP Procs., 2012/10000-5, and 2018/15425-0).

LITERATURE CITED

Acosta-Galvis, A. R. 2012. Anfibios de los enclaves secos en la ecorregión de La Tatacoa y su área de influencia, alto Magdalena, Colombia. Biota Colombiana 13 (2):182–210.

Acosta-Galvis, A.R., and M. Vargas-Ramírez. 2018. A new species of *Hyloxalus* Jiménez De La Espada, 1871 ‘‘1870’’ (Anura: Dendrobatidae: Hyloxalinae) from a cloud forest near Bogotá, Colombia, with comments on the *subpunctatus* clade. Vertebrate Zoology 68:123–141.

Acosta-Galvis, A.R., and A. Pinzón. 2018. Una nueva rana nodriza (Anura: Dendrobatidae) de los bosques de niebla asociados a la cuenca del Orinoco de Colombia. Biota Colombia 19 (2018):160–190.

Acosta-Galvis, A.R., M. Vargas-Ramírez, M. Anganoy-Criollo, O. A. Ibarra, and S. Gonzáles. 2020. Description of a new diminutive *Hyloxalus* (Anura: Dendrobatidae: Hyloxalinae) from the Magdalena Valley of Colombia. Zootaxa 4758:83–102.

Abdala, V., M.C. Vera, L.I. Amador, G. Fontanarrosa, J. Fratani, and M.L. Ponssa. 2019. Sesamoids in tetrapods: the origin of new skeletal morphologies. Biological Reviews 94:2011–2032.

Aichinger, M. 1991. A new species of poison-dart frog (Anura: Dendrobatidae) from the Serranía de Sira, Peru. Herpetologica 47:1–5.

Amézquita, A., R. Márquez, R. Medina, D. Mejía-Vargas, T.R. Kahn, G. Suárez, and L. Mazariegos 2013. A new species of Andean poison frog, *Andinobates* (Anura: Dendrobatidae), from the northwestern Andes of Colombia. Zootaxa 3620: 163–178.

Andrade, S.P., E.P. Victor-Júnior, W. Vaz-Silva. 2013. Distribution extension, new state record and geographic distribution map of *Ameerega berohoka* Vaz-Silva and Maciel, 2011 (Amphibia, Anura, Dendrobatidae) in Central Brazil. Herpetology Notes 6: 337–338.

Anganoy-Criollo, M. 2013. Tadpoles of the high-Andean *Hyloxalus subpunctatus* (Anura: Dendrobatidae) with description of larval variation and species distinction by larval morphology. Papéis Avulsos de Zoologia 53:211–224.

Anganoy-Criollo, M. 2014. Exploración y análisis de caracteres filogenéticos en el condrocráneo de los renacuajos de los géneros de las ranas venenosas neotropicales (Anura: Dendrobatoidea) de Colombia. M.Sc. dissertation, Universidad Nacional de Colombia.

Anganoy-Criollo, M., and B. Cepeda-Quilindo. 2017. Redescription of the tadpoles of *Epipedobates narinensis* and *E. boulengeri* (Anura: Dendrobatidae). Phyllomedusa 16:155–182.

Anganoy-Criollo, M., A. Viuche-Lozano, M.P. Enciso-Calle, M.H. Bernal, and T. Grant. *in press*. The enigmatic *Hyloxalus edwardsi* species group (Anura: Dendrobatidae): Phylogenetic position and a new species. Herpetologica, 00:000 – 000.

Arch, V.S., D.D. Simmons, P.M. Quiñones, A.S. Feng, J. Jiang, B.L. Stuart, J.-X. Shen, C. Blair, P.M. Narins. 2012. Inner ear morphological correlates of ultrasonic hearing in frog. Hearing Research 283:70–79.

Ardila-Robayo, M.C., A.R. Acosta-Galvis, L.A. Coloma. 2000 “1999”. Una nueva especie de *Colostethus* Cope 1867 (Amphibia: Anura: Dendrobatidae) de la Cordillera Oriental de Colombia. Revista de la Academia Colombiana de Ciencias Exactas, Físicas y Naturales 23:239–244.

Barbour, T., and G.K. Noble. 1920. Some amphibians from northwestern Perú, with a revision of the genera *Phyllobates* and *Telmatobius*. Bulletin of the Museum of Comparative Zoology 63:395–427.

Barnes, W.J.P., M. Baum, H. Peisker, and S.N. Gorb. 2013. Comparative Cryo-SEM and AFM studies of hylid and rhacophorid tree frog toe pads. Journal of Morphology 274:1384–1396.

Barrio-Amorós, C.L., J.C. Santos, and C.R. Molina. 2010. An addition to the diversity of dendrobatid frogs in Venezuela: description of three new collared frogs (Anura: Dendrobatidae: Mannophryne). Phyllomedusa 9:3–35.

Barrio-Amorós, C.L., R. Rivero, and J.C. Santos. 2011. A new striking dendrobatid frog (Dendrobatidae: Aromobatinae, Aromobates) from the Venezuelan Andes. Zootaxa 3063:39–52.

Batista, A., A C.A. Jaramillo, M. Ponce, A.J. Crawford. 2014. A new species of *Andinobates* (Amphibia: Anura: Dendrobatidae) from west central Panama. Zootaxa 3866: 333–352.

Bauer, L. 1994. New names in the family Dendrobatidae (Anura, Amphibia). Ripa. Netherlands Fall: 1–6.

Bhaduri, J.L. 1953. A study of the urogenital system of Salientia. Proceedings of the Zoological Society of Bengal 6:1–111.

Bentley, P. J., and A.R. Main. 1972. Zonal differences in permeability of the skin of some anuran Amphibia. American Journal of Physiology 223:361–362.

Bernal, M.H., V.F. Luna-Mora, O. Gallego, A. Quevedo. 2007. A new species of poison frog (Amphibia: Dendrobatidae) from the Andean mountains of Tolima, Colombia. Zootaxa 1638:59–68.

Blotto, B., M. Pereira, T. Grant, J. Faivovich. 2020. Hand and foot musculature of Anura: structure, homology, terminology, and synapomorphies for major clades. Bulletin of the American Museum of Natural History 443:1–155.

Boulenger, G.A. 1882a. Account of the reptiles and batrachians collected by Mr. Edward Whymper in Ecuador in 1879–80. Annals and Magazine of Natural History Series 5:457–467.

Boulenger, G.A. 1882b. Catalogue of the Batrachia Salientia s. Ecaudata in the collection of the British Museum. London: Taylor and Francis.

Boulenger, G.A. 1898. An account of the reptiles and batrachians collected by Mr. W.F.H. Rosenberg in western Ecuador. Proceedings of the Zoological Society of London 1898:107–126.

Boulenger, G.A. 1899. Descriptions of new batrachians in the collection of the British Museum (Natural History). Annals and Magazine of Natural History Series 7:273–277.

Boulenger, G.A. 1918. Descriptions of south-American batrachians. Annals and Magazine of Natural History Series 9:427–433.

Boulenger, G. A. 1919. Descriptions of two new lizards and a new frog from the Andes of Colombia. Proceedings of the Zoological Society of London 1919:79–81.

Bremer, K. 1988. The limits of aminoacid sequence data in angiosperm phylogenetic reconstruction. Evolution 42:795–803.

Brown, J.L., and E. Twomey. 2009. Complicated histories: three new species of poison frogs of the genus *Ameerega* (Anura: Dendrobatidae) from north-central Peru. Zootaxa 2049:1–38.

Brown, J.L., E. Twomey, A. Amézquita, M.B. Souza, J.P. Caldwell, S. Lötters, R. von May, P.R. Melo-Sampaio, D. Mejía-Vargas, P. Perez-Peña, M. Pepper, E.H.

Poelman, M. Sanchez-Rodriguez, and K. Summers. 2011. A taxonomic revision of the neotropical poison frog genus *Ranitomeya* (Amphibia: Dendrobatidae). Zootaxa 3083:1–120.

Brown, J.L., K. Siu-Ting, R. Von May, E. Twomey, W.X. Guillory, M.S. Deutsch, and G. Chávez. 2019. Systematics of the *Ameerega rubriventris* complex (Anura: Dendrobatidae) with descriptions of two new cryptic species from the East-Andean versant of Peru. Zootaxa 4712:211–235.

Burton, T.C. 1980. Phylogenetic and functional significance of cutaneous muscles in Microhylid frogs. Herpetologica 36:256–264.

Burton, T.C. 1998a. Pointing the way: The distribution and evolution of some characters of the finger muscles of frogs. American Museum Novitates, 3229:1–13.

Burton, T.C. 1998b. Are the distal extensor muscles of the fingers of anurans an adaptation to arboreality?. Journal of Herpetology 32:611–617.

Cabra-García, J., and G. Hormiga. 2019. Exploring the impact of morphology, multiple sequence alignment and choice of optimality criteria in phylogenetic inference: a case study with the Neotropical orb-weaving spider genus *Wagneriana* (Araneae: Araneidae). Zoological Journal of the Linnean Society 2019:1–176.

Caldwell, J.P. 2005. A new Amazonian species of *Cryptophyllobates* (Anura: Dendrobatidae). Herpetologica 61:449–461.

Caldwell, J.P., and C.W. Myers. 1990. A new poison frog from Amazonian Brazil, with further revision of the *quinquevittatus* group of *Dendrobates*. American Museum Novitates 2988:1–21.

Caldwell, J.P., A.P. Lima, and G.M. Biavatia. 2002. Descriptions of tadpoles of *Colostethus marchesianus* and *Colostethus caeruleodactylus* (Anura: Dendrobatidae) from their type localities. Copeia 2002:166–172.

Castillo-Trenn P., and L.A. Coloma. 2008. Notes on behaviour and reproduction in captive *Allobates kingsburyi* (Anura: Dendrobatidae), with comments on evolution of reproductive amplexus. International Zoo Yearbook 42:58–70.

Cavalcanti, I.R.S., M.C. Luna, J. Faivovich, and T. Grant. 2021. Structure and evolution of the sexually dimorphic integumentary swelling on the hands of dendrobatid poison frogs and their relatives (Amphibia: Anura: Dendrobatoidea). Journal of Anatomy 2021:1–19.

Cisneros, D.F., and R. W. McDiarmid. 2007. Revision of the characters of Centrolenidae (Amphibia: Anura: Athesphatanura), with comments on its taxonomy and the description of new taxa of glassfrogs 1572:1–82.

Clavijo-Garzón, S., J.A. Romero-García, M.P. Enciso-Calle, A. Viuche-Lozano, J. Herrán-Medina, M.A. Vejarano-Delgado, and M.H. Bernal. 2018. Lista actualizada de los anfibios del departamento del Tolima, Colombia. Biota Colombiana 19:64–72.

Clark, D.L., and S.E. Peters. 2006. Isometric contractile properties of sexually dimorphic forelimb muscles in the marine toad *Bufo marinus* Linnaeus 1758: functional analysis and implications for amplexus. The journal of Experimental Biology 209: 3448–3456.

Clough, M., and K. Summers. 2000. Phylogenetic systematics and biogeography of the poison frogs: Evidence from mitochondrial DNA sequences. Biological Journal of the Linnean Society 70:515–540.

Cochran, D.M., and C.J. Goin. 1970. Frogs of Colombia. Bulletin of the U.S. National Museum 288:1–655.

Coloma, L.A. 1995. Ecuadorian frogs of the genus *Colostethus* (Anura: Dendrobatidae). The University of Kansas Natural History Museum Miscellaneous Publication 87:1–72.

Cope, E.D. 1865. Sketch of the primary groups of Batrachia Salientia. Natural History Review, New Series, 5:97–120.

Cope, E.D. 1866a. Fourth contribution to the herpetology of tropical America. Proceedings of the Academy of Natural Sciences of Philadelphia 18:123–132.

Cope, E.D. 1899. Contributions to the herpetology of New Granada and Argentina, with descriptions of new forms. The Philadelphia Museums Scientific Bulletin 1:2–22.

Costa, R.C., K.G. Facure, and A.A. Giaretta. 2006. Courtship, vocalization, and tadpole description of *Epipedobates flavopictus* (Anura: Dendrobatidae) in southern Goiás, Brazil. Biota Neotropica 6.

Daly et al. 1978. Classification of skin alkaloids from neotropical poison-dart frogs (Dendrobatidae). Toxicon 16:163–188.

Davis, M., and T. Burton. 1982. Osteology and myology of the gastric brooding frog *Rheobatrachus silus* Liem (Anura: Leptodactylidae). Australian Journal of Zoology 30:503–521.

de la Riva, I., C. Lansac, B. Cepeda, G. Cantillo, J. de Luca, L. González, R. Márquez, and P.A. Burrowes. 2020. Forensic bioacoustics? The advertisement calls of two locally extinct frogs from Colombia. Amphibian and Reptile Conservation 14: 177–188.

de Sá, R.O., T. Grant, A. Camargo, W.R. Heyer, M.L. Ponssa, and E. Stanley. 2014. Systematics of the neotropical genus *Leptodactylus* Fitzinger, 1826 (Anura:

Leptodactylidae): Phylogeny, the relevance of non-molecular evidence, and species accounts. South American Journal of Herpetology 9:S1–S128.

Dias, P.H.D.S., M. Anganoy-Criollo, J.M. Guayasamin, and T. Grant. 2018a, The tadpole of *Epipedobates darwinwallacei* Cisneros-Heredia and Yánez-Muñoz, 2011 (Dendrobatidae: Colostethinae), with new synapomorphies for *Epipedobates*. South American Journal of Herpetology 13:54–63.

Dias, P.H.D.S. 2018b. Evolution of larval characters in Dendrobatoidea Cope, 1865 (Amphibia; Anura; Dendrobatidae and Aromobatidae). Ph.D., dissertation. Universidade de São Paulo, Brazil.

Dias, P.H.D.S., A.P. Brandão, T. Grant. 2018c, The buccopharyngeal morphology of the tadpole of *Ameerega flavopicta* (Anura: Dendrobatidae: Colostethinae), with a redescription of its external morphology. Herpetologica 74:323–328.

Dias, P.H.D.S., M. Anganoy-Criollo, M. Rada, T. Grant. 2021. The tadpoles of the funnel-mouthed dendrobatids (Anura: Dendrobatidae: Colostethinae: *Silverstoneia*): external morphology, musculoskeletal anatomy, buccopharyngeal cavity, and new synapomorphies. Journal of Zoological Systematics and Evolutionary Research 2021:1–27.

Dingerkus, G., and L.D. Uhler. 1977. Enzyme clearing of alcian blue stained whole small vertebrates for demonstration of cartilage. Stain Technology 52:229–232.

Diogo, R., and J.M. Ziermann. 2014. Development of fore- and hindlimb muscles in frogs: Morphogenesis, homeotic transformations, digit reduction, and the forelimb–hindlimb enigma. Journal of Experimental Zoology (Mol. Dev. Evol) 322B:86–105.

Drewes, R.C., M.S. Hedrick, S.S. Hillman, and P.C. Witthers. 2007. Unique role of skeletal muscle contraction in vertical lymph movement in anurans. Journal of Experimental Biology 210:3931–3939. https://doi:10.1242/jeb.009548

Drewes, R.C., S.S. Hillman, M.S. Hedrick, and P.C. Withers. 2013. Evolutionary implications of the distribution and variation of the skeletal muscles of the anuran lymphatic system. Zoomorphology 132:339–349. https://doi:10.1007/s00435-013-0190-7

Dubois, A. 2017. The nomenclatural status of *Hysaplesia*, *Hylaplesia*, *Dendrobates* and related nomina (Amphibia, Anura), with general comments on zoological nomenclature and its governance, as well as on taxonomic databases and websites. Bionomina 11:1–48.

Dubois, A., A. Ohler, A. Pyron. 2021. New concepts and methods for phylogenetic taxonomy and nomenclature in zoology, exemplified by a new ranked cladonomy of recent amphibians (Lissamphibia). Megataxa 5:1–738.

Duellman, W.E. 2004. Frogs of the genus *Colostethus* (Anura; Dendrobatidae) in the Andes of northern Peru. Scientific Papers Natural History Museum, The University of Kansas 35:1–49.

Duellman, W.E., and E. Lehr. 2009. Terrestrial-breeding frogs (Strabomantidae) in Peru. Nature und Tier Verlag, Münster, Germany.

Duellman, W.E., and J.E. Simmons. 1988. Two new species of dendrobatid frogs, genus *Colostethus*, from the Cordillera del Cóndor, Ecuador. Proceedings of the Academy of Natural Sciences of Philadelphia 140:115–124.

Duellman, W.E., and L. Trueb. 1994. Biology of Amphibians. McGraw Hill. Inc. New York, USA.

Duellman, W.E., and E.R. Wild. 1993. Anuran amphibians from the Cordillera de Huancabamba, northern Peru: systematics, ecology, and biogeography. Occasional Papers of the Museum of Natural History University of Kansas 157:1–53.

Duellman, W.E., I. de la Riva, E. Wild. 1997. Frogs of the *Hyla armata* and *Hyla pulchella* groups in the Andes of South America, with definitions and analyses of phylogenetic relationships of Andean groups of Hyla. Scientific Papers, Natural History Museum, University of Kansas 3:1–41.

Dunlap, D.G. 1966. The development of the musculature of the hindlimb in the frog, *Rana pipiens*. Journal of Morphology 119:241–258.

Ecker, A., and G. Haslam. 1889. The Anatomy of the Frog. Oxford, Clarendon Press, USA.

Dunn, E.R. 1924. Some Panamanian frogs. Occasional Papers of the Museum of Zoology, University of Michigan 151:1–17.

Dunn E.R. 1957. Neotropical frog genera: *Prostherapis* versus *Hyloxalus*, with remarks on *Phyllobates*. Copeia 1957:77–78.

Ecker, A., and G. Haslam. 1889. Anatomy of the frogs. Clarendon Press, Oxford.

Edwards, S.R. 1971. Taxonomic notes on South American *Colostethus* with descriptions of two new species (Amphibia, Dendrobatidae). Proceedings of the Biological Society of Washington 84:147–162.

Edwards, S.R. 1974. Taxonomic notes on south American dendrobatid frogs of the genus *Colostethus*. Occasional Papers of the Museum of Natural History, The University of Kansas 30:1–14.

Elias-Costa, A.J., R. Montesinos, T. Grant, J. Faivovich. 2017. The vocal sac of Hylodidae (Amphibia, Anura): Phylogenetic and functional implications of a unique morphology. Journal of Morphology 2017:1–11.

Eterovick, P.C., A.M. de Souza, I. Sazima.. 2020. Anfíbios anuros da Serra do Cipó, Minas Gerais, Brasil. Bios Consultoria e Réplicas Eireli. Brasil.

Fabrezi M., and P. Alberch. 1996. The carpal elements of anurans. Herpetologica 52:188–204.

Fabrezi, M., A.S. Manzano, V. Abdala, F. Lobo. 2014. Anuran locomotion: ontogeny and morphological variation of a distinctive set of muscles. Evolutionary Biology 41:308–326.

Fandiño, M.C., H. Luddecke, and A. Amézquita. 1997. Vocalization and larval transportation of male *Colostethus subpunctatus* (Anura: Dendrobatidae). Amphibia-Reptilia 18: 39–48.

Fedorov, A., R. Beichel, J. Kalpathy-Cramer, J. Finet, J.-C. Fillion-Robin, S. Pujol, C. Bauer, D. Jennings, F. Fennessy, M. Sonka, J. Buatti, S. Aylward, J.V. Miller, S. Pieper, and R. Kikinis. 2012. 3D Slicer as an image computing platform for the Quantitative Imaging Network. Magnetic Resonance Imaging 30:1323–1341.

Fidalgo, G., K. Paiva, G. Mendes, R. Barcellos, G. Colaço, G. Sena, A. Pickler, C.L. Mota1, G. Tromba, L.P. Nogueira, D. Braz, H.R. Silva, M.V. Colaço, and R.C. Barroso. Synchrotron microtomography applied to the volumetric analysis of internal structures of Thoropa miliaris tadpoles. Scientific Report Nature 10:18934.

Forti, L.R., C. Strüssmann, T. Mott. 2010. Acoustic communication and vocalization microhabitat in *Ameerega braccata* (Steindachner, 1864) (Anura, Dendrobatidae) from midwestern Brazil. Brazilian Journal of Biology 70:211–216.

Fouquet, A., S.M. Souza, P.M.S. Nunes, P.J.R. Kok, F.F. Curcio, C.M. de Carvalho, T. Grant, M.T. Rodrigues. 2015. Two new endangered species of *Anomaloglossus* (Anura: Aromobatidae) from Roraima State, northern Brazil. Zootaxa 3926:191–210.

Fouquet, A., J-P. Vacher, E.A. Courtois, B.Villette, H. Reizine, P. Gaucher, R. Jairam, P. Ouboter, and P.J.R. Kok. 2018. On the brink of extinction: two new species of *Anomaloglossus* from French Guiana and amended definitions of *Anomaloglossus degranvillei* and *A. surinamensis* (Anura: Aromobatidae). Zootaxa 4379:1–23.

Fouquet, A., B. Ferrier, J. Salmona, S. Tirera, J-P. Vacher, E.A. Courtois, P. Gaucher, J. Dias Lima, P.M.S. Nunes, S.M. de Souza, M.T. Rodrigues, B. Noonan, B. de Thoisy. 2019. Phenotypic and life-history diversification in Amazonian frogs despite past introgressions. Molecular Phylogenetics and Evolution 130:169–180.

Fox, H. 1994. Structure of the integument. Pp. 1–32 in Amphibian Biology, volume I (Heatwole, H., and G. T. Barthalmus eds.). Surrey Beatty and Sons, New South Wales, Australia.

French, C.M., C. Burkette, S. Reichle, and J.L. Brown. 2019. The tadpole of *Ameerega boehmei* in southeastern Bolivia. Zootaxa 4661:197–200.

Frost, D.R. 1986. A new species of *Colostethus* (Anura: Dendrobatidae) from Ecuador. Proceedings of the Biological Society of Washington 99:214–217.

Frost, D.R. 2021. Amphibian species of the world: An online reference. Version 6.1 (01/12/2021). Electronic Database accessible at https://amphibiansoftheworld.amnh.org/index.php. American Museum of Natural History, New York, USA. doi.org/10.5531/db.vz.0001

Frost, D.R., T. Grant, J. Faivovich, R.H. Bain, A. Haas, C.F.B. Haddad , R.O. de Sá, S.C. Donnellan, C.J. Raxworthy, M. Wilkinson, A. Channing, J.A. Campbell, B.L. Blotto, P. Moler, R.C. Drewes, R.A. Nussbaum, J.D. Lynch, D. Green, and W.C. Wheeler.. 2006. The amphibian tree of life. Bulletin of the American Museum of Natural History 297:1–370.

Gaupp E. 1896. A. Ecker's und R. Wiedersheim's Anatomie des Frosches. I. Braunschweig: Friedrich Vieweg und Sohn.

Gaupp, E. 1904. Lehre von integument und von den sinnesorganen. Pp.3–439 in Anatomie des Frosches (A. Ecker's and R. Wiederseim's, eds.). Friedrich Vieweg und Sohn, Braunschweig, Germany.

Giribet, G. 2015. Morphology should not be forgotten in the era of genomics—a phylogenetic perspective. Zoologischer Anzeiger 256:96–103.

Goloboff, P.A. 1996. Methods for faster parsimony analysis. Cladistics 12:199–220.

Goloboff, P.A. 1999. Analyzing large data sets in reasonable times, solutions for composite optima. Cladistics 24:774–786.

Goloboff, P.A., and S.A. Catalano. 2016. TNT version 1.5, including a full implementation of phylogenetic morphometrics. Cladistics 32:221–238.

Goloboff, P.A., J.S. Farris, and K.C. Nixon. 2008. TNT, a free program for phylogenetic analysis. Cladistics 24:774–786.

Goodman, M., C.B. Olson, J.E. Beeber, J. Czelusniak. 1982. New perspectives in the molecular biological analysis of mammalian phylogeny. Acta Zoologica Fennica 169:19–35.

Gosner, K.L. 1960. A simplified table for staging anuran embryos and larvae with notes on identification. Herpetologica 16:183–190.

Grant, T. 2007. A new, toxic species of *Colostethus* (Anura: Dendrobatidae: Colostethinae) from the Cordillera Central of Colombia. Zootaxa 1555:39–51.

Grant, T. 2019. Outgroup sampling in phylogenetics: Severity of the test and successive outgroup expansion. Journal of Zoological Systematics and Evolutionary Research 2019:1–16. https://doi.org/10.1111/jzs.12317

Grant, T., and M.C. Ardila-Robayo. 2002. A new species of *Colostethus* (Anura: Dendrobatidae) from the eastern slopes of the Cordillera Oriental of Colombia. Herpetologica, 58: 252–260.

Grant, T., and W. Bolivar-G. 2014. A new species of semiarboreal toad with a salamander-like ear (Anura: Bufonidae: *Rhinella*). Herpetologica, 70:198–210.

Grant, T., and F. Castro-Herrera. 1998. The cloud forest *Colostethus* (Anura, Dendrobatidae) of a region of the Cordillera Occidental of Colombia. Journal of Herpetology 32:378– 392.

Grant, T., and A.G. Kluge. 2003. Data exploration in phylogenetic inference: Scientific, heuristic, or neither. Cladistics 19:379–418.

Grant, T., and A.G. Kluge. 2004. Transformation series as an ideographic character concept. Cladistics, 20:23–31.

Grant, T., and A.G. Kluge. 2008a. Clade support measures and their adequacy. Cladistics 24:1051–1064.

Grant, T., and A.G. Kluge. 2008b. Credit where credit is due: The Goodman-Bremer support metric. Molecular Phylogenetics and Evolution 49:405–406.

Grant, T., and A.G. Kluge. 2009. Parsimony, explanatory power, and dynamic homology testing. Systematics and biodiversity 7:357–363. https://doi.org/10.1017/S147720000999017X

Grant T., and Myers C.W. 2013. Review of the frog genus *Silverstoneia*, with descriptions of five new species from the Colombian Chocó (Dendrobatidae: Colostethinae). American Museum Novitates 3784:1–58.

Grant, T., and L.O. Rodríguez. 2001. Two new species of frogs of the genus *Colostethus* (Dendrobatidae) from Peru and a redescription of *C. trilineatu*s (Boulenger, 1883). American Museum Novitates 3355:1–24.

Grant, T., E.C. Humphrey, and C.W. Myers. 1997. The median lingual process of frogs: A bizarre character of Old World ranoids discovered in South American dendrobatids. American Museum Novitates 3212:1–40.

Grant, T., D.R. Frost, J.P. Caldwell, R. Gagliardo, C.F.B. Haddad, P.J.R. Kok, and W.C. Wheeler. 2006. Phylogenetic systematics of dart-poison frogs and their relatives (Anura: Athesphatanura: Dendrobatidae). Bulletin of the American Museum of Natural History 299:1–262.

Grant T., A.R. Acosta-Galvis, and M. Rada. 2007. A name for the species of *Allobates* (Anura: Dendrobatoidea: Aromobatidae) from the Magdalena Valley of Colombia. Copeia 2007:844–854.

Grant, T., M. Rada, M. Anganoy-Criollo, A. Batista, P.H. Dias, A.M. Jeckel, D.J. Machado, and J.V. Rueda-Almonacid. 2017. Phylogenetic systematics of dart-poison frogs and their relatives revisited (Anura: Dendrobatoidea). South American Journal of Herpetology 12:1–90.

Guillory, W.X., M.R. Muell, K. Summers, and J.L. Brown. 2019. Phylogenomic reconstruction of the neotropical poison frogs (Dendrobatidae) and their conservation. Diversity 2019:1–14.

Guillory, W.X., C.M. French, E.M. Twomey, G. Chávez, I. Prates, R. von May, I. de la Riva, S. Lötters, S. Reichle, S.J. Serrano-Rojas, A. Whitworth, J.L. Brown. 2020. Phylogenetic relationships and systematics of the Amazonian poison frog genus *Ameerega* using ultraconserved genomic elements. Molecular Phylogenetics and Evolution 142:1–13.

Haas, A. 1995. Cranial features of dendrobatid larvae (Amphibia: Anura: Dendrobatidae). Journal of Morphology 224:241–264.

Haas, A. 1997. The larval hyobranchial apparatus of discoglossoid frogs: its structure and bearing on the systematics of the Anura (Amphibia: Anura). Journal Zoological Systematics and Evolutionary Research 35:179–197.

Haas, A. 2001. Mandibular arch musculature of anuran tadpoles, with comments on homologies of amphibian jaw muscles. Journal of Morphology, 247:1–33.

Haas, A., J. Pohlmeyer, D.S. McLeod, T. Kleinteich, S.T. Hertwig, I. Das, D.R. Buchholz. 2014. Extreme tadpoles II: The highly derived larval anatomy of *Occidozyga baluensis* (Boulenger, 1896), an obligate carnivorous tadpole. Zoomorphology 133:321–342.

Haddad, C.F.B., and M. Martins. 1994. Four species of Brazilian poison frogs related to *Epipedobates pictus* (Dendrobatidae): Taxonomy and natural history. Herpetologica 50:282–295.

Haddad, C.F.B., and J.P. Pombal Jr. 1995. A new species of *Hylodes* from southeastern Brazil (Amphibia: Leptodactylidae). Herpetologica 51:279–286.

Heath, T.A., S.M. Hedtke, and D.M. Hillis. 2008. Taxon sampling and the accuracy of phylogenetic analyses. Journal of Systematics and Evolution 46:239–257. https://doi.org/10.3724/SP.J.1002.2008.08016

Hellmich W. 1940. Beiträge zur Kenntnis der Gattung *Hyloxalus* (Brachycephalidae, Amphibia). Zoologischer Anzeiger 131:113–128.

Hennig, W. 1966. Phylogenetic systematics. Chicago: University of Illinois Press.

Hillis, D.M. 1998. Taxonomic sampling, phylogenetic accuracy, and investigator bias. Systematic Biology 47:3–8. https://doi. org/10.1080/106351598260987

Hillis, D.M., D.D. Pollock, J.A. McGuire, and D.J. Zwickl. 2003. Is sparse taxon sampling a problem for phylogenetic inference?. Systematic Biology 52:124–126.

Holland, B.R., D. Penny, and M.D. Hendy. 2003. Outgroup misplacement and phylogenetic inaccuracy under a molecular clock—a simulation study. Systematic Biology 52:229–238.

Hoyos, J.M., and L. Salgar. 2016. New conditions and intraspecific variation of some muscles of hands and feet of *Dendropsophus labialis* (Peters, 1863) (Anura, Hylidae). Acta Zoologica 97: 143–153.

Hutter, C.R., J.M. Guayasamin, and J.J. Wiens. 2013. Explaining Andean megadiversity: the evolutionary and ecological causes of glassfrog elevational richness patterns. Ecology Letters 16:1135–1144.

Hutter, C.R., S.M. Lambert, and J.J. Wiens. 2017. Rapid diversification and time explain amphibian richness at different scales in the tropical Andes, earth's most biodiverse hotspot. The American Naturalist 190:828–843.

Jaramillo. A.J., G. Gagliardi-Urrutia, P.I. Simões, and S. Castroviejo-Fisher. 2021. Redescription and phylogenetics of *Allobates trilineatus* (Boulenger 1884 "1883") (Anura: Aromobatidae) based on topotypic specimens. Zootaxa 4951: 201–235.

Jetz, W., and A. Pyron. 2018. The interplay of past diversification and evolutionary isolation with present imperilment across the amphibian tree of life. Nature Ecology and Evolution 2:850–858.

Jiménez de la Espada, M. 1871 "1870". Fauna neotropicalis species quaedam nondum cognitae. Jornal se Sciencias, Mathematicas, Physicas e Naturaes 3:57–65.

Jiménez de la Espada M. 1875. Vertebrados del viaje al Pacífico verificado de 1862 a 1865 por una comisión de naturalistas enviada por el gobierno Español. Batracios. Imprenta de Miguel Ginesta, Madrid.

Kaplan, M. 1997. A new species of *Colostethus* from the Sierra Nevada de Santa Marta (Colombia) with comments on inter-generic relationships within the Dendrobatidae. Journal of Herpetology 31:369–375.

Kaplan, M. 2004. Evaluation and redefinition of the states of anuran pectoral girdle architecture. Herpetologica 60:84–97.

Klein, B. R.A.Regnet, M. Krings, and D. Rödder. 2020. Larval development and morphology of six neotropical poison-dart frogs of the genus *Ranitomeya* (Anura: Dendrobatidae) based on captive-raised specimens. Bonn Zoological Bulletin 69:191–223.

Kluge, A.G. 1989. A concern for evidence and a phylogenetic hypothesis of relationships among *Epicrates* (Boidae, Serpentes). Systematic Biology 38:7–25.

Kluge, A.G. 2004. On total evidence: for the record. Cladistics 20:205– 207.

Kluge, A.G. 2009. Explanation and falsification in phylogenetic inference: Exercises in Popperian philosophy. Acta Biotheorica 57:171–186.

Kluge, A.G., and T. Grant. 2006. From conviction to anti-superfluity: Old and new justifications for parsimony in phylogenetic inference. Cladistics 22:276–288.

Kneller, M., and K. Henle. 1985. Ein neuer blattsteiger-frosch (Salientia: Dendrobatidae: *Phyllobates*) aus Peru. Salamandra 21:62–69.

Koch, C., P.J. Venegas, D. Rödder. 2011. Advertisement call of *Hyloxalus elachyhistus* (Edwards, 1971) (Anura, Dendrobatidae). Salamandra 47:116–119.

Kok, P.J.R. 2010. A redescription of *Anomaloglossus praderioi* (La Marca, 1998) (Anura: Aromobatidae: Anomaloglossinae), with description of its tadpole and call. Papéis Avulsos de Zoologia 50:51–68.

Kok, P.J.R., and M. Kalamandeen. 2008. Introduction to the taxonomy of the amphibians of Kaieteur National Park, Guyana. Abc Taxa, The Journal Dedicated to Capacity Building in Taxonomy and Collection Management 5:1–278.

Kok, P.J.R., R.D. MacCulloch, P. Gaucher, E.H. Poelman, G.R. Bourne, A. Lathrop, G.L. Lenglet. 2006a. A new species of *Colostethus* (Anura, Dendrobatidae) from French Guiana with a redescription of *Colostethus beebei* (Noble, 1923) from its type locality. Phyllomedusa 5:43–66.

Kok P.J.R., H. Sambhu, I. Roopsind, G.L. Lenglet, G.R Bourne. 2006b. A new species of *Colostethus* (Anura: Dendrobatidae) with maternal care from Kaieteur National Park, Guyana. Zootaxa 1238:35–61.

Kohler, J., A. John, and W. Böhme. 2006. Notes on amphibians recently collected in the Yungas de La Paz region, Bolivia. Salamandra 42:21–27.

La Marca, E. 1989. A new species of collared frog (Anura: Dendrobatidae: *Colostethus*) from Serrania de Portuguesa, Andes of Estado Lara, Venezuela. Amphibia–Reptilia 10:175–183.

La Marca, E. 1994. Descripción de un nuevo género de ranas (Amphibia: Dendrobatidae) de la Cordillera de Mérida, Venezuela. Anuario de Investigación 1991:39–41.

La Marca, E. 1995. Biological and systematic synopsis of a genus of frogs from northern mountains of South America (Anura: Dendrobatidae: *Mannophryne*). Bulletin of the Maryland Herpetological Society 31:40–78.

Lee, J.C. 2001. Evolution of a secondary sexual dimorphism in the toad, *Bufo marinus*. Copeia 4:928–935.

Lee, M.S.Y, and A. Palci. 2015. Morphological phylogenetics in the genomic age. Current Biology 25:922–929.

Lima, A.P., and J.P. Caldwell. 2001. A new amazonian species of *Colostethus* with sky blue digits. Herpetologica, 57: 180–189.

Lima, A.P., J.P. Caldwell, C. Strussmann. 2009. Redescription of *Allobates brunneus* (Cope) 1887 (Anura: Aromobatidae: Allobatinae), with a description of the tadpole, call, and reproductive behavior. Zootaxa 16:1–16.

Limese, C.E. 1964. La musculatura del muslo en los ceratofrinidos y formas afines, con un análisis crítico sobre la significación de los caracteres miológicos en la sistemática de los anuros superiores. Contribuciones Cientificas–Serie Zoología 1964:193–245.

Lips, K.R., P.A. Burrowes, J.R. Mendelson. 2005. Amphibian population declines in latin America: A synthesis. Biotropica 37:222–226.

Liu, C.e.C. 1935. Types of vocal sac in the Salientia. Proceedings of the Boston Society of Natural History 41:19–40.

Lötters, S., K.-H. Jungfer, A. Widmer. 2000. A new genus of aposematic poison frog (Amphibia: Anura: Dendrobatidae) from the upper Amazon basin, with notes on its reproductive behaviour and tadpole morphology. Jahreshefte der Gesellschaft für Naturkunde in Wurttemberg 156:233–243.

Lötters S., A. Schmitz, S. Reichle. 2005. A new cryptic species of poison frog from the Bolivian Yungas (Anura: Dendrobatidae: *Epidedobates*). Herpetozoa 18:115–124.

Lötters S., K.-H. Jungfer, F.W. Henkel, W. Schmidt. 2007. Poison frogs. Edition Chimaira, Frankfurt.

Lötters S., A. Schmitz, S. Reichle, D. Rödder, V. Quennet. 2009. Another case of cryptic diversity in poison frogs (Dendrobatidae: *Ameerega*)—description of a new species from Bolivia. Zootaxa 2028:20–30.

Lynch, J.D. 1982. Two new species of poison-dart frogs (*Colostethus*) from Colombia. Herpetologica 38:366–374.

Lynch, J.D. 1998. New species of *Eleutherodactylus* from the Cordillera Occidental of western Colombia with a synopsis of the distributions of species in western Colombia. Revista de la Academia Colombiana de Ciencias Exactas, Físicas y Naturales 22:117–148.

Lynch, J.D., and W.E. Duellman. 1997. Frogs of the genus *Eleutherodactylus* in western Ecuador. Systematics, ecology, and biogeography. Special Publication Natural History Museum University of Kansas 23:1– 236.

Lynch, J.D., and T. Grant. 1998. Dying frogs in western Colombia: Catastrophe or trivial observation?. Revista de la Academia Colombiana de Ciencias Exactas, Físicas y Naturales 22:149–152.

Lyra, M.L., A.C.C. Lourenço, P.D.P. Pinheiro, T.L. Pezzuti, D. Baêta, A. Barlow, M. Hofreiter, J.P. Pombal Jr, C.F.B. Haddad, and J. Faivovich. 2020. High-throughput DNA sequencing of museum specimens sheds light on the long-missing species of the *Bokermannohyla claresignata* group (Anura: Hylidae: Cophomantini). Zoological Journal of the Linnean Society XX:1–21.

Machado, D.J. 2015. YBYRÁ facilitates comparison of large phylogenetic trees. BMC Bioinformatics 16: 204.

Maddison W.P., and D.R. Maddison. 2016. Mesquite: A modular system for evolutionary analysis, Version 3.04. Available from: http:// mesquiteproject.org.

Magalhães R.F., J.V.A. Lacerda, L.P. Reis, P.C.A. Garcia, P.D.P. Pinheiro. 2018. Sexual dimorphism in *Bokermannohyla martinsi* (Bokermann, 1964) (Anura, Hylidae) with a report of male–male combat. South American Journal of Herpetology 13:202–209. http://doi.org/10.2994/SAJH-D-17-00039.1

Magrini, L., K.G. Facure, A.A. Giaretta, W. R. da Silva, and R.C. Costa. 2010. Geographic call variation and further notes n on habitat of *Ameerega flavopicta* (Anura, Dendrobatidae). Studies on Neotropical Fauna and Environment 45:89–94. DOI: 10.1080/01650521.2010.494025.

Malagoli, L.R., F.P. de Sá, C. Canedo, and C.F.B. Haddad. 2017. A new species of *Hylodes* (Anura, Hylodidae) from Serra do Mar, southeastern Brazil: The fourth with nuptial thumb tubercles. Herpetologica, 73:136–147.

Manzano, A.S., V. Abdala, and A. Herrel. 2008. Morphology and function of the forelimb in arboreal frogs: specializations for grasping ability?. Journal of Anatomy 213:296–307.

Marin, C.M., C. Molina-Zuluaga, A. Restrepo, E. Cano, and J.M. Daza. 2018. A new species of *Leucostethus* (Anura: Dendrobatidae) from the eastern versant of the Central Cordillera of Colombia and the phylogenetic status of *Colostethus fraterdanieli*. Zootaxa 4461:359–380.

Martins, M. 1989. Nova espécie de *Colostethus* da Amazônia central (Amphibia: Dendrobatidae). Revista Brasileira de Biologia 49:1009–1012.

Mason, M.J. 2007. Pathways from sound transmission to the inner ear in amphibians. Pp. 147–183. in Hearing and Sound Communication in Amphibians (Narins, P., A. Feng, R.R. Fay, A. Popper., eds). Springer, USA.

McDiarmid, R.W. 1971. Comparative morphology and evolution of frogs of the Neotropical genera *Atelopus*, *Dendrophryniscus*, *Melanophryniscus*, and *Oreophrynella*. Bulletin of the Los Angeles County Museum of Natural History Science 12:1–66.

McDiarmid, R.W. 1994. Preparing amphibians as scientific specimens. Pp. 289–296. In Measuring and Monitoring Biological Diversity. Standard Methods for

Amphibians (Heyer W.R., M.A. Donnelly, R.W. McDiarmid, L.C. Hayek and M.S. Foster, eds.). Smithsonian Institution Press, USA.

McDiarmid, R.W., and R. Altig (eds.) 1999. Tadpoles: The biology of anuran larvae. Chicago: University of Chicago Press.

Melo-Sampaio, P.R., I. Prates, P.L.V. Peloso, R. Recoder, F.D. Vechio, S. Marques-Souza, and M.T. Rodrigues. 2020. A new nurse frog from southwestern amazonian highlands, with notes on the phylogenetic affinities of *Allobates alessandroi* (Aromobatidae), Journal of Natural History 54:43–62. DOI: 10.1080/00222933.2020.1727972

Morales, V.R. 1994. Taxonomía sobre algunos *Colostethus* (Anura: Dendrobatidae) de Sudamerica, con descripción de dos especies nuevas. Revista Española de Herpetologia 8:95–103.

Morales, V.R. 1998. Observaciones sobre la historia natural del *Colostethus littoralis* (Amphibia, Anura, Dendrobatidae). Universidad Nacional Mayor de San Marcos, Museo de Historia Natural, serie de divulgación 11:211–216.

Morales, V. 2002 “2000”. Sistemática y biogeografía del grupo *trilineatus* (Amphibia, Anura, Dendrobatidae, *Colostethus*) con descripción de once nuevas especies. Publicaciones de la Asociación de Amigos de Doñana 13:1–59.

Mudrack, W. 1969. Pflege und zucht eines blattsteiger frosches der gattung *Phyllobates* aus Ecuador. Salamandra, 5:81–84.

Mueses-Cisneros, J.J., B. Cepeda-Quilindo, V. Moreno-Quintero. 2008. Una nueva especie de *Epipedobates* (Anura: Dendrobatidae) del suroccidente de Colombia. Papéis Avulsos de Zoologia 48:1–10.

Muñoz-Ortiz, A., Á.A. Velásquez-Álvarez, C.E. Guarnizo, and A.J. Crawford. 2015. Of peaks and valleys: testing the roles of orogeny and habitat heterogeneity in

driving allopatry in mid-elevation frogs (Aromobatidae: *Rheobates*) of the northern Andes. Journal of Biogeography 42:193–205.

Myers, C.W. 1982. Spotted poison frogs: Descriptions of three new *Dendrobates* from western Amazonia, and resurrection of a lost species from "Chiriqui." American Museum Novitates 2721:1–23.

Myers, C.W. 1987. New generic names for some neotropical poison frogs (Dendrobatidae). Papéis Avulsos de Zoologia 36:301–306.

Myers, C.W. 1991. Distribution of the dendrobatid frog *Colostethus chocoensis* and description of a related species occurring macrosympatrically. American Museum Novitates, 3010: 1–15.

Myers, C.W., and P.A. Burrowes. 1987. A new poison frog (*Dendrobates*) from Andean Colombia, with notes on a lowland relative. American Museum Novitates 2899:1–17.

Myers, C.W., and J.W. Daly. 1976a. A new species of poison frog (*Dendrobates*) from Andean Ecuador, including an analysis of its skin toxins. Occasional Papers of the Museum of Natural History, the University of Kansas 59: 1–12.

Myers, C.W., and J.W. Daly. 1976b. Preliminary evaluation of skin toxins and vocalizations in taxonomic and evolutionary studies of poison-dart frogs (Dendrobatidae). Bulletin of the American Museum of Natural History 157: 173–262.

Myers, C.W., and J.W. Daly. 1979. A name for the poison frog of Cordillera Azul, eastern Peru, with notes on its biology and skin toxins (Dendrobatidae). American Museum Novitates 2674:1–24.

Myers, C.W., and J.W. Daly. 1980. Taxonomy and ecology of *Dendrobates bombetes*, a new Andean frog with new skin toxins. American Museum Novitates 2692:1–23.

Myers, C.W., and M.A. Donnelly. 1997. A tepui herpetofauna on a granitic mountain (Tamacuari) in border land between Venezuela and Brazil: report from the Phipps Tapirapeco Expedition. American Museum Novitates 3213: 1–71.

Myers, C.W., and M.A. Donnelly. 2001. Herpetofauna of the Yutajé-Corocoro massif, Venezuela: Second report from the Robert G. Goelet American Museum-Terramar Expedition to the northwestern tepuis. Bulletin of the American Museum of Natural History 261: 1–85.

Myers, C.W., and W.E. Duellman. 1982. A new species of *Hyla* from Cerro Colorado, and the other tree frog records and geographical notes from western Panama. American Museum Novitates 2752:1–32.

Myers, C.W., and L.S. Ford. 1986. On *Atopophrynus*, a recently described frog wrongly assigned to the Dendrobatidae. American Museum Novitates 2843:1–15.

Myers, C.W., and T. Grant. 2009. *Anomaloglossus confusus*, a new Ecuadorian frog formerly masquerading as "*Colostethus*" *chocoensis* (Dendrobatoidea: Aromobatidae). American Museum Novitates 3659:1–12.

Myers, C.W., J.W. Daly, and B. Malkin. 1978. A dangerously toxic new frog (*Phyllobates*) used by Emberá Indians of western Colombia, with discussion of blowgun fabrication and dart poisoning. Bulletin of the American Museum of Natural History161:307–366.

Myers C.W., O.A. Paolillo, and J.W. Daly. 1991. Discovery of malodorous and nocturnal frog in the family Dendrobatidae: Phylogenetic significance of a new genus and species from the Venezuela Andes. American Museum Novitates 3002:1–33.

Myers, C.W., L.O. Rodríguez, and J. Icochea. 1998. *Epipedobates simulans*, a new cryptic species of poison frog from southeastern Peru, with notes on *E. macero* and *E. petersi* (Dendrobatidae). American Museum Novitates 3238:1–20.

Myers, C.W., D. R. Ibáñez, T. Grant T, C.A. Jaramillo. 2012. Discovery of the frog genus *Anomaloglossus* in Panama, with descriptions of two new species from the Chagres Highlands (Dendrobatoidea: Aromobatidae). American Museum Novitates 3763:1–20.

Myers, N., R.A. Mittermeier, C.G. Mittermeier, G.A.B. da Fonseca, and J. Kent. Biodiversity hotspots for conservation priorities. Nature 403:853–858.

Navas, C.A., and R.S. James. 2007. Sexual dimorphism of extensor carpi radialis muscle size, isometric force, relaxation rate and stamina during the breeding season of the frog *Rana temporaria* Linnaeus 1758. The Journal of Experimental Biology 210:715–721.

Neves, M.O., L. A. da Silva, P.S. Akieda, R. Cabrera, R. Koroiva, and D.J. Santana. 2017. A new species of poison frog, genus *Ameerega* (Anura: Dendrobatidae), from the southern Amazonian rain forest. Salamandra 53: 485–493.

Nixon, K.C. 1999. The parsimony ratchet, a new method for rapid parsimony analysis. Cladistics 15, 407–414.

Noble, G.K. 1922. The phylogeny of the Salientia I. The osteology and the thing musculature; their bearing on classification and phylogeny. Bulletin of the American Museum of Natural History 46:1–87.

Noble, G.K. 1923. New batrachians from the Tropical Research Station, British Guiana. Zoologica 3:288–299.

Noble, G.K. 1931. The biology of the Amphibia. New York: McGraw-Hill.

Noble, G.K., and M.E. Jaeckle. 1928. The digital pads of the tree frogs. A study of the phylogenesis of an adaptation structure. Journal of Morphology and Physiology 45:259–292.

Ogushi, Y., A. Tsuzuki, M. Sato, H. Mochida, R. Okada, M. Suzuki, S.D. Hillyard, and S. Tanaka. 2010. The water-absorption region of ventral skin of several semiterrestrial and aquatic anuran amphibians identified by aquaporins. Am. J. Physiol. Regul. Integr. Comp. Physiol. 299:R1150–R1162.

Oka, O., R. Ohtani, M. Satou, and K. Ueda. 1984. Sexually dimorphic muscles in the forelimb of the japanese toad, *Bufo japonicus*. Journal of Morphology 180:297–308.

Ospina-Sarria, J.J., and T. Angarita-Sierra. 2020. A new species of *Pristimantis* (Anura: Strabomantidae) from the eastern slope of the Cordillera Oriental, Arauca, Colombia. Herpetologica, 76:83–92.

Ospina-Sarria, J.J., and W.E. Duellman. 2019. Two new species of *Pristimantis* (Amphibia: Anura: Strabomantidae) from southwestern Colombia. Herpetologica 75:85–95.

Ovalle-Pacheco, A., C. Camacho-Rozo, S. Arroyo. 2019. Amphibians from Serrania de Las Quinchas, in the mid-Magdalena river valley, Colombia. Check List 15:387–404.

Páez-Vacas, M.I., L.A. Coloma, and J.C. Santos. 2010. Systematics of the *Hyloxalus bocagei* complex (Anura: Dendrobatidae), description of two new cryptic species, and recognition of *H. maculosus*. Zootaxa 75:1–75.

Padial, J.M., T. Grant, and D.R. Frost. 2014. Molecular systematics of terraranas (Anura: Brachycephaloidea) with an assessment of the effects of alignment and optimality criteria. Zootaxa 3825:1–132.

Pardo J.D., M. Szostakiwskyj, P.E. Ahlberg, and J.S. Anderson. 2017. Hidden morphological diversity among early tetrapods. Nature Letters 546:642–646.

Péfaur, J.E. 1984. A new species of dendrobatid frog from the coast of Peru. Journal of Herpetology 18:492–494.

Pereyra, M.O., M.C. Womack, J.S. Barrionuevo, B.L. Blotto, D. Baldo , M. Targino, J.J. Ospina-Sarria, J.M. Guayasamin, L.A. Coloma, K.L. Hoke, T. Grant, and J. Faivovich. 2016. The complex evolutionary history of the tympanic middle ear in frogs and toads (Anura). Scientific Reports 6: 34130.

Peters, S.E., and D.A. Aulner. 2000. Sexual dimorphism in forelimb muscles of the bullfrog, *Rana catesbeiana*: a functional analysis of isometric contractile properties. The Journal of Experimental Biology 203: 3639–3654.

Pinheiro, P.D.P., B.L. Blotto, S.R. Ron, E.L. Stanley, P.C.A. Garcia, C.F.B. Haddad, T. Grant, and J. Faivovich. 2021. Prepollex diversity and evolution in Cophomantini (Anura: Hylidae: Hylinae). Zoological Journal of the Linnean Society XX:1–27.

Pirani, R.M., S. Mângia, D.J. Santana, B. de Assis, R.N. Feio. 2010. Rediscovery, distribution extension and natural history notes of *Hylodes babax* (Anura, Hylodidae) with comments on southeastern Brazil biogeography. South American Journal of Herpetology, 5:83–88.

Poelman, E.H., J.C. Verkade, R.P.A van Wijngaarden, and C. Félix-Novoa . 2010. Descriptions of the tadpoles of two poison frogs, *Ameerega parvula* and *Ameerega bilinguis* (Anura: Dendrobatidae) from Ecuador. Journal of Herpetology 44: 409–417.

Ponssa, M.L., J. Goldberg, and V. Abdala. 2010. Sesamoids in anurans: New data, old issues. The Anatomical Record 293:1646–1668.

Popper, K. 1963. Conjectures and Refutations: The growth of scientific knowledge. Routledge and Kegan Paul, London.

Prikryl T., P. Aerts, P. Havelková, A. Herrel, and Z. Roc ek. 2009. Pelvic and thigh musculature in frogs (Anura) and origin of anuran jumping locomotion . Journal of Anatomy 214:100–139.

Puslednik, L., and J.M. Serb. 2008. Molecular phylogenetics of the Pectinidae (Mollusca: Bivalvia) and effect of increased taxon sampling and outgroup selection on tree topology. Molecular Phylogenetics and Evolution 48:1178–1188.

Pyron, R.A. 2014. Biogeographic analysis reveals ancient continental vicariance and recent oceanic dispersal in amphibians. Systematic Biology 63:779–797.

Pyron, R.A. 2015. Post-molecular systematics and the future of phylogenetics. Trends in Ecology and Evolution XX:1–6.

Pyron, R.A., and J.J. Wiens. 2011. A large-scale phylogeny of Amphibia including over 2800 species, and a revised classification of extant frogs, salamanders, and caecilians. Molecular Phylogenetics and Evolution 61:543–583. https://doi: 10.1016/j.ympev.2011.06.012.

Quiguango-Ubillús, A., and L.A. Coloma. 2008. Notes on behaviour, communication and reproduction in captive *Hyloxalus toachi* (Anura: Dendrobatidae), an endangered Ecuadorian frog. International Zoo Yearbook 42:78–89.

Rancilhac, L., T. Bruy, M.D. Scherz, E. Almeida Pereira, M. Preick, N. Straube, M.L. Lyra, A. Ohler, J.W. Streicher, F.Andreone, A. Crottini, C.R. Hutter, J.C. Randrianantoandro, A. Rakotoarison, F. Glaw, M. Hofreiter, and M. Vences. 2020. Target-enriched DNA sequencing from historical type material enables a partial revision of the Madagascar giant stream frogs (genus *Mantidactylus*). Journal Of Natural History 54:87–118.

Rejaud, A., M.T. Rodrigues, A.J. Crawford, S. Castroviejo-Fisher, A.F. Jaramillo, J.C. Chaparro, F. Glaw, G. Gagliardi-Urrutia, J. Moravec, I.J. de la Riva, P. Perez, A.P. Lima, F.P. Werneck, T. Hrbek, S.R. Ron, R. Ernst, P.J. R. Kok, A. Driskel, J. Chave, A. Fouquet. 2020. Historical biogeography identifies a possible role of Miocene wetlands in the diversification of the Amazonian rocket frogs (Aromobatidae: *Allobates*). Journal of Biogeography 2020:1–11.

Rivero, J.A. 1991a. New *Colostethus* (Amphibia, Dendrobatidae) from South America. Breviora, 493:1–28.

Rivero, J.A. 1991b. New Ecuadorean [sic] *Colostethus* (Amphibia, Dendrobatidae) in the collection of National Museum of Natural History, Smithsonian Institution. Caribbean Journal of Science 27:1–22.

Rivero, J.A., and H. Granados-Díaz. 1990 ‘‘1989’’. Nuevos *Colostethus* (Amphibia, Dendrobatidae) del departamento de Cauca, Colombia. Caribbean Journal of Science 25:148–152.

Rivero, J.A., and M.A. Serna. 1986. Dos nuevas especies de *Colostethus* (Amphibia, Dendrobatidae) de Colombia. Caldasia XV:71–75.

Rivero, J.A., and M.A. Serna. 2000 ‘‘1995’’. Nuevos *Colostethus* (Amphibia, Dendrobatidae) del departamento de Antioquia, Colombia, con la descripción del renacuajo de *Colostethus fraterdanieli*. Revista de Ecología Latinoamericana 2:45–58.

Rokas, A., and S. B. Carroll. 2005. More genes or more taxa? the relative contribution of gene number and taxon number to phylogenetic accuracy. Molecular Biology and Evolution 22:1337–1344.

Rokas, A., B.L. Williams, N. King, and S. B. Carroll. 2003. Genome-scale approaches to resolving incongruence in molecular phylogenies . Nature 425:798–804.

Rodríguez, L.O., and C.W. Myers. 1993. A new poison frog from from Manu National Park, southeastern Peru (Dendrobatidae, *Epipedobates*). American Museum Novitates 3068: 1–15.

Rueda-Almonacid, J.V., M. Rada, S.J. Sánchez-Pacheco, Á.A. Velásquez Álvarez , A. Quevedo. 2006. Two new and exceptional poison dart frogs of the genus *Dendrobates* (Anura: Dendrobatidae) from the Northeastern Flank of the cordillera Central of Colombia. Zootaxa 54:39–54.

Ruiz-Carranza, P.M., M.C. Ardila-Robayo, J.D. Lynch. 1996. Lista actualizada de la fauna Amphibia de Colombia. Revista de la Academia Ciencias Exactas, Físicas y Naturales 20:365–415.

Salles, R.O.L., L.N. Weber, and T. Silva-Soares. 2009. Amphibia, Anura, Parque Natural Municipal da Taquara, municipality of Duque de Caxias, state of Rio de Janeiro, southeastern Brazil. Check List 5:840–854,.

Sánchez, D.A. 2013. Larval morphology of dart-poison frogs (Anura: Dendrobatoidea: Aromobatidae and Dendrobatidae). Zootaxa 3637:569–591.

Sánchez-Pacheco, S.J., O. Torres-Carvajal, V. Aguirre-Peñafiel, P.M. Nunes, L. Verrastro, G.A. Rivas, M.T. Rodrigues, T. Grant, and R.W. Murphy. 2017. Phylogeny of *Riama* (Squamata: Gymnophthalmidae), impact of phenotypic evidence on molecular datasets, and the origin of the Sierra Nevada de Santa Marta endemic fauna. Cladistics 34:260–291.

Sankoff, D. 1975. Minimal mutation trees of sequences. SIAM Journal on Applied Mathematics 28:35–42.

Sankoff, D., and R.J. Cedergren.1983. Simultaneous comparison of three or more sequences related by a tree. Pp. 253–263 in Time Warps, String Edits, and

Macromolecules: The Theory and Practice of Sequence Comparison (Sankoff, D., and J. B. Kruskal, eds.). Addison-Wesley Pub, USA.

Santos, J.C., and D.C. Cannatella. 2011. Phenotypic integration emerges from aposematism and scale in poison frogs. Proceeding of the National Academy of Sciences United States of America 108:6175–6180. https://doi.org/10.1073/pnas.1010952108

Santos, J.C., L.A. Coloma, and D.C. Cannatella. 2003. Multiple, recurring origins of aposematism and diet specialization in poison frogs. Proceedings of the National Academy of Sciences of the United States of America 100:12792–12797. https://doi.org/10.1073/pnas.2133521100

Santos, J.C., L.A. Coloma, K. Summers, J.P. Caldwell, R. Ree, and D.C. Cannatella. 2009. Amazonian amphibian diversity is primarily derived from late Miocene andean lineages. PLOS Biology 7:1–14. https://doi.org/10.1371/journal.pbio.1000056

Santos, J.C., M. Baquero, C. Barrio-Amoros, L.A. Coloma, L.K. Erdtmann, A.P. Lima, and D.C. Cannatella. 2014. Aposematism increases acoustic diversification and speciation in poison frogs. Proceedings of the Royal Society B: Biological Sciences 281:20141761–2014176. https://doi.org/10.1098/rspb.2014.1761

Savage, J.M. 1968. The dendrobatid frogs of Central America. Copeia 1968:745–776.

Savage, J.M. 2002. The amphibians and reptiles of Costa Rica: A herpetofauna between two continents, between two seas. University of Chicago Press, Chicago.

Schulze, A., M. Jansen, and G. Köhler . 2015. Tadpole diversity of Bolivia's lowland anuran communities: molecular identification, morphological characterization, and ecological assignment. Zootaxa 4016:1–111.

Silverstone, P.A. 1971. Status of certain frogs of the genus *Colostethus*, with descriptions of new species. Los Angeles County Museum Contributions in Science 215:1–8.

Silverstone, P.A. 1975. A revision of the poison– arrow frogs of the genus *Dendrobates* Wagler. Natural History Museum of Los Angeles County Science Bulletin 21:1–55.

Silverstone, P.A. 1976. A revision of the poison-arrow frogs of the genus *Phyllobates* Bibron in Sagra (family Dendrobatidae). Natural History Museum of Los Angeles County 27:1–53.

Stebbins, R., and J. Hendrickson. 1959. Field studies of amphibians in Colombia, South America. Univesity of California Publications in Zoology 56:497–540.

Targino, M., A.J. Elias-Costa, C. Taboada, and J. Faivovich. 2019. Novel morphological structures in frogs: vocal sac diversity and evolution in Microhylidae (Amphibia: Anura). Zoological Journal of the Linnean Society 187:479–493.

Tihen, J.A. 1960. Two new genera of african bufonids, with remarks on the phylogeny of related genera . Copeia 1960:225–233.

Trewavas, E. 1933. The hyoid and larynx of the Anura. Philosophical Transactions of the Royal Society of London, B 222: 401–527.

Trueb, L. 1993. Patterns of cranial diversification among the Lissamphibia. Pp. 255–343 in The Skull (J. Hanken, and B.K. Hall eds). University of Chicago Press, Chicago.

Twomey, E. and J.L. Brown. 2008. Spotted poison frogs: Rediscovery of a lost species and a new genus (Anura: Dendrobatidae) from northwestern Peru. Herpetologica 64:121–137.

Tyler, M.J. 1971. The phylogenetic significance of vocal sac structure in hylid frogs. Occasional Papers of the Museum of Natural History, the University of Kansas 19: 319–360.

Vacher, J.P, P.J.R. Kok, M.T. Rodrigues, J.D. Lima, A. Lorenzini, Q. Martinez, M. Fallet, E.A. Courtois, M. Blanc, P. Gaucher, M. Dewynter, R. Jairam, P. Ouboter, C. Thébaud, A. Fouquet, 2017. Cryptic diversity in Amazonian frogs: Integrative taxonomy of the genus *Anomaloglossus* (Amphibia: Anura: Aromobatidae) reveals a unique case of diversification within the Guiana Shield. Molecular Phylogenetics and Evolution 112:158–173.

Van Dijk, D.E. 1955. The 'tail' of *Ascaphus*: A historical résumé and new histological-anatomical details. Annals of the University of Stellenbosch 31:1–71.

Van Dijk, D.E. 1959. On the cloacal region of Anura in particular of larval *Ascaphus*. Annals of the University of Stellenbosch 35:169–249.

Varón, A., and W.C. Wheeler. 2012. The tree alignment problem. BMC Bioinformatics 13:1–14. https://doi:10.1186/1471-2105-13-293

Varón, A., and W.C. Wheeler. 2013. Local search for the tree alignment problem. BMC Bioinformatics 14:1–12. https://doi:10.1186/1471-2105-14-66.

Vaz-Silva, W., and N.M. Maciel. 2011. A new cryptic species of *Ameerega* (Anura: Dendrobatidae) from Brazilian Cerrado. Zootaxa 68:57–68.

Vences, M., J. Kosuch, S. Lötters, A. Widmer, K.H. Jungfer, J. Kohler, and M. Veith. 2000. Phylogeny and classification of poison frogs (Amphibia: Dendrobatidae), based on mitochondrial 16S and 12S ribosomal RNA gene sequences. Molecular Phylogenetics and Evolution 15:34–40. https://doi:10.1006/mpev.1999.0738.

Vigle, G.O., and K. Miyata. 1980. A new species of *Dendrobates* (Anura: Dendrobatidae) from the lowland rain forests of western Ecuador. Breviora 459:1–7.

Vigle, G.O., L.A. Coloma, J.C. Santos, S. Hernandez-Nieto, H.M. Ortega-Andrade, D.J. Paluh, and M. Read. 2020. A new species of *Leucostethus* (Anura: Dendrobatidae) from the Cordillera Mache-Chindul in northwestern Ecuador, with comments on similar *Colostethus* and *Hyloxalus*. Zootaxa 4896:342–372 .

von May, R., M. Medina-Müller, M.A. Donnelly, and K. Summers. 2008. The tadpole of the bamboo-breeding poison frog *Ranitomeya biolat* (Anura: Dendrobatidae). Zootaxa 1857:66–68.

Wassersug, R.J., and W.R. Heyer. 1988. A survey of internal oral features of leptodactyloid larvae (Amphibia: Anura) . Smithsonian Contribution to Zoology 457:1–99.

Wells, K.D. 2007. The ecology and behavior of amphibians. The University of Chicago Press, Chicago and London.

Werner, F. 1899. Ueber Reptilien und Batrachier aus Columbien und Trinidad. Verhandlungen des Zoologisch-Botanischen Vereins in Wien 49:470–484.

Werner, F. 1916. Bemerkungen über einige niedere Wirbeltiere der Anden von Kolumbien mit Beschreibung neuer Arten. Zoologischer Anzeiger 47:301–304.

Wever, E.G. 1985. The amphibian ear. Princeton University Press.

Wheeler, W.C. 1990. Nucleic acid sequence phylogeny and random outgroups. Cladistics 6:363–367.

Wheeler, W.C. 1994. Sources of ambiguity in nucleic acid sequence alignment. Pp. 323–352 in Molecular ecology and evolution: Approaches and applications (Schierwater, B., B. Streit, G.P. Wagner, and R. De Salle eds.). Basel: Birkhauser.

Wheeler, W.C. 1996. Optimization alignment: The end of multiple sequence alignment in phylogenetics? Cladistics 12:1–9.

Wheeler, W.C. 2003a. Implied alignment: A synapomorphy-based multiple sequence alignment method. Cladistics 19:261–268.

Wheeler, W.C. 2003b. Iterative pass optimization of sequence data. Cladistics 19:254–260.

Wheeler, W.C., N. Lucaroni, L. Hong, L.M. Crowley, and A. Varón. 2015. POY version 5: Phylogenetic analysis using dynamic homologies under multiple optimality criteria. Cladistics 31:189–196

Wheeler, W.C., L. Aagesen, C.P. Arango, J. Faivovich, T. Grant, C. D'Haese, D. Janies, W.L. Smith, A. Varon, and G. Giribet. 2006. Dynamic homology and phylogenetic systematics: A unified approach using POY. American Museum Novitates, American Museum of Natural History, USA.

Young, J.E., K.A. Christian, S. Donnellan, C.R. Tracy, and D. Parry. 2005. Comparative analysis of cutaneous evaporative water loss in frogs demonstrates correlation with ecological habits. Physiological and Biochemical Zoology 78: 847–856 .

Zimmermann, H., and E. Zimmermann. 1988. Etho-taxonomie und zoogeographische artengruppenbildung bei pfeilgiftfröschen (Anura: Dendrobatidae). Salamandra 24:125–160.

Zwickl, D.J., and D.M. Hillis. 2002. Increased taxon sampling greatly reduces the phylogenetic error. Systematic Biology 51:588–598.

TABLES

TABLE 1.—Field trips made to search key *Hyloxalus* species and other poison frogs. An asterisk mark "*" designated unnamed species.

Species	Locality	Year	Result
Colostethus mertensi	Quintana, Popayan, Cauca, Colombia	2016	Negative
Colostethus ucumari	Reserva Natural Lisbran, Pereira, Risaralda, Colombia	2017	Negative
Ectopoglossus confusus	San Francisco de las Pampas, Ecuador Tantí, Santo Domingo de los Tsachilas, Ecuador	2018	Negative
Hyloxalus cepedai	Villavicencio, Meta, Colombia	2015	Positive
Hyloxalus edwardsi	Cuevas las Moyas, Cundinamarca, Colombia	2015	Negative
	Villarica, Tolima, Colombia	2017	Positive*
Hyloxalus marmoreoventris	Río Negro, Tungurahua, Ecuador	2019	Negative
Hyloxalus pinguis	Totoro, Cauca, Colombia	2016	Positive
Hyloxalus ruizi	Quebrada Agua Bonita, Silvania, Cundinamarca, Colombia	2015, 2016, 2017	Negative
Hyloxalus vergeli	Fusagasuga, Cundinamarca Colombia	2009	Negative

	Ibague, Tolima, Colombia	2018	Positive*
Paruwrobates andinus	Ricaurte, Nariño, Colombia	2017, 2018	Negative
Paruwrobates whymperi	San Francisco de las Pampas, Cotopaxi, Ecuador	2018	Negative
	Tantí, Santo Domingo de los Tsachilas, Ecuador	2018	Negative

TABLE 2.—Number and percentage of the species examined for phenotypic data of the adult and tadpoles of the *Hyloxalus* and other Dendrobatoidea. In bold type is the ingroup.

Family	Subfamily	Genus	N° spp. Genus	Adults		Larvae	
				N° spp.	% spp.	N° spp.	% spp.
Dendrobatidae		*Ectopoglossus*	7	6	86	0	0
	Hyloxalinae	***Hyloxalus***	**63**	**53**	**84**	**30**	**47**
		Paruwrobates	3	3	100	1	33
	Colostethinae	*Ameerega*	29	26	90	14	48
		Colostethus	15	6	40	6	40
		Epipedobates	8	4	50	7	88
		Leucostethus	7	3	43	1	14
		Silverstoneia	8	2	25	3	38
	Dendrobatinae	*Adelphobates*	3	3	100	3	100
		Andinobates	15	2	13	8	53
		Dendrobates	5	3	60	4	80
		Excidobates	3	0	0	3	100
		Minyobates	1	1	100	1	100
		Oophaga	12	4	33	7	58
		Phyllobates	5	4	80	5	100

		Ranitomeya	16	4	25	11	69
		"Colostethus" ruthveni group	2	2	100	1	50
Aromobatidae	Allobatinae	*Allobates*	57	14	25	23	40
	Anomalogloss inae	*Anomaloglossus*	32	5	16	12	38
		Rheobates	2	1	50	1	50
	Aromobatinae	*Aromobates*	18	3	17	3	17
		Mannophryne	20	4	20	10	50
Un-ranked		*"Colostethus" poecilonotus*	1	1	100	0	0

TABLE 3.—Genes and number of terminals per gene used in this study. Names follow the Gene Nomenclature Committee HUGO.

Gene	No. Terminals
H-strand transcription unit 1 (H1: MT-RNR1, MT-TV, and MT-RNR2), MT-TL2, MT-ND1, MT-TI, MT-TQ, MT-TM, and MT-ND2	564
mitochondrially encoded cytochrome b (MT-CYB)	330
mitochondrially encoded cytochrome c oxidase I (MT-CO1)	218
H3 histone family member 3C (H3F3C)	192
rhodopsin (RHO)	189
siah E3 ubiquitin protein ligase 1 (SIAH1)	156
recombination activating 1 (RAG1)	161
28S ribosomal RNA (RNA28S)	159
tyrosinase (TYR)	130
proopiomelanocortin (POMC)	69
solute carrier family 8 member A1 (SLC8A1)	59
brain derived neurotrophic factor (BDNF)	55
bone morphogenetic protein 2 (BMP2)	54
3’-nucleotidase (NT3)	54
zinc Finger E-box binding homeobox 2 (ZEB2)	54

TABLE 4.—Primers used in this study.

Gene Region	Primer	Direction	Primer sequence (5' to 3')	Reference
16S rDNA	AR	Forward	CGCCTGTTTATCAAAAACAT	Palumbi et al. 1991
	BR	Reverse	CCGGTCTGAACTCAGATCACGT	Palumbi et al. 1991
	Wilkinson2	Reverse	GACCTGGATTACTCCGGTCTGA	Wilkinson et al. 1996
	L2A	Forward	CCAAACGAGCCTAGTGATAGCTGGTT	Hedges 1994
	H10	Reverse	TGATTACGCTACCTTTGCACGGT	Hedges 1994
	L13	Forward	TTAGAAGAGGCAAGTCGTAACATGGTA	Feller and Hedges 1998
	TITUS 1	Reverse	GGTGGCTGCTTTTAGGCC	Feller and Hedges 1998
12S rDNA	MVZ59	Forward	ATAGCACTGAAAAYGCTDAGATG	Graybeal 1997
	MVZ50	Reverse	TYTCGGTGTAAGYGARAKGCTT	Graybeal 1997
	12S A-L	Forward	AAACTGGGATTAGATACCCCACTAT	Goebel et al. 1999
	TRNAval-H	Reverse	GGTGTAAGCGARAGGCTTTKGTTAAG	Goebel et al. 1999
Cytochr	ANF1	Forward	ACHAAYCAYAAAGAYATYGG	Lyra et al. 2017

ome oxidase subunit 1	ANF2	Reverse	CCRAARAATCARAADARRTGTTG	Lyra et al. 2017
Cytochrome b	MVZ15	Forward	GAACTAATGGCCCACACWWTACGNAA	Moritz et a. 1992
	CytB2	Reverse	AAACTGCAGCCCCTCAGAAATGATATTTGTCCTCA	
Rhodopsin exon 1	Rhod1A	Forward	ACCATGAACGGAACAGAAGGYCC	Bossuyt and Milinkovitch, 2000
	Rhod1C	Reverse	CCAAGGGTAGCGAAGAARCCTTC	Bossuyt and Milinkovitch, 2000
Tyrosinase exon 1	TyrC	Forward	GGCAGAGGAWCRTGCCAAGATGT	Bossuyt and Milinkovitch, 2000
	TyrG	Reverse	TGCTGGCRTCTCTCCARTCCCA	Bossuyt and Milinkovitch, 2000
Histone H3	H3F	Forward	ATGGCTCGTACCAAGCAGACVGC	Colgan et al. 1999
	H3R	Reverse	ATATCCTTRGGCATRATRGTGAC	Colgan et al. 1999
28S rDNA	28sV	Forward	AAGGTAGCCAAATGCCTCATC	Hillis and Dixon 1991
	28sJJ	Reverse	AGTAGGGTAAAACTAACCT	Hillis and Dixon 1991

Recombination activing gene 1	RAG1TG1F	Forward	CCAGCTGGAAATAGGAGAAGTCTA	Grant et al. 2006
	RAG1TG1R	Reverse	CTGAACAGTTTATTACCGGACTCG	Grant et al. 2006
Seven in absentia	SIA1	Forward	TCGAGTGCCCCGTGTGYTTYGAYTA	Bonacum et al. 2001
	SIA2	Reverse	GAAGTGGAAGCCGAAGCAGSWYTGCATCAT	Bonacum et al. 2001

TABLE 5.—Details of the successive outgroup expansion analysis, and search stats in the POY and TNT analyses. # is the total number of terminals used in each analysis. In Taxa, in parenthesis is the number of terminals added to the anterior analysis. For all analyses in POY were used 40 CPU and 11 nodes so the time in POY search is expressed in hours/CPU/nodes. * "*Colostethus*" *poecilonotus* was found part of *Hyloxalus*, for this, it is excluded from the outgroup count. IP is the tree length after iterative pass optimization.

Analysis	**Outgroup**		**Root**	**POY**				**TNT**	
	#	**Taxa**		**Search time**	**# trees**	**Tree length**	**IP**	**# trees**	**Tree length**
1	6	*Ectopoglossus* (5), *Paruwrobates* (1)	*Phyllobates lugubris*	2200	2	18657	18636	345	18636
2	18	+ Dendrobatinae (12)	*Silverstoneia flotator*	2640	1	21708	21685	305	21685
3	26	+ Dendrobatinae (3), Colostethinae (4) "*Colostethus*" *poecilonotus* (1)	*Rheobates palmatus*	3520	2	24666	24639	371	24639
4	35*	+ Dendrobatinae (5), Colostethinae (5)	*Rheobates palmatus*	3960	1	28953	28912	339	28912
5	66	+ Dendrobatinae (8), Colostethinae (23)	*Rheobates palmatus*	4400	1	34064	34018	380	34018
6	78	+ Colostethinae (5), Aromobatidae (4), Hylodidae (1), Bufonidae (1), Cycloramphidae (1)	*Boana boans*	6600	1	38751	38692	371	38692

7	95	+ Colostethinae (7), Aromobatidae (10)	*Boana boans*	7040	1	43642	43578	320	43577
8	118	+ Colostethinae (6), Aromobatidae (17)	*Boana boans*	28160	1	48005	47942	365	47942
9	136	+ Aromobatidae (11), Alsodidae (1), Bufonidae (1), Cycloramphidae (2), Hylodidae (3)	*Boana boans*	29600	1	54749	54672	345	54671

TABLE 6.—Sesamoid (s) and bone projection (p) on the hand bones in poison frogs from micro-computed tomography reconstructions. A white cell is a flattened subarticular tubercle, a gray cell is a projected subarticular tubercle, and dark gray is a polymorphism between a flat or projected tubercle. s/p condition is reported when micro-CT does not allow distinction between s or p. "0" denoted insufficient reconstructions to know the conditions. Other abbreviations: Mtc: metacarpal bone. Prox.Ph: proximal phalanx.

Species	Mtc II	Mtc III	Mtc IV	Mtc FV	Prox.Ph IV	Prox.Ph V
Allobates insperatus	s/p	s/p	s/p	s/p	0	0
Allobates juanii	s/p	s/p	s/p	s/p	s/p	s/p
Allobates talamancae	s/p	s/p	s/p	s/p	0	0
Allobates trilineatus	s/p	s/p	s/p	s/p	0	0
Ameerega parvula	s/p	s/p	s/p	s/p	p	p
Ameerega petersi	s/p	s/p	s/p	s/p	s/p	s/p
Ameerega trivittata	s/p	s/p	s/p	s/p	s/p	s/p
Anomaloglossus baeobatrachus	0	s/p	s/p	s/p	0	0
Anomaloglossus stepheni	s/p	s/p	s/p	s/p	0	0
Aromobates haydeeae	p	s/p	0	s/p	0	0
Aromobates mayorgai	0	0	0	s/p	0	0
Leucostethus sp.	s	s	s	s/p	0	0

fraterdanieli complex						
Colostethus inguinalis	s	s	s	s	0	s/p
Colostethus mertensi	p	0	0	p	0	0
Colostethus panamensis	s	s/p	s/p	s	0	0
"Colostethus" ruthveni-like	0	0	s/p	s/p	0	0
Colostethus ucumari	p	0	0	0	0	0
Ectopoglossus confusus	0	0	0	s/p	0	0
Ectopoglossus saxatilis	0	0	0	0	0	0
Epipedobates machalilla	s/p	s/p	s/p	s/p	s/p	0
Hyloxalus abditaurntius	0	0	0	0	0	0
Hyloxalus anthracinus	s/p	s/p	s/p	s/p	s/p	s/p
Hyloxalus breviquartus	s/p	s/p	s/p	s/p	0	p
Hyloxaus cepedai	0	0	0	0	0	0
Hyloxalus edwardsi	0	0	0	0	0	0
Hyloxalus excisus	0	0	0	0	0	0
Hyloxalus jhoncito spnov	0	0	0	0	0	0
Hyloxalus lehmanni	s/p	s/p	s/p	s/p	0	0
Hyloxalus maculosus	0	0	0	0	0	0
Hyloxalus nexipus	0	s/p	s/p	s/p	0	0
Hyloxalus pinguis	s/p	s/p	s/p	s/p	0	p

Hyloxalus pulchellus	s/p	s	s	s	0	p
Hyloxalus ruizi	s	s	s	s	0	0
Hyloxalus saltuarius	s	s	s	s/p	0	s/p
Hyloxalus sanctamariensis	s/p	0	0	0	0	0
Hyloxalus subpunctatus	s/p	s/p	p	s/p	0	0
Hyloxalus vergeli	0	0	0	p	0	0
Hyloxalus sp_LVP	0	0	0	0	0	0
Hyloxalus sp_R	s/p	0	0	0	0	0
Hyloxalus felixcoperari	s/p	s/p	s/p	s/p	0	0
Hyloxalus sp_Tambo	s/p	s/p	s/p	s/p	p	p
Leucostethus fugax	s	s	s	s	s/p	s/p
Oophaga pumilio	0	0	0	0	0	0
Paruwrobates andinus	0	s/p	s/p	s/p	0	0
Phyllobates vitattus	0	0	s	0	0	0

TABLE 7.—Results of the successive outgroup expansion analysis. Affected ingroup topological position respect to the previous analysis is reported. *Hyloxalus*, the ingroup have 188 terminals in the first to third analysis, but from fourth analysis onward, there is 189 terminals because "*Colostethus*" *poecilonotus* is an ingroup member. Conventions: "-": No apply.

Analysis	**# Taxa**	**Affected clade**		
		Sufamily/Genus	**Clade**	**Species**
1	6	-	-	-
2	18	-	*Hyloxalus bocagei*, *H. sylvaticus–H.pulcherrimus*, *H. nexipus*, *H. azureiventris*	-
3	26	-	*Hyloxalus bocagei*, *H. sylvaticus–H.pulcherrimus*, *H. delatorreae* (KU220621)–*H. jacobuspetersi*, *H. nexipus*, *H. azureiventris*, *Hyloxalus* sp. Bongara–*Hyloxalus* sp. PAV	*H. anthracinus*
4	35	Hyloxalinae	*Hyloxalus bocagei*, *H. sylvaticus–H.pulcherrimus*, *H. delatorreae* (KU220621)–*H. jacobuspetersi*, *H. nexipus*, *H. shuar–H.idiomelus*, *Hyloxalus* sp. Bongara–*Hyloxalus* sp. PAV	*H. anthracinus, H. elachyhistus*
5	66	Hyloxalinae, *Hyloxalus*	*Hyloxalus bocagei*, *H. nexipus*, *H. shuar–H. idiomelus,* clade compose by *H. bocagei, H. leucophaeus, H. maculosus, H.sauli, H.*	*H. elachyhistus, H.maculosus, H.picachos,*

			sordidatus, Hyloxalus sp. Amazonas	*Hyloxalus* sp.ElCopal, *"C" poecilonotus*
6	78	Hyloxalinae	*Hyloxalus bocagei*, *H. sylvaticus–H.pulcherrimus*, *H. nexipus*, *H. azureiventris*, *H. shuar–H.idiomelus,* clade compose by *H. bocagei, H. leucophaeus, H. maculosus, H.sauli, H. sordidatus, Hyloxalus* sp. Amazonas	*H. elachyhistus, H. maculosus, H. picachos*
7	95	-	*Hyloxalus bocagei*, *H. sylvaticus–H.pulcherrimus*, *H. nexipus*, *H. azureiventris*, *Hyloxalus* sp. Bongara–*Hyloxalus* sp. PAV, *H. shuar–H. Idiomelus,* clade compose by *H. bocagei, H. leucophaeus, H. maculosus, H.sauli, H. sordidatus, Hyloxalus* sp. Amazonas	*H. elachyhitus, H. picachos*
8	118	-	*Hyloxalus nexipus*, *Hyloxalus* sp. Bongara–*Hyloxalus* sp. PAV, *H. sylvaticus–H. puchlerrimus*, *H. delatorreae* (KU220621)–*H. jacobuspetersi*, *H. shuar–H. idiomelus*	*H. anthracinus*
9	136	-	*Hyloxalus nexipus*, *Hyloxalus* sp. Bongara–*Hyloxalus* sp. PAV, *H. shuar–H. Idiomelus*, clade compose by *H. bocagei, H. leucophaeus, H. maculosus, H.sauli, H. sordidatus, Hyloxalus* sp. Amazonas	*H. picachos*

TABLE 8.—Percent of the uncorrected pairwise distance between 16S sequences of the populations considered as *Hyloxalus vergeli*. Lines separate species.

	Terminals	1	2	3	4	5	6	7	8	9	10	11	12	13
1	*Hyloxalus_sp_Inza_LVP386*	-												
2	*Hyloxalus_sp_Inza_LVP389*	0,0	-											
3	*Hyloxalus_sp_Inza_Gigante_GFM1579*	0,0	0,0	-										
4	*Hyloxalus_sp_Inza_LVP402*	0,4	0,4	0,4	-									
5	*Hyloxalus_sp_Inza_Tamarindo_MUJ4298*	0,6	0,6	0,6	0,5	-								
6	*Hyloxalus_sp_Inza_Tamarindo_MUJ5017*	0,6	0,6	0,6	0,5	0,0	-							
7	*Hyloxalus_sp_Inza_Tamarindo_MUJ5018*	0,3	0,3	0,3	0,4	0,3	0,3	-						
8	*Hyloxalus_vergeli_Ibague_DFZ409*	3,4	3,4	3,4	2,1	3,4	3,4	3,5	-					
9	*Hyloxalus_vergeli_Ibague_LHUTMT28*	3,3	3,3	3,3	2,1	3,2	3,2	3,4	0,1	-				
10	*Hyloxalus_vergeli_Ibague_MAA1376*	3,3	3,3	3,3	2,1	3,2	3,2	3,4	0,1	0,0	-			
11	*Hyloxalus_vergeli_Ibague_MAA1373*	3,3	3,3	3,3	2,1	3,2	3,2	3,4	0,1	0,1	0,1	-		

12	*Hyloxalus_vergeli_Ibague_Chaparral_LHUTMT13*	3,0	3,0	3,0	2,1	2,9	2,0	3,0	0,3	0,2	0,2	0,2	-	
13	*Hyloxalus_vergeli_Quinchas_ALOP191*	6,8	6,8	6,8	5,8	8,0	6,7	6,6	6,9	6,8	6,8	6,8	6,4	-

TABLE 9.—Percent of the uncorrected pairwise distance between 16S sequences of the populations of the three cis-Andean *Hyloxalus*, *H. cepedai*, *H. picachos*, and *H. sanctamariensis*. Lines separate species.

	Terminals	1	2	3	4	5	6	7	8	9	10	11	12	13
1	*Hyloxalus_cepedai_MAA574*	-												
2	*Hyloxalus_cepedai_MAA1003*	0,1	-											
3	*Hyloxalus_cepedai_Medina_EQB107*	0,3	0,2	-										
4	*Hyloxalus_cepedai_Medina_ALH36*	0,3	0,2	0,0	-									
5	*Hyloxalus_cepedai_StaMaria_MLC1426*	0,9	0,8	0,6	0,6	-								
6	*Hyloxalus_cepedai_AguaAzul_TNHCFS4940*	1,8	1,8	1,6	1,6	1,5	-							
7	*Hyloxalus_cepedai_CasanareAR_MAA528*	1,7	1,6	1,4	1,4	1,4	0,4	-						
8	*Hyloxalus_picachos_MCL1171*	11,9	11,8	11,6	11,6	11,9	11,2	11,4	-					
9	*Hyloxalus_picachos_MCL813*	11,8	11,8	11,6	11,6	11,8	11,2	11,4	0,2	-				
10	*Hyloxalus_sanctamariensis_MAA1402*	10,9	11,0	10,8	10,8	10,6	10,6	10,7	11,6	11,5	-			
11	*Hyloxalus_sanctamariensis_AJC6369*	11,1	11,1	10,9	10,9	10,7	10,5	10,6	11,3	11,2	1,1	-		

12	*Hyloxalus_sanctamariensis_ANDESA6370*	11,3	11,2	11,0	11,0	10,8	10,7	10,7	11,5	11,4	1,1	0,1	-	
13	*Hyloxalus_sanctamariensis_MLC1438*	11,4	11,3	11,1	11,1	11,0	10,8	10,8	11,6	11,5	1,2	0,2	0,1	-

TABLE 10.—Percent of the uncorrected pairwise distance between 16S sequences of the populations similar to *Hyloxalus subpunctatus*. Lines separate localities and/or species.

	Terminals	1	2	3	4	5	6	7	8	9	10	11	12	13	14	15	16	17	18
1	*Hyloxalus_sp_Aguabonita_MAA1197*	-																	
2	*Hyloxalus_sp_Aguabonita_MAA1213*	0,1	-																
3	*Hyloxalus_sp_Aguabonita_MAA1241A*	0,1	0,2	-															
4	*Hyloxalus_felixcoperari_Supata_DAS_384*	1,1	1,2	1,2	-														
5	*Hyloxalus_felixcoperari_IAvHAm14540*	1,0	1,0	1,0	0,8	-													
6	*Hyloxalus_sp_QuebradaWolf_CZUT_2178*	1,5	1,6	1,6	1,5	1,7	-												
7	*Hyloxalus_sp_QuebradaWolf_MAA_1263*	1,4	1,6	1,6	1,4	1,6	0,2	-											
8	*Hyloxalus_sp_QuebradaWolf_MAA_1270*	1,5	1,6	1,6	1,5	1,6	0,4	0,3	-										

9	*Hyloxalus_sp_QuebradaWolf_MAA_1267*	1,4	1,5	1,5	1,3	1,3	0,2	0,1	0,2	-									
10	*Hyloxalus_subpunctatus_MAA1054*	2,7	2,8	2,8	2,4	2,2	2,7	2,6	2,7	2,5	-								
11	*Hyloxalus_subpunctatus_ss_MAA167*	2,6	2,7	2,7	2,2	2,1	2,6	2,5	2,6	2,4	0,1	-							
12	*Hyloxalus_subpunctatus_TNHCFS4957*	2,8	2,8	2,8	2,9	3,3	3,0	2,9	3,0	2,8	2,8	2,6	-						
13	*Hyloxalus_walesi_SVR_013*	3,9	3,9	4,2	3,9	4,2	4,1	4,2	4,3	4,1	4,2	4,1	3,9	-					
14	*Hyloxalus_walesi_SVR_015*	2,3	2,3	2,3	2,1	2,3	2,1	2,1	2,3	2,1	2,5	2,3	3,0	0,0	-				
15	*Hyloxalus_walesi_SVR_014*	2,5	2,5	2,5	2,3	2,5	2,3	2,3	2,5	2,3	2,6	2,5	3,0	0,4	0,4	-			
16	*Hyloxalus_walesi_SVR_016*	2,3	2,3	2,3	2,1	2,3	2,1	2,1	2,3	2,1	2,5	2,3	2,8	0,2	0,2	0,2	-		
17	*Hyloxalus_sp_Junin_MAA_1077*	3,7	3,8	4,1	3,9	3,9	4,1	4,0	4,2	3,9	3,9	3,8	3,9	3,3	1,6	1,9	1,8	-	
18	*Hyloxalus_sp_Junin_MAA_1086*	3,7	3,8	4,1	3,9	3,9	4,1	4,0	4,2	3,9	3,9	3,8	3,9	3,3	1,6	1,9	1,8	0,0	-

TABLE 11.—Percent of the uncorrected pairwise distance between 16S sequences of the populations of *Hyloxalus nexipus*. Lines separate localities and species.

	Terminals	Locality	1	2	3	4	5	6
1	*Hyloxalus_nexipus_KU211807*	San Martín, Peru	-					
2	*Hyloxalus_nexipus_KU211808*	San Martín, Peru	0,1	-				
3	*Hyloxalus_nexipus_KU212486*	San Martín, Peru	0,2	0,2	-			
4	*Hyloxalus_nexipus_KU211806*	San Martín, Peru	0,1	0,1	0,1	-		
5	*Hyloxalus_nexipus_QCAZ16534*	Morona Santiago, Ecuador	4,6	4,5	4,4	4,4	-	
6	*Hyloxalus_nexipus_QCAZ16537*	Morona Santiago, Ecuador	4,9	4,9	4,7	4,8	3,8	-

TABLE 12.—Percent of the uncorrected pairwise distance between 16S sequences of the *Hyloxalus pinguis* and their close relatives. Lines separate species.

	Terminals	1	2	3	4	5	6	7	8	9	10	11
1	*Hyloxalus_pinguis_MAA_1248*	-										
2	*Hyloxalus_pinguis_MAA_1249*	0,0	-									
3	*Hyloxalus_pinguis_MAA1250*	0,1	0,1	-								
4	*Hyloxalus_pinguis_GAP_195*	0,7	0,7	0,6	-							
5	*Hyloxalus_sp_MonteOlivo_KU220666*	3,4	3,6	3,5	3,8	-						
6	*Hyloxalus_delatorreae_KJ940457*	5,1	5,1	5,2	5,4	4,7	-					
7	*Hyloxalus_delatorreae_KU220619*	5,2	5,2	5,2	5,4	4,8	0,1	-				
8	*Hyloxalus_sp_SanMiguelDeSalcedo_KU202833*	5,0	5,0	5,1	5,4	4,3	1,8	1,6	-			
9	*Hyloxalus_pulchellus_QCAZ15964*	5,9	5,9	5,9	6,1	5,3	4,5	4,6	4,7	-		
10	*Hyloxalus_vertebralis_QCAZ16553*	8,2	8,2	8,2	8,7	7,6	7,3	7,4	7,4	7,4	-	
11	*Hyloxalus_vertebralis_QCAZ16554*	8,2	8,2	8,2	8,7	7,6	7,4	7,5	7,6	7,5	0,1	-

TABLE 13.—Percent of the uncorrected pairwise distance between 16S sequences of the *Hyloxalus lehamnni–H. arliensis* complex. Lines separate species.

	Terminals	1	2	3	4	5	6	7	8	9	10	11	12	13	14	15	16	17
1	*Hyloxalus_arliensis_DFZ_411*	-																
2	*Hyloxalus_arliensis_MUJ3564*	0,1	-															
3	*Hyloxalus_arliensis_MAR105*	0,3	0,5	-														
4	*Hyloxalus_arliensis_Caparrapi_RC_1423*	0,5	0,6	0,8	-													
5	*Hyloxalus_arliensis_Caparrapi_RC_1439*	0,4	0,5	0,8	0,1	-												
6	*Hyloxalus_arliensis_MAA_1381*	0,5	0,6	0,8	0,5	0,5	-											
7	*Hyloxalus_arliensis_MAA_1400B*	0,5	0,6	0,8	0,5	0,5	0,1	-										
8	*Hyloxalus_arliensis_DFZ_413*	0,4	0,5	0,7	0,5	0,4	0,1	0,1	-									
9	*Hyloxalus_arliensis_ARA2520*	0,4	0,5	0,6	0,5	0,4	0,2	0,2	0,1	-								
10	*Hyloxalus_arliensis_TG1959*	0,4	0,5	0,7	0,5	0,4	0,5	0,5	0,4	0,4	-							
11	*Hyloxalus_sp_MesasGalilea_MAA_1281*	6,8	6,9	7,4	6,9	6,8	6,6	6,6	6,5	6,7	6,7	-						

12	*Hyloxalus_sp_MesasGalilea_MAA_1283*	8,2	8,3	10,0	8,2	8,1	7,9	7,9	7,9	8,0	5,7	0,2	-				
13	*Hyloxalus_sp_MesasGalilea_MAA_1272*	6,7	6,8	7,3	6,7	6,7	6,5	6,5	6,4	6,5	6,6	0,1	0,3	-			
14	*Hyloxalus_sp_Alban_ANDESA_2923*	7,5	7,7	8,9	7,8	7,7	7,6	7,6	7,6	7,6	7,6	7,8	9,2	7,6	-		
15	*Hyloxalus_lehmanni_FC_656*	8,3	8,4	8,2	8,5	8,4	8,5	8,5	8,4	8,4	8,3	7,6	8,9	7,6	9,3	-	
16	*Hyloxalus_lehmanni_FC_657*	8,2	8,4	8,2	8,4	8,4	8,4	8,4	8,4	8,4	8,2	7,6	8,8	7,6	9,2	0,1	-
17	*Hyloxalus_lehmanni_MAR2675*	6,7	6,7	7,8	6,9	6,9	6,9	6,9	6,9	6,9	6,7	6,2	7,5	6,1	7,8	6,6	6,6	-

TABLE 14.—Percent of the uncorrected pairwise distance between 12S sequences of the *Hyloxalus craspedoceps*. Lines separate localities and potential species.

	Terminals	1	2	3	4
1	*Hyloxalus_craspedoceps_Chazuta_MNCN47538*	-			
2	*Hyloxalus_craspedoceps_Chazuta_MNCN47539*	0,0	-		
3	*Hyloxalus_craspedoceps_Lamas_CORBIDI_6804*	5,9	5,9	-	
4	*Hyloxalus_craspedoceps_MHNSM22882*	5,6	5,6	0,4	-

TABLE 15.—Percent of the uncorrected pairwise distance between 16S sequences of the *Hyloxalus elachyhistus*. Lines separate localities and potential species.

	Terminal	1	2	3	4	5	6	7	8	9	10	11	12	13	14	15	16	17	18
1	*Hyloxalus_elachyhistus_Cajamarca_KU212522*	-																	
2	*Hyloxalus_elachyhistus_Cajamarca_KU212524*	0,1	-																
3	*Hyloxalus_elachyhistus_Cajamarca_KU212523*	0,1	0,1	-															
4	*Hyloxalus_elachyhistus_CORBIDI_4201*	6,2	6,3	6,1	-														
5	*Hyloxalus_elachyhistus_CORBIDI_4205*	6,1	6,2	6,1	0,1	-													
6	*Hyloxalus_elachyhistus_Piura_KU219749*	6,2	6,3	6,1	0,1	0,1	-												
7	*Hyloxalus_elachyhistus_CORBIDI_4234*	6,4	6,4	6,3	1,0	0,9	0,9	-											
8	*Hyloxalus_elachyhistus_CORBIDI_4236*	6,4	6,4	6,3	1,0	0,9	0,9	0,0	-										
9	*Hyloxalus_elachyhistus_CORBIDI_13260*	6,6	6,6	6,5	0,9	0,9	0,8	0,3	0,3	-									

10	*Hyloxalus_elachyhistus_Piura_KU212514*	6,5	6,6	6,4	1,1	1,1	1,1	1,1	1,1	1,1	-									
11	*Hyloxalus_elachyhistus_Piura_KU212517*	6,5	6,6	6,4	1,1	1,1	1,1	1,1	1,1	1,1	0,0	-								
12	*Hyloxalus_elachyhistus_Piura_KU212515*	6,5	6,6	6,5	1,1	1,1	1,1	1,1	1,1	1,1	0,3	0,3	-							
13	*Hyloxalus_elachyhistus_Piura_KU212516*	6,5	6,6	6,5	1,1	1,1	1,1	1,1	1,1	1,1	0,3	0,3	0,0	-						
14	*Hyloxalus_elachyhistus_QCAZ16517*	6,6	6,8	6,6	2,3	2,2	2,3	2,4	2,4	2,3	2,2	2,2	2,1	2,1	-					
15	*Hyloxalus_elachyhistus_QCAZ16518*	6,6	6,8	6,6	2,3	2,2	2,3	2,4	2,4	2,3	2,2	2,2	2,1	2,1	0,0	-				
16	*Hyloxalus_elachyhistus_CORBIDI_3719*	6,9	6,8	6,6	2,4	2,3	2,4	2,4	2,4	2,4	2,3	2,3	2,2	2,2	0,2	0,2	-			
17	*Hyloxalus_elachyhistus_Lambayaque_CORBIDI_4292*	5,3	5,3	5,2	5,7	5,6	5,7	5,9	5,9	5,9	5,7	5,7	5,7	5,7	5,7	5,7	5,7	-		
18	*Hyloxalus_elachyhistus_ElOro_KU212507*	5,3	5,4	5,2	5,9	5,8	5,9	6,1	6,1	6,1	5,9	5,9	5,9	5,9	5,9	5,9	5,9	0,1	-	

TABLE 16.—Percent of the uncorrected pairwise distance between 16S sequences of the *Hyloxalus littoralis* and *H. insulatus*. Lines separate localities and species.

	Terminal	1	2	3	4	5	6	7	8	9	10	11	12	13
1	*Hyloxalus_littoralis_CORBIDI_16094*	-												
2	*Hyloxalus_littoralis_Huanuco_CORBIDI_13350*	0,1	-											
3	*Hyloxalus_littoralis_Huanuco_CORBIDI_8658*	0,1	0,0	-										
4	*Hyloxalus_littoralis_Huanuco_CORBIDI_8642*	0,1	0,0	0,0	-									
5	*Hyloxalus_littoralis_Huanuco_CORBIDI_9017*	0,1	0,0	0,0	0,0	-								
6	*Hyloxalus_littoralis_CORBIDI_6880*	0,1	0,0	0,0	0,0	0,0	-							
7	*Hyloxalus_littoralis_KST_650*	0,5	0,5	0,5	0,5	0,5	0,5	-						
8	*Hyloxalus_littoralis_LIMA*	0,5	0,6	0,6	0,6	0,6	0,6	0,1	-					
9	*Hyloxalus_insulatus_Cajamarca_CORBIDI_5656*	1,3	1,2	1,2	1,2	1,2	1,2	1,4	1,5	-				
10	*Hyloxalus_sp_LaLibertad_CORBIDI_5650*	1,3	1,2	1,2	1,2	1,2	1,2	1,4	1,5	0,1	-			

11	*Hyloxalus_insulatus_Amazonas_KU211878*	2,2	2,1	2,1	2,1	2,1	2,1	2,4	2,4	2,4	2,3	-		
12	*Hyloxalus_insulatus_Amazonas_KU211877*	2,2	2,1	2,1	2,1	2,1	2,1	2,4	2,4	2,4	2,3	0,0	-	
13	*Hyloxalus_insulatus_Amazonas_CORBIDI1961*	2,5	2,4	2,4	2,4	2,4	2,4	2,8	2,8	2,8	2,8	0,0	0,0	-

APPENDICES

APPENDIX 1.

List of the phenotypic Characters.

A) Characters from Grant et al. (2006, 2017).

0 Dorsal skin texture: (0) smooth, (1) posteriorly granular, (2) strongly granular, (3) spiculate.

1 Palmar skin: (0) taut, (1) loose,

2 Paired dorsal digital scutes: (0) absent, (1) present.

3 Supernumerary tubercles on hand: (0) absent, (1) present.

4 Digital discs: (0) absent, (1) present.

5 Finger disc II: (0) unexpanded, (1) weakly expanded, (2) moderately expanded. Additive.

6 Finger disc III: (0) unexpanded, (1) weakly expanded, (2) moderately expanded, (3) greatly expanded. Additive.

7 Finger disc IV: (0) unexpanded, (1) weakly expanded, (2) moderately expanded, (3) greatly expanded. Additive.

8 Finger disc V: (0) unexpanded, (1) weakly expanded, (2) moderately expanded, (3) greatly expanded. Additive.

9 Finger fringe: II preaxial: (0) absent, (1) present.

10 Finger fringe: IIpostaxial: (0) absent, (1) present.

11 Finger fringe: III preaxial: (0) absent, (1) present.

12 Finger fringe: III postaxial: (0) absent, (1) present.

13 Finger fringe: IV preaxial: (0) absent, (1) present.

14 Finger fringe: IV postaxial: (0) absent, (1) present.

15 Finger fringe: V preaxial: (0) absent, (1) present.

16 Finger fringe: V postaxial: (0) absent, (1) present.

17 Metacarpal ridge/fold: (0) absent, (1) present.

18 Carpal pad: (0) absent, (1) present.

19 Male nuptial excrescenses on Finger II: (0) absent, (1) present.

20 Morphology of male nuptial excrescenses on thumb: (0) large, cornified spines; (1) small, uncornified spines; (2) non-spinous asperities. Additive.

21 Female nuptial excrescences on Finger II: (0) absent, (1) present.

22 Thenar tubercle: (0) absent or small, inconspicuous swelling, (1) large, conspicuous, well defined tubercle.

23 Tarsal keel: (0) absent, (1) present.

24 Morphology of tarsal keel: (0) straight or weakly curved, extending proximolaterad from inner metatarsal tubercle, (1) tuberclelike, strongly curved at proximal end, extending from metatarsal tubercle, (2) short, tuberclelike, curved or directed transversely across tarsus, not extending from metatarsal tubercle, (3) weak, short dermal thickening, not extending from metatarsal tubercle. Additive.

25 Tarsal fringe: (0) absent, (1) present.

26 Toe disc I: (0) unexpanded, (1) weakly expanded, (2) moderately expanded. Additive.

27 Toe disc II: (0) unexpanded, (1) weakly expanded, (2) moderately expanded. Additive.

28 Toe disc III: (0) unexpanded, (1) weakly expanded, (2) moderately expanded. Additive.

29 Toe disc IV: (0) unexpanded, (1) weakly expanded, (2) moderately expanded, (3) greatly expanded. Additive.

30 Toe disc V: (0) unexpanded, (1) weakly expanded, (2) moderately expanded. Additive.

31 Webbing: Toe I Preaxial: (0) absent, (1) fringe.

32 Webbing: Toe I Postaxial: (0) absent, (1) fringe, (2) 2, (3) 1.5, (4) 1, (5) 0. Additive.

33 Webbing: Toe II Preaxial: (0) absent, (1) 2.5, (2) 2; (3) 1, (4) 0. Additive

34 Webbing: Toe II Postaxial: (0) absent, (1) 2, (2) 2 (with fringe), (3) 1.5, (4) 1, (5) 0. Additive.

35 Webbing: Toe III Preaxial: (0) absent, (1) fringe, (2) 3.5, (3) 3.5 (with fringe), (4) 3, (5) 2.5, (6) 2, (7) 1.5, (8) 1. Additive.

36 Webbing: Toe III Postaxial: (0) absent, (1) 3, (2) 3 (with fringe), (3) 2.5, (4) 2, (5) 1.5, (6) 1. Additive.

37 Webbing: Toe IV Preaxial: (0) absent, (1) 4, (2) 4 (with fringe), (3) 3.5, (4) 3, (5) 2.5, (6) 2, (7) 1. Additive.

38 Webbing: Toe IV Postaxial: (0) absent, (1) fringe, (2) 4, (3) 3.5, (4) 3, (5) 2.5, (6) 2, (7) 1. Additive.

39 Webbing: Toe V Preaxial: (0) absent, (1) fringe, (2) 2.5, (3) 2, (4) 1.5, (5) 1. Additive.

40 Webbing: Toe V Postaxial: (0) absent, (1) fringe.

41 Cloacal tubercles: (0) absent, (1) present.

42 Iridescent orange or golden spot at dorsal limb insertions: (0) absent, (1) present.

43 Pale paracloacal mark: (0) absent, (1) present.

44 Thigh dorsal coloration: (0) pale with dark spots (forming reticulum when spots close together), (1) solid dark, (2) dark with pale spots/bands, (3) solid pale, (4)

brown with dark brown bands/blotches, (5) dark with pale longitudinal stripe. Nonadditive.

45 Pale proximoventral calf spot: (0) absent, (1) present.

46 Dorsolateral stripe A occurrence (does not drop to thigh): (0) absent, (1) present.

47 Dorsolateral stripe A length: (0) anterior only (extending from eye to area above arm insertion); (1) complete (extending from eye well past area above arm insertion).

48 Dorsoloteral stripe A structure: (0) series of discrete spots, (1) solid.

49 Dorsolateral stripe A ontogeny: (0) present in juveniles only (i.e., lost ontogenetically), (1) present in adults and juveniles.

50 Dorsolateral stripe B (drops to top of thigh, not groin): (0) absent, (1) present.

51 Oblique lateral stripe: (0) absent, (1) present.

52 Oblique lateral stripe length: (0) partial, (1) complete.

53 Oblique lateral stripe structure: (0) solid, (1) series of spots, (2) diffuse. Nonadditive.

54 Gular-chest markings: (0) absent, (1) present.

55 Dermal collar: (0) absent, (1) present.

56 Dark lower labial stripe: (0) absent, (1) present.

57 Male throat (vocal sac) color: (0) pale, free or almost free of melanophores, (1) dark due to absence of iridophores, (2) evenly stippled, (3) pale with discrete dark spotting/reticulation/marbling, (4) solid dark, (5) dark with discrete pale spotting/reticulation/marbling, (6) irregular (clumped) stippling or faint, diffuse spotting. Nonadditive.

58 Female throat color: (0) pale, free or almost free of melanophores, (1) irregular (clumped) stippling or faint, diffuse spotting, (2) solid dark, (3) dark with discrete pale spotting/reticulation/marbling, (4) pale with discrete dark

spotting/reticulation/marbling, (5) dark with pale medial longitudinal stripe, (6) evenly stippled. Nonadditive.

59 Male abdomen color: (0) pale, free or almost free of melanophores, (1) pale with discrete dark spotting/reticulation/marbling, (2) evenly stippled, (3) dark with discrete pale spotting/reticulation/marbling, (4) irregular (clumped) stippling or faint, diffuse spotting, (5) solid dark. Nonadditive.

60 Female abdomen color: (0) pale, free or almost free of melanophores, (1) pale with discrete dark spotting/reticulation/marbling, (2) solid dark, (3) dark with discrete pale spotting/reticulation/marbling, (4) irregular (clumped) stippling or faint, diffuse spotting, (5) evenly stippled. Nonadditive.

61 Iris coloration: (0) lacking metallic pigmentation and pupil ring, (1) with metallic pigmentation and pupil ring.

62 Large intestine color: (0) unpigmented, (1) pigmented anteriorly, (2) pigmented entirely. Additive.

63 Adult testis color: (0) unpigmented, (1) pigmented medially only, (2) entirely pigmented. Additive.

64 Color of mature oocytes: (0) unpigmented (white or creamy yellow), (1) pigmented (animal pole brown).

65 M. semitendinosus insertion: (0) "bufonid type" (ventrad), (1) "ranid type" (dorsad).

66 M. semitendinosus binding tendon: (0) absent, (1) present.

67 M. adductor mandibulae externus superficialis: (0) undivided (s), (1) divided (s+e).

68 M. depressor mandibulae dorsal flap: (0) dorsal flap absent, (1) dorsal flap present.

69 M. depressor mandibulae origin posterior to squamosal: (0) absent, (1) present.

70 M. depressor mandibulae origin on annulus tympanicus: (0) no fibers originating from annulus tympanicus, (1) some fibers originating from annulus tympanicus.

71 Tympanum and m. depressor mandibulae relation: (0) tympanum superficial to m. depressor mandibulae, (1) tympanum concealed superficially by m. depressor mandibulae.

72 Vocal sac occurrence: (0) absent, (1) present.

73 Vocal sac structure (sensu Liu, 1935): (0) median, subgular, (1) paired lateral,

74 M. intermandubularis supplementary element occurrence: (0) absent, (1) present.

75 M. intermandibularis supplementary element orientation: (0) anterolateral, (1) anteromedial,

76 Median lingual process (MLP): (0) absent, (1) present.

77 MLP shape: (0) short, bumplike, (1) elongate.

78 MLP tip: (0) blunt, (1) tapering to point.

79 MLP texture: (0) smooth, (1) rugose.

80 MLP orientation when protruded: (0) upright, (1) posteriorly reclined.

81 MLP retractility: (0) nonretractile, (1) retractile.

82 MLP associated pit: (0) absent, (1) present.

83 MLP epithelium: (0) glandular, (1) nonglandular.

84 Larval caudal coloration: (0) vertically striped, (1) scattered melanophores clumped to form diffuse blotches and retic, (2) evenly pigmented. Additive.

85 Larval oral disc occurrence: (0) absent, (1) present.

86 Larval oral disc morphology: (0) "normal", (1) umbelliform, (0) suctorial.

87 Lateral emargination of larval oral disc: (0) absent (not emarginate), (1) present (emarginate).

88 Larval marginal labial papillae size: (0) short, (1) enlarged, (2) greatly enlarged. Additive.

89 Larval jaw sheaths: (0) absent, (1) lower only, not keratinized, (2) entire, keratinized. Additive.

90 Advertisement calls: (0) buzz, (1) chirp, (2) trill, (3) retarded trill, (4) retarded chirp. Nonadditive.

91 Male courtship: Stereotyped strut: (0) absent, (1) present.

92 Male courtship: Jumping up and down: (0) absent, (1) present.

93 Female courtship: Crouching: (0) absent, (1) present.

94 Female courtship: Sliding under male: (0) absent, (1) present.

95 Timing of sperm deposition: (0) after oviposition; (1) prior to oviposition.

96 Reproductive amplexus occurrence: (0) absent, (1) present.

97 Reproductive amplexus position: (0) axillary, (1) cephalic.

98 Cloaca-cloaca touching: (0) absent, (1) present.

99 Egg deposition site: (0) aquatic; (1) terrestrial: leaf litter, soil, on or under stones; (2) terrestrial: phytotelmata. Additive.

100 Egg clutch attendance occurrence: (0) absent, (1) present.

101 Egg clutch attendant sex: (0) male, (1) female, (2) both.

102 Dorsal tadpole transport: (0) absent, (1) present.

103 Sex of nurse frog: (0) male, (1) female, (2) both.

104 Larval habitat: (0) pool or stream; (1) phytotelmata; (1) nidicolous. Nonadditive.

105 Larval trophic guild: (0) exotrophic, (1) endotrophic.

106 Exotrophic larval diet: (0) detritivorous; (1) predaceous; (2) oophagous. Nonadditive.

107 Egg provisioning for larval oophagy: (0) both sexes involved, (1) female only.

108 Adult habitat selection: (0) aquatic, (1) riparian (<3 m from water), (2) independent of streams (up to ca. 30 m or more from water). Additive

109 Diel activity: (0) nocturnal, (1) diurnal.

110 Toe trembling: (0) absent, (1) present.

111 Hyalia anterior process: (0) absent, (1) present.

112 Shape of terminal phalanges: (0) T-shaped, (1) knobbed.

113 Epicoracoid fusion in adults: (0) entirely fused (Kaplan E), (1) anteriorly fused, posteriorly free (Kaplan C), (2) fused at anterior extreme, free posteriorly (Kaplan A). Additive.

114 Epicoracoid overlap in adults: (0) no overlap (Kaplan B), (1) partial overlap (Kaplan E), (2) partial overlap (Kaplan C), (3) partial overlap (Kaplan A). Nonadditive.

115 Angle of clavicles: (0) directed laterad, perpendicular to sagittal plane, (1) directed posteriad, (2) directed anteriad. Nonadditive.

116 Acromion process: (0) cartilaginous, distinct; (1) fully calcified/ossified, continuous with clavicle and scapula.

117 Prezonal element (omosternun): (0) absent, (1) present.

118 Prezonal element (omosternum) anterior expansion: (0) not expanded distally, tapering to tip, (1) weakly expanded, to 2.5x style at base of cartilage or equivalent, (2) extensively expanded distally, 3.5x or greater. Additive.

119 Prezonal element (omosternun) shape of anterior terminus: (0) rounded or irregularly shaped, (1) distinctly bifid.

120 Prezonal element (omosternum) shape of posterior terminus: (0) simple, (1) notched, forming two struts continuous with epicoracoid cartilage.

121 Prezonal element (omosternum) ossification: (0) entirely cartilaginous, (1) medially ossified (cartilaginous base and tip), (2) basally ossified (cartilaginous tip), (3) entirely ossified. Additive.

122 Suprascapula anterior projection: (0) cartilaginous, (1) heavily calcified.

123 Sternum shape: (0) simple, ovoid, or irregular, (1) medially divided, bifid.

124 Zygomatic ramus of squamosal: (0) elongate, slender, pointed, (1) very long and slender, (2) robust, truncate, and elongate, (3) shorter and less robust but still well defined, (4) well defined, moderate length, abruptly directed ventrad, (5) inconspicuous, poorly differentiated, (6) very small, inconspicuous, hook-like, (7) miniscule bump, (8) robust, elongate, in broad contact with the maxilla. Nonadditive.

125 Orientation of alary process of premaxilla: (0) tilted anteriorly, (1) directed dorsally (vertical, not tilted), (2) tilted posteriorly. Additive.

126 Palatines: (0) absent, (1) present.

127 Quadratojugal-maxilla relation: (0) overlapping, (1) separated.

128 Nasal-maxilla relation: (0) separated, (1) in contact.

129 Nasal-sphenethmoid relation: (0) separate, (1) overlapping or fused.

130 Frontoparietal fusion: (0) entirely free (articulating, but not fused), (1) fused posteriorly, (2) fused along entire length. Additive.

131 Frontoparietal-otoccipital relation: (0) free, articulating but not fused, (1) fused.

132 Exoccipitals: (0) free, separate, (1) fused sagitally.

133 Maxillary teeth: (0) absent, (1) present.

134 Maxillary tooth structure: (0) pedicelate, (1) nonpedicelate.

135 Vomerine teeth: (0) absent, (1) present.

136 Retroarticular process of mandible: (0) absent, (1) present.

137 Expansion of sacral diapophyses: (0) unexpanded, (1) weakly expanded (1.5-2.5X), (2) strongly expanded. Additive

138 Vertebra 8 and sacrum: (0) free, (1) fused.

139 Vertebae 1 and 2: (0) free, (1) fused.

140 Vertebae 2 and 3: (0) free, (1) fused.

141 Ability to sequester liophilic alkaloids: (0) absent, (1) present.

142 Batrachotoxins (BTX): (0) absent, (1) present.

143 Histrionicotoxins (HTX): (0) absent, (1) present.

144 Pumiliotoxins (PTX): (0) absent, (1) present.

145 Allopumiliotoxins: (0) absent, (1) present.

146 Homopumiliotoxins: (0) absent, (1) present.

147 Decahydroquinolines (DHQ): (0) absent, (1) present.

148 3,5-Disubstituted pyrrolizidines (3,5-P): (0) absent, (1) present.

149 3,5-Disubstituted indolizidines (3,5-I): (0) absent, (1) present.

150 5,8-disubstituted indolizidines (5,8-I): (0) absent, (1) present.

151 Dehydro-5,8-Indolizidines (Dehydro-5,8-I): (0) absent, (1) present.

152 5,6,8-Trisubstituted indolizidines (5,6,8-I): (0) absent, (1) present.

153 4,6-Disubstituted quinolizidines (4,6-Q): (0) absent, (1) present.

154 1,4-Disubstituted quinolizidines (1,4-Q): (0) absent, (1) present.

155 Lehmizidines (Lehm): (0) absent, (1) present.

156 Epiquinamide: (0) absent, (1) present.

157 2,5-Disubstituted pyrrolidines (PYR): (0) absent, (1) present.

158 2,6-Disubstituted piperidines (Pip): (0) absent, (1) present.

159 Gephyrotoxins (GTX): (0) absent, (1) present.

160 Coccinelline-like tricyclics (Tricyclic): (0) absent, (1) present.

161 Cyclopentylquinolizidines (CPQ): (0) absent, (1) present.

162 Spiropyrrolizidines (SpiroP): (0) absent, (1) present.

163 Indolic alkaloids: (0) absent, (1) present.

164 Epibatidines: (0) absent, (1) present.

165 Noranabasamine: (0) absent, (1) present.

166 N-methyldecahydroquinolines (N-MeDHQ): (0) absent, (1) present.

167 Pumiliotoxin 7-hydroxylase: (0) absent, (1) present.

168 Tetrodotoxin (TTX): (0) absent, (1) present.

169 Chromosome number (2n): (0) 18, (1) 20, (1) 22, (2) 24, (3) 26, (4) 28, (5) 30. Additive.

B) New characters.

170 Ventral body skin, texture: (0) smooth, (1) granular, (2) warty.

171 Ventrolateral body skin, texture: (0) smooth, (1) granular, (2) warty.

172 Internal tympanic membrane, occurrence: (0) present, (1) absent.

173 Skin on the tympanic middle ear: (0) adhered, (1) loose.

174 Distal subarticular tubercle on Finger II, occurrence: (0) absent, (1) present.

175 Distal subarticular tubercle on Finger III, occurrence: (0) absent, (1) present.

176 Subarticular tubercles on Finger IV: (0) basal, (1) basal+distal, (2) basal+distal+hyperdistal. Additive.

177 Subarticular tubercles on Finger V: basal (0); basal+distal (1); basal+distal+hyperdistal (2). Additive.

178 Basal subarticular tubercle of Finger II, protrusiveness: (0) flattened, (1) projected.

179 Basal subarticular tubercle of Finger III, protrusiveness: (0) flattened, (1) projected.

180 Basal subarticular tubercle of Finger IV protrusiveness: (0) flattened, (1) projected.

181 Basal subarticular tubercle of Finger V, protrusiveness: (0) flattened, (1) projected.

182 Distal subarticular tubercle of Finger IV protrusiveness: (0) flattened, (1) projected.

183 Distal subarticular tubercle of Finger V, protrusiveness: (0) flattened, (1) projected.

184 Basal subarticular tubercle of Finger II, shape: (0) rounded, (1) elongated.

185 Basal subarticular tubercle of Finger III, shape: (0) rounded, (1) elongated.

186 Relation between basal subarticular tubercle width of finger II and its finger width: (0) lesser or equal than finger width, (1) wider than finger width.

187 Relation between basal subarticular tubercle width of finger III and its finger width: (0) lesser or equal than finger width, (1) wider than finger width.

188 Relation between thenar tubercle and the basal subarticular tubercle of finger II: lesser (0), equal (1), or larger (2) than the basal subarticular tubercle.

189 Thenar tubercle, shape: (0) rounded, (1) elongated.

190 Finger III length: (0) not reaching the distal subarticular tubercle of finger IV, (1) reaching the distal subarticular tubercle of finger IV.

191 Finger V length: (0) barely surpassing the basal subarticular tubercle of finger IV, (1) extending to just before of the distal subarticular tubercle of finger IV, (2) reaching or at same level than distal subarticular tubercle of finger IV, (3) surpassing the distal subarticular tubercle of finger IV, (4) reaching the hyperdistal subarticular tubercle or the disc of finger IV. Additive.

192 Metacarpal ridge/fold, morphology: (0) ridge/fold, (1) tubercle-like.

193 Metacarpal ridge/fold, distal extension: (0) reaching and continuous with postaxial fringe of Finger V, (1) no reaching, non-continuous with postaxial fringe of Finger V.

194 Metacarpal ridge/fold, proximal extension: (0) reaching one-half of palm, (1) reaching two-third of palm, (2) in contact with the palmar tubercle.

195 Phalangeal swelling on finger II of adult males, occurrence: (0) absent, (1) present.

196 Phalangeal swelling on finger III of adult males, occurrence: (0) absent, (1) present.

197 Phalangeal swelling on finger IV of adult males, occurrence: (0) absent, (1) present.

198 Phalangeal swelling on finger IV of adult males, expansion: (0) dorsal and preaxial, (1) dorsal, preaxial, and postaxial.

199 Preaxial phalangeal swelling on finger IV of adult males, degree: (0) weak, (1) strong.

200 Basal swelling on finger IV of adult males, occurrence: (0) absent, (1) present.

201 Metacarpal swelling in adult males, occurrence: (0) absent, (1) present.

202 Phalangeal swelling on finger V of adult males: (0) absent, (1) present.

203 Ulnar tubercle, occurrence: (0) absent, (1) present.

204 Ulnar tubercles, structure: (0) one tubercle, antebrachial, (1) row of tubercles.

205 Distal swelling of the upper arm of adult males, occurrence: (0) absent, (1) present.

206 Distal swelling of the upper arm of adult males, extension: (0) restricted to distal end of the upper arm, (1) distal end of the upper arm, extending to the proximal lower arm.

207 Basal subarticular tubercle of toe IV, occurrence: (0) absent, (1) present.

208 Relation between basal and proximal subarticular tubercle of toe IV, size: (0) small (≤1/2), (1) slightly lesser or equal (>3/4).

209 Basal subarticular tubercle of toe I, protrusiveness: (0) flattened, (1) projected.

210 Basal subarticular tubercle of toe II, protrusiveness: (0) flattened, (1) projected.

211 Basal subarticular tubercle of toe III, protrusiveness: (0) flattened, (1) projected.

212 Basal subarticular tubercle of toe IV, protrusiveness: (0) flattened, (1) projected.

213 Basal subarticular tubercle of toe V, protrusiveness: (0) flattened, (1) projected.

214 Proximal subarticular tubercle of toe III, protrusiveness: (0) flattened, (1) projected.

215 Proximal subarticular tubercle of toe IV, protrusiveness: (0) flattened, (1) projected.

216 Proximal subarticular tubercle of toe V, protrusiveness: (0) flattened, (1) projected.

217 Distal subarticular tubercle of toe IV, protrusiveness: (0) flattened, (1) projected.

218 Basal subarticular tubercle of toe II, shape: (0) rounded or ovoid, (1) elongated.

219 Basal subarticular tubercle of toe III, shape: (0) rounded or ovoid, (1) elongated.

220 Basal subarticular tubercle of toe IV, shape: (0) rounded or ovoid, (1) elongated.

221 Inner metatarsal tubercle, shape: (0) rounded or ovoid, (1) elongated.

222 Metatarsal fold, occurrence: (0) absent, (1) present.

223 Metatarsal fold, degree: (0) weak, (1) strong.

224 Metatarsal fold, extension: (0) reaching half of plantar surface, (1) reaching the proximal 2/3 of plantar surface, (2) reaching the outer metatarsal tubercle level.

225 Toe III length: (0) reaching antepenultimate subarticular tubercle of toe IV, (1) surpassing antepenultimate subarticular tubercle of toe IV. Additive

226 Toe V length: (0) not reaching proximal subarticular tubercle of toe IV; (1) reaching proximal subarticular tubercle of toe IV; (2) surpassing proximal subarticular tubercle of toe IV. Additive.

227 Ventrolateral stripe A occurrence: (0) absent, (1) present.

228 Ventrolateral stripe A, structure: (0) wavy series of elongate spots, (1) straight.

229 Ventrolateral stripe B occurrence: (0) absent, (1) present.

230 Ventrolateral stripe B structure: (0) wavy series of elongate spots, (1) straight.

231 Adult testis, size: (0) small, 0.2–0.6 of kidney length, (1) large, 0.9–1 of kidney length.

232 M. compressor cloacae, anterior portion insertion: (0) inserting ventrally, covered by the m. pyriformis, (1) inserting anteriorly, uncovered by the m. pyriformis.

233 M. sphincter ani cloacalis, distal slip occurrence: (0) absent, (1) present.

234 M. sphincter ani cloacalis, slip, ventral insertion: (0) proximal, ventral to cloaca, on dermis, (1) distal, pubic symphysis level, on dermis and posterior branch of the m. rectus abdominis tendon origin.

235 Posterior branch of the m. rectus abdominis tendon origin, occurrence: (0) absent, (1) present.

236 M. tensor faciae latae, origin: (0) anterior, (1) medial, (2) posterior.

237 Second origin of m. gracilis minor, from dermis: (0) absent, (1) present.

238 M. extensor carpi radialis, origin width of internal slip: (0) thin, (1) robust.

239 M. extensor carpi radialis, insertion of internal slip: (0) at about distal two-third. of external slip, (1) at the external slip distal tendon, roughly at radiale level.

C) Larval characters.

240 Oral disc position: (0) ventral, 0° angle, (1) anteroventral, 45° angle, (2) anterior, 90° angle. Additive.

241 Medial emargination of the lower lip: (0) absent, (1) present.

242 Medial emargination of the upper lip: (0) absent, (1) present.

243 Marginal papillae, dorsolateral on upper lip, occurrence: (0) absent, (1) present.

244 Marginal papillae, lateroventral on lower lip, occurrence: (0) absent, (1) present.

245 Marginal papillae, medial on lower lip, occurrence: (0) absent, (1) present.

246 Submarginal papillae on the central portion of the lower lip: (0) absent, (1) present.

247 Submarginal papillae on the ventrolateral portion of the lower lip: (0) absent, (1) present.

248 Submarginal papillae on the dorsolateral portion of the upper lip: (0) absent, (1) present.

249 Labial dermal ridge on A2, occurrence: (0) absent, (1) present.

250 Labial dermal ridge on P1, occurrence: (0) absent, (1) present.

251 Labial dermal ridge on P2, occurrence: (0) absent, (1) present.

252 Labial dermal ridge on P3, occurrence: (0) absent, (1) present.

253 Gap on A1, occurrence: (0) absent, (1) present.

254 Gap on A2, occurrence: (0) absent, (1) present.

255 Gap on A2, size: (0) small, (1) large.

256 Gap on P1, occurrence: (0) absent, (1) present.

257 Labial teeth on A1, occurrence: (0) absent, (1) present.

258 Labial teeth on P1, occurrence: (0) absent, (1) present.

259 Margin of the upper jaw sheath, structure: (0) smooth, (1) with a medial notch.

260 Shape of the upper jaw sheath: (0) arch, (1) trapezoid, (2) inverted V, (3) cylindrical.

261 Lateral process of the upper jaw sheath, occurrence: (0) absent, (1) present.

262 Shape of the lower jaw sheath: (0) arch, (1) V-shaped, (2) cylindrical.

263 Robustness of the jaw sheaths: (0) thin, less than 50% OD height, (1) massive, more than 60% OD height.

264 Major axis of the jaw sheaths: (0) horizontal, (1) vertical.

265 Shelf, occurrence: (0) absent, (1) present.

266 Shape of the body on dorsal view: (0) elliptical, (1) cylindrical, (2) globular.

267 Shape of the body on lateral view: (0) ovoid, (1) depressed.

268 Bumps, anterior ventral surface of body: (0) absent, (1) present.

269 Bumps, lateroventral surface of body: (0) absent, (1) present.

270 Anterior, medial, body depression: (0) absent, (1) present.

271 Dark transverse band on ventral body: (0) absent, (1) present.

272 Spiracle, occurrence: (0) absent, (1) present.

273 Spiracular shape: (0) tubular, (1) conical.

274 Inner wall of the spiracle, occurrence: (0) absent, (1) present.

275 Inner wall of spiracle, fusion degree: (0) completely fused, (1) free medial to distally, (2) free distally, (3) border free only.

276 Spiracle margin, structure: (0) smooth, (1) irregular.

277 Spiracle, position regarding to medial longitudinal axis of body: (0) below, (1) very low, dislodged.

278 Relation of spiracle: longitudinal axis, angle: (0) parallel, (1) inclined, on 30-45°.

279 Relation spiracle opening: spiracle height: (0) equal, (1) smaller.

280 Spiracle pigmentation: (0) free of pigmentation, (1) melanophores and border with iridophores, (1) only melanophores.

281 Eyes position: (0) dorsal, (1) lateral.

282 Eyes orientation: (0) lateral, (1) anterolateral.

283 White ring on iris, occurrence: (0) absent, (1) present.

284 External nares orientation: (0) lateral, (1) anterolateral, (2) anterior.

285 Narial opening, shape: (0) elliptical, (1) rounded, (2) reniform.

286 Fleshy rim on narial opening, occurrence: (0) absent, (1) present.

287 Projection on inner margin of nares: (0) absent, (1) present.

288 Vent tube, opening: (0) open, (1) close.

289 Vent tube respect to ventral fin, position: (0) medial, (1) dextral.

290 Vent tube, shape: (0) conical, (1) tubular, (2) enlarged distally.

291 Left wall of vent tube, attachment to ventral fin : (0) fully attached, (1) medially attached, (2) basis attached.

292 Vent tube regard to ventral fin margin: (0) above, (1) at level.

293 Vent tube in lateral view, inclination: (0) parallel to longitudinal axis, (1) ventrally directed, 30-45°.

294 Dorsal fin, origin: (0) at body/tail junction, (1) at body, posterior third, (2) at tail, from first third.

295 Tail tip, shape: (0) rounded, (1) acute.

296 Tail muscles, posterior extension: (0) not reaching the tail tip, (1) reaching the tail tip.

297 Dorsal fin, shape: (0) arch-shaped, (1) straight line, (2) sigmoid, proximally low.

298 Ventral fin, shape: (0) arch-shaped, (1) straight line.

299 Stitches of supraorbital lateral line: (0) absent, (1) present.

300 Stitches of anterior pit line: (0) absent, (1) present.

301 Stitches of infraorbital lateral line: (0) absent, (1) present.

302 Stitches of middle pit line: (0) absent, (1) present.

303 Stitches of preopercular lateral line: (0) absent, (1) present.

304 Stitches of gular pit line: (0) absent, (1) present.

305 Stitches of jugal lateral line: (0) absent, (1) present.

306 Stitches of mandibular lateral line: (0) absent, (1) present.

307 Stitches of angular lateral line: (0) absent, (1) present.

308 Stitches of oral lateral line: (0) absent, (1) present.

309 Stitches of temporal lateral line: (0) absent, (1) present.

310 Stitches of supratemporal lateral line: (0) absent, (1) present.

311 Stitches of dorsal trunk line: (0) absent, (1) present.

312 Stitches of middle trunk line: (0) absent, (1) present.

313 Stitches of ventral trunk line: (0) absent, (1) present.

314 White spots on posterolateral body surface, occurrence: (0) absent, (1) present.

315 White spots on posteroventral body surface, occurrence: (0) absent, (1) present.

316 White spots on anterolateral body surface, occurrence: (0) absent, (1) present.

317 White spots on anteroventral body surface, occurrence: (0) absent, (1) present.

318 Gut coiling, axis: (0) perpendicular to longitudinal body axis, (1) laterally dislocated to left, sinistral.

319 Gut coiling, morphology: (0) long, concealing other organs, (1) short, revealing other organs.

320 Partes corpora, medial fusion: (0) not fused, (1) fused distally, (2) fused proximally, (3) fused medially, (4) fused entirely, (5) fused almost distally.

321 Partes corpora, inclination in frontal view: (0) parallel, (1) converging distally, V-shaped.

322 Pars corporis, proximal internal margin: (0) smooth, (1) serrated, or process.

323 Pars corporis, width along its length: (0) uniform, (1) distally expanded.

324 Pars corporis, width: (0) thin, (1) wider.

325 Fusion between pars corporis and pars alaris: (0) not fused, (1) fused proximally, (2) fused distally, (3) fused proximal and distally, with fenestra.

326 Processus anterior dorsalis: (0) absent, (1) present.

327 Processus anterior dorsalis, size: (0) short, wider than longer, (1) medial, as wide as long, (2) large, longer than wider. Additive.

328 Processus anterior dorsalis tip: (0) acuminate, (1) rounded.

329 Processus posterior dorsalis, occurrence: (0) absent, (1) present.

330 Processus posterior dorsalis, size: (0) short, wider than longer, (1) medial, as wide as long, (2) large, longer than wider. Additive.

331 Processus posterior dorsalis tip: (0) acuminate, (1) rounded.

332 Adrostral elements: (0) absent, (1) adrostral tissue mass, ATM, (2) ATM+adrostral cartilage. Additive.

333 Pars alaris, distal margin: (0) straight, (1) rounded, (2) acuminate.

334 Pars corporis shape: (0) vertically rectangular, (1) horizontal rectangular, (2) quadrangular.

335 Pars alaris shape: (0) rectangular, (1) subtriangular, (2) quadrangular.

336 Cornua trabeculae width: (0) uniform, (1) distally expanded.

337 Processus lateralis trabeculae: (0) absent, (1) present.

338 Fusion between cornua trabeculae and suprarostral: (0) absent, (1) present.

339 Processus orbitonasalis, occurrence: (0) absent, (1) present.

340 Processus orbitonasalis, size: (0) short (1) moderate, (2) large. Additive.

341 Relation cartilago orbitalis/otic capsule dorsal margin height: (0) low, (1) at same level, (2) high.

342 Contact between cartilago orbitalis and otic capsule: (0) absent, fenestra prootica, (1) present. foramen prooticum.

343 Arcus praeoccipitalis, orientation in ventral view: (0) posterolateral, (1) dorsad, parallel to vertical axis.

344 Medial projection of the arcus praeoccipitalis: (0) absent, (1) present.

345 Larval crista parotica: (0) inconspicuous, (1) conspicuous, well-development.

346 Processus anterolateralis of the crista parotica, occurrence: (0) absent, (1) present.

347 Processus anterolateralis of the crista parotica, size: (0) short (1) moderate, (2) large.

348 Processus anterolateralis tip, shape: (0) acuminated, (1) rounded.

349 Processus anterolateralis, orientation in dorsal view: (0) anterolateral, (0) anterior.

350 Processus posterolateralis of the crista parotica: (0) absent, (1) present.

351 Taenia tecti medialis: (0) absent, (1) partially developed, (2) fully developed. Additive.

352 Taenia tecti transversalis: (0) absent, (1) partially developed, (2) fully developed. Additive.

353 Processus antorbitalis, size: (0) short (1) moderate, (2) large.

354 Processus quadratoethmoidalis: (0) absent, (1) present.

355 Processus quadratoethmoidalis, size: (0) short, (1) moderate, (1) large. Additive.

356 Processus pseudopterygoideus: (0) absent, (1) present.

357 Processus pseudopterygoideus, size: (0) short, (1) large. Additive.

358 Contact between processus muscularis and processus antorbitalis: (0) absent, (1) present.

359 Hole on posterior arcus subocularis: (0) absent, (1) present.

360 Posterolateral margin of the palatoquadrate: (0) flat, (1) concave.

361 Processus ascendens attachment: (0) low, (1) intermediate, (2) high.

362 Posterior process of palatoquadrate: (0) absent, (1) present.

363 Thickness of the infrarostral cartilage: (0) uniform, (1) thin at its extremities, (2) thin medially.

364 Free basihyal: (0) absent, (1) present.

365 Fusion of the CB II with hypobranchial: (0) absent, (1) present.

366 Fusion of the CB III with hypobranchial: (0) absent, (1) present.

367 Fusion of the CB IV with hypobranchial: (0) absent, (1) present.

368 Spicule I–IV, occurrence: (0) absent, (1) present.

369 Processus anterior hyalis, occurrence: (0) absent, (1) present.

370 Processus anterior hyalis, size: (0) short, (1) large.

371 Processus anterolateralis hyalis, occurrence: (0) absent, (1) present.

372 Processus anterolateralis hyalis, size: (0) short, (1) large.

373 Processus of the crista lateralis hyalis: (0) absent, (1) present.

374 Condilus articularis, internal end: (0) short, no visible from frontal view, (1) large, visible from frontal view.

375 Processus anterior branchialis: (0) short, (1) large.

APPENDIX 2

Phenotypic Matrix of the *Hyloxalus* Used to Test the Phylogenetic Relationships.

See the attached file: Hyloxalus_Phenotypic_Matrix

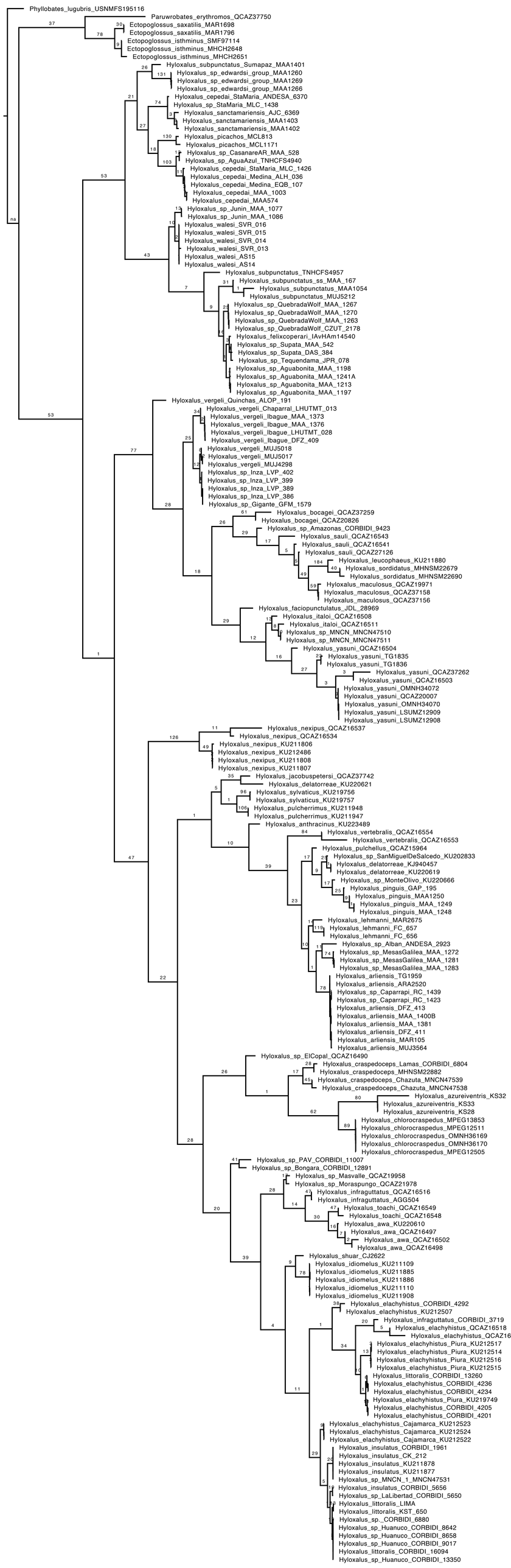
Phyllobates_lugubris_USNMFS195116
Paruwrobates_erythromos_QCAZ37750
Ectopoglossus_saxatilis_MAR1698
Ectopoglossus_saxatilis_MAR1796
Ectopoglossus_isthminus_SMF97114
Ectopoglossus_isthminus_MHCH2648
Ectopoglossus_isthminus_MHCH2651
Hyloxalus_subpunctatus_Sumapaz_MAA1401
Hyloxalus_sp_edwardsi_group_MAA1260
Hyloxalus_sp_edwardsi_group_MAA1269
Hyloxalus_sp_edwardsi_group_MAA1266
Hyloxalus_cepedai_StaMaria_ANDESA_6370
Hyloxalus_sp_StaMaria_MLC_1438
Hyloxalus_sanctamariensis_AJC_6369
Hyloxalus_sanctamariensis_MAA1403
Hyloxalus_sanctamariensis_MAA1402
Hyloxalus_picachos_MCL813
Hyloxalus_picachos_MCL1171
Hyloxalus_sp_CasanareAR_MAA_528
Hyloxalus_sp_AguaAzul_TNHCFS4940
Hyloxalus_cepedai_StaMaria_MLC_1426
Hyloxalus_cepedai_Medina_ALH_036
Hyloxalus_cepedai_Medina_EQB_107
Hyloxalus_cepedai_MAA_1003
Hyloxalus_cepedai_MAA574
Hyloxalus_sp_Junin_MAA_1077
Hyloxalus_sp_Junin_MAA_1086
Hyloxalus_walesi_SVR_016
Hyloxalus_walesi_SVR_015
Hyloxalus_walesi_SVR_014
Hyloxalus_walesi_SVR_013
Hyloxalus_walesi_AS15
Hyloxalus_walesi_AS14
Hyloxalus_subpunctatus_TNHCFS4957
Hyloxalus_subpunctatus_ss_MAA_167
Hyloxalus_subpunctatus_MAA1054
Hyloxalus_subpunctatus_MUJ5212
Hyloxalus_sp_QuebradaWolf_MAA_1267
Hyloxalus_sp_QuebradaWolf_MAA_1270
Hyloxalus_sp_QuebradaWolf_MAA_1263
Hyloxalus_sp_QuebradaWolf_CZUT_2178
Hyloxalus_felixcoperari_IAvHAm14540
Hyloxalus_sp_Supata_MAA_542
Hyloxalus_sp_Supata_DAS_384
Hyloxalus_sp_Tequendama_JPR_078
Hyloxalus_sp_Aguabonita_MAA_1198
Hyloxalus_sp_Aguabonita_MAA_1241A
Hyloxalus_sp_Aguabonita_MAA_1213
Hyloxalus_sp_Aguabonita_MAA_1197
Hyloxalus_vergeli_Quinchas_ALOP_191
Hyloxalus_vergeli_Chaparral_LHUTMT_013
Hyloxalus_vergeli_Ibague_MAA_1373
Hyloxalus_vergeli_Ibague_MAA_1376
Hyloxalus_vergeli_Ibague_LHUTMT_028
Hyloxalus_vergeli_Ibague_DFZ_409
Hyloxalus_vergeli_MUJ5018
Hyloxalus_vergeli_MUJ5017
Hyloxalus_vergeli_MUJ4298
Hyloxalus_sp_Inza_LVP_402
Hyloxalus_sp_Inza_LVP_399
Hyloxalus_sp_Inza_LVP_389
Hyloxalus_sp_Inza_LVP_386
Hyloxalus_sp_Gigante_GFM_1579
Hyloxalus_bocagei_QCAZ37259
Hyloxalus_bocagei_QCAZ20826
Hyloxalus_sp_Amazonas_CORBIDI_9423
Hyloxalus_sauli_QCAZ16543
Hyloxalus_sauli_QCAZ16541
Hyloxalus_sauli_QCAZ27126
Hyloxalus_leucophaeus_KU211880
Hyloxalus_sordidatus_MHNSM22679
Hyloxalus_sordidatus_MHNSM22690
Hyloxalus_maculosus_QCAZ19971
Hyloxalus_maculosus_QCAZ37158
Hyloxalus_maculosus_QCAZ37156
Hyloxalus_faciopunctulatus_JDL_28969
Hyloxalus_italoi_QCAZ16508
Hyloxalus_italoi_QCAZ16511
Hyloxalus_sp_MNCN_MNCN47510
Hyloxalus_sp_MNCN_MNCN47511
Hyloxalus_yasuni_QCAZ16504
Hyloxalus_yasuni_TG1835
Hyloxalus_yasuni_TG1836
Hyloxalus_yasuni_QCAZ37262
Hyloxalus_yasuni_QCAZ16503
Hyloxalus_yasuni_OMNH34072
Hyloxalus_yasuni_QCAZ20007
Hyloxalus_yasuni_OMNH34070
Hyloxalus_yasuni_LSUMZ12909
Hyloxalus_yasuni_LSUMZ12908
Hyloxalus_nexipus_QCAZ16537
Hyloxalus_nexipus_QCAZ16534
Hyloxalus_nexipus_KU211806
Hyloxalus_nexipus_KU212486
Hyloxalus_nexipus_KU211808
Hyloxalus_nexipus_KU211807
Hyloxalus_jacobuspetersi_QCAZ37742
Hyloxalus_delatorreae_KU220621
Hyloxalus_sylvaticus_KU219756
Hyloxalus_sylvaticus_KU219757
Hyloxalus_pulcherrimus_KU211948
Hyloxalus_pulcherrimus_KU211947
Hyloxalus_anthracinus_KU223489
Hyloxalus_vertebralis_QCAZ16554
Hyloxalus_vertebralis_QCAZ16553
Hyloxalus_pulchellus_QCAZ15964
Hyloxalus_sp_SanMiguelDeSalcedo_KU202833
Hyloxalus_delatorreae_KJ940457
Hyloxalus_delatorreae_KU220619
Hyloxalus_sp_MonteOlivo_KU220666
Hyloxalus_pinguis_GAP_195
Hyloxalus_pinguis_MAA1250
Hyloxalus_pinguis_MAA_1249
Hyloxalus_pinguis_MAA_1248
Hyloxalus_lehmanni_MAR2675
Hyloxalus_lehmanni_FC_657
Hyloxalus_lehmanni_FC_656
Hyloxalus_sp_Alban_ANDESA_2923
Hyloxalus_sp_MesasGalilea_MAA_1272
Hyloxalus_sp_MesasGalilea_MAA_1281
Hyloxalus_sp_MesasGalilea_MAA_1283
Hyloxalus_arliensis_TG1959
Hyloxalus_arliensis_ARA2520
Hyloxalus_sp_Caparrapi_RC_1439
Hyloxalus_sp_Caparrapi_RC_1423
Hyloxalus_arliensis_DFZ_413
Hyloxalus_arliensis_MAA_1400B
Hyloxalus_arliensis_MAA_1381
Hyloxalus_arliensis_DFZ_411
Hyloxalus_arliensis_MAR105
Hyloxalus_arliensis_MUJ3564
Hyloxalus_sp_ElCopal_QCAZ16490
Hyloxalus_craspedoceps_Lamas_CORBIDI_6804
Hyloxalus_craspedoceps_MHNSM22882
Hyloxalus_craspedoceps_Chazuta_MNCN47539
Hyloxalus_craspedoceps_Chazuta_MNCN47538
Hyloxalus_azureiventris_KS32
Hyloxalus_azureiventris_KS33
Hyloxalus_azureiventris_KS28
Hyloxalus_chlorocraspedus_MPEG13853
Hyloxalus_chlorocraspedus_MPEG12511
Hyloxalus_chlorocraspedus_OMNH36169
Hyloxalus_chlorocraspedus_OMNH36170
Hyloxalus_chlorocraspedus_MPEG12505
Hyloxalus_sp_PAV_CORBIDI_11007
Hyloxalus_sp_Bongara_CORBIDI_12891
Hyloxalus_sp_Masvalle_QCAZ19958
Hyloxalus_sp_Morasapungo_QCAZ21978
Hyloxalus_infragluttatus_QCAZ16516
Hyloxalus_infragluttatus_AGG504
Hyloxalus_toachi_QCAZ16549
Hyloxalus_toachi_QCAZ16548
Hyloxalus_awa_KU220610
Hyloxalus_awa_QCAZ16497
Hyloxalus_awa_QCAZ16502
Hyloxalus_awa_QCAZ16498
Hyloxalus_shuar_CJ2622
Hyloxalus_idiomelus_KU211109
Hyloxalus_idiomelus_KU211885
Hyloxalus_idiomelus_KU211886
Hyloxalus_idiomelus_KU211110
Hyloxalus_idiomelus_KU211908
Hyloxalus_elachyhistus_CORBIDI_4292
Hyloxalus_elachyhistus_KU212507
Hyloxalus_infragluttatus_CORBIDI_3719
Hyloxalus_elachyhistus_QCAZ16518
Hyloxalus_elachyhistus_QCAZ16
Hyloxalus_elachyhistus_Piura_KU212517
Hyloxalus_elachyhistus_Piura_KU212514
Hyloxalus_elachyhistus_Piura_KU212516
Hyloxalus_elachyhistus_Piura_KU212515
Hyloxalus_littoralis_CORBIDI_13260
Hyloxalus_elachyhistus_CORBIDI_4236
Hyloxalus_elachyhistus_CORBIDI_4234
Hyloxalus_elachyhistus_Piura_KU219749
Hyloxalus_elachyhistus_CORBIDI_4205
Hyloxalus_elachyhistus_CORBIDI_4201
Hyloxalus_elachyhistus_Cajamarca_KU212523
Hyloxalus_elachyhistus_Cajamarca_KU212524
Hyloxalus_elachyhistus_Cajamarca_KU212522
Hyloxalus_insulatus_CORBIDI_1961
Hyloxalus_insulatus_CK_212
Hyloxalus_insulatus_KU211878
Hyloxalus_insulatus_KU211877
Hyloxalus_sp_MNCN_1_MNCN47531
Hyloxalus_insulatus_CORBIDI_5656
Hyloxalus_sp_LaLibertad_CORBIDI_5650
Hyloxalus_littoralis_LIMA
Hyloxalus_littoralis_KST_650
Hyloxalus_sp._CORBIDI_6880
Hyloxalus_sp_Huanuco_CORBIDI_8642
Hyloxalus_sp_Huanuco_CORBIDI_8658
Hyloxalus_sp_Huanuco_CORBIDI_9017
Hyloxalus_littoralis_CORBIDI_16094
Hyloxalus_sp_Huanuco_CORBIDI_13350

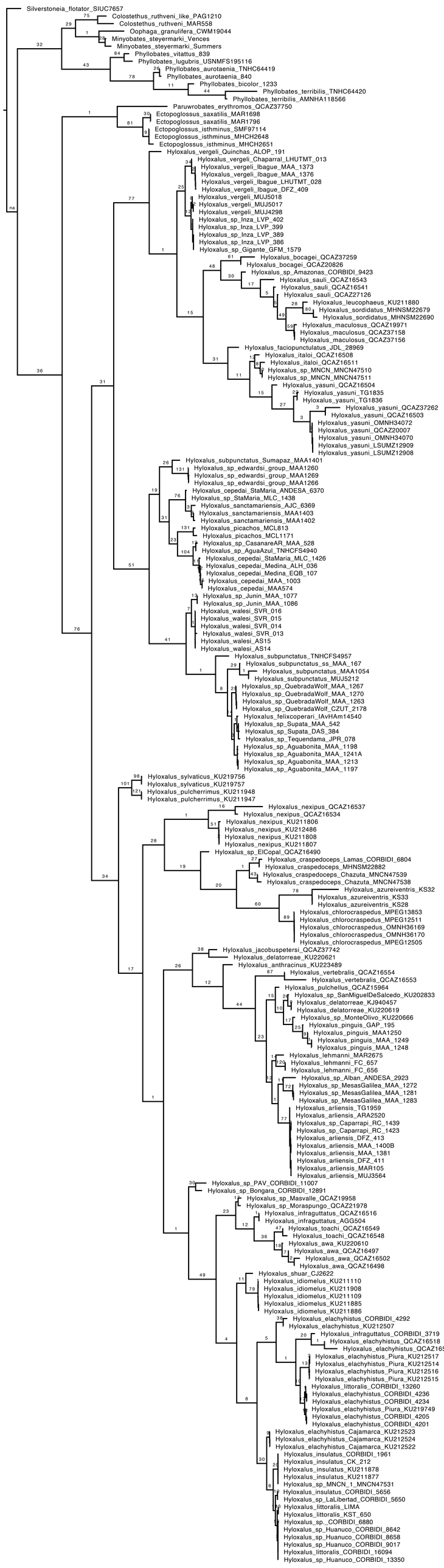
Silverstoneia_flotator_SIUC7657
Colostethus_ruthveni_like_PAG1210
Colostethus_ruthveni_MAR558
Oophaga_granulifera_CWM19044
Minyobates_steyermarki_Vences
Minyobates_steyermarki_Summers
Phyllobates_vittatus_839
Phyllobates_lugubris_USNMFS195116
Phyllobates_aurotaenia_TNHC64419
Phyllobates_aurotaenia_840
Phyllobates_bicolor_1233
Phyllobates_terribilis_TNHC64420
Phyllobates_terribilis_AMNHA118566
Paruwrobates_erythromos_QCAZ37750
Ectopoglossus_saxatilis_MAR1698
Ectopoglossus_saxatilis_MAR1796
Ectopoglossus_isthminus_SMF97114
Ectopoglossus_isthminus_MHCH2648
Ectopoglossus_isthminus_MHCH2651
Hyloxalus_vergeli_Quinchas_ALOP_191
Hyloxalus_vergeli_Chaparral_LHUTMT_013
Hyloxalus_vergeli_Ibague_MAA_1373
Hyloxalus_vergeli_Ibague_MAA_1376
Hyloxalus_vergeli_Ibague_LHUTMT_028
Hyloxalus_vergeli_Ibague_DFZ_409
Hyloxalus_vergeli_MUJ5018
Hyloxalus_vergeli_MUJ5017
Hyloxalus_vergeli_MUJ4298
Hyloxalus_sp_Inza_LVP_402
Hyloxalus_sp_Inza_LVP_399
Hyloxalus_sp_Inza_LVP_389
Hyloxalus_sp_Inza_LVP_386
Hyloxalus_sp_Gigante_GFM_1579
Hyloxalus_bocagei_QCAZ37259
Hyloxalus_bocagei_QCAZ20826
Hyloxalus_sp_Amazonas_CORBIDI_9423
Hyloxalus_sauli_QCAZ16543
Hyloxalus_sauli_QCAZ16541
Hyloxalus_sauli_QCAZ27126
Hyloxalus_leucophaeus_KU211880
Hyloxalus_sordidatus_MHNSM22679
Hyloxalus_sordidatus_MHNSM22690
Hyloxalus_maculosus_QCAZ19971
Hyloxalus_maculosus_QCAZ37158
Hyloxalus_maculosus_QCAZ37156
Hyloxalus_faciopunctulatus_JDL_28969
Hyloxalus_italoi_QCAZ16508
Hyloxalus_italoi_QCAZ16511
Hyloxalus_sp_MNCN_MNCN47510
Hyloxalus_sp_MNCN_MNCN47511
Hyloxalus_yasuni_QCAZ16504
Hyloxalus_yasuni_TG1835
Hyloxalus_yasuni_TG1836
Hyloxalus_yasuni_QCAZ37262
Hyloxalus_yasuni_QCAZ16503
Hyloxalus_yasuni_OMNH34072
Hyloxalus_yasuni_QCAZ20007
Hyloxalus_yasuni_OMNH34070
Hyloxalus_yasuni_LSUMZ12909
Hyloxalus_yasuni_LSUMZ12908
Hyloxalus_subpunctatus_Sumapaz_MAA1401
Hyloxalus_sp_edwardsi_group_MAA1260
Hyloxalus_sp_edwardsi_group_MAA1269
Hyloxalus_sp_edwardsi_group_MAA1266
Hyloxalus_cepedai_StaMaria_ANDESA_6370
Hyloxalus_sp_StaMaria_MLC_1438
Hyloxalus_sanctamariensis_AJC_6369
Hyloxalus_sanctamariensis_MAA1403
Hyloxalus_sanctamariensis_MAA1402
Hyloxalus_picachos_MCL813
Hyloxalus_picachos_MCL1171
Hyloxalus_sp_CasanareAR_MAA_528
Hyloxalus_sp_AguaAzul_TNHCFS4940
Hyloxalus_cepedai_StaMaria_MLC_1426
Hyloxalus_cepedai_Medina_ALH_036
Hyloxalus_cepedai_Medina_EQB_107
Hyloxalus_cepedai_MAA_1003
Hyloxalus_cepedai_MAA574
Hyloxalus_sp_Junin_MAA_1077
Hyloxalus_sp_Junin_MAA_1086
Hyloxalus_walesi_SVR_016
Hyloxalus_walesi_SVR_015
Hyloxalus_walesi_SVR_014
Hyloxalus_walesi_SVR_013
Hyloxalus_walesi_AS15
Hyloxalus_walesi_AS14
Hyloxalus_subpunctatus_TNHCFS4957
Hyloxalus_subpunctatus_ss_MAA_167
Hyloxalus_subpunctatus_MAA1054
Hyloxalus_subpunctatus_MUJ5212
Hyloxalus_sp_QuebradaWolf_MAA_1267
Hyloxalus_sp_QuebradaWolf_MAA_1270
Hyloxalus_sp_QuebradaWolf_MAA_1263
Hyloxalus_sp_QuebradaWolf_CZUT_2178
Hyloxalus_felixcoperari_IAvHAm14540
Hyloxalus_sp_Supata_MAA_542
Hyloxalus_sp_Supata_DAS_384
Hyloxalus_sp_Tequendama_JPR_078
Hyloxalus_sp_Aguabonita_MAA_1198
Hyloxalus_sp_Aguabonita_MAA_1241A
Hyloxalus_sp_Aguabonita_MAA_1213
Hyloxalus_sp_Aguabonita_MAA_1197
Hyloxalus_sylvaticus_KU219756
Hyloxalus_sylvaticus_KU219757
Hyloxalus_pulcherrimus_KU211948
Hyloxalus_pulcherrimus_KU211947
Hyloxalus_nexipus_QCAZ16537
Hyloxalus_nexipus_QCAZ16534
Hyloxalus_nexipus_KU211806
Hyloxalus_nexipus_KU212486
Hyloxalus_nexipus_KU211808
Hyloxalus_nexipus_KU211807
Hyloxalus_sp_ElCopal_QCAZ16490
Hyloxalus_craspedoceps_Lamas_CORBIDI_6804
Hyloxalus_craspedoceps_MHNSM22882
Hyloxalus_craspedoceps_Chazuta_MNCN47539
Hyloxalus_craspedoceps_Chazuta_MNCN47538
Hyloxalus_azureiventris_KS32
Hyloxalus_azureiventris_KS33
Hyloxalus_azureiventris_KS28
Hyloxalus_chlorocraspedus_MPEG13853
Hyloxalus_chlorocraspedus_MPEG12511
Hyloxalus_chlorocraspedus_OMNH36169
Hyloxalus_chlorocraspedus_OMNH36170
Hyloxalus_chlorocraspedus_MPEG12505
Hyloxalus_jacobuspetersi_QCAZ37742
Hyloxalus_delatorreae_KU220621
Hyloxalus_anthracinus_KU223489
Hyloxalus_vertebralis_QCAZ16554
Hyloxalus_vertebralis_QCAZ16553
Hyloxalus_pulchellus_QCAZ15964
Hyloxalus_sp_SanMiguelDeSalcedo_KU202833
Hyloxalus_delatorreae_KJ940457
Hyloxalus_delatorreae_KU220619
Hyloxalus_sp_MonteOlivo_KU220666
Hyloxalus_pinguis_GAP_195
Hyloxalus_pinguis_MAA1250
Hyloxalus_pinguis_MAA_1249
Hyloxalus_pinguis_MAA_1248
Hyloxalus_lehmanni_MAR2675
Hyloxalus_lehmanni_FC_657
Hyloxalus_lehmanni_FC_656
Hyloxalus_sp_Alban_ANDESA_2923
Hyloxalus_sp_MesasGalilea_MAA_1272
Hyloxalus_sp_MesasGalilea_MAA_1281
Hyloxalus_sp_MesasGalilea_MAA_1283
Hyloxalus_arliensis_TG1959
Hyloxalus_arliensis_ARA2520
Hyloxalus_sp_Caparrapi_RC_1439
Hyloxalus_sp_Caparrapi_RC_1423
Hyloxalus_arliensis_DFZ_413
Hyloxalus_arliensis_MAA_1400B
Hyloxalus_arliensis_MAA_1381
Hyloxalus_arliensis_DFZ_411
Hyloxalus_arliensis_MAR105
Hyloxalus_arliensis_MUJ3564
Hyloxalus_sp_PAV_CORBIDI_11007
Hyloxalus_sp_Bongara_CORBIDI_12891
Hyloxalus_sp_Masvalle_QCAZ19958
Hyloxalus_sp_Moraspungo_QCAZ21978
Hyloxalus_infragutttatus_QCAZ16516
Hyloxalus_infragutttatus_AGG504
Hyloxalus_toachi_QCAZ16549
Hyloxalus_toachi_QCAZ16548
Hyloxalus_awa_KU220610
Hyloxalus_awa_QCAZ16497
Hyloxalus_awa_QCAZ16502
Hyloxalus_awa_QCAZ16498
Hyloxalus_shuar_CJ2622
Hyloxalus_idiomelus_KU211110
Hyloxalus_idiomelus_KU211908
Hyloxalus_idiomelus_KU211109
Hyloxalus_idiomelus_KU211885
Hyloxalus_idiomelus_KU211886
Hyloxalus_elachyhistus_CORBIDI_4292
Hyloxalus_elachyhistus_KU212507
Hyloxalus_infragutttatus_CORBIDI_3719
Hyloxalus_elachyhistus_QCAZ16518
Hyloxalus_elachyhistus_QCAZ16
Hyloxalus_elachyhistus_Piura_KU212517
Hyloxalus_elachyhistus_Piura_KU212514
Hyloxalus_elachyhistus_Piura_KU212516
Hyloxalus_elachyhistus_Piura_KU212515
Hyloxalus_littoralis_CORBIDI_13260
Hyloxalus_elachyhistus_CORBIDI_4236
Hyloxalus_elachyhistus_CORBIDI_4234
Hyloxalus_elachyhistus_Piura_KU219749
Hyloxalus_elachyhistus_CORBIDI_4205
Hyloxalus_elachyhistus_CORBIDI_4201
Hyloxalus_elachyhistus_Cajamarca_KU212523
Hyloxalus_elachyhistus_Cajamarca_KU212524
Hyloxalus_elachyhistus_Cajamarca_KU212522
Hyloxalus_insulatus_CORBIDI_1961
Hyloxalus_insulatus_CK_212
Hyloxalus_insulatus_KU211878
Hyloxalus_insulatus_KU211877
Hyloxalus_sp_MNCN_1_MNCN47531
Hyloxalus_insulatus_CORBIDI_5656
Hyloxalus_sp_LaLibertad_CORBIDI_5650
Hyloxalus_littoralis_LIMA
Hyloxalus_littoralis_KST_650
Hyloxalus_sp._CORBIDI_6880
Hyloxalus_sp_Huanuco_CORBIDI_8642
Hyloxalus_sp_Huanuco_CORBIDI_8658
Hyloxalus_sp_Huanuco_CORBIDI_9017
Hyloxalus_littoralis_CORBIDI_16094
Hyloxalus_sp_Huanuco_CORBIDI_13350

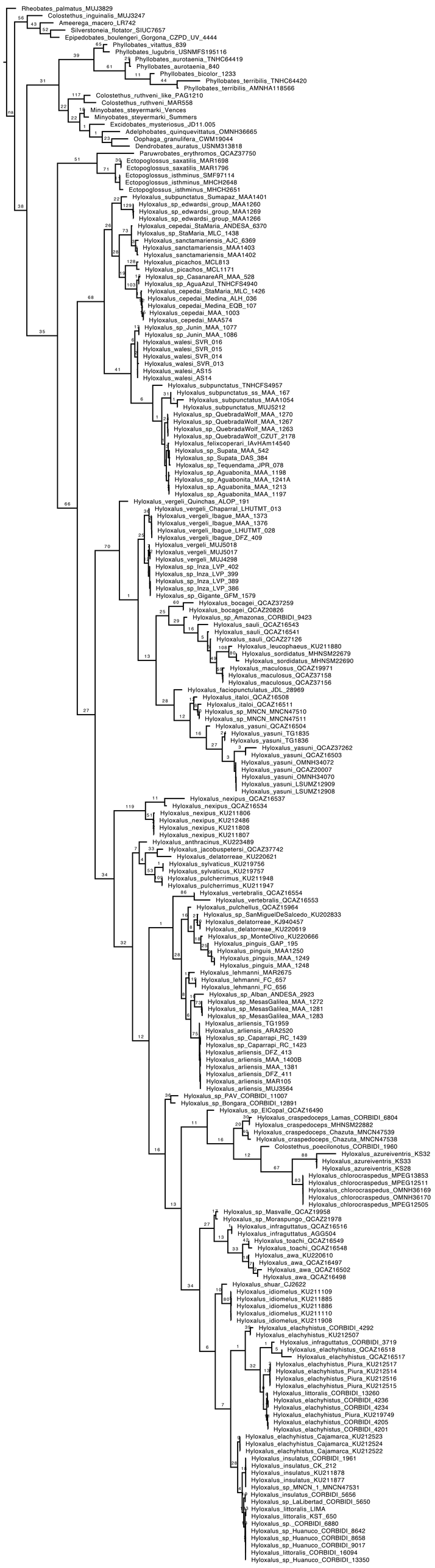
Rheobates_palmatus_MUJ3829
Colostethus_inguinalis_MUJ3247
Ameerega_macero_LR742
Silverstoneia_flotator_SIUC7657
Epipedobates_boulengeri_Gorgona_CZPD_UV_4444
Phyllobates_vitattus_839
Phyllobates_lugubris_USNMFS195116
Phyllobates_aurotaenia_TNHC64419
Phyllobates_aurotaenia_840
Phyllobates_bicolor_1233
Phyllobates_terribilis_TNHC64420
Phyllobates_terribilis_AMNHA118566
Colostethus_ruthveni_like_PAG1210
Colostethus_ruthveni_MAR558
Minyobates_steyermarki_Vences
Minyobates_steyermarki_Summers
Excidobates_mysteriosus_JD11.005
Adelphobates_quinquevittatus_OMNH36665
Oophaga_granulifera_CWM19044
Dendrobates_auratus_USNM313818
Paruwrobates_erythromos_QCAZ37750
Ectopoglossus_saxatilis_MAR1698
Ectopoglossus_saxatilis_MAR1796
Ectopoglossus_isthminus_SMF97114
Ectopoglossus_isthminus_MHCH2648
Ectopoglossus_isthminus_MHCH2651
Hyloxalus_subpunctatus_Sumapaz_MAA1401
Hyloxalus_sp_edwardsi_group_MAA1260
Hyloxalus_sp_edwardsi_group_MAA1269
Hyloxalus_sp_edwardsi_group_MAA1266
Hyloxalus_cepedai_StaMaria_ANDESA_6370
Hyloxalus_sp_StaMaria_MLC_1438
Hyloxalus_sanctamariensis_AJC_6369
Hyloxalus_sanctamariensis_MAA1403
Hyloxalus_sanctamariensis_MAA1402
Hyloxalus_picachos_MCL813
Hyloxalus_picachos_MCL1171
Hyloxalus_sp_CasanareAR_MAA_528
Hyloxalus_sp_AguaAzul_TNHCFS4940
Hyloxalus_cepedai_StaMaria_MLC_1426
Hyloxalus_cepedai_Medina_ALH_036
Hyloxalus_cepedai_Medina_EQB_107
Hyloxalus_cepedai_MAA_1003
Hyloxalus_cepedai_MAA574
Hyloxalus_sp_Junin_MAA_1077
Hyloxalus_sp_Junin_MAA_1086
Hyloxalus_walesi_SVR_016
Hyloxalus_walesi_SVR_015
Hyloxalus_walesi_SVR_014
Hyloxalus_walesi_SVR_013
Hyloxalus_walesi_AS15
Hyloxalus_walesi_AS14
Hyloxalus_subpunctatus_TNHCFS4957
Hyloxalus_subpunctatus_ss_MAA_167
Hyloxalus_subpunctatus_MAA1054
Hyloxalus_subpunctatus_MUJ5212
Hyloxalus_sp_QuebradaWolf_MAA_1270
Hyloxalus_sp_QuebradaWolf_MAA_1267
Hyloxalus_sp_QuebradaWolf_MAA_1263
Hyloxalus_sp_QuebradaWolf_CZUT_2178
Hyloxalus_felixcoperari_IAvHAm14540
Hyloxalus_sp_Supata_MAA_542
Hyloxalus_sp_Supata_DAS_384
Hyloxalus_sp_Tequendama_JPR_078
Hyloxalus_sp_Aguabonita_MAA_1198
Hyloxalus_sp_Aguabonita_MAA_1241A
Hyloxalus_sp_Aguabonita_MAA_1213
Hyloxalus_sp_Aguabonita_MAA_1197
Hyloxalus_vergeli_Quinchas_ALOP_191
Hyloxalus_vergeli_Chaparral_LHUTMT_013
Hyloxalus_vergeli_Ibague_MAA_1373
Hyloxalus_vergeli_Ibague_MAA_1376
Hyloxalus_vergeli_Ibague_LHUTMT_028
Hyloxalus_vergeli_Ibague_DFZ_409
Hyloxalus_vergeli_MUJ5018
Hyloxalus_vergeli_MUJ5017
Hyloxalus_vergeli_MUJ4298
Hyloxalus_sp_Inza_LVP_402
Hyloxalus_sp_Inza_LVP_399
Hyloxalus_sp_Inza_LVP_389
Hyloxalus_sp_Inza_LVP_386
Hyloxalus_sp_Gigante_GFM_1579
Hyloxalus_bocagei_QCAZ37259
Hyloxalus_bocagei_QCAZ20826
Hyloxalus_sp_Amazonas_CORBIDI_9423
Hyloxalus_sauli_QCAZ16543
Hyloxalus_sauli_QCAZ16541
Hyloxalus_sauli_QCAZ27126
Hyloxalus_leucophaeus_KU211880
Hyloxalus_sordidatus_MHNSM22679
Hyloxalus_sordidatus_MHNSM22690
Hyloxalus_maculosus_QCAZ19971
Hyloxalus_maculosus_QCAZ37158
Hyloxalus_maculosus_QCAZ37156
Hyloxalus_faciopunctulatus_JDL_28969
Hyloxalus_italoi_QCAZ16508
Hyloxalus_italoi_QCAZ16511
Hyloxalus_sp_MNCN_MNCN47510
Hyloxalus_sp_MNCN_MNCN47511
Hyloxalus_yasuni_QCAZ16504
Hyloxalus_yasuni_TG1835
Hyloxalus_yasuni_TG1836
Hyloxalus_yasuni_QCAZ37262
Hyloxalus_yasuni_QCAZ16503
Hyloxalus_yasuni_OMNH34072
Hyloxalus_yasuni_QCAZ20007
Hyloxalus_yasuni_OMNH34070
Hyloxalus_yasuni_LSUMZ12909
Hyloxalus_yasuni_LSUMZ12908
Hyloxalus_nexipus_QCAZ16537
Hyloxalus_nexipus_QCAZ16534
Hyloxalus_nexipus_KU211806
Hyloxalus_nexipus_KU212486
Hyloxalus_nexipus_KU211808
Hyloxalus_nexipus_KU211807
Hyloxalus_anthracinus_KU223489
Hyloxalus_jacobuspetersi_QCAZ37742
Hyloxalus_delatorreae_KU220621
Hyloxalus_sylvaticus_KU219756
Hyloxalus_sylvaticus_KU219757
Hyloxalus_pulcherrimus_KU211948
Hyloxalus_pulcherrimus_KU211947
Hyloxalus_vertebralis_QCAZ16554
Hyloxalus_vertebralis_QCAZ16553
Hyloxalus_pulchellus_QCAZ15964
Hyloxalus_sp_SanMiguelDeSalcedo_KU202833
Hyloxalus_delatorreae_KJ940457
Hyloxalus_delatorreae_KU220619
Hyloxalus_sp_MonteOlivo_KU220666
Hyloxalus_pinguis_GAP_195
Hyloxalus_pinguis_MAA1250
Hyloxalus_pinguis_MAA_1249
Hyloxalus_pinguis_MAA_1248
Hyloxalus_lehmanni_MAR2675
Hyloxalus_lehmanni_FC_657
Hyloxalus_lehmanni_FC_656
Hyloxalus_sp_Alban_ANDESA_2923
Hyloxalus_sp_MesasGalilea_MAA_1272
Hyloxalus_sp_MesasGalilea_MAA_1281
Hyloxalus_sp_MesasGalilea_MAA_1283
Hyloxalus_arliensis_TG1959
Hyloxalus_arliensis_ARA2520
Hyloxalus_sp_Caparrapi_RC_1439
Hyloxalus_sp_Caparrapi_RC_1423
Hyloxalus_arliensis_DFZ_413
Hyloxalus_arliensis_MAA_1400B
Hyloxalus_arliensis_MAA_1381
Hyloxalus_arliensis_DFZ_411
Hyloxalus_arliensis_MAR105
Hyloxalus_arliensis_MUJ3564
Hyloxalus_sp_PAV_CORBIDI_11007
Hyloxalus_sp_Bongara_CORBIDI_12891
Hyloxalus_sp_ElCopal_QCAZ16490
Hyloxalus_craspedoceps_Lamas_CORBIDI_6804
Hyloxalus_craspedoceps_MHNSM22882
Hyloxalus_craspedoceps_Chazuta_MNCN47539
Hyloxalus_craspedoceps_Chazuta_MNCN47538
Colostethus_poecilonotus_CORBIDI_1960
Hyloxalus_azureiventris_KS32
Hyloxalus_azureiventris_KS33
Hyloxalus_azureiventris_KS28
Hyloxalus_chlorocraspedus_MPEG13853
Hyloxalus_chlorocraspedus_MPEG12511
Hyloxalus_chlorocraspedus_OMNH36169
Hyloxalus_chlorocraspedus_OMNH36170
Hyloxalus_chlorocraspedus_MPEG12505
Hyloxalus_sp_Masvalle_QCAZ19958
Hyloxalus_sp_Moraspungo_QCAZ21978
Hyloxalus_infrauttatus_QCAZ16516
Hyloxalus_infrauttatus_AGG504
Hyloxalus_toachi_QCAZ16549
Hyloxalus_toachi_QCAZ16548
Hyloxalus_awa_KU220610
Hyloxalus_awa_QCAZ16497
Hyloxalus_awa_QCAZ16502
Hyloxalus_awa_QCAZ16498
Hyloxalus_shuar_CJ2622
Hyloxalus_idiomelus_KU211109
Hyloxalus_idiomelus_KU211885
Hyloxalus_idiomelus_KU211886
Hyloxalus_idiomelus_KU211110
Hyloxalus_idiomelus_KU211908
Hyloxalus_elachyhistus_CORBIDI_4292
Hyloxalus_elachyhistus_KU212507
Hyloxalus_infrauttatus_CORBIDI_3719
Hyloxalus_elachyhistus_QCAZ16518
Hyloxalus_elachyhistus_QCAZ16517
Hyloxalus_elachyhistus_Piura_KU212517
Hyloxalus_elachyhistus_Piura_KU212514
Hyloxalus_elachyhistus_Piura_KU212516
Hyloxalus_elachyhistus_Piura_KU212515
Hyloxalus_littoralis_CORBIDI_13260
Hyloxalus_elachyhistus_CORBIDI_4236
Hyloxalus_elachyhistus_CORBIDI_4234
Hyloxalus_elachyhistus_Piura_KU219749
Hyloxalus_elachyhistus_CORBIDI_4205
Hyloxalus_elachyhistus_CORBIDI_4201
Hyloxalus_elachyhistus_Cajamarca_KU212523
Hyloxalus_elachyhistus_Cajamarca_KU212524
Hyloxalus_elachyhistus_Cajamarca_KU212522
Hyloxalus_insulatus_CORBIDI_1961
Hyloxalus_insulatus_CK_212
Hyloxalus_insulatus_KU211878
Hyloxalus_insulatus_KU211877
Hyloxalus_sp_MNCN_1_MNCN47531
Hyloxalus_insulatus_CORBIDI_5656
Hyloxalus_sp_LaLibertad_CORBIDI_5650
Hyloxalus_littoralis_LIMA
Hyloxalus_littoralis_KST_650
Hyloxalus_sp_CORBIDI_6880
Hyloxalus_sp_Huanuco_CORBIDI_8642
Hyloxalus_sp_Huanuco_CORBIDI_8658
Hyloxalus_sp_Huanuco_CORBIDI_9017
Hyloxalus_littoralis_CORBIDI_16094
Hyloxalus_sp_Huanuco_CORBIDI_13350

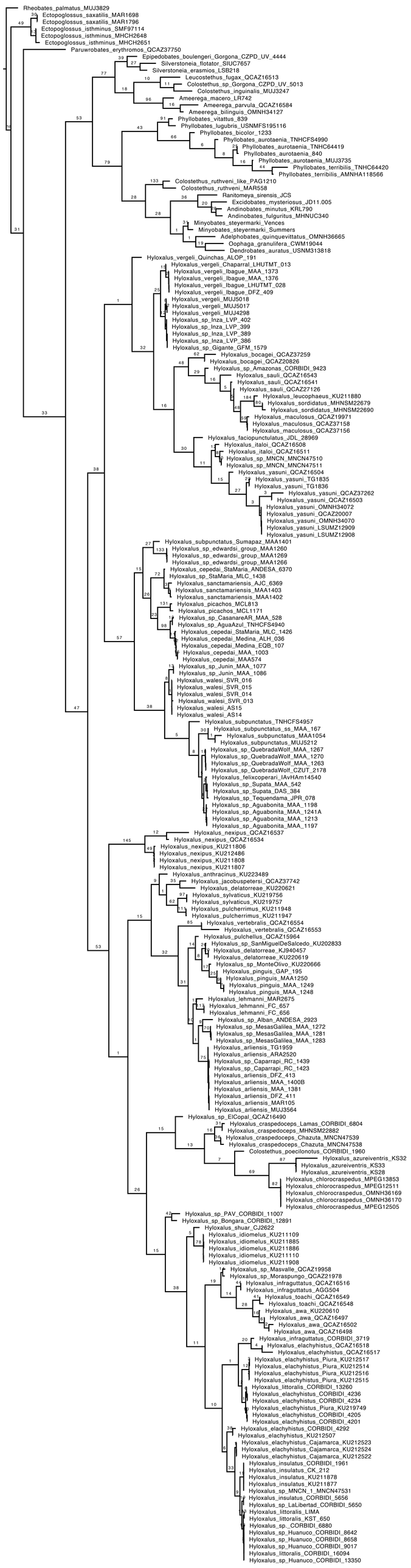
Rheobates_palmatus_MUJ3829
Ectopoglossus_saxatilis_MAR1698
Ectopoglossus_saxatilis_MAR1796
Ectopoglossus_isthminus_SMF97114
Ectopoglossus_isthminus_MHCH2648
Ectopoglossus_isthminus_MHCH2651
Paruwrobates_erythromos_QCAZ37750
Epipedobates_boulengeri_Gorgona_CZPD_UV_4444
Silverstoneia_flotator_SIUC7657
Silverstoneia_erasmios_LSB218
Leucostethus_fugax_QCAZ16513
Colostethus_sp_Gorgona_CZPD_UV_5013
Colostethus_inguinalis_MUJ3247
Ameerega_macero_LR742
Ameerega_parvula_QCAZ16584
Ameerega_bilinguis_OMNH34127
Phyllobates_vittatus_839
Phyllobates_lugubris_USNMFS195116
Phyllobates_bicolor_1233
Phyllobates_aurotaenia_TNHCFS4990
Phyllobates_aurotaenia_TNHC64419
Phyllobates_aurotaenia_840
Phyllobates_aurotaenia_MUJ3735
Phyllobates_terribilis_TNHC64420
Phyllobates_terribilis_AMNHA118566
Colostethus_ruthveni_like_PAG1210
Colostethus_ruthveni_MAR558
Ranitomeya_sirensis_JCS
Excidobates_mysteriosus_JD11.005
Andinobates_minutus_KRL790
Andinobates_fulguritus_MHNUC340
Minyobates_steyermarki_Vences
Minyobates_steyermarki_Summers
Adelphobates_quinquevittatus_OMNH36665
Oophaga_granulifera_CWM19044
Dendrobates_auratus_USNM313818
Hyloxalus_vergeli_Quinchas_ALOP_191
Hyloxalus_vergeli_Chaparral_LHUTMT_013
Hyloxalus_vergeli_Ibague_MAA_1373
Hyloxalus_vergeli_Ibague_MAA_1376
Hyloxalus_vergeli_Ibague_LHUTMT_028
Hyloxalus_vergeli_Ibague_DFZ_409
Hyloxalus_vergeli_MUJ5018
Hyloxalus_vergeli_MUJ5017
Hyloxalus_vergeli_MUJ4298
Hyloxalus_sp_Inza_LVP_402
Hyloxalus_sp_Inza_LVP_399
Hyloxalus_sp_Inza_LVP_389
Hyloxalus_sp_Inza_LVP_386
Hyloxalus_sp_Gigante_GFM_1579
Hyloxalus_bocagei_QCAZ37259
Hyloxalus_bocagei_QCAZ20826
Hyloxalus_sp_Amazonas_CORBIDI_9423
Hyloxalus_sauli_QCAZ16543
Hyloxalus_sauli_QCAZ16541
Hyloxalus_sauli_QCAZ27126
Hyloxalus_leucophaeus_KU211880
Hyloxalus_sordidatus_MHNSM22679
Hyloxalus_sordidatus_MHNSM22690
Hyloxalus_maculosus_QCAZ19971
Hyloxalus_maculosus_QCAZ37158
Hyloxalus_maculosus_QCAZ37156
Hyloxalus_faciopunctulatus_JDL_28969
Hyloxalus_italoi_QCAZ16508
Hyloxalus_italoi_QCAZ16511
Hyloxalus_sp_MNCN_MNCN47510
Hyloxalus_sp_MNCN_MNCN47511
Hyloxalus_yasuni_QCAZ16504
Hyloxalus_yasuni_TG1835
Hyloxalus_yasuni_TG1836
Hyloxalus_yasuni_QCAZ37262
Hyloxalus_yasuni_QCAZ16503
Hyloxalus_yasuni_OMNH34072
Hyloxalus_yasuni_QCAZ20007
Hyloxalus_yasuni_OMNH34070
Hyloxalus_yasuni_LSUMZ12909
Hyloxalus_yasuni_LSUMZ12908
Hyloxalus_subpunctatus_Sumapaz_MAA1401
Hyloxalus_sp_edwardsi_group_MAA1260
Hyloxalus_sp_edwardsi_group_MAA1269
Hyloxalus_sp_edwardsi_group_MAA1266
Hyloxalus_cepedai_StaMaria_ANDESA_6370
Hyloxalus_sp_StaMaria_MLC_1438
Hyloxalus_sanctamariensis_AJC_6369
Hyloxalus_sanctamariensis_MAA1403
Hyloxalus_sanctamariensis_MAA1402
Hyloxalus_picachos_MCL813
Hyloxalus_picachos_MCL1171
Hyloxalus_sp_CasanareAR_MAA_528
Hyloxalus_sp_AguaAzul_TNHCFS4940
Hyloxalus_cepedai_StaMaria_MLC_1426
Hyloxalus_cepedai_Medina_ALH_036
Hyloxalus_cepedai_Medina_EQB_107
Hyloxalus_cepedai_MAA_1003
Hyloxalus_cepedai_MAA574
Hyloxalus_sp_Junin_MAA_1077
Hyloxalus_sp_Junin_MAA_1086
Hyloxalus_walesi_SVR_016
Hyloxalus_walesi_SVR_015
Hyloxalus_walesi_SVR_014
Hyloxalus_walesi_SVR_013
Hyloxalus_walesi_AS15
Hyloxalus_walesi_AS14
Hyloxalus_subpunctatus_TNHCFS4957
Hyloxalus_subpunctatus_ss_MAA_167
Hyloxalus_subpunctatus_MAA1054
Hyloxalus_subpunctatus_MUJ5212
Hyloxalus_sp_QuebradaWolf_MAA_1267
Hyloxalus_sp_QuebradaWolf_MAA_1270
Hyloxalus_sp_QuebradaWolf_MAA_1263
Hyloxalus_sp_QuebradaWolf_CZUT_2178
Hyloxalus_felixcoperari_IAvHAm14540
Hyloxalus_sp_Supata_MAA_542
Hyloxalus_sp_Supata_DAS_384
Hyloxalus_sp_Tequendama_JPR_078
Hyloxalus_sp_Aguabonita_MAA_1198
Hyloxalus_sp_Aguabonita_MAA_1241A
Hyloxalus_sp_Aguabonita_MAA_1213
Hyloxalus_sp_Aguabonita_MAA_1197
Hyloxalus_nexipus_QCAZ16537
Hyloxalus_nexipus_QCAZ16534
Hyloxalus_nexipus_KU211806
Hyloxalus_nexipus_KU212486
Hyloxalus_nexipus_KU211808
Hyloxalus_nexipus_KU211807
Hyloxalus_anthracinus_KU223489
Hyloxalus_jacobuspetersi_QCAZ37742
Hyloxalus_delatorreae_KU220621
Hyloxalus_sylvaticus_KU219756
Hyloxalus_sylvaticus_KU219757
Hyloxalus_pulcherrimus_KU211948
Hyloxalus_pulcherrimus_KU211947
Hyloxalus_vertebralis_QCAZ16554
Hyloxalus_vertebralis_QCAZ16553
Hyloxalus_pulchellus_QCAZ15964
Hyloxalus_sp_SanMiguelDeSalcedo_KU202833
Hyloxalus_delatorreae_KJ940457
Hyloxalus_delatorreae_KU220619
Hyloxalus_sp_MonteOlivo_KU220666
Hyloxalus_pinguis_GAP_195
Hyloxalus_pinguis_MAA1250
Hyloxalus_pinguis_MAA_1249
Hyloxalus_pinguis_MAA_1248
Hyloxalus_lehmanni_MAR2675
Hyloxalus_lehmanni_FC_657
Hyloxalus_lehmanni_FC_656
Hyloxalus_sp_Alban_ANDESA_2923
Hyloxalus_sp_MesasGalilea_MAA_1272
Hyloxalus_sp_MesasGalilea_MAA_1281
Hyloxalus_sp_MesasGalilea_MAA_1283
Hyloxalus_arliensis_TG1959
Hyloxalus_arliensis_ARA2520
Hyloxalus_sp_Caparrapi_RC_1439
Hyloxalus_sp_Caparrapi_RC_1423
Hyloxalus_arliensis_DFZ_413
Hyloxalus_arliensis_MAA_1400B
Hyloxalus_arliensis_MAA_1381
Hyloxalus_arliensis_DFZ_411
Hyloxalus_arliensis_MAR105
Hyloxalus_arliensis_MUJ3564
Hyloxalus_sp_ElCopal_QCAZ16490
Hyloxalus_craspedoceps_Lamas_CORBIDI_6804
Hyloxalus_craspedoceps_MHNSM22882
Hyloxalus_craspedoceps_Chazuta_MNCN47539
Hyloxalus_craspedoceps_Chazuta_MNCN47538
Colostethus_poecilonotus_CORBIDI_1960
Hyloxalus_azureiventris_KS32
Hyloxalus_azureiventris_KS33
Hyloxalus_azureiventris_KS28
Hyloxalus_chlorocraspedus_MPEG13853
Hyloxalus_chlorocraspedus_MPEG12511
Hyloxalus_chlorocraspedus_OMNH36169
Hyloxalus_chlorocraspedus_OMNH36170
Hyloxalus_chlorocraspedus_MPEG12505
Hyloxalus_sp_PAV_CORBIDI_11007
Hyloxalus_sp_Bongara_CORBIDI_12891
Hyloxalus_shuar_CJ2622
Hyloxalus_idiomelus_KU211109
Hyloxalus_idiomelus_KU211885
Hyloxalus_idiomelus_KU211886
Hyloxalus_idiomelus_KU211110
Hyloxalus_idiomelus_KU211908
Hyloxalus_sp_Masvalle_QCAZ19958
Hyloxalus_sp_Morasputungo_QCAZ21978
Hyloxalus_infraguttatus_QCAZ16516
Hyloxalus_infraguttatus_AGG504
Hyloxalus_toachi_QCAZ16549
Hyloxalus_toachi_QCAZ16548
Hyloxalus_awa_KU220610
Hyloxalus_awa_QCAZ16497
Hyloxalus_awa_QCAZ16502
Hyloxalus_awa_QCAZ16498
Hyloxalus_infraguttatus_CORBIDI_3719
Hyloxalus_elachyhistus_QCAZ16518
Hyloxalus_elachyhistus_QCAZ16517
Hyloxalus_elachyhistus_Piura_KU212517
Hyloxalus_elachyhistus_Piura_KU212514
Hyloxalus_elachyhistus_Piura_KU212516
Hyloxalus_elachyhistus_Piura_KU212515
Hyloxalus_littoralis_CORBIDI_13260
Hyloxalus_elachyhistus_CORBIDI_4236
Hyloxalus_elachyhistus_CORBIDI_4234
Hyloxalus_elachyhistus_Piura_KU219749
Hyloxalus_elachyhistus_CORBIDI_4205
Hyloxalus_elachyhistus_CORBIDI_4201
Hyloxalus_elachyhistus_CORBIDI_4292
Hyloxalus_elachyhistus_KU212507
Hyloxalus_elachyhistus_Cajamarca_KU212523
Hyloxalus_elachyhistus_Cajamarca_KU212524
Hyloxalus_elachyhistus_Cajamarca_KU212522
Hyloxalus_insulatus_CORBIDI_1961
Hyloxalus_insulatus_CK_212
Hyloxalus_insulatus_KU211878
Hyloxalus_insulatus_KU211877
Hyloxalus_sp_MNCN_1_MNCN47531
Hyloxalus_insulatus_CORBIDI_5656
Hyloxalus_sp_LaLibertad_CORBIDI_5650
Hyloxalus_littoralis_LIMA
Hyloxalus_littoralis_KST_650
Hyloxalus_sp._CORBIDI_6880
Hyloxalus_sp_Huanuco_CORBIDI_8642
Hyloxalus_sp_Huanuco_CORBIDI_8658
Hyloxalus_sp_Huanuco_CORBIDI_9017
Hyloxalus_littoralis_CORBIDI_16094
Hyloxalus_sp_Huanuco_CORBIDI_13350

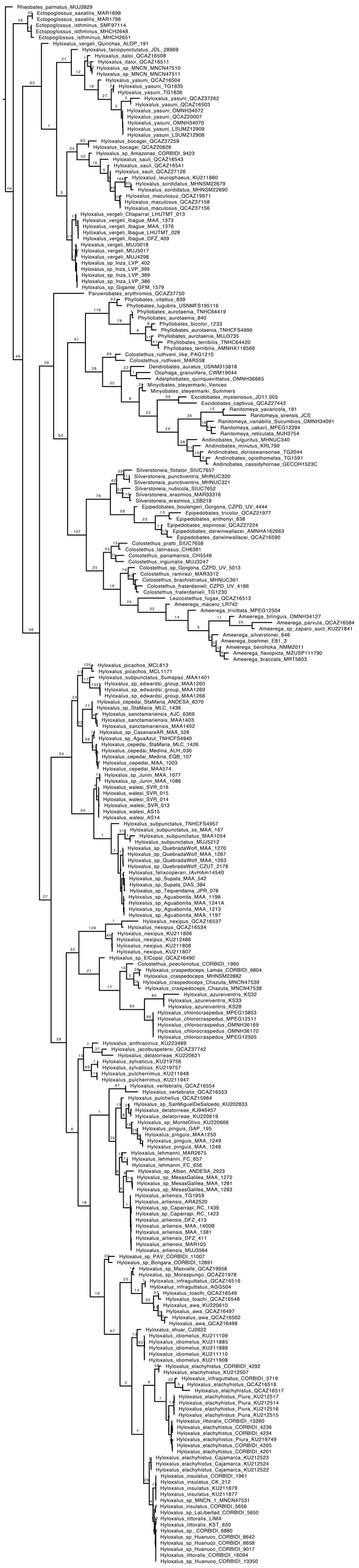
Rheobates_palmatus_MUJ3829
Ectopoglossus_saxatilis_MAR1698
Ectopoglossus_saxatilis_MAR1796
Ectopoglossus_isthminus_SMF97114
Ectopoglossus_isthminus_MHCH2648
Ectopoglossus_isthminus_MHCH2651
Hyloxalus_vergeli_Quinchas_ALOP_191
Hyloxalus_faciopunctulatus_JDL_28969
Hyloxalus_italoi_QCAZ16508
Hyloxalus_italoi_QCAZ16511
Hyloxalus_sp_MNCN_MNCN47510
Hyloxalus_sp_MNCN_MNCN47511
Hyloxalus_yasuni_QCAZ16504
Hyloxalus_yasuni_TG1835
Hyloxalus_yasuni_TG1836
Hyloxalus_yasuni_QCAZ37262
Hyloxalus_yasuni_QCAZ16503
Hyloxalus_yasuni_OMNH34072
Hyloxalus_yasuni_QCAZ20007
Hyloxalus_yasuni_OMNH34070
Hyloxalus_yasuni_LSUMZ12909
Hyloxalus_yasuni_LSUMZ12908
Hyloxalus_bocagei_QCAZ37259
Hyloxalus_bocagei_QCAZ20826
Hyloxalus_sp_Amazonas_CORBIDI_9423
Hyloxalus_sauli_QCAZ16543
Hyloxalus_sauli_QCAZ16541
Hyloxalus_sauli_QCAZ27126
Hyloxalus_leucophaeus_KU211880
Hyloxalus_sordidatus_MHNSM22679
Hyloxalus_sordidatus_MHNSM22690
Hyloxalus_maculosus_QCAZ19971
Hyloxalus_maculosus_QCAZ37158
Hyloxalus_maculosus_QCAZ37156
Hyloxalus_vergeli_Chaparral_LHUTMT_013
Hyloxalus_vergeli_Ibague_MAA_1373
Hyloxalus_vergeli_Ibague_MAA_1376
Hyloxalus_vergeli_Ibague_LHUTMT_028
Hyloxalus_vergeli_Ibague_DFZ_409
Hyloxalus_vergeli_MUJ5018
Hyloxalus_vergeli_MUJ5017
Hyloxalus_vergeli_MUJ4298
Hyloxalus_sp_Inza_LVP_402
Hyloxalus_sp_Inza_LVP_399
Hyloxalus_sp_Inza_LVP_389
Hyloxalus_sp_Inza_LVP_386
Hyloxalus_sp_Gigante_GFM_1579
Paruwrobates_erythromos_QCAZ37750
Phyllobates_vittatus_839
Phyllobates_lugubris_USNMFS195116
Phyllobates_aurotaenia_TNHC64419
Phyllobates_aurotaenia_840
Phyllobates_bicolor_1233
Phyllobates_aurotaenia_TNHCFS4990
Phyllobates_aurotaenia_MUJ3735
Phyllobates_terribilis_TNHC64420
Phyllobates_terribilis_AMNHA118566
Colostethus_ruthveni_like_PAG1210
Colostethus_ruthveni_MAR558
Dendrobates_auratus_USNM313818
Oophaga_granulifera_CWM19044
Adelphobates_quinquevittatus_OMNH36665
Minyobates_steyermarki_Vences
Minyobates_steyermarki_Summers
Excidobates_mysteriosus_JD11.005
Excidobates_captivus_QCAZ27442
Ranitomeya_yavaricola_181
Ranitomeya_sirensis_JCS
Ranitomeya_variabilis_Sucumbios_OMNH34091
Ranitomeya_uakarii_MPEG12394
Ranitomeya_reticulata_MJH3754
Andinobates_fulguritus_MHNUC340
Andinobates_minutus_KRL790
Andinobates_dorisswansonae_TG2044
Andinobates_opisthomelas_TG1591
Andinobates_cassidyhornae_GECOH1523C
Silverstoneia_flotator_SIUC7657
Silverstoneia_punctiventris_MHNUC320
Silverstoneia_punctiventris_MHNUC321
Silverstoneia_nubicola_SIUC7652
Silverstoneia_erasmios_MAR33316
Silverstoneia_erasmios_LSB218
Epipedobates_boulengeri_Gorgona_CZPD_UV_4444
Epipedobates_tricolor_QCAZ21977
Epipedobates_anthonyi_838
Epipedobates_espinosai_QCAZ27224
Epipedobates_darwinwallacei_AMNHA162663
Epipedobates_darwinwallacei_QCAZ16590
Colostethus_pratti_SIUC7658
Colostethus_latinasus_CH6381
Colostethus_panamansis_CH5546
Colostethus_inguinalis_MUJ3247
Colostethus_sp_Gorgona_CZPD_UV_5013
Colostethus_ramirezi_MAR3312
Colostethus_brachistriatus_MHNUC361
Colostethus_fraterdanieli_CZPD_UV_4186
Colostethus_fraterdanieli_TG1230
Leucostethus_fugax_QCAZ16513
Ameerega_macero_LR742
Ameerega_trivittata_MPEG12504
Ameerega_bilinguis_OMNH34127
Ameerega_parvula_QCAZ16584
Ameerega_sp_zaparo_auct_KU221841
Ameerega_silverstonei_646
Ameerega_boehmei_E81_3
Ameerega_berohoka_NMM2011
Ameerega_flavopicta_MZUSP111790
Ameerega_braccata_MRT5603
Hyloxalus_picachos_MCL813
Hyloxalus_picachos_MCL1171
Hyloxalus_subpunctatus_Sumapaz_MAA1401
Hyloxalus_sp_edwardsi_group_MAA1260
Hyloxalus_sp_edwardsi_group_MAA1269
Hyloxalus_sp_edwardsi_group_MAA1266
Hyloxalus_cepedai_StaMaria_ANDESA_6370
Hyloxalus_sp_StaMaria_MLC_1438
Hyloxalus_sanctamariensis_AJC_6369
Hyloxalus_sanctamariensis_MAA1403
Hyloxalus_sanctamariensis_MAA1402
Hyloxalus_sp_CasanareAR_MAA_528
Hyloxalus_sp_AguaAzul_TNHCFS4940
Hyloxalus_cepedai_StaMaria_MLC_1426
Hyloxalus_cepedai_Medina_ALH_036
Hyloxalus_cepedai_Medina_EOB_107
Hyloxalus_cepedai_MAA_1003
Hyloxalus_cepedai_MAA574
Hyloxalus_sp_Junin_MAA_1077
Hyloxalus_sp_Junin_MAA_1086
Hyloxalus_walesi_SVR_016
Hyloxalus_walesi_SVR_015
Hyloxalus_walesi_SVR_014
Hyloxalus_walesi_SVR_013
Hyloxalus_walesi_AS15
Hyloxalus_walesi_AS14
Hyloxalus_subpunctatus_TNHCFS4957
Hyloxalus_subpunctatus_ss_MAA_167
Hyloxalus_subpunctatus_MAA1054
Hyloxalus_subpunctatus_MUJ5212
Hyloxalus_sp_QuebradaWolf_MAA_1270
Hyloxalus_sp_QuebradaWolf_MAA_1267
Hyloxalus_sp_QuebradaWolf_MAA_1263
Hyloxalus_sp_QuebradaWolf_CZUT_2178
Hyloxalus_felixcoperari_IAvHAm14540
Hyloxalus_sp_Supata_MAA_542
Hyloxalus_sp_Supata_DAS_384
Hyloxalus_sp_Tequendama_JPR_078
Hyloxalus_sp_Aguabonita_MAA_1198
Hyloxalus_sp_Aguabonita_MAA_1241A
Hyloxalus_sp_Aguabonita_MAA_1213
Hyloxalus_sp_Aguabonita_MAA_1197
Hyloxalus_nexipus_QCAZ16537
Hyloxalus_nexipus_QCAZ16534
Hyloxalus_nexipus_KU211806
Hyloxalus_nexipus_KU212486
Hyloxalus_nexipus_KU211808
Hyloxalus_nexipus_KU211807
Hyloxalus_sp_ElCopal_QCAZ16490
Colostethus_poecilonotus_CORBIDI_1960
Hyloxalus_craspedocoeps_Lamas_CORBIDI_6804
Hyloxalus_craspedocoeps_MHNSM22882
Hyloxalus_craspedocoeps_Chazuta_MNCN47539
Hyloxalus_craspedocoeps_Chazuta_MNCN47538
Hyloxalus_azureiventris_KS32
Hyloxalus_azureiventris_KS33
Hyloxalus_azureiventris_KS28
Hyloxalus_chlorocraspedus_MPEG13853
Hyloxalus_chlorocraspedus_MPEG12511
Hyloxalus_chlorocraspedus_OMNH36169
Hyloxalus_chlorocraspedus_OMNH36170
Hyloxalus_chlorocraspedus_MPEG12505
Hyloxalus_anthracinus_KU223489
Hyloxalus_jacobuspeterseni_QCAZ37742
Hyloxalus_delatorreae_KU220621
Hyloxalus_sylvaticus_KU219756
Hyloxalus_sylvaticus_KU219757
Hyloxalus_pulcherrimus_KU211948
Hyloxalus_pulcherrimus_KU211947
Hyloxalus_vertebralis_QCAZ16554
Hyloxalus_vertebralis_QCAZ16553
Hyloxalus_pulchellus_QCAZ15964
Hyloxalus_sp_SanMiguelDeSalcedo_KU202833
Hyloxalus_delatorreae_KJ940457
Hyloxalus_delatorreae_KU220619
Hyloxalus_sp_MonteOlivo_KU220666
Hyloxalus_pinguis_GAP_195
Hyloxalus_pinguis_MAA1250
Hyloxalus_pinguis_MAA_1249
Hyloxalus_pinguis_MAA_1248
Hyloxalus_lehmanni_MAR2675
Hyloxalus_lehmanni_FC_657
Hyloxalus_lehmanni_FC_656
Hyloxalus_sp_Alban_ANDESA_2923
Hyloxalus_sp_MesasGalilea_MAA_1272
Hyloxalus_sp_MesasGalilea_MAA_1281
Hyloxalus_sp_MesasGalilea_MAA_1283
Hyloxalus_arliensis_TG1959
Hyloxalus_arliensis_ARA2520
Hyloxalus_sp_Caparrapi_RC_1439
Hyloxalus_sp_Caparrapi_RC_1423
Hyloxalus_arliensis_DFZ_413
Hyloxalus_arliensis_MAA_1400B
Hyloxalus_arliensis_MAA_1381
Hyloxalus_arliensis_DFZ_411
Hyloxalus_arliensis_MAR105
Hyloxalus_arliensis_MUJ3564
Hyloxalus_sp_PAV_CORBIDI_11007
Hyloxalus_sp_Bongara_CORBIDI_12891
Hyloxalus_sp_Masvalle_QCAZ19958
Hyloxalus_sp_Moraspungo_QCAZ21978
Hyloxalus_infraguttatus_QCAZ16516
Hyloxalus_infraguttatus_AGG504
Hyloxalus_toachi_QCAZ16549
Hyloxalus_toachi_QCAZ16548
Hyloxalus_awa_KU220610
Hyloxalus_awa_QCAZ16497
Hyloxalus_awa_QCAZ16502
Hyloxalus_awa_QCAZ16498
Hyloxalus_shuar_CJ2622
Hyloxalus_idiomelus_KU211109
Hyloxalus_idiomelus_KU211885
Hyloxalus_idiomelus_KU211886
Hyloxalus_idiomelus_KU211110
Hyloxalus_idiomelus_KU211908
Hyloxalus_elachyhistus_CORBIDI_4292
Hyloxalus_elachyhistus_KU212507
Hyloxalus_infraguttatus_CORBIDI_3719
Hyloxalus_elachyhistus_QCAZ16518
Hyloxalus_elachyhistus_QCAZ16517
Hyloxalus_elachyhistus_Piura_KU212517
Hyloxalus_elachyhistus_Piura_KU212514
Hyloxalus_elachyhistus_Piura_KU212516
Hyloxalus_elachyhistus_Piura_KU212515
Hyloxalus_littoralis_CORBIDI_13260
Hyloxalus_elachyhistus_CORBIDI_4236
Hyloxalus_elachyhistus_CORBIDI_4234
Hyloxalus_elachyhistus_Piura_KU219749
Hyloxalus_elachyhistus_CORBIDI_4205
Hyloxalus_elachyhistus_CORBIDI_4201
Hyloxalus_elachyhistus_Cajamarca_KU212523
Hyloxalus_elachyhistus_Cajamarca_KU212524
Hyloxalus_elachyhistus_Cajamarca_KU212522
Hyloxalus_insulatus_CORBIDI_1961
Hyloxalus_insulatus_CK_212
Hyloxalus_insulatus_KU211878
Hyloxalus_insulatus_KU211877
Hyloxalus_sp_MNCN_1_MNCN47531
Hyloxalus_insulatus_CORBIDI_5656
Hyloxalus_sp_LaLibertad_CORBIDI_5650
Hyloxalus_littoralis_LIMA
Hyloxalus_littoralis_KST_650
Hyloxalus_sp_CORBIDI_6880
Hyloxalus_sp_Huanuco_CORBIDI_8642
Hyloxalus_sp_Huanuco_CORBIDI_8658
Hyloxalus_sp_Huanuco_CORBIDI_9017
Hyloxalus_littoralis_CORBIDI_16094
Hyloxalus_sp_Huanuco_CORBIDI_13350


Boana_boans_RWM117746
Thoropa_taophora_CFBH3239
Melanophryniscus_setiba_CFBH15748
Crossodactylus_schmidti_MLPA1414
Allobates_olfersioides_MNRJ79897
Rheobates_palmatus_MUJ3829
Anomaloglossus_tamacuarensis_MNRJ38049
Anomaloglossus_degranvillei_Vences
Paruwrobates_erythromos_QCAZ37750
Ectopoglossus_saxatilis_MAR1698
Ectopoglossus_saxatilis_MAR1796
Ectopoglossus_isthminus_SMF97114
Ectopoglossus_isthminus_MHCH2648
Ectopoglossus_isthminus_MHCH2651
Phyllobates_vitattus_839
Phyllobates_lugubris_USNMFS195116
Phyllobates_bicolor_1233
Phyllobates_aurotaenia_TNHCFS4990
Phyllobates_aurotaenia_TNHC64419
Phyllobates_aurotaenia_840
Phyllobates_aurotaenia_MUJ3735
Phyllobates_terribilis_TNHC64420
Phyllobates_terribilis_AMNH118566
Colostethus_ruthveni_like_PAG1210
Colostethus_ruthveni_MAR558
Dendrobates_auratus_USNM313818
Oophaga_granulifera_CWM19044
Adelphobates_quinquevittatus_OMNH36665
Minyobates_steyermarki_Vences
Minyobates_steyermarki_Summers
Excidobates_mysteriosus_JD11.005
Excidobates_captivus_QCAZ27442
Ranitomeya_yavaricola_181
Ranitomeya_sirensis_JCS
Ranitomeya_variabilis_Sucumbios_OMNH34091
Ranitomeya_uakarii_MPEG12394
Ranitomeya_reticulata_MJH3754
Andinobates_fulguritus_MHNUC340
Andinobates_minutus_KRL790
Andinobates_dorisswansonae_TG2044
Andinobates_opisthomelas_TG1591
Andinobates_cassidyhornae_GECOH1523C
Silverstoneia_flotator_SIUC7657
Silverstoneia_punctiventris_MHNUC320
Silverstoneia_punctiventris_MHNUC321
Silverstoneia_nubicola_SIUC7652
Silverstoneia_erasmios_MAR33316
Silverstoneia_erasmios_LSB218
Epipedobates_boulengeri_Gorgona_CZPD_UV_4444
Epipedobates_tricolor_QCAZ21977
Epipedobates_anthonyi_838
Epipedobates_espinosai_QCAZ27224
Epipedobates_darwinwallacei_AMNHA162663
Epipedobates_darwinwallacei_QCAZ16590
Colostethus_pratti_SIUC7658
Colostethus_latinasus_CH6381
Colostethus_panamansis_CH5546
Colostethus_inguinalis_MUJ3247
Ameerega_macero_LR742
Ameerega_silverstonei_646
Ameerega_bilinguis_OMNH34127
Ameerega_parvula_QCAZ16584
Ameerega_sp_zaparo_auct_KU221841
Ameerega_trivittata_MPEG12504
Ameerega_boehmei_E81_3
Ameerega_berohoka_NMM2011
Ameerega_flavopicta_MZUSP111790
Ameerega_braccata_MRT5603
Leucostethus_fugax_QCAZ16513
Leucostethus_argyrogaster_MHNSM22877
Leucostethus_jota_MHUAA9244
Colostethus_sp_Gorgona_CZPD_UV_5013
Leucostethus_bilsa_CJ7213
Leucostethus_fraterdanieli_MHUAA8082
Colostethus_ramirezi_MAR3312
Colostethus_fraterdanieli_CZPD_UV_4186
Colostethus_fraterdanieli_TG1230
Colostethus_brachistriatus_TNHCFS4977
Colostethus_brachistriatus_MHNUC361
Hyloxalus_vergeli_Quinchas_ALOP_191
Hyloxalus_bocagei_QCAZ37259
Hyloxalus_bocagei_QCAZ20826
Hyloxalus_sp_Amazonas_CORBIDI_9423
Hyloxalus_sauli_QCAZ16543
Hyloxalus_sauli_QCAZ16541
Hyloxalus_sauli_QCAZ27126
Hyloxalus_leucophaeus_KU211880
Hyloxalus_sordidatus_MHNSM22679
Hyloxalus_sordidatus_MHNSM22690
Hyloxalus_maculosus_QCAZ19971
Hyloxalus_maculosus_QCAZ37158
Hyloxalus_maculosus_QCAZ37156
Hyloxalus_vergeli_Chaparral_LHUTMT_013
Hyloxalus_vergeli_Ibague_MAA_1373
Hyloxalus_vergeli_Ibague_MAA_1376
Hyloxalus_vergeli_Ibague_LHUTMT_028
Hyloxalus_vergeli_Ibague_DFZ_409
Hyloxalus_vergeli_MUJ5018
Hyloxalus_vergeli_MUJ5017
Hyloxalus_vergeli_MUJ4298
Hyloxalus_sp_Inza_LVP_402
Hyloxalus_sp_Inza_LVP_389
Hyloxalus_sp_Inza_LVP_389
Hyloxalus_sp_Inza_LVP_386
Hyloxalus_sp_Gigante_GFM_1579
Hyloxalus_faciopunctulatus_JDL_28969
Hyloxalus_italoi_QCAZ16508
Hyloxalus_italoi_QCAZ16511
Hyloxalus_sp_MNCN_MNCN47510
Hyloxalus_sp_MNCN_MNCN47511
Hyloxalus_yasuni_QCAZ16504
Hyloxalus_yasuni_TG1835
Hyloxalus_yasuni_TG1836
Hyloxalus_yasuni_QCAZ37262
Hyloxalus_yasuni_QCAZ16503
Hyloxalus_yasuni_OMNH34072
Hyloxalus_yasuni_QCAZ20007
Hyloxalus_yasuni_OMNH34070
Hyloxalus_yasuni_LSUMZ12909
Hyloxalus_yasuni_LSUMZ12908
Hyloxalus_subpunctatus_Sumapaz_MAA1401
Hyloxalus_sp_edwardsi_group_MAA1260
Hyloxalus_sp_edwardsi_group_MAA1269
Hyloxalus_sp_edwardsi_group_MAA1266
Hyloxalus_cepedai_StaMaria_ANDESA_6370
Hyloxalus_sp_StaMaria_MLC_1438
Hyloxalus_sanctamariensis_AJC_6369
Hyloxalus_sanctamariensis_MAA1403
Hyloxalus_sanctamariensis_MAA1402
Hyloxalus_picachos_MCL813
Hyloxalus_picachos_MCL1171
Hyloxalus_sp_CasanareAR_MAA_528
Hyloxalus_sp_AguaAzul_TNHCFS4940
Hyloxalus_cepedai_StaMaria_MLC_1426
Hyloxalus_cepedai_Medina_ALH_036
Hyloxalus_cepedai_Medina_EQB_107
Hyloxalus_cepedai_MAA_1003
Hyloxalus_cepedai_MAA574
Hyloxalus_sp_Junin_MAA_1077
Hyloxalus_sp_Junin_MAA_1086
Hyloxalus_walesi_SVR_016
Hyloxalus_walesi_SVR_015
Hyloxalus_walesi_SVR_014
Hyloxalus_walesi_SVR_013
Hyloxalus_walesi_AS15
Hyloxalus_walesi_AS14
Hyloxalus_subpunctatus_TNHCFS4957
Hyloxalus_subpunctatus_ss_MAA_167
Hyloxalus_subpunctatus_MAA1054
Hyloxalus_subpunctatus_MUJ5212
Hyloxalus_sp_QuebradaWolf_MAA_1270
Hyloxalus_sp_QuebradaWolf_MAA_1267
Hyloxalus_sp_QuebradaWolf_MAA_1263
Hyloxalus_sp_QuebradaWolf_CZUT_2178
Hyloxalus_felixcoperari_IAvHAm14540
Hyloxalus_sp_Supata_MAA_542
Hyloxalus_sp_Supata_DAS_384
Hyloxalus_sp_Tequendama_JPR_078
Hyloxalus_sp_Aguabonita_MAA_1198
Hyloxalus_sp_Aguabonita_MAA_1241A
Hyloxalus_sp_Aguabonita_MAA_1213
Hyloxalus_sp_Aguabonita_MAA_1197
Hyloxalus_sylvaticus_KU219756
Hyloxalus_sylvaticus_KU219757
Hyloxalus_pulcherrimus_KU211948
Hyloxalus_pulcherrimus_KU211947
Hyloxalus_anthracinus_KU223489
Hyloxalus_jacobuspetersi_QCAZ37742
Hyloxalus_delatorreae_KU220621
Hyloxalus_vertebralis_QCAZ16554
Hyloxalus_vertebralis_QCAZ16553
Hyloxalus_pulchellus_QCAZ15964
Hyloxalus_sp_SanMiguelDeSalcedo_KU202833
Hyloxalus_delatorreae_KJ940457
Hyloxalus_delatorreae_KU220619
Hyloxalus_sp_MonteOlivo_KU220666
Hyloxalus_pinguis_GAP_195
Hyloxalus_pinguis_MAA1250
Hyloxalus_pinguis_MAA_1249
Hyloxalus_pinguis_MAA_1248
Hyloxalus_lehmanni_MAR2675
Hyloxalus_lehmanni_FC_657
Hyloxalus_lehmanni_FC_656
Hyloxalus_sp_Alban_ANDESA_2923
Hyloxalus_sp_MesasGalilea_MAA_1272
Hyloxalus_sp_MesasGalilea_MAA_1281
Hyloxalus_sp_MesasGalilea_MAA_1283
Hyloxalus_arliensis_TG1959
Hyloxalus_arliensis_ARA2520
Hyloxalus_sp_Caparrapi_RC_1439
Hyloxalus_sp_Caparrapi_RC_1423
Hyloxalus_arliensis_DFZ_413
Hyloxalus_arliensis_MAA_1400B
Hyloxalus_arliensis_MAA_1381
Hyloxalus_arliensis_DFZ_411
Hyloxalus_arliensis_MAR105
Hyloxalus_arliensis_MUJ3564
Hyloxalus_sp_PAV_CORBIDI_11007
Hyloxalus_sp_Bongara_CORBIDI_12891
Hyloxalus_nexipus_QCAZ16537
Hyloxalus_nexipus_QCAZ16534
Hyloxalus_nexipus_KU211806
Hyloxalus_nexipus_KU212486
Hyloxalus_nexipus_KU211808
Hyloxalus_nexipus_KU211807
Colostethus_poecilonotus_CORBIDI_1960
Hyloxalus_craspedocoeps_Lamas_CORBIDI_6804
Hyloxalus_craspedocoeps_MHNSM22882
Hyloxalus_craspedocoeps_Chazuta_MNCN47539
Hyloxalus_craspedocoeps_Chazuta_MNCN47538
Hyloxalus_azureiventris_KS32
Hyloxalus_azureiventris_KS33
Hyloxalus_azureiventris_KS28
Hyloxalus_chlorocraspedus_MPEG13853
Hyloxalus_chlorocraspedus_MPEG12511
Hyloxalus_chlorocraspedus_OMNH36169
Hyloxalus_chlorocraspedus_OMNH36170
Hyloxalus_chlorocraspedus_MPEG12505
Hyloxalus_sp_ElCopal_QCAZ16490
Hyloxalus_shuar_CJ2622
Hyloxalus_idiomelus_KU211109
Hyloxalus_idiomelus_KU211885
Hyloxalus_idiomelus_KU211886
Hyloxalus_idiomelus_KU211110
Hyloxalus_idiomelus_KU211908
Hyloxalus_sp_Masvalle_QCAZ19958
Hyloxalus_sp_Moraspungo_QCAZ21978
Hyloxalus_infragguttatus_QCAZ16516
Hyloxalus_infragguttatus_AGG504
Hyloxalus_toachi_QCAZ16549
Hyloxalus_toachi_QCAZ16548
Hyloxalus_awa_KU220610
Hyloxalus_awa_QCAZ16497
Hyloxalus_awa_QCAZ16502
Hyloxalus_awa_QCAZ16498
Hyloxalus_infragguttatus_CORBIDI_3719
Hyloxalus_elachyhistus_QCAZ16518
Hyloxalus_elachyhistus_QCAZ16517
Hyloxalus_elachyhistus_Piura_KU212517
Hyloxalus_elachyhistus_Piura_KU212514
Hyloxalus_elachyhistus_Piura_KU212516
Hyloxalus_elachyhistus_Piura_KU212515
Hyloxalus_littoralis_CORBIDI_13260
Hyloxalus_elachyhistus_CORBIDI_4236
Hyloxalus_elachyhistus_CORBIDI_4234
Hyloxalus_elachyhistus_Piura_KU219749
Hyloxalus_elachyhistus_CORBIDI_4205
Hyloxalus_elachyhistus_CORBIDI_4201
Hyloxalus_elachyhistus_CORBIDI_4292
Hyloxalus_elachyhistus_KU212507
Hyloxalus_elachyhistus_Cajamarca_KU212523
Hyloxalus_elachyhistus_Cajamarca_KU212524
Hyloxalus_elachyhistus_Cajamarca_KU212522
Hyloxalus_insulatus_CORBIDI_1961
Hyloxalus_insulatus_CK_212
Hyloxalus_insulatus_KU211878
Hyloxalus_insulatus_KU211877
Hyloxalus_sp_MNCN_1_MNCN47531
Hyloxalus_insulatus_CORBIDI_5656
Hyloxalus_sp_LaLibertad_CORBIDI_5650
Hyloxalus_littoralis_LIMA
Hyloxalus_littoralis_KST_650
Hyloxalus_sp_CORBIDI_6880
Hyloxalus_sp_Huanuco_CORBIDI_8642
Hyloxalus_sp_Huanuco_CORBIDI_8658
Hyloxalus_sp_Huanuco_CORBIDI_9017
Hyloxalus_littoralis_CORBIDI_16094
Hyloxalus_sp_Huanuco_CORBIDI_13350


Boana_boans_RWM17746
Melanophryniscus_setiba_CFBH15748
Thoropa_taophora_CFBH3239
Crossodactylus_schmidti_MLPA1414
Rheobates_palmatus_MUJ3829
Anomaloglossus_tamacuarensis_MNRJ38049
Anomaloglossus_degranvillei_Vences
Aromobates_ornatissimus_WES626
Aromobates_nocturnus_AMNHA130041
Mannophryne_herminae_TNHCFS5676
Mannophryne_leonardoi_WES1034
Mannophryne_leonardoi_TNHCFS5659
Allobates_olfersioides_MNRJ79897
Allobates_undulatus_AMNHA159139
Allobates_talamancae_QCAZ16551
Allobates_talamancae_OMNH33237
Allobates_juanii_TNHCFS4978
Allobates_juanii_ARA2394
Silverstoneia_nubicola_SIUC7652
Silverstoneia_erasmios_MAR33316
Silverstoneia_erasmios_LSB218
Silverstoneia_punctiventris_MHNUC320
Silverstoneia_punctiventris_MHNUC321
Silverstoneia_flotator_TNHCFS4804
Silverstoneia_flotator_SIUC7657
Epipedobates_boulengeri_Gorgona_TNHCFS4941
Epipedobates_boulengeri_Gorgona_CZPD_UV_4444
Epipedobates_espinosai_QCAZ27224
Epipedobates_darwinwallacei_AMNHA162663
Epipedobates_darwinwallacei_QCAZ16590
Epipedobates_anthonyi_QCAZ16597
Epipedobates_anthonyi_838
Epipedobates_tricolor_QCAZ21977
Epipedobates_machalilla_KU220631
Epipedobates_machalilla_QCAZ16527
Colostethus_pratti_SIUC7658
Colostethus_latinasus_CH6381
Colostethus_panamansis_CH5546
Colostethus_inguinalis_MUJ3247
Leucostethus_fugax_QCAZ16513
Leucostethus_argyrogaster_MHNSM22877
Leucostethus_jota_MHUAA9244
Colostethus_sp_Gorgona_CZPD_UV_5013
Leucostethus_bilsa_CJ7213
Leucostethus_fraterdanieli_MHUAA8082
Colostethus_ramirezi_MAR3312
Colostethus_fraterdanieli_CZPD_UV_4186
Colostethus_fraterdanieli_TG1230
Colostethus_brachistriatus_TNHCFS4977
Colostethus_brachistriatus_MHNUC361
Ameerega_macero_LR742
Ameerega_silverstonei_646
Ameerega_parvula_QCAZ16584
Ameerega_sp_zaparo_auct_KU221841
Ameerega_bilinguis_QCAZ28835
Ameerega_bilinguis_OMNH34127
Ameerega_trivittata_MPEG12504
Ameerega_hahneli_QCAZ19240
Ameerega_boehmei_E81_3
Ameerega_berohoka_NMM2011
Ameerega_flavopicta_MZUSP111790
Ameerega_braccata_MRT5603
Phyllobates_vitattus_839
Phyllobates_lugubris_USNMFS195116
Phyllobates_aurotaenia_TNHC64419
Phyllobates_aurotaenia_840
Phyllobates_bicolor_1233
Phyllobates_aurotaenia_TNHCFS4990
Phyllobates_aurotaenia_MUJ3735
Phyllobates_terribilis_TNHC64420
Phyllobates_terribilis_AMNHA118566
Colostethus_ruthveni_like_PAG1210
Colostethus_ruthveni_MAR558
Dendrobates_auratus_USNM313818
Oophaga_granulifera_CWM19044
Adelphobates_quinquevittatus_OMNH36665
Minyobates_steyermarki_Vences
Minyobates_steyermarki_Summers
Excidobates_mysteriosus_JD11.005
Excidobates_captivus_QCAZ27442
Ranitomeya_yavaricola_181
Ranitomeya_sirensis_JCS
Ranitomeya_variabilis_Sucumbios_OMNH34091
Ranitomeya_uakarii_MPEG12394
Ranitomeya_reticulata_MJH3754
Andinobates_fulguritus_MHNUC340
Andinobates_minutus_KRL790
Andinobates_dorisswansonae_TG2044
Andinobates_opisthomelas_TG1591
Andinobates_cassidyhornae_GECOH1523C
Paruwrobates_erythromos_QCAZ37750
Ectopoglossus_saxatilis_MAR1698
Ectopoglossus_saxatilis_MAR1796
Ectopoglossus_isthminus_SMF97114
Ectopoglossus_isthminus_MHCH2648
Ectopoglossus_isthminus_MHCH2651
Hyloxalus_vergeli_Quinchas_ALOP_191
Hyloxalus_vergeli_Chaparral_LHUTMT_013
Hyloxalus_vergeli_Ibague_MAA_1373
Hyloxalus_vergeli_Ibague_MAA_1376
Hyloxalus_vergeli_Ibague_LHUTMT_028
Hyloxalus_vergeli_Ibague_DFZ_409
Hyloxalus_vergeli_MUJ5018
Hyloxalus_vergeli_MUJ5017
Hyloxalus_vergeli_MUJ4298
Hyloxalus_sp_Inza_LVP_402
Hyloxalus_sp_Inza_LVP_399
Hyloxalus_sp_Inza_LVP_389
Hyloxalus_sp_Inza_LVP_386
Hyloxalus_sp_Gigante_GFM_1579
Hyloxalus_bocagei_QCAZ37259
Hyloxalus_bocagei_QCAZ20826
Hyloxalus_sp_Amazonas_CORBIDI_9423
Hyloxalus_sauli_QCAZ16543
Hyloxalus_sauli_QCAZ16541
Hyloxalus_sauli_QCAZ27126
Hyloxalus_leucophaeus_KU211880
Hyloxalus_sordidatus_MHNSM22679
Hyloxalus_sordidatus_MHNSM22690
Hyloxalus_maculosus_QCAZ19971
Hyloxalus_maculosus_QCAZ37158
Hyloxalus_maculosus_QCAZ37156
Hyloxalus_faciopunctulatus_JDL_28969
Hyloxalus_italoi_QCAZ16508
Hyloxalus_italoi_QCAZ16511
Hyloxalus_sp_MNCN_MNCN47510
Hyloxalus_sp_MNCN_MNCN47511
Hyloxalus_yasuni_QCAZ16504
Hyloxalus_yasuni_TG1835
Hyloxalus_yasuni_TG1836
Hyloxalus_yasuni_QCAZ37262
Hyloxalus_yasuni_QCAZ16503
Hyloxalus_yasuni_OMNH34072
Hyloxalus_yasuni_QCAZ20007
Hyloxalus_yasuni_OMNH34070
Hyloxalus_yasuni_LSUMZ12909
Hyloxalus_yasuni_LSUMZ12908
Hyloxalus_picachos_MCL813
Hyloxalus_picachos_MCL1171
Hyloxalus_subpunctatus_Sumapaz_MAA1401
Hyloxalus_sp_edwardsi_group_MAA1260
Hyloxalus_sp_edwardsi_group_MAA1269
Hyloxalus_sp_edwardsi_group_MAA1266
Hyloxalus_cepedai_StaMaria_ANDESA_6370
Hyloxalus_sp_StaMaria_MLC_1438
Hyloxalus_sanctamariensis_AJC_6369
Hyloxalus_sanctamariensis_MAA1403
Hyloxalus_sanctamariensis_MAA1402
Hyloxalus_sp_CasanareAR_MAA_528
Hyloxalus_sp_AguaAzul_TNHCFS4940
Hyloxalus_cepedai_StaMaria_MLC_1426
Hyloxalus_cepedai_Medina_ALH_036
Hyloxalus_cepedai_Medina_EQB_107
Hyloxalus_cepedai_MAA_1003
Hyloxalus_cepedai_MAA574
Hyloxalus_sp_Junin_MAA_1077
Hyloxalus_sp_Junin_MAA_1086
Hyloxalus_walesi_SVR_016
Hyloxalus_walesi_SVR_015
Hyloxalus_walesi_SVR_014
Hyloxalus_walesi_SVR_013
Hyloxalus_walesi_AS15
Hyloxalus_walesi_AS14
Hyloxalus_subpunctatus_TNHCFS4957
Hyloxalus_subpunctatus_ss_MAA_167
Hyloxalus_subpunctatus_MAA1054
Hyloxalus_subpunctatus_MUJ5212
Hyloxalus_sp_QuebradaWolf_MAA_1267
Hyloxalus_sp_QuebradaWolf_MAA_1270
Hyloxalus_sp_QuebradaWolf_MAA_1263
Hyloxalus_sp_QuebradaWolf_CZUT_2178
Hyloxalus_felixcoperari_IAvHAm14540
Hyloxalus_sp_Supata_MAA_542
Hyloxalus_sp_Supata_DAS_384
Hyloxalus_sp_Tequendama_JPR_078
Hyloxalus_sp_Aguabonita_MAA_1198
Hyloxalus_sp_Aguabonita_MAA_1241A
Hyloxalus_sp_Aguabonita_MAA_1213
Hyloxalus_sp_Aguabonita_MAA_1197
Hyloxalus_nexipus_QCAZ16537
Hyloxalus_nexipus_QCAZ16534
Hyloxalus_nexipus_KU211806
Hyloxalus_nexipus_KU212486
Hyloxalus_nexipus_KU211808
Hyloxalus_nexipus_KU211807
Hyloxalus_anthracinus_KU223489
Hyloxalus_jacobuspetersi_QCAZ37742
Hyloxalus_delatorreae_KU220621
Hyloxalus_sylvaticus_KU219756
Hyloxalus_sylvaticus_KU219757
Hyloxalus_pulcherrimus_KU211948
Hyloxalus_pulcherrimus_KU211947
Hyloxalus_vertebralis_QCAZ16554
Hyloxalus_vertebralis_QCAZ16553
Hyloxalus_pulchellus_QCAZ15964
Hyloxalus_sp_SanMiguelDeSalcedo_KU202833
Hyloxalus_delatorreae_KJ940457
Hyloxalus_delatorreae_KU220619
Hyloxalus_sp_MonteOlivo_KU220666
Hyloxalus_pinguis_GAP_195
Hyloxalus_pinguis_MAA1250
Hyloxalus_pinguis_MAA_1249
Hyloxalus_pinguis_MAA_1248
Hyloxalus_lehmanni_MAR2675
Hyloxalus_lehmanni_FC_657
Hyloxalus_lehmanni_FC_656
Hyloxalus_sp_Alban_ANDESA_2923
Hyloxalus_sp_MesasGalilea_MAA_1272
Hyloxalus_sp_MesasGalilea_MAA_1281
Hyloxalus_sp_MesasGalilea_MAA_1283
Hyloxalus_arliensis_TG1959
Hyloxalus_arliensis_ARA2520
Hyloxalus_sp_Caparrapi_RC_1439
Hyloxalus_sp_Caparrapi_RC_1423
Hyloxalus_arliensis_DFZ_413
Hyloxalus_arliensis_MAA_1400B
Hyloxalus_arliensis_MAA_1381
Hyloxalus_arliensis_DFZ_411
Hyloxalus_arliensis_MAR105
Hyloxalus_arliensis_MUJ3564
Hyloxalus_sp_ElCopal_QCAZ16490
Hyloxalus_craspedoceps_Lamas_CORBIDI_6804
Hyloxalus_craspedoceps_MHNSM22882
Hyloxalus_craspedoceps_Chazuta_MNCN47539
Hyloxalus_craspedoceps_Chazuta_MNCN47538
Colostethus_poecilonotus_CORBIDI_1960
Hyloxalus_azureiventris_KS32
Hyloxalus_azureiventris_KS33
Hyloxalus_azureiventris_KS28
Hyloxalus_chlorocraspedus_MPEG13853
Hyloxalus_chlorocraspedus_MPEG12511
Hyloxalus_chlorocraspedus_OMNH36169
Hyloxalus_chlorocraspedus_OMNH36170
Hyloxalus_chlorocraspedus_MPEG12505
Hyloxalus_sp_PAV_CORBIDI_11007
Hyloxalus_sp_Bongara_CORBIDI_12891
Hyloxalus_shuar_CJ2622
Hyloxalus_idiomelus_KU211109
Hyloxalus_idiomelus_KU211885
Hyloxalus_idiomelus_KU211886
Hyloxalus_idiomelus_KU211110
Hyloxalus_idiomelus_KU211908
Hyloxalus_sp_Masvalle_QCAZ19958
Hyloxalus_sp_Moraspungo_QCAZ21978
Hyloxalus_infraguttatus_QCAZ16516
Hyloxalus_infraguttatus_AGG504
Hyloxalus_toachi_QCAZ16549
Hyloxalus_toachi_QCAZ16548
Hyloxalus_awa_KU220610
Hyloxalus_awa_QCAZ16497
Hyloxalus_awa_QCAZ16502
Hyloxalus_awa_QCAZ16498
Hyloxalus_elachyhistus_CORBIDI_4292
Hyloxalus_elachyhistus_KU212507
Hyloxalus_infraguttatus_CORBIDI_3719
Hyloxalus_elachyhistus_QCAZ16518
Hyloxalus_elachyhistus_QCAZ1651
Hyloxalus_elachyhistus_Piura_KU212517
Hyloxalus_elachyhistus_Piura_KU212514
Hyloxalus_elachyhistus_Piura_KU212516
Hyloxalus_elachyhistus_Piura_KU212515
Hyloxalus_littoralis_CORBIDI_13260
Hyloxalus_elachyhistus_CORBIDI_4236
Hyloxalus_elachyhistus_CORBIDI_4234
Hyloxalus_elachyhistus_Piura_KU219749
Hyloxalus_elachyhistus_CORBIDI_4205
Hyloxalus_elachyhistus_CORBIDI_4201
Hyloxalus_elachyhistus_Cajamarca_KU212523
Hyloxalus_elachyhistus_Cajamarca_KU212524
Hyloxalus_elachyhistus_Cajamarca_KU212522
Hyloxalus_insulatus_CORBIDI_1961
Hyloxalus_insulatus_CK_212
Hyloxalus_insulatus_KU211878
Hyloxalus_insulatus_KU211877
Hyloxalus_sp_MNCN_1_MNCN47531
Hyloxalus_insulatus_CORBIDI_5656
Hyloxalus_sp_LaLibertad_CORBIDI_5650
Hyloxalus_littoralis_LIMA
Hyloxalus_littoralis_KST_650
Hyloxalus_sp._CORBIDI_6880
Hyloxalus_sp_Huanuco_CORBIDI_8642
Hyloxalus_sp_Huanuco_CORBIDI_8658
Hyloxalus_sp_Huanuco_CORBIDI_9017
Hyloxalus_littoralis_CORBIDI_16094
Hyloxalus_sp_Huanuco_CORBIDI_13350


Boana_boans_RWM17746
Melanophryniscus_setiba_CFBH15748
Thoropa_taophora_CFBH3239
Crossodactylus_schmidti_MLPA1414
Allobates_olfersioides_MNRJ79897
Allobates_undulatus_AMNHA159139
Allobates_talamancae_QCAZ16551
Allobates_talamancae_OMNH33237
Allobates_peruvianus_MHNSM22923
Allobates_zaparo_QCAZ16603
Allobates_zaparo_USNM546405
Allobates_femoralis_Acre02_PortoWalter_OMNH36070
Allobates_femoralis_femo04_Yurimaguas
Allobates_juanii_TNHCFS4978
Allobates_juanii_ARA2394
Allobates_tapajos_APL12965
Allobates_trilineatus_MJH7477
Allobates_trilineatus_KU215175
Rheobates_palmatus_MUJ3829
Anomaloglossus_tamacuarensis_MNRJ38049
Anomaloglossus_baeobatrachus_PK737.4
Anomaloglossus_stepheni_MJH3928
Anomaloglossus_degranvillei_Vences
Anomaloglossus_rufulus_CLBA
Anomaloglossus_kaiei_VUB3106
Anomaloglossus_kaiei_279
Aromobates_ornatissimus_WES626
Aromobates_nocturnus_AMNHA130041
Aromobates_molinarii_VencesLaMarca
Aromobates_meridensis_CVULA7399
Mannophryne_olmonae_UWIZM2732
Mannophryne_leonardoi_WES1034
Mannophryne_leonardoi_TNHCFS5659
Mannophryne_herminae_TNHCFS5676
Mannophryne_cordilleriana_TNHCFS5589
Silverstoneia_nubicola_SIUC7652
Silverstoneia_erasmios_MAR33316
Silverstoneia_erasmios_LSB218
Silverstoneia_punctiventris_MHNUC320
Silverstoneia_punctiventris_MHNUC321
Silverstoneia_flotator_TNHCFS4804
Silverstoneia_flotator_SIUC7657
Epipedobates_boulengeri_Gorgona_TNHCFS4941
Epipedobates_boulengeri_Gorgona_CZPD_UV_4444
Epipedobates_espinosai_QCAZ27224
Epipedobates_darwinwallacei_AMNHA162663
Epipedobates_darwinwallacei_QCAZ16590
Epipedobates_anthonyi_QCAZ16597
Epipedobates_anthonyi_838
Epipedobates_tricolor_QCAZ21977
Epipedobates_machalilla_KU220631
Epipedobates_machalilla_QCAZ16527
Colostethus_pratti_SIUC7658
Colostethus_latinasus_CH6381
Colostethus_panamansis_CH5546
Colostethus_inguinalis_MUJ3247
Leucostethus_fugax_QCAZ16513
Leucostethus_argyrogaster_MHNSM22877
Leucostethus_jota_MHUAA9244
Colostethus_sp_Gorgona_CZPD_UV_5013
Leucostethus_bilsa_CJ7213
Leucostethus_fraterdanieli_MHUAA8082
Colostethus_ramirezi_MAR3312
Colostethus_fraterdanieli_CZPD_UV_4186
Colostethus_fraterdanieli_TG1230
Colostethus_brachistriatus_TNHCFS4977
Colostethus_brachistriatus_MHNUC361
Ameerega_trivittata_MPEG12504
Ameerega_picta_TNHCFS5642
Ameerega_picta_BPN1074
Ameerega_silverstonei_646
Ameerega_bassleri_MHNSM22600
Ameerega_parvula_QCAZ16584
Ameerega_sp_zaparo_auct_KU221841
Ameerega_bilinguis_QCAZ28835
Ameerega_bilinguis_OMNH34127
Ameerega_petersi_MJH3715
Ameerega_macero_LR742
Ameerega_hahneli_QCAZ19240
Ameerega_rubriventris_KS37
Ameerega_simulans_EsimQuinceviii63
Ameerega_boehmei_E81_3
Ameerega_berohoka_NMM2011
Ameerega_flavopicta_MZUSP111790
Ameerega_braccata_MRT5603
Phyllobates_vitattus_839
Phyllobates_lugubris_USNMFS195116
Phyllobates_aurotaenia_TNHC64419
Phyllobates_aurotaenia_840
Phyllobates_bicolor_1233
Phyllobates_aurotaenia_TNHCFS4990
Phyllobates_aurotaenia_MUJ3735
Phyllobates_terribilis_TNHC64420
Phyllobates_terribilis_AMNHA118566
Colostethus_ruthveni_like_PAG1210
Colostethus_ruthveni_MAR558
Dendrobates_auratus_USNM313818
Oophaga_granulifera_CWM19044
Adelphobates_quinquevittatus_OMNH36665
Minyobates_steyermarki_Vences
Minyobates_steyermarki_Summers
Excidobates_mysteriosus_JD11.005
Excidobates_captivus_QCAZ27442
Ranitomeya_yavaricola_181
Ranitomeya_sirensis_JCS
Ranitomeya_variabilis_Sucumbios_OMNH34091
Ranitomeya_uakarii_MPEG12394
Ranitomeya_reticulata_MJH3754
Andinobates_fulguritus_MHNUC340
Andinobates_minutus_KRL790
Andinobates_dorisswansonae_TG2044
Andinobates_opisthomelas_TG1591
Andinobates_cassidyhornae_GECOH1523C
Paruwrobates_erythromos_QCAZ37750
Ectopoglossus_saxatilis_MAR1698
Ectopoglossus_saxatilis_MAR1796
Ectopoglossus_isthminus_SMF97114
Ectopoglossus_isthminus_MHCH2648
Ectopoglossus_isthminus_MHCH2651
Hyloxalus_vergeli_Quinchas_ALOP_191
Hyloxalus_vergeli_Chaparral_LHUTMT_013
Hyloxalus_vergeli_Ibague_MAA_1373
Hyloxalus_vergeli_Ibague_MAA_1376
Hyloxalus_vergeli_Ibague_LHUTMT_028
Hyloxalus_vergeli_Ibague_DFZ_409
Hyloxalus_vergeli_MUJ5018
Hyloxalus_vergeli_MUJ5017
Hyloxalus_vergeli_MUJ4298
Hyloxalus_sp_Inza_LVP_402
Hyloxalus_sp_Inza_LVP_399
Hyloxalus_sp_Inza_LVP_389
Hyloxalus_sp_Inza_LVP_386
Hyloxalus_sp_Gigante_GFM_1579
Hyloxalus_bocagei_QCAZ37259
Hyloxalus_bocagei_QCAZ20826
Hyloxalus_sp_Amazonas_CORBIDI_9423
Hyloxalus_sauli_QCAZ16543
Hyloxalus_sauli_QCAZ16541
Hyloxalus_sauli_QCAZ27126
Hyloxalus_leucophaeus_KU211880
Hyloxalus_sordidatus_MHNSM22679
Hyloxalus_sordidatus_MHNSM22690
Hyloxalus_maculosus_QCAZ19971
Hyloxalus_maculosus_QCAZ37158
Hyloxalus_maculosus_QCAZ37156
Hyloxalus_faciopunctulatus_JDL_28969
Hyloxalus_italoi_QCAZ16508
Hyloxalus_italoi_QCAZ16511
Hyloxalus_sp_MNCN_MNCN47510
Hyloxalus_sp_MNCN_MNCN47511
Hyloxalus_yasuni_QCAZ16504
Hyloxalus_yasuni_TG1835
Hyloxalus_yasuni_TG1836
Hyloxalus_yasuni_QCAZ37262
Hyloxalus_yasuni_QCAZ16503
Hyloxalus_yasuni_OMNH34072
Hyloxalus_yasuni_QCAZ20007
Hyloxalus_yasuni_OMNH34070
Hyloxalus_yasuni_LSUMZ12909
Hyloxalus_yasuni_LSUMZ12908
Hyloxalus_picachos_MCL813
Hyloxalus_picachos_MCL1171
Hyloxalus_subpunctatus_Sumapaz_MAA1401
Hyloxalus_sp_edwardsi_group_MAA1260
Hyloxalus_sp_edwardsi_group_MAA1269
Hyloxalus_sp_edwardsi_group_MAA1266
Hyloxalus_cepedai_StaMaria_ANDESA_6370
Hyloxalus_sp_StaMaria_MLC_1438
Hyloxalus_sanctamariensis_AJC_6369
Hyloxalus_sanctamariensis_MAA1403
Hyloxalus_sanctamariensis_MAA1402
Hyloxalus_sp_CasanareAR_MAA_528
Hyloxalus_sp_AguaAzul_TNHCFS4940
Hyloxalus_cepedai_StaMaria_MLC_1426
Hyloxalus_cepedai_Medina_ALH_036
Hyloxalus_cepedai_Medina_EQB_107
Hyloxalus_cepedai_MAA_1003
Hyloxalus_cepedai_MAA574
Hyloxalus_sp_Junin_MAA_1077
Hyloxalus_sp_Junin_MAA_1086
Hyloxalus_walesi_SVR_016
Hyloxalus_walesi_SVR_015
Hyloxalus_walesi_SVR_014
Hyloxalus_walesi_SVR_013
Hyloxalus_walesi_AS15
Hyloxalus_walesi_AS14
Hyloxalus_subpunctatus_TNHCFS4957
Hyloxalus_subpunctatus_ss_MAA_167
Hyloxalus_subpunctatus_MAA1054
Hyloxalus_subpunctatus_MUJ5212
Hyloxalus_sp_QuebradaWolf_MAA_1267
Hyloxalus_sp_QuebradaWolf_MAA_1270
Hyloxalus_sp_QuebradaWolf_MAA_1263
Hyloxalus_sp_QuebradaWolf_CZUT_2178
Hyloxalus_felixcoperari_IAvHAm14540
Hyloxalus_sp_Supata_MAA_542
Hyloxalus_sp_Supata_DAS_384
Hyloxalus_sp_Tequendama_JPR_078
Hyloxalus_sp_Aguabonita_MAA_1198
Hyloxalus_sp_Aguabonita_MAA_1241A
Hyloxalus_sp_Aguabonita_MAA_1213
Hyloxalus_sp_Aguabonita_MAA_1197
Hyloxalus_sylvaticus_KU219756
Hyloxalus_sylvaticus_KU219757
Hyloxalus_pulcherrimus_KU211948
Hyloxalus_pulcherrimus_KU211947
Hyloxalus_jacobuspetersi_QCAZ37742
Hyloxalus_delatorreae_KU220621
Hyloxalus_anthracinus_KU223489
Hyloxalus_vertebralis_QCAZ16554
Hyloxalus_vertebralis_QCAZ16553
Hyloxalus_pulchellus_QCAZ15964
Hyloxalus_sp_SanMiguelDeSalcedo_KU202833
Hyloxalus_delatorreae_KJ940457
Hyloxalus_delatorreae_KU220619
Hyloxalus_sp_MonteOlivo_KU220666
Hyloxalus_pinguis_GAP_195
Hyloxalus_pinguis_MAA1250
Hyloxalus_pinguis_MAA_1249
Hyloxalus_pinguis_MAA_1248
Hyloxalus_lehmanni_MAR2675
Hyloxalus_lehmanni_FC_657
Hyloxalus_lehmanni_FC_656
Hyloxalus_sp_Alban_ANDESA_2923
Hyloxalus_sp_MesasGalilea_MAA_1272
Hyloxalus_sp_MesasGalilea_MAA_1281
Hyloxalus_sp_MesasGalilea_MAA_1283
Hyloxalus_arliensis_TG1959
Hyloxalus_arliensis_ARA2520
Hyloxalus_sp_Caparrapi_RC_1439
Hyloxalus_sp_Caparrapi_RC_1423
Hyloxalus_arliensis_DFZ_413
Hyloxalus_arliensis_MAA_1400B
Hyloxalus_arliensis_MAA_1381
Hyloxalus_arliensis_DFZ_411
Hyloxalus_arliensis_MAR105
Hyloxalus_arliensis_MUJ3564
Hyloxalus_sp_PAV_CORBIDI_11007
Hyloxalus_sp_Bongara_CORBIDI_12891
Hyloxalus_nexipus_QCAZ16537
Hyloxalus_nexipus_QCAZ16534
Hyloxalus_nexipus_KU211806
Hyloxalus_nexipus_KU212486
Hyloxalus_nexipus_KU211808
Hyloxalus_nexipus_KU211807
Hyloxalus_sp_ElCopal_QCAZ16490
Hyloxalus_craspedoceps_Lamas_CORBIDI_6804
Hyloxalus_craspedoceps_MHNSM22882
Hyloxalus_craspedoceps_Chazuta_MNCN47539
Hyloxalus_craspedoceps_Chazuta_MNCN47538
Colostethus_poecilonotus_CORBIDI_1960
Hyloxalus_azureiventris_KS32
Hyloxalus_azureiventris_KS33
Hyloxalus_azureiventris_KS28
Hyloxalus_chlorocraspedus_MPEG13853
Hyloxalus_chlorocraspedus_MPEG12511
Hyloxalus_chlorocraspedus_OMNH36169
Hyloxalus_chlorocraspedus_OMNH36170
Hyloxalus_chlorocraspedus_MPEG12505
Hyloxalus_sp_Masvalle_QCAZ19958
Hyloxalus_sp_Moraspungo_QCAZ21978
Hyloxalus_infraguttatus_QCAZ16516
Hyloxalus_infraguttatus_AGG504
Hyloxalus_toachi_QCAZ16549
Hyloxalus_toachi_QCAZ16548
Hyloxalus_awa_KU220610
Hyloxalus_awa_QCAZ16497
Hyloxalus_awa_QCAZ16502
Hyloxalus_awa_QCAZ16498
Hyloxalus_shuar_CJ2622
Hyloxalus_idiomelus_KU211109
Hyloxalus_idiomelus_KU211885
Hyloxalus_idiomelus_KU211886
Hyloxalus_idiomelus_KU211110
Hyloxalus_idiomelus_KU211908
Hyloxalus_elachyhistus_CORBIDI_4292
Hyloxalus_elachyhistus_KU212507
Hyloxalus_infraguttatus_CORBIDI_3719
Hyloxalus_elachyhistus_QCAZ16518
Hyloxalus_elachyhistus_QCAZ16517
Hyloxalus_elachyhistus_Piura_KU212517
Hyloxalus_elachyhistus_Piura_KU212514
Hyloxalus_elachyhistus_Piura_KU212516
Hyloxalus_elachyhistus_Piura_KU212515
Hyloxalus_littoralis_CORBIDI_13260
Hyloxalus_elachyhistus_CORBIDI_4236
Hyloxalus_elachyhistus_CORBIDI_4234
Hyloxalus_elachyhistus_Piura_KU219749
Hyloxalus_elachyhistus_CORBIDI_4205
Hyloxalus_elachyhistus_CORBIDI_4201
Hyloxalus_elachyhistus_Cajamarca_KU212523
Hyloxalus_elachyhistus_Cajamarca_KU212524
Hyloxalus_elachyhistus_Cajamarca_KU212522
Hyloxalus_insulatus_CORBIDI_1961
Hyloxalus_insulatus_CK_212
Hyloxalus_insulatus_KU211878
Hyloxalus_insulatus_KU211877
Hyloxalus_sp_MNCN_1_MNCN47531
Hyloxalus_insulatus_CORBIDI_5656
Hyloxalus_sp_LaLibertad_CORBIDI_5650
Hyloxalus_littoralis_LIMA
Hyloxalus_littoralis_KST_650
Hyloxalus_sp._CORBIDI_6880
Hyloxalus_sp_Huanuco_CORBIDI_8642
Hyloxalus_sp_Huanuco_CORBIDI_8658
Hyloxalus_sp_Huanuco_CORBIDI_9017
Hyloxalus_littoralis_CORBIDI_16094
Hyloxalus_sp_Huanuco_CORBIDI_13350

Boana_boans_RWM17746
Cycloramphus_boraceiensis_CFBH5757
Thoropa_miliaris_AF1434
Thoropa_taophora_CFBH3239
Limnomedusa_macroglossa_MACN38641
Atelopus_zeteki_UMFS11492
Melanophryniscus_setiba_CFBH15748
Megaelosia_jordanensis_MCP11575
Crossodactylus_schmidti_MLPA1414
Hylodes_phyllodes_MCL00015
Hylodes_perere_CFBHT15413
Allobates_olfersioides_MNRJ79897
Allobates_undulatus_AMNHA159139
Allobates_talamancae_QCAZ16551
Allobates_talamancae_OMNH33237
Allobates_kingsburyi_QCAZ16523
Allobates_peruvianus_MHNSM22923
Allobates_zaparo_QCAZ16603
Allobates_zaparo_USNM546405
Allobates_femoralis_Acre02_PortoWalter_OMNH36070
Allobates_femoralis_femo04_Yurimaguas
Allobates_magnussoni_MPEG11923
Allobates_juanii_TNHCFS4978
Allobates_juanii_ARA2394
Allobates_insperatus_QCAZ16533
Allobates_trilineatus_MJH7477
Allobates_trilineatus_KU215175
Allobates_chalcopis_Alca1
Allobates_tapajos_APL12965
Allobates_algorei_TNHCFS5551
Anomaloglossus_tamacuarensis_MNRJ38049
Anomaloglossus_wothuja_VUB3736
Anomaloglossus_megacephalus_ROM39637
Anomaloglossus_baeobatrachus_PK737.4
Anomaloglossus_stepheni_MJH3928
Anomaloglossus_degranvillei_Vences
Anomaloglossus_rufulus_CLBA
Anomaloglossus_beebei_ROM39631
Anomaloglossus_kaiei_VUB3106
Anomaloglossus_kaiei_279
Rheobates_palmatus_MUJ3829
Rheobates_pseudopalmatus_MHUA5162
Aromobates_ornatissimus_WES626
Aromobates_nocturnus_AMNHA130041
Aromobates_molinarii_VencesLaMarca
Aromobates_meridensis_CVULA7399
Aromobates_ericksonae_CVULA8308
Mannophryne_olmonae_UWIZM2732
Mannophryne_leonardoi_WES1034
Mannophryne_leonardoi_TNHCFS5659
Mannophryne_herminae_TNHCFS5676
Mannophryne_yustizi_TNHCFS5604
Mannophryne_cordilleriana_TNHCFS5589
Silverstoneia_nubicola_SIUC7652
Silverstoneia_erasmios_MAR33316
Silverstoneia_erasmios_LSB218
Silverstoneia_punctiventris_MHNUC320
Silverstoneia_punctiventris_MHNUC321
Silverstoneia_flotator_TNHCFS4804
Silverstoneia_flotator_SIUC7657
Epipedobates_boulengeri_Gorgona_TNHCFS4941
Epipedobates_boulengeri_Gorgona_CZPD_UV_4444
Epipedobates_espinosai_QCAZ27224
Epipedobates_darwinwallacei_AMNHA162663
Epipedobates_darwinwallacei_QCAZ16590
Epipedobates_anthonyi_QCAZ16597
Epipedobates_anthonyi_838
Epipedobates_tricolor_QCAZ21977
Epipedobates_machalilla_KU220631
Epipedobates_machalilla_QCAZ16527
Colostethus_pratti_SIUC7658
Colostethus_latinasus_CH6381
Colostethus_panamansis_CH5546
Colostethus_inguinalis_MUJ3247
Leucostethus_fugax_QCAZ16513
Leucostethus_argyrogaster_MHNSM22877
Leucostethus_jota_MHUAA9244
Colostethus_sp_Gorgona_CZPD_UV_5013
Leucostethus_bilsa_CJ7213
Leucostethus_fraterdanieli_MHUAA8082
Colostethus_ramirezi_MAR3312
Colostethus_fraterdanieli_CZPD_UV_4186
Colostethus_fraterdanieli_TG1230
Colostethus_brachistriatus_TNHCFS4977
Colostethus_brachistriatus_MHNUC361
Ameerega_trivittata_MPEG12504
Ameerega_picta_TNHCFS5642
Ameerega_picta_BPN1074
Ameerega_silverstonei_646
Ameerega_bassleri_MHNSM22600
Ameerega_parvula_QCAZ16584
Ameerega_sp_zaparo_auct_KU221841
Ameerega_bilinguis_QCAZ28835
Ameerega_bilinguis_OMNH34127
Ameerega_petersi_MJH3715
Ameerega_macero_LR742
Ameerega_hahneli_QCAZ19240
Ameerega_rubriventris_KS37
Ameerega_simulans_EsimQuinceviii63
Ameerega_boehmei_E81_3
Ameerega_berohoka_NMM2011
Ameerega_flavopicta_MZUSP111790
Ameerega_braccata_MRT5603
Phyllobates_vitattus_839
Phyllobates_lugubris_USNMFS195116
Phyllobates_aurotaenia_TNHC64419
Phyllobates_aurotaenia_840
Phyllobates_bicolor_1233
Phyllobates_aurotaenia_TNHCFS4990
Phyllobates_aurotaenia_MUJ3735
Phyllobates_terribilis_TNHC64420
Phyllobates_terribilis_AMNHA118566
Colostethus_ruthveni_like_PAG1210
Colostethus_ruthveni_MAR558
Dendrobates_auratus_USNM313818
Oophaga_granulifera_CWM19044
Adelphobates_quinquevittatus_OMNH36665
Minyobates_steyermarki_Vences
Minyobates_steyermarki_Summers
Excidobates_mysteriosus_JD11.005
Excidobates_captivus_QCAZ27442
Ranitomeya_yavaricola_181
Ranitomeya_sirensis_JCS
Ranitomeya_variabilis_Sucumbios_OMNH34091
Ranitomeya_uakarii_MPEG12394
Ranitomeya_reticulata_MJH3754
Andinobates_fulguritus_MHNUC340
Andinobates_minutus_KRL790
Andinobates_dorisswansonae_TG2044
Andinobates_opisthomelas_TG1591
Andinobates_cassidyhornae_GECOH1523C
Paruwrobates_erythromos_QCAZ37750
Ectopoglossus_saxatilis_MAR1698
Ectopoglossus_saxatilis_MAR1796
Ectopoglossus_isthminus_SMF97114
Ectopoglossus_isthminus_MHCH2648
Ectopoglossus_isthminus_MHCH2651
Hyloxalus_vergeli_Quinchas_ALOP_191
Hyloxalus_vergeli_Chaparral_LHUTMT_013
Hyloxalus_vergeli_Ibague_MAA_1373
Hyloxalus_vergeli_Ibague_MAA_1376
Hyloxalus_vergeli_Ibague_LHUTMT_028
Hyloxalus_vergeli_Ibague_DFZ_409
Hyloxalus_vergeli_MUJ5018
Hyloxalus_vergeli_MUJ5017
Hyloxalus_vergeli_MUJ4298
Hyloxalus_sp_Inza_LVP_402
Hyloxalus_sp_Inza_LVP_399
Hyloxalus_sp_Inza_LVP_389
Hyloxalus_sp_Inza_LVP_386
Hyloxalus_sp_Gigante_GFM_1579
Hyloxalus_bocagei_QCAZ37259
Hyloxalus_bocagei_QCAZ20826
Hyloxalus_sp_Amazonas_CORBIDI_9423
Hyloxalus_sauli_QCAZ16543
Hyloxalus_sauli_QCAZ16541
Hyloxalus_sauli_QCAZ27126
Hyloxalus_leucophaeus_KU211880
Hyloxalus_sordidatus_MHNSM22679
Hyloxalus_sordidatus_MHNSM22690
Hyloxalus_maculosus_QCAZ19971
Hyloxalus_maculosus_QCAZ37158
Hyloxalus_maculosus_QCAZ37156
Hyloxalus_faciopunctulatus_JDL_28969
Hyloxalus_italoi_QCAZ16508
Hyloxalus_italoi_QCAZ16511
Hyloxalus_sp_MNCN_MNCN47510
Hyloxalus_sp_MNCN_MNCN47511
Hyloxalus_yasuni_QCAZ16504
Hyloxalus_yasuni_TG1835
Hyloxalus_yasuni_TG1836
Hyloxalus_yasuni_QCAZ37262
Hyloxalus_yasuni_QCAZ16503
Hyloxalus_yasuni_OMNH34072
Hyloxalus_yasuni_QCAZ20007
Hyloxalus_yasuni_OMNH34070
Hyloxalus_yasuni_LSUMZ12909
Hyloxalus_yasuni_LSUMZ12908
Hyloxalus_subpunctatus_Sumapaz_MAA1401
Hyloxalus_sp_edwardsi_group_MAA1260
Hyloxalus_sp_edwardsi_group_MAA1269
Hyloxalus_sp_edwardsi_group_MAA1266
Hyloxalus_cepedai_StaMaria_ANDESA_6370
Hyloxalus_sp_StaMaria_MLC_1438
Hyloxalus_sanctamariensis_AJC_6369
Hyloxalus_sanctamariensis_MAA1403
Hyloxalus_sanctamariensis_MAA1402
Hyloxalus_picachos_MCL813
Hyloxalus_picachos_MCL1171
Hyloxalus_sp_CasanareAR_MAA_528
Hyloxalus_sp_AguaAzul_TNHCFS4940
Hyloxalus_cepedai_StaMaria_MLC_1426
Hyloxalus_cepedai_Medina_ALH_036
Hyloxalus_cepedai_Medina_EQB_107
Hyloxalus_cepedai_MAA_1003
Hyloxalus_cepedai_MAA574
Hyloxalus_sp_Junin_MAA_1077
Hyloxalus_sp_Junin_MAA_1086
Hyloxalus_walesi_SVR_016
Hyloxalus_walesi_SVR_015
Hyloxalus_walesi_SVR_014
Hyloxalus_walesi_SVR_013
Hyloxalus_walesi_AS15
Hyloxalus_walesi_AS14
Hyloxalus_subpunctatus_TNHCFS4957
Hyloxalus_subpunctatus_ss_MAA_167
Hyloxalus_subpunctatus_MAA1054
Hyloxalus_subpunctatus_MUJ5212
Hyloxalus_sp_QuebradaWolf_MAA_1267
Hyloxalus_sp_QuebradaWolf_MAA_1270
Hyloxalus_sp_QuebradaWolf_MAA_1263
Hyloxalus_sp_QuebradaWolf_CZUT_2178
Hyloxalus_felixcoperari_IAvHAm14540
Hyloxalus_sp_Supata_MAA_542
Hyloxalus_sp_Supata_DAS_384
Hyloxalus_sp_Tequendama_JPR_078
Hyloxalus_sp_Aguabonita_MAA_1198
Hyloxalus_sp_Aguabonita_MAA_1241A
Hyloxalus_sp_Aguabonita_MAA_1213
Hyloxalus_sp_Aguabonita_MAA_1197
Hyloxalus_nexipus_QCAZ16537
Hyloxalus_nexipus_QCAZ16534
Hyloxalus_nexipus_KU211806
Hyloxalus_nexipus_KU212486
Hyloxalus_nexipus_KU211808
Hyloxalus_nexipus_KU211807
Hyloxalus_sylvaticus_KU219756
Hyloxalus_sylvaticus_KU219757
Hyloxalus_pulcherrimus_KU211948
Hyloxalus_pulcherrimus_KU211947
Hyloxalus_jacobuspetersi_QCAZ37742
Hyloxalus_delatorreae_KU220621
Hyloxalus_anthracinus_KU223489
Hyloxalus_vertebralis_QCAZ16554
Hyloxalus_vertebralis_QCAZ16553
Hyloxalus_pulchellus_QCAZ15964
Hyloxalus_sp_SanMiguelDeSalcedo_KU202833
Hyloxalus_delatorreae_KJ940457
Hyloxalus_delatorreae_KU220619
Hyloxalus_sp_MonteOlivo_KU220666
Hyloxalus_pinguis_GAP_195
Hyloxalus_pinguis_MAA1250
Hyloxalus_pinguis_MAA_1249
Hyloxalus_pinguis_MAA_1248
Hyloxalus_lehmanni_MAR2675
Hyloxalus_lehmanni_FC_657
Hyloxalus_lehmanni_FC_656
Hyloxalus_sp_Alban_ANDESA_2923
Hyloxalus_sp_MesasGalilea_MAA_1272
Hyloxalus_sp_MesasGalilea_MAA_1281
Hyloxalus_sp_MesasGalilea_MAA_1283
Hyloxalus_arliensis_TG1959
Hyloxalus_arliensis_ARA2520
Hyloxalus_sp_Caparrapi_RC_1439
Hyloxalus_sp_Caparrapi_RC_1423
Hyloxalus_arliensis_DFZ_413
Hyloxalus_arliensis_MAA_1400B
Hyloxalus_arliensis_MAA_1381
Hyloxalus_arliensis_DFZ_411
Hyloxalus_arliensis_MAR105
Hyloxalus_arliensis_MUJ3564
Hyloxalus_sp_PAV_CORBIDI_11007
Hyloxalus_sp_Bongara_CORBIDI_12891
Hyloxalus_sp_ElCopal_QCAZ16490
Hyloxalus_craspedoceps_Lamas_CORBIDI_6804
Hyloxalus_craspedoceps_MHNSM22882
Hyloxalus_craspedoceps_Chazuta_MNCN47539
Hyloxalus_craspedoceps_Chazuta_MNCN47538
Colostethus_poecilonotus_CORBIDI_1960
Hyloxalus_azureiventris_KS32
Hyloxalus_azureiventris_KS33
Hyloxalus_azureiventris_KS28
Hyloxalus_chlorocraspedus_MPEG13853
Hyloxalus_chlorocraspedus_MPEG12511
Hyloxalus_chlorocraspedus_OMNH36169
Hyloxalus_chlorocraspedus_OMNH36170
Hyloxalus_chlorocraspedus_MPEG12505
Hyloxalus_shuar_CJ2622
Hyloxalus_idiomelus_KU211110
Hyloxalus_idiomelus_KU211908
Hyloxalus_idiomelus_KU211109
Hyloxalus_idiomelus_KU211885
Hyloxalus_idiomelus_KU211886
Hyloxalus_sp_Masvalle_QCAZ19958
Hyloxalus_sp_Moraspungo_QCAZ21978
Hyloxalus_infraguttatus_QCAZ16516
Hyloxalus_infraguttatus_AGG504
Hyloxalus_toachi_QCAZ16549
Hyloxalus_toachi_QCAZ16548
Hyloxalus_awa_KU220610
Hyloxalus_awa_QCAZ16497
Hyloxalus_awa_QCAZ16502
Hyloxalus_awa_QCAZ16498
Hyloxalus_elachyhistus_CORBIDI_4292
Hyloxalus_elachyhistus_KU212507
Hyloxalus_infraguttatus_CORBIDI_3719
Hyloxalus_elachyhistus_QCAZ16518
Hyloxalus_elachyhistus_QCAZ16517
Hyloxalus_elachyhistus_Piura_KU212517
Hyloxalus_elachyhistus_Piura_KU212514
Hyloxalus_elachyhistus_Piura_KU212516
Hyloxalus_elachyhistus_Piura_KU212515
Hyloxalus_littoralis_CORBIDI_13260
Hyloxalus_elachyhistus_CORBIDI_4236
Hyloxalus_elachyhistus_CORBIDI_4234
Hyloxalus_elachyhistus_Piura_KU219749
Hyloxalus_elachyhistus_CORBIDI_4205
Hyloxalus_elachyhistus_CORBIDI_4201
Hyloxalus_elachyhistus_Cajamarca_KU212523
Hyloxalus_elachyhistus_Cajamarca_KU212524
Hyloxalus_elachyhistus_Cajamarca_KU212522
Hyloxalus_insulatus_CORBIDI_1961
Hyloxalus_insulatus_CK_212
Hyloxalus_insulatus_KU211878
Hyloxalus_insulatus_KU211877
Hyloxalus_sp_MNCN_1_MNCN47531
Hyloxalus_insulatus_CORBIDI_5656
Hyloxalus_sp_LaLibertad_CORBIDI_5650
Hyloxalus_littoralis_LIMA
Hyloxalus_littoralis_KST_650
Hyloxalus_sp._CORBIDI_6880
Hyloxalus_sp_Huanuco_CORBIDI_8642
Hyloxalus_sp_Huanuco_CORBIDI_8658
Hyloxalus_sp_Huanuco_CORBIDI_9017
Hyloxalus_littoralis_CORBIDI_16094
Hyloxalus_sp_Huanuco_CORBIDI_13350

APPENDIX 3

Length Relation Between the Finger II and the Finger IV.

Values are in percentage (%). In Interspecific Variation, the species are ordered from the lower to the higher finger II/IV value.

Intraspecified Variation

Species	**Collection Number/Source**	**II/IV**
Oophaga sylvatica	MZUSP 55661	74
Oophaga sylvatica	MZUSP 56308	72
Adelphobates quinquevittatus	MZUSP 100208	63
Adelphobates quinquevittatus	MZUSP 100210	65
Minyobates steyermarki	MZUSP 58304	70
Minyobates steyermarki	MZUSP 58305	73
Dendrobates leucomelas	MZUSP 69777	65
Dendrobates leucomelas	MZUSP 63311	70
Ranitomeya variabilis	MZUSP 50711	57
Ranitomeya variabilis	MZUSP 50720	58
Ranitomeya variabilis	MZUSP 100151	58
Aromobates orostoma	MZUSP 106702	73
Aromobates orostoma	MZUSP 106701	70
Hyloxalus pinguis	KU 181163	74
Hyloxalus pinguis	ICN 7670	73

Hyloxalus pinguis	ICN 7682	76
Hyloxalus pinguis	ICN 32794	74
Hyloxalus pinguis	ICN 7646	74
Hyloxalus vergeli	KU 12477	69
Hyloxalus vergeli	ICN 35431	69
Hyloxalus vergeli	ICN 2482	70
Hyloxalus vergeli	ICN 35423	70
Hyloxalus vergeli	ICN 22504	69
Hyloxalus vergeli	ICN 2477	69
Hyloxalus sp_R	CZUT-A 1501	72
Hyloxalus sp_R	ICN 9213	69
Hyloxalus sp_R	ICN 9209	71
Hyloxalus sp_R	ICN 22524	70
Hyloxalus sp_R	ICN 43963	70
Hyloxalus cepedai	MAA 577	76
Hyloxalus cepedai	MAA 576	76
Hyloxalus cepedai	ICN 44492	76
Hyloxalus cepedai	MAA 271	75
Hyloxalus cepedai	ICN 44495	76
Hyloxalus cepedai	MAA 574	76
Interspecified Variation		

Ranitomeya variabilis	MZUSP 50711	57
Ranitomeya variabilis	MZUSP 100151	58
Ranitomeya variabilis	MZUSP 50720	58
Ranitomeya reticulata	MZUSP 58302	59
Oophaga pumilio	PD 50	62
Andinobates viridis	KU 152921	62
Ranitomeya amazonica	MZUSP 149345	63
Adelphobates quinquevittatus	MZUSP 100208	63
Andinobates cassidyhornae	ANDES-A1095, Amezquita et al. 2013	64
Andinobates dorisswansoni	ICN 53279, Rueda-A et al. 2006	64
Andinobates tolimensis	CZUT-A 0990	64
Adelphobates quinquevittatus	MZUSP 100210	65
Adelphobates castaneoticus	MZUSP 147796	65
Andinobates abditus	KU 143093	65
Adelphobates castaneoticus	MZUSP 64763, Caldwell & Myers1990	65
Oophaga granulifera	KU 43874	65
Andinobates bombetes	KU 139647	65
Colostethus agilis	KU 181164	68
Hyloxalus maculosus	ICN 24249	68

*Hyloxalus exasperatus*_like	KU 106240	68
Paruwrobates andinus	PSO-CZ 623	68
Hyloxalus excisus	ICN 15813	69
Dendrobates leucomelas	MZUSP 69777	69
Hyloxalus vergeli	ICN 2477	69
Oophaga lehmanni	KU 152919	69
Oophaga occultator	KU 152923	69
Hyloxalus vergeli	ICN 35431	69
Hyloxalus sp_R	ICN 9213	69
Allobates talamancae	PD 49	69
Hyloxalus vergeli	ICN 22504	69
Aromobates orostoma	MZUSP 106702	69
Hyloxalus nexipus	KU 211810	69
Ectopoglossus confusus	KU 166157	69
Colostethus ucumari	KU 133309	69
Hyloxalus vergeli	KU 124777	69
Ectopoglossus absconditus	KU 189526	70
Allobates zaparo	KU 120660	70
Minyobates steyermarki	MZUSP 58304	70
Minyobates steyermarki	MZUSP 58305	70

Hyloxalus fallax	USNM 282669	70
Hyloxalus peculiaris	USNM 282666	70
Colostethus praderioi	IRSNB 14403 in Kok 2010	70
Hyloxalus fasciopunctulatus	MZUSP 56284	70
Colostethus kaiei	IRSNB 1938 in Kok et al. 2006a	70
Colostethus bebei	Kok et al. 2006b	70
Anomaloglossus tamacuarensis	Amnh131347, Myers & Donelly 1997	70
Dendrobates leucomelas	MZUSP 63311	70
Hyloxalus vergeli	ICN 35423	70
Anomaloglossus tepequen	MZUSP 63310, Fouquet et al. 2015	70
Hyloxalus sp_R	ICN 43963	70
Hyloxalus bocagei	KU 166106	70
Hyloxalus vergeli	ICN 2482	70
Aromobates orostoma	MZUSP 106701	70
Hyloxalus sp_R	ICN 22524	70
Mannophryne cordillerana	MZUSP 94591	71
Hyloxalus fuliginosus	KU 143087	71
Hyloxalus infraguttatus	KU 142392	71

Hyloxalus azureiventris	KU 211976	71
Anomaloglossus apiau	MZUSP 155833, Fouquet et al. 2015	71
Hyloxalus leucophaeus	KU 211879	71
Hyloxalus sp_R	ICN 9209	71
Hyloxalus vertebralis	KU 142416	71
Hyloxalus delatorreae	KU 182197	72
Hyloxalus sauli	KU 122217	72
Hyloxalus abditaurantius	ICN 21579	72
Hyloxalus maquipucuna	KU 202882	72
Hyloxalus jacobuspetersi	KU 132309	72
Hyloxalus sylvaticus	KU 181672	72
Allobates tapajos	INPA-H 34425, Lima et al. 2015	72
Anomaloglossus megacephalus	Kok et al. 2010	72
Hyloxalus pulchellus	KU 142976	72
Hyloxalus mittermeieri	KU 211944	72
Hyloxalus craspedoceps	KU 211957	72
Ectopoglossus lacrimosus	KU 170243	72
Oophaga sylvatica	MZUSP 56308	72
*Hyloxalus lehmanni*_LaPlanada	KU 200258	72

Hyloxalus sp_R	CZUT-A 1501	72
Hyloxalus exasperatus	KU 147100	72
Hyloxalus mystax	KU 147095	72
Rheobates palmatus	KU 133238	73
Allobates wayuu	ICN 43234	73
Hyloxalus awa	KU 166085	73
Paruwrobates whymperi	KU 221620	73
Mannophryne trujillensis	MZUSP 106688	73
Colostethus mertensi	KU 139596	73
Hyloxalus aeroginosus	KU 211940	73
Dendrobates auratus	MZUSP 100174	73
Hyloxalus insulatus	KU 211857	73
Hyloxalus pinguis	ICN 7670	73
Hyloxalus sp_walesi	ICN 12739	74
Hyloxalus elachyhistus	KU 120540	74
Ectopoglossus atopoglossus	KU 289251	74
Allobates olfersioides	KU 93157	74
Ectopoglossus saxatilis	IAvH 14613	74
Hyloxalus pinguis	ICN 32794	74
Hyloxalus pinguis	ICN 7646	74

Hyloxalus eletherodactylus	KU 211813	74
Hyloxalus shuar	KU 147091	74
Anomaloglossus baeobatrachus	MZUSP 69178	74
Oophaga sylvatica	MZUSP 55661	74
Anomaloglossus stepheni	MZUSP 69178	74
Allobates kingsburgyi	KU 182122	74
Colostethus ruthveni	ICN 35712	74
Hyloxalus chlorocraspedus	mcz36169	74
Hyloxalus pinguis	KU 181163	74
Mannophryne vulcano	MZUSP 31386	75
Hyloxalus cepedai	MAA 271	75
Dendrobates tinctorius	MZUSP 139803	75
Hyloxalus fascianigrus	KU 289247	76
Phyllobates lugubris	MZUSP 100124	76
Ameerega hahneli	ZUEC 9049, Haadad & Martins1994	76
Paruwrobates erythromops	MCZ 96382	76
Hyloxalus jhoncito	MAA 1260	76
Aromobates meridensis	CVULA 7399 in Barrio et al. 2010	76
Aromobates ornatissimus	EBRG 5292 in Barrio-Amoros	76

	et al. 2010	
Hyloxalus cepedai	ICN 44492	76
Hyloxalus cepedai	ICN 44495	76
Hyloxalus pulcherrimus	KU 211946	76
Hyloxalus cepedai	MAA 577	76
Hyloxalus pinguis	ICN 7682	76
Ameerega berohoka	mnrj67262	76
Hyloxalus cepedai	MAA 576	76
Ameerega boehmei	zfmk77444	76
Hyloxalus cepedai	MAA 574	76
Hyloxalus parcus	USNM 282533	76
Hyloxalus sordidatus	KU 211960	77
Hyloxalus edwardsi	ICN 21936	77
Ameerega imasmari	MUSM-H 35670 in Brown et al. 2019	77
Hyloxalus idiomelus	KU 211887	77
Colostethus ruthveni like	ICN 35211	77
Ameerega macero	MHNSM 3837 in Rodriguez & Myers1993	77
Ameerega simulans	MUSM 15505 in Myers et al. 1998	77

Hyloxalus subpunctatus ss	ICN 110484	77
Aromobates nocturnus	KU 220983	77
Phyllobates vittatus	MZUSP 99986	81
Ameerega flavopicta	MZUSP 100112	81
Ameerega braccata	MZUSP 100230	81
Allobates trilineatus	MHNSM 40420 in Jaramillo et al. 2021	81
Ameerega picta	ZUEC 9055, Haddad & Martins 1994	81
Amereega yungicola	CBF 3900 in Serrano et al. 2017	81
Ameerega shihuemoy	MHNC 15488 in Serrano et al. 2017	81
Allobates femoralis	KU 205284	81
Ameerega bilinguis	ZFMK 49073	81
Hyloxalus borjai	KU 189439	81
Hyloxalus breviquartus	ICN 21667	81
Hyloxalus arliensis	DFZ 341	81
Phyllobates bicolor	MZUSP 106692	82
Ameerega pulchripecta	MZUSP 69846	82
Allobates magnussoni	INPA-H 32960 in Lima et al.	82

	2014	
Hyloxalus toachi	KU 202891	82
Epipedobates machalilla	KU 142483	83
Hyloxalus anthracinus	KU 120643	83
Hyloxalus ruizi	ICN 5416	83
Colostethus inguinalis	ICN 47692	84
Epipedobates anthonyi	KU 219764	84
Epipedobates darwinwallacei	MZUSP 78213	84
Colostethus fugax	KU 146237	84
Ameerega silverstonei	AMNH 91844, Myers & Daly. 1979	85
Anomaloglossus surinamensis	KU 220993	86
Silverstoneia erasmios	MAR 3590	86

APPENDIX 4

Trees of the Successive Outgroup Expansion Analysis (SOE).

Nine SOE analyses were done (1–9th). Number on the nodes are Goodman-Bremer value.

See the attached file: Appendix_4_1.0-1.8_SOE_GB.pdf

APPENDIX 5

Phylogenetic Relationships of the Genus *Hyloxalus* and the Superfamily Dendrobatoidea.

Optimal most parsimonious tree of the poison frogs, obtained from the ninth SOE analysis after iterative pass optimization. Tree show minimum branch-length, unsupported nodes collapsed, supported nodes with Goodman-Bremen value. Tree length 54672 steps.

See attached file: Appendix_5_Phylogeny_ALL_GB

APPENDIX 6

Unambiguously Phenotypic Synapomorphies

List of the unambiguously phenotypic synapomorphies optimizing in all most parsimonious trees. Character and character-state transformations for each species and/or node are specified.

See the attached file: Appendix_6_ybyra_synaphomorphies.csv

APPENDIX 5

Optitimal most parsimonious tree of the poison frogs, Dendrobatoidea, to test the *Hyloxalus* relationships. Tree show minimum branch-length, unsupported nodes collapsed, supported nodes with Goodman-Bremen value. Tree length 54672 steps.

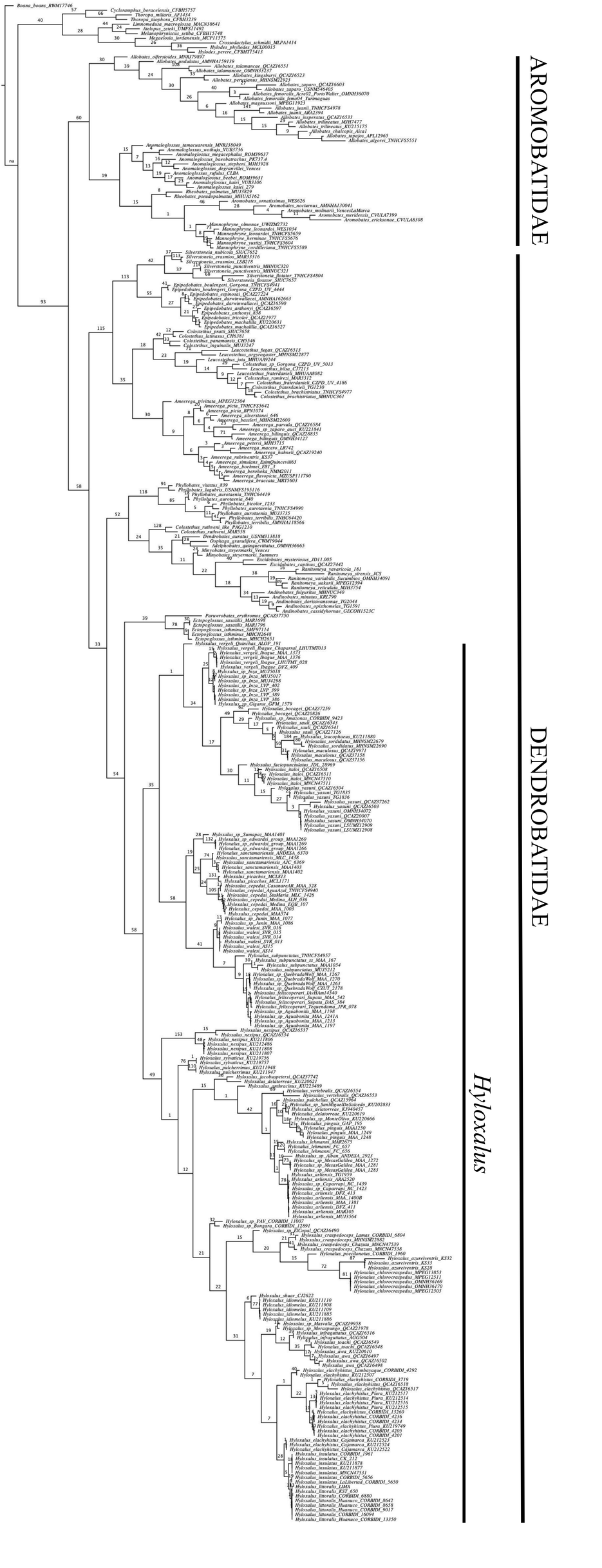

APPENDIX 6

Unambiguously Phenotypic Synapomorphies.

'NON-AMBIGUOUS SYNAPOMORPHIES FOR EACH NODE

'Hyloxalus_faciopunctulatus_JDL_28969','0(1-0)', '9(0-1)', '10(0-1)', '12(0-1)', '14(0-1)', '15(0-1)', '16(0-1)', '28(1-0)', '35(5-6)', '124(6-4)', '191(3-2)'

'Hyloxalus_cepedai_StaMaria_ANDESA_6370'

'Colostethus_poecilonotus_CORBIDI_1960','6(1-0)', '17(0-1)', '56(0-1)', '191(3-1)', '212(0-1)', '215(0-1)', '216(0-1)', '217(0-1)', '224(2-1)', '237(1-0)'

'Silverstoneia_nubicola_SIUC7652','11(0-1)', '13(0-1)', '250(1-0)', '276(1-0)'

'Ranitomeya_yavaricola_181','44(0-2)', '56(0-1)', '57(3-0)', '58(4-0)'

'Ranitomeya_variabilis_Sucumbios_OMNH34091','152(0-1)', '154(1-0)', '262(1-0)', '280(0-1)', '283(0-1)', '294(2-0)', '297(1-2)'

'Ranitomeya_uakarii_MPEG12394','56(0-1)', '253(0-1)'

'Ranitomeya_sirensis_JCS','6(2-3)', '23(1-0)', '27(0-2)', '28(1-2)', '88(0-1)'

'Ranitomeya_reticulata_MJH3754','6(2-1)', '7(3-2)', '50(1-0)'

'Phyllobates_vitattus_839','17(0-1)', '27(2-1)', '28(2-1)', '29(2-1)', '44(2-1)', '124(6-3)', '144(1-0)', '148(0-1)', '150(0-1)', '156(0-1)', '160(0-1)', '227(0-1)'

'Phyllobates_lugubris_USNMFS195116','60(2-13)','115(0-1)', '118(2-1)', '149(1-0)', '152(0-1)', '158(0-1)', '222(1-0)', '265(0-1)'

'Phyllobates_bicolor_1233','17(0-1)','30(1-0)', '49(1-0)', '58(2-0)', '59(5-0)', '60(2-0)', '100(1-0)', '129(0-1)', '130(0-1)', '139(0-1)', '150(0-1)', '163(0-1)', '252(1-0)', '256(0-1)', '259(1-0)', '266(0-2)', '267(0-1)', '274(1-0)', '277(0-1)', '287(1-0)', '297(2-0)', '299(1-0)', '301(1-0)', '304(0-1)', '306(0-1)', '311(1-0)', '312(1-0)'

'Paruwrobates_erythromos_QCAZ37750','5(01-2)', '6(1-2)', '30(1-2)', '124(6-5)', '137(0-1)', '141(0-1)', '189(0-1)', '190(1-0)', '191(3-2)', '222(1-0)'

'Oophaga_granulifera_CWM19044','0(0-2)','28(2-1)', '44(0-1)', '57(3-4)', '59(1-5)', '60(1-2)', '88(0-1)', '103(0-1)', '157(0-1)', '169(0-1)', '170(0-1)', '171(0-1)', '226(0-1)', '249(1-0)', '251(1-0)', '252(1-0)', '253(0-1)', '262(1-0)', '266(2-0)', '295(0-1)'

'Mannophryne_olmonae_UWIZM2732','52(0-1)', '59(0-2)', '185(0-1)', '240(0-1)', '315(0-1)'

'Mannophryne_herminae_TNHCFS5676','7(01-2)', '8(1-2)', '17(0-1)', '59(0-2)',
'60(0-4)', '186(0-1)', '222(1-0)', '256(0-1)', '284(1-0)', '294(0-1)',
'299(1-0)', '300(1-0)', '301(1-0)', '303(1-0)', '305(1-0)', '307(1-0)',
'308(1-0)', '310(1-0)', '311(1-0)', '312(1-0)', '313(1-0)'

'Mannophryne_cordilleriana_TNHCFS5589','6(1-0)', '8(1-0)', '26(2-1)', '27(2-1)',
'28(2-1)', '29(2-1)', '39(2-34)', '46(1-0)', '240(0-1)', '273(1-0)'

'Hyloxalus_vergeli_Quinchas_ALOP_191','131(1-0)', '188(1-0)', '229(0-1)'

'Hyloxalus_subpunctatus_Sumapaz_MAA1401','17(0-1)', '56(0-1)', '212(0-1)'

'Hyloxalus_shuar_CJ2622','5(0-1)', '26(0-1)', '27(0-1)', '30(0-1)', '58(1-3)',
'108(1-2)', '182(0-1)', '197(0-1)', '204(0-1)', '209(0-1)', '210(0-1)',
'211(0-1)', '212(0-1)', '214(0-1)', '215(0-1)', '216(0-1)', '217(0-1)',
'295(0-1)', '301(1-0)', '305(1-0)', '308(1-0)', '309(1-0)', '311(1-0)',
'312(1-0)', '313(1-0)'

'Hyloxalus_pulchellus_QCAZ15964','30(0-2)', '57(2-5)', '184(0-1)', '189(0-1)',
'193(0-1)', '203(1-0)', '224(2-1)', '318(1-0)'

'Hyloxalus_leucophaeus_KU211880','5(1-0)', '6(1-0)', '36(6-4)', '59(2-0)',
'224(1-2)', '226(1-0)', '232(0-1)', '247(0-1)', '248(0-1)'

'Hyloxalus_jacobuspetersi_QCAZ37742','60(0-3)', '178(1-0)', '179(1-0)', '180(1-0)',
'181(1-0)', '190(0-1)', '195(0-1)', '196(0-1)', '197(0-1)', '202(0-1)',
'203(1-0)', '224(2-1)', '287(0-1)'

'Hyloxalus_infraguttatus_CORBIDI_3719','6(1-0)', '11(1-0)', '13(1-0)', '17(1-0)',
'28(0-1)', '29(0-1)', '31(1-0)', '33(2-1)', '38(12-0)', '39(1-0)',
'40(1-0)', '124(5-4)', '127(0-1)', '129(1-0)', '130(1-0)', '131(1-0)',
'132(1-0)', '190(1-0)', '191(3-2)', '203(0-1)', '209(1-0)', '210(1-0)',
'211(1-0)', '212(1-0)', '213(1-0)', '214(1-0)', '215(1-0)', '216(1-0)',
'217(1-0)', '221(0-1)', '223(1-0)', '237(0-1)', '248(1-0)', '256(0-1)',
'270(1-0)', '273(0-1)', '276(1-0)', '282(0-1)', '283(1-0)', '287(0-1)',
'290(1-0)', '297(2-0)', '303(1-0)', '304(1-0)', '315(0-1)', '321(0-1)',
'322(0-1)', '331(0-1)', '341(0-1)', '347(2-1)', '367(1-0)', '373(1-0)'
'Hyloxalus_delatorreae_KU220621','27(0-1)', '108(1-2)', '188(1-0)', '191(3-2)',
'226(1-0)', '229(0-1)', '240(0-1)', '293(0-1)', '314(0-1)', '316(0-1)',
'375(1-0)'

'Hyloxalus_anthracinus_KU223489','57(2-4)', '115(0-1)', '124(35-4)', '200(0-1)',
'201(0-1)', '205(0-1)', '206(0-1)', '259(1-0)', '270(0-1)', '280(2-0)',
'287(0-1)', '314(0-1)', '316(0-1)'

'Excidobates_mysteriosus_JD11.005','0(0-2)', '5(0-1)', '8(2-1)'

'Excidobates_captivus_QCAZ27442','27(0-2)', '42(0-1)', '46(0-1)', '87(1-0)',
'282(1-0)', '294(2-0)', '297(1-2)'

'Epipedobates_tricolor_QCAZ21977','125(0-1)', '275(3-0)', '344(1-0)'

'Epipedobates_espinosai_QCAZ27224','43(0-1)', '52(1-0)', '189(0-1)', '300(1-0)',
'304(1-0)', '305(1-0)', '306(1-0)', '309(1-0)', '310(1-0)', '313(1-0)',
'315(1-0)'

'Dendrobates_auratus_USNM313818','24(3-0)', '151(0-1)', '159(0-1)', '160(0-1)',
'162(0-1)', '261(1-0)', '274(1-0)', '279(1-0)', '280(0-2)', '284(1-2)',
'290(1-2)'

'Cycloramphus_boraceiensis_CFBH5757','0(1-3)', '11(0-1)', '12(0-1)', '13(0-1)',
'14(0-1)', '31(0-1)', '32(0-4)', '34(0-4)', '35(0-5)', '40(0-1)',
'56(0-1)', '112(0-1)', '116(1-0)', '120(0-2)', '124(2-1)', '132(1-0)',
'266(0-1)', '278(1-0)', '286(1-0)', '296(0-1)'

'Crossodactylus_schmidti_MLPA1414','5(1-0)', '21(0-1)', '27(2-1)', '28(2-1)',
'29(2-1)', '30(1-0)', '88(0-1)', '109(1-0)', '118(1-2)', '120(0-2)',
'189(0-1)'

'Colostethus_ruthveni_like_PAG1210','27(2-1)', '31(0-1)', '37(0-2)', '38(0-1)',
'39(0-1)', '40(0-1)', '75(1-0)', '129(1-0)', '183(0-1)', '219(0-1)',
'223(0-1)', '237(1-0)'

'Colostethus_ruthveni_MAR558','30(1-2)', '32(0-2)', '33(0-1)', '116(1-0)', '124(6-4)',
'128(0-1)', '131(1-0)', '137(0-1)', '189(0-1)', '190(1-0)'

'Colostethus_pratti_SIUC7658','43(0-1)', '46(0-1)'

'Colostethus_panamansis_CH5546','58(0-4)', '116(1-0)', '139(0-1)', '198(0-1)',
'224(1-2)', '259(1-0)', '270(1-0)', '275(2-3)', '287(1-0)', '299(1-0)',
'301(1-0)', '304(1-0)', '305(1-0)', '306(1-0)', '307(1-0)', '308(1-0)',
'309(1-0)', '310(1-0)', '311(1-0)', '312(1-0)', '313(1-0)', '314(1-0)',
'317(1-0)'

'Colostethus_latinasus_CH6381','7(1-2)', '17(1-0)', '58(0-3)', '60(0-13)'

'Colostethus_inguinalis_MUJ3247','7(1-2)', '26(1-2)', '30(1-2)', '59(0-5)', '256(1-0)',
'285(0-1)', '293(0-1)', '303(0-1)'

'Leucostethus_fugax_QCAZ16513','17(1-0)', '36(1-2)', '37(1-2)', '38(0-1)',
'39(0-1)', '40(0-1)', '189(0-1)', '191(2-1)', '221(1-0)'

'Leucostethus_argyrogaster_MHNSM22877','8(1-0)', '27(2-1)', '28(2-1)', '197(1-0)'

'Aromobates_ornatissimus_WES626','5(1-0)', '6(1-0)', '7(1-0)', '8(1-0)',
'11(1-0)', '13(1-0)', '17(0-1)', '24(0-1)', '26(1-0)', '30(1-0)',
'31(1-0)', '32(4-0)', '33(1-0)', '34(3-0)', '35(4-0)', '37(3-0)',
'40(1-0)', '108(1-2)', '191(3-2)', '199(1-0)'

'Aromobates_nocturnus_AMNHA130041','33(1-3)', '35(4-8)', '37(3-7)', '59(03-4)',
'60(03-4)', '108(1-0)', '109(1-0)', '119(0-1)', '124(3-2)', '128(0-1)',
'240(0-1)', '247(0-1)', '259(1-0)', '266(0-2)', '270(0-1)', '282(1-0)'

'Aromobates_molinarii_VencesLaMarca','27(1-2)', '28(1-2)', '29(1-2)', '56(0-1)', '58(01-3)'

'Aromobates_meridensis_CVULA7399','46(1-0)'

'Anomaloglossus_wothuja_VUB3736','240(0-1)', '256(0-1)', '275(3-2)', '291(0-1)'

'Anomaloglossus_tamacuarensis_MNRJ38049','17(0-1)', '198(0-1)', '273(0-1)', '275(3-2)', '283(0-1)', '294(0-1)', '295(1-0)', '327(1-2)', '333(2-0)', '348(0-1)', '349(0-1)'

'Anomaloglossus_stepheni_MJH3928','7(1-0)', '8(1-0)', '30(1-0)', '53(1-0)', '102(1-0)', '124(3-4)', '196(0-1)', '201(0-1)', '218(0-1)'

'Anomaloglossus_rufulus_CLBA','0(1-0)', '32(24-0)', '33(1-0)', '34(3-0)', '35(3-0)', '36(2-0)', '37(3-0)', '57(02-35)', '58(0-34)', '59(0-13)', '60(0-13)', '63(0-2)'

'Anomaloglossus_degranvillei_Vences','1(0-1)', '33(1-2)', '35(3-5)', '36(2-4)', '41(0-1)', '57(6-5)', '60(0-3)', '64(1-0)', '108(2-1)', '197(1-0)', '272(1-0)'

'Anomaloglossus_beebei_ROM39631','6(1-2)', '7(1-2)', '8(1-2)', '34(3-1)', '35(3-2)', '36(2-3)', '37(3-1)', '87(1-0)', '104(0-1)', '259(1-0)', '263(0-1)', '266(0-2)', '267(0-1)', '268(0-1)', '269(0-1)', '270(0-1)', '273(0-1)', '277(0-1)', '287(0-1)', '297(2-1)', '318(1-0)'

'Anomaloglossus_baeobatrachus_PK737.4','128(0-1)', '223(1-0)', '270(0-1)', '271(0-1)', '294(0-2)'

'Anomaloglossus_megacephalus_ROM39637','58(0-1)', '270(0-1)', '294(0-1)', '299(1-0)', '301(1-0)', '303(1-0)', '307(1-0)', '311(1-0)', '312(1-0)', '313(1-0)'

'Andinobates_opisthomelas_TG1591','6(1-2)', '27(0-1)', '58(3-2)', '245(1-0)', '262(0-1)'

'Andinobates_minutus_KRL790','27(0-1)', '88(0-1)', '152(0-1)', '267(1-0)', '270(0-1)', '273(0-1)', '280(0-1)', '287(0-1)', '293(0-1)', '297(1-0)', '299(0-1)', '300(0-1)', '301(0-1)', '304(0-1)', '305(0-1)', '306(0-1)', '307(0-1)', '308(0-1)', '311(0-1)', '312(0-1)', '313(0-1)', '319(1-0)'

'Andinobates_fulguritus_MHNUC340','22(1-0)', '51(0-1)', '124(6-5)', '128(0-1)', '130(2-1)', '147(1-0)', '154(1-0)', '275(3-2)', '277(1-0)', '285(0-1)', '290(1-0)', '297(1-2)', '317(0-1)', '337(1-0)'

'Andinobates_dorisswansonae_TG2044','28(1-0)', '29(1-0)'

'Andinobates_cassidyhornae_GECOH1523C','7(2-1)', '8(2-1)', '256(1-0)', '275(3-2)'

'Ameerega_trivittata_MPEG12504','62(0-1)', '130(1-0)', '133(1-0)', '144(1-0)', '158(0-1)', '162(0-1)', '184(0-1)', '185(0-1)', '187(0-1)', '197(1-0)', '221(1-0)', '267(0-1)', '273(0-1)', '282(1-0)', '283(0-1)', '284(1-0)',

'296(0-1)', '298(0-1)', '318(1-0)', '344(1-0)', '359(0-1)'

'Ameerega_simulans_EsimQuinceviii63','29(1-2)'

'Ameerega_silverstonei_646','5(0-1)', '6(0-1)', '51(1-0)', '56(0-1)', '116(1-0)',
'129(1-0)', '130(1-0)', '131(1-0)', '132(1-0)', '143(1-0)', '147(1-0)',
'160(0-1)', '164(0-1)', '270(0-1)', '273(0-1)', '318(1-0)'

'Ameerega_rubriventris_KS37','45(0-1)', '266(0-1)', '267(0-1)'

'Ameerega_petersi_MJH3715','225(1-0)', '275(2-3)', '280(0-2)', '299(1-0)', '301(1-0)'

'Ameerega_macero_LR742','26(0-1)', '52(1-0)', '90(3-2)', '144(1-0)', '145(0-1)',
'148(0-1)', '162(0-1)', '197(1-0)', '208(1-0)', '271(0-1)', '276(1-0)',
'279(0-1)', '297(2-0)', '302(0-1)', '310(0-1)', '314(0-1)', '317(0-1)'

'Ameerega_hahneli_QCAZ19240','24(0-2)', '45(0-1)', '57(35-4)', '58(3-2)', '146(0-1)',
'152(0-1)', '164(0-1)', '186(1-0)', '188(0-1)', '190(1-0)', '191(2-3)',
'221(1-0)', '224(2-1)', '229(0-1)', '249(1-0)', '252(1-0)', '273(0-1)',
'278(1-0)', '281(0-1)', '282(1-0)', '284(1-0)', '287(0-1)', '294(0-2)',
'296(0-1)', '298(0-1)'

'Ameerega_flavopicta_MZUSP111790','24(2-1)', '187(0-1)', '190(1-0)', '229(1-0)',
'256(0-1)', '259(1-0)', '294(2-1)'

'Ameerega_braccata_MRT5603','17(0-1)', '28(0-12)', '221(1-0)', '240(1-0)'

'Ameerega_boehmei_E81_3','17(0-1)', '187(0-1)', '197(1-0)', '221(1-0)'

'Ameerega_berohoka_NMM2011','44(5-4)', '45(0-1)', '57(3-4)', '230(0-1)'

'Ameerega_bassleri_MHNSM22600','8(1-0)', '45(1-0)', '122(0-1)', '151(0-1)',
'153(0-1)', '154(0-1)', '287(0-1)', '290(1-0)'

'Allobates_tapajos_APL12965','0(1-2)', '5(1-0)', '6(1-0)', '34(0-1)', '35(0-2)',
'57(2-0)'

'Allobates_olfersioides_MNRJ79897','5(1-0)', '6(1-0)', '7(1-0)', '8(1-0)',
'27(2-1)', '28(2-1)', '29(2-1)', '43(0-1)', '86(0-1)', '122(0-1)',
'127(0-1)', '177(1-0)', '187(0-1)', '188(1-0)', '190(1-0)', '197(0-1)',
'221(1-0)', '265(0-1)', '267(0-1)', '283(0-1)', '295(1-0)', '301(1-0)',
'304(1-0)', '305(1-0)', '307(1-0)', '308(1-0)', '309(1-0)', '310(1-0)',
'313(1-0)'

'Allobates_magnussoni_MPEG11923','228(1-0)', '232(0-1)', '293(0-1)', '294(0-1)',
'296(0-1)'

'Allobates_insperatus_QCAZ16533','59(0-2)', '115(0-1)', '128(1-0)', '211(1-0)',
'214(1-0)', '271(0-1)', '279(1-0)', '280(0-1)', '287(1-0)', '304(1-0)',
'342(0-1)', '349(0-1)', '361(1-2)'

'Allobates_chalcopis_Alca1','7(01-2)', '26(0-1)', '29(2-1)', '47(1-0)', '51(1-0)',

'57(2-4)', '59(0-4)', '87(1-0)', '89(2-1)', '105(0-1)', '191(0-1)',
'277(0-1)', '281(0-1)', '289(1-0)', '290(1-0)', '294(0-2)', '295(1-0)',
'296(0-1)', '297(2-1)'

'Allobates_algorei_TNHCFS5551','36(1-0)','37(1-0)'

'Adelphobates_quinquevittatus_OMNH36665','22(1-0)', '42(0-1)', '50(0-1)', '154(1-0)',
'178(0-1)', '179(0-1)', '180(0-1)', '181(0-1)', '182(0-1)', '209(0-1)',
'210(0-1)', '211(0-1)', '212(0-1)', '213(0-1)', '214(0-1)', '215(0-1)',
'217(0-1)', '222(1-0)', '225(1-0)', '227(0-1)', '229(0-1)', '232(1-0)',
'256(0-1)', '294(2-0)'

Node_327 327','56(0-1)'

Node_328 328','6(1-0)', '52(0-1)', '108(1-2)', '122(0-1)', '124(6-3)', '171(0-1)',
'178(0-1)', '179(0-1)', '180(0-1)', '181(0-1)', '197(0-1)', '232(0-1)',
'282(1-0)', '285(0-1)', '290(1-0)', '328(1-0)'

Node_329 329','293(0-1)', '300(0-1)', '302(0-1)'

Node_330 330','226(0-1)'

Node_331 331','209(1-0)', '210(1-0)'

Node_332 332','37(4-0)', '118(1-2)', '287(0-1)', '344(0-1)'

Node_334 334','34(1-0)', '36(1-0)', '37(1-0)', '203(1-0)'

Node_335 335','191(3-2)', '196(1-0)', '197(1-0)', '202(1-0)'

Node_336 336','17(0-1)', '212(0-1)'

Node_337 337','39(5-23)', '223(0-1)'

Node_338 338','237(1-0)'

Node_339 339','11(0-1)', '13(0-1)', '31(0-1)', '32(0-4)', '33(0-2)', '38(0-34)',
'39(0-5)', '40(0-1)', '126(0-1)', '129(1-0)'

Node_340 340','8(1-0)', '35(5-6)', '75(1-0)', '129(0-1)', '130(0-1)', '171(0-1)',
'203(0-1)', '218(0-1)', '219(0-1)', '220(0-1)'

Node_341 341','29(2-1)', '43(0-1)', '130(0-2)', '137(0-1)', '183(0-1)', '184(0-1)',
'189(0-1)', '190(1-0)', '218(0-1)', '219(0-1)', '226(1-0)', '232(1-0)'

Node_342 342','75(1-0)', '191(3-12)', '207(1-0)', '263(0-1)', '284(1-0)', '300(1-0)',
'303(1-0)', '304(1-0)', '305(1-0)', '307(1-0)', '308(1-0)', '309(1-0)',
'310(1-0)', '313(1-0)', '315(1-0)', '317(1-0)', '322(0-1)', '323(0-1)',
'333(2-1)', '336(0-1)', '361(1-0)'

Node_343 343','27(0-1)', '191(3-2)', '226(1-0)'

Node_344 344','108(1-2)', '293(0-1)', '317(1-0)'

Node_345 345','6(1-0)', '8(1-0)', '209(0-1)', '210(0-1)', '211(0-1)', '212(0-1)', '214(0-1)', '215(0-1)', '216(0-1)', '217(0-1)'

Node_346 346','273(0-1)', '300(0-1)', '348(0-1)', '364(1-0)', '373(1-0)'

Node_347 347','190(1-0)'

Node_348 348','52(0-1)', '178(0-1)', '179(0-1)', '180(0-1)', '181(0-1)', '232(0-1)', '280(0-2)', '287(1-0)'

Node_349 349','221(1-0)'

Node_350 350','6(0-1)', '23(1-0)', '31(0-1)', '32(0-4)', '33(0-3)', '34(1-4)', '36(1-4)', '37(1-4)', '38(0-4)', '39(0-3)', '40(0-1)', '108(2-0)', '109(1-0)', '129(1-0)', '171(1-0)', '175(0-1)', '176(1-2)', '177(1-2)', '178(1-0)', '179(1-0)', '180(1-0)', '181(1-0)', '189(0-1)', '191(3-4)', '224(1-2)', '225(1-0)', '234(0-1)', '235(0-1)', '236(2-1)', '238(0-1)', '239(0-1)'

Node_351 351','56(0-1)', '57(2-5)'

Node_352 352','116(1-0)'

Node_353 353','182(0-1)', '209(0-1)', '210(0-1)', '211(0-1)', '214(0-1)'

Node_354 354','58(0-3)', '87(1-0)', '114(0-3)', '129(1-0)', '135(0-1)', '259(1-0)', '262(1-2)', '267(0-1)', '274(1-0)', '279(1-0)', '289(1-0)', '294(0-2)', '299(1-0)', '301(1-0)', '304(1-0)', '305(1-0)', '307(1-0)', '308(1-0)', '309(1-0)', '310(1-0)', '311(1-0)', '312(1-0)', '313(1-0)', '332(1-0)'

Node_355 355','11(0-1)', '13(0-1)', '57(2-3)', '58(0-4)', '59(0-1)', '60(0-1)'

Node_356 356','62(0-1)', '86(0-1)', '227(0-1)', '241(0-1)', '243(1-0)', '244(1-0)', '245(1-0)', '246(0-1)', '247(0-1)', '248(0-1)', '249(1-0)', '251(1-0)', '252(1-0)', '256(0-1)', '259(1-0)', '261(1-0)', '291(0-1)', '321(1-0)', '324(0-1)', '332(1-2)', '341(1-2)', '345(1-0)', '346(1-0)', '375(1-0)'

Node_357 357','36(0-1)', '37(0-1)'

Node_358 358','52(0-1)', '130(0-1)', '192(0-1)', '193(0-1)', '197(0-1)'

Node_359 359','57(2-4)', '242(0-1)'

Node_360 360','17(0-1)'

Node_361 361','17(0-1)', '59(0-125)', '65(1-0)', '294(1-2)', '296(0-1)', '297(2-0)', '298(0-1)', '300(0-1)', '302(0-1)', '303(0-1)'

Node_362 362','226(0-1)', '300(0-1)', '302(0-1)'

Node_363 363','11(0-1)', '13(0-1)', '24(2-0)', '31(0-1)', '32(0-4)', '34(0-34)', '35(0-4)', '40(0-1)', '189(0-1)', '209(1-0)', '210(1-0)', '361(1-0)'

Node_364 364','351(1-0)', '367(1-0)'

Node_365 365','30(0-2)', '90(0-2)'

Node_366 366','7(2-3)', '50(0-1)'

Node_367 367','27(2-0)', '149(1-0)', '222(1-0)', '237(1-0)', '256(0-1)', '319(0-1)'

Node_368 368','5(1-0)', '44(4-0)', '130(0-2)', '133(1-0)', '221(1-0)', '232(0-1)', '259(1-0)', '263(0-1)', '266(0-2)', '267(0-1)', '268(0-1)', '269(0-1)', '311(1-0)', '312(1-0)', '324(0-1)', '333(2-0)', '335(1-2)', '339(1-0)', '342(0-1)', '343(0-1)', '344(1-0)', '361(1-0)', '363(2-1)', '370(1-0)', '372(1-0)'

Node_369 369','63(0-2)'

Node_370 370','341(1-0)'

Node_371 371','276(1-0)'

Node_372 372','130(0-1)', '146(0-1)', '270(0-1)', '276(1-0)', '297(2-0)', '299(1-0)', '301(1-0)', '311(1-0)', '312(1-0)'

Node_373 373','44(4-2)', '57(2-4)', '60(0-2)', '142(0-1)', '319(0-1)'

Node_374 374','30(1-0)', '44(2-3)', '49(1-0)', '57(4-2)', '58(2-0)', '59(5-0)', '60(2-0)', '84(2-1)', '100(1-0)', '119(0-1)', '123(0-1)', '124(5-6)', '130(0-1)', '143(1-0)', '144(1-0)', '147(1-0)', '163(0-1)', '256(0-1)', '267(0-1)', '274(1-0)', '277(0-1)', '287(1-0)', '297(2-0)', '299(1-0)', '301(1-0)', '304(0-1)', '306(0-1)', '311(1-0)', '312(1-0)'

Node_375 375','84(1-2)', '124(6-5)', '128(0-1)', '165(0-1)', '255(0-1)', '279(1-0)', '282(1-0)'

Node_376 376','60(0-1)'

Node_377 377','27(2-1)', '87(1-0)', '233(1-0)'

Node_378 378','148(0-1)', '150(0-1)', '152(0-1)', '289(1-0)'

Node_379 379','6(12-0)', '56(0-1)', '59(1-4)', '96(0-1)', '116(1-0)', '130(2-1)', '147(1-0)', '270(0-1)', '275(3-1)', '276(1-0)', '279(1-0)', '280(0-2)', '285(0-1)', '293(0-1)'

Node_380 380','32(4-3)'

Node_381 381','26(1-2)', '55(0-1)'

Node_382 382','33(2-1)', '37(4-3)', '46(0-1)'

Node_383 383','6(1-0)', '29(2-1)', '34(3-1)', '36(34-1)', '37(3-1)', '38(2-1)', '39(2-1)', '46(1-0)'

Node_384 384','323(0-1)', '355(2-0)', '367(1-0)'

Node_385 385','17(1-0)', '40(1-0)', '53(0-1)', '58(0-3)', '224(1-2)'

Node_386 386','62(0-1)', '118(2-1)', '122(0-1)', '123(1-0)', '190(0-1)', '224(2-1)', '268(0-1)', '282(1-0)', '283(0-1)', '304(1-0)', '305(1-0)', '306(1-0)', '307(1-0)', '308(1-0)', '347(1-2)', '348(1-0)', '352(1-0)', '355(0-2)', '356(0-1)', '361(0-1)'

Node_387 387','131(1-0)', '188(1-0)', '224(1-2)', '229(0-1)', '237(0-1)'

Node_388 388','24(1-2)', '54(1-0)', '58(1-0)', '59(3-0)', '60(3-0)', '63(0-2)', '93(0-1)', '108(1-2)', '182(0-1)', '184(0-1)', '190(0-1)', '192(0-1)', '193(0-1)', '209(0-1)', '210(0-1)', '211(0-1)', '214(0-1)', '215(0-1)', '216(0-1)', '217(0-1)', '226(1-0)', '229(0-1)', '240(1-0)', '265(0-1)', '270(0-1)', '280(0-2)', '284(1-0)', '295(0-1)', '317(1-0)', '332(1-2)'

Node_389 389','5(0-1)', '26(0-1)', '27(0-2)', '28(1-2)', '37(2-1)', '56(1-0)', '208(1-0)', '232(1-0)', '279(0-1)'

Node_390 390','280(2-0)', '300(0-1)', '364(1-0)'

Node_391 391','37(0-2)', '54(0-1)', '56(0-1)', '60(0-3)', '224(2-1)'

Node_392 392','7(1-0)'

Node_393 393','6(1-0)', '8(1-0)', '37(0-2)'

Node_394 394','0(1-0)', '27(0-2)', '30(0-2)', '60(0-5)', '64(1-0)', '186(0-1)', '188(1-0)', '276(1-0)', '290(1-0)', '292(1-0)', '295(0-1)', '303(1-0)', '304(1-0)', '305(1-0)', '306(1-0)', '307(1-0)', '308(1-0)', '313(1-0)'

Node_395 395','11(1-0)', '13(1-0)', '223(1-0)', '297(2-0)'

Node_396 396','24(1-0)', '27(1-0)', '30(1-0)', '32(3-4)', '34(3-4)', '36(3-6)', '37(3-4)', '38(2-4)', '39(2-5)', '171(1-0)', '184(1-0)', '208(1-0)', '240(1-0)', '256(0-1)', '298(1-0)'

Node_397 397','294(0-1)'

Node_398 398','232(1-0)', '304(1-0)'

Node_399 399','0(1-0)', '17(0-1)', '56(0-1)', '57(2-3)', '60(0-3)', '189(0-1)', '191(3-2)', '209(0-1)', '210(0-1)', '211(0-1)', '212(0-1)'

Node_400 400','28(1-2)', '43(0-1)', '184(0-1)', '190(1-0)', '225(1-0)', '226(1-0)', '232(1-0)'

Node_401 401','8(1-2)', '11(0-1)', '13(0-1)', '31(0-1)', '32(0-4)', '33(0-2)', '36(01-5)', '37(0-3)', '38(0-4)', '39(0-5)', '40(0-1)', '60(0-3)', '188(1-0)', '200(0-1)', '205(0-1)', '273(0-1)', '282(1-0)', '319(0-1)'

Node_402 402','6(1-2)', '7(1-2)', '8(1-2)', '53(0-1)', '56(0-1)', '203(0-1)', '219(0-1)', '237(1-0)', '273(0-1)', '315(0-1)', '316(0-1)'

Node_403 403','27(1-2)', '62(0-1)', '183(1-0)', '189(0-1)', '191(2-1)', '203(1-0)', '206(0-1)', '233(0-1)', '273(1-0)', '275(3-2)', '280(2-0)', '293(1-0)', '304(1-0)', '308(1-0)', '309(1-0)', '311(1-0)', '312(1-0)', '313(1-0)'

Node_404 404','5(0-1)', '6(0-1)', '8(0-1)', '205(0-1)', '229(0-1)', '295(0-1)'

Node_405 405','240(0-1)', '273(0-1)', '314(0-1)'

Node_406 406','6(1-0)', '7(1-0)', '8(1-0)', '32(3-2)', '34(3-1)', '56(1-0)', '59(3-4)', '191(3-1)', '232(1-0)', '273(0-1)', '275(3-2)', '279(0-1)', '280(0-2)', '292(1-0)', '297(2-0)'

Node_407 407','33(0-2)', '209(0-1)', '210(0-1)', '211(0-1)', '212(0-1)', '214(0-1)', '215(0-1)', '216(0-1)', '217(0-1)', '221(1-0)', '248(0-1)', '270(0-1)', '283(0-1)', '321(1-0)', '341(1-0)', '347(1-2)'

Node_408 408','6(1-0)', '33(0-1)', '127(0-1)', '129(1-0)', '131(1-0)', '256(0-1)', '304(1-0)'

Node_409 409','6(1-0)', '8(1-0)', '32(0-2)', '33(0-1)', '34(0-1)', '59(3-4)', '60(3-4)', '178(1-0)', '179(1-0)', '180(1-0)', '181(1-0)', '191(3-2)', '248(0-1)', '265(0-1)', '273(0-1)', '279(0-1)', '283(0-1)', '293(0-1)', '297(2-0)', '302(0-1)'

Node_410 410','8(1-2)', '28(1-2)', '53(0-2)', '59(3-0)', '181(1-0)', '188(1-0)', '191(3-2)', '203(1-0)', '205(0-1)', '225(1-0)', '271(0-1)', '280(2-0)', '287(0-1)', '293(0-1)', '304(1-0)', '306(1-0)', '314(0-1)'

Node_411 411','24(2-0)', '51(1-0)', '59(3-5)', '263(0-1)', '266(0-2)', '268(0-1)', '279(0-1)'

Node_412 412','0(1-2)', '61(1-0)'

Node_413 413','52(0-1)', '53(0-1)', '58(0-14)', '188(1-0)', '270(0-1)', '273(0-1)', '287(1-0)', '297(2-0)', '323(0-1)', '355(2-0)', '367(1-0)'

Node_414 414','8(1-2)', '26(0-1)', '28(1-2)', '30(0-1)', '203(1-0)', '232(1-0)', '297(2-0)'

Node_415 415','8(1-2)', '101(0-2)', '103(0-2)', '115(0-1)', '178(1-0)', '179(1-0)', '180(1-0)', '181(1-0)', '315(1-0)', '323(0-1)', '330(2-0)', '333(2-1)', '339(1-0)', '347(1-2)', '351(1-0)'

Node_416 416','64(1-0)'

Node_417 417','120(0-1)'

Node_418 418','57(2-5)', '58(5-3)', '182(0-1)', '183(0-1)', '217(0-1)', '280(0-2)', '297(2-0)'

Node_419 419','30(1-0)', '34(0-1)'

Node_420 420','27(2-1)', '28(2-1)', '29(2-1)', '58(0-5)', '59(0-3)', '60(0-3)', '141(0-1)', '265(0-1)', '271(0-1)', '300(0-1)', '315(0-1)', '356(0-1)'

Node_421 421','5(1-0)', '6(1-0)', '43(0-1)', '57(5-0)', '58(3-0)', '59(3-0)', '60(3-0)', '115(0-1)', '124(5-3)', '130(1-0)', '132(1-0)', '141(1-0)', '280(2-1)', '285(0-1)'

Node_422 422','188(1-0)', '225(1-0)', '273(0-1)', '293(0-1)'

Node_423 423','5(1-0)', '6(1-0)', '7(1-0)', '8(1-0)', '75(1-0)', '130(1-0)', '137(0-1)', '271(1-0)', '280(0-1)', '316(0-1)'

Node_424 424','130(1-0)', '131(1-0)', '203(0-1)', '229(0-1)', '276(1-0)', '282(1-0)', '283(0-1)', '284(1-0)', '285(0-2)', '296(0-1)', '302(0-1)', '327(0-2)', '328(1-0)', '333(2-1)', '340(0-2)'

Node_425 425','0(1-0)', '101(0-2)', '103(0-2)', '153(0-1)', '162(0-1)', '276(1-0)', '359(0-1)'

Node_426 426','6(1-0)', '11(0-1)', '13(0-1)', '17(0-1)', '48(1-0)', '56(0-1)', '79(0-1)', '176(1-0)', '225(1-0)'

Node_427 427','0(1-0)', '1(0-1)', '27(2-1)', '31(0-1)', '32(0-4)', '36(0-6)', '37(0-6)', '38(0-6)', '39(0-5)', '40(0-1)', '76(0-1)'

Node_428 428','191(3-4)', '223(0-1)', '226(1-2)'

Node_429 429','36(0-1)', '37(0-1)'

Node_430 430','137(0-1)', '256(0-1)', '270(0-1)', '314(0-1)'

Node_431 431','17(0-1)', '333(2-1)', '340(0-2)', '364(1-0)'

Node_432 432','170(0-1)', '171(0-1)', '178(0-1)', '179(0-1)', '180(0-1)', '181(0-1)', '196(0-1)', '197(0-1)', '203(0-1)'

Node_433 433','24(2-1)', '56(0-1)', '58(0-14)', '203(0-1)', '226(0-1)', '237(1-0)'

Node_434 434','62(0-1)'

Node_435 435','52(1-0)', '103(0-1)', '178(1-0)', '179(1-0)', '240(1-0)', '276(1-0)'

Node_436 436','24(2-0)', '31(0-1)', '32(0-23)', '34(0-2)', '35(0-4)', '36(0-3)', '37(0-2)', '38(0-2)', '39(0-2)', '40(0-1)', '108(2-1)', '124(4-5)', '192(1-0)', '193(1-0)', '203(0-1)', '223(0-1)', '229(0-1)'

Node_437 437','5(1-0)', '6(1-0)', '184(0-1)', '225(1-0)'

Node_438 438','27(2-1)', '28(2-1)', '29(2-1)'

Node_439 439','222(1-0)'

Node_440 440','297(2-0)'

Node_441 441','37(4-3)'

Node_442 442','76(0-1)', '190(1-0)', '194(1-2)', '197(0-1)', '344(0-1)'

Node_443 443','5(1-0)', '6(1-0)', '26(1-0)', '43(0-1)', '85(1-0)', '89(2-0)', '173(0-1)', '267(0-1)', '281(0-1)', '297(2-1)'

Node_444 444','37(3-2)', '57(02-6)', '189(1-0)', '282(1-0)'

Node_445 445','33(2-1)', '35(4-3)', '108(1-2)'

Node_446 446','11(1-0)', '13(1-0)', '51(1-0)', '78(1-0)'

Node_447 447','5(1-0)', '24(0-1)', '26(1-0)', '39(0-2)', '41(0-1)', '43(0-1)', '240(0-1)', '276(0-1)', '319(0-1)'

Node_448 448','46(0-1)'

Node_449 449','0(0-2)'

Node_450 450','116(1-0)', '137(0-1)', '148(0-1)', '279(1-0)'

Node_451 451','150(0-1)', '262(1-0)', '298(0-1)'

Node_452 452','0(1-2)', '27(2-1)', '28(2-1)', '29(2-1)', '59(0-3)', '60(0-3)', '141(0-1)', '180(0-1)', '181(0-1)', '182(0-1)', '183(0-1)', '186(0-1)', '212(0-1)', '217(0-1)', '304(1-0)', '305(1-0)', '307(1-0)', '308(1-0)', '309(1-0)', '310(1-0)', '311(1-0)', '312(1-0)'

Node_453 453','27(1-0)', '28(1-0)', '58(3-4)', '59(3-1)', '60(3-1)'

Node_454 454','17(1-0)', '294(0-2)'

Node_455 455','188(1-0)', '287(1-0)', '313(1-0)'

Node_456 456','17(1-0)', '27(1-0)', '28(1-0)', '29(1-0)', '58(3-2)', '60(3-2)', '158(0-1)', '275(2-3)', '276(1-0)'

Node_457 457','5(1-0)', '6(1-0)', '45(0-1)', '294(0-1)'

Node_458 458','7(1-0)', '8(1-0)', '116(1-0)', '159(0-1)', '160(0-1)', '162(0-1)', '187(0-1)', '229(0-1)', '252(1-0)', '271(0-1)', '297(2-0)', '299(1-0)', '301(1-0)'

Node_459 459','28(1-2)', '29(1-2)', '137(0-1)', '319(0-1)'

Node_460 460','52(1-0)', '88(0-1)', '240(1-0)', '291(0-1)', '294(1-2)'

Node_461 461','27(1-2)', '88(0-1)', '266(0-1)', '267(0-1)', '283(0-1)', '304(0-1)', '305(0-1)', '307(0-1)', '308(0-1)', '309(0-1)', '311(0-1)', '312(0-1)', '313(0-1)'

Node_462 462','7(1-0)', '37(0-1)'

Node_463 463','8(1-0)', '226(0-1)'

Node_464 464','3(0-1)', '5(1-0)', '6(1-0)', '44(1-5)', '229(0-1)'

Node_465 465','144(1-0)', '145(1-0)', '150(1-0)', '182(1-0)', '183(1-0)', '187(0-1)', '192(1-0)', '193(1-0)', '266(0-1)', '267(0-1)', '282(1-0)', '284(1-0)', '285(0-1)', '287(0-1)', '299(1-0)', '301(1-0)', '333(0-2)', '340(0-1)', '353(2-0)'

Node_466 466','188(1-0)', '190(1-0)'

Node_467 467','0(1-2)', '6(1-2)', '7(1-2)', '51(1-0)', '57(2-4)', '58(0-2)', '187(0-1)', '229(0-1)'

Node_468 468','108(1-2)', '287(0-1)', '297(2-0)'

Node_469 469','37(4-1)', '128(0-1)', '180(0-1)', '181(0-1)', '208(1-0)', '227(0-1)', '255(0-1)', '282(1-0)'

Node_470 470','6(1-0)', '208(0-1)', '256(1-0)', '275(2-3)', '282(1-0)', '284(1-0)'

Node_471 471','267(0-1)', '297(0-2)'

Node_472 472','43(0-1)', '177(1-0)', '282(0-1)'

Node_473 473','28(2-1)', '221(1-0)', '222(1-0)', '259(1-0)'

Node_474 474','5(1-2)', '8(1-2)', '116(1-0)', '118(1-2)'

FIGURES CAPTIONS

FIGURE 1.—Palmar view of *Anomaloglossus surinamensis* (KU 220993). See the loose skin on hand.

FIGURE 2.—Supernumerary tubercles on the hand of *Ameerega braccata*, in palmar and lateroventral view. Scale = 1 mm.

FIGURE 3.—The median lingual process in *Paruwrobates andinus*. Adult male and its tongue, PSO-CZ 623 (A – D). Tongue of the adult female PSOCZ624 (E). Note the MLP in C and D, and a pit in E.

FIGURE 4.—Ventral body skin texture. Warty skin in *Rheobates palmatus* in a live specimens from Caqueza, Cundinamarca, Colombia (A), and in the preserved specimen MZUSP 106695 (B). Granular ventrolateral flank in *Hyloxalus cepedai*, ICN 55839 (C). Scale = 1 mm.

FIGURE 5.—Tympanic middle ear in poison frogs. Observe the common condition, the tympanic middle ear structures visible externally in *Allobates talamancae*, PD 49 (A) and *Hyloxalus vergeli*, ICN 35428 (C), or no visible in *A. wayuu*, ICN 43248 (B). Tympanic membrane (TM) and tympanic annulus (TA) in Hylodes sp. RFB484 (D), note the extracolumella (Co) under TM. Raised skin in *A. talamancae* shows the connective tissue disc, Ct. (E), and raised TM in Rhinella ornata, uncatalogued specimens (F). Scale = 1 mm.

FIGURE 6.—Subarticular tubercles shape on the fingers. Flattened tubercles in lateroventral view of the hand of *Hyloxalus walesi*, ICN 6318 (A). Rounded (B)

and elongated (C) basal subarticular tubercle of the finger II and III in *H. subpunctatus* ICN 55855, and *Aromobates nocturnus* KU 220983, respectively. Scale = 1 mm.

FIGURE 7.—Sesamoids in poison frogs (Arrow). Present on the finger II of the *Ameerega flavopicta*, MZUSP 100108 (A), and absent in *Hyloxalus* sp_R, DFZ 409 (B). Projection or sesamoids in all fingers of *A. trivittata*, ZUEC 17661 (C), and *Hyloxalus breviquartus* ICN 21667 (D) are observed. In A and B the bones are stained with alizarin red, and C y D are micro-CT reconstructions. Scale = 1 mm.

FIGURE 8.—Basal subarticular tubercle regard to the finger I width (A and B; character 186 and 187), thenar tubercle respect the basal subarticular tubercle (A, C and D; character 188), and thenar tubercle shape (A and D; character 189). Character 186 –187: state 0 (A) and state 1 (B). Character 188: state 0 (C), state 1 (B), and state 2 (A). Character 189: state 0 (D), and state 1 (A). Species are *Colostethus agilis*, KU 181164 (A), *Ameerega pulchripecta*, MZUSP 69846 (B), *Colostethus delatorreae*, KU 192197, and *Hyloxalus* sp. R, DFZ 407 (D). Scale = 1 mm.

FIGURE 9.—Finger III and V length, character 190 and 191 respectively. Character 190: state 0 (A), and state 1 (B). Character 191: state 0 (C), state 1 (D), state 2 (E), state 3 (B), and state 4 (F). Species are *Hyloxalus awa*, MZUSP 122127 (A), *H. maculosus*, ICN 24249 (B), *Anomaloglossus stepheni*, MZUSP 69178 (C), *H. breviquartus*, ICN 21667 (D), *H. arliensis*, DFZ 341 (E), and *H. edwardsi*, ICN 21936 (F). Scale = 1 mm.

FIGURE 10.—Metacarpal ridge/fold (characters 192 – 194). Character 192, state 0, ridge (A), and state 1, tubercle-like (E, F). Character 193, state 0, distal extension reaching/continuous with the postaxial fringe of finger V (A, B), and state 1, no reaching/continuous (D). Character 194, state 0, reaching one-half of palm (B), state 1, reaching two-thirds of palm (A, D), state 2, in contact with the palmar tubercle (C). Species are *Hyloxalus pinguis*, ICN 7670 (A), *Aromobates nocturnus*, KU 220986 (B), *Anomaloglossus baeobatrachus*, MZUSP 122137 (C), *H. pulchellus*, KU 117970 (D), *H. toachi*, MZUSP 76317 (E), and *Ameerega pulchripecta*, MZUSP 69846 (E). Scale = 1 mm.

FIGURE 11.—Swelling on the fingers (Characters 195–202). Phalangeal swelling is present on finger III (196: state 1, A), finger IV (197: state 1, A, F), and finger V (202: state 1, A). Basal swelling on finger IV (200: state 1, B, C, E). Metacarpal swelling (201: state 1, E). Compare sexual differences in D. Species are *Hyloxalus walesi*, adult male ICN 6318 (A, E) and adult female ICN 12739 (E), *H. anthracinus*, adult male KU 120643 (B, E), *H. nexipus*, adult male KU 211810 (C), *H. jacobuspetersi*, adult male MZUSP 132308 (F). Scale = 1 mm.

FIGURE 12.—Ulnar tubercles on the forearm (Characters 203–204). An ulnar tubercle row occurs in *Hyloxalus aeruginosus,* KU 211940 (A, B), and only the antebrachial tubercle is present in *H. anthracinus*, KU 202813 (C). Arrow indicates the tubercle. Scale = 1 mm.

FIGURE 13.—Swelling on the distal end of the upper arm and lower arm (character 205–206). Swelling is restricted to the distal end of the upper arm (A, B), but it extends to the proximal lower arm, see a dark brown area on the internal

forearm (C). Note the un-noticed dull-white swelling on B (arrow), and to confirm was necessary histological evaluation. Species: *Hyloxalus craspedoceps*, adult male KU 211953, ventral view (A), *H. pinguis*, adult male ICN 7682, posteroventral view (B), *H. anthracinus*, adult male KU 202813, lateroventral view (C). Scale = 1 mm.

FIGURE 14.—Occurrence, size, and shape of the basal subarticular tubercle (characters 207–208, 218–220) and shape of the inner metatarsal tubercle (character 221). Character 207: state 0, absent (B, arrow), state 1, present (A, arrow). Character 208: state 0, small (C, arrow), state 1, lesser/equal (A). Character 218 – 220: state 0, rounded/ovoid (A), state 1, elongated (C, D, red circle). Character 221: state 0, rounded/ovoid (A), state 1, elongated (E, red circle). Species: *Hyloxalus subpunctatus*, ICN 55855 (A), *Ectopoglossus saxatilis*, IAvH14613 (B), *Hyloxalus* sp. R, DFZ 407 (C, E), *Aromobates nocturnus*, KU 220983 (D). Scale = 1 mm.

FIGURE 15.—Protrusiveness of the subarticular tubercles of the toes (character 209 – 217). Projected tubercles in *Ameerega flavopicta*, MZUSP 100112, state 1 (A), and flattened tubercles in *Hyloxalus maculosus*, KU 141528, state 0 (B). Foot in lateroventral view. Scale = 1 mm.

FIGURE 16.—Metatarsal fold extension (character 224). The arrow shows the end of the fold. Metatarsal fold reaching half of the plantar surfaces in *Aromobates nocturnus*, KU 220986, state 0 (A), reaching the proximal 2/3 of plantar surface in *Hyloxalus subpunctatus*, ICN 55855, state 1 (B), and reaching the outer metatarsal tubercle level in *Paruwrobates andinus*, PSO-CZ 623, state 2 (C). Scale = 1 mm.

FIGURE 17.—Toe III and V length (character 225–226). Character 225, toe III reaching (state 0, A) or surpassing (state 1, B) the proximal subarticular tubercle of toe IV. Character 226, toe V not reaching (state 0, A), reaching (state 1, B), or surpassing (state 2, C) the proximal subarticular tubercle of toe IV. *Paruwrobates andinus*, PSO-CZ 623 (A), *Hyloxalus subpunctatus*, ICN 55855 (B), *H. edwardsi*, ICN 21936 (C). Scale = 1 mm.

FIGURE 18.—The two types of ventrolateral stripe in a live *Allobates femoralis*. A-type runs by the upper end of the ventrolateral body flank, extending from groin to arm insertion region. B-type runs on lower end of the ventrolateral flanks, from groin to arm insertion region. QCAZ 63892 (A) and QCAZ 48728 (B). Photos from Fauna Web Ecuador, use authorized by S. Ron.

FIGURE 19.—A and B-type ventrolateral stripes in preserved specimens (characters 227–230). Presence of A-type, character 227: state 1 (A). Presence of B-type, character 229, state 1 (A–C). A wavy series of elongate spots (character 230: 0, B) or straight (230: 1, C) ventrolateral stripe. *Allobates femoralis*, MZUSP 77740 (A), *Hyloxalus mittermeieri*, KU 211944 (B), and *Rheobates palmatus*, MZUSP 106695 (C). Scale = 1 mm.

FIGURE 20.—Testis size (character 231). A small testis, 0.2–0.6 of kidney length in *Hyloxalus pinguis,* ICN 7682 (A), and a large testis, 0.9–1 of kidney length in *H. edwardsi*, ICN 21937 (B). Scale = 1 mm.

FIGURE 21.—Insertion of the *m. compressor cloacae* (CC) anterior portion (character 232). CC inserting ventrally and covered by the *m. pyriformis* (P), compare

(A) and (B), where the last muscle was removed (state 0). Anterior portion of the CC inserting anteriorly, uncovered by the *m. pyriformis* (state 1, C). In B, the dotted red line delimited the CC. *Hyloxalus maculosus*, ICN 24253 (A, B), *H. elachyhistus* KU 142376 (C). Other abbreviation: CI, *m. coccygeoiliacus*. U, urostyle. SAC, *m. sphincter ani cloacali*.

FIGURE 22—Absence of the distal slip of the *m. sphincter ani cloacalis* in *Colostethus mertensi*, ICN 8220, in lateral (A) in ventral view (B). Scale = 1mm. Abbreviations: C, cloacal tube. GM, *m. gracilis major*. P, *m. pyriformis*. U, urostyle. RA, *m. rectus abdominis*, SAC, *m. sphincter ani cloacali*. Scale = 1 mm.

FIGURE 23.—Origin of the *m. tensor fascia latae* (TFL, character 236). A posterior origin is shown in A and B (state 2), and a medial origin in B and D (state 1). ICN 55863 (A), ICN 55887 (B), PD 49 (C), KU 133272, *Leucostethus* sp. *fraterdanieli* complex (D). Scale = 1 mm.

FIGURE 24.—*M. gracilis minor* (GMi) showing the second origin on the dermis (inset; character 237: state 1). Ventral view of the left thigh of the *Hyloxalus pinguis*, ICN 7670. *M. gracilis major* (GM). Scale = 1 mm.

FIGURE 25.—The *m. extensor carpi radialis* (ECR) in three poison frogs (characters 238–239). Thin (character 238: 0; A) and robust (character 238: 1; B, C) origin of the internal slip of ECR (isECR in red color). isECR inserting at about distal two-thirds of external slip (esECR or in blue, character 239: 0; A), or at the external slip distal tendon, roughly at radiale level (character 239: 1; B, C). *Rheobates palmatus*, ICN 55887 (A), *Hyloxalus edwardsi*, ICN 21942 (B), *H. ruizi*, ICN 5416

(C). Other muscles: APL, *m. abductor pollicis longus*. ECU, *m. extensor carpi ulnaris*. EDCL, *m. extensor digitorius communis longus*. Scale = 1 mm.

FIGURE 26.—Pattern coloration of the *Hyloxalus azureiventris* (KU 211976; A) and *Ameerega braccata* (MZUSP 100230; B), shows the supralabial line. Scale = 1 mm.

FIGURE 27.—Trees of the first to fifth (1–5th) successive outgroup expansion analysis show the effect on the ingroup topology. Names are *Hyloxalus* clades (details in the text). In the first analysis, the outgroup same as the sister group (*Ectopoglossus* and *Paruwrobates*, Pw). "Ou" denoted outgroup. Note that the Hyloxalinae and *Hyloxalus* monophyly was lost in the fourth and fifth analysis, respectively. Values at nodes are Goddman-Bremer support.

FIGURE 28.—Trees of the sixth to ninth (6–9th) successive outgroup expansion analysis showing the effect on the ingroup topology. Names are *Hyloxalus* clades (details in the text). "Ou" denoted outgroup, Hs is *H. shuar*, EC is *Hyloxalus* sp. ElCopal. Values at nodes are Goddman-Bremer supports.

FIGURE 29.—Effect of the successive outgroup expansion into three *Hyloxalus* clades: *H. bocagei* clade (purple), *H. subpunctatus* clade (blue), and *H. elachyhistus* clade (orange). A dark shade denotes the clade that changes the position. Ordinal numbers below the tree correspond to the number of analysis. Goodman-Bremer on the branch corresponds to the fourth, fifth and sixth SOE analysis in A, the fourth and fifth analysis in B, and the third and fourth analysis in C. *H. bocagei* + indicate the clade composed of *H. bocagei*, *H. leucophaeus*, *H. maculosus*, *H.sauli*,

H. sordidatus, and *Hyloxalus* sp. Amazonas. “Other” designate the remaining members in the *H. subpunctatus* and *H. elachyhistus* clade. See details and support in **Appendix 4.**

FIGURE 30.—Summary of the Hyloxalinae subfamily relationships, obtained from the most parsimonious optimal tree found in the larger evidence analysis to the ingroup relationships. Numbers on the supported nodes are Goodman-Bremer value and unambiguous phenotypic synapomorphies are specify on the select clades (Red square: unambiguous, non-private synapomorphies. Blue square: unambiguous, private synapomorphies. Numbers below square is the character, and numbers into square are primitive–derive character-states transformation).

FIGURE 31.—Optimal hypothesis of relationships of the Aromobatidae family. The most parsimonious tree shows minimum branch-length, unsupported nodes collapsed, supported nodes with Goodman-Bremen value, and select nodes show unambiguous phenotypic synapomorphies (Red square: unambiguous, non-private synapomorphies. Blue square: unambiguous, private synapomorphies. Black square: unambiguous, and non-homoplastic synapomorphies. Numbers below square is the character, and the numbers into the square are primitive–derive character-states transformation).

FIGURE 32.—Optimal hypothesis of relationships of dendrobatids subfamilies, Colostethinae and Dendrobatinae. The most parsimonious tree shows minimum branch-length, unsupported nodes collapsed, supported nodes with Goodman-Bremen value, and select nodes show unambiguous phenotypic synapomorphies (Red square: unambiguous, non-private synapomorphies. Blue

square: unambiguous, private synapomorphies. Black square: unambiguous, and non-homoplastic synapomorphies. Numbers below square is the character, and the numbers into the square are primitive–derive character-states transformation).

FIGURE 33.—A condense *Hyloxalus* phylogeny from the most parsimonious tree of the large ingroup analysis. Only species and candidate species are shown (see text for discussion). For a detailed phylogeny, with support see Appendix 5. Synapomorphies are in Appendix 6.

FIGURE 34.—Optimal hypothesis of relationships of *Hyloxalus bocagei* clade. The most parsimonious tree shows minimum branch-length, unsupported nodes collapsed, supported nodes with Goodman-Bremen value, and select nodes show unambiguous phenotypic synapomorphies (Red square: unambiguous, non-private synapomorphies. Blue square: unambiguous, private synapomorphies. Numbers below square is the character, and the numbers into the square are primitive–derive character-states transformation).

FIGURE 35.—Optimal hypothesis of relationships of *Hyloxalus subpunctatus* clade. The most parsimonious tree shows minimum branch-length, unsupported nodes collapsed, supported nodes with Goodman-Bremen value, and select nodes show unambiguous phenotypic synapomorphies (Red square: unambiguous, non-private synapomorphies. Blue square: unambiguous, private synapomorphies. Black square: unambiguous, and non-homoplastic synapomorphies. Numbers below the square is the character, and the numbers in the square are primitive–derive character-states transformation).

FIGURE 36.—Optimal hypothesis of relationships of a part of *Hyloxalus pulchellus* clade. Clades *H. nexipus, H. sylvaticus–H. pulcherrimus, H. jacobuspetersi–H. delatorreae, H. anthracinus,* and the *H. pulchellus* group. The most parsimonious tree shows minimum branch-length, unsupported nodes collapsed, supported nodes with Goodman-Bremen value, and select nodes show unambiguous phenotypic synapomorphies (Red square: unambiguous, non-private synapomorphies. Numbers below the square is the character, and the numbers in the square are primitive–derive character-states transformation).

FIGURE 37.—Optimal hypothesis of relationships of a part of *Hyloxalus pulchellus* clade. Clades *Hyloxalus* sp. Bongara–*Hyloxalus* sp. PAV, and *H. azureiventris*. The most parsimonious tree shows minimum branch-length, unsupported nodes collapsed, supported nodes with Goodman-Bremen value, and select nodes show unambiguous phenotypic synapomorphies (Red square: unambiguous, non-private synapomorphies. Number below the square is the character, and numbers in the square are primitive–derive character-states transformation).

FIGURE 38.—Optimal hypothesis of relationships of a part of *Hyloxalus pulchellus* clade. Clades *H. shuar–H. idiomelus,* and the *H. infraguttatus*. The most parsimonious tree shows minimum branch-length, unsupported nodes collapsed, supported nodes with Goodman-Bremen value, and select nodes show unambiguous phenotypic synapomorphies (Red square: unambiguous, non-private synapomorphies. Number below the square is the character, and the numbers in the square are primitive–derive character-states transformation).

FIGURE 39.—Optimal hypothesis of relationships of a part of *Hyloxalus pulchellus* clade. Clade *H. elachyhistus*. The most parsimonious tree shows minimum branch-length, unsupported nodes collapsed, supported nodes with Goodman-Bremen value, and select nodes show unambiguous phenotypic synapomorphies (Red square: unambiguous, non-private synapomorphies. Number below the square is the character, and numbers in the square are primitive–derive character-states transformation).

FIGURE 1.—Palmar view of *Anomaloglossus surinamensis* (KU 220993). See the loose skin on hand.

FIGURE 2.—Supernumerary tubercles on the hand of *Ameerega braccata*, in palmar and lateroventral view. Scale = 1 mm.

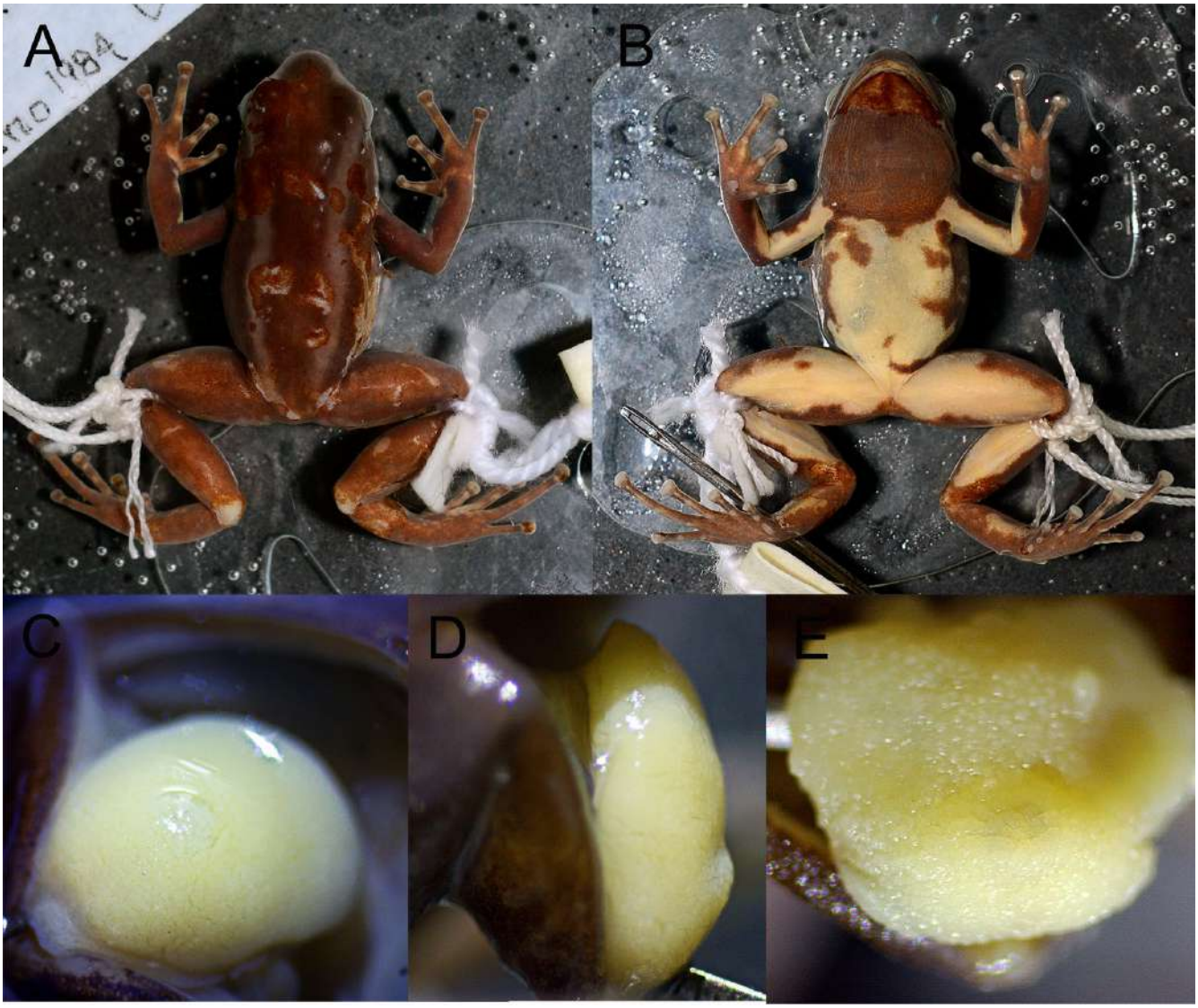

FIGURE 3.—The median lingual process in *Paruwrobates andinus*. Adult male and its tongue, PSO-CZ 623 (A – D). Tongue of the adult female PSOCZ624 (E). Note the MLP in C and D, and a pit in E.

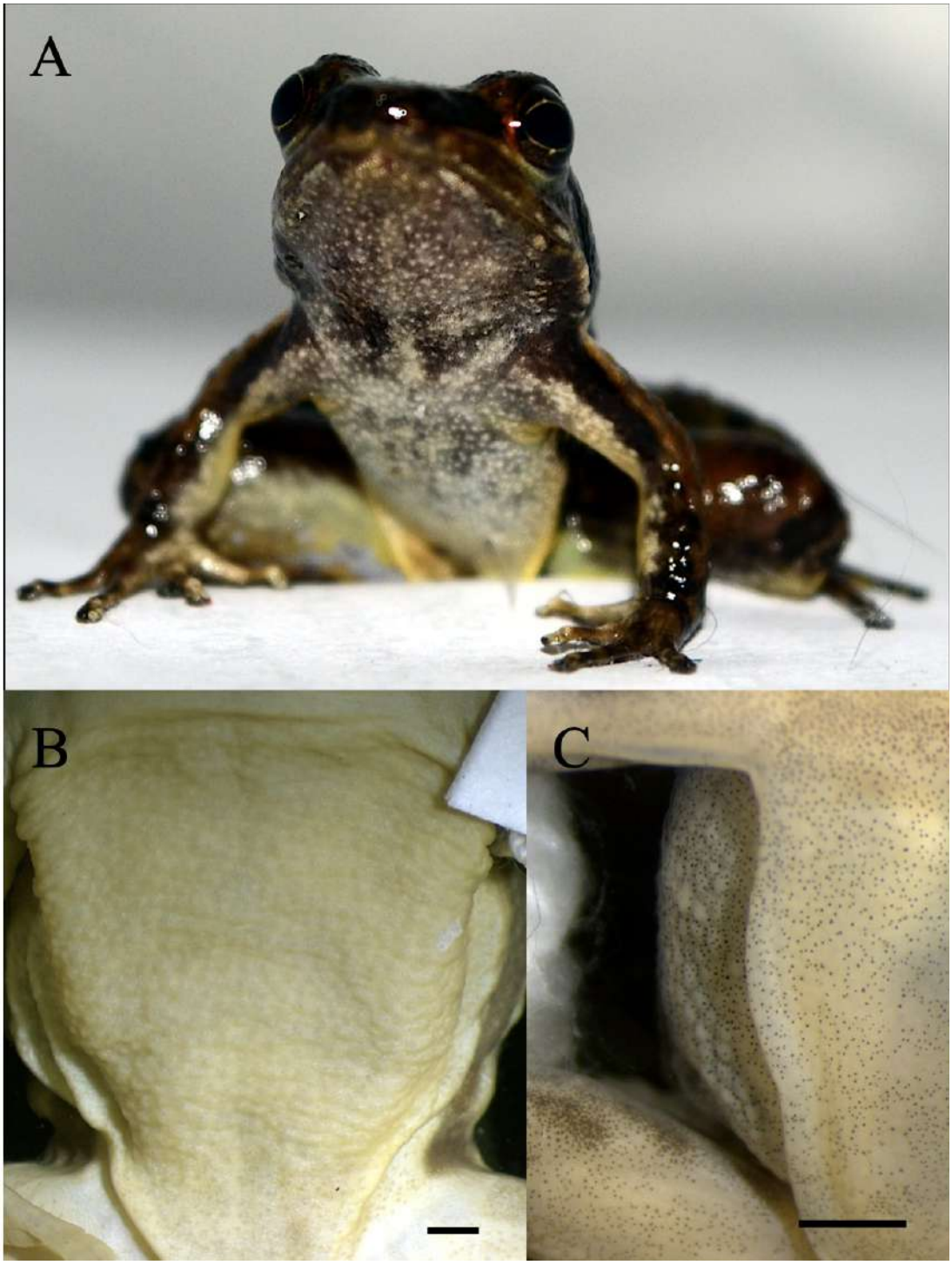

FIGURE 4.—Ventral body skin texture. Warty skin in *Rheobates palmatus* in a live specimens from Caqueza, Cundinamarca, Colombia (A), and in the preserved specimen MZUSP 106695 (B). Granular ventrolateral flank in *Hyloxalus cepedai*, ICN 55839 (C). Scale = 1 mm.

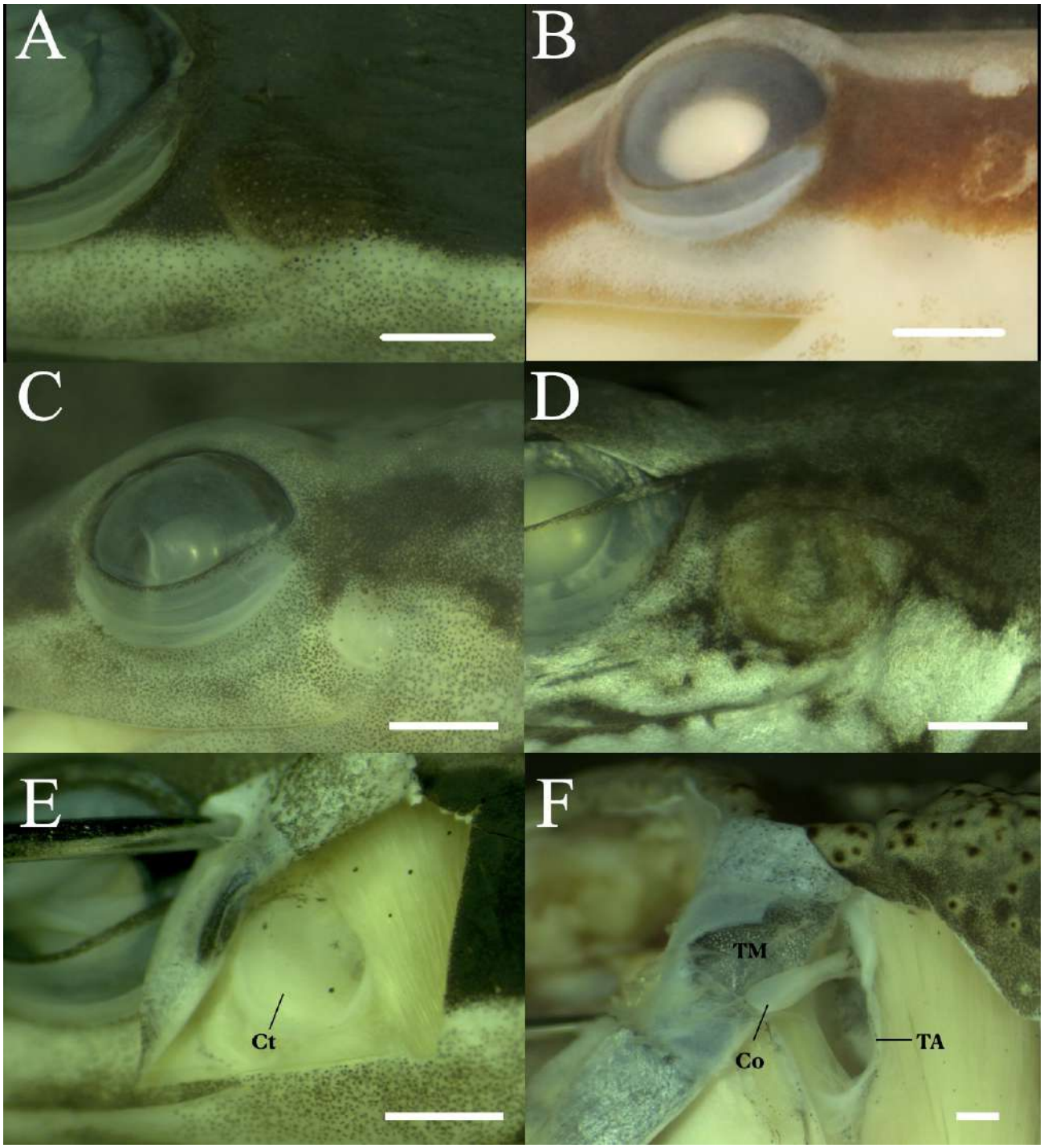

FIGURE 5.—Tympanic middle ear in poison frogs. Observe the common condition, the tympanic middle ear structures visible externally in *Allobates talamancae*, PD 49 (A) and *Hyloxalus vergeli*, ICN 35428 (C), or no visible in *A. wayuu*, ICN 43248 (B). Tympanic membrane (TM) and tympanic annulus (TA) in *Hylodes* sp. RFB484 (D), note the extracolumella (Co) under TM. Raised skin in *A.*

talamancae show the connective tissue disc, Ct. (E), and raised TM in *Rhinella ornata*, uncatalogued specimens (F). Scale = 1 mm.

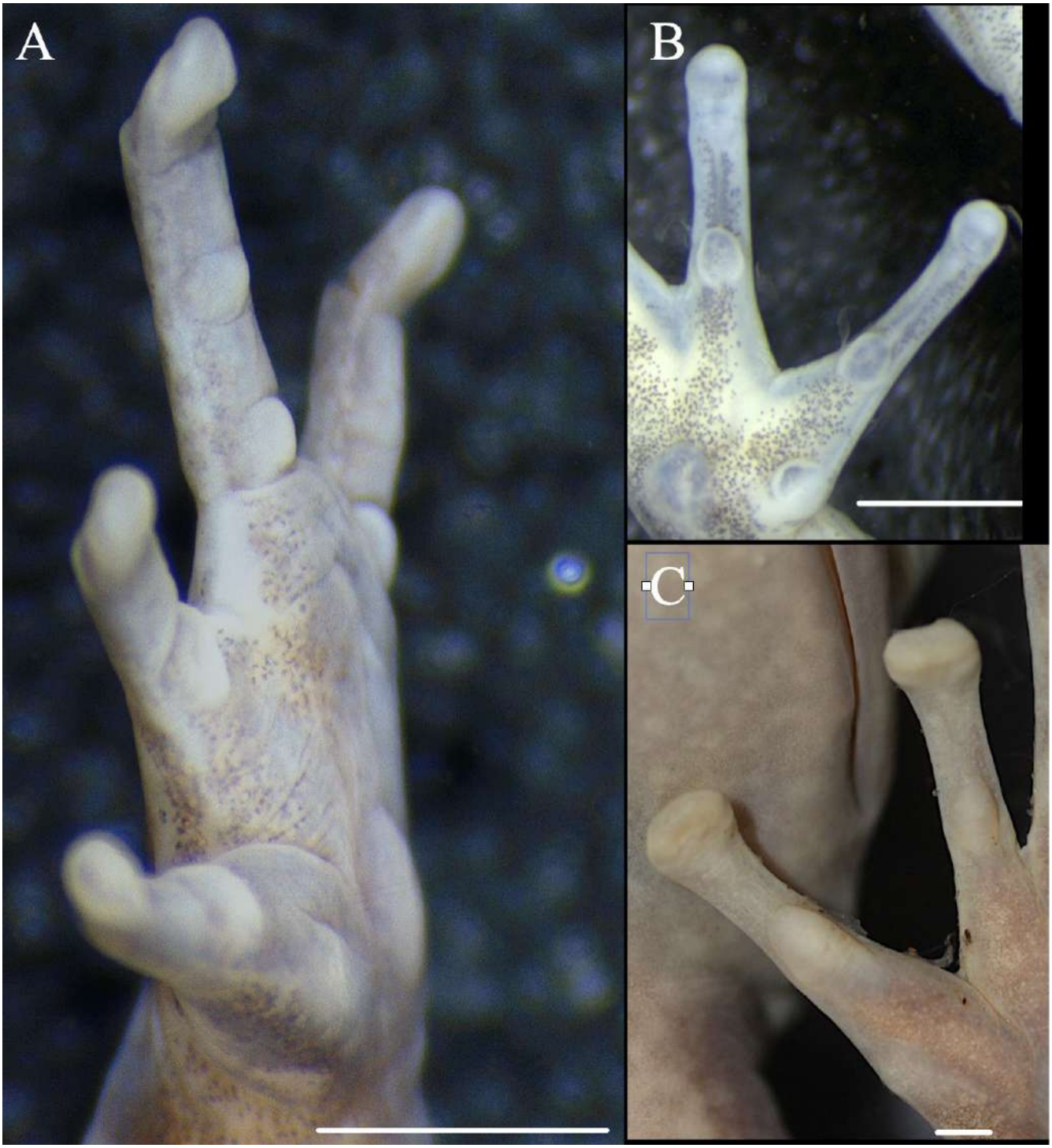

FIGURE 6.—Subarticular tubercles shape on the fingers. Flattened tubercles in lateroventral view of the hand of *Hyloxalus walesi*, ICN 6318 (A). Rounded (B) and elongated (C) basal subarticular

tubercle of the finger II and III in *H. subpunctatus* ICN 55855, and *Aromobates nocturnus* KU 220983, respectively. Scale = 1 mm.

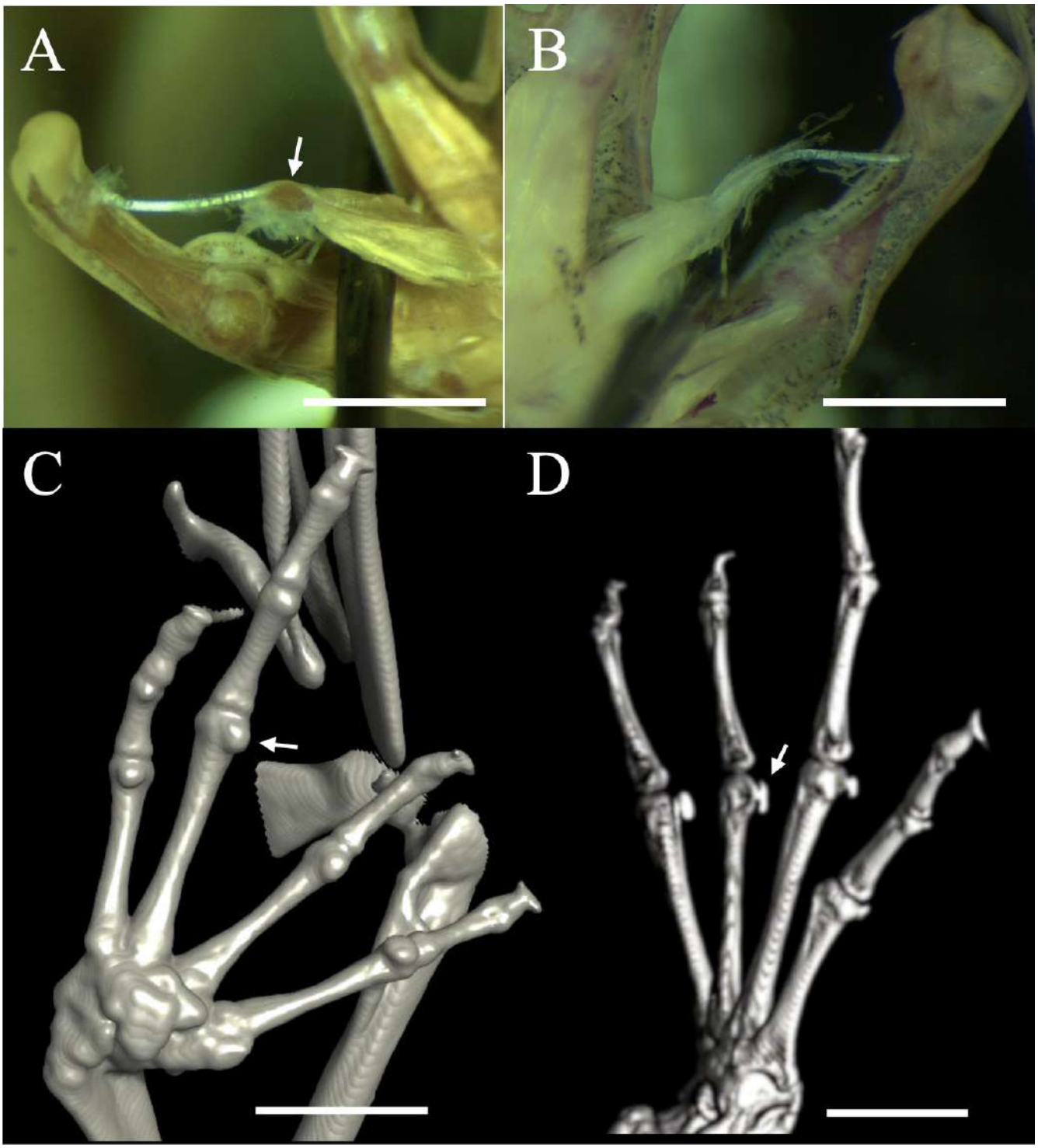

FIGURE 7.—Sesamoids in poison frogs (Arrow). Present on the finger II of the *Ameerega flavopicta*, MZUSP 100108 (A), and absent in *Hyloxalus* sp_R, DFZ 409 (B). Projection or sesamoids in all fingers of *A. trivittata*, ZUEC 17661 (C), and *Hyloxalus breviquartus* ICN 21667 (D) are observed. In A and B the bones stained with alizarin red, and C y D are micro-CT reconstructions. Scale = 1 mm.

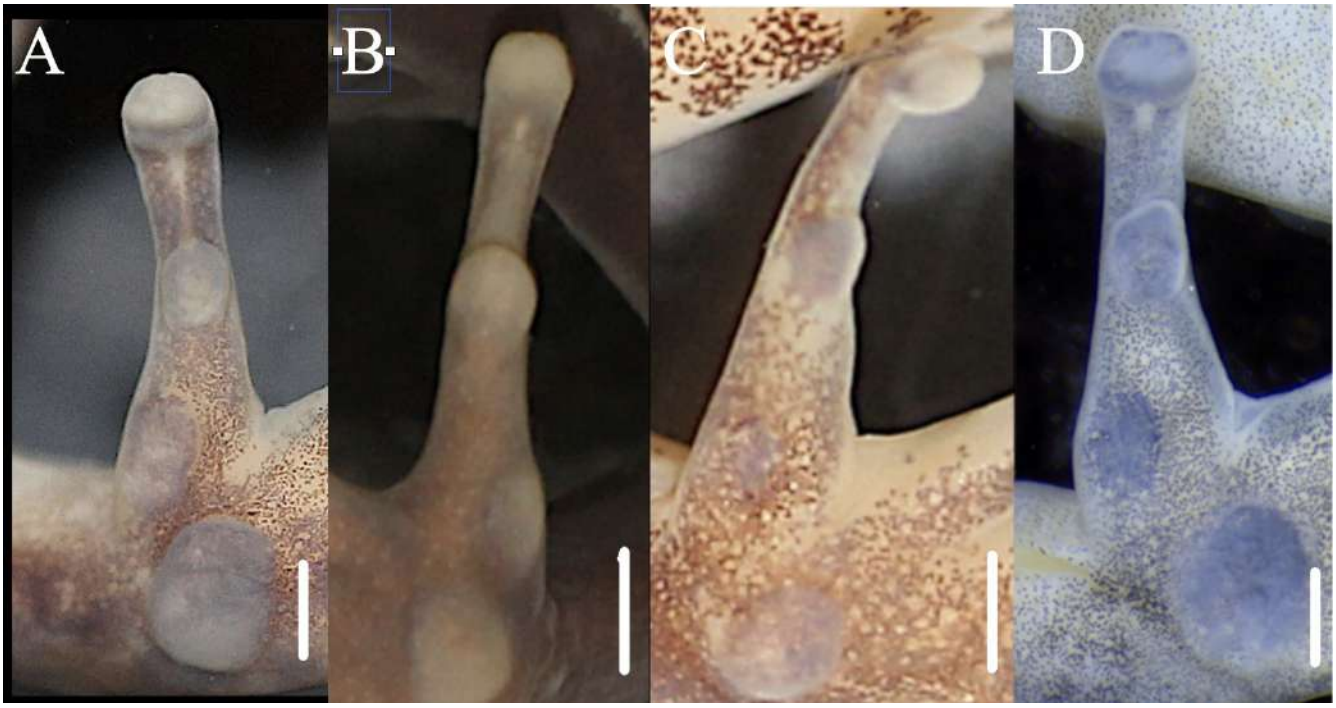

FIGURE 8.—Basal subarticular tubercle regard to the finger I width (A and B; character 186 and 187), thenar tubercle respect the basal subarticular tubercle (A, C and D; character 188), and thenar tubercle shape (A and D; character 189). Character 186 –187: state 0 (A) and state 1 (B). Character 188: state 0 (C), state 1 (B), and state 2 (A). Character 189: state 0 (D), and state 1 (A). Species are: *Colostethus agilis*, KU 181164 (A), *Ameerega pulchripecta*, MZUSP 69846 (B), *Colostethus delatorreae*, KU 192197, and *Hyloxalus* sp. R, DFZ 407 (D). Scale = 1 mm.

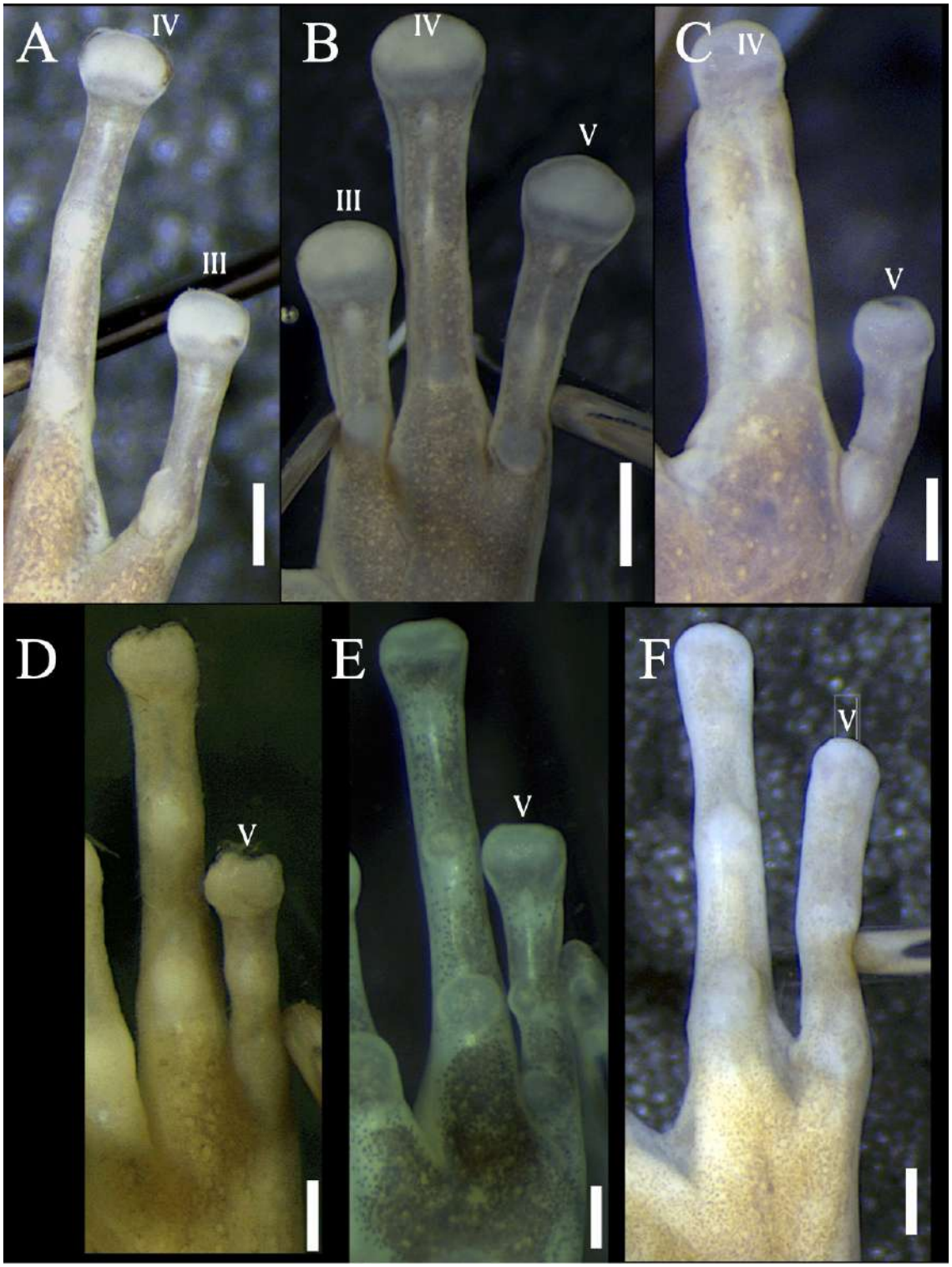

FIGURE 9.—Finger III and V length, character 190 and 191 respectively. Character 190: state 0 (A), and state 1 (B). Character 191: state 0 (C), state 1 (D), state 2 (E), state 3 (B), and state 4 (F). Species are Hyloxalus awa, MZUSP 122127 (A), H. maculosus, ICN 24249 (B), Anomaloglossus stepheni,

MZUSP 69178 (C), H. breviquartus, ICN 21667 (D), H. arliensis, DFZ 341 (E), and H. edwardsi, ICN 21936 (F). Scale = 1 mm.

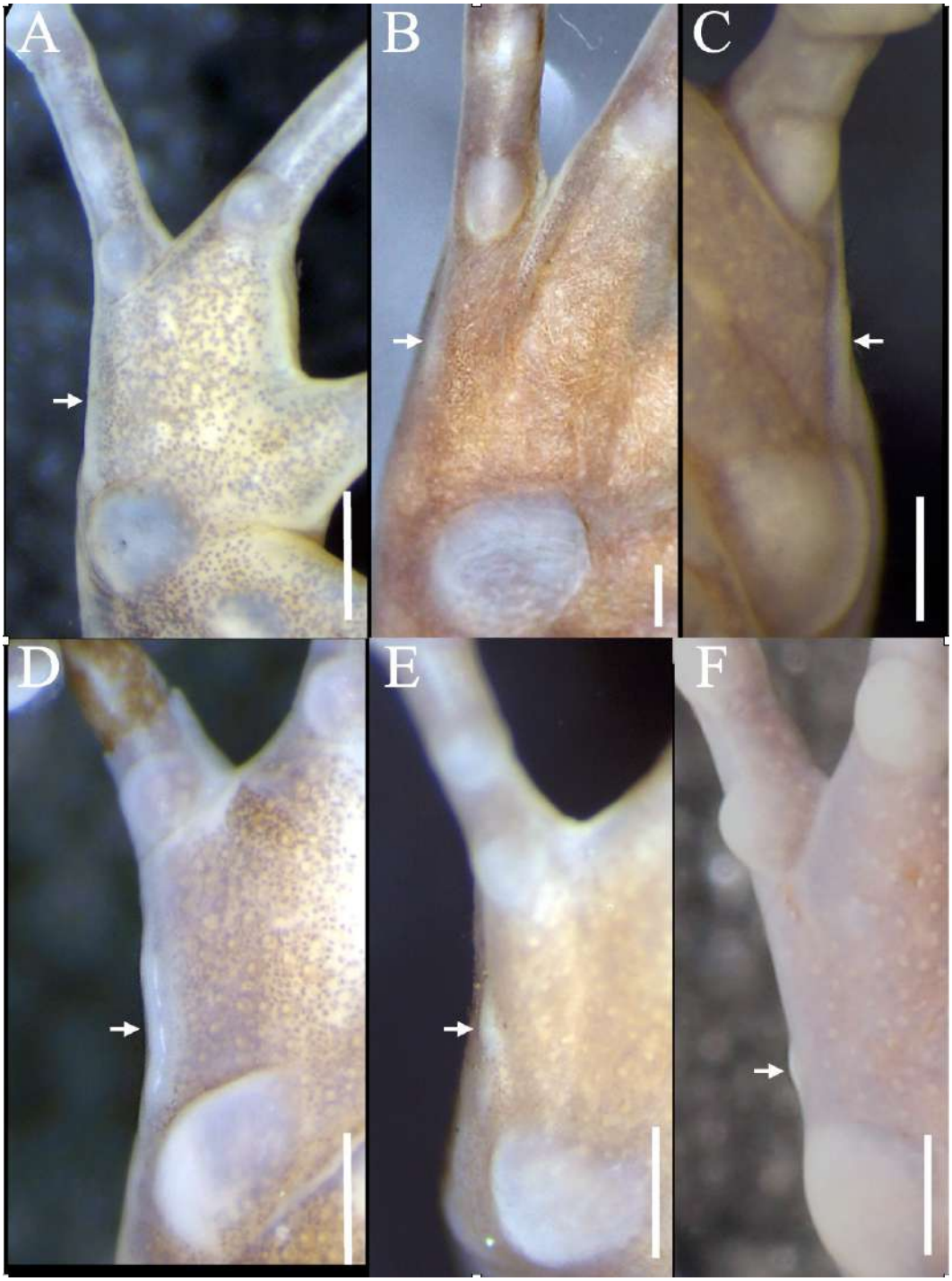

FIGURE 10.—Metacarpal ridge/fold (characters 192 – 194). Character 192, state 0, ridge (A), and state 1, tubercle-like (E, F). Character 193, state 0, distal extension reaching/continuous with postaxial fringe of finger V (A, B), and state 1, no reaching/continuous (D). Character 194, state 0, reaching one-half of palm (B), state 1, reaching two-third of palm (A, D), state 2, in contact with the palmar tubercle (C). Species are *Hyloxalus pinguis*, ICN 7670 (A), *Aromobates nocturnus*, KU 220986 (B),

Anomaloglossus baeobatrachus, MZUSP 122137 (C), *H. pulchellus*, KU 117970 (D), *H. toachi*, MZUSP 76317 (E), and *Ameerega pulchripecta*, MZUSP 69846 (E). Scale = 1 mm.

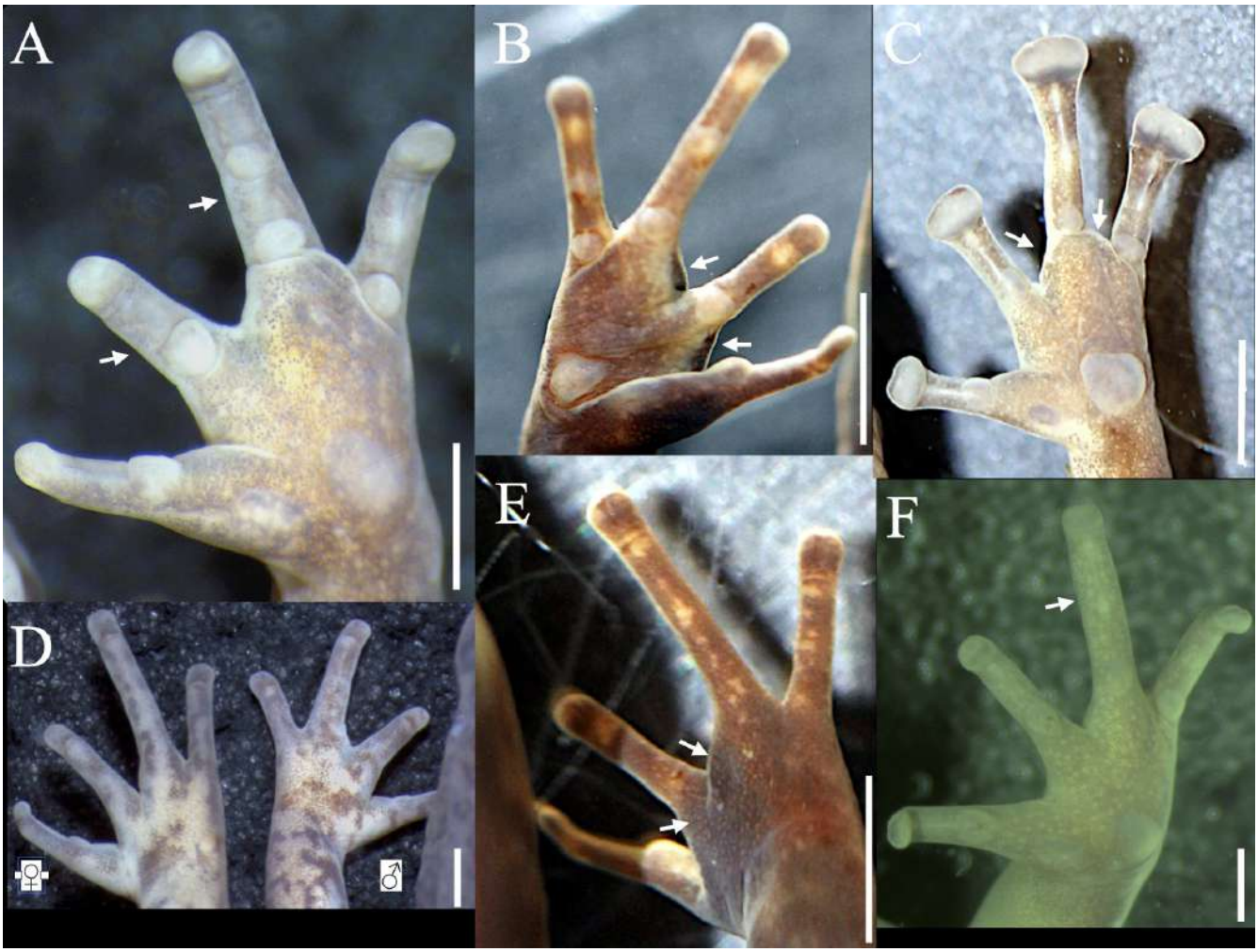

FIGURE 11.—Swelling on the fingers (Characters 195–202). Phalangeal swelling present on finger III (196: state 1, A), on finger IV (197: state 1, A, F) and on finger V (202: state 1, A). Basal swelling on finger IV (200: state 1, B, C, E). Metacarpal swelling (201: state 1, E). Compare sexual differences in D. Species are *Hyloxalus walesi*, adult male ICN 6318 (A, E) and adult female ICN 12739 (E), *H. anthracinus*, adult male KU 120643 (B, E), *H. nexipus*, adult male KU 211810 (C), *H. jacobuspetersi*, adult male MZUSP 132308 (F). Scale = 1 mm.

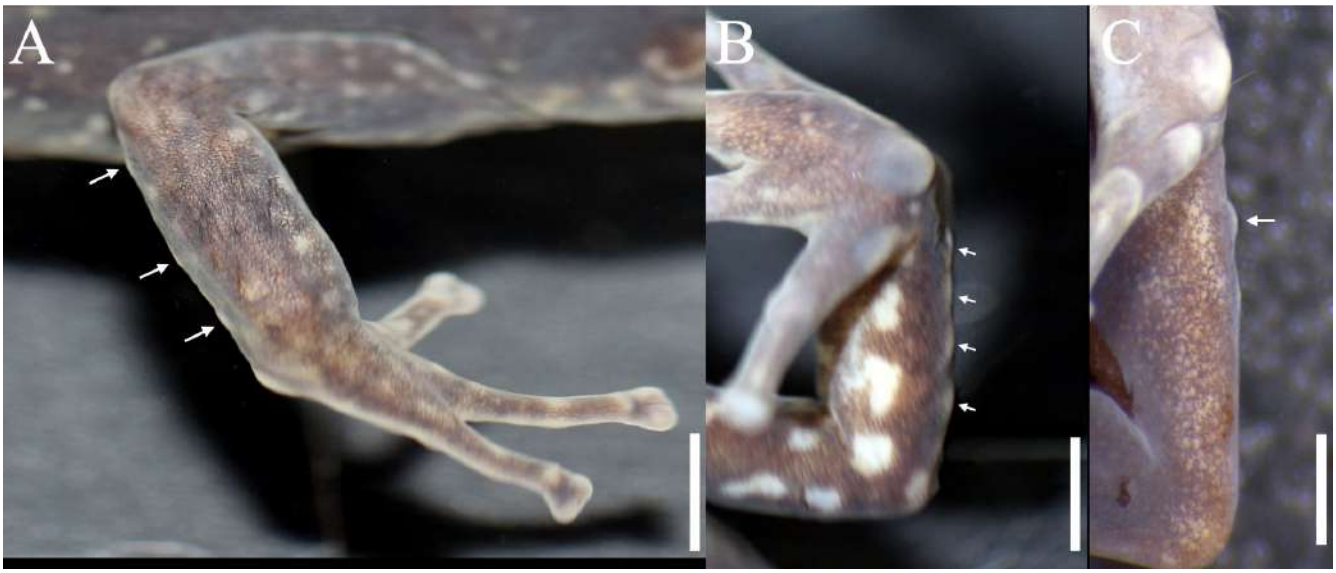

FIGURE 12.—Ulnar tubercles on forearm (Characters 203–204). An ulnar tubercles row occur in *Hyloxalus aeruginosus*, KU 211940 (A, B), and only the antebrachial tubercle is present in *H. anthracinus*, KU 202813 (C). Arrow indicate the tubercle. Scale = 1 mm.

FIGURE 13.—Swelling on the distal end of the upper arm and lower arm (character 205–206). Swelling restricted to the distal end of the upper arm (A, B), but it extends to the proximal lower arm, see dark brown area on internal forearm (C). Note the un-notice dull white swelling on B (arrow), and to confirm was necessary histological evaluation. Species: *Hyloxalus craspedoceps*, adult male KU 211953, ventral view (A), *H. pinguis*, adult male ICN 7682, posteroventral view (B), *H. anthracinus*, adult male KU 202813, lateroventral view (C). Scale = 1 mm.

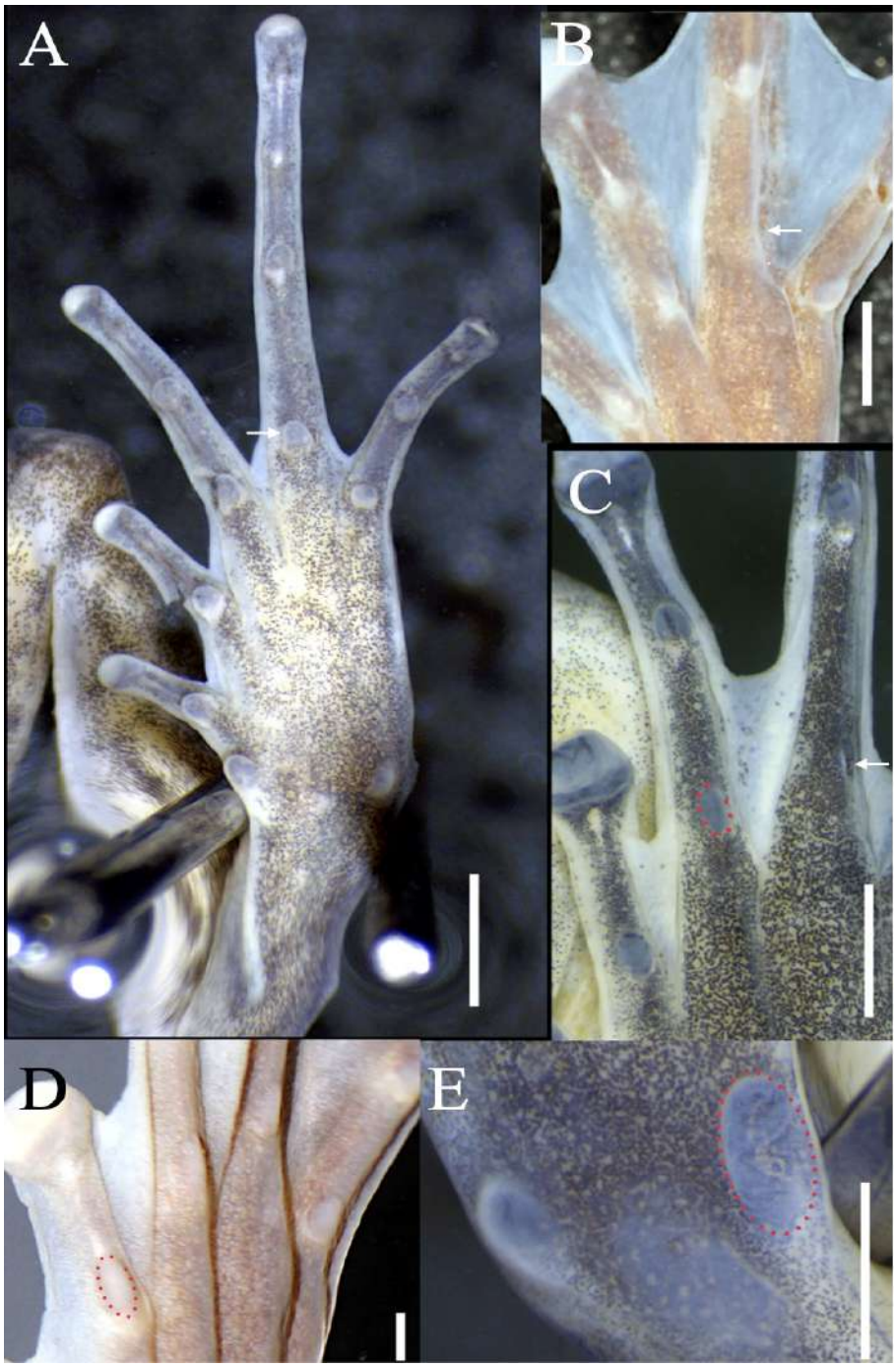

FIGURE 14.—Occurrence, size and shape of the basal subarticular tubercle (characters 207–208, 218–220) and shape of the inner metatarsal tubercle (character 221). Character 207: state 0, absent (B, arrow), state 1, present (A, arrow). Character 208: state 0, small (C, arrow), state 1, lesser/equal (A). Character 218 – 220: state 0, rounded/ovoid (A), state 1, elongated (C, D, red circle). Character 221: state 0, rounded/ovoid (A), state 1, elongated (E, red circle). Species: *Hyloxalus subpunctatus*, ICN

55855 (A), *Ectopoglossus saxatilis*, IAvH14613 (B), *Hyloxalus* sp. R, DFZ 407 (C, E), *Aromobates nocturnus*, KU 220983 (D). Scale = 1 mm.

FIGURE 15.—Protrusiveness of the subarticular tubercles of the toes (character 209 – 217). Projected tubercles in Ameerega flavopicta, MZUSP 100112, state 1 (A), and flattened tubercles in Hyloxalus maculosus, KU 141528, state 0 (B). Foot in lateroventral view. Scale = 1 mm.

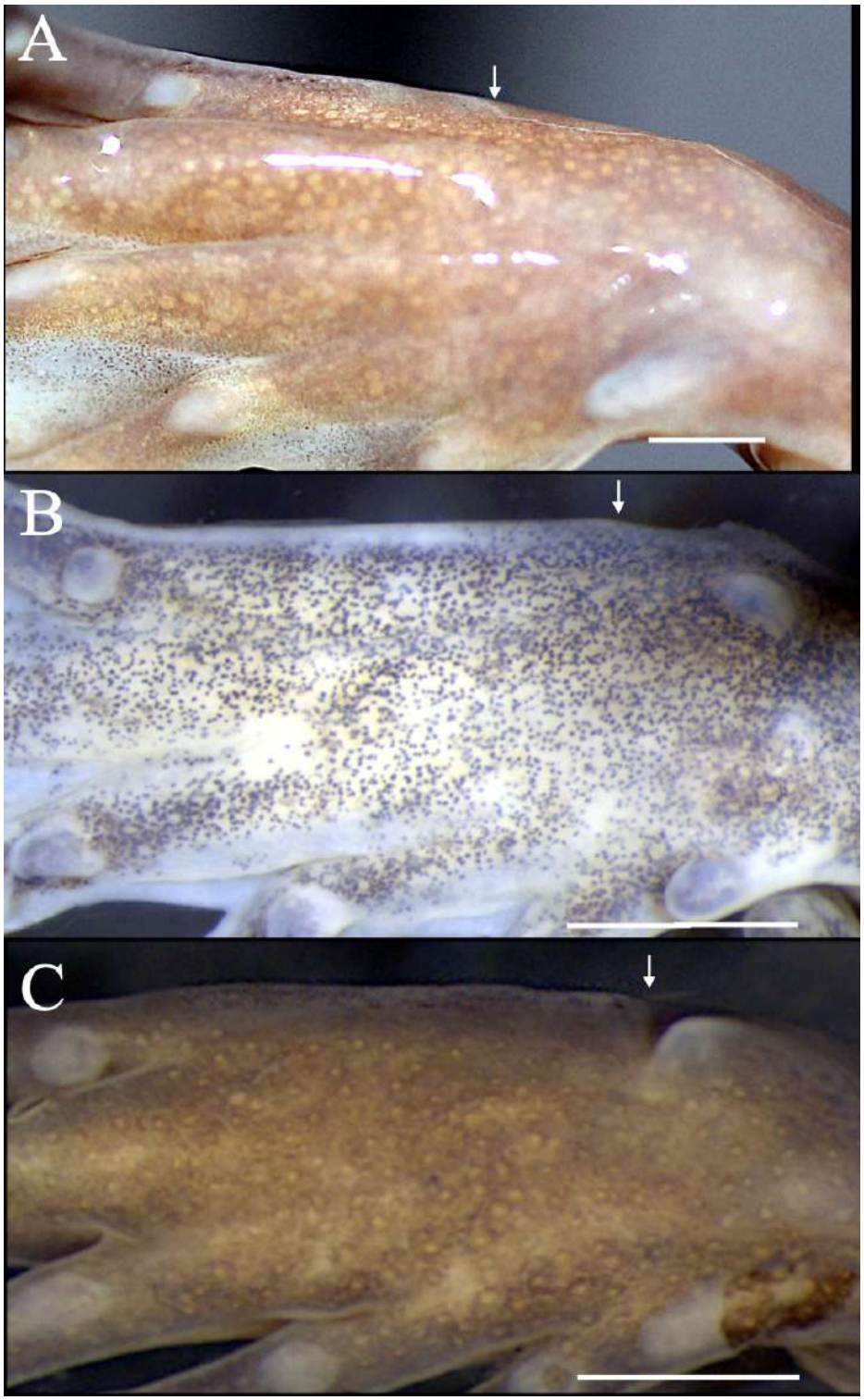

FIGURE 16.—Metatarsal fold extension (character 224). Arrow show the end of the fold. Metatarsal fold reaching half of plantar surfaces in *Aromobates nocturnus*, KU 220986, state 0 (A), reaching the proximal 2/3 of plantar surface in *Hyloxalus subpunctatus*, ICN 55855, state 1 (B), and reaching the outer metatarsal tubercle level in *Paruwrobates andinus*, PSO-CZ 623, state 2 (C). Scale = 1 mm.

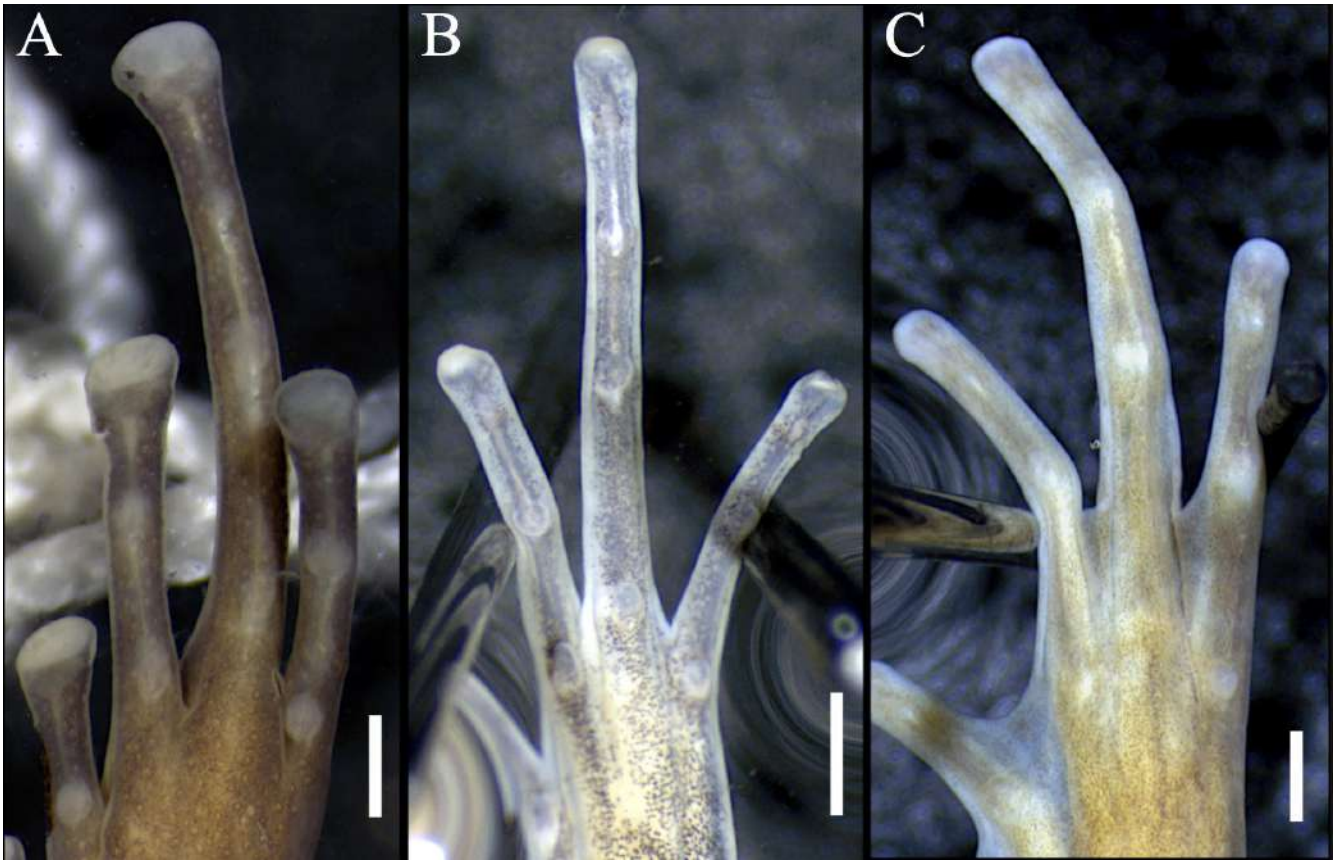

FIGURE 17.—Toe III and V length (character 225–226). Character 225, toe III reaching (state 0, A) or surpassing (state 1, B) the proximal subarticular tubercle of toe IV. Character 226, toe V not reaching (state 0, A), reaching (state 1, B), or surpassing (state 2, C) the proximal subarticular tubercle of toe IV. *Paruwrobates andinus*, PSO-CZ 623 (A), *Hyloxalus subpunctatus*, ICN 55855 (B), *H. edwardsi*, ICN 21936 (C). Scale = 1 mm.

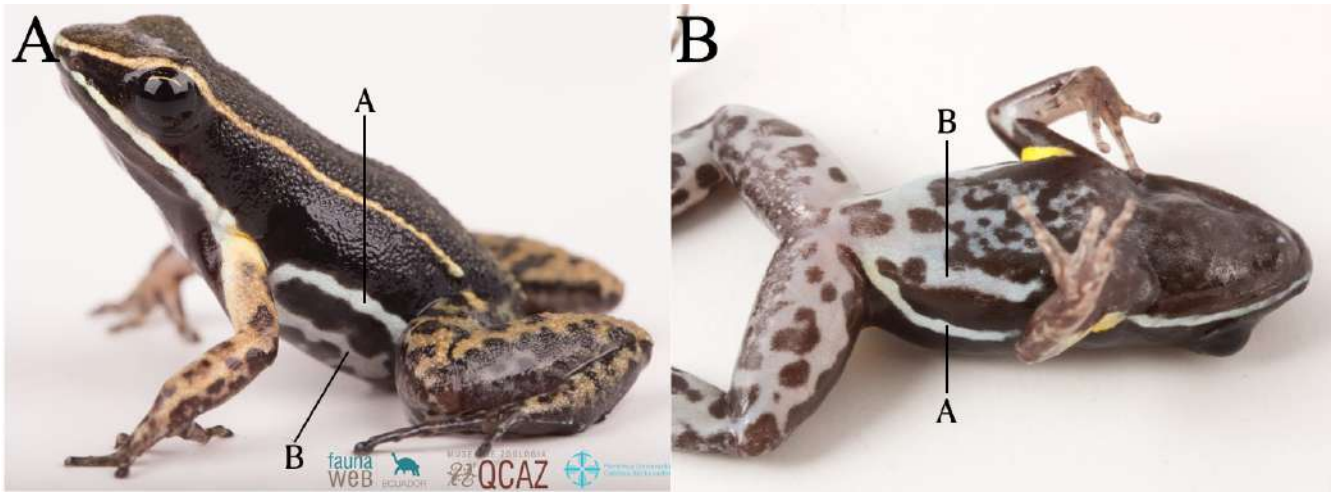

FIGURE 18.—The two types of ventrolateral stripe in a live *Allobates femoralis*. A-type runs by the upper end of the ventrolateral body flank, extending from groin to arm insertion region. B-type runs on lower end of the ventrolateral flanks, from groin to arm insertion region. QCAZ 63892 (A) and QCAZ 48728 (B). Photos from Fauna Web Ecuador, use authorized by S. Ron.

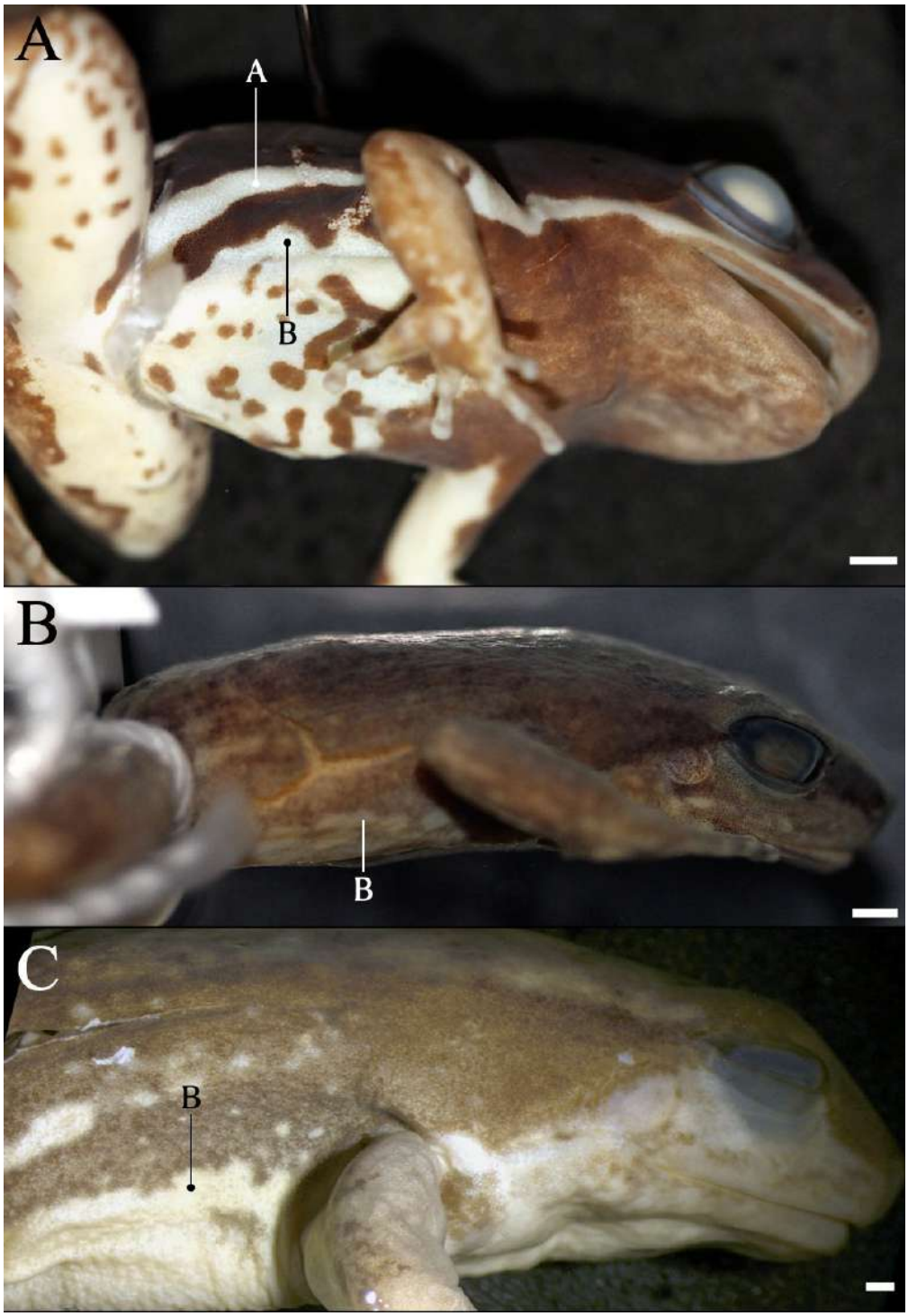

FIGURE 19.—A and B-type ventrolateral stripes in preserved specimens (characters 227–230). Presence of A-type, character 227: state 1 (A). Presence of B-type, character 229, state 1 (A–C). A wavy series of elongate spots (character 230: 0, B) or straight (230: 1, C) ventrolateral stripe. *Allobates femoralis*, MZUSP 77740 (A), *Hyloxalus mittermeieri*, KU 211944 (B), and *Rheobates palmatus*, MZUSP 106695 (C). Scale = 1 mm.

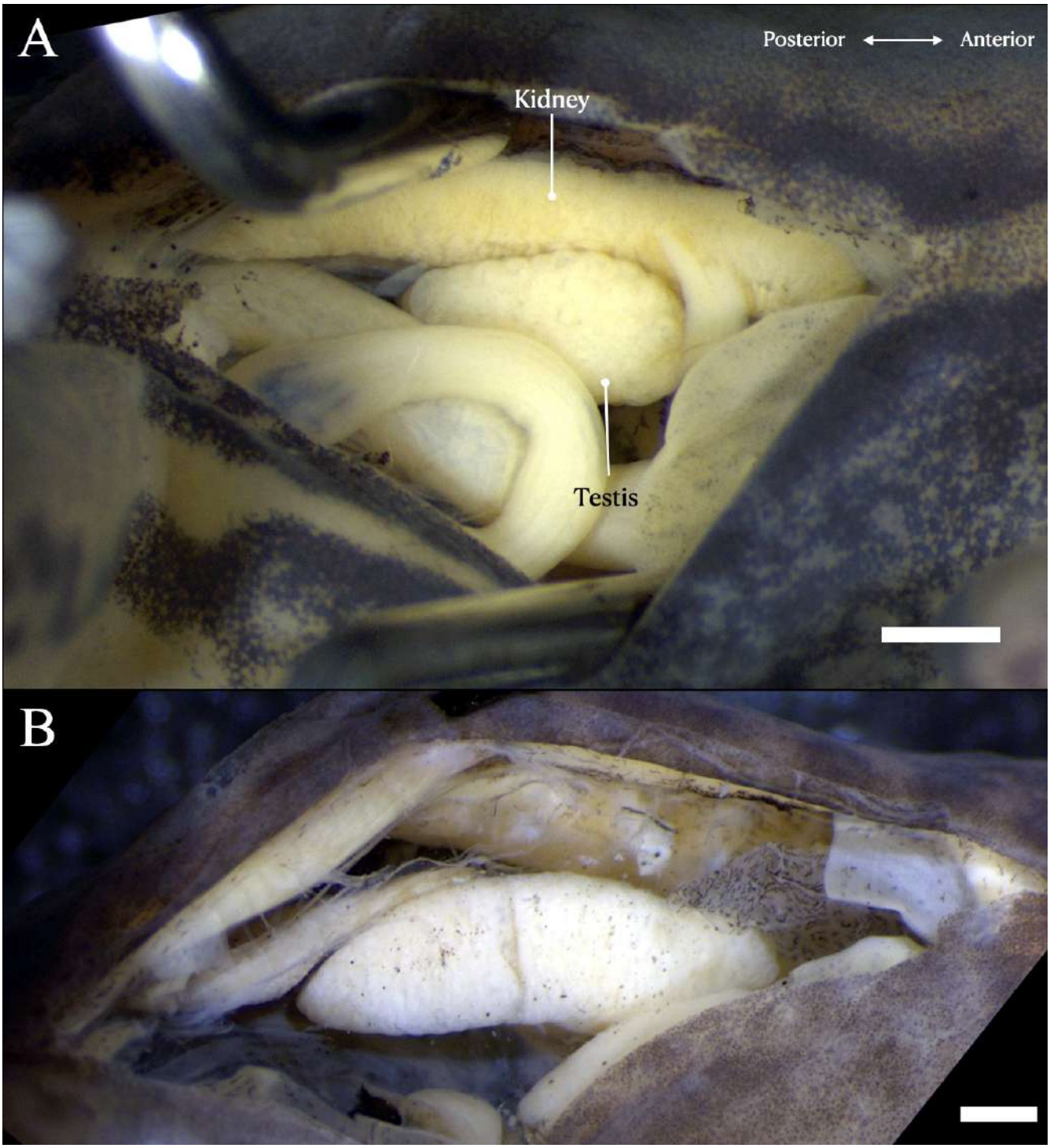

FIGURE 20.—Testis size (character 231). A small testis, 0.2–0.6 of kidney length in *Hyloxalus pinguis,* ICN 7682 (A), and a large testis, 0.9–1 of kidney length in *H. edwardsi,* ICN 21937 (B). Scale = 1 mm.

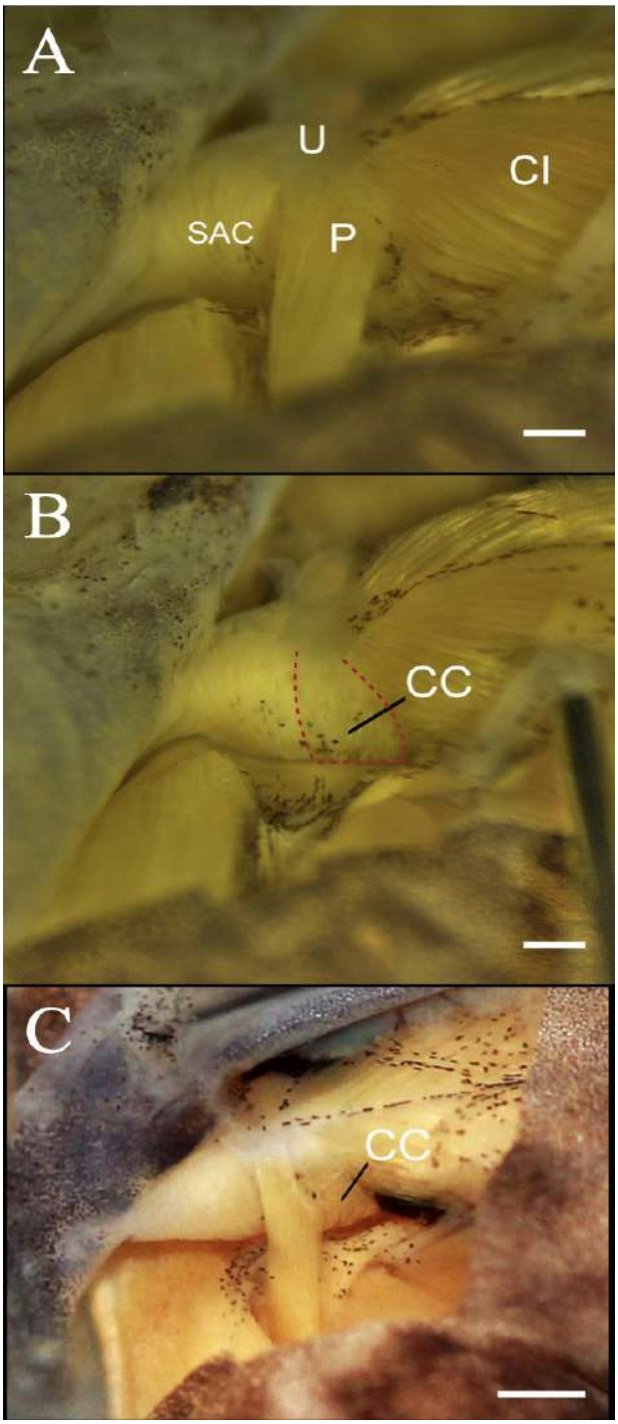

FIGURE 21.—Insertion of the *m. compressor cloacae* (CC) anterior portion (character 232). CC inserting ventrally and covered by the *m. pyriformis* (P), compare (A) and (B), where the last muscle was removed (state 0). Anterior portion of the CC inserting anteriorly, uncovered by the *m. pyriformis* (state 1, C). In B, dotted red line delimited the CC. *Hyloxalus maculosus*, ICN 24253 (A, B), *H. elachyhistus* KU 142376 (C). Other abbreviation: CI, *m. coccygeoiliacus*. U, urostyle. SAC, *m. sphincter ani cloacali*.

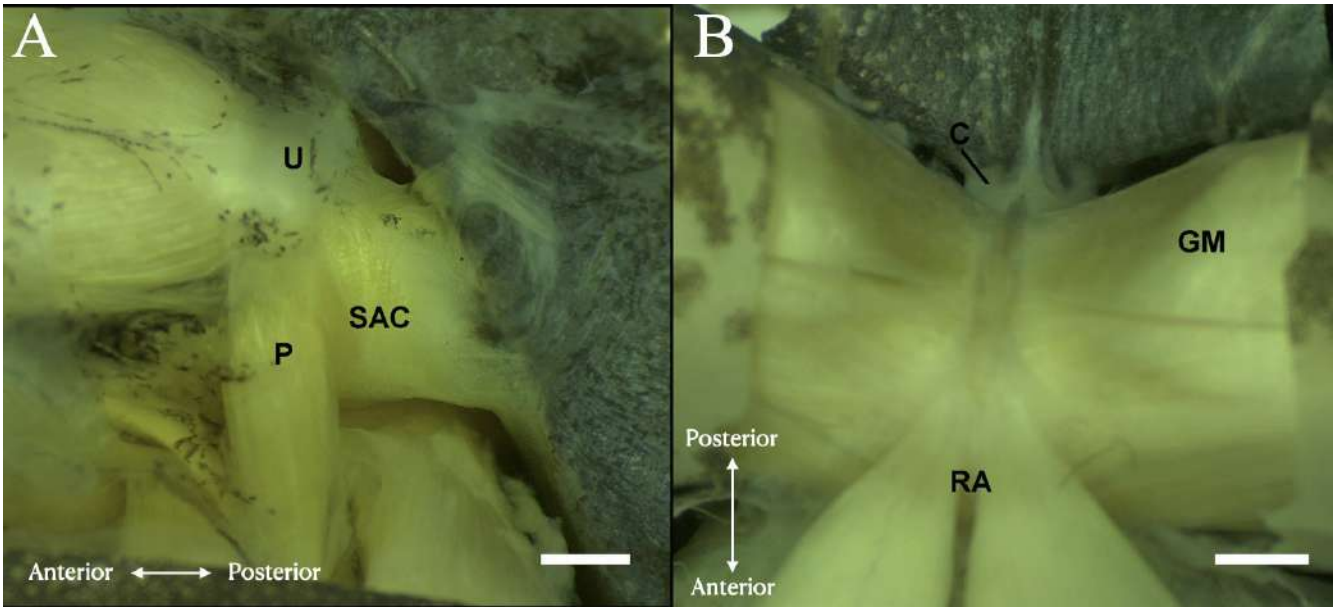

FIGURE 22—Absence of the distal slip of the *m. sphincter ani cloacalis* in *Colostethus mertensi*, ICN 8220, in lateral (A) in ventral view (B). Scale = 1mm. Abbreviations: C, cloacal tube. GM, m. gracilis major. P, *m. pyriformis*. U, urostyle. RA, *m. rectus abdominis*, SAC, *m. sphincter ani cloacali*. Scale = 1 mm.

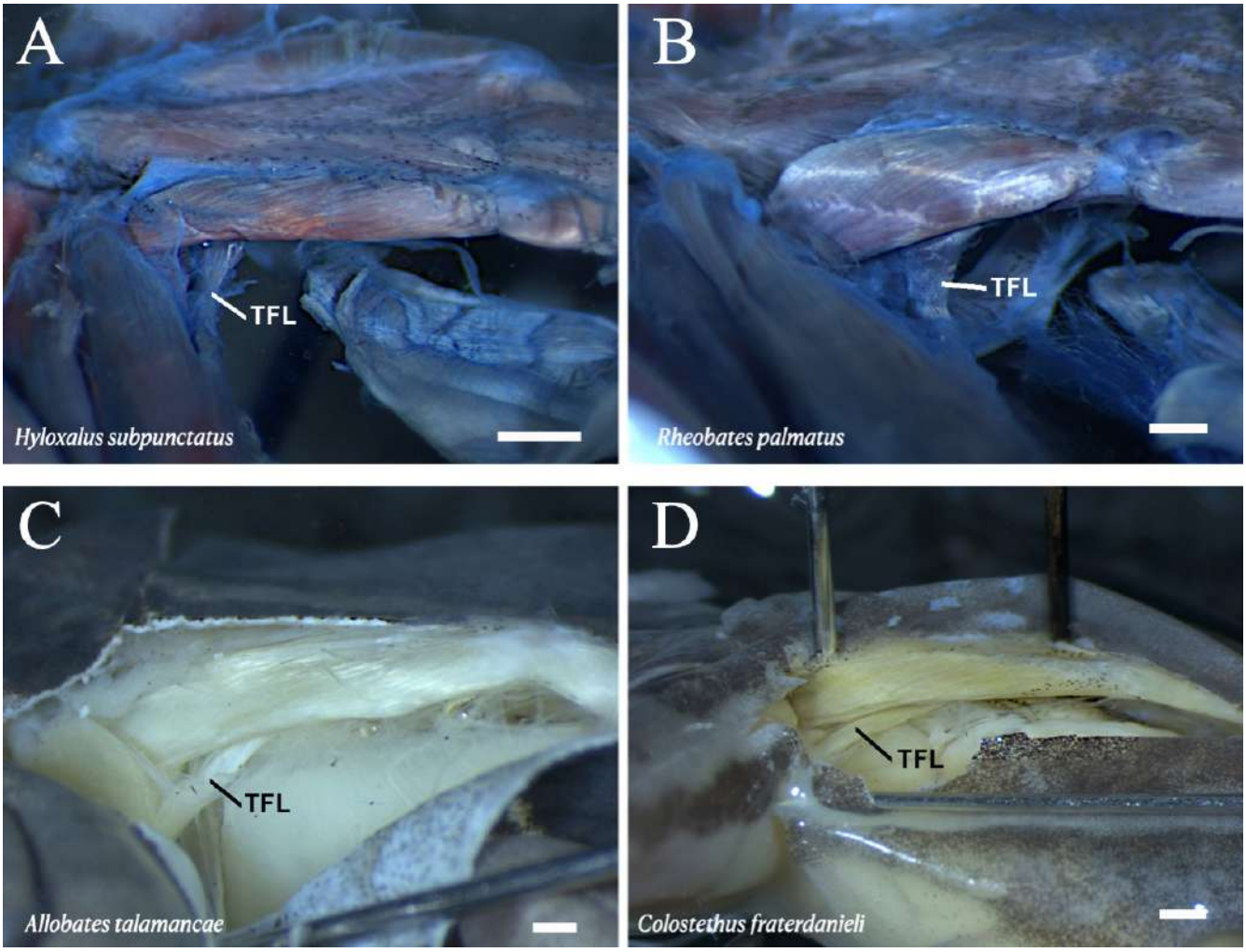

FIGURE 23.—Origin of the *m. tensor fascia latae* (TFL, character 236). A posterior origin is show in A and B (state 2), and a medial origin in B and D (state 1). ICN 55863 (A), ICN 55887 (B), PD 49 (C), KU 133272, *Leucostethus* sp. *fraterdanieli* complex (D). Scale = 1 mm.

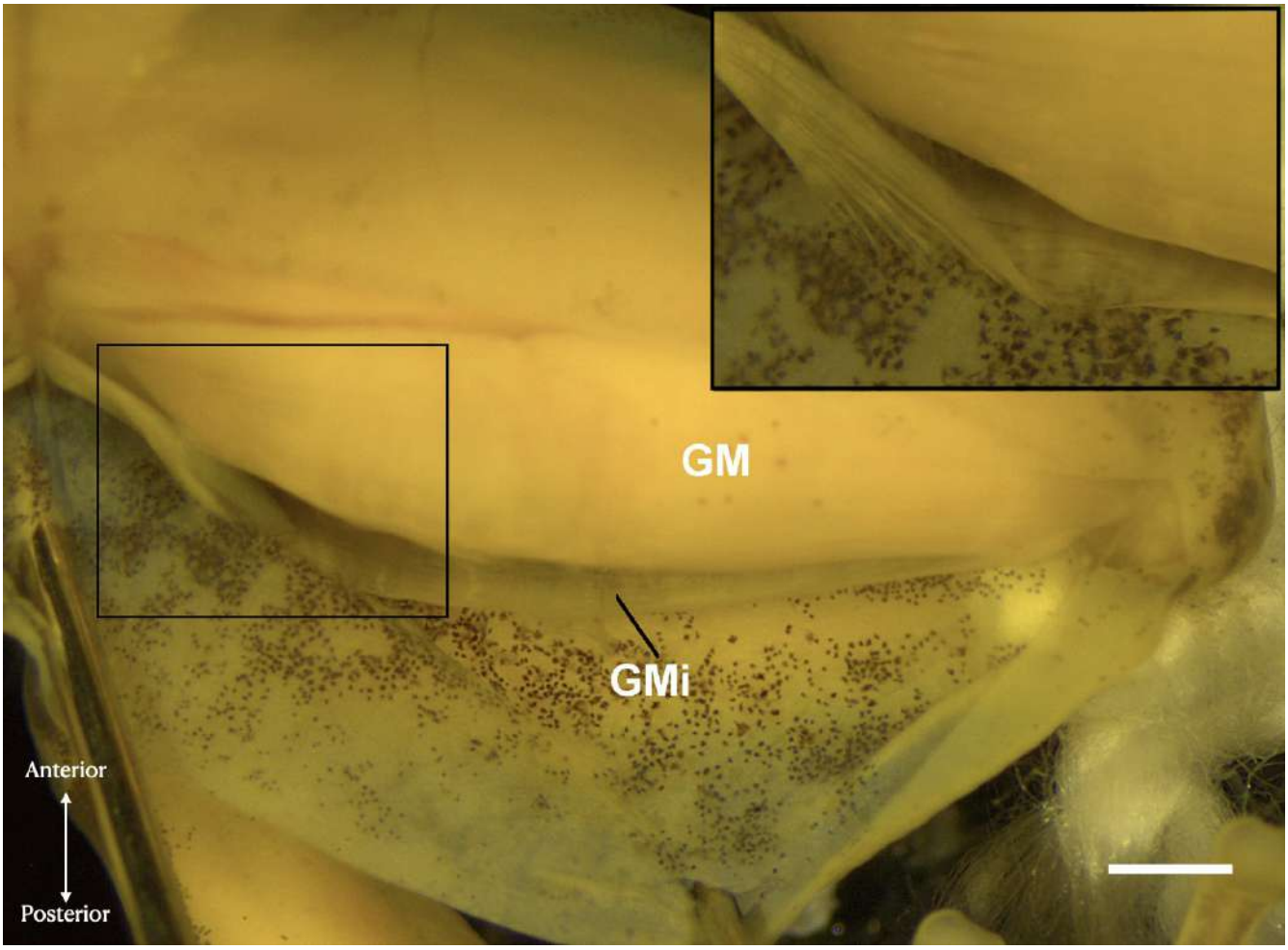

FIGURE 24.—*M. gracilis minor* (GMi) showing the second origin on the dermis (inset; character 237: state 1). Ventral view of the left thigh of the *Hyloxalus pinguis*, ICN 7670. *M. gracilis major* (GM). Scale = 1 mm.

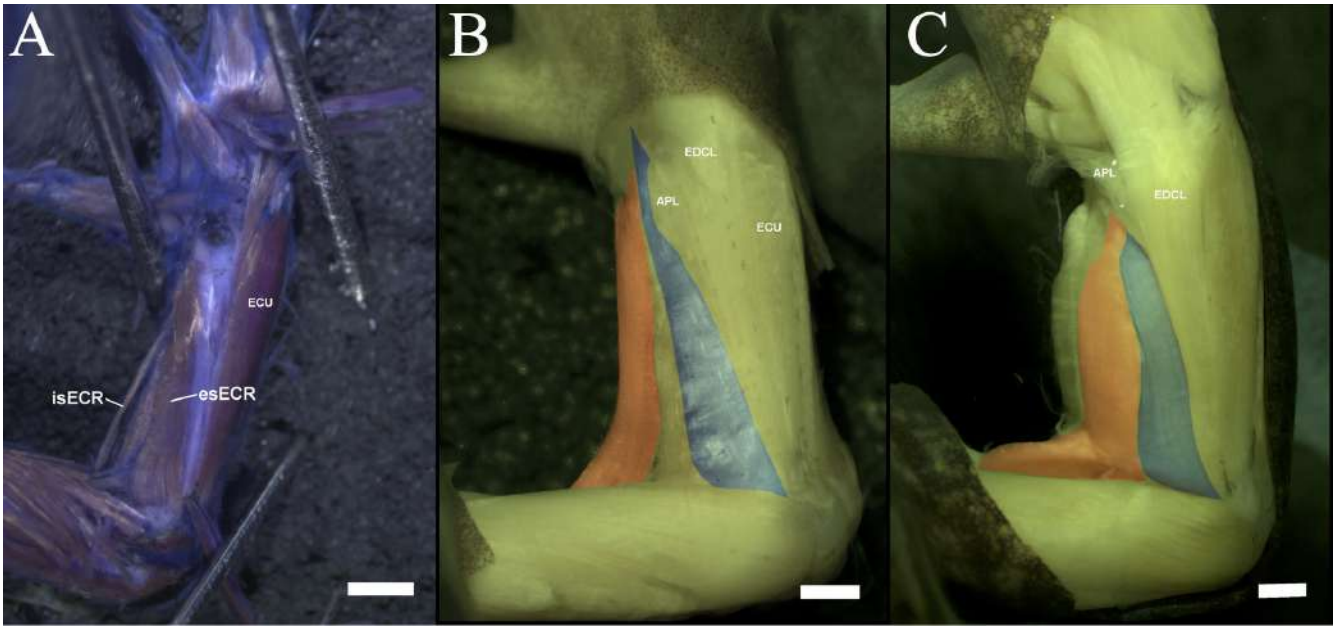

FIGURE 25.—The *m. extensor carpi radialis* (ECR) in three poison frogs (characters 238–239). Thin (character 238: 0; A) and robust (character 238: 1; B, C) origin of the internal slip of ECR (isECR in red color). isECR inserting at about distal two-third of external slip (esECR or in blue, character 239: 0; A), or at the external slip distal tendon, roughly at radiale level (character 239: 1; B, C). *Rheobates palmatus*, ICN 55887 (A), *Hyloxalus edwardsi*, ICN 21942 (B), *H. ruizi*, ICN 5416 (C). Other muscles: APL, *m. abductor pollicis longus*. ECU, *m. extensor carpi ulnaris*. EDCL, *m. extensor digitorius communis longus*. Scale = 1 mm.

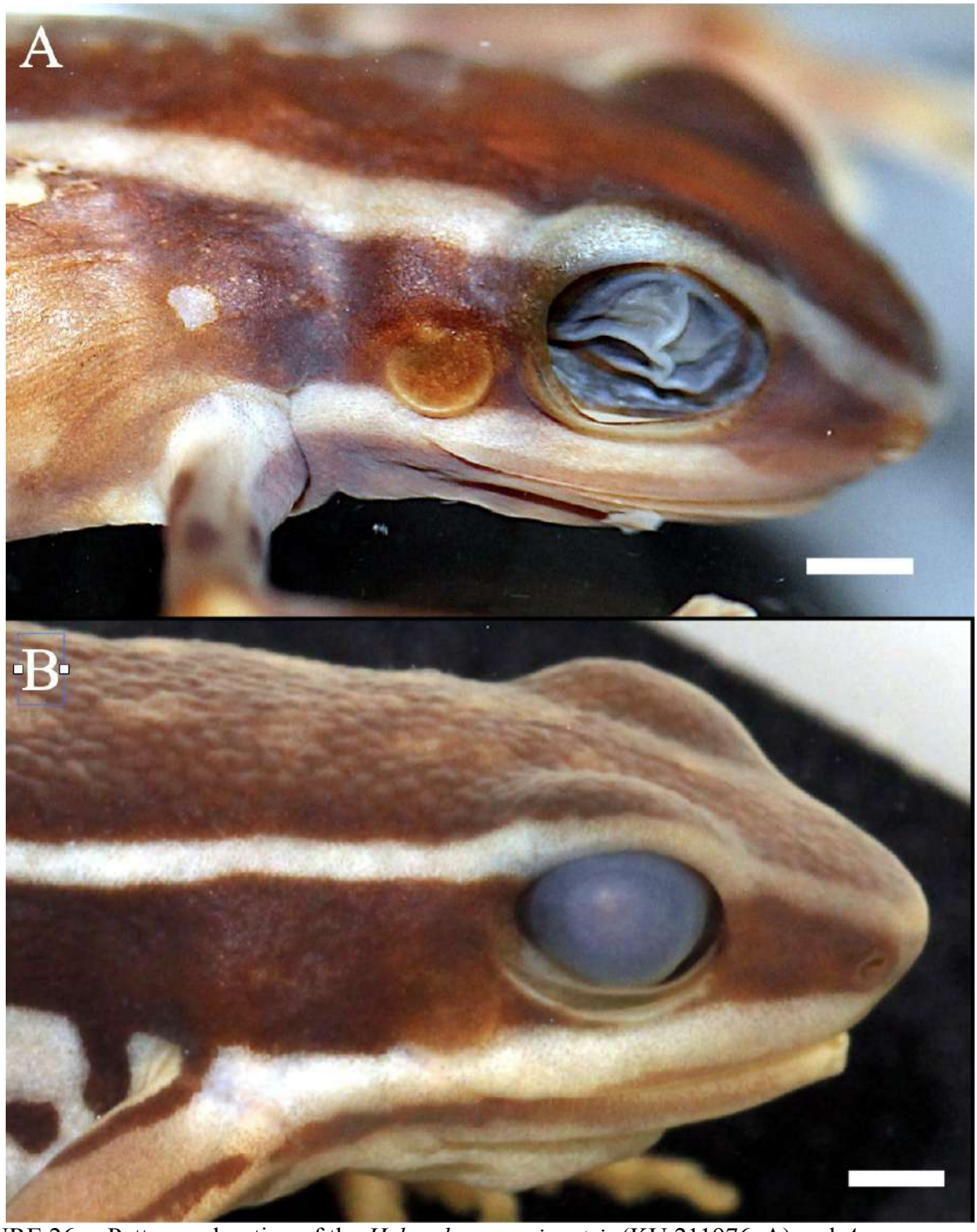

FIGURE 26.—Pattern coloration of the *Hyloxalus azureiventris* (KU 211976; A) and *Ameerega braccata* (MZUSP 100230; B), showing the supralabial line. Scale = 1 mm.

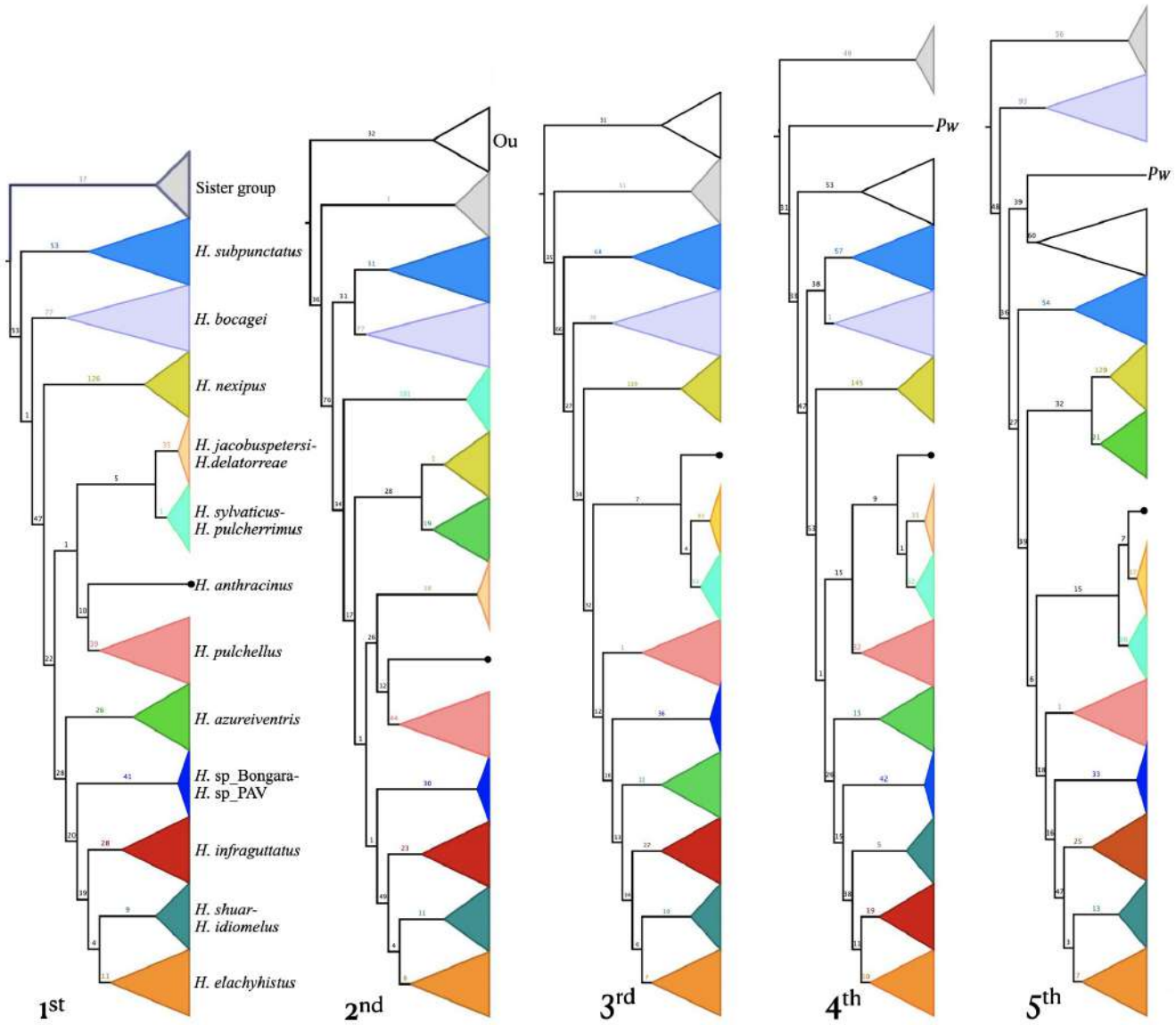

FIGURE 27.—Trees of the first to fifth (1–5th) successive outgroup expansion analysis showing the effect on the ingroup topology. Names are *Hyloxalus* clades (details in the text). In the first analysis, the outgroup same as sister group (*Ectopoglossus* and *Paruwrobates*, Pw). "Ou" denoted outgroup. Note that the Hyloxalinae and *Hyloxalus* monophyly was loss in the fourth and fifth analysis, respectively. Values at nodes are Goddman-Bremer support.

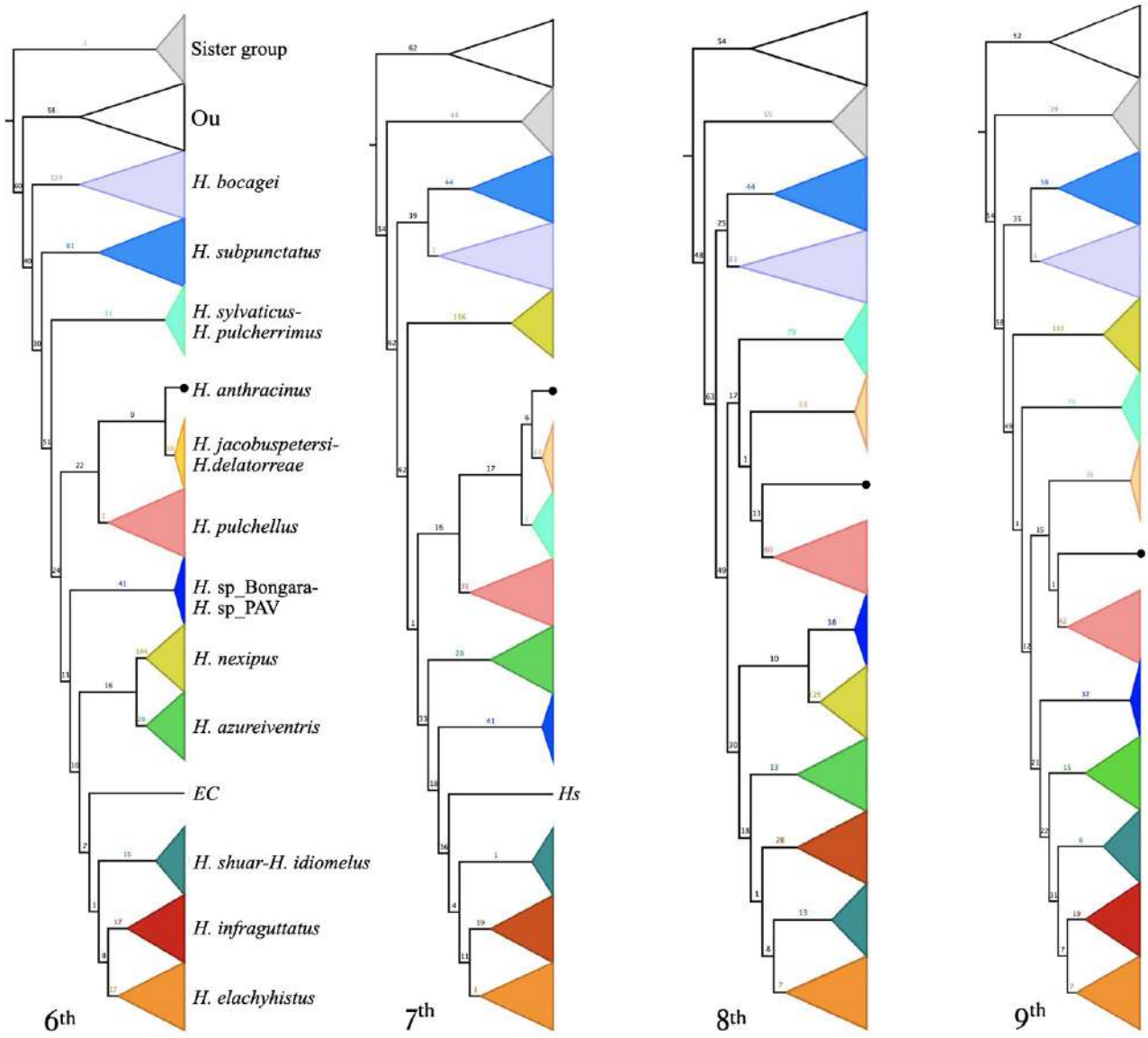

FIGURE 28.—Trees of the sixth to ninth (6–9th) successive outgroup expansion analysis showing the effect on the ingroup topology. Names are *Hyloxalus* clades (details in the text). "Ou" denoted outgroup, Hs is *H. shuar*, EC is Hyloxalus sp. ElCopal. Values at nodes are Goddman-Bremer supports.

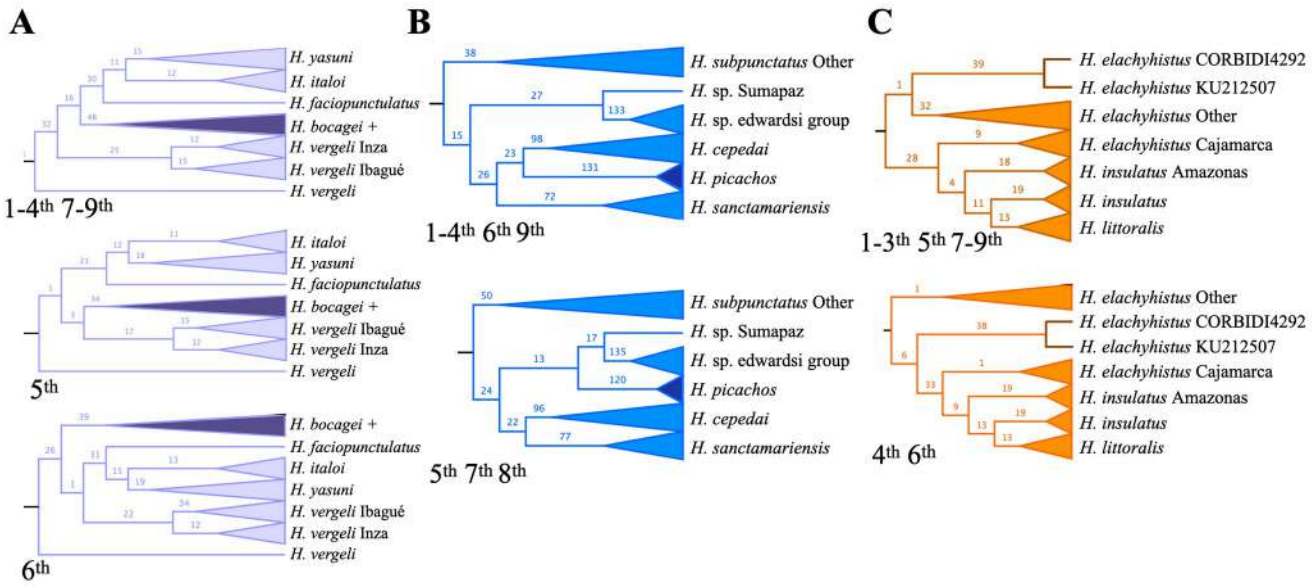

FIGURE 29.—Effect of the successive outgroup expansion into three *Hyloxalus* clades: *H. bocagei* clade (purple), *H. subpunctatus* clade (blue) and *H. elachyhistus* clade (orange). A dark shade denote the clade changing the position. Ordinal numbers below the tree correspond to the number of analysis. Goodman-Bremer on the branch are of the fourth, fifth and sixth analysis in A, the fourth and fifth analysis in B, and third and fourth analysis is C. *H. bocagei* + indicate the clade compose by *H. bocagei*, *H. leucophaeus*, *H. maculosus*, *H.sauli*, *H. sordidatus*, and *Hyloxalus* sp. Amazonas. "Other" word designate the remaining members in the *H. subpunctatus* and *H. elachyhistus* clade. See details and supports in Appendix 4.

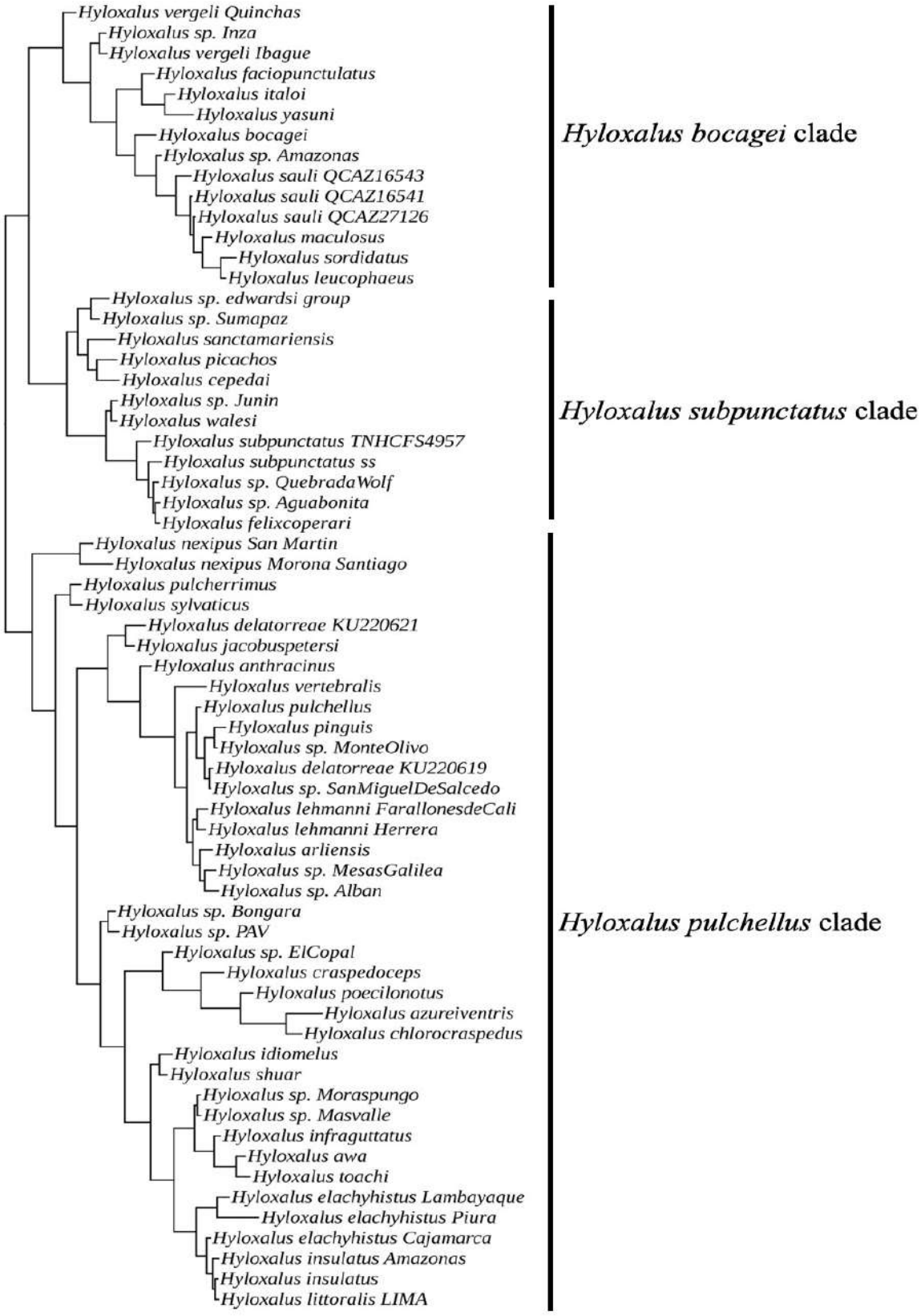
Hyloxalus vergeli Quinchas
Hyloxalus sp. Inza
Hyloxalus vergeli Ibague
Hyloxalus faciopunctulatus
Hyloxalus italoi
Hyloxalus yasuni
Hyloxalus bocagei
Hyloxalus sp. Amazonas
Hyloxalus sauli QCAZ16543
Hyloxalus sauli QCAZ16541
Hyloxalus sauli QCAZ27126
Hyloxalus maculosus
Hyloxalus sordidatus
Hyloxalus leucophaeus
Hyloxalus sp. edwardsi group
Hyloxalus sp. Sumapaz
Hyloxalus sanctamariensis
Hyloxalus picachos
Hyloxalus cepedai
Hyloxalus sp. Junin
Hyloxalus walesi
Hyloxalus subpunctatus TNHCFS4957
Hyloxalus subpunctatus ss
Hyloxalus sp. QuebradaWolf
Hyloxalus sp. Aguabonita
Hyloxalus felixcoperari
Hyloxalus nexipus San Martin
Hyloxalus nexipus Morona Santiago
Hyloxalus pulcherrimus
Hyloxalus sylvaticus
Hyloxalus delatorreae KU220621
Hyloxalus jacobuspetersi
Hyloxalus anthracinus
Hyloxalus vertebralis
Hyloxalus pulchellus
Hyloxalus pinguis
Hyloxalus sp. MonteOlivo
Hyloxalus delatorreae KU220619
Hyloxalus sp. SanMiguelDeSalcedo
Hyloxalus lehmanni FarallonesdeCali
Hyloxalus lehmanni Herrera
Hyloxalus arliensis
Hyloxalus sp. MesasGalilea
Hyloxalus sp. Alban
Hyloxalus sp. Bongara
Hyloxalus sp. PAV
Hyloxalus sp. ElCopal
Hyloxalus craspedoceps
Hyloxalus poecilonotus
Hyloxalus azureiventris
Hyloxalus chlorocraspedus
Hyloxalus idiomelus
Hyloxalus shuar
Hyloxalus sp. Moraspungo
Hyloxalus sp. Masvalle
Hyloxalus infraguttatus
Hyloxalus awa
Hyloxalus toachi
Hyloxalus elachyhistus Lambayaque
Hyloxalus elachyhistus Piura
Hyloxalus elachyhistus Cajamarca
Hyloxalus insulatus Amazonas
Hyloxalus insulatus
Hyloxalus littoralis LIMA
Hyloxalus bocagei clade
Hyloxalus subpunctatus clade
Hyloxalus pulchellus clade

FIGURE 30—A condense *Hyloxalus* phylogeny from the most parsimonious tree of the large ingroup analysis. Only species and candidate species are show (see text for discussion). For a detailed phylogeny, with support see the Appendix 5. Synapomorphies are in Appendix 6.

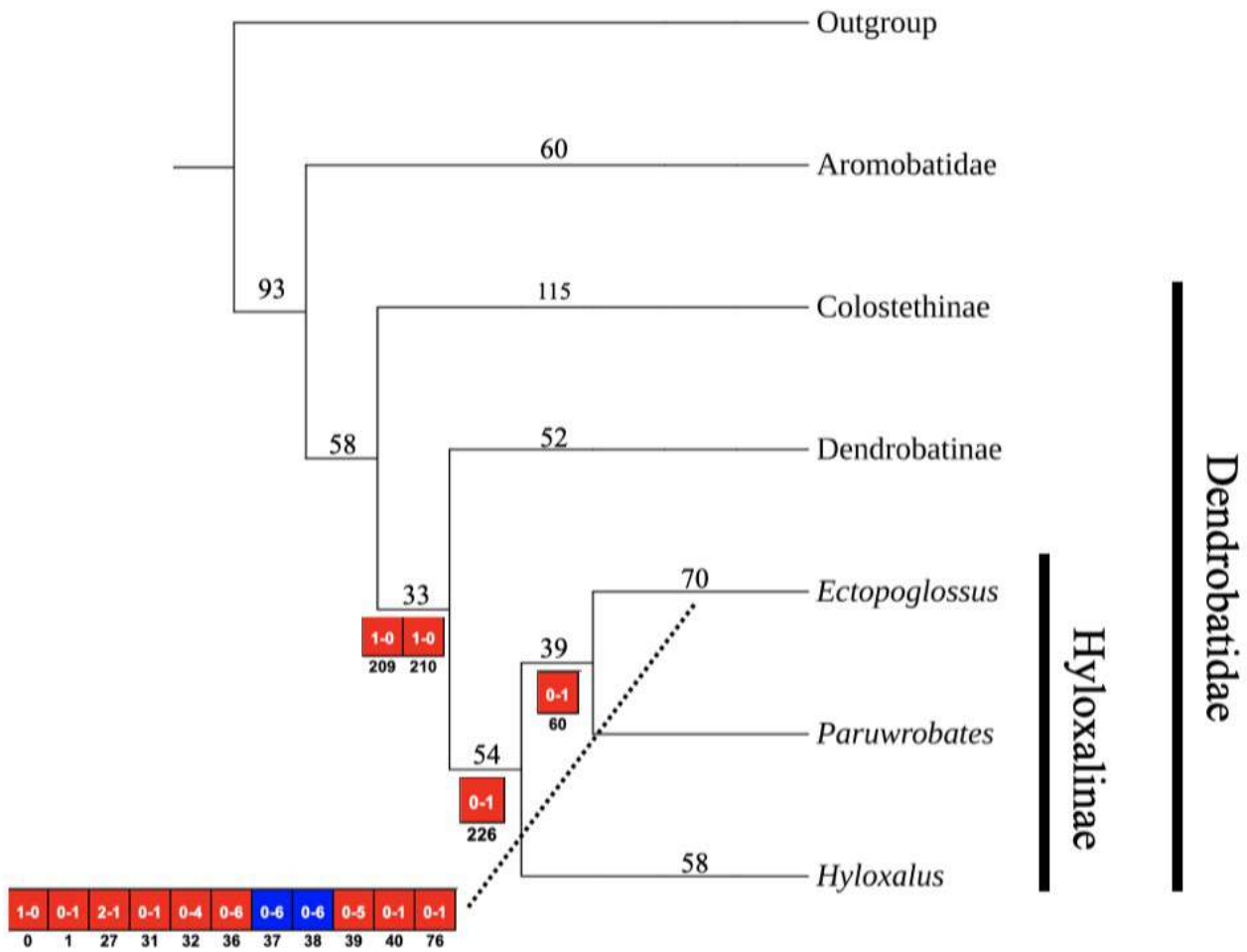

FIGURE 31.—Summary of the Hyloxalinae subfamily relationships, obtained from the most parsimonious optimal tree found larger evidence analysis to the ingroup relationships. Numbers on the supported nodes are Goodman-Bremer value and unambiguous phenotypical synapomorphies are specify on the select clades (Red square: unambiguous, non-private synapomorphies. Blue square: unambiguous, private synapomorphies. Numbers below square is the character, and numbers into square are primitive–derive character-states transformation).

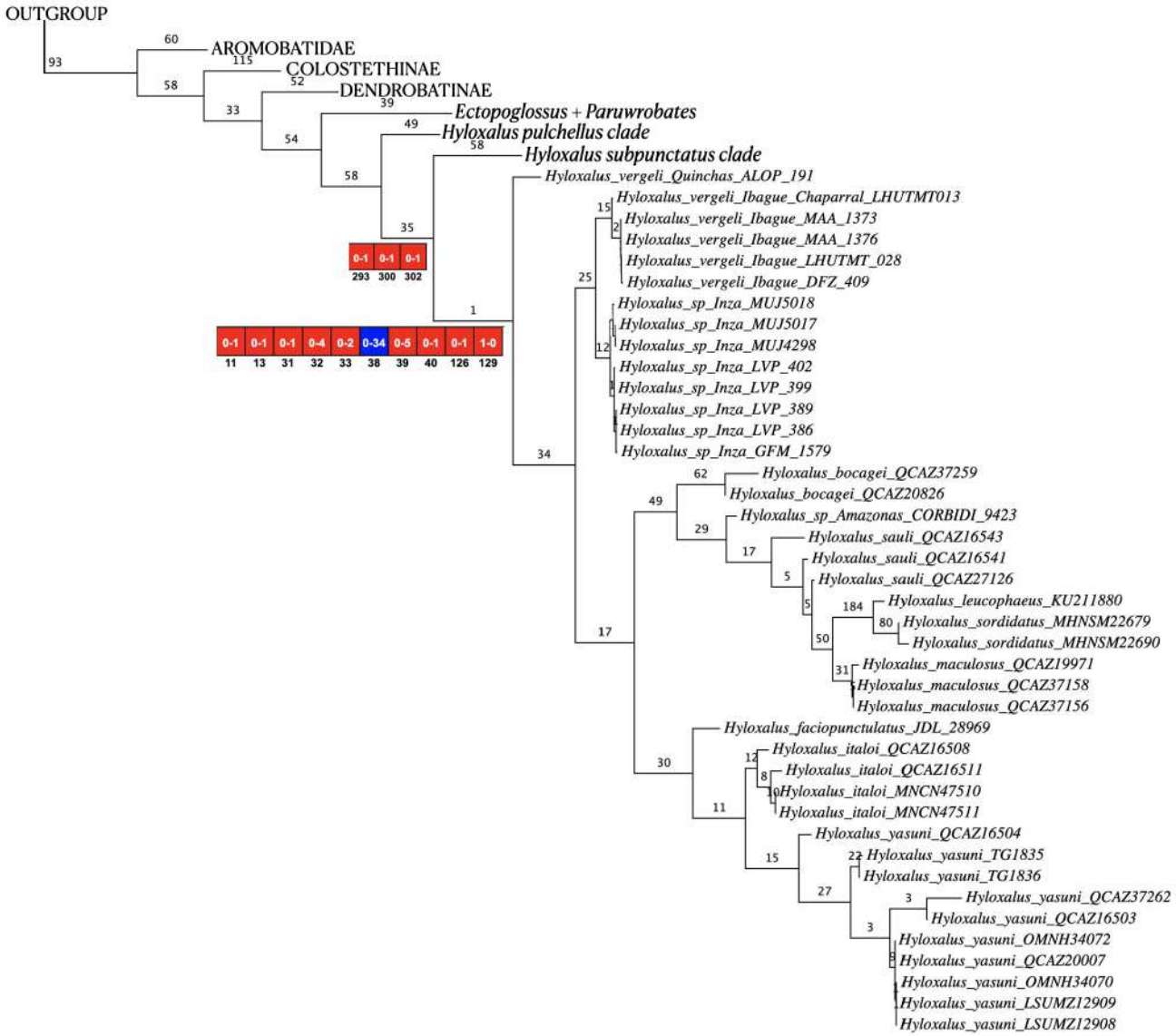

FIGURE 32.—Optimal hypothesis of relationships of *Hyloxalus bocagei* clade. The most parsimonious tree show minimum branch-length, unsupported nodes collapsed, supported nodes with Goodman-Bremen value, and select nodes show unambiguous phenotypic synapomorphies (Red square: unambiguous, non-private synapomorphies. Blue square: unambiguous, private synapomorphies. Numbers below square is the character, and numbers into square are primitive–derive character-states transformation).

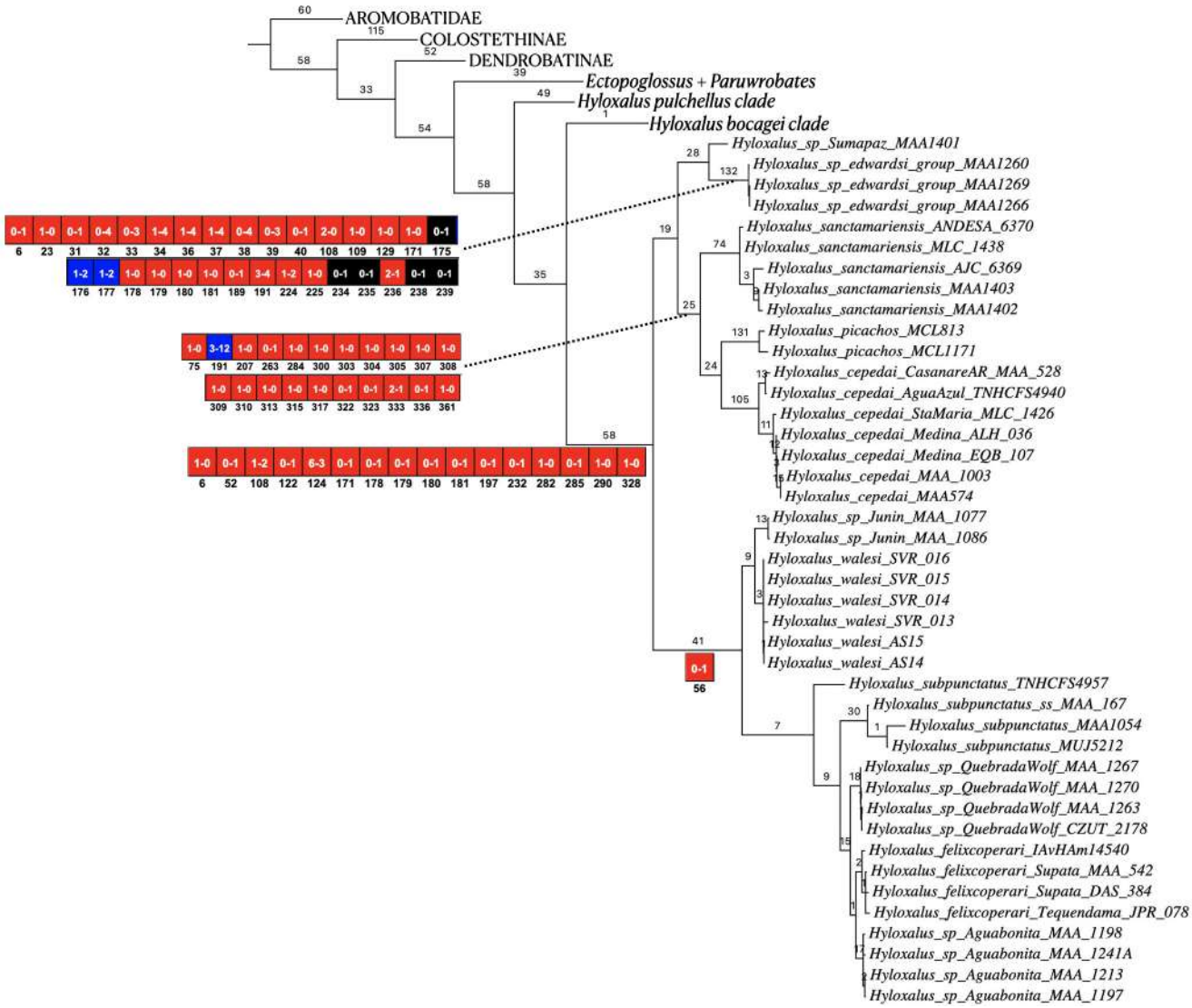

FIGURE 33.—Optimal hypothesis of relationships of *Hyloxalus subpunctatus* clade. The most parsimonious tree show minimum branch-length, unsupported nodes collapsed, supported nodes with Goodman-Bremen value, and select nodes show unambiguous phenotypic synapomorphies (Red square: unambiguous, non-private synapomorphies. Blue square: unambiguous, private synapomorphies. Black square: unambiguous, and non-homoplastic synapomorphies. Numbers below square is the character, and numbers into square are primitive–derive character-states transformation).

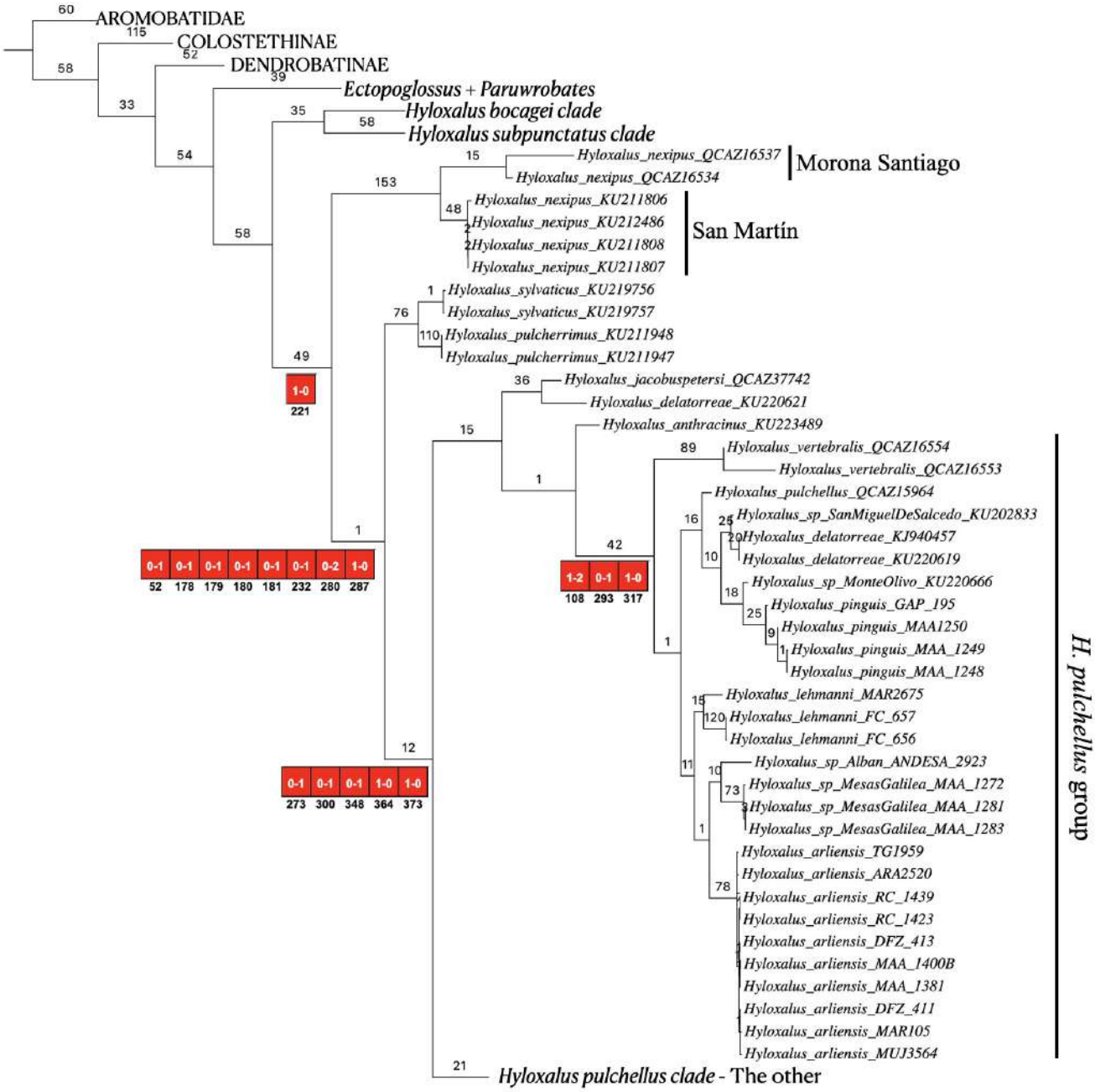

FIGURE 34.—Optimal hypothesis of relationships of a part of *Hyloxalus pulchellus* clade. Clades *H. nexipus, H. sylvaticus–H. pulcherrimus, H. jacobuspetersi–H. delatorreae,* and *H. anthracinus* and the *H. pulchellus group*. The most parsimonious tree show minimum branch-length, unsupported nodes collapsed, supported nodes with Goodman-Bremen value, and select nodes show unambiguous phenotypic synapomorphies (Red square: unambiguous, non-private synapomorphies. Numbers below square is the character, and numbers into square are primitive–derive character-states transformation).

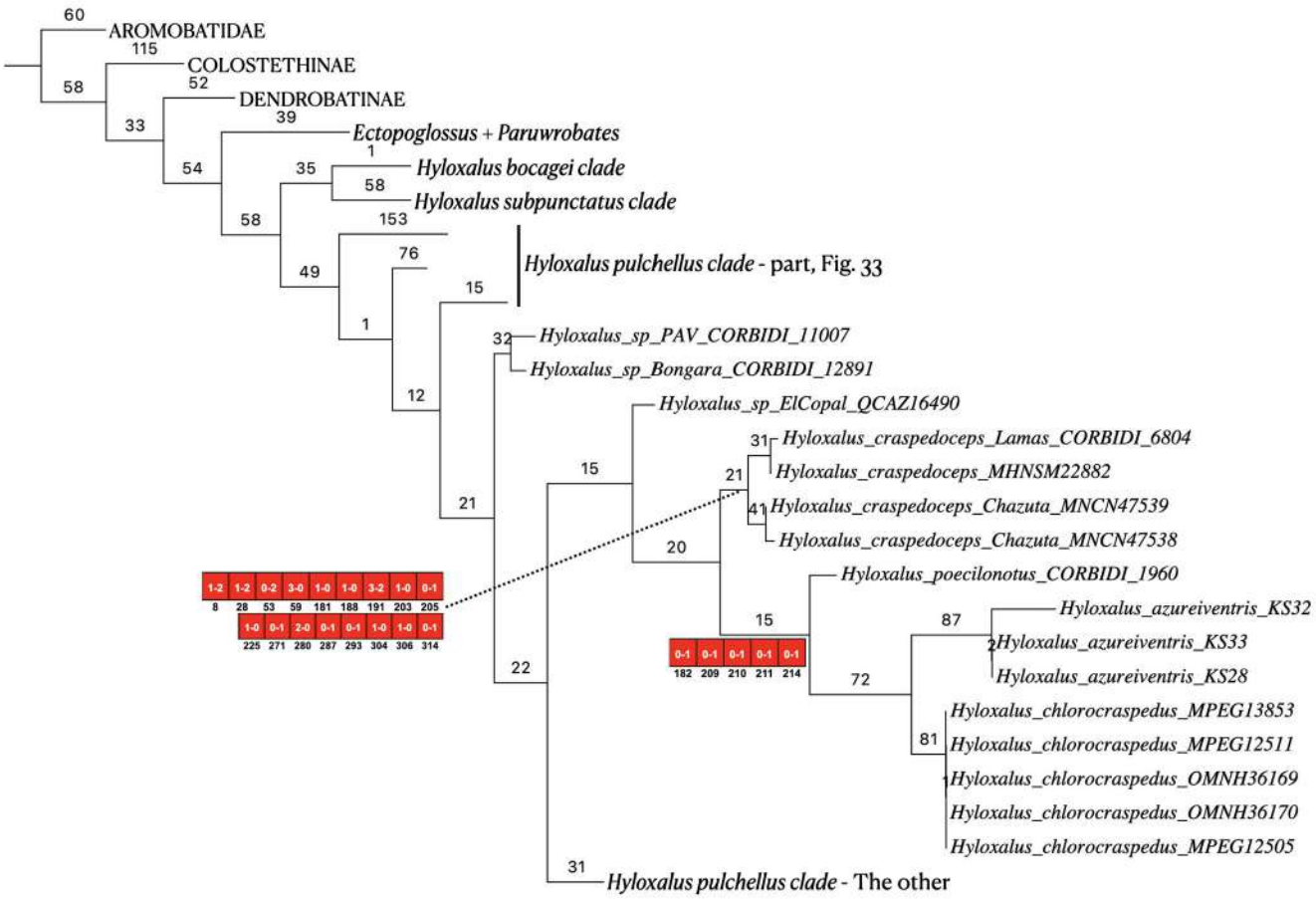

FIGURE 35.—Optimal hypothesis of relationships of a part of *Hyloxalus pulchellus* clade. Clades *Hyloxalus* sp. Bongara–*Hyloxalus* sp. PAV, and *H. azureiventris*. The most parsimonious tree show minimum branch-length, unsupported nodes collapsed, supported nodes with Goodman-Bremen value, and select nodes show unambiguous phenotypic synapomorphies (Red square: unambiguous, non-private synapomorphies. Numbers below square is the character, and numbers into square are primitive–derive character-states transformation).

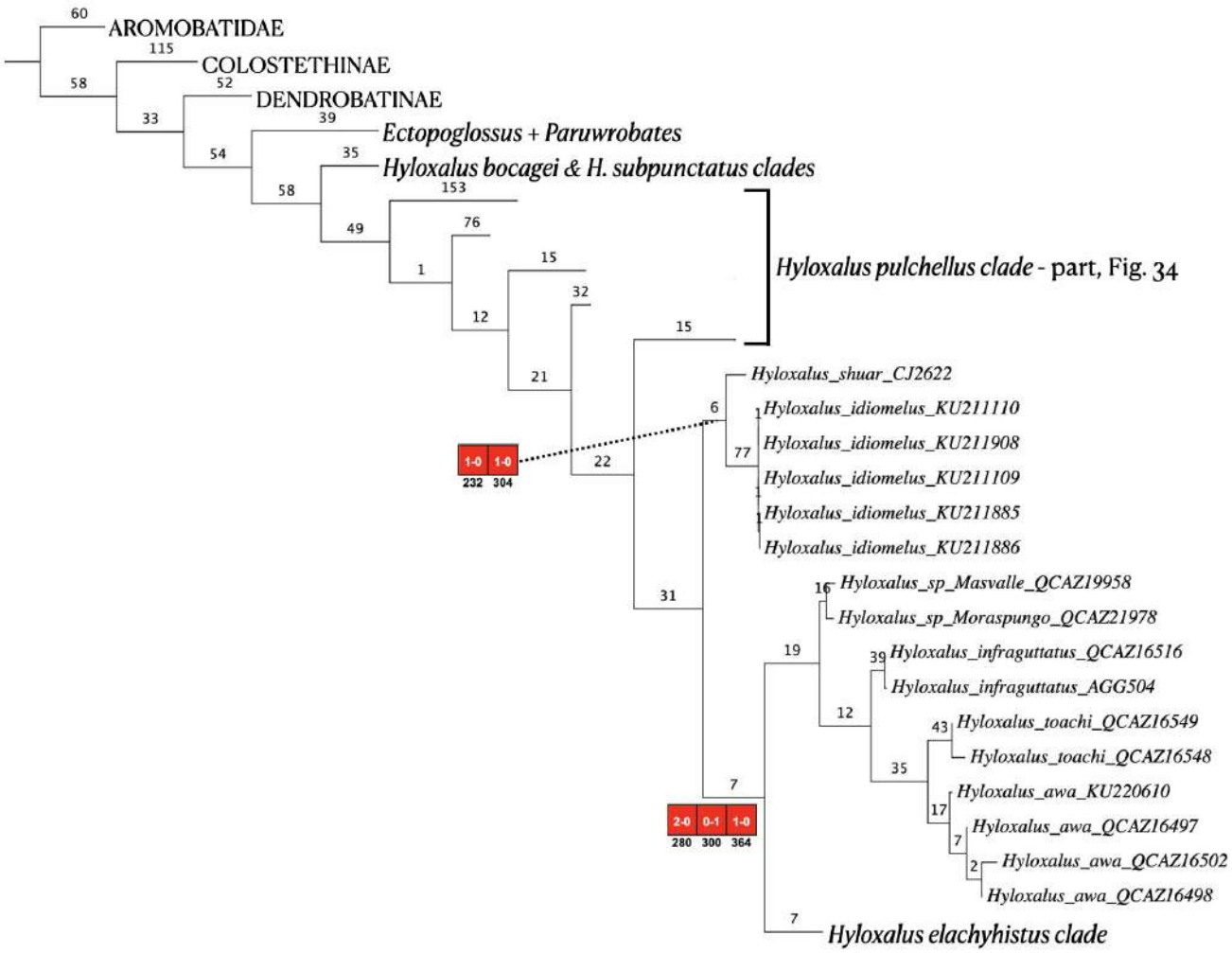

FIGURE 36.—Optimal hypothesis of relationships of a part of *Hyloxalus pulchellus* clade. Clades *H. shuar–H. idiomelus,* and the *H. infraguttatus*. The most parsimonious tree show minimum branch-length, unsupported nodes collapsed, supported nodes with Goodman-Bremen value, and select nodes show unambiguous phenotypic synapomorphies (Red square: unambiguous, non-private synapomorphies. Numbers below square is the character, and numbers into square are primitive–derive character-states transformation).

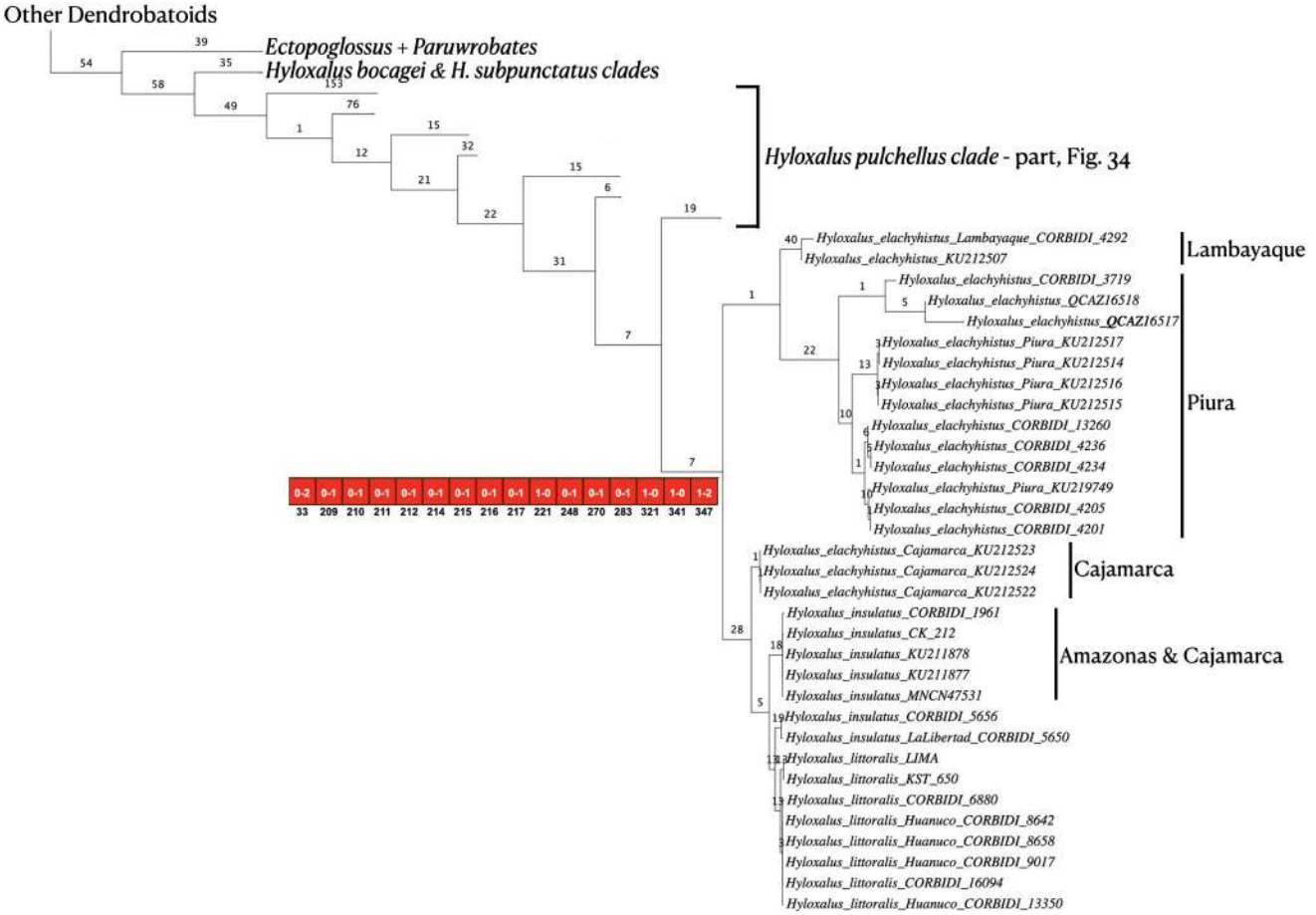

FIGURE 37.—Optimal hypothesis of relationships of a part of *Hyloxalus pulchellus* clade. Clade *H. elachyhistus*. The most parsimonious tree show minimum branch-length, unsupported nodes collapsed, supported nodes with Goodman-Bremen value, and select nodes show unambiguous phenotypic synapomorphies (Red square: unambiguous, non-private synapomorphies. Numbers below square is the character, and numbers into square are primitive–derive character-states transformation).

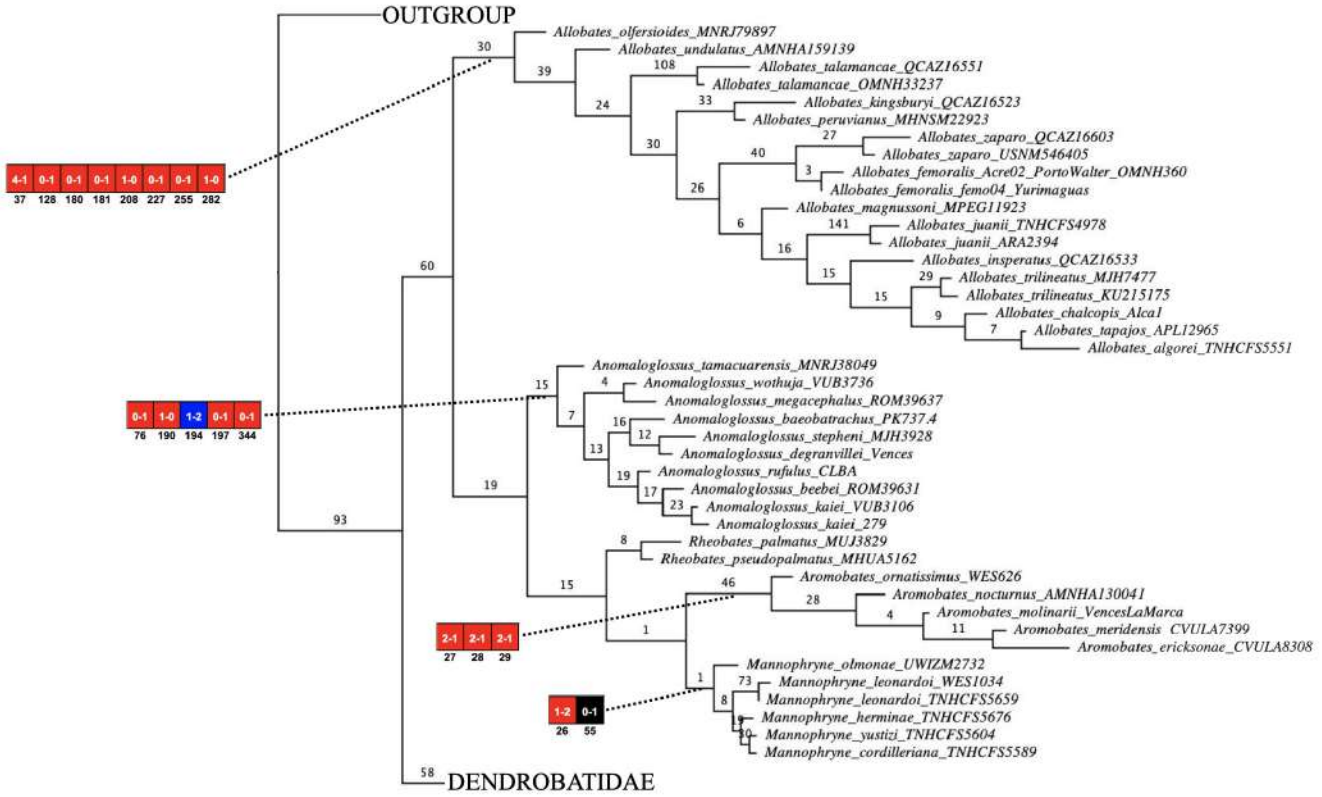

FIGURE 38.—Optimal hypothesis of relationships of Aromobatidae family. The most parsimonious tree show minimum branch-length, unsupported nodes collapsed, supported nodes with Goodman-Bremen value, and select nodes show unambiguous phenotypic synapomorphies (Red square: unambiguous, non-private synapomorphies. Blue square: unambiguous, private synapomorphies. Black square: unambiguous, and non-homoplastic synapomorphies. Numbers below square is the character, and numbers into square are primitive–derive character-states transformation).

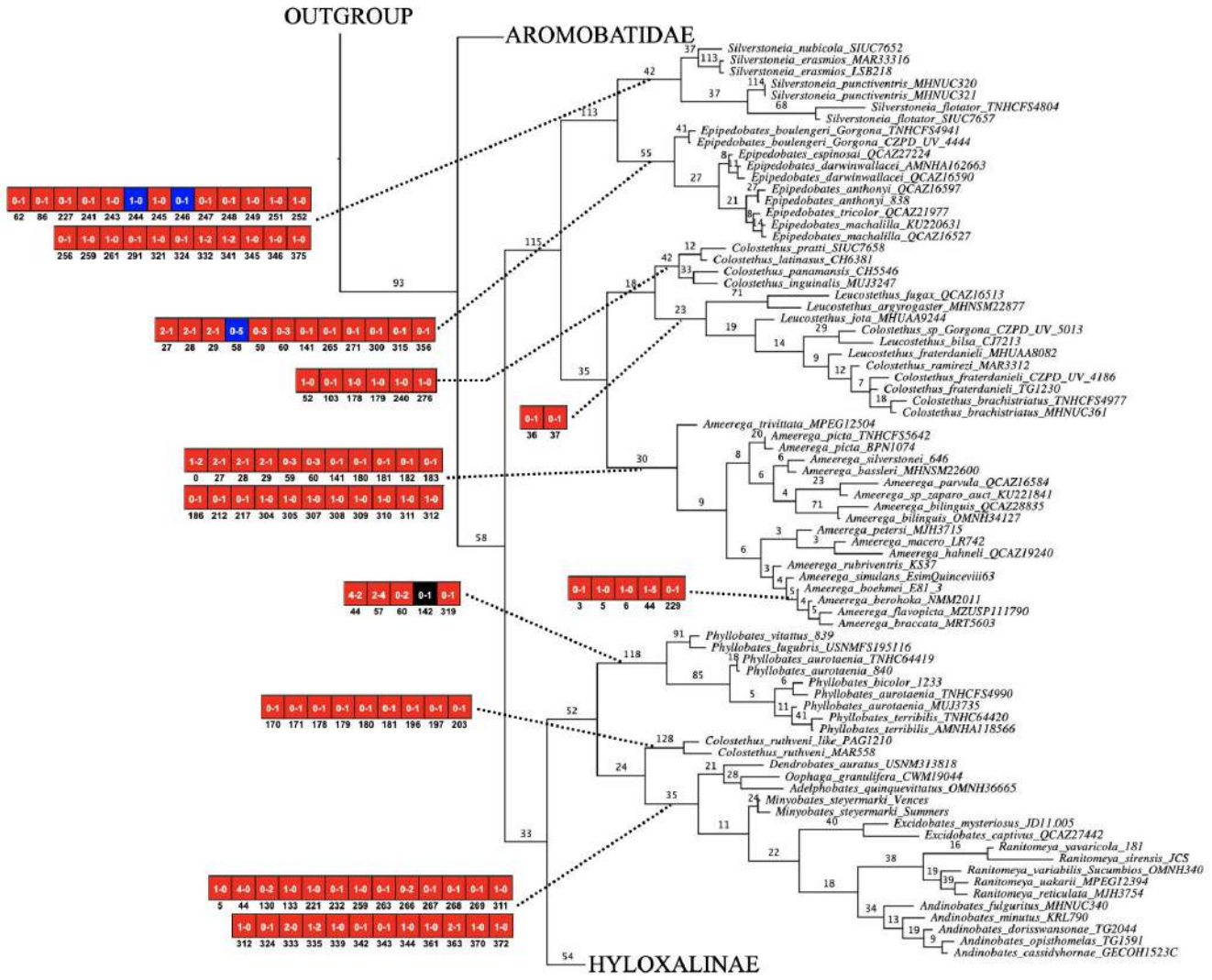

FIGURE 39.—Optimal hypothesis of relationships of dendrobatids subfamilies, Colostethinae and Dendrobatinae. The most parsimonious tree show minimum branch-length, unsupported nodes collapsed, supported nodes with Goodman-Bremen value, and select nodes show unambiguous phenotypic synapomorphies (Red square: unambiguous, non-private synapomorphies. Blue square: unambiguous, private synapomorphies. Black square: unambiguous, and non-homoplastic synapomorphies. Numbers below square is the character, and numbers into square are primitive–derive character-states transformation).

Capítulo 3

The arm swelling of *Hyloxalus* (Anura: Dendrobatidae): A histological approach with systematic implications.

MARVIN ANGANOY-CRIOLLO[1], ISABELA RODRIGUES DE SOUZA CAVALCANTI[1], PEDRO HENRIQUE DOS SANTOS DIAS[1], & TARAN GRANT[1]

[1] Universidade de São Paulo, Departamento de Zoologia, Instituto de Biociências, Rua do Matão n° 101, CEP 05508-090, São Paulo, SP, Brazil.

ABSTRACT: The arm swelling (or black arm gland, black arm band) is a protrusion on the internal surface of the skin at the distal end of the upper arm and proximal end of the lower arm. This varies in coloration, extension, and protuberance degree both intra- and inter-specifically, but this is only present in adult males of nine species of *Hyloxalus.* In concordance with observed variation was hypothesized that the arm swelling could be glandular, under hormonal control, and involved in the reproductive amplexus. Moreover, the occurrence of this swelling was used to define the putative *H. ramosi* group (then-*Colostethus*); nevertheless, in the recent Dendrobatoidea phylogenetic analysis was revealed that this is homoplastic because four species of this group are not close relatives. For this reason, was suspected anatomical differences in the arm swelling. In this research, we study the integument nature in six species (three described and three undescribed) of the former *H. ramosi* group using external observation and histological methods, to analyze the anatomical variation, and propose transformation series (i.e., characters). Also, we discussed the homology, evolution, and the systematic and biological implications of our findings.

Results show that this swelling occurs in seven additional species, with a complex integumentary structure between species, because there is a cluster, packed or close specialized exocrine glands in most of the examined species, with others associated dermal and hypodermal modifications, including the melanophores accumulation in the *stratum spongiosum* and the *tela subpuctanea*, and an enlarged lymphatic space in this last layer. Glandular integument is present both in species with external protrusion and in one species with almost undetectable swelling. This integument sometimes is conformed by a mixture of specialized mucous and serous glands, and in other species only either by mucous or serous glands. Integumentary differences were grouped into four arm swelling types. Optimization of the external characters shows independent acquisition and synapomorphy for a restricted clade in the *Hyloxalus pulchellus* group (as defined in Chapter 2). Based on the specialized glands and the integumentary modifications, we provided evidence that the arm swelling is involved in reproduction; however, we cannot corroborate its participation in the sexual amplexus due to the lack of the natural history data and others for most species.

Key words: Black Arm Gland, Specialized Glands, *Tela Subcutanea*, Hyloxalinae, Dendrobatoidea.

INTRODUCTION

The amphibian integument is characterized by the presence of exocrine glands, involve in different functions, such as dehydration avoidance, thermoregulation, reproductive behavior, social interactions, and chemical defense (Lillywhite 1971, Neuwirth et al. 1979, Toledo and Jared 1995, Daly et al. 2005; Brunetti et al. 2014). Two exocrine gland types are common in the amphibian integument, mucous and granular or serous glands (Toledo and Jared 1995, Delfino et

al. 1985, Brizzi et al. 2002, 2003). Both types of glands are composed of a duct, the neck, and the secretory portion. The secretory portion is filled by granules in serous glands, while the mucous gland is composed of columnar or cuboidal epithelium with a medial lumen. Mucous glands are smaller and more numerous than serous glands (Toledo and Jared 1995, Brizzi et al. 2003, Luna et al. 2018). Functionally, serous glands produce toxic and repellent secretion (Neuwirth et al. 1979, Toledo and Jared 1995, Delfino et al. 1999, Brunetti et al. 2016); in change, mucous glands generate mucins, threonines, carbohydrates, gycosaminoglycans, and noxious and toxic components, and are implicit in diverse function as pH balance, skin lubrication and moisture, thermoregulation, reproduction and in antipredatory defense (Toledo and Jared 1995, Brizzi et al. 2002).

When glands has specialized functions are considered specialized exocrine glands (Brizzi et al. 2003, Brunetti et al. 2014, Luna et al. 2018). These specialized glands are large, clustered and packed in determined body regions, sometimes morphologically modified, protruding the skin as patches, plicae, swollen areas, or macroglands. In change, the ordinary exocrine glands are scattered throughout the body without skin modification (Thomas et al. 1993, Toledo and Jared 1995, Brizzi et al. 2002). In amphibian anurans, glands involve in reproductive amplexus are known as specialized dimorphic sexual glands (SDSGs, Thomas et al. 1993), which are commonly found in sexual dimorphic characters (e.g., nuptial pads; Duellman and Trueb 1994, Luna et al. 2018). Histochemical studies show that specialized exocrine glands are mucous or serous glands (SMGs or SSGs, respectively) and are found in different body regions (Thomas et al. 1993, Brizzi et al. 2003; Brunetti et al. 2012, 2014, Luna et al. 2018, 2019).

The arm swelling or before named black arm gland (or blank arm band; Grant and Castro 1998) is a dull gray to black swelling of the ventral and anterior skin

surface at the distal end of the upper arm, sometimes extending to the inner surfaces of the lower arm, present only in the adult males of nine dendrobatid species of the genus *Hyloxalus—H. anthracinus, H. arliensis, H. cevallosi, H. exasperatus, H. fascianigrus, H. lehmanni, H. ramosi, H. nexipus,* and *H. saltuarius* (Grant and Castro 1998, Grant and Ardila-Robayo 2002, Grant et al. 2006, 2017, Acosta-Galvis et al. 2020). Adult females and juvenile of those species lack it, and the protrusion in the adult males of those species varies from unnoticed to males with slightly or large swelling (Grant and Castro 1998, Grant et al. 2006, 2017). Given this variation in the arm swelling, that is, a sexually dimorphic character, marked protruding in sexually active males, a glandular integument composition, under hormonal control, implicit in the reproductive amplexus was presumed (Grant and Castro 1998); however, the glandular nature, gland types and secretion, and amplexus occurrence in those species remain unknown to date.

Arm swelling became important in the systematic of Dendrobatoidea because this was used to define a natural group within then-*Colostethus sensu lato* (now in *Hyloxalus*)—the *H. ramosi* group (Grant and Castro 1998; see also Grant et al. 2006). Nevertheless, the homology of this swelling and monophyly of this group was roundly rejected by Grant et al. (2017), because they found that four species of this group, *H. anthracinus, H. arliensis* (referred as *Hyloxalus* sp. "Ibagué"), *H. lehmanni* and *H. nexipus*, are not close allied, and this swelling arises independently at least three times within *Hyloxalus*, one time shared by the sister species *H. arliensis* and *H. lehmanni*, the second time in *H. anthracinus* and finally in *H. nexipus*. This finding allowed Grant et al. suspect integumentary difference in the black arm gland.

Recently, Cavalcanti et al. (2021) analyzed the finger swelling integument of the poison frogs. They found at least four specialized sexually dimorphic mucous glands on the four fingers and the wrist, responsible to produce the swelling on these.

Sometimes, despite the occurrence of these specialized glands, the swelling is almost imperceptible externally. Furthermore, they did not find other dermal modifications in the swelling. Based on these data, they formulated 15 transformation series, analyzed the evolution, and found phenotypic synapomorphies for poison frogs. Moreover, they deduce that these glands in males, like the nuptial pads, deliver sexual hormones to stimulate the female in the cephalic amplexus.

Given the reported variation and homoplastic nature of the arm swelling, and the finding in the other sexual dimorphic character in the poison frogs, in this research we reviewed the external morphology of the arm swelling, and studied and compared the anatomical structure of the swelling integument of six *Hyloxalus* species (three described and three undescribed), using histological and histochemical techniques, to test the glandular nature hypothesis. We characterize the arm swelling integument to identify transformation series (i.e., characters) in the observed variation. The possible systematic, evolutionary, and functional implications of the characters and the arm swelling are analyzed.

MATERIALS AND METHODS

Species studied.—We examined the external morphology of the arm swelling in adult males of *Hyloxalus anthracinus, H. arliensis, H. cevallosi*, *H. craspedoceps, H. exasperatus*, *H. fascianigrus*, *H. lehmanni*, *H. nexipus, H. ramosi* (photos of holotype)*, H. saltuarius,* and in five undescribed species similar to *H. lehmanni*. *Hyloxalus* sp. Albán (from Albán, Cundinamarca), *Hyloxalus* sp. *fascianigrus*-like (from Tambo, Cauca), *Hyloxalus* sp. Icononzo (from Icononzo, Tolima), *Hyloxalus* sp. MesasGalilea (Las Mesas de Galilea, Villarica, Tolima), and *Hyloxalus* sp. Samaná (Samaná, Caldas). The same region in juveniles of both sexes and adult females also were observed. When necessary, gross dissections were employed. Due

to the intraspecific variation in the arm swelling, i.e., some adult males lack the swelling, while others have (a few, commonly), we included all or a large amount of the adult males available for those species in the revised amphibians collections to treat to identify the swelling occurrence. For comparison, we reviewed the adult males and females of 53 species of *Hyloxalus* and also other Dendrobatoidea (**Appendix 1,** specimens examined).

For histology, we analyzed the serial cuts of the arm swelling in the one adult male and equivalent region in one adult female of the *Hyloxalus lehmanni, H. nexipus,* and *Hyloxalus* sp. *fascianigrus*-like*,* and just one adult male of the *H. anthracinus, Hyloxalus* sp. Icononzo and *Hyloxalus* sp. Samaná. Adult males with prominent swelling were selected. To compare the swelling integument with a species without swelling, serial cuts of the equivalent region of the one adult male and one adult female of the *H. pinguis* were analyzed. The adult males of this species lack arm swelling. Additionally, the serial cuts of the *H. lehmanni, H. pinguis,* and *Hyloxalus* sp. *fascianigrus*-like include forelimb areas where there is no arm swelling—the elbow, posterior surface of the upper arm, and external surface of the lower arm. This information was contrasted with the published available integument and glands data of the other dendrobatoids species (i.e., Prates et al. 2012, Moreno-Goméz et al. 2014, Grant et al. 2017, Cavalcanti et al. 2021).

Histological and histochemical procedures.—All arm swelling region, and equivalent portion in females, was extracted in those seven species. Samples were dehydrated in ascending ethanol series (25%, 50%, 75%, 100%), transferred to an infiltrate solution of historesine (Leica) plus 100% ethanol (1:1), and after, these were placed in pure historesine at vacuum chamber by twelve hours. Finally, the samples were included in a solution of the historesine plus hardener. 5 μm was the thickness of each cut, and these were mounted on a microscopy slide. Serial cuts were stained with

toluidine blue with basic fuchsin stain to the visualized general structure, and naphthol yellow with the periodic acid Schiff stain (PAS+NY) was used to identify proteins and neutral mucopolisacarids, respectively. Histochemical reaction of glands was coded follows Brunetti et al. (2014) as: strongly positive with “++”, positive with “+”, negative with “-”, and equivocal with "+/-” when in some samples there is staining affinity uncertainty due to different preservation methods. Gland quantification in the integument was done by counting the gland number in 1 linear mm as Brunetti et al. (2016), and for the gland size, the length was taken at their larger axis, the longitudinal axis for mucous glands, and the perpendicular axis for serous glands. Observations and photos were done with a microscope Leica DM 750, with a built-in camera Leica ICC50 W. Terminology follows Jared and Toledo (1995) for mucous and serous glands. The distinction between common and specialized glands follows Brizzi et al. (2003). Thomas et al. (1993) and Brunetti et al. (2012) were used for specialized dimorphic sexual glands (SDSGs).

Characters evolution.—All phenotypic independent variation observed in the lineages were infer as manifestation of the same evolutionary transformation series (Grant and Kluge 2004). Therefore, the independent macroscopical and microscopical morphological variation occurring in the arm swelling in all species evaluated were coded as alternative character-states of the defined characters. Multi-states characters were treated as unordered due to lack of auxiliary evidence (e.g., ontogeny). The character of the Grant et al. (2006: character 27, the black arm gland occurrence) was evaluated and considered as the starting point.

Although there is intraspecific variation in the arm swelling, apparently correlated with sexual activity, we coded only the swelling presence if it occurs in at least one adult male (see Campbell and Frost 1993: 63). The defined characters were

optimized in the most recent *Hyloxalus* phylogeny, revised in **Chapter 2**, to analyze the homology hypotheses and characters evolution, and to identify synapomorphies.

Edition of the matrix and the optimization of the characters were did in Mesquite 3.4 (Maddison and Maddison 2019) to reconstruct the ancestral states by a Fitch (1971) parsimony. When optimization was ambiguous, the delayed and accelerate optimization are discussed, giving the lack of the valid argument to prefer one over the other (Farris 1970, Agnarsson and Miller 2008). Ideally, character evolution should be studied with the most complete phylogeny; however, data of the histological characters are only of four species present in the phylogeny (i.e., *Hyloxalus anthracinus, H. lehmanni, H. pinguis*, and *H. nexipus*), while the data of the external morphology characters come from most species presents in the tree; therefore, the evolution is only analyzed for external morphology. Nonetheless, histological characters are also discussed. Due to species is the evolutionary unit, the phylogeny was pruned to one terminal by species.

RESULTS

External Morphology of the Arm Swelling

Our observations agree with Grant and Castro 1998 (see also Acosta et al. 2020), because the arm swelling (or black arm gland, BAG) varies intraspecifically in coloration degree, swelling extension (restricted to the distal end of upper arm, or also extending to the proximal lower arm), swelling protrusion (the adult females and juveniles without external protrusion, and adult males with arm swelling). A few adult males express the swelling, while others not. Additional to the species reported with the arm swelling (or BAG), we confirm the presence in the adult males of *H. craspedoceps*, and in five undescribed species similar to *H. lehmanni* (*Hyloxalus* sp. Albán, *Hyloxalus* sp. Icononzo, *Hyloxalus* sp. MesasGalilea, *Hyloxalus* sp. Samaná,

and *Hyloxalus* sp. *fascianigrus*-like). *H. pinguis* also have the arm swelling, but this was detected after histological analysis, because swelling is almost undetectable externally (see below. **Figure 1**).

In magnification, commonly many melanophores covering the arm swelling, and sometimes, the glands are perceivable. In adult males of the *H. pinguis* this region is white. Despite the coloration variation, some adult males of *Hyloxalus anthracinus*, *H. cevallosi*, *H. exasperatus, H. fascianigrus*, *H. lehmanni*, *H. ramosi, H. saltuarius*, and *Hyloxalus* sp. *fascianigrus*-like express the solid black arm swelling, while the darkest coloration reaching in the preserved specimens of *H. arliensis*, *H. craspedoceps,* and *H. nexipus* is light gray/brown (although in *H. arliensis* is black in life. **Figure 1H**). Moreover, the swelling in the last three species is restricted to the distal end of the upper arm, not extending to the proximal lower arm.

Internally between the integument and the fascia muscular, the branchial blood vessels are tied to the dermis of the arm swelling, and beneath the dermis there is a translucent tissue with melanophores (**Figure 1F)**. The quantity of these melanophores varies from a few (in species with light gray/brown BAG) to many melanophores (in species with black swelling; e.g., *H. anthracinus* and *H. lehmanni*). These pigments do not extend or covers adjacent non-swelling areas.

General Features of the Arm Integument

In general, the integument structure of the distal end of the upper arm and proximal lower arm is relatively similar in the species evaluated. The epidermis has three to four cellular layers, and the external surface is undulated to notably wavy in the male of *Hyloxalus lehmanni*. In the dermis, there are two exocrine gland types, mucous and serous (or granular) glands, blood capillaries, nerves, and melanophores. The *stratum spongiosum* and the *stratum compactum* are separated by the well-

defined Eberth-Katschenko layer, which is inconspicuous in *H. anthracinus*. The deepest layer, *tela subacutanea* is the lymphatic narrow lining beneath the dermis, with small and narrow spaces for blood vessels and nerves (Elkan 1968, 1976, Toledo and Jared 1993, Amey and Grig 1995). It is composed of elastic fibers (Schwinger et al. 2001). Melanophores are found in the *stratum spongiosum* of the dermis, scattered and close to the epidermis, and rarely associates with glands when these occur. Iridophores and xanthophores were not detected in the samples evaluated (**Figure 2**).

The exocrine glands of this integument are composed of an unbranched duct, the intercalary region (neck), and the secretory portion. In all glands, there is a bilayer of the nearly elongated cells in the intercalary region and the duct of mucous glands, except that the duct internal cells are flats. A single layer of the elongated cells composes the duct of the serous glands. The secretory portion varies between gland types. The secretory portion of the ordinary mucous glands (OMGs) is alveolar to elongated, composed of one layer of low, roughly square epithelial cells with rounded nucleus disposed at its base commonly, and this delimited the empty lumen. In ordinary serous glands (OSGs), the secretory portion is alveolar, but sometimes is elongated; the syncytial cytoplasm is filled with rounded granules. The secretory portion of the OMGs and OSGs is surrounded by a contractile sheath of myoepithelial thin cells. A few epithelial cells of the OMGs react positive to the presence of neutral mucopolysaccharides and rarely does the lumen show proteins (naphthol yellow positive). The secretory portion of the OSGs reacts slightly for neutral mucopolysaccharides and sometimes the syncytium is stained slightly for proteins (**Table 2**). Both types of ordinary glands are scattered in the evaluated skin regions of the females, and adjacent integument to the arm swelling region. There are more OMGs than OSGs, and the former is smaller than the latter, generally (**Figure 2, Appendix 2**).

Integument in the Arm Swelling

There is no increase in the epidermis thickness in the arm swelling region with respect to adjacent skin areas without swelling (i.e, elbow, posterior skin surface of upper arm, and lower arm) in each species; but, there is sexual dimorphism in *Hyloxalus lehmanni* and *Hyloxalus* sp. *fascianigrus*-like, being slightly thinner in males than females. Interspecifically, the epidermis of the male of *H. pinguis* (a species without notable swelling) is thicker than the epidermis of the arm swelling in other species evaluated (64.7–76.5 µm in *H. pinguis,* and 23.5–41.2 µm in males with BAG. **Table 1**). Epidermis is invaginated in some regions of the swelling in *H. anthracinus,* sometimes connected with the gland ducts.

The dermis thickness varies between regions, sex and species. In all species, the dermis is thicker than other evaluated forelimb regions. Only, *Hyloxalus pinguis* do not have sexual dimorphism in dermis thickness in the arm swelling; however, the dermis of the species with swelling is one time thicker in males than females. Interspecifically, the dermis of the *H. lehmanni*, *Hyloxalus* sp. *fascianigrus*-like, *Hyloxalus* sp. Samaná and *Hyloxalus* sp. Icononzo is from one time to twice thicker than the dermis of the *H. anthracinus* and *H. pinguis* (without external swelling. **Table 1**). There are melanophores accumulation in the *stratum spongiosum* of the arm swelling region, covering most exocrine glands, unlike in the male of *H. pinguis*, where these are scarce and glands are almost pigments free. The thickness of the dermis is due to increasing of *stratum spongiosum* thickness, because of the presence of the cluster, packed or closely large glands, and the melanophores accumulation in this layer (**Figure 3**).

The *tela subcutanea* forms a wide lymphatic space with blood capillaries, nerves, and many melanophores in the arm swelling region. This enlarged space and melanophores accumulation in this layer are not found in other evaluated regions of

the forelimb, and also is absent in females of those species and both sex of *Hyloxalus pinguis*. Melanophores in this layer are located beneath the dermis and quantity varies interspecifically. Thus, there are a few melanophores in *H. nexipus*, *Hyloxalus* sp. *fascianigrus*-like, *Hyloxalus* sp.Icononzo, and in *Hyloxalus* sp. Samaná; in change, there are many melanophores in *H. lehmanni* and *H. anthracinus*. In this last species, these form a black thin layer close to the dermis.

In the integument of the arm swelling region, including the equivalent area of the adult male of *H. pinguis*, the exocrine glands are disposed in a cluster, closely or packed glands usually (except in *H. anthracinus*). Mucous and serous glands in this region are larger than ordinary glands of the adjacent areas (**Figure 4, Table 1**). These hypertrophied glands are absent in females evaluated, and there are more hypertrophied exocrine glands in males (8–11 glands/mm.) than ordinary glands in females at the equivalent region (5–7 glands/mm.). Moreover, there is interspecific variation in the gland type composition in the arm swelling integument of the adult males. In *H. nexipus* predominated hypertrophied serous glands (SGs), with a few OMGs (7–8 SGs/mm., and 1–2 OMGs/mm.); while, the hypertrophied mucous glands prevail in *H. pinguis*, and rarely there are OSGs (5–9 MGs/mm., and 0–1 OSGs/mm.); in change, a mixture of the hypertrophied MGs and SGs are found in *H. lehmanni*, *Hyloxalus* sp. Samaná, *Hyloxalus* sp. *fascianigrus*-like, and *Hyloxalus* sp. Icononzo, although the large SGs are in less quantity. The arm swelling of the *H. anthracinus* has some scattered ordinary mucous and serous glands only.

A rounded to ovoid secretory portion is found in the hypertrophied mucous glands. Their epithelium is conform by trapezoid or rectangle cells, larger and higher than the epithelial cells of the OMGs, with rounded nucleus located at the base or in the middle of the epithelial cell. The lumen in these glands tends to be smalls (**Figure 5**). These epithelial cells are positive for neutral mucopolysacharides, with greater

concentration in most, or in some cells, or at the tips of these in *H. lehmanni* and *Hyloxalus* sp. Samaná. These differential secretory composition is also showed with different affinity degrees to the toluidine dye. Despite the morphology of the epithelial cells of the *H. pinguis*, *Hyloxalus* sp. *fascianigrus*-like and *Hyloxalus* sp. Icononzo is similar to *H. lehmanni* and *Hyloxalus* sp. Samaná, their cells does not stained strongly positive for PAS+NY. Hypertrophied MGs reacts to proteins rarely (**Table 2**).

Morphology of the hypertrophied serous glands is like to the OSGs, except for the largest size and a rounded adenomero. In addition to the granules, the syncytium in the glands of the *H. nexipus*, show one, two to three semicircular regions or compartments, where granules are not obvious and externally appear be texture homogeneous (**Figure 5**). Granules of these glands sometimes are slightly positive for neutral mucopolysaccharides. Proteins (naphthol yellow positive) were only detected in the syncytium of the *H. lehmanni* and *H. nexipus* (**Table 2**).

Also hypertrophied mucous and serous glands differ in morphology and histochemical reaction from ordinary glands; moreover, despite unknown the specific function of these glands, their dimorphic sexual occurrence, suggests that these can act as an extension of the reproduction as suspected previously (Grant and Castro 1998). On the basis of these differences, we considered these hypertrophied mucous and serous glands of the arm swelling integument as specialized glands (SMGs and SSGs, respectively).

Types of the Arm Swelling

The histological data reveals at least four types of the arm swelling:

Type I.—This type of swelling is found in *H. lehmanni*, *Hyloxalus* sp. *fascianigrus*-like, *Hyloxalus* sp. Icononzo and *Hyloxalus* sp. Samaná (type I). These undescribed species are similar to *H. lehmanni*. Histologically, this type is

characterized and differentiated from other types by the presence of the glandular integument with a mixture of the cluster and packed SMGs and SSGs, melanophores accumulation in the dermis, and the *tela subcutanea.* This last layer is as enlarged lymphatic spaces. Hypertrophied glands and enlarged lymphatic space produce the swelling that extends on the distal end of the upper arm and the proximal end of the lower arm. The great melanophores quantity generates the external dark coloration.

Type II.—This type is found in *Hyloxalus pinguis*; although, this species was considered without swelling (see Grant et al. 2017). The integument is glandular, composed of clustered and closely SMGs. Other dermal and hypodermal modifications are absent and similar to the integument of the adult females, i.e., the melanophores are scarce in the dermis and lack in the *tela subcutanea*, and this last layer does not show an enlarged lymphatic space. Nevertheless, the epidermis is thick than other species with swelling. Swelling externally is white, very low, and almost un-noticeable externally, restricted to the distal end of the upper arm. This species was confused with *H. pulchellus* (Ruiz-Carranza et al. 1996: 378, Acosta-Galvis 2000: 297–298; Anganoy-Criollo 2013), but these differ in morphological features, genetic distances, and topological position (**see Chapter 2**). A close inspection of the forelimb of the adult male of *H. pulchellus* shows a very low, white protuberance in the anteroventral surface of the distal end of the upper arm, surrounded by cream or dull white skin with dark brown stippled. A macroscopical dissection in this area reveals that the integument is thicker than adjacent skin areas; however, below the integument, there is no enlarged lymphatic space with melanophores. On the basis of the swelling similarities between *H. pinguis* and *H. pulchellus*, we anticipate the glandular swelling presence in *H. pulchellus*. Serial cuts are necessary to confirm the occurrence of specialized glands.

Type III.—Present in *Hyloxalus nexipus.* The swelling is glandular, filled by cluster and closely SSGs, with melanophores accumulated in the dermis and in the *tela subcutanea*. The last layer is modified as enlarged lymphatic space. The SSGs has a semicircular regions or compartments without obvious granules in the syncytium. The swelling is generated by the large serous glands and the enlarged lymphatic space, while melanophores cause the dark coloration. Externally, the dark swelling is restricted to the distal end of the upper arm.

Type IV.—This type of arm swelling occurs in *Hyloxalus anthracinus.* This species posses a black arm swelling, extending on the distal upper arm and the proximal lower arm. The black coloration is product of a great quantity of the melanophores in the dermis and in the enlarged lymphatic space of the *tela subcutanea*, forming a thin dark layer in the *tela subcutanea.* However, the integument is not glandular, because this posses scarce, scattered OMGs and OSGs. In this type, melanophores layers and enlarged lymphatic space yield the protuberance (Figure 3C, Appendix 2.5).

Characters

On the basis of our results, we proposed two characters from external morphology and six from integument of the arm swelling.

External morphology.—On the basis of the integument variation found in the *Hyloxalus* evaluated (see above), the black arm gland (Grant and Castro 1998, and Grant and Ardila 2002, Grant et al. 2006, 2017) is not always glandular or black (referring to dark or black coloration); because, the swelling of *H. anthracinus* have some scattered ordinary exocrine glands, and therefore the integument is not glandular. Contrastingly, although the swelling is almost un-noticeable, there is a glandular integument with hypertrophied mucous glands at the distal end of the upper arm in the adult male of the *H. pinguis*; moreover, their skin is white, given that the

dermis have scarce melanophores. This variation shows distinct types of the swelling, and the name black arm gland do not embrace these exceptions. Therefore, we suggest to change the name by the *arm swelling*, which include broadly all swelling types observed in *Hyloxalus*.

Character 1: Arm swelling in the adult males, occurrence: absent (0), present (1) (**Figure 1**).

Adult males of the former *Hyloxalus ramosi* group have a slightly to pronounced swelling at the distal end of the upper arm, sometimes extending to the proximal lower arm (state 1). This swelling is absent in most *Hyloxalus* and other species of the Dendrobatidae and Aromobatidae families, that is, the skin of the distal end of the arm is not protuberant, and no dermal modifications are observed (state 0). This character is equivalent to character 27 of Grant et al. (2006); however, we are not considering the dark coloration, because there is independent variation in the melanophores accumulation in two layers of the integument, and their interaction cause different external dark degrees. Additionally to the previously reported species with arm swelling (before black arm gland/band), we confirm the presence in the adult male of the *Hyloxalus craspedoceps, H. pinguis* (by mean of the histological analysis), and *H. pulchellus* (by mean of the gross dissection), and also in the undescribed species *Hyloxalus* sp. Albán, *Hyloxalus* sp. Icononzo, *Hyloxalus* sp. MesasGalilea, and *Hyloxalus* sp. Samaná.

Character 2: Arm swelling in the adult males, extension: (0) restricted to the distal end of the upper arm, (1) on the distal end of the upper arm, extending to the proximal lower arm (Figure 1C, E).

To evaluate this character is need observations in various adult males because there is intraspecific variation in the swelling extension (see Grant and Castro 1998, Acosta-Galvis et al. 2020, and our data). Our data come from various adult males *H.*

anthracinus, H. arliensis, H. lehmanni, H. nexipus, H. pinguis, and *Hyloxalus* sp. *fascianigrus*-like. Despite this variation, in five species (*H. arliensis, H. craspedoceps, H. nexipus, H. saltuarius, H. pinguis, H. pulchellus*, and *Hyloxalus* sp. MesasGalilea), the swelling is restricted to the distal end of the upper arm, no extending to the forearm (state 0); in change, in the remains species the swelling extends distad, on the inner surface of the proximal lower arm (state 1).

Integument.—The following characters are proposed based on six *Hyloxalus* species, *H. anthracinus, H. lehmanni, H. nexipus, H. pinguis, Hyloxalus* sp. Icononzo, and *Hyloxalus* sp. Samaná. Even though the reduced taxon sampling, variation of the characters not overlapped, and this is independent.

Character 3: Specialized mucous glands in the glandular integument, occurrence: (0) absent, (1) present (Figure 5A–C).

Character 4: Specialized serous glands in the glandular integument, occurrence: (0) absent, (1) present (Figure 5D–F).

The semicircular regions or compartment and size of the SSGs of the *H. nexipus* differ from SSGs of the other species (i.e., *H. lehmanni*, *Hyloxalus* sp. *fascianigrus*-like, *Hyloxalus* sp. Icononzo, and *Hyloxalus* sp. Samaná). This insinuate possible differences between these glands—distinct specialized serous glands. Nevertheless, our data are not sufficient to confirm this; therefore, we assumed that all SSGs of the swelling are homologous. Further analysis and evidence are necessary to characterize and determine differences.

Character 5: Enlarged lymphatic space of the *tela subcutanea* in the arm swelling, occurrence: absent (0), present (1) (Figure 3C).

Tela subcutanea is the deepest and narrow lymphatic layer of the skin (Elkan 1968, 1976, Toledo and Jared 1993, Haslam et al. 2014). Although not specified, there is interspecific variation in the lymphatic space size in some species of Anura (Elkan

op.cit.). In some *Hyloxalus* with arm swelling, the *tela subcutanea* forms an enlarged lymphatic space under the swelling integument, surpassing half of the integument thickness or sometimes as higher as it (state 1). In change, as in many anurans, the enlarged lymphatic space is absent in other *Hyloxalus* with or without swelling. In this case, this is a narrow lining of the dermis, leaving small lymphatic spaces (state 0). Evaluation of the enlarged space occurrence can be done by means of macroscopical dissection, given that the enlarged space is visible as translucent dark "connective tissue" between the skin and muscular fascia at the distal end of the arm.

Character 6: Density of the melanophores in the dermis: few, scarce (0), many, numerous (1) (Figure 3A, 3B).

Melanophores are a common chromatophore in the amphibian integument. These participate in metachrosis, darkening the integument when a large quantity of these are accumulated (Bagnara et al. 1968, Thibaudeau and Altig 2014). The dark coloration of the arm swelling is due to the melanophores accumulation in the dermis, and also in the *tela subcutanea*, but variation in quantity and distribution support independence of the dark pigments in each layer. In the state 0, there are few or scarce melanophores on the dermis. In this case, the swelling is white externally. In state 1, the density of melanophores is large, with many pigments, sometimes forming a dark thin layer on the glandular integument (state 1). In this case, the swelling is from slightly dark to black, externally. Despite the melanophores movement capacity (Bagnara et al. 1968; Hoffman and Blouin 2000), the state 0 does not reach the state 1, because the amount of melanophores is not sufficient to cover all glandular region.

Acosta et al. (2020) considered coloration differences in the swelling based on external appearance, delimiting the pale and black arm gland conditions; however, given the dependence between integument melanophores and the external coloration,

we do not considered this proposal. In change, we proposed independent characters in each integument layer, based on the melanophores variation (see below).

Character 7: Melanophores in the *tela subcutanea* of the arm swelling, occurrence: absent (0), present (1) (Figure 3B, 3C).

Commonly, in the *tela subcutanea* of the distal upper arm and proximal lower arm, there are no melanophores. This condition is also observed in species with arm swelling (state 0). Contrarily, other species with arm swelling present melanophores. These pigments are disposed close, beneath the dermis (state 1). Like than enlarged lymphatic space of the *tela subcutanea*, this character can be evaluated from macroscopical dissection with maximum magnification.

Character 8: Thin melanophores layer at the *tela subcutanea* of the arm swelling, occurrence: absent (0), present (1) (Figure 3C).

There is variation in the amount of melanophores in the *tela subcutanea*, but we were unable to delimit objectively the character states. However, the melanophores accumulation forms a thin, continuous dark layer below the dermis of the arm swelling in *H. anthracinus* (state 1). In other species, this is absent despite the presence of the melanophores (state 0).

Evolution of the Arm Swelling

The phylogeny included nine species from 16 *Hyloxalus* with arm swelling. These are: *H. anthracinus, H. arliensis, H. craspedoceps, H. lehmanni, H. nexipus, H. pinguis, H. pulchellus, Hyloxalus* sp. Albán, and *Hyloxalus* sp. MesasGalilea. These are not closely related relatives, as found by Grant et al. (2017), because *H. craspedoceps* and *H. nexipus* are not nested with those other *Hyloxalus. H. nexipus* is an independent clade, sister to all *Hyloxalus*, except the *H. bocagei* and *H. subpunctatus* clades; while, *H. craspedoceps* is related with *H. azureiventris, H. chlorocraspedus, Hyloxalus* sp. ElCopal, and with *Hyloxalus poecilonotus* (see

Chapter 2). All of these species are without arm swelling. The remains species conform a heterogeneous clade—the *H. pulchellus* group (see **Chapter 2**) because this also included species without arm swelling, such as *H. delatorreae, H. vertebralis, Hyloxalus* sp. MonteOlivo, and *Hyloxalus* sp. SanMiguelDeSalcedo (**Figure 6A**).

Due to the topological position of the species without arm swelling in *H. puchellus* clade, the optimization of the presence of arm swelling is ambiguous at the base of its node, and the swelling may have been acquired independently three times in an accelerated optimization or four times in a delayed optimization within this clade. In both cases, there is a secondary loss in the species that lack swelling (**Figure 6A**). Despite this, the presence optimizes as synapomorphy for the restricted clade, composed of *H. arliensis, H. delatorreae, H. lehmanni, H. pinguis, H. pulchellus, Hyloxalus* sp. Albán, and *Hyloxalus* sp. MesasGalilea, *Hyloxalus* sp. MonteOlivo, and *Hyloxalus* sp. SanMiguelDeSalcedo. Within this clade, two species (*H. lehmanni* and *H. pinguis*) show a glandular integument with SMGs only or with SSGs in the arm swelling.

A swelling covering the distal end of the upper arm and the proximal lower arm is only found in *Hyloxalus anthracinus, H. lehmanni*, and *Hyloxalus* sp. Albán, while the other remaining species have the swelling restricted to the upper arm. The last is also optimized as a synapomorphy for the restricted clade within the *H. pulchellus* group (see above), except *H. vertebralis* (**Figure 6B**).

DISCUSSION

Limitations, Integument and Specialized Glands

Although our histological study have some limitations related with the reduce taxa and individuals sampled, lack of comparison between the arm integument with

integument from the other body regions by species, and the additional histochemical stains, all data were compare with integument and glands information available for anurans. Moreover, the characters were propose only when there were a clear discrete variation. Given our aim—to test the glandular nature hypothesis of the arm swelling, and identify characters in the integument, these limitations did not prevent us to achieve this. We are aware that is necessary included additional samples (serial cuts, individuals, species), specially these species with arm swelling to corroborate findings and test characters, homology hypothesis, and evolution of the characters.

The ordinary mucous and serous glands was reported from the ventral and the dorsal integument in the poison frog *Andinobates virolinensis, Ameerega picta, Dendrobates auratus, Hyloxalus faciopunctulatus,* and *Phyllobates bicolor* (de Pérez et al. 1992; Angel et al. 2003: Fig.1A–B; Delfino et al. 2010: 1F; Prates et al. 2012:Fig. 3; Moreno-Gómez et al. 2014: 00, Grant et al. 2017: Fig.15B); however, the most broadly revision of the ordinal and specialized cutaneous glands of the hand integument, including multiple species of Dendrobatoidea, were done by Cavalcanti et al. (2021). The comparison of the ordinary glands of the forelimb of the six *Hyloxalus* species reviewed herein with ordinary glands types reported previously revealed no major differences between these glands.

Specialized cutaneous glands in anurans are morphology and histochemical different regard to the ordinary glands. These are large, restricted to some body parts, forming clusters or packlike glandular integument (Thomas et al. 1993, Brizzi et al. 2003). In dendrobatoids, specialized mucous glands have hypertrophy in the secretory portion, epithelial cells are cubic or columnar, enveloping the large or small lumen; and the secretory portion has an alveolar or tubular shape. These react positively to PAS and NY commonly (Cavalcanti et al. 2021). Hypertrophied mucous glands of the arm swelling are not equal that those reported by Cavalcanti et al. (2021) because the

secretory portion does not exhibit these mentioned morphological modifications. However, the secretory portion of the glands (serous and mucous) in the arm swelling of the five *Hyloxalus* differs in morphology, size, and histochemical reaction from the ordinary glands found in the adjacent area to the arm swelling; moreover, these are sexually dimorphic, disposed in a cluster of the closing or packed hypertrophied exocrine glands in the arm swelling integument in comparison with the scattered ordinary glands found in the forelimb of adult of both males and females.

Nevertheless, although differences in histochemical reaction between hypertrophied glands were observed in this study, this can be explained by differences in the preservation history of specimens. Thus, the epithelial cells of the hypertrophied mucous glands of *H. lehmanni* and *Hyloxalus* sp. Samaná are densely stained for neutral mucopolysaccharides and show a differential toluidine stained degree. But, the hypertrophied glands found in *H. pinguis*, *Hyloxalus* sp. *fascianigrus*-like and *Hyloxalus* sp. Icononzo does not react strongly to PAS+NY, although these glands are similar in morphology and toluidine affinity degree to those last two species, and these appear not be preserved by standard techniques. Therefore, on the basis of the morphological and histochemical differences, the hypertrophied glands of the arm swelling in those five species are recognized as specialized glands.

Although in other anuran groups, the cluster of the specialized glands produce external skin modification (e.g., swelling, macroglands, plicae; Brizzi et al. 2003), there are cases where the skin is not obvious modified. For example, commonly the specialized mucous glands swollen the fingers and the wrist in dendrobatoids; however, although specialized glands occur, some species in this superfamily show fingers without evident swelling (Cavalcanti et al. 2021). Likewise, the skin of the dorsum of the ranids *Rana dalmatina, R. italica,* and *Pelophylax perezi* possess specialized mucous glands, but the skin is unmodified externally (Brizzi et al. 2002),

and the mental gland in some *Hyloscirtus* and *Hypsiboas*, although has specialized glands, seem to be absent externally (Brunetti et al. 2014). Likewise, the specialized exocrine glands, in conjunction with other dermal and hypodermal modifications yield a notable protuberance in some *Hyloxalus* with arm swelling; while in another case, only the specialized mucous glands do not generate obvious external protuberance, as in *H. pinguis*. But, on the other hand, only melanophores accumulation and enlarged lymphatic space of the *tela subcutanea* are sufficient to produce swelling in the forelimb of *H. anthracinus*.

Specialized glands are involve in specific biological roles (Brizzi et al. 2003), specifically the cutaneous glands are implicit in the reproduction, found in the secondary sexual characters. These glands are known as sexual dimorphic skin glands (SDSGs; Thomas et al. 1993). Both mucous and serous glands can be SDSGs (Thomas et al. 1993, Brizzi et al. 2003; Brunetti et al. 2012; Luna et al. 2019). These are part of the sexual characters found in various body regions of the anurans, such as nuptial pads, and the abdominal, mental, lateral and labial glands (Duellman and Trueb 1994, Thomas et al. 1993, Brunetti et al. 2014, Luna et al. 2018, 2019). Nevertheless, the specific function of the arm swelling glands in those *Hyloxalus* is unknown and unfortunately, as most *Hyloxalus* (see Grant et al. 2006: 97), the reproductive natural history data of these species are absent. Despite this, Grant and Castro (1998: 389) hypothesized that arm swelling is used in reproductive amplexus given this protuberance is expressed only in a some adult males active reproductive, analogous to the fingers swelling. This imply that the specialized glands in the arm swelling are SDSGs. Our morphological and histological data, and the findings of the Cavalcanti et al. (2021) indirectly, offers support for that statement. However, if these glands are SDSGs remains hypothetic.

In the sexual dimorphic characters is common that exocrine glands are specialized, but sometimes there is the modification in the other dermal structures; for instance, the mental glands of hylids present thickness increasing in the *stratum spongiosum* (by the occurrence of hypertrophied specialized glands) with a reduction of the *stratum compactum*, while in the laterals gland do not (Brunetti et al. 2014). Sometimes, there is a thickness increase in both strata in the nuptial pad (Luna et al. 2018). In poison frogs conversely, the sexual dimorphic swelling of the fingers and wrist has no additional dermal modifications (Cavalcanti et al. 2021). Despite this, the arm swelling of *Hyloxalus* is accompanied by a great melanophores accumulation associated with the specialized exocrine glands, sometimes observed as a thin layer just beneath the epidermis. Remarkably, the melanophores are found in the *tela subcutanea* also and with the thick *tela subcutanea* forming an enlarged lymphatic space.

Unlike the almost un-noticeable arm swelling of *H. pinguis* (and also *H. pulchellus*) that has few melanophores only in the dermis and a narrow lining layer *tela subcutanea*, with small lymphatic spaces, as in many anurans (see Elkan 1968). Few is known about the *tela subcutanea* in anurans, but iridophores accumulation has been reported in the ventral integument of the body of *Hyperolius viridiflavus* (Kobelt and Linsenmair 1986), and there are some species with a thicker layer; for example, in the dorsal and ventral integument of the body of *Discoglossus pictus* and *Telmatobius macrostomus* (Elkan 1968: Fig. 16, 28).

Despite the limited samples, the result clearly shows that arm swelling is a heterospecific complex structure, involving modifications in the integument. In most species evaluated, the integument is glandular, with specialized exocrine glands, there is melanophores accumulation in the *stratum spongiosum* and the *tela subcutanea*, and the last layer forms an enlarged lymphatic space. These features are not the

generality, because there is nongladular arm swelling, and in other species only there are specialized exocrine glands.

Arm Swelling, Characters and Systematic Implication

Our revision finds the arm swelling (before known as black arm gland) in other eight additional species (viz., *Hyloxalus craspedoceps, H. pinguis, H. pulchellus, Hyloxalus* sp. Albán, *Hyloxalus* sp. *fascianigrus*-like, *Hyloxalus* sp. Icononzo, *Hyloxalus* sp. MesasGalilea, and *Hyloxalus* sp. Samaná), for a total 17 *Hyloxalus* species with swelling on the forelimb.

Our findings has implications on that is known as black arm gland (BAG), because the swelling can be glandular or not, and despite coloration variation, there are white swelling, due to scarce melanophores in the dermis. Previous studies considered external features mainly to named the swelling. Thus Grant and Castro (1998) adopted the name black arm band based on the dark external coloration of the swelling; after that, Grant et al. (2017) changes to the current name, assuming that swelling in all species was glandular, although without evidences for that. Nevertheless, based on their phylogenetic result, where four *Hyloxalus* with swelling are not close related, they suggested possible integumentary differences in this homoplastic character. Our results confirm it, because the swelling on the arm differ interspecifically in dermal and hypodermal structures. Thus, although most species has a glandular integument, externally dark, the swelling of the *H. anthracinus* lack of the specialized glands, while there is a very low, white protuberance in *H. pinguis* and *H. pulchellus*. Therefore, the former names not embrace all swelling types, and in consequence, we propose the name “Arm swelling” to include all external arm protuberances observed in those seventeen *Hyloxalus*.

Recently, another name was proposed by Acosta et al. (2020). Despite the broad external color variation, they used this variation to name it as arm gland,

delimiting the “pale” condition for light gray/brown swelling, and the black state for dark-colored swelling. However, in addition to the glandular integument not yielding all swelling, our extensive revision of adult show that species with “pale” swelling also has dark and black coloration (see **Figure 1H**). Therefore, we do not recognize this character-states given the dependence on the external coloration and pigments, but instead of this we proposed transformation series for the dark pigments in each integumentary layer, given the independence in the topological position in the integument and the melanophores variation.

Structurally, the arm swelling is complex and heterogeneous morphological structure in *Hyloxalus.* Based on this variation, we proposed nine characters (two from external morphology and seven from integument) from the single character proposed by Grant et al. (2006: character 27, 2017). Nevertheless, due to the limited histological samples, the homology and evolution of the integumentary characters was not evaluated. Despite this, there appear to be a relation between the arm swelling types, the integumentary characters and the current phylogenetic relationships.

The *Hyloxalus pulchellus* group is composed of *H. arliensis*, *H. delatorreae* (KJ940457, KU220619–20), *H. lehmanni*, *H. pinguis*, *H. pulchellus*, *H. vertebralis*, the undetermined *Hyloxalus* sp. MonteOlivo and *Hyloxalus* sp. SanMiguelDeSalcedo, and the undescribed *Hyloxalus* sp. Albán and *Hyloxalus* sp. MesasGalilea (for definition see **Chapter 2**). Optimization of the presence of the arm swelling is ambiguous for the node of this clade, but this is derived and shared for a restricted clade that excludes *H. vertebralis*. The arm swelling occurs in most species of this clade, minus in *H. delatorreae,* and is unconfirmed in *Hyloxalus* sp. MonteOlivo and *Hyloxalus* sp. SanMiguelDeSalcedo. Two arm swelling types are found in this clade, type I in *H. lehmmani* and type II in *H. pinguis*.

Type I is also found in three non-sequenced undescribed species, *Hyloxalus* sp. *fascianigrus*-like, *Hyloxalus* sp. Icononzo, and *Hyloxalus* sp. Samaná. These are phenotypically similar to *H. lehmanni* (see Grant and Ardila 2002, Grant et al. 2017), likewise as their sister species (*H. arliensis, Hyloxalus* sp. Albán, and *Hyloxalus* sp. MesasGalilea). If histological data or phylogenetic relationships will be as expected, that is, unsequenced species are closed related to the *H. lehmanni*, and the sister species has arm swelling type I, then glandular integument features of this type (i.e., SMGs and SSGs occurrence, with many melanophores in the dermis, and with pigments in the enlarged lymphatic space of the *tela subcutanea*) could be synapomorphic for this clade, evolving independently at its node. Concerning type II, further studies are necessary to corroborate the swelling type in *H. pulchellus* and the occurrence in the closely related species (i.e., *H. delatorreae, Hyloxalus* sp. MonteOlivo, and *Hyloxalus* sp. SanMiguelDeSalcedo) to unravel the evolution of this arm swelling type. Moreover, the fact that *H. pinguis*—a species with almost un-noticeable swelling, has a glandular integument, opens the possibility that other species without protuberant swelling, really have this.

The gains of the arm swelling and integumentary modifications evolve independently in *Hyloxalus nexipus*. At least two species are in *H. nexipus* (see Grant et al. 2006, Santos et al. 2014, and chapter 2). The San Martin, Perú population is a distinct lineage from those of Morona Santiago, Ecuador. The histological analyzed specimen with glandular arm swelling is from San Martín, Perú (KU 211827). One adult male from Morona Santiago, Ecuador also has arm swelling (QCAZ 26240), but histological confirmation is necessary. This species is the only one exhibiting arm swelling type III. On the other hand, the arm swelling type III is populated by SSGs, also found in the arm swelling type I; however, the relationships reveal homoplasy in this character.

Furthermore, these serous glands of type I and III exhibit differences in the syncytium, because there are semicircular regions or compartments in type III of *H. nexipus*. This feature also differ from the serous gland of Anura, for the reason that their syncytium is relatively homogeneous, filled with granules varying in density and size (Toledo and Jared 1995, Delfino et al. 2001, Terreni et al. 2002; Brunetti et al. 2016). However, in other amphibians, such as salamanders and caecilians, there is regionalization in the glands (Mauricio et al. 2021). Further studies are necessary in the syncytium of the serous gland of the *H. nexipus* and other *Hyloxalus* to characteriz the syncytium, determine the differences, and try to understand their function.

The arm swelling of the *Hyloxalus anthracinus*, peculiarly, lack of the specialized glands, but the swelling is generate by the great melanophores accumulation in the dermis and in the enlarged lymphatic space of the *tela subcutanea*. Until now, this arm swelling type is only found in this species, and given the topological position of the species, some integumentary features of this type are autapomorphies (e.g., melanophores disposed in a thin layer in the *tela subcutanea*). Nevertheless, additional samples are required to corroborate our findings. For the case of the arm swelling occurrence, given the ambiguity in the optimization, it is unclear if arm swelling of *H. anthracinus* is homologous with the arm swelling type I and II, or otherwise, if this represent an evolutionary novelty.

Sexual dimorphic characters present one specialized gland type. For instance, in hylids, the specialized mucous and serous glands occur independently; however, both specialized gland types co-occur in mental and lateral glands of some Cophomantinae (Brunetti et al. 2012, 2014, Luna et al. 2019). Likewise, the *Hyloxalus* with an arm swelling type I has a mixture of the specialized mucous and serous glands in the glandular integument. Nonetheless, the arm swelling type II and

III, like the finger and the wrist swelling (see Cavalcanti et al. 2021) has one specialized gland type.

Implications in the Arm Swelling Function

Presumably, the arm swelling is involve in the reproductive amplexus (Grant and Castro 1998). However, this behavior is unknown for most species with arm swelling (except *H. fascianigrus*), and this data type is available for a few *Hyloxalus* species (Lotter et al. 2000*,* Grant et al. 2006, Quiguango and Coloma 2008). Amplexus is cephalic in two species of the genus (*H. fascianigrus* and *H. toachi*), like as many aromobatids and dendrobatids (Myers et al. 1991, Grant et al. 2006, 2017), but this is absent in *H. azureiventris* (Lotters et al. 2000, Grant et al. 2006, Quiguango and Coloma 2008). This show that there is variation if this character within the genus, which suggest caution with a generalization. Despite this, exocrine glands and the dermal modification found in the studied arm swelling types can be provide some clues about its function.

Specialized dimorphic sexual glands (SDSGs) participate in and enhance different reproduction instances; for example, courtship, nuptial hug, and mating, as well as in eggs and larvae transport (Conaway and Metter 1967, Duellman and Trueb 1994; see reference in Brizzi et al. 2003). Moreover, serous glands produce toxic and noxious secretions, as well as odorous volatile compounds that are involved in chemical defense (Toledo and Jared 1995, Smith et al. 2004, Delfino et al. 2010; Brunetti et al. 2016; Myers et al. 1991; Means and Savage 2007); however, both mucous and serous glands can be a type of SDSGs (Thomas et al. 1998, Luna et al. 2019). Although histochemical data are limited, the presence of the glandular integument with specialized mucous and/or serous glands in the dimorphic arm swelling type I–III agrees with the idea that this protuberance is implicit in reproduction.

On the other hand, the analogous branchial gland found in the adult male of the brachycephalid *Niceforonia adenobrachia* shows a great melanophores quantity in the thick *stratum spongiosum*, but this structure lack*s* the specialized glands. The great thickness of the dermis with melanophores causes the enlarged branchial gland which helps the male fasten the female in the reproductive amplexus (Romero de Perez and Ruiz-Carranza 1996). In the same way, there is quite tempting to think that the enlarged lymphatic space in the *tela subcutanea* and the melanophores accumulated in the dermis and hypodermis of the arm swelling type I, III, and IV can provide surface increase to enhance the fastness in the cephalic amplexus. However, additional behavior, histology, and biochemical data are necessary to corroborate the arm swelling function.

It is important to consider that arm swelling in *H. nexipus* (type III) is packed by hypertrophied serous glands. In poison frogs, these glands stored the alkaloids employed in the antipredatory strategy (Neuwirth et al., 1979, Daly et al. 1987, Myers and Daly 1983, Saporito et al. 2010); however, despite the bright coloration (shades from red-orange) on dorsolateral and oblique lateral stripes, alkaloid sequestration capacity is absent in *H. nexipus* (Santos and Cannatella 2011), discarding that arm swelling participate in this function.

As recognized by Cavalcanti et al. (2021), poison frogs lack the nuptial pads, but these frogs have three sexual dimorphic characters, all located in distinct forelimb regions—(1) the finger IV swelling (also present in other fingers, extending to wrist), widespread distributed taxonomically; (2) the arm swelling of some *Hyloxalus* (or black arm gland); (3) and the carpal pad restricted to *Allobates undulatus* and two *Anomaloglossus* (*A. saramaka, A. vackeri*; Fouquet et al. 2020). Likewise, they pointed the co-occurrence of the former (as basal finger and metacarpal swelling) and the second swelling in *H. nexipus* and *H. anthracinus*. In both species, the finger base

and metacarpal region of the hand is filled with specialized mucous glands (Cavalcanti et al. 2021), while the arm swelling of the *H. nexipus* possesses hypertrophied serous glands discarding glands homology; but contrarily, in *H. anthracinus* the arm swelling integument is not glandular. The remaining species with arm swelling do not present another sexual dimorphic character on the forelimb.

The histochemical data and the reproductive behavior sustained that finger IV swelling is involved in cephalic amplexus, whereas the function of the arm swelling in reproductive amplexus is hypothetic. In case the last is confirmed, then the occurrence the both sexual dimorphic characters in *H. nexipus* allow entails interesting questions about function because we do not know if both sexual dimorphic characters participate simultaneously or sequentially in cephalic amplexus, or whether arm swelling is implicit for other courtship instances. Concerning the arm swelling type I and II, if its specialized mucous glands come from the same transformation event as finger IV swelling or represent evolutionary novelties and by consequence, the arm swelling is its substitute is an interest unresolved topic.

Many questions arise with our findings, which invite to further histochemical, biochemical and behavioral studies in *Hyloxalus* and other poison frogs. Moreover, a large gap in natural history data in this genus precludes infers function of the sexual dimorphic arm swelling and the integumentary modifications that it entails, which natural history studies in this genus are necessary. At moment, our study provide evidence of non-homologous and convergent evolution of the arm swelling, and given the current phylogenetic scenario, it is plausible to think that arm swelling are immerse in distinct functions; however, until now the morphological and histological evidence provided support to that these are a functional extension in the reproductive amplexus. To test all of these questions, we recommended more extensive revision of the integument and glands of the species with arm swelling, or the distal upper arm

and proximal lower arm of the other *Hyloxalus* and poison frogs to elucidate homology, characters and evolutionary aspect, and their systematics and biological implications in the Dendrobratoidea.

Acknowledgement.—We thanks to the Dr. Andrés Brunetti, Dra. Adriana Jeckel, Dra. Carola Yovanovich and the technicians Phillip Lenktaitis and Enio Mattos for you help with the histological procedures and results. We grateful to curator and/or managers Andrew Crawford (ANDES-A), John D. Lynch (ICN), Manuel Bernal and Sigifredo Clavijo (CZUT-A), Rafe Brown, Richard Glor, and Melissa Mayhew (KU), Aline Staskowian Benetti and Hussam Zaher (MZUSP), Belisario Cepeda and Fernando Santander (PSO-CZ) by specimens loans and allow us to obtain the skin samples. To Duvan Zambrano and Jhon Jairo Ospina, they provided variation data and photos from *Hyloxalus arliensis* and *H. saltuarius*, respectively. Grant doctoral scholarship of M. Anganoy was provided by the Fundación Centro de Estudios Interdisciplinarios Básicos y Aplicados – CEIBA (2016), and partial economical support was provided by the Brazilian Coordenação de Aperfeiçoamento de Pessoal de Nível Superior (CAPES Finance Code 001) and São Paulo Research Foundation (FAPESP Procs., 2012/10000-5, and 2018/15425-0).

LITERATURE CITED

Acosta-Galvis, A.R. 2000. Ranas, salamandras y caecilias (Tetrapoda: Amphibia) de Colombia. Biota Colombiana 1(3):289–319.

Acosta-Galvis, A.R., M. Vargas-Ramírez, M. Anganoy-Criollo, O. A. Ibarra, and S. Gonzáles. 2020. Description of a new diminutive *Hyloxalus* (Anura: Dendrobatidae: Hyloxalinae) from the Magdalena Valley of Colombia. Zootaxa 4758:83–102.

Agnarsson, I., and J.A. Miller. 2008. Is ACCTRAN better than DELTRAN? Cladistics 24:1032–1038.

Amey, A.P., and G.C. Grig. 1995. Lipid-reduced evaporative water loss in two arboreal hylid frogs. Comparative Biochemistry and Physiology 111A(2):283–291.

Anganoy-Criollo, M. 2013. Tadpoles of the high-Andean *Hyloxalus subpunctatus* (Anura: Dendrobatidae) with description of larval variation and species distinction by larval morphology. Papéis Avulsos de Zoologia 53:211–224.

Angel, R., G., Delfino, and G. Parra. 2003. Ultrastructural patterns of secretory activity in poison cutaneous glands of larval and juvenile *Dendrobates auratus* (Amphibia, Anura). Toxicon 41:29–39. doi:10.1016/s0041-0101(02)00206-4

Bagnara, J.T., J.D. Taylor, and M.E. Hadley. 1968. The dermal chromatophore unit. The Journal of Cell Biology 38:67–79.

Brizzi, R., G. Delfino, and R. Pellegrini. 2002. Specialized mucous glands and their possible adaptive role in the males of some species of *Rana* (Amphibia, Anura). Journal of Morphology 254:328–341.

Brizzi, X., G. Delfino, and S. Jantra. 2003. An overview of breeding glands. Pp. 254 – 317. in Reproductive biology and phylogeny of Anura (Jamieson, B., ed). Science Publishers, Inc., UK.

Brunetti, A.E., G.N. Hermida, and J. Faivovich. 2012. New insights into sexually dimorphic skin glands of anurans: The structure and ultrastructure of the mental and lateral glands in *Hypsiboas punctatus* (Amphibia: Anura: Hylidae). Journal of Morphology 273:1257–1271.

Brunetti, A.E., G.N. Hermida, M.C. Luna, A.M.G. Barsotti, C. Jared, M.M. Antoniazzi,M. Rivera-Correa, B.V.M. Berneck, and J. Faivovich. 2014. Diversity and evolution of sexually dimorphic mental and lateral glands in Cophomantini

treefrogs (Anura: Hylidae: Hylinae). Biological Journal of the Linnean Society 114:12–34.

Brunetti, A.E., G.N. Hermida, M.G. Lurman, and J. Faivovich. 2016. Odorous secretions in anurans: morphological and functional assessment of serous glands as a source of volatile compounds in the skin of the treefrog *Hypsiboas pulchellus* (Amphibia: Anura: Hylidae). Journal of Anatomy 228:430–442.

Campbell, J.A., and D.R. Frost. 1993. Anguid lizards of the genus *Abronia*: Revisionary notes, descriptions of four new species, a phylogenetic analysis, and key. Bulletin of the American Museum of Natural History 216:1–121.

Cavalcanti, I.R.S., M.C. Luna, J. Faivovich, and T. Grant. 2021. Structure and evolution of the sexually dimorphic integumentary swelling on the hands of dendrobatid poison frogs and their relatives (Amphibia: Anura: Dendrobatoidea). Journal of Anatomy 2021:1–19.

Conaway, C. H. and D. E. Metter. 1967. Skin glands associated with breeding in *Microhyla carolinensis*. Copeia 1967:672–673.

Daly, J.W., C.W. Myers, and N. Whittaker. 1987. Further classification of skin alkaloids from neotropical poison frogs (Dendrobatidae), with ageneral survey of toxic/noxious substances in the Amphibia. Toxicon 25(10):1023–1095.

Daly, J.W., T.F. Spande, and H.M. Garraffo. 2005. Alkaloids from amphibian skin: A tabulation of over eight-hundred compounds. Journal of Natural Products 68:1556–1575.

Delfino, G., R. Brizzi, and C. Calloni. 1985. Dermo-epithelial interactions during the development of cutaneous gland anlagen in Amphibia: a light and electron microscope study on several species with some cytochemical findings. Z. Mikrosk. Anat. Forsch. 99(2):225–53.

Delfino, G., R. Brizzi, B.B. Alvarez, and M. Gentili. 1999. Granular cutaneous glands in the frog *Physalaemus biligonigerus* (Anura, Leptodactylidae): Comparison between ordinary serous and ‘inguinal’ glands. Tissue & Cell 31(6):576–586.

Delfino, G., D. Nosi, and F. Giachi. 2001. Secretory granule-cytoplasm relationships in serous glands of anurans: Ultrastructural evidence and possible functional role. Toxicon 39:1161–1171.

Delfino, G., F. Giachi, D. Nosi, and C. Malentacchi. 2010. Serous cutaneous glands in *phyllobates bicolor* (Anura: Dendrobatidae): An ontogenetic, ultrastructural study on secretory product biosynthesisand maturation. Copeia 2010:27–37.

de Pérez, G.R., P.M. Ruiz-Carranza, M.P. Ramírez-Pinilla. 1992. Modificaciones tegumentarias de larvas y adultos durante el cuidado parental en *Minyobates virolinensis* (Amphibia: Anura: Dendrobatidae). Caldasia 17:75–86.

Duellman, W.E., and L. Trueb. 1994. Biology of Amphibians. McGraw Hill. Inc., USA

Elkan, E. 1968. Mucopolysaccharides in the anuran defence against desiccation. Journal of Zoology of London 155:19–53.

Elkan, E. 1976. Ground substance: An anuran defense against desiccation. Pp. 101–110 in Physiology of the Amphibia (Lofts, B. Ed.). Academic Press.

Farris, J.S. 1970. Methods for computing Wagner trees. Systematic Zoology 19:83–92.

Fitch, W.M. 1971. Toward defining the course of evolution: minimum change for a specific tree topology. Systematic Zoology 20:406–416.

Fouquet, A., R. Jairam, P. Ouboter, and P.J. R. Kok. 2020. Two new species of *Anomaloglossus* (Anura: Aromobatidae) of the *stepheni* group from Suriname. Zootaxa 4820:147–164.

Grant, T., and M.C. Ardila-Robayo. 2002. A new species of *Colostethus* (Anura: Dendrobatidae) from the eastern slopes of the Cordillera Oriental of Colombia. Herpetologica 58:252–260.

Grant, T., and F. Castro-Herrera. 1998. The cloud forest *Colostethus* (Anura, Dendrobatidae) of a region of the Cordillera Occidental of Colombia. Journal of Herpetology, 32:378–392.

Grant, T., and A.G. Kluge. 2004. Transformation series as an ideographic character concept. Cladistics, 20:23–31.

Grant, T., D.R. Frost, J.P. Caldwell, R. Gagliardo, C.F.B. Haddad, P.J.R. Kok, and W.C. Wheeler. 2006. Phylogenetic systematics of dart-poison frogs and their relatives (Anura: Athesphatanura: Dendrobatidae). Bulletin of the American Museum of Natural History 299:1–262.

Grant, T., M. Rada, M. Anganoy-Criollo, A. Batista, P.H. Dias, A.M. Jeckel, D.J. Machado, and J.V. Rueda-Almonacid. 2017. Phylogenetic systematics of dart-poison frogs and their relatives revisited (Anura: Dendrobatoidea). South American Journal of Herpetology 12:1–90.

Haslam, I.S., E.W. Roubos, M.L. Mangoni, K. Yoshizato, H. Vaudry, J.E. Kloepper, D.M. Pattwell, P.F.A. Maderson, and R. Paus. 2014. From frog integument to human skin: Dermatological perspectives from frog skin biology. Biological Reviews 89:618–655.

Hoffman, E.A., and M.S. Blouin. 2000. A review of colour and pattern polymorphismsin anurans. Biological Journal of the Linnean Society 70:633–665.

Kobelt, F., and K.E. Linsenmair. 1986. Adaptations of the reed frog *Hyperolius viridiflavus*(Amphibia, Anura, Hyperoliidae) to its arid environmentI. The skin of *Hyperolius viridiflavus nitidulus* in wet and dry season conditions. Oecologia 68:533–541.

Lillywhite, H.B. 1971. Thermal modulation of cutaneous mucus discharge as a determinant of evaporative water loss in the frog, *Rana catesbeiana*. Z. vergl. Physiol. 73:84–104.

Lötters, S., K.-H. Jungfer, A. Widmer. 2000. A new genus of aposematic poison frog (Amphibia: Anura: Dendrobatidae) from the upper Amazon basin, with notes on its reproductive behaviour andtadpole morphology. Jahreshefte der Gesellschaft für Naturkunde in Wurttemberg 156:233–243.

Luna, M.C., R.W. Mcdiarmid, and J. Faivovich. 2018. From erotic excrescences to pheromone shots: Structure and diversity of nuptial pads in anurans. Biological Journal of the Linnean Society 20:1–44.

Luna, M.C., C.R. Vásquez-Almazán, J. Faivovich, A.E. Brunetti. 2019. Gland composition in sexually dimorphic skin structures of two species of Hylid frogs: *Plectrohyla guatemalensis* and *Ptychohyla hypomykter.* Amphibia-Reptilia 2019:1–7.

Maddison, W. P. and D.R. Maddison. 2019. Mesquite: A modular system for evolutionary analysis. Version 3.61 http://www.mesquiteproject.org

Mauricio, B., P. L. Mailho-Fontana, L.A. Sato, F. F. Barbosa, R.M. Astray, A. Kupfer, E.D. Brodie, Jr., C. Jared, and M.M. Antoniazzi. 2021. Morphology of the cutaneous poison and mucous glands in amphibians with particular emphasis on caecilians (*Siphonops annulatus*). Toxins 13, 779. https://doi.org/10.3390/toxins13110779

Means, B. and J.M. Savage. 2007. Three new malodorous rainfrogs of the genus *Pristimantis* (Anura: Brachycephalidae) from the Wokomung Massif in west-central Guyana, South America. Zootaxa 1658:39–55.

Moreno-Gómez, F., T. Duque, L. Fierro, J. Arango, X. Peckham, and H. Asencio-Santofimio. Histological description of the skin glands of *Phyllobates bicolor*

(Anura: Dendrobatidae) using three staining techniques. International Journal of Morphology 32(3):882–888.

Myers, C.W., and J.W. Daly. 1983. Dart-poison frogs. Scientific American 248(2):120–133.

Myers C.W., O.A. Paolillo, and J.W. Daly. 1991. Discovery of malodorous and nocturnal frog in the family Dendrobatidae: Phylogenetic significance of a new genus and species from the Venezuela Andes. American Museum Novitates 3002:1–33.

Neuwirth, M., J.W. Daly, C.W. Myers, and L.W. Tice. 1979. Morphology of the granularsecretory glands in skin of poison-dart frogs (Dendrobatidae). Tissue and Cell 11(4):755–771.

Prates, I., M.M. Antoniazzi, J.M. Sciani, D.C. Pimenta, L.F. Toledo, C.F.B. Haddad, and C.Jared. 2012. Skin glands, poison and mimicry in dendrobatid and leptodactylid amphibians. Journal of Morphology 273:279–290.

Quiguango-Ubillús, A., and L.A. Coloma. 2008. Notes on behaviour, communication and reproduction in captive *Hyloxalus toachi* (Anura: Dendrobatidae), an endangered Ecuadorian frog. International Zoo Yearbook 42:78–89.

Romero de Perez, G., and P.M. Ruiz-Carranza 1996. Histología, histoquímica y estructura fina de la glándula mentoniana de dos especies de *Hyla* (grupo *bogotensis*) y del antebrazo de *Phrynopus adenobrachius*. Revista de la Academia Colombiana de Ciencias Exactas, Físicas y Naturales 20(78): 575–584.

Ruiz-Carranza, P.M., M.C. Ardila-Robayo, J.D. Lynch. 1996. Lista actualizada de la fauna Amphibia de Colombia. Revista de la Academia Ciencias Exactas, Físicas y Naturales 20:365–415.

Santos, J.C., and D.C. Cannatella. 2011. Phenotypic integration emerges from aposematism and scale in poison frogs. Proceeding of the National Academy of

Sciences United States of America 108:6175–6180. https://doi.org/10.1073/pnas.1010952108

Santos, J.C., M. Baquero, C. Barrio-Amoros, L.A. Coloma, L.K. Erdtmann, A.P. Lima, and D.C. Cannatella. 2014. Aposematism increases acoustic diversification and speciation in poison frogs. Proceedings of the Royal Society B: Biological Sciences 281:20141761–2014176. https://doi.org/10.1098/rspb.2014.1761

Saporito, R. A., M. Isola, V.C. Maccachero, K. Condon, and M.A. Donnelly. 2010. Ontogenetic scaling of poison glands in a dendrobatid poison frog. Journal of Zoology 282:238–245.

Schwinger, G., K. Zanger, H. Greven. 2001. Structural and mechanical aspects of the skin of *Bufo marinus* (Anura, Amphibia). Tissue and Cell 33(5):541–547.

Smith, B.P.C., C.R. Williams, M.J. Tyler, B.D. Williams. 2004. A survey of frog odorous secretions, their possible functions and phylogenetic significance. Applied Herpetology 2: 47–82.

Terreni, A., D. Nosi, R. Brizzi, and G. Delfino. 2002. Cutaneous serous glands in South□American anurans: An ultrastructural comparison between hylid and pseudid species. Italian Journal of Zoology 69:2:115–123.

Thibaudeau, G., and R. Altig. 2014. Coloration of anuran tadpoles (Amphibia): Development, dynamics, function, and hypotheses. International Scholarly Research Network Zoology 2012:1–16.

Thomas, E.O., L. Tsang, and P. Licht. 1993. Comparative histochemistry of the sexually dimorphic skin glands of anuran amphibians. Copeia 1993:133–143.

Toledo, R.C., and C. Jared. 1993. Cutaneous adaptations to water balance in amphibians. Comparative Biochemistry and Physiology 105A(4):593–608.

Toledo, R.C., and C. Jared. 1995. Cutaneous granular glands and amphibian venoms. Comparative Biochemistry and Physiology 111A:l–29.

TABLE 1.—Thickness of integument layers and glands size in the arm swelling (former black arm gland, BAG) and the adjacent skin regions (ASR) of the forelimb. OMGs and OSGs are ordinary mucous and serous glands, respectively; MGs and SGs are hypertrophied mucous and serous glands in the arm swelling, respectively. ∅ no data or absent. * see text for discussion.

Species	Sex	External protuberance (or BAG)	Glands Density (glands/mm.)		Ordinary glands size (µm)		BAG glands size (µm)		Integument thickness (µm)		Epidermis thickness (µm)	Dermis thickness (µm)	
			BAG	ASR	OMGs	OSGs	MGs	SGs	BAG	ASR	BAG	BAG	ASR
H.anthracinus	♂	+	5 – 7	∅	57.3 – 77.9	36,8 – 52,9	∅	∅	88,2 – 105,9	∅	29.4 – 41.2	47,0 – 70,6	58.8 – 82.3
H.fascianigrus	♂	+	8 – 11	5	52.9 – 64.7	29.4 – 50.0	73.5 – 95.5	45.7 – 52.8	111,7 – 147,0	58,8 – 76,4	23.5 – 29.4	88,2 – 123,5	29.4 – 58.8
	♀	–	5	2	39.7 – 52.9	29.4 – 51.4	∅	∅	82,3 – 93,5	64,7 – 88,2	23.5 – 41.2	52,3 – 58,8	29.4 –

												64.7
H.lehmanni	♂	+	10 – 13	9	47.0 – 61.7	29.4 – 42.6	73.5 – 95.6	58.8 – 79.4	135,3 – 158,8	75,8 – 82,3	23.5 – 29.4	105,9 – 135,3	52.3 – 58.8
	♀	–	4	5	45.6 – 58.8	32.3 – 58.8	∅	∅	94,1 – 135,2	52,9 – 58,8	23.5 – 47	70,6 – 88,2	29.4 – 35.3
H.nexipus	♂	+	9	∅	38.2 – 50.0	∅	48.5 – 73.5	72.0 – 95.6	129,4 – 152,9	∅	29.4 – 41.2	88,2 – 117,6	∅
	♀	–	6	7	32.3 – 51.4	36.7 – 54.4	58.8 – 79.4	44.1 – 55.8	100,0 – 117,6	69,9 – 82,3	23.5 – 35.3	70,6 – 82,3	41.2 – 64.7
Hyloxalus sp.Icononzo	♂	+	8 – 9	5	44.4 – 55.6	55.6 – 77.8	61.7 – 88.2	94.0	58,8 – 105,9	∅	11.8 – 23.5	52,9 – 94,1	∅

Hyloxalus sp.Samaná	♂	+	7 – 10	4	55.6 – 72.2	66.7 – 72.2	73.5 – 107.3	55.6 – 77.8	88,2 – 164,7	∅	17.6 – 29.4	70,6 – 105,8	∅
H.pinguis	♂	– *	7 – 9	3	17.6 – 35.3	27.9 – 42.6	51.4 – 98.5	∅	123,6 – 164,7	82,4 – 94,1	64.7 – 76.5	70,6 – 88,2	35.3 – 58.2
	♀	–	5 – 6	5	47.0 – 61.7	22.0 – 48.5	∅	∅	111,8 – 117,7	82,4 – 94,1	41.2 – 41.8	70,6 – 76,5	41.2 – 58.8

TABLE 2.—Histochemistry of the ordinary and hypertrophied exocrine glands in the distal end of the upper arm and proximal end of the lower arm to the periodic acid Schiff (PAS) and naphthol yellow (NY) stain. Ordinary mucous and serous glands are OMG and OSG, and hypertrophied mucous and serous glands are MG and SG. The dye affinity is coded as strongly positive (++), positive (+), negative (-), and equivocal or variable (+/-). Other abbreviations: not apply (na), and unknown data (?).

Species	ID #	Sex	PAS				NY			
			OMG	OSG	SMG	SSG	OMG	OSG	SMG	SSG
H. lehmanni	ICN 16281	♂	+	+	++	+	-	-	-	+
	ICN 21966	♀	+	+	na	na	-	-	na	na
H. fascianigrus	ICN 35527	♂	+	+	+	-	-	-	+/-	-
	ICN 32803	♀	+	+	na	na	+	+	na	na
H. pinguis	ICN 7670	♂	+	+	+	na	+	+	-	na
	ICN 32794	♀	+	+	na	na	-	-	na	na
H. anthracinus	KU 202813	♂	+	+	na	na	?	?	na	na
H. nexipus	KU 211827	♂	?	?	na	+	?	?	na	+
H. sp. Icononzo	ICN 35516	♂	+	+	+	+	+	+	-	-
H. sp. Samaná	PR 14890	♂	+	+	++	-	+	+	+	-

APPENDICES

APPENDIX 1

Specimens Examined

Individual with an asterisk mark was used for histological procedures.

Hyloxalus anthracinus: KU 207512–13, KU 132129, KU 142976, KU 202813*, KU 120637 – 38, KU 132527, KU 142544, KU 142546 – 47, KU 120635 – 36, KU 182210 – 11, KU 166118 – 20, KU 202827, KU 120656 – 58, KU 141563, KU 142545, KU 223489, KU 120639- 55, KU 121031.

Hyloxalus arliensis: IAvH-Am 8851, IAvH-Am 8853–54, IAvH-Am 8855, MUJ 5002, ICN 39106–07, ICN 39105, IAvH-Am 6554.

Hyloxalus cevallosi: USNM 282648.

Hyloxalus craspedoceps: KU 215609 – 10, KU 211952 – 59.

Hyloxalus exasperatus: KU 146240 – 41, KU 147100, KU 209650, KU 209648.

Hyloxalus fascianigrus: KU 289246 – 50.

Hyloxalus lehmanni: ICN 21966*, ICN 16280, ICN 16281*, ICN 16282 – 83, ICN 16286, ICN 18425 – 26, ICN 18428 – 31, ICN 19825 – 31, ICN 39045 – 47.

Hyloxalus pinguis: ICN 7670*, ICN 32794*, KU 189519 – 20, KU 189522 – 23.

Hyloxalus pulchellus: KU 143053, 143521 – 23, KU 143525 – 28, KU 166121 – 38, KU 166245, KU 166248.

Hyloxalus nexipus: KU 196727 – 30, KU 209397 – 98, KU 202822 – 24, KU 211811 – 12, KU 211815 – 17, KU 211819 – 21, KU 211823 – 26, KU 211827*, KU 211828 – 31, KU 211832*, KU 215594 – 96.

Hyloxalus saltuarius: ICN 42663–70, ICN 43464–65, ICN 43467, ICN 43466.

Hyloxalus sp. Albán: Andes-A2923, ICN 21945–47, ICN 21954 – 59.

Hyloxalus sp. fascianigrus-like: ICN 35527, ICN 32803*, ICN 32804 – 17, ICN 32819.

Hyloxalus sp. Icononzo: ICN 35516.

Hyloxalus sp. MesasGalilea: MAA 1271 – 77, MAA 1281.

Hyloxalus sp. Samaná: PR 14890.

APPENDIX 2

Integument of the Distal End of the Upper Arm and the Proximal End of the Lower Arm of the Species Studied of *Hyloxalus*.

See file: Plates_of _integument.

APPENDIX 2.1.—Integumentary features of the adult female (A) and adult male (B) of the *Hyloxalus pinguis*. A is skin without arm swelling, and B is skin with almost un-noticeable arm swelling. Abbreviations: Ep = epidermis, M and S = ordinary mucous and serous gland, M* = hypertrophied mucous gland, Me = melanophores, Mye = myoepithelial cells, Sc = stratum compactum, Ss = *stratum spongiosum*, Ts = *tela subcutanea*. Scale = 50 μm.

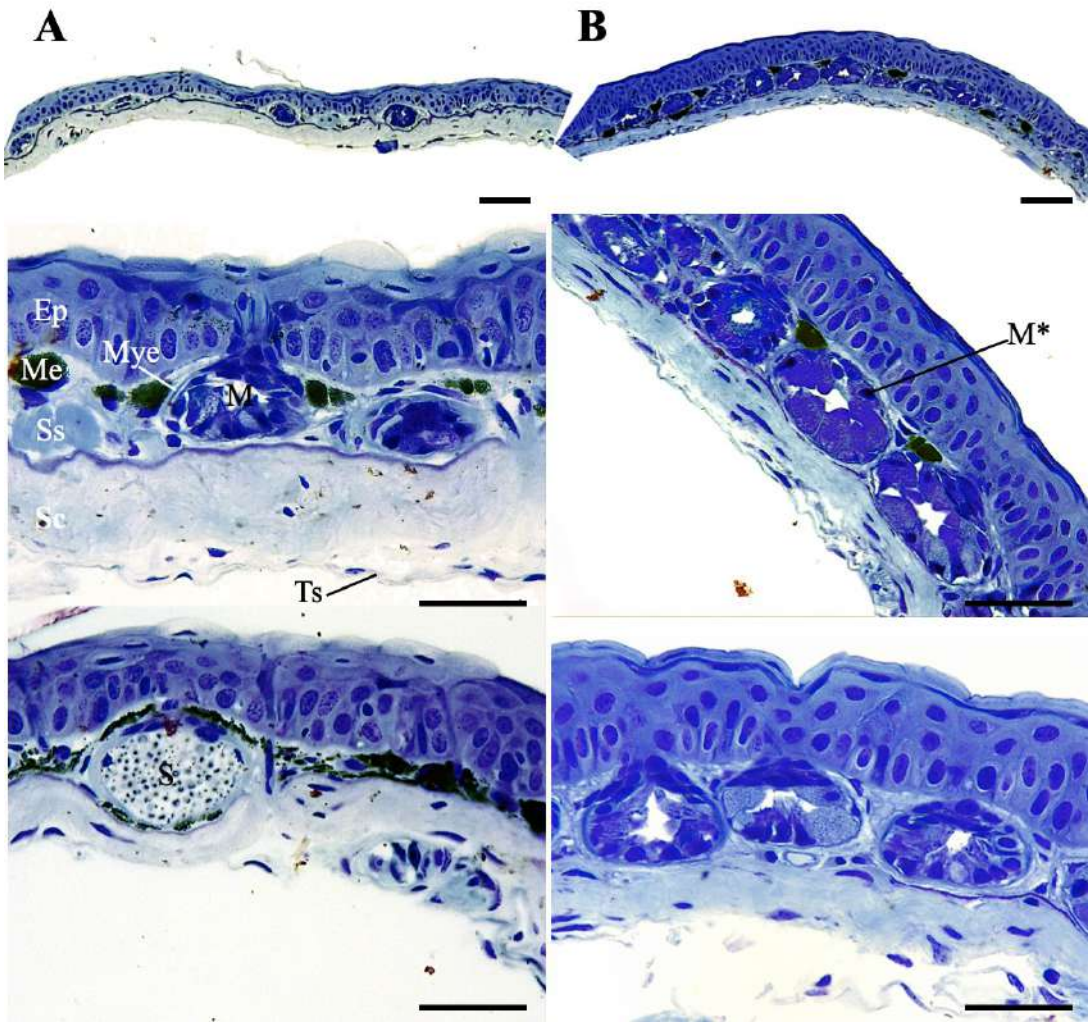

APPENDIX 2.2.—Integumentary features of the adult female (A, B, C) and adult male (D, E, F, G) of the *Hyloxalus lehmanni.* A, B, and C is skin without arm swelling, and D, E, F, and G is skin with arm swelling. D and G were stained with periodic acid schiff with naphthol yellow (PAS+NY). Abbreviations: M and S = ordinary mucous and serous gland, M* and S* = hypertrophied mucous and serous gland, Me = melanophores, Ts = *tela subcutanea*. Scale = 50 μm.

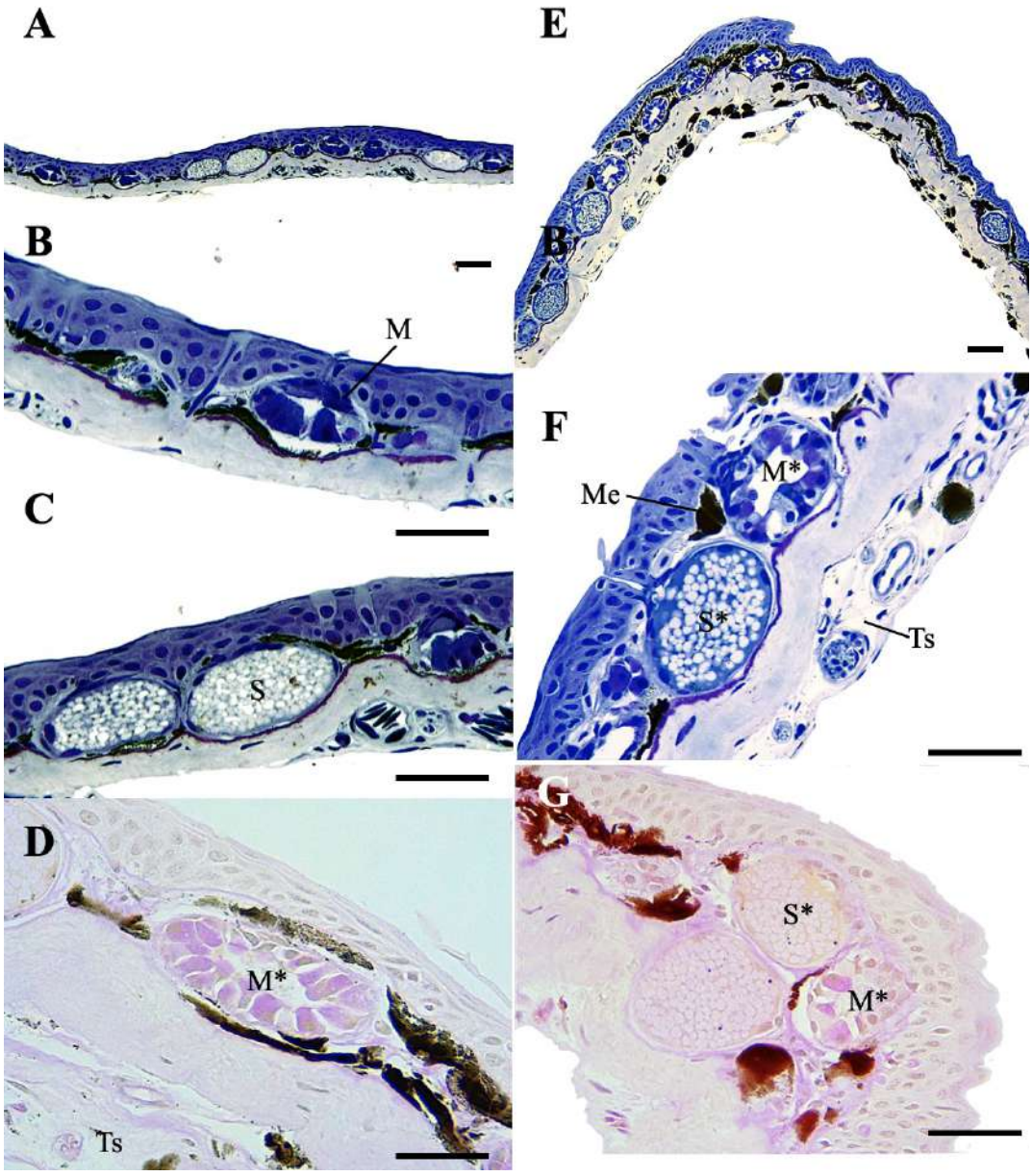

APPENDIX 2.3.—Integumentary features of the adult female (A and B) and adult male (C, D, E) of the *Hyloxalus* sp. *fascianigrus*-like. A, and B is skin without arm swelling, and C–E is skin with arm swelling. E was stained with periodic acid schiff with naphthol yellow (PAS+NY). Abbreviations: M and S = ordinary mucous and serous gland, M* and S* = hypertrophied mucous and serous gland. Scale = 50 µm.

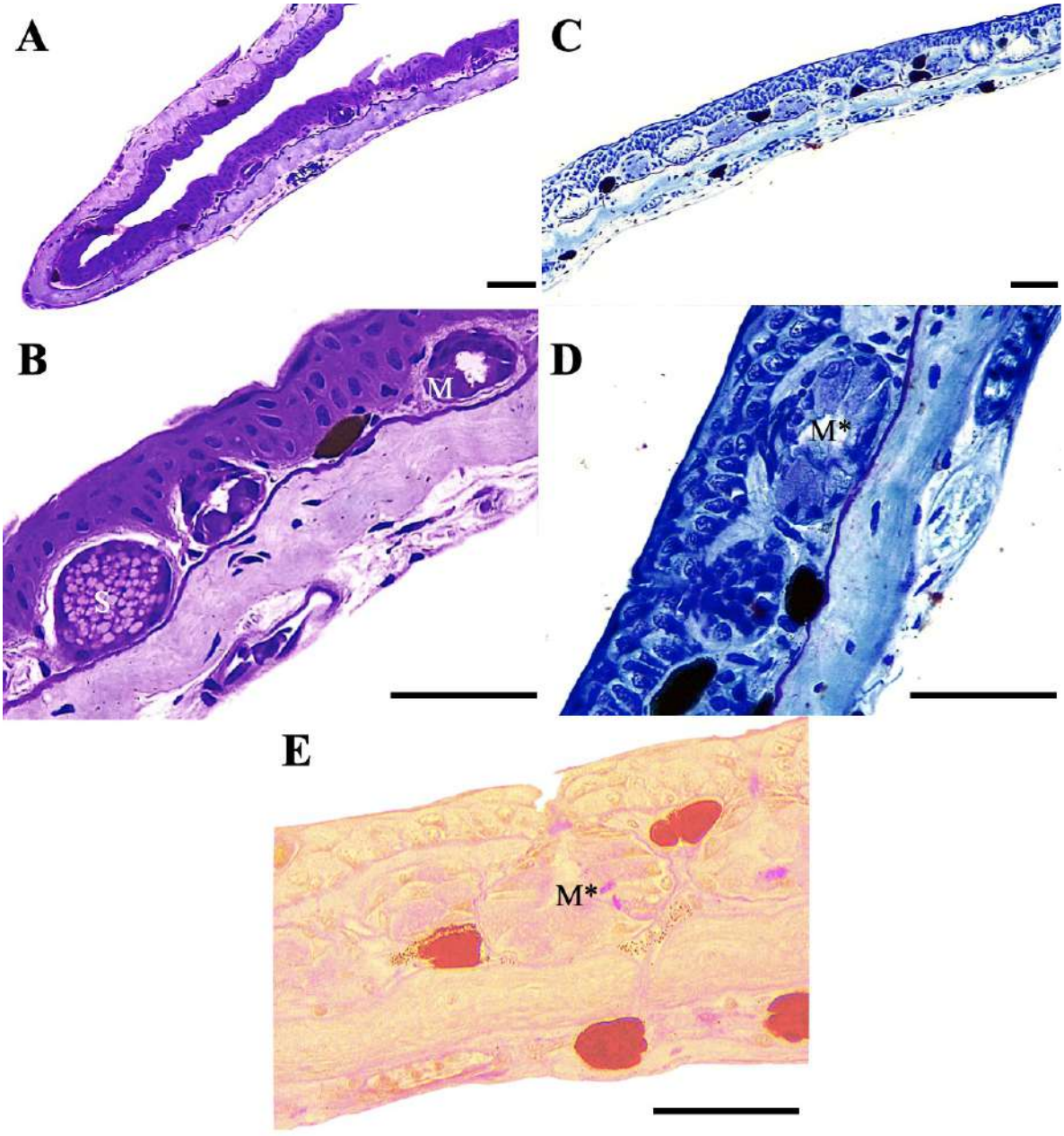

APPENDIX 2.4.—Integumentary features of the adult female (A) and adult male (B) of the *Hyloxalus nexipus*. A is skin without arm swelling, and B is skin with arm swelling. Abbreviations: M and S = ordinary mucous and serous gland, M* and S* = hypertrophied mucous and serous gland. White arrow show the semicircular region or compartment in the syncytium. Scale = 50 µm.

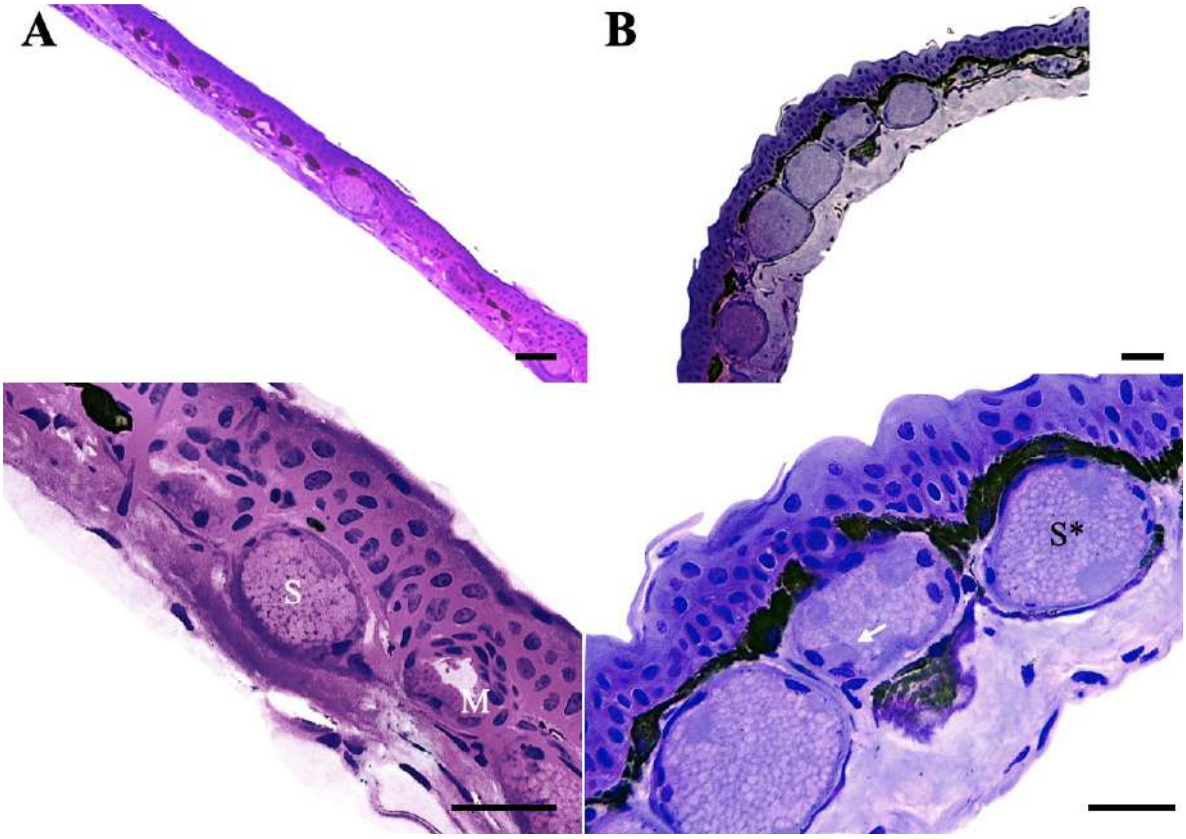

APPENDIX 2.5. —Integumentary features of the adult male of the *Hyloxalus anthracinus* (A), *Hyloxalus* sp. Icononzo (B), and *Hyloxalus* sp. Samaná (C). All samples are from skin with arm swelling. Abbreviations: Ep = epidermis, De = dermis, M and S = ordinary mucous and serous gland, M* and S* = hypertrophied mucous and serous gland, Ts = *tela subcutanea*. Scale = 50 µm.

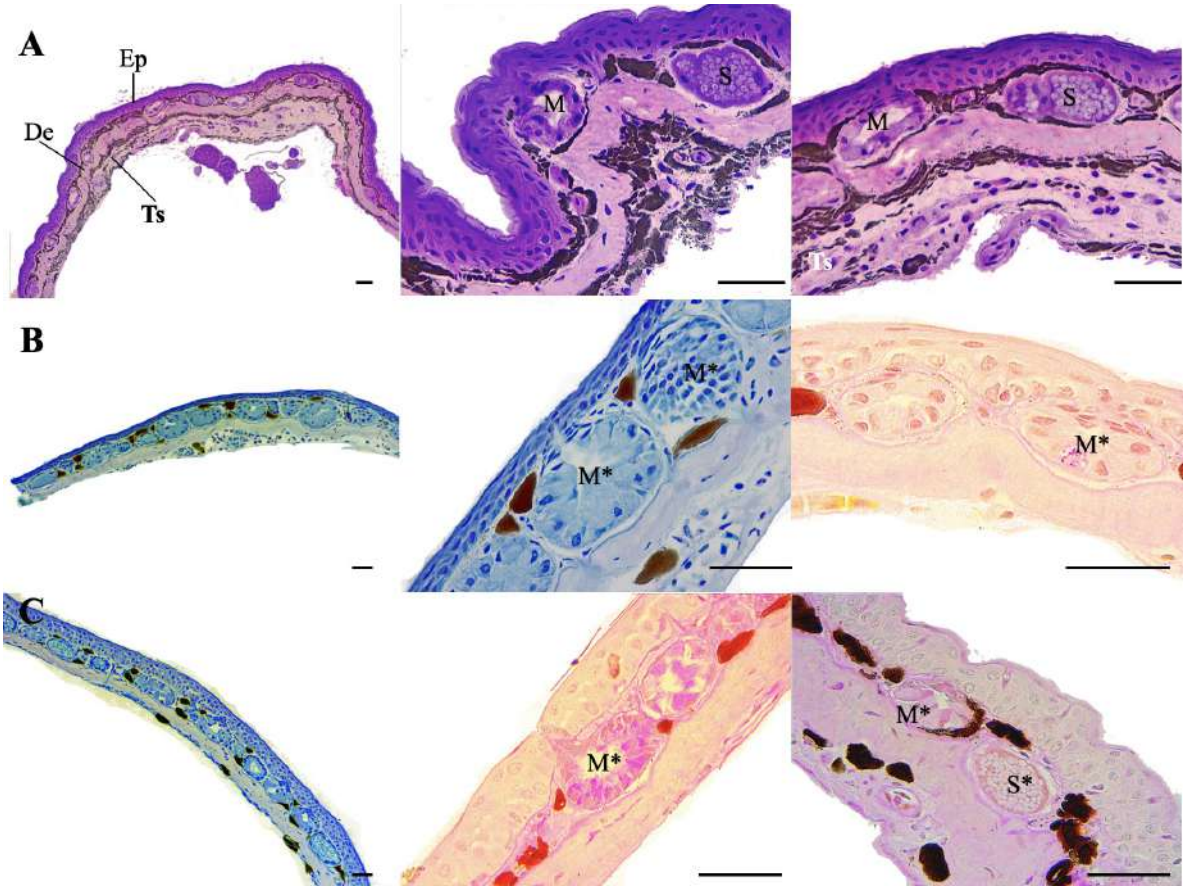

FIGURES CAPTIONS

FIGURE 1.—Arm swelling (former black arm gland, BAG) in *Hyloxalus*. Sexual dimorphism in *Hyloxalus pinguis* (A male, and B female) and *H. lehmanni* (C males, and D female). Interspecific differences between A, C, E, and G. Compare the white, almost un-noticeable swelling in *H. pinguis*, delimited by a dotted circle (A), with the dark (brown or black) swelling in *H. lehmanni* (C), *H. craspedoceps* (E), and *H. anthracinus* (G). Arm swelling is restricted to the distal end of the upper arm in A and E, or also it is extending to the lower arm in C (delimited by arrows) and G. Connective tissue with melanophores beneath the arm swelling in *H. saltuarius* (F. Not scale). The black arm swelling in life in *H. arliensis* (H. Not scale). Scale: 1 mm.

FIGURE 2.—Non-glandular integument with ordinary exocrine glands of skin without swelling of the distal end of the upper arm in the adult female (left) and the adult male (right) of the *Hyloxalus pinguis* (A) and *H. lehmanni* (B). Abbreviations: M = mucous gland, S = serous gland, Ep = epidermis, Sp = *stratum spongiosum*, Sc = *stratum compactum*, Ts = *tela subcutanea*. Scale = 50 μm.

FIGURE 3.—Integument from the arm swelling in three *Hyloxalus*, *H. pinguis* (A), *H. lehmanni* (B), and *H. anthracinus* (C). A glandular integument is observed in A and B. Note the melanophores accumulation in the dermis and the *tela subcutanea* in B and C, and the enlarged lymphatic space in the last layer in C. Scale = 50 μm.

FIGURE 4.—Size of the mucous glands (A) and serous glands (B). OMG and OSG are ordinary mucous and serous glands, and MG and SG are hypertrophied

mucous and serous glands, respectively. Size refers to the larger axis of the glands, longitudinal in the mucous gland and perpendicular in the serous gland.

FIGURE 5.—Specialized hypertrophied exocrine glands from the arm swelling in *Hyloxalus pinguis* (A), *H. lehmanni* (B, D), *Hyloxalus* sp. Samaná (C, E), and *H. nexipus* (F). B, C, D, and E stained with periodic acid Schiff and naphthol yellow. The semicircular region or compartment in the syncytium of the serous gland is shown with an arrow in F. Abbreviations: M* = hypertrophied mucous gland, S* = hypertrophied serous gland, Me = melanophores, Mye = myoepithelial cells. Scale = 50 μm.

FIGURE 6.—Evolution of the external morphology characters of the arm swelling in *Hyloxalus*. A. Character 1: arm swelling occurrence: absent in light blue, present in red. B. Character 2: arm swelling extension: restricted to the distal end of the upper arm in orange, and on the distal end of the upper arm, extending to the proximal lower arm in green. In blue square is the *H. pulchellus* group. Gray color in A is unknown condition, and in B is inapplicable.

General Discussion and Conclusions

The revision of the *Hyloxalus* revealed that there are additional phenotypic characters in poison frogs. The variation found in this anuran group allowed me to re-formulate some characters previously proposed, and also define new characters, which optimized as unambiguous synapomorphies at different clades of *Hyloxalus*, and of other clades of Dendrobatoidea (e.g., *Anomaloglossus*, *Ameerega*, Dendrobatoidea). For example, characters of the extrinsic musculature of the cloacal sheath are shared by the species of the *H. edwardsi* group; and the study of the arm swelling integument shows that there are heterospecific features in dermal and hypodermal layers and provided synapomorphies for a clade within of the *H. pulchellus* group. Thus, the phenotypic variation of *Hyloxalus* and Dendrobatoidea is a rich evidence source that can be useful both in systematic and phylogenetic studies, even more, in the present genomic era, where genotypic data tend to be common and widely used to infer relationships, while the phenotype evidence is increasingly limited.

The topological relationships within *Hyloxalus* were severely tested with the successive outgroup expansion. This revealed that with the addition of a single species the known *Hyloxalus* relationships are affected because the relationships of this species and its sister species changes topologically. This impact also was found when was incorporated more terminals and characters of the ingroup to the phylogeny; however, the impact was larger because some clades remain sensitive to the outgroup in the finals analysis rounds. Nevertheless, given most ingroup relationships become stable or insensitive in the three last expansion rounds, this suggesting that these changing clades in their topological position are due to the ingroup evidence of each clade (i.e., terminals and character) rather outgroup effect.

Thus the successive outgroup expansion allows identifying the weak regions of the tree where is necessary more evidence to unveil their relationships.

Three monophyletic large clades within *Hyloxalus* were identified: the *H. bocagei, H. pulchellus*, and the *H. subpunctatus* clades. These groups were recovered in the last three final rounds of the successive outgroup expansion, and also have been previously recovered (Grant et al. 2017). Likewise, other proposed Dendrobatoidea relationships were recovered. In addition to the molecular evidence, each of one these three groups are supported in phenotypic synapomorphies. Moreover, this study showed that there are additional undescribed species in each one of these clades, therefore their diversity is larger than formally described. On the other hand, with the available phenotype synapomorphies, some unsequenced species were allocated in one of these three clades, but in another case, this was not possible. Thus, on the basis of the phylogenetic evidence and the divrecuperatedersity of each clade, in Chapter 2 were proposed a new monophyletic taxonomy for *Hyloxalus* that mirror their phylogenetic relationships, recognizing *H. bocagei*, *H. pulchellus*, and *H. subpunctatus* clades as generic unit, as was predicted by Grant et al. (2006).

The evolutionary analysis of the phenotype shows that some synapomorphies are related to habitat. For instance, the *Hyloxalus* inhabiting riparian habitats have flat subarticular tubercles on hand and smooth skin on the ventrolateral body flanks; in change, those that occupy terrestrial habitats have projected subarticular tubercles on hand and granular ventrolateral body flanks. However, there are exceptions to this pattern outside *Hyloxalus,* because the terrestrial Dendrobatinae has flat subarticular tubercles. Unfortunately, the function for most phenotypic features in Dendrobratoidea is unknown or for a few cases, this is suspected.

The life history is complex in poison frogs with elaborated reproductive behavior and social interactions, but this knowledge come from a few groups (e.g., Oophaga, Dendrobates), and in *Hyloxalus* there is a larger gap in that because the behavioral data only have been described for four species, obfuscating the evolutionary study of the many phenotypic characters. To illustrate this, the reproductive function of the dimorphic arm swelling present in some *Hyloxalus* is suspected, given that the reproductive amplexus was documented for one species (*H. fascianigrus*) with arm swelling. Nonetheless, the use of the other tools and technicals can help to understand the character evolution, because in this case the histological characterization of the exocrine glands and the integument supply some insight into the reproductive function of this character. However, more natural history studies like phenotypic characters evaluations are recommended.

Finally, the *Hyloxalus* and dendrobatoids systematic is a fruitful field that supplies data to the continuous discussion in phylogeny and evolution of this anuran group and amphibians in general; additionally, these provide empirical evidence to the homology and characters theoretical debate. An interesting non-evaluated aspect in this study is the impact of the phenotypic evidence on phylogeny, which has provided arguments in favor of the phenotypic evidence in phylogenetic systematic. This is recommended for further studies. On the other hand, although this research treats to resolve some problems of the *Hyloxalus* systematic and phylogenetic, new questions arose from the results, invite to new and further tests in different aspects of poison frogs, such as taxonomic problems in complex species, relationships, phenotype evolution, natural history, and behavioral studies, among others biological aspect. Therefore, I expect that this study generates additional experiments and research that enrich the knowledge of Dendrobatoidea.

Resumo

Com 63 espécies, *Hyloxalus* é o gênero mais diverso de rãs venenosas neotropicais da superfamília Dendrobatoidea. As espécies deste gênero habitam diversos ecossistemas desde o nível do mar até os ecossistemas alto-andinos, da Colombia, Ecuador e Peru. Há vários problemas na sistemática e na filogenia deste grupo, como por exemplo: taxonomia não resolvida de diferentes complexos de espécies, falta de sinapomorfias fenotípicas para o gênero, inconsistências entre filogenias propostas quanto às relações de parentesco, variação fenotípica subestimada mesmo se conhecendo variação notável na morfologia (e.g., espécies menores sem membrana no pé, e com linhas laterais, ou espécies maiores com membrana no pé, mas sem linhas laterais), além de que o 50% das espécies (31 espécies) atribuídas ao gênero tentativamente. Alem disso, há déficit no conhecimento da diversidade, na filogenia, e na evolução de *Hyloxalus*, o que se toma evidente quando se compara este grupo com outros géneros de dendrobatoides (e.g., *Allobates*). Assim, neste estudo são avaliadas as relações filogenéticas de *Hyloxalus*, e também se tenta resolver alguns desses problemas mencionados, utilizando como fontes de evidência caracteres de adultos e de girinos, e também sequências de DNA. Para isso, a morfologia e a anatomia da maioria de espécies do gênero e de outros dendrobatoideos foi explorada e qualificada para procurar variação independente, afim de se testar caracteres e hipóteses de homologia já propostos, e além de formular novos caracteres filogenéticos. Novas sequências de DNA foram geradas tanto para cinco espécies até então não amostradas, como para novas amostras de espécies já conhecidas deste este ponto de vista. Sendo assim, essa evidencia foi montada em um dataset junto com outros dados de evidência molecular e fenotípica disponível de representantes de espécies de *Hyloxalus* e outras rãs venenosas. Este dataset foi

explorado para testar a monofilia de *Hyloxalus* e suas relações filogenéticas em uma análise de evidência total utilizando a máxima parcimônia como critério de otimalidade.

De acordo com os objetivos e os resultados, esta tese foi dividida em três capítulos: O primeiro deles discorre sobre a posição filogenética e avaliação do grupo de *Hyloxalus edwardsi* e sinapomorfias do mesmo. Os resultados mostram que, como foi suposto, o grupo é parte de *Hyloxalus*, irmão da espécie cis-Andina *H. picachos.* São propostas novas sinapomorfias fenotípicas para o grupo além da descrição de uma nova espécie para o mesmo. No segundo capítulo, é realizada a mais completa análise filogenética de *Hyloxalus* até hoje. A análise inclui 326 terminais em total, dos quais o grupo interno, *Hyloxalus*, inclui 189 como representantes de 38 espécies nominais e de 24 de espécies não descritas do gênero. O grupo externo inclui 137 terminais como representantes de 110 espécies de outros dendrobatoideos bem como de outras famílias. A hipótese recupera algumas relações monofiléticas bem suportadas dentro do grupo interno, mas demostra que *Hyloxalus* é parafiletico. Os clados internos de *Hyloxalus* estão sustentados com sinapomorfias fenotípicas não ambíguas, além de outros caracteres fenotípicos que otimizam como sinapomorfias em distintos clados em Dendrobatoidea. Também é revelado uma diversidade críptica em espécies de ampla distribuição no gênero. Nestes dois primeiros capítulos, também foi examinado o efeito de grupo externo na topologia e nas hipóteses de homologia do grupo interno, utilizando o método de expansões sucessivas do grupo externo (ou successive outgroup expansion em inglês). Para isso foram feitas seis e nove análises no primeiro e segundo capítulo, respetivamente. Nestas análises, o grupo externo foi ampliado gradativamente com a adição de terminais selecionados que tenham a capacidade de refutar as hipóteses. Em cada rodada a topologia do

grupo interno é afetada em diferentes níveis de inclusão, e em alguns casos, a monofilia de *Hyloxalus* e rejeitada. No terceiro capítulo, é estudada a histologia do tegumento e a homologia da glândula preta do braço em seis espécies do gênero. Essa glândula pode ser vista como um inchaço no braço, um caracter homoplástico historicamente relevante para a sistemática do gênero, com a hipótese de ter a função associada ao amplexo nupcial. Os cortes histológicos revelam glândulas exócrinas especializadas e modificações na derme e na hipoderme na região do referido inchaço da maioria das espécies estudadas. A variação da morfologia externa e do tegumento foi codificada em novos caracteres. Os caracteres de morfologia externa foram otimizados na filogenia obtida no anterior capítulo e revelaram aquisições independentes em *Hyloxalus* e, portanto, homoplasias. Entretanto, um dos tipo de inchaço do braço encontrados é derivado e compartilhado pelo grupo de espécies *H. puchellus*. A análise dessas modificações tegumentárias dá suporte para a hipótese funcional de o inchaço participar no amplexo nupcial. Outros tipos de estudo tais como histoquímica, bioquímica e de história natural são necessários para entender a evolução e função do inchaço. Os resultados demostram que a sistemática de *Hyloxalus* é uma área rica em evidencia para compreender as relações filogenéticas, a evolução e a biologia deste gênero e das rãs venenosas em geral.

Palavras-chave: Caracteres fenotípicos, Evidencia total, Expansões sucessivas do grupo externo, Dendrobatoidea, Hyloxalinae.

Abstract

With 63 species, *Hyloxalus* is the most speciose genus of the superfamily Dendrobatoidea, which comprises the neotropical poison-dart frogs and their relatives. Species of this genus inhabit diversity of environments from almost sea level to high-Andean ecosystems in Colombia, Ecuador, and Peru. The genus has several problems regarding its systematics and phylogeny. For example, unresolved taxonomy of species complexes, lack of the phenotypic synapomorphies for the genus, inconsistencies in the phylogenetic relationships between previous studies, underestimated phenotypic variation despite there are notorious morphological differences (e.g., small species without toe webbing and with lateral stripes, or large species with toe webbing and without lateral stripes), and a half of species (31 species) being assigned to the genus only tentatively. Moreover, progress about our knowledge about its diversity, phylogeny, and evolution is slow, which is evident when contrasting our knowledge of the group with other dendrobatoid genera (e.g., *Allobates*). Therefore, the present study evaluates the phylogenetic relationships of *Hyloxalus* and attempts to solve some of these problems, employing as evidence phenotypic characters of both adult and larvae as well as molecular DNA sequences. Accordingly, the morphology and anatomy of most species of this genus and several other dendrobatoids species were explored and assessed to search for independent variation. This variation was used to test characters and homology hypotheses previously formulated, and to propose new characters. Also, I generated molecular DNA data from five species that have never been sequenced before, and from additional populations of the other nominal species. All evidence was analyzed in a phylogenetic analysis together with the available phenotype and genotype data of

Hyloxalus and the poison frogs in general, in a total evidence analysis with parsimony as optimality criteria, to test the monophyly and the relationships of this genus.

Based on the aims and the results, this study was divided into three chapters, as follows: The first chapter evaluates the phylogenetic position and tests the monophyly of the *Hyloxalus edwardsi* group and its synapomorphies. Results show that this group is embedded within *Hyloxalus*, as proposed, sister to the cis-Andean species, *H. picachos*. New phenotypic synapomorphies for this group are provided, and a new species is described. The most comprehensive phylogeny of *Hyloxalus* to date is displayed in the second chapter, based on a total evidence approach and the direct optimization of genotypical and phenotypic evidence. The largest hypothesis contains 326 terminals, of which 189 belong to the ingroup, *Hyloxalus*, representing 38 nominal species (from a total of 63) plus 24 undescribed species of the ingroup. The outgroup has 137 terminals representing 110 species of Dendrobatidae and other anuran families. The resulting phylogeny shows a well-supported and monophyletic *Hyloxalus*. Internal clades are supported by unambiguously optimized phenotypic synapomorphies, and other phenotype synapomorphies optimized for different taxonomical levels for other clades in Dendrobatoidea. Hidden diversity within this genus is recognized. Additionally, for the first and second chapters, the outgroup effect on the ingroup homology and topology hypotheses is examined by means of the successive outgroup expansion method. Either six and nine analyses of the sequential outgroup terminals addition were performed on each chapter, respectively. Ingroup topology is impacted at different inclusiveness levels in each round, even compromising *Hyloxalus* monophyly in some cases. In the third chapter, the homology and the integumentary structure of the homoplastic, dimorphic black arm gland—a relevant character for systematic in *Hyloxalus*, because it is homoplastic,

with hypothesize function related to the reproductive amplexus—is assessed in six species through the use of histological techniques. Serial cuts show that specialized hypertrophied exocrine glands together with other dermal and hypodermal modifications fill the arm swelling in most of the six species examined. New characters from the external morphology and the integument are proposed. Optimization of the external morphology character disclosed independent evolutionary acquisition of the arm swelling and therefore homoplasies. However, an external swelling type is derived and shared in the *H. pulchellus* group. Furthermore, the analysis of the integumentary features provides support for the proposed functional hypothesis, that is, arm swelling is involved in the reproductive amplexus. Nevertheless, further histochemical, biochemical, and natural history studies are necessary to elucidate the evolution and function of the arm swelling. In general, all of these results highlight that *Hyloxalus* systematics is a rich source of evidence to understand the phylogenetic relationships, evolution, and biology of the genus and the poison frogs in general.

Key words: Phenotypic characters, Total evidence, Successive outgroup expansion, Dendrobatoidea, Hyloxalinae.

Literature Cited

Acosta-Galvis, A.R., and M. Vargas-Ramírez. 2018. A new species of *Hyloxalus* Jiménez De La Espada, 1871 ‘‘1870’’ (Anura: Dendrobatidae: Hyloxalinae) from a cloud forest near Bogotá, Colombia, with comments on the *subpunctatus* clade. Vertebrate Zoology 68:123–141.

Anganoy-Criollo, M. 2013. Tadpoles of the high-Andean *Hyloxalus subpunctatus* (Anura: Dendrobatidae) with description of larval variation and species distinction by larval morphology. Papéis Avulsos de Zoologia 53:211–224.

Coloma, L.A. 1995. Ecuadorian frogs of the genus *Colostethus* (Anura: Dendrobatidae). The University of Kansas Natural History Museum Miscellaneous Publication 87:1–72.

Dias, P.H.D.S., M. Anganoy-Criollo, M. Rada, T. Grant. 2021. The tadpoles of the funnel-mouthed dendrobatids (Anura: Dendrobatidae: Colostethinae: *Silverstoneia*): external morphology, musculoskeletal anatomy, buccopharyngeal cavity, and new synapomorphies. Journal of Zoological Systematics and Evolutionary Research 2021:1–27.

Duellman, W.E. 2004. Frogs of the genus *Colostethus* (Anura; Dendrobatidae) in the Andes of northern Peru. Scientific Papers Natural History Museum, The University of Kansas 35:1–49.

Frost, D.R. 2021. Amphibian species of the world: An online reference. Version 6.1 (31/01/2022). Electronic Database accessible at https://amphibiansoftheworld.amnh.org/index.php. American Museum of Natural History, New York, USA. doi.org/10.5531/db.vz.0001

Grant, T. 2019. Outgroup sampling in phylogenetics: Severity of the test and successive outgroup expansion. Journal of Zoological Systematics and Evolutionary Research 2019:1–16. https://doi.org/10.1111/jzs.12317

Grant, T., and M.C. Ardila-Robayo. 2002. A new species of *Colostethus* (Anura: Dendrobatidae) from the eastern slopes of the Cordillera Oriental of Colombia. Herpetologica, 58: 252–260.

Grant, T., and F. Castro-Herrera. 1998. The cloud forest *Colostethus* (Anura, Dendrobatidae) of a region of the Cordillera Occidental of Colombia. Journal of Herpetology 32:378– 392.

Grant, T., D.R. Frost, J.P. Caldwell, R. Gagliardo, C.F.B. Haddad, P.J.R. Kok, and W.C. Wheeler. 2006. Phylogenetic systematics of dart-poison frogs and their relatives (Anura: Athesphatanura: Dendrobatidae). Bulletin of the American Museum of Natural History 299:1–262.

Grant, T., M. Rada, M. Anganoy-Criollo, A. Batista, P.H. Dias, A.M. Jeckel, D.J. Machado, and J.V. Rueda-Almonacid. 2017. Phylogenetic systematics of dart-poison frogs and their relatives revisited (Anura: Dendrobatoidea). South American Journal of Herpetology 12:1–90.

Guillory, W.X., M.R. Muell, K. Summers, and J.L. Brown. 2019. Phylogenomic reconstruction of the neotropical poison frogs (Dendrobatidae) and their conservation. Diversity 2019:1–14.

Guillory, W.X., C.M. French, E.M. Twomey, G. Chávez, I. Prates, R. von May, I. de la Riva, S. Lötters, S. Reichle, S.J. Serrano-Rojas, A. Whitworth, J.L. Brown. 2020. Phylogenetic relationships and systematics of the Amazonian poison frog genus *Ameerega* using ultraconserved genomic elements. Molecular Phylogenetics and Evolution 142:1–13.

Haas, A. 1995. Cranial features of dendrobatid larvae (Amphibia: Anura: Dendrobatidae). Journal of Morphology 224:241–264.

Haas, A. 2003. Phylogeny of frogs as inferred from primarily larval characters (Amphibia: Anura). Cladistics 19:23–89.

Jetz, W., and A. Pyron. 2018. The interplay of past diversification and evolutionary isolation with present imperilment across the amphibian tree of life. Nature Ecology and Evolution 2:850–858.

Lynch, J.D. 1982. Two new species of poison-dart frogs (*Colostethus*) from Colombia. Herpetologica 38:366–374.

Muell, M.R., G. Chávez, I. Prates, W.X. Guillory, T.R. Kahn, E.M. Twomey, M.T. Rodrigues, J.L. Brown. 2022. Phylogenomic analysis of evolutionary relationships in *Ranitomeya* poison frogs (Family Dendrobatidae) using ultraconserved elements. Molecular Phylogenetics and Evolution 168:107389.

Myers, C.W. 1987. New generic names for some neotropical poison frogs (Dendrobatidae). Papéis Avulsos de Zoologia 36:301–306.

Myers, C.W., D. R. Ibáñez, T. Grant T, C.A. Jaramillo. 2012. Discovery of the frog genus *Anomaloglossus* in Panama, with descriptions of two new species from the Chagres Highlands (Dendrobatoidea: Aromobatidae). American Museum Novitates 3763:1–20.

Páez-Vacas, M.I., L.A. Coloma, and J.C. Santos. 2010. Systematics of the *Hyloxalus bocagei* complex (Anura: Dendrobatidae), description of two new cryptic species, and recognition of *H. maculosus*. Zootaxa 75:1–75.

Pyron, R.A. 2014. Biogeographic analysis reveals ancient continental vicariance and recent oceanic dispersal in amphibians. Systematic Biology 63:779–797.

Pyron, R.A., and J.J. Wiens. 2011. A large-scale phylogeny of Amphibia including over 2800 species, and a revised classification of extant frogs, salamanders, and caecilians. Molecular Phylogenetics and Evolution 61:543–583. https://doi: 10.1016/j.ympev.2011.06.012.

Rivero, J.A. 1991a. New *Colostethus* (Amphibia, Dendrobatidae) from South America. Breviora, 493:1–28.

Rivero, J.A. 1991b. New Ecuadorean [sic] *Colostethus* (Amphibia, Dendrobatidae) in the collection of National Museum of Natural History, Smithsonian Institution. Caribbean Journal of Science 27:1–22.

Rivero, J.A., and H. Granados-Díaz. 1990 ‘‘1989’’. Nuevos *Colostethus* (Amphibia, Dendrobatidae) del departamento de Cauca, Colombia. Caribbean Journal of Science 25:148–152.

Rivero, J.A., and M.A. Serna. 1986. Dos nuevas especies de *Colostethus* (Amphibia, Dendrobatidae) de Colombia. Caldasia XV:71–75.

Rivero, J.A., and M.A. Serna. 2000 ‘‘1995’’. Nuevos *Colostethus* (Amphibia, Dendrobatidae) del departamento de Antioquia, Colombia, con la descripción del renacuajo de *Colostethus fraterdanieli*. Revista de Ecología Latinoamericana 2:45–58.

Sánchez, D.A. 2013. Larval morphology of dart-poison frogs (Anura: Dendrobatoidea: Aromobatidae and Dendrobatidae). Zootaxa 3637:569–591.

Santos, J.C., and D.C. Cannatella. 2011. Phenotypic integration emerges from aposematism and scale in poison frogs. Proceeding of the National Academy of Sciences United States of America 108:6175–6180. https://doi. org/10.1073/pnas.1010952108

Santos, J.C., L.A. Coloma, K. Summers, J.P. Caldwell, R. Ree, and D.C. Cannatella. 2009. Amazonian amphibian diversity is primarily derived from late Miocene andean lineages. PLOS Biology 7:1–14. https://doi.org/10.1371/journal.pbio.1000056

Santos, J.C., M. Baquero, C. Barrio-Amoros, L.A. Coloma, L.K. Erdtmann, A.P. Lima, and D.C. Cannatella. 2014. Aposematism increases acoustic diversification and speciation in poison frogs. Proceedings of the Royal Society B: Biological Sciences 281:20141761–2014176. https://doi.org/10.1098/rspb.2014.1761